



HAL
open science

Perspective multi-échelle des tendances du changement climatique dans l'Océan Indien Sud : potentiels impacts sur les écosystèmes pélagiques et implications pour la gestion de la biodiversité

Clara Azarian

► To cite this version:

Clara Azarian. Perspective multi-échelle des tendances du changement climatique dans l'Océan Indien Sud : potentiels impacts sur les écosystèmes pélagiques et implications pour la gestion de la biodiversité. Océan, Atmosphère. Sorbonne Université, 2024. Français. NNT : 2024SORUS393 . tel-04901733

HAL Id: tel-04901733

<https://theses.hal.science/tel-04901733v1>

Submitted on 20 Jan 2025

HAL is a multi-disciplinary open access archive for the deposit and dissemination of scientific research documents, whether they are published or not. The documents may come from teaching and research institutions in France or abroad, or from public or private research centers.

L'archive ouverte pluridisciplinaire **HAL**, est destinée au dépôt et à la diffusion de documents scientifiques de niveau recherche, publiés ou non, émanant des établissements d'enseignement et de recherche français ou étrangers, des laboratoires publics ou privés.

SORBONNE UNIVERSITÉ

**Multi-scale perspective on climate
change trends in the Southern Indian
Ocean: potential impacts on pelagic
ecosystems and implications for
biodiversity management**

by

Clara Azarian

Under the supervision of Francesco D'OVIDIO and Laurent BOPP

A thesis submitted for the
degree of Doctor of Oceanography

in the
Faculté des Sciences et Ingénierie
ED129: Sciences de l'environnement de l'île-de-France

October 2024

Jury :

Francis Codron (président)
Rosemary MORROW (rapportrice)
Alice DELLA PENNA (rapportrice)
Nicole HILL (examinatrice)
Philippe KOUBBI (invité)
Francesco D'OVIDIO (directeur de thèse)
Laurent BOPP (co-directeur de thèse)

Declaration of Authorship

I, Clara Azarian, declare that this thesis titled, ‘Multi-scale perspective on climate change trends in the Southern Indian Ocean: potential impacts on pelagic ecosystems and implications for biodiversity management’ and the work presented in it are my own. I confirm that:

- This work was done wholly or mainly while in candidature for a research degree at this University.
- Where any part of this thesis has previously been submitted for a degree or any other qualification at this University or any other institution, this has been clearly stated.
- Where I have consulted the published work of others, this is always clearly attributed.
- Where I have quoted from the work of others, the source is always given. With the exception of such quotations, this thesis is entirely my own work.
- I have acknowledged all main sources of help.
- Where the thesis is based on work done by myself jointly with others, I have made clear exactly what was done by others and what I have contributed myself.

Signed:



Date: 20/05/2024

“Accroche-toi à tout, toi qui n’es rien. D’aucuns parlent de poussières d’étoile, d’autres de chair et d’os. Je ne suis qu’enchaînement de molécules, symbioses de bactéries, particules soi-disant ordonnées pour former ce tout qui est le moi. Ce moi qui étudie les autres moi ou les autres tout, particuliers et ordonnés. Je prends, je regarde. Je trie, je décortique. Dans mon arrogance, j’affirme. Dans mon humilité, je questionne. En tout temps, je cherche.”

Abstract

Significant physical changes have been observed in the Southern Ocean these last decades, notably through the subsurface accumulation and storage of heat at subantarctic latitudes. However, large uncertainties remain on climate change impacts on pelagic ecosystems, which can hinder climate change adaptation strategies in conservation and fisheries management. To investigate climate change impacts, especially for open ocean ecosystems, understanding better the physical and temporal complexity of changes is crucial. In this regard, important knowledge gaps remain concerning climate change impacts on 3D pelagic habitats and on fine scales features of ecological importance. The aim of this PhD thesis is to address these gaps through a multi-scale approach focused on the Southern Indian Ocean, which is a climate change hotspot and an interesting case study for biodiversity management. To do so, we investigate different spatial and temporal scales, focusing on physical features of ecological importance, through both satellite and *in situ* observations in the past and climate models projections in the future, also discussing relevant metrics and management strategies. First, an analysis of the spatial heterogeneity of current and projected warming and marine heatwaves characteristics over the Southern Indian Ocean is provided. Second, the impacts of marine heatwaves and long-term global warming on a subsurface water mass that plays a key role for top predators foraging strategy (so-called “winter waters”) are investigated. Third, the question of the potential impacts of climate change on the local circulation over and around the Kerguelen Plateau, which contributes to Patagonian toothfish (*Dissostichus eleginoides*) early-life stages transport, is addressed. Overall, this PhD thesis points out the projected increased exposure of subantarctic pelagic ecosystems to warming and marine heatwaves, with a projected southward shift of a water mass of key ecological importance (“winter waters”), especially west of the Kerguelen Plateau. Ocean circulation and the topography appear to modulate the spatial and temporal heterogeneity of change. In particular, the east of the Kerguelen Plateau stands out as an offshore temporary climate refugium. This refugium is also a potential recruitment area for Patagonian toothfish. This thesis highlights the high interannual variability of connectivity between potential spawning areas west of the Plateau and this possible recruitment area east of Kerguelen, as well as the non-linearity over time of climate change potential impacts on such connectivity. Scientific perspectives based on this work are discussed as well as further societal implications regarding the effective consideration of climate change in biodiversity management.

Résumé en français

Des changements physiques significatifs ont été observés dans l’océan austral ces dernières décennies, notamment du fait de l’accumulation et du stockage de chaleur aux latitudes subantarctiques. Cependant, de fortes incertitudes demeurent concernant les impacts de ces changements sur les écosystèmes pélagiques, ce qui peut freiner la prise en considération du changement climatique pour la conservation et la gestion des pêches. Mieux comprendre la complexité spatiale et temporelle de ces changements est crucial pour étudier les impacts, en particulier pour les écosystèmes pélagiques. Des lacunes subsistent sur les potentiels impacts du changement climatique sur les habitats pélagiques en 3D et sur les processus de plus fines échelles qui modulent la biodiversité localement. L’objectif de cette thèse est d’étudier ces questions à travers une approche multi-échelle appliquée à l’Océan Indien Sud, région pour laquelle une forte augmentation du contenu de chaleur dans la colonne d’eau subantarctique a été observée ces dernières décennies et qui est un cas d’étude intéressant pour la gestion de la biodiversité. Nous étudions, à travers différentes échelles spatiales et temporelles, les potentiels impacts du changement climatique sur des caractéristiques physiques d’importance écologique, en utilisant des observations satellite et *in situ* dans le passé et des projections de modèles climatiques dans le futur et en discutant également des mesures pertinentes de conservation et des stratégies de gestion adaptées pour prendre en compte cet environnement changeant. Tout d’abord nous analysons l’hétérogénéité spatiale des tendances actuelles et projetées du réchauffement et des caractéristiques des vagues de chaleur marines dans l’Océan Indien Sud. Ensuite, les impacts de ces vagues de chaleur marines et du réchauffement global sur une masse d’eau de subsurface, qui joue un rôle important dans la stratégie d’alimentation de grands prédateurs (les “eaux d’hiver”), sont étudiés. Enfin, la question des impacts potentiels du changement climatique sur la circulation océanique au niveau du Plateau de Kerguelen, qui contribue au transport des premiers stades de vie de la légine australe (*Dissostichus eleginoides*), est examinée. Cette thèse permet de mettre en évidence l’exposition accrue, projetée dans le futur, des écosystèmes pélagiques subantarctiques au réchauffement et aux vagues de chaleur marines, avec notamment un déplacement vers le sud projeté de masses d’eau d’importance écologique (les “eaux d’hiver”) en particulier à l’ouest du Plateau de Kerguelen. La circulation océanique et la topographie modulent l’hétérogénéité spatiale et temporelle des changements observés et projetés. En particulier, l’est du Plateau de Kerguelen est identifié comme une zone de “refuge climatique” pélagique temporaire. Cette zone de refuge pourrait aussi être une zone de recrutement pour la légine australe. La forte variabilité interannuelle de la connectivité entre des potentielles zones de frayères à l’ouest du Plateau et cette possible zone de recrutement à l’est de Kerguelen ainsi que la non-linéarité dans le temps des impacts potentiels du changement climatique sur cette connectivité sont aussi mises en

évidence. Les perspectives scientifiques de ces travaux sont discutées ainsi que les implications sociétales concernant la prise en compte effective du changement climatique dans la gestion de la biodiversité.

Acknowledgements

Un grand merci à mon jury de thèse: Rosemarry Morrow et Alice Della Penna (rapportrices) pour leur lecture attentive, leurs conseils et leur intérêt pour mes travaux; également Nicole Hill (examinatrice), Francis Codron (Président du Jury) et Philippe Koubbi (invité) pour leur implication et les discussions riches le jour de la soutenance.

Je tiens à remercier mes directeurs de thèse, Francesco d'Ovidio et Laurent Bopp pour leurs conseils et toutes les discussions scientifiques passionnantes que nous avons pu avoir. Merci de m'avoir permis de faire cette thèse et de m'avoir laissé une grande liberté dans le choix des sujets mais aussi de m'avoir guidée scientifiquement et avec bienveillance. Ce travail s'est également fait grâce à un grand nombre de collaborateurs avec lesquels j'ai eu un grand plaisir à travailler, notamment: Jean-Baptiste Sallée, Alice Pietri, Sebastiaan Swart, Christophe Guinet, Louise Rousselet, Jilda Caccavo, Philippe Koubbi, Félix Massiot-Granier, Mouna Chambon, Cam Ly Rintz, Camille Merland et Fanny Ouzoulias. Merci à mon comité de suivi composé de David Nerini, Thierry Penduff et Marion Gehlen pour leur intérêt et leurs conseils sur le déroulement de ma thèse.

Je tiens également à remercier les chercheurs du LOCEAN, du MNHN et d'autres laboratoires pour les discussions très enrichissantes, notamment Juliette Mignot, Julie Deshayes, Marina Lévy, Xavier Capet, Fabien Roquet et Clara Péron. En particulier, merci à Marc Eléaume pour m'avoir permis de participer à plusieurs événements dans le cadre de la CCAMLR et à Cédric Cotté pour m'avoir incluse dans l'équipe THEMISTO lors de la campagne ObsAustral 2024. Merci à toutes les équipes scientifiques et non-scientifiques de cette campagne pour cette expérience incroyable et unique!

Un grand merci aussi à tous les doctorants, post-doctorants et stagiaires du LOCEAN, qui contribuent à faire de ce laboratoire un espace de travail accueillant et bienveillant. Sara Sergi, Gina et Georges Baaklini, Pierre Chabert, Antoine Nasser, Lloyd Izard, Clément Haëck, Diego Cortes-Morales, Clovis Thouvenin-Masson, Léa Poli, Kenza Himmich, Gaston Irrmann, Robin Rolland, Linus Vogt, Kirtana Naeck, Yoania Povea-Perez, Cinthia Arellano, Shanshan Pang, Batoul Geara, Léonard Barthélémy, Ines Mangolte, Luther Ollier, Valentin Deteix, Nicolas Michalezyk, Adélie Antoine, Margaux Perhirin, Matthias Noel, Matthieu Delteil, Léna Champiot-Bayard, Maud Tissot, Auguste Gaudin, Stéphane Doléac, Matthis Guyomard, Alex Nalivaev, Lou Gauthier, Eeva Piedagnel, Elise Ortega, Ana Parracho et bien d'autres!

Merci à mes amis pour leur soutien et leur bonne humeur, les rires et les questions existentielles, notamment à Diane Lenormand, Madeline Petit et Laurent Le; mais aussi à mes amies d'enfance de Feucherolles. Un grand merci plein de tendresse à ma famille:

mes parents pour leur soutien sans faille et pour m'avoir donné le goût des sciences très tôt mais aussi la volonté de travailler pour l'intérêt général, à mon frère et à ma grand-mère pour leur curiosité sur tout ce que j'ai pu entreprendre. Merci tout particulièrement à Joris Verstraten pour avoir partagé ma vie pendant ces trois ans, les hauts, les bas, et avoir toujours cru en moi.

Contributions during the PhD

Peer-reviewed scientific publications

- **Azarian, C.**, Bopp, L., Sallée, J.-B., Swart, S., Guinet, C., and d'Ovidio, F. (2024). “Marine heatwaves and global warming impacts on winter waters in the Southern Indian Ocean”. *Journal of Marine Systems*. <https://10.1016/j.jmarsys.2023.103962>.
- **Azarian, C.**, Bopp, L., Pietri, A., Sallée, J.-B. and d'Ovidio, F. (2023) “Current and projected patterns of warming and marine heatwaves in the Southern Indian Ocean”. *Progress in Oceanography*. <https://doi.org/10.1016/j.pocean.2023.103036>.
- Chambon, M., Wambiji, N., Alvarez Fernandez, S., **Azarian, C.**, Ngunu Wandiga, Vialard, J., Ziveri, P., and Reyes-Garcia, V. (under review). “Weaving Scientific and Local Knowledge on Climate Change Impacts in Coastal Kenya, Western Indian Ocean.” *Environmental Science and Policy*.
- Merland, C., **Azarian, C.**, d'Ovidio, F. and Cotté, C. (under review). “Physical and biogeochemical regionalisations and climate velocities in the epipelagic and mesopelagic Southern Indian Ocean.” *CCAMLR Science*.
- **Azarian, C.**, Bopp, L., Massiot-Granier, F., Rousselet, L., Koubbi, P., Caccavo, J. and d'Ovidio, F. (in preparation) “Assessing the Potential Influence of Climate Change on Life History Connectivity of the Patagonian Toothfish over the Northern Kerguelen Plateau”.
- Rintz, C.L., Koubbi, P., Ramiro-Sánchez, B., **Azarian, C.**, Caccavo, J., Cotté, C., Goberville, E., Godet, C., Hulley P. A., Le Goff, R., Leprieur, F., Robuchon, M., Serandour, B., Leroy, B.. “Predicting biogeographical regions of lanternfishes in the Southern Ocean and their future distribution under climate change” (in preparation).

Policy briefs

- **Azarian, C.**, Bopp, L., d'Ovidio, F. “Climate change patterns in the Southern Indian Ocean: warming and marine heatwaves.” WG-EMM-2022/12.
- Nalivaev, A., **Azarian, C.**, Bopp, L., d'Ovidio, F. “Climate change patterns in the Southern Indian Ocean: primary production changes.” WG-EMM-2022/13.

- **Azarian, C.**, Bopp, L, d'Ovidio, F. "Climate change impacts vary with depth: what can be the consequences for pelagic ecosystems and for conservation ? Examples from the Southern Indian Ocean." WS-CC-2023/04.
- **Azarian, C.**, Bopp, L, d'Ovidio, F. "Potential implications of climate change on the Patagonian toothfish fisheries management." WS-CC-2023/05.

Other publications

- **Azarian, C.**, Fernández, P., Coimbra, P.H., Noyelle, R., Raillard, L. (2023). Journée scientifique "Comprendre et s'appropriier les messages clés du 6e rapport du Giec". La Météorologie, 120, 25-30. 10.37053/lameteorologie-2023-0013
- **Azarian, C.** (February 2024). "Vagues de chaleur marines." Bulletin scientifique des pêches australes. Bulletin édité par Nicolas Gasco, Muséum national d'Histoire Naturelle. ISSN 2777-8282.
- Vuillemein Tusseau, M-H., Meyssignac, B., **Azarian, C.** (January 2024). "Changement climatique : l'océan sous pression." La Jaune et la Rouge.
- **Azarian, C.**, Bopp, L. and d'Ovidio, F. (submitted May 2024). "Enjeux du changement climatique pour les écosystèmes pélagiques dans l'océan Indien Sud". Colloque sur les Terres Australes et Antarctiques Françaises, soumis aux éditions Pédone.
- Gauthier, L., Mignot, J., **Azarian, C.**, Koubbi, P., Barnerias, C., Marras, P. and d'Ovidio, F. "La protection de la biodiversité en haute mer : défis scientifiques et juridiques autour d'un cas d'étude dans l'Austral". La Météorologie (in preparation).

Seminars and international conferences

- Scientific Committee on Antarctic Research (SCAR) Open Science Conference, 2022 (10 min presentation, online).
- CCAMLR Ecosystem Management and Monitoring meeting, 2022 (3 min presentation, online).
- FilaChange, 2022 (30 min keynote speaker presentation, Paris, France): "How can fine scales modulate the impact of climate change on open ocean ecosystems ?"
- Kertrend, 2022 (15 min presentation, Paris, France).

- Effects of Climate Change on the World Ocean (ECCWO), 2023 (10 min presentation, Bergen, Norway).
- Climate change workshop CCAMLR, 2023 (2 presentations of 5 min, French hub online).

Co-supervisions

- Lou Gauthier - 6-month internship (M2; May - October 2023) : “La protection de la biodiversité en haute mer : défis scientifiques et juridiques autour d’un cas d’étude dans l’Austral”.
- Alex Nalivaev - 6-month internship (M1; 2022): “Investigating the response of Southern Indian Ocean phytoplankton abundance to climate change using CMIP6 projections under different SSP scenarios”.
- Short internships:
 - Elsa Bernard (June 2024): global response of chlorophyll to MHWs in recent simulations.
 - Thomas Gauthier (June 2024): physical connectivity between Prince Edward and Crozet islands and implications for the Patagonian toothfish populations.
 - Charlotte Loir (L3; 2023): exploring spatial patterns of warming in the Southern Ocean from satellite data.
 - Juliette Poilvet (L2; 2022) : literature on climate change in the Southern Ocean.

Outreach

- Participation to an intervention for the master “Audiovisuel Journalisme et Communication Scientifiques” for the preparation of a student play on the theme “Océan, préservation ou exploitation”.
- Intervention on climate and oceanographic research in a high school with the association Declics.
- Presentations for middle and high school students visiting LOCEAN.
- Participation at “La Fête de la Science” for the LOCEAN-IPSL stand in October 2021, 2022 and 2023.

At-sea experience

- ObsAustral oceanographic campaign (January - March 2024)
 - biological acoustic monitoring and scientific trawling within THEMISTO program.
 - drifters deployment to study surface currents of the Baleiniers Gulf within the MARGO program.

Other PhD-related activities

- Complementary Mission at the French Ministry of Agriculture (May to July 2023).
- Poster presentation at IMBeR CLimEco summer school (June 2023).
- Laboratory visit at the University of Gothenburg in Sebastiaan Swart team (1 week, April 2023).
- Delegate for PhD students at the Ecole Doctorale 129 (2022-2023).

Contents

Declaration of Authorship	i
Abstract	iii
Résumé en français	iv
Acknowledgements	vi
Contributions during the PhD	viii
List of Figures	xv
Abbreviations	xviii
1 Introduction	1
1.1 Research context and challenges	1
1.1.1 What is climate change?	1
1.1.2 Observed changes in the Southern Ocean these last decades	2
1.1.2.1 Regional warming and changes in the circulation	6
1.1.2.2 Observed changes in the vertical structure of the water column	8
1.1.2.3 Biogeochemical changes	10
1.1.3 The complexity to attribute mixed ecological trends to climate change	13
1.1.4 Uncertainties on climate change impacts on ecosystems hinder the development of climate-adapted conservation and fisheries management	17
1.1.4.1 Growing need to account for climate change in conservation and fisheries management	17
1.1.4.2 The case of the Southern Indian Ocean	20
1.1.5 Towards a more mechanistic understanding of climate change impacts on pelagic ecosystems at subantarctic latitudes	27
1.1.5.1 The importance of accounting for a 3D habitat	29
1.1.5.2 The importance of accounting for finer scale processes	34
1.2 Objectives and structure of the thesis	37
2 Data and methods	39

2.1	Data	40
2.1.1	Satellite observations	40
2.1.1.1	Altimetry	41
2.1.1.2	Sea surface temperature	42
2.1.1.3	Chlorophyll	43
2.1.2	<i>In situ</i> data	43
2.1.3	Reanalyses products	45
2.1.4	CMIP 6 models	46
2.2	Methods	51
2.2.1	Computing climate velocity	51
2.2.2	Detecting marine heatwaves	52
2.2.2.1	Definition	52
2.2.2.2	Marine heatwaves subsurface characteristics	52
2.2.3	Lagrangian analyses	54
2.2.4	Detecting winter waters and the Polar Front position	56
2.2.4.1	Winter waters detection	58
2.2.4.2	Decomposition of the thermohaline structure	58
3	Current and projected warming and marine heatwaves patterns in the Southern Indian Ocean	62
3.1	Context	62
3.2	Key results	64
3.3	Main study	65
3.4	Science and society : Climate velocities are useful tools to inform conservation in the Southern Indian Ocean	85
4	Marine heatwaves and global warming impacts on winter waters in the Southern Indian Ocean	91
4.1	Context	91
4.2	Key results	93
4.3	Main study	94
4.4	Science and society: Characterizing temporary refugia	109
5	Assessing the potential influence of climate change on life history connectivity of the Patagonian toothfish over and around the Northern Kerguelen Plateau	115
5.1	Context	115
5.2	Key results	119
5.3	Main study	120
5.4	Science and society: Identifying ecologically important areas to maximize Patagonian toothfish stock resilience.	153
6	Conclusions, limits and perspectives	159
6.1	Main findings	159
6.2	Scientific perspectives	165
6.2.1	Improving the mechanistic understanding of physical drivers of change	165
6.2.2	Towards (re)defining extreme events at depth	169

6.2.2.1	Further characterizing marine heatwaves impacts at depth	169
6.2.2.2	Can there be “hidden MHWs”?	170
6.2.3	Further characterizing the potential ecological impacts	176
6.2.3.1	Do elephant seals change or adapt their behaviors in response to extreme events?	176
6.2.3.2	Can the local circulation modulate the conditions of development for Patagonian toothfish early-life stages?	178
6.3	Societal perspectives	186
6.3.1	Climate change management implications on the Patagonian toothfish fishery in the Southern Indian Ocean	186
6.3.1.1	Climate change: a rising issue on the agenda of intergovernmental fisheries management	186
6.3.1.2	Leads for climate-adaptive management actions	187
6.3.2	Are scientific uncertainties a real barrier to the operational consideration of climate change in the management of marine biodiversity?	191
A	Supplementary Material Azarian et al., 2023	203
B	Supplementary Material Azarian et al., 2024	212
C	Supplementary Material Azarian et al., in preparation	233
D	Syntheses on the implications of climate change for the Patagonian toothfish fishery management in the Southern Indian Ocean	242
	Bibliography	295

List of Figures

1.1	Earth’s energy balance: comparing the flows of incoming and outgoing energy to the climate system.	3
1.2	Southern Ocean circulation and water masses	4
1.3	Schematic of some of the major Southern Ocean changes assessed in the IPCC Special Report on the ocean and cryosphere in a changing climate	5
1.4	Compound upper-ocean impact drivers	12
1.5	Summary of ecological assessments from the Marine Ecosystem Assessment of the Southern Ocean from Constable et al. (2023) - part I	16
1.6	Summary of ecological assessments from the Marine Ecosystem Assessment of the Southern Ocean from Constable et al. (2023) - part II	17
1.7	Observed trends in ocean heat content over 0-2000 m	21
1.8	Apparent fishing effort based on Automatic Identification System (AIS) data from the Global Fishing Watch between 2013 and 2024.	21
1.9	Map of the current key biodiversity areas, important marine mammals areas and ecologically and biologically significant areas in the Southern Indian Ocean.	24
1.10	Patagonian toothfish catches off the Kerguelen islands and in CCAMLR areas	25
1.11	Spatial distribution and life cycle of the Patagonian toothfish (<i>Dissostichus eleginoides</i>)	26
1.12	Schematic illustrating the current knowledge gap regarding the complexity of the physical disturbances under climate change	30
1.13	Spatial and temporal scales of oceanographic and ecosystem processes from Carr et al. (2011)	31
1.14	Examples of top predators targeting subsurface and mesopelagic layers to forage.	33
1.15	Schematics of Antarctic Circumpolar Current fronts	35
1.16	Examples of studies highlighting spatial patterns of ecologically important areas	36
2.1	Schematic of our multi-scale approach, investigating both last decades variability and emerging trends and future projections under different emission scenarios.	40
2.2	Satellite observations relies on different technologies, targeting different wavelength depending on the metric studied	41
2.3	Different products are derived from satellite altimetry, for instance absolute dynamic topography, resulting from satellite sea surface height measurements, and geostrophic velocities derived from it	42

2.4	Spatial and temporal distributions of MEOP-CTD and Argo hydrographic profiles complete down to 900 m	45
2.5	Schematic of climate models components and Shared-Socioeconomic Pathways	48
2.6	Schematic of the different approaches to combine climate models' outputs.	50
2.7	Spatial and temporal complementarity of the datasets used in this PhD thesis.	50
2.8	Marine heatwaves definition and associated physical processes	53
2.9	Definition of temperature anomaly depth and cumulative temperature anomaly	54
2.10	Schematic illustrating the use of altimetry data to conduct Lagrangian analyses.	57
2.11	Winter water detection based on temperature profiles.	59
3.1	Climate velocity as calculated in Azarian et al. (2023), masked by SST signal-to-noise ratio as defined in Auger et al. (2021)	85
3.2	Climate residence time over each epipelagic and mesopelagic regions determined with the regionalisation approach using a functional principal analysis in Merland et al. (under review).	87
3.3	Identification of the habitat shearing threat.	88
3.4	Overview of the main projected temperature-related changes under climate change in the Southern Indian Ocean determined in Chapter 3.	89
4.1	Winter waters ecological role and mean probability of presence in the Southern Indian Ocean.	92
4.2	Changes in the Polar Front position, as defined as the northernmost extension of the winter waters, at the circumpolar scale.	111
4.3	Evolution of the mean Polar Front position under a strong emission scenario and an overshoot scenario.	112
4.4	Examples using the climate model GFDL-CM4 of the evolution of winter water probability of presence, in small areas near the Kerguelen Plateau, under a strong emission scenario.	113
5.1	Schematic of fish life cycle adapted from Harden-Jones (1968)	117
5.2	Current knowledge on the local circulation and the spatial distribution of the Patagonian toothfish over and around the Kerguelen Plateau	118
5.3	Arrival points density in log10 scale after 3 months or 6 months advections from potential spawning areas either from the Skiff area or the west of Heard	155
5.4	Ratio of the standard deviation over the mean of arrival points density after 3 months or 6 months advections from potential spawning areas either from the Skiff area or the west of Heard	157
5.5	Arrival points density in log10 scale after 6 months advections from potential spawning areas either from the Skiff area (A) or west of Heard overlapped with no-take zones currently implemented.	157
6.1	Summary figure of the climate change impacts on physical features of ecological importance for pelagic ecosystems identified in Chapter 3, 4 and 5.	162

6.2	Identification of a pelagic climate refugium offshore east of Kerguelen shelf break.	164
6.3	Spread in volume transport of the ACC through the Drake Passage and in the historical sea ice area across different CMIP6 models.	167
6.4	Figures extracted from recent peer-reviewed literature on MHWs extent at depth (Fragkopoulou et al., 2023; Sun et al., 2023; Zhang et al., 2023).	171
6.5	Seasonal characteristics of marine heatwaves, detected with OSTIA dataset and sampled by Argo floats.	172
6.6	Probability of “hidden” marine heatwaves (MHWs) and examples of MHWs detected at depth in CNRM-ESM2-1 under a historical simulation.	173
6.7	Historical and projected MHW intensity on T/S diagrams using CNRM-ESM2-1.	175
6.8	Examples of elephant seals trajectory overlapped with mean MHW intensity over the period of the trajectory	178
6.9	Schematic illustrating potential research leads associated with investigating the conditions of development for Patagonian toothfish larvae over the Kerguelen Plateau	179
6.10	Empirical Orthogonal Function (EOF) analysis on the “distance metric” as defined in Chapter 5.	181
6.11	Summer chlorophyll-a composites depending on the level of connectivity between the west of Heard and the east of Kerguelen.	182
6.12	Schematic illustrating the differences between an Eulerian and a Lagrangian approach of climate change impacts on physical oceanography leading to different types of ecological impacts.	184
6.13	Complementary analyses on recent years (2022-2023).	185
6.14	Schematic of the key steps in Patagonian toothfish management.	189
6.15	Schematic illustrating the need for climate-responsive management features	195
6.16	Schematic illustrating the two main timescales of a theoretical risk management approach to account for climate change impacts on ecosystems	197
6.17	Schematic providing a simplified overview of the different potential strategies to account for climate change in biodiversity management	200
6.18	Summary of the focus of this PhD work and its scientific and societal perspectives.	201

Abbreviations

AABW	Antarctic Bottom Waters
AAIW	Antarctic Intermediate Waters
AASW	Antarctic Surface Waters
ACC	Antarctic Circumpolar Current
ADT	Absolute Dynamic Topography
BBNJ	Biodiversity Beyond National Jurisdiction
CCAMLR	Commission for the Conservation of Antarctic Marine Living Resources
CDW	Circumpolar Deep Water
CMEMS	Copernicus Marine Environment Monitoring Service
CMIP	Coupled Model Intercomparison Project
CRT	Climate Residence Time
CV	Climate Velocity
EBSA	Ecologically and Biologically Significant Area
EEZ	Exclusive Economic Zone
EOF	Empirical Orthogonal Function
FCPA	Functional Principal Component Analysis
GWL	Global Warming Level
HNLC	High Nutrient Low Chlorophyll
ILD	Isothermal Depth Layer
IMMA	Important Marine Mammals Area
IPCC	Intergovernmental Panel on Climate Change
IUCN	International Union for the Conservation of Nature
KBA	Key Biodiversity Area
LAMTA	Lagrangian Manifolds Tracking Algorithm
LCDW	Lower Circumpolar Deep Water

MEOP	M arine M ammals E xploring the O ceans P ole to P ole
MLD	M ixed L ayer D epth
MPA	M arine P rotected A rea
MHW	M arine H eat W ave
NPP	N et P rimary P roduction
OISO	O céan I ndien S ystème d' O bservation
PC	P rincipal C omponent
PF	P olar F ront
RCP	R epresentative C oncentration P athways
SAF	S ub- A ntarctic F ront
SSH	S ea S urface H eight
SSP	S hared S ocioeconomic P athway
SST	S ea S urface T emperature
TAC	T otal A llowable C atch
THEMISTO	T oward H ydroacoustics and E cology of M id-trophic levels in I ndian and S ou T hern O cean
UCDW	U pper C ircumpolar D eep W ater
WGCM	W orking G roup on C oupled M odelling
WW	W inter W ater

Chapter 1

Introduction

“Ainsi, toujours poussés vers de
nouveaux rivages,
Dans la nuit éternelle emportés sans
retour,
Ne pourrons-nous jamais sur l’océan
des âges,
Jeter l’ancre un seul jour ?”

A. De Lamartine, “Le Lac”

1.1 Research context and challenges

1.1.1 What is climate change?

According to the Intergovernmental Panel on Climate Change (IPCC), climate change is defined as “a change in the state of the climate that can be identified (e.g., by using statistical tests) by changes in the mean and/or the variability of its properties and that persists for an extended period, typically decades or longer” (IPCC, 2023). Climate change can be due to natural internal processes (e.g. volcanic eruptions), external forcings (e.g. solar cycles) and anthropogenic changes in the composition of the atmosphere or in land use. A scientific consensus has been reached on the occurrence of climate change today and its anthropogenic causes. The increase in atmospheric anthropogenic greenhouse gases has decreased the energy flux re-emitted by the Earth toward space,

meaning that the Earth radiative budget is imbalanced, receiving more energy from the Sun than it re-emits toward space (Forster et al. (2021) ; Figure 1.1). As a consequence, this energy is stored as heat which is responsible for global warming. Climate change consists in this transitory period until a new energy balance is reached, that is, until the Earth energy emissions to space compensates the energy received from the Sun (Forster et al., 2021; Gulev et al., 2021).

The climate system has five main components - the atmosphere, the ocean, the cryosphere, land masses and the biosphere - that interact with each other. Among these components, the ocean plays a major regulating role for the climate as it absorbs 20 to 30 percent of the anthropogenic CO_2 and around 91 percent of the anthropogenic heat (Canadell et al., 2021; Fox-Kemper et al., 2021). Due to the high ocean heat capacity, global warming is thus slower than it would be without the ocean.

The excess of greenhouse gases in the atmosphere has two main consequences for the ocean : i) it contributes to atmospheric warming and the majority of this heat is absorbed by the ocean, ii) part of the atmospheric CO_2 is dissolved in the ocean and contributes to ocean acidification (Fox-Kemper et al., 2021). From ocean warming, other physical and biogeochemical changes can arise (e.g. changes in ocean circulation, ocean deoxygenation; Meredith et al. (2019); Fox-Kemper et al. (2021)) but climate change trends and impacts are spatially and temporally heterogeneous, notably as climate change signal can emerge (i.e. trend larger than than the amplitude of natural or internal variations) earlier in some areas compared to others (Silvy et al., 2020).

1.1.2 Observed changes in the Southern Ocean these last decades

The Southern Ocean, which covers 30 % of the world's ocean, plays a key role in the Earth system, both in terms of heat and carbon absorption, while hosting a rich and partly endemic biodiversity. This remote area is lacking from *in situ* observations compared to the rest of the world but sustained monitoring efforts have contributed to better understand the Southern Ocean physics and biology and, increasingly, to better understand the changes occurring under climate change. Here, we present current evidence on physical changes observed in the Southern Ocean these last decades, also pointing out remaining uncertainties.

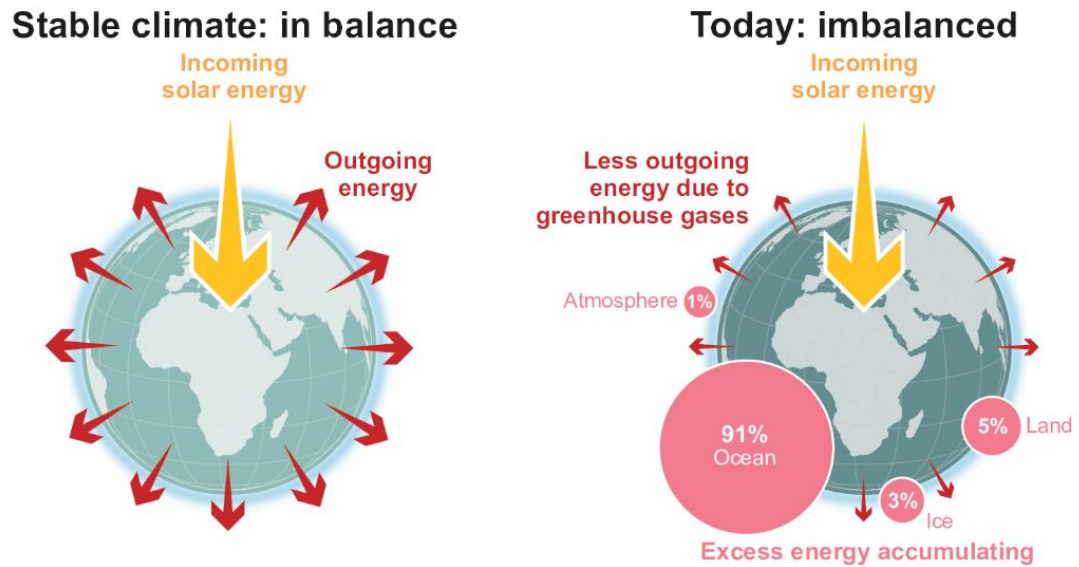


FIGURE 1.1: **Earth's energy balance: comparing the flows of incoming and outgoing energy to the climate system.** Since at least the 1970s, less energy is flowing out than is flowing in, which leads to excess energy being absorbed by the ocean, land, ice and atmosphere, with the ocean absorbing 91%; from [Forster et al. \(2021\)](#)

Box. 1.1.1: The Antarctic Circumpolar Current

The Southern Ocean hosts the strongest current in the world: the Antarctic Circumpolar Current (ACC), flowing eastward and transporting between 140 and 170 Sv around the Antarctic continent ([Xu et al. \(2020\)](#); Figure 1.2). This current connects the different ocean basins but also isolates the Antarctic continent by limiting meridional exchanges.

The key ingredients to explain the Southern Ocean circulation are: wind and buoyancy forcing, eddies, stratification, and topography ([Rintoul and Naveira Garabato, 2013](#); [Rintoul, 2018](#)). The eastward flow is driven by both strong westerlies and buoyancy forcing tilting isopycnals. Density surfaces indeed shoal to the south, leading to denser waters being closer to the surface at high latitudes. The potential energy stored in sloping isopycnals can give rise to an energetic eddy field, with eddies that contribute to poleward heat transport ([Wolfe et al., 2008](#)). Because of the deep-reaching nature of the flow within the ACC system and due to the weak stratification of the Southern Ocean, bottom topography also modulates the circulation, by mostly weakening the flow ([de Boer et al., 2022](#)) and contributing to the vorticity balance ([Rintoul, 2018](#)).

The Antarctic Circumpolar Current is associated with dynamic jets and a systems of fronts. From north to south: the Northern Boundary (NB), the Subantarctic Front (SAF), the Polar Front (PF), the Southern ACC front (SACCF) and the Southern Boundary (SB; [Park and Durand \(2019\)](#)).

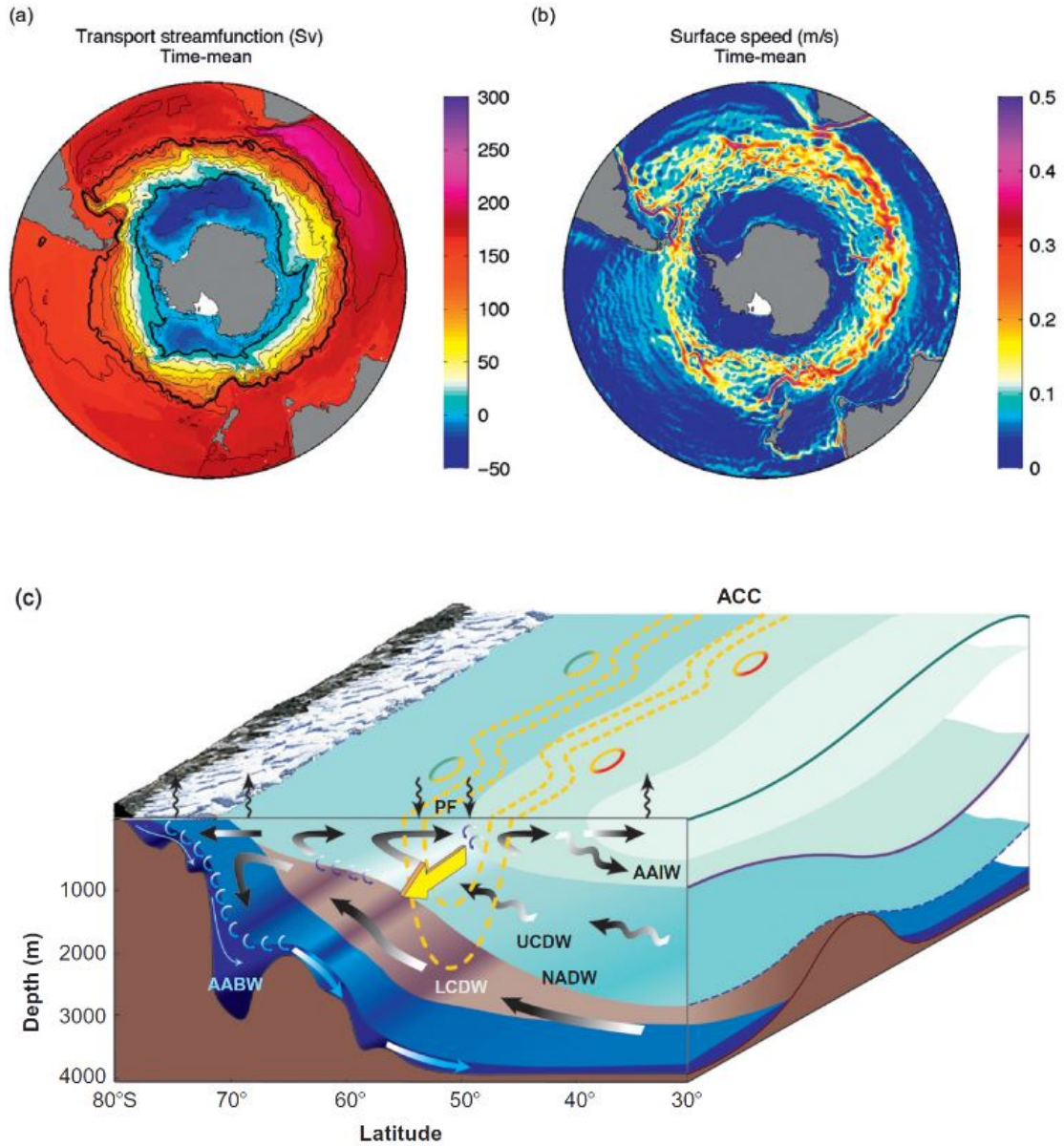


FIGURE 1.2: **Southern Ocean circulation and water masses.** Five-year mean (2005–2009) vertically integrated transport streamfunction (A) and mean surface velocity (B). The bold contour on panel A mark the northernmost and southernmost streamlines to pass through Drake Passage. (C) Schematic view of the Southern Ocean circulation. Figures from [Rintoul and Naveira Garabato \(2013\)](#).

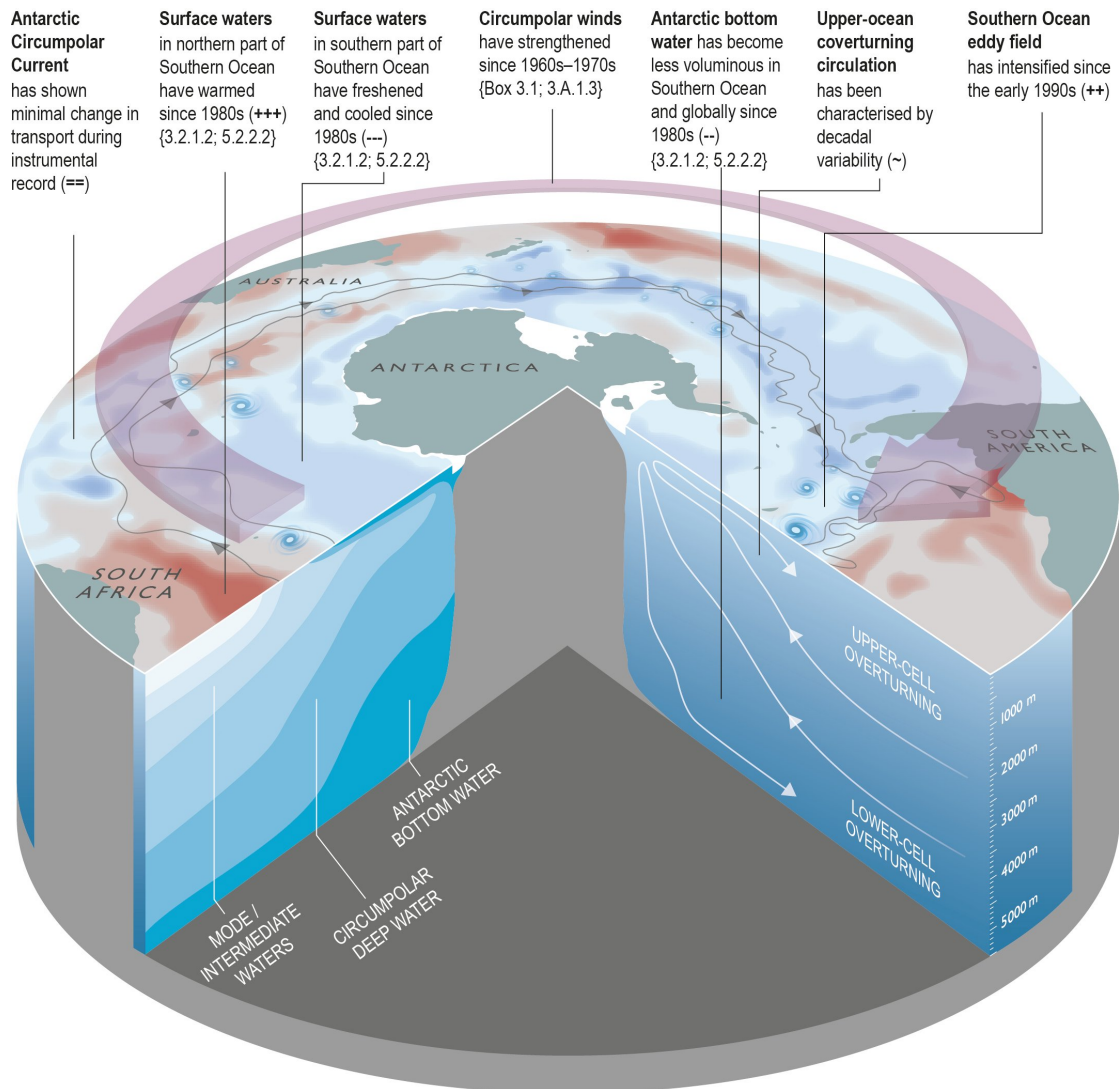


FIGURE 1.3: Schematic of some of the major Southern Ocean changes assessed in the IPCC Special Report on the ocean and cryosphere in a changing climate (Meredith et al., 2019). Assessed changes are marked as positive (+), neutral (=), negative (–), or dominated by variability (~). The number of symbols used indicates confidence, from low (1) through medium (2) to high (3); from Meredith et al. (2019)

Box. 1.1.2: Southern Ocean overturning circulation

The Southern Ocean overturning circulation plays a key role in meridional heat transport. The common description of this circulation identifies two cells (Figure 1.2 C). The lower cell, at depth, consists in dense water (Lower Circumpolar Deep Water or LCDW, see Box 1.1.3) spreading poleward and outcropping at the surface near the sea ice edge. As the upwelled water interacts with the cold

atmosphere and sea ice, it becomes denser and dives to the bottom of the ocean, then spreading equatorward. The upper cell consists in lighter water (Upper Circumpolar Deep Water or UCDW, see Box 1.1.3) outcropping at subantarctic latitudes within the ACC system and being transported equatorward through Ekman transport (driven by the westerlies) and contributing to the formation of less dense mode and intermediate waters through interactions with the atmosphere.

1.1.2.1 Regional warming and changes in the circulation

Increasing evidence show that significant changes have occurred in the Southern Ocean, especially at subantarctic latitudes (60°-30°S). A surface warming north of the Antarctic Circumpolar Current (ACC) and a surface cooling south of the ACC have been observed these last decades (Sallée (2018) ; Figure 1.3).

South of the ACC, a surface cooling has been observed up to 2016, associated with increased sea ice extent (Eayrs et al., 2021). Heat uptake by upwelled waters south of the ACC may have been largely balanced by anomalous northward heat transport, mostly contributing to warming the ocean interior (Armour et al., 2016). Since 2016, the sea ice trend has been reversed and record low ice states were observed in 2022 (Turner et al., 2022; Raphael and Handcock, 2022) and in 2023 (Purich and Doddridge, 2023; Gilbert and Holmes, 2024). The mechanisms driving these events and their attribution to climate change is still an active research question, although recent studies point out the potential role of subsurface ocean warming (Zhang et al., 2022; Purich and Doddridge, 2023).

Warming is generally either caused by an increased heat uptake at the surface and/or by a change in advective heat transport (Frölicher et al., 2015; Armour et al., 2016; Morrison et al., 2016). The Southern Indian Ocean is a region with an important recent upper ocean warming, with one of the largest heat uptakes, especially around 40°S (Llovel and Terray, 2016; Garcia-Soto et al., 2021), mostly due a convergence of heat modulated by the ocean circulation. Accumulated heat south of 50°S can be advected by enhanced northward wind-induced Ekman transport (Sallée, 2018) which can also affect deeper layers (Cai et al., 2010). This heat accumulates within and north of the ACC where eddies could then contribute to redistribute heat southward along isopycnal (Wolfe et al.,

2008) but, as warming increases, this southward eddy-mediated transport is less efficient and heat accumulates even more north of the ACC (Morrison et al., 2016). An increase in oceanic mesoscale activity at high latitudes has also been observed these last decades, which could impact ocean circulation and heat transport in the future (Martínez-Moreno et al. (2019); Martínez-Moreno et al. (2021); Figure 1.3).

Ocean warming may have in turn impacted the Southern Ocean circulation. Ocean warming has been associated with strengthening and poleward shifting trends of westerlies (Toggweiler, 2009; Swart and Fyfe, 2012; Thomas et al., 2015). Besides, the observed ACC acceleration could be stronger due to increased buoyancy forcing associated with warming than to a direct impact of westerly intensification (Shi et al., 2021). Despite those recent observations, further evidence is needed to support and estimate the ACC transport sensitivity in response to wind and buoyancy fluxes in the future (Fox-Kemper et al. (2021), Figure 1.3).

In addition to long-term changes, extreme events are a growing concern in the Southern Ocean. Antarctic extreme events related to sea-ice extent or ice-shelves collapses are identified as major threats to Antarctic ecosystems (Siegert et al., 2023). Extreme events of ocean temperature, also called “marine heatwaves” (MHW, Hobday et al. (2016)), may also be detrimental to marine species as their intensity and frequency are expected to increase (Smale et al., 2019; Smith et al., 2023). A global increase of around 0.57 events/decade (Oliver et al. (2018), over 1982-2015) or 0.52 annual events/decade (Plecha and Soares (2020), over 1982-2018), as well as an increase in mean surface MHW intensity between 0.03 °C/decade (Plecha and Soares, 2020) and 0.085°C/decade (Oliver et al., 2018) have been estimated. Particular extreme events in the Southern Ocean have been identified: for instance the 1997 MHW west of the Southern Indian Ocean that was associated with a southward shift of the Polar Front (Bost et al., 2015) or the 2016 MHW that was associated with a decrease in sea ice extent (Meehl et al., 2019). The recent abundant productivity of scientific research on extreme events reflects the growing concern about such events and their impacts on ecosystems.

1.1.2.2 Observed changes in the vertical structure of the water column

Box. 1.1.3: Southern Ocean waters masses

- At the surface, the Antarctic Surface Waters (AASW) are formed at high latitudes and extend up to the Polar Front. Antarctic Surface Waters are generally characterized by negative temperatures but they can reach 2.5°C near the Polar Front (Carter et al., 2008). Between the Polar and Subantarctic fronts the surface waters have transitional properties between AASW and Subantarctic Surface Waters (SASW): between 3 and 8°C and between 34 and 34.4 psu, depending on the level of mixing. Subantarctic Surface Waters, between 6°C and 12°C, are found north of the Subantarctic Front and Subtropical Surface Waters north of the Subtropical Front where the temperature and salinity gradients are quite high (rise of 4–5°C and 0.5 psu northward; Carter et al. (2008)).
- Winter waters (WWs) are formed from the cold surface waters of the winter mixed layer of the subpolar regions, which are capped by a warmer and fresher surface layer in spring-summer. This seasonal cycle leaves behind a cold water mass in the subsurface (100 - 400 m) with temperatures ranging between -2°C and 3°C (Toole, 1981; Park et al., 1998).
- North of the Subantarctic Front, the Subantarctic Surface Waters subside forming the Subantarctic Mode Waters (SAMW; McCartney (1977); Morris et al. (2001); Rintoul et al. (2001)) down to 500 m deep. The Antarctic Intermediate Waters (AAIW) sink under the SAMW down to 1400 m deep. AAIW are usually formed from the sinking of Antarctic Surface Waters near the Polar Front, with temperatures between 3°C and 7°C and are characterised by a salinity minimum (34.3–34.5 psu; Carter et al. (2008)). The coldest, densest, least saline AAIWs are formed in the South-East Pacific, and advected at depth around Antarctica by the ACC (Talley (2011)).
- Below the AAIW are found the most voluminous water mass in the Southern Ocean, the Circumpolar Deep Waters (CDW), which extend between 1400 m to 3500 m deep but outcrop near the Antarctic continental margin. This water mass is commonly distinguished in two layers: the Upper Circumpolar

Deep Waters (UCDW) and the Lower Circumpolar Deep Waters (LCDW). The UCDW extend down to 2500 m and are characterised by an oxygen minimum and high nutrient concentrations. The LCDW are characterised by a salinity maximum (34.70–34.75 psu; [Gordon \(1975\)](#); [Orsi et al. \(1995\)](#)).

- The Antarctic Bottom Waters (AABW) carpet the ocean floor with temperatures ranging between -0.9°C and 2°C , but this water mass does not spread far from Antarctica before mixing with other waters ([Orsi et al., 1999](#)). In particular, in deep western boundary currents, the AABW are mixed with CDW ([Carter et al., 2008](#)). The freshest (salinity <34.64) and coldest (temperature $<-1^{\circ}\text{C}$) AABW have been observed in the Weddell Sea.

Ocean warming and dynamical changes in the circulation (e.g. ACC dynamics, westerlies strengthening) are linked to changes throughout the water column. We present here observed trends on ocean stratification and on deeper water masses in the Southern Ocean.

The surface mixed layer, the layer with relatively homogeneous properties due to mixing mostly through the action of wind, is an important characteristic that can modulate the heat and carbon uptake of the ocean as well as the primary production. Below the mixed layer is found the pycnocline where the density gradient is maximal in the water column. Depending on the strength of this gradient, also named stratification, mixing between the vertical layers fluctuates. In the Southern Ocean, the mixed layer can extend deeper than in other ocean basins and can reach 400 m in winter ([Sallée et al., 2021](#)).

The observed and projected strengthening of the westerlies and ocean warming have different consequences on the vertical structure of the water column. On the one hand, increasing winds would tend to deepen the mixed layer and enhance upper-ocean turbulence; on the other hand, ocean warming would tend to increase surface stratification. Observations have revealed both a deepening of the summertime mixed layer between 1970 and 2018 (several metres per decade; [Sallée et al. \(2021\)](#)) and an increase of Southern Ocean stratification between 1960 and 2018 ([Li et al., 2020](#)).

The vertical structure of the water column in the Southern Ocean can also be impacted through changes of the water masses characteristics. The Southern Ocean is vertically

divided in several water masses that varies depending on the latitude (Box 1.1.3). Recent studies have observed significant changes in the Subantarctic Mode Waters (SAMW) properties, as the SAMW layer has warmed, freshened and potentially thickened and deepened, depending on the SAMW definition used (Roemmich et al., 2015; Gao et al., 2018; Kolodziejczyk et al., 2019; Portela et al., 2020; Xu et al., 2021). SAMW subduction rates have been increasing these last 15 years, probably due to wind-induced deepening of the mixed layer (Qu et al., 2020). Variations in SAMW may differ depending on the basin and SAMW thickness appears to be mostly modulated by wind stress curl variability in the Southern Indian Ocean (Wang et al., 2022). While the volume of SAMW has been found to increase, the volume of Antarctic Intermediate Waters (AAIW) has been decreasing, with the strongest volume loss in the South Indian and South Atlantic basins north of the ACC (Portela et al., 2020). South of the ACC, the AAIW volume trend is reversed in those basins, with the strongest volume increases between the Subantarctic and the Polar Fronts (Portela et al., 2020).

Contrasting trends for the AABW properties have been observed between the east and the west of the Southern Indian Ocean, with observed faster warming and fresher water east compared to the west of the basin (Choi and Nam, 2022). Those warming trends impact the poleward transport of AABW. Compared to the 1990s, the deep flow toward the Indian Ocean in the 2010s has been weakening east of the Southern Indian Ocean. Such contrasting trends can be due to different processes affecting the different origins of the AABW closer to the Antarctic (Solodoch et al., 2022). Climate models from the Coupled Model Intercomparison Project 6 (CMIP6) project a circumpolar warming of AABW that could be partly influenced by Circumpolar Deep Water warming (Purich and England, 2021). Significant trends of warming and shoaling of Upper Circumpolar Deep Water have already been observed, especially close to the Antarctic continent (Schmidtke et al., 2014; Auger et al., 2021; Herraiz-Borreguero and Naveira Garabato, 2022).

1.1.2.3 Biogeochemical changes

Physical changes in the ocean circulation and vertical structure are generally coupled with biogeochemical changes. Observing trends in biogeochemical variables, such as pH, oxygen concentration or primary production, requires multi-decadal timeseries to

distinguish climate trend from natural variability (Henson et al., 2016). In the Southern Ocean, long-term monitoring programs are barely starting to reach those timescales, but, along with the ongoing development of biogeochemical modelling, they can provide insights on what are the current trends of various biogeochemical variables that are key for ecosystems functioning. Three main variables are considered here: pH (acidification), primary productivity and oxygen concentration (deoxygenation).

First, ocean acidification is directly linked to the ocean uptake of CO_2 and can be modulated by ocean circulation and primary productivity. In the Southern Indian Ocean, surface fCO_2 and pH have been measured since 1998 through long-term programs such as the “Ocean Indien Système d’Observation” (OISO). Decrease in pH (i.e. acidification) has been observed in summer over 1998-2019, ranging from $-0,0015$ to $-0,0043$ /yr (Leseurre et al., 2022). This trend is also spatially heterogeneous. It was observed that pH decreased faster in the fertilised waters around Crozet and Kerguelen islands (between $-0,0023$ and $-0,0043$ /yr), mainly driven by the accumulation of anthropogenic CO_2 in the ocean (Leseurre et al., 2022).

Second, changes in primary productivity can result from multiple factors, most often region-specific. The Southern Ocean is mainly a high-nutrient low-chlorophyll (HNLC) area with hotspots of productivity, most probably due to the iron inputs from islands, seamounts and continental shelves (Blain et al., 2001; Ardyna et al., 2017; Sergi et al., 2020). Long-term observations have shown that iron stress increased between 1996 and 2021 (Ryan-Keogh et al., 2023). This could induce a decrease in net primary production (NPP) but trends in NPP are unclear as other factors such as temperature or stratification are changing as well, in an area where primary production is also limited by light (Deppeler and Davidson, 2017). Recent studies suggest a significant increase in chlorophyll-a satellite observations over the Southern Ocean, notably in the subantarctic area (Del Castillo et al., 2019; Pinkerton et al., 2021) but trends are more mixed in the diatom-dominated silicate-rich waters in the southern subantarctic and antarctic zones (Pinkerton et al., 2021). While climate models from the Coupled Model Intercomparison Project 5 (CMIP5) project a decrease in NPP in the subantarctic region due to deeper summertime mixed layer depths and thus less incident photosynthetically active radiation for photosynthesis (Leung et al., 2015), CMIP6 models project an increase in NPP (Kwiatkowski et al., 2020) as the wind stress representation improved from CMIP5 to

CMIP6 (Bracegirdle et al., 2020), modifying the patterns of mixed layer depths. Future changes in primary production patterns in the Southern Ocean thus remain uncertain.

Third, deoxygenation can be enhanced by surface warming and increased stratification. However, deoxygenation is considered to be less of an issue for Southern Ocean ecosystems. Although the deoxygenation rates are higher at high latitudes, where the signal has clearly emerged (Andrews et al., 2013; Long et al., 2016), the oxygen concentrations are much higher too (Schmidtko et al., 2017; Levin, 2018), and the risks of hypoxia are thus low.

So far the physical and biogeochemical changes have been presented separately but their co-occurrence (“compound stressors”) can exacerbate climate change impacts on ecosystems (Zscheischler et al., 2018). CMIP6 projections show that the future occurrence of compound stressors is limited in the Southern Ocean, the main biogeochemical stressor being acidification (Kwiatkowski et al. (2020); Gruber et al. (2021) ; Figure 1.4).

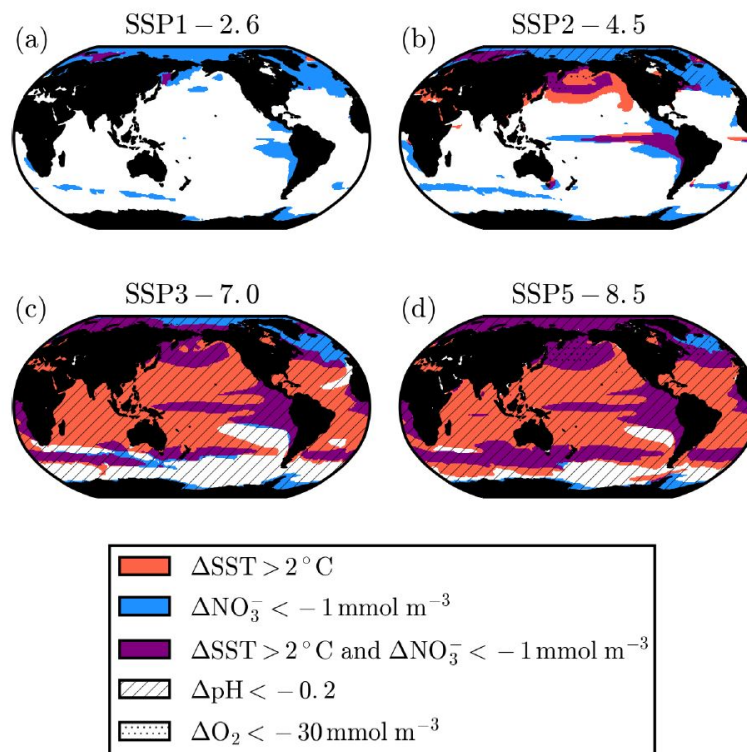


FIGURE 1.4: **Compound upper-ocean impact drivers.** Regions where projected CMIP6 sea surface warming exceeds 2°C , euphotic-zone (0–100 m) NO_3^- decline exceeds 1 mmol.m^{-3} , surface ocean pH decline exceeds 0.2, and subsurface (100–600 m) dissolved O_2 concentration decline exceeds 30 mmol.m^{-3} in (a) SSP1-2.6, (b) SSP2-4.5, (c) SSP3-7.0, and (d) SSP5-8.5. The exceedance of driver thresholds is determined from 2080 to 2099 anomalies relative to 1995–2014 values. Figures and caption from Kwiatkowski et al. (2020).

Key point

There is abundant evidence that the physical and biogeochemical environments in the Southern Ocean both at the surface and at depth are changing. Heterogeneity of climate change trends is observed both latitudinally across the system of ACC fronts and longitudinally across basins.

1.1.3 The complexity to attribute mixed ecological trends to climate change

Climate change is a major threat to biodiversity (Stock et al., 2019; Williamson and Guinder, 2021). Yet, despite the observed climate signals in the Southern Ocean, climate change impacts on ecosystems are complex to determine, especially at subantarctic latitudes. Strong relations between environmental variables and ecological processes can enlighten on potential climate change impacts but ecosystems are often driven by multiple factors, both biotic and abiotic. Besides, abiotic factors can play a key role at different levels (e.g. physiology of an individual, species, communities).

In the Antarctic region, the link between sea-ice changes and sea-ice dependent ecosystems vulnerabilities has been well established (Rogers et al., 2020; Constable et al., 2023). For instance, sea-ice extent plays an important role, among other environmental variables, on krill (*Euphausia superba*) populations variability (e.g., Loeb et al. (1997); Quetin and Ross (2003); Atkinson et al. (2004, 2019)). A poleward contraction of krill distribution has been observed in the Atlantic sector of the Southern Ocean over the last decades, associated with positive Southern Annular Mode (SAM) anomalies (e.g., Atkinson et al. (2004, 2019)). Habitat modeling using different emission scenario also project further habitat contraction and population decline (e.g., Hill et al. (2013); Pinones and Fedorov (2016); Klein et al. (2018); Hill et al. (2019)), although climate change might also increase suitable habitats extent for the first overwintering period for krill (Melbourne-Thomas et al., 2016).

Trends are even less clear for subantarctic ecosystems. Continued efforts to monitor the subantarctic islands ecosystems has fed decadal timeseries which are essential to study ecological trends over the last decades. For instance, penguins monitoring in the French Southern Lands has started in the early 1950s. The Marine Ecosystem Assessment

for the Southern Ocean (MEASO) summarizes trend assessments for several species and shows a wide range of observed trends depending on the species and depending on the regions (Figures 1.5 and 1.6; Constable et al. (2023)). Three of the four main species of southern elephant seals, those at South Georgia, the Valdes Peninsula, and Kerguelen, are either currently stable or increasing slightly (Hindell et al., 2016), while the Macquarie Island population in the southern Pacific is decreasing (McMahon et al., 2005). In addition, most penguins populations breeding in the French Southern Lands increased or were stable over the past 30–60 years, except for the northern rockhopper penguin, king and gentoo penguins on Crozet and the emperor penguin (Barbraud et al., 2020). A massive decline of the king penguin colony of Morne du Tamaris on Ile aux Cochons in the Crozet archipelago by 85 % over the past 30 years has been observed (Weimerskirch et al., 2018). In the Indian sector, an increase in fur seals and adelic penguins has been observed while a decrease in emperor penguins and antarctic and Cape petrels was found.

The ecological reasons behind several trends are still poorly understood. Both physical changes at finer scales and the vulnerabilities of subantarctic species are quite uncertain. For species such as elephant seals, increasing trends can be partly due to recovery from past exploitation (Aubert De La Rue, 1932; Laws, 1977; Heupink et al., 2012; Southwell et al., 2015; Barbraud et al., 2020). In addition, it can be challenging to differentiate the effects of climate change from those caused by other human activities, such as fishing activities, notably in case of cumulative effects (Bestley et al., 2020).

Climate change impacts can also occur through trophic interactions. The mid-trophic chain communities might be impacted, although the uncertainty is again high over subantarctic latitudes (Pinkerton et al., 2020). These communities seem to be strongly structured by the frontal system, with the highest abundances found between the subantarctic front and the northern annual limit of sea-ice (Pinkerton et al., 2020). There are still knowledge gaps on those communities distributions and their relation to oceanographic variability which hinder our understanding of potential climate change impacts on this biodiversity. Besides, trends over the last decades vary depending on the geographical location and zooplankton groups. There has been a patchy increase in habitat range for groups such as *Oithona similis*, Copepoda (Calanoida), Euphausiidae, Foraminifera, and Fritillaria species, notably between the subantarctic front and the southern boundary of the ACC (Pinkerton et al., 2020). Habitat suitability for

pteropods has improved in the subantarctic zone but worsened over the last 20 years over the Ross Sea shelf (Pinkerton et al., 2020). As for lanternfish, which are an abundant prey field for top predators, Antarctic species with restricted thermal niches may be the most vulnerable to climate change. A general shift in myctophids community structure is expected along a southward shift of subantarctic species (Freer et al., 2019).

Climate change can also fragilize populations by impacting key life stages. Ocean warming might increase egg and larval mortality for fish species (Meredith et al., 2019) and could also impact dispersal patterns and thus connectivity between populations, through changes in the local circulation. Those local changes might then affect the ability of some populations to adapt to climate change (Young et al., 2018; Meredith et al., 2019).

Since trends mostly provide mixed information regarding long-term impacts, it can be useful to focus on the impacts of extreme events. Most of the studied impacts of extreme events have been related to a shift in the foraging areas of top predators. For instance, the summer of 1997 was characterised by an intense, large and prolonged MHW west of the Southern Indian Ocean (around 50°-54°E). Over the whole Southern Indian Ocean, the mean MHW intensity of this event remained greater than 0.5°C for 36 days (Azarian et al., 2023). The abnormal large scale warming was associated with an extreme positive Subtropical Atlantic and Indian Oceans dipole and with a southward shift of the Polar Front, which marks the position of favored foraging areas for top predators such as king penguins or elephant seals (Bost et al., 2015). High mortality was observed that year for king penguins from Crozet, probably due to the increased foraging distance (Bost et al., 2015). Important SST anomalies were also detected during the summer of 1987-1988, as well as a southward shift of the Polar Front over the period 1982-1998 using an SST-gradient based definition of the front (Moore et al., 1999), which was associated with a decreased breeding success of some seabirds species, depending on the location of their foraging areas (Inchausti et al., 2003).

To better understand future climate change impacts on ecosystems, many studies have focused on evaluating species niches and projecting future habitats using climate models (Melo-Merino et al., 2020). Those studies help provide a general understanding of the direction of change and contribute to understanding whether habitats are shifting, expanding or shrinking. However, other ecological processes related to species life cycle and behaviors may also play a crucial role and are often coupled to the ocean finer

scale dynamic, especially in the open ocean at subantarctic latitudes. The uncertainties around those impacts at a scale relevant for management may currently hinder the development of climate-adapted conservation and fisheries management.

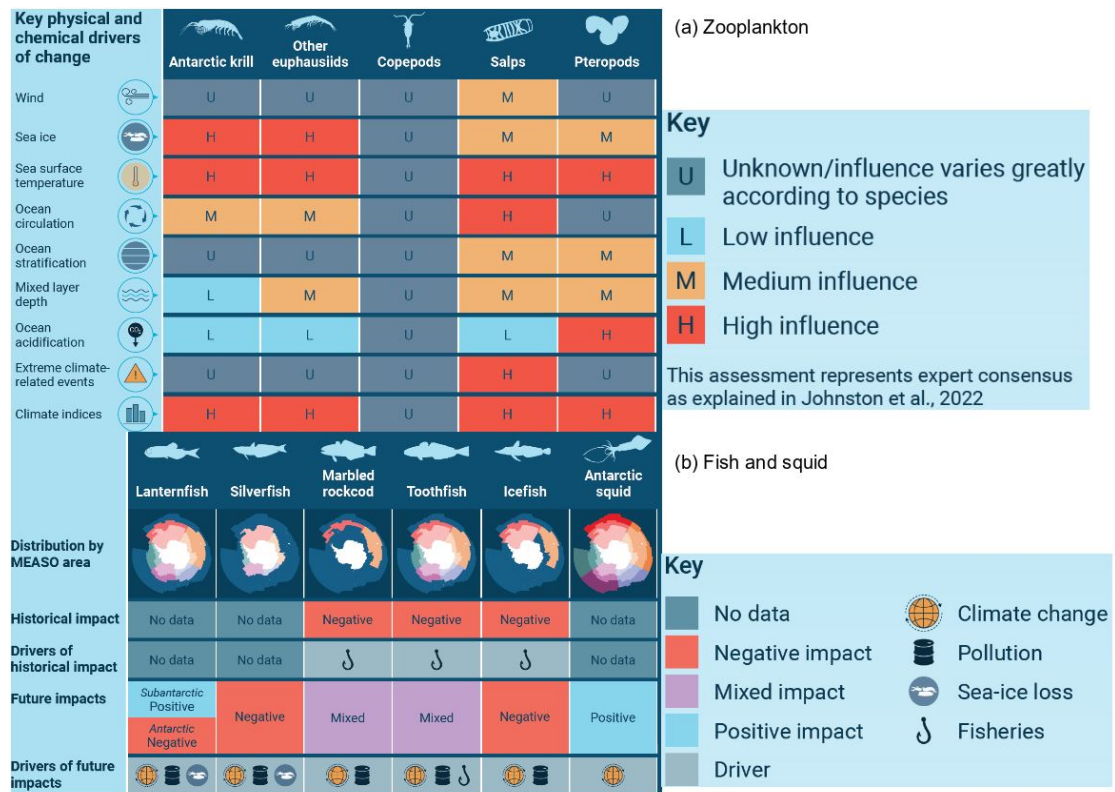


FIGURE 1.5: Summary of ecological assessments from the Marine Ecosystem Assessment of the Southern Ocean from Constable et al. (2023) - part I. Drivers impacting (A) krill and zooplankton, adapted from Johnston et al. (2022) and (B) fish and squid, adapted from Caccavo et al. (2021).

Key point

Through long-term monitoring efforts, ecological trends, at each level of the trophic web, have been investigated and show mixed impacts of environmental changes, depending on species, ecological parameters, regions and so on. Climate change impacts on ecosystems is complex to estimate because of the interactions between biotic and abiotic drivers, on various timescales. Mechanistic understandings of how climate change can impact pelagic ecosystems are needed.

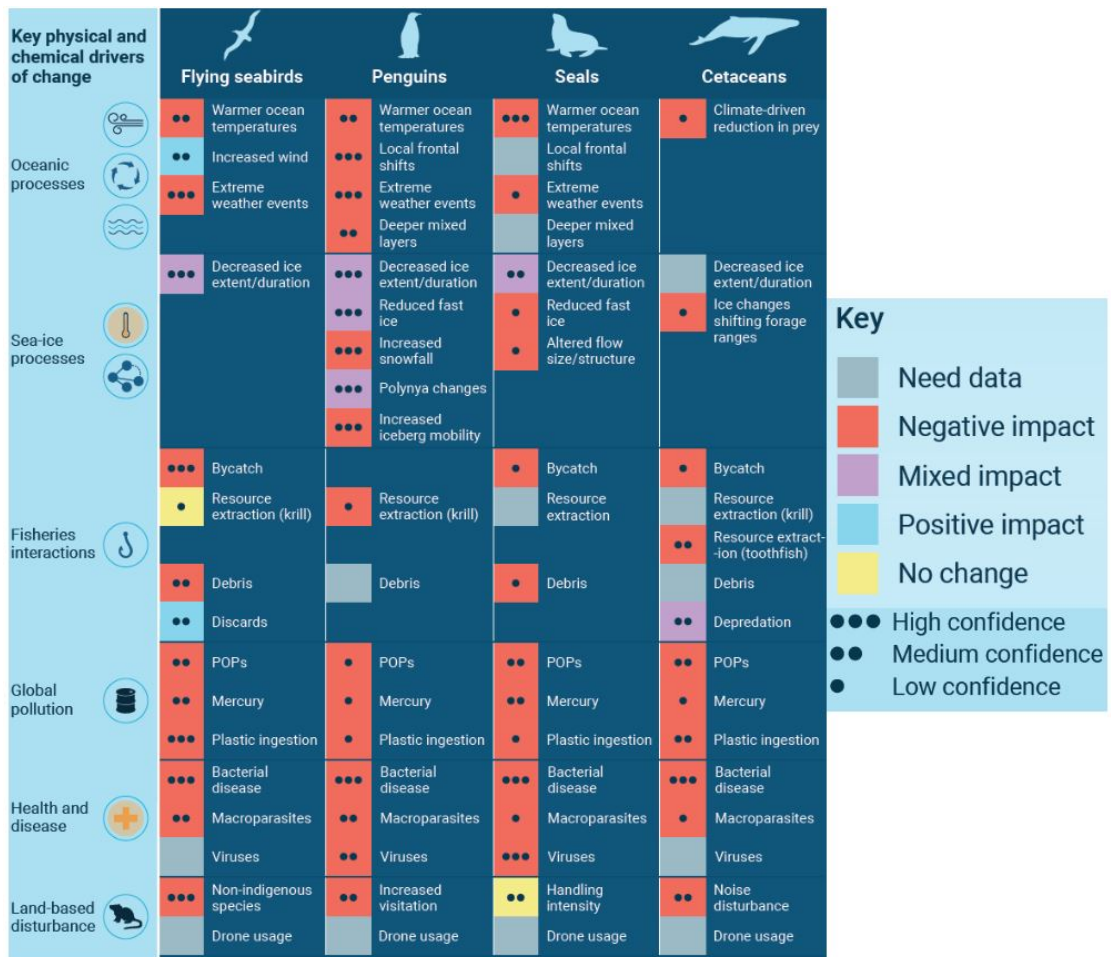


FIGURE 1.6: Summary of ecological assessments from the Marine Ecosystem Assessment of the Southern Ocean from [Constable et al. \(2023\)](#) - part II. Drivers impacting Southern Ocean birds and marine mammals, adapted from [Bestley et al. \(2020\)](#).

1.1.4 Uncertainties on climate change impacts on ecosystems hinder the development of climate-adapted conservation and fisheries management

1.1.4.1 Growing need to account for climate change in conservation and fisheries management

Both conservation and fisheries management aim at regulating human activities so that marine biodiversity is either protected or sustainably exploited. Both conservation and fisheries management are thus generally developed based on an underlying understanding of the ecosystem state and functioning. Climate change can generate a disturbance to that understanding and functioning, that often questions the current management

assumptions and induces uncertainty on the future management efficiency. Global studies indicate that the benefits of marine protected areas might be reduced under climate change (Bruno et al., 2018) and the additional threat represented by climate change for fisheries sustainability has also been well documented (Brander, 2010; Sumaila et al., 2011; Ruby and Ahilan, 2018; Barange et al., 2018; Cheung, 2018). Fisheries can be impacted by both species migration and decrease in stock biomass (Cheung, 2018).

Climate change has different implications for conservation and fisheries management. For conservation, the fundamental question is: what do we want to conserve and from which threat(s)? Scientific expertise is then provided to delineate areas of ecological significance or biodiversity hotspots, overlapping that information with known anthropogenic activities. There are several ways that climate change could be included in spatial planning depending on the state of knowledge and on the conservation targets. Developing a “refugium” approach in conservation (i.e. protecting areas less impacted by climate change) can be considered as a way to mitigate climate change impacts (Jones et al., 2016; Keppel et al., 2015). Other studies highlight the benefits of accounting for spatial heterogeneity of biotic and abiotic characteristics to ensure ecosystem resilience (Jones et al., 2016). Increasing connectivity to enable migration due to changing conditions might also be a way to alleviate pressure on ecosystems (Gaines et al., 2010), although the efficiency of this approach is limited by the magnitude of changes. A key action is also to reduce other human stressors to minimize cumulative impacts and to increase ecosystem resilience (McLeod et al., 2019). There are therefore different ways to establish priority sites (Wilson et al., 2020) that might be regionally specific.

For fisheries management, climate change generates two straightforward concerns: (i) will the stock migrate? (ii) Will the stock biomass decline? However, answering these two questions requires knowledge on the species vulnerability to changing environmental conditions. Global studies provide projections of biomass shifts and trends based on increased modelling efforts and international collaborations (e.g. FISH-MIP, Tittensor et al. (2018)), notably with the aim to highlight and estimate climate change impacts on fisheries (Cheung et al., 2009; Cheung, 2018; Bryndum-Buchholz et al., 2019; Lotze et al., 2018; Fernandes et al., 2020). If trends of decline are already observed, attributing them to environmental changes can be difficult, as their effects could be intertwined with fishing pressure impacts. If not, projections are often used but can be difficult to

communicate to policy-makers due to the associated uncertainties. A main issue for fisheries management is that policy-making institutions are often not adapted to anticipate changes in the long term and are mostly managing on short timescales which can be, in some cases, contradictory when the management target is to ensure sustainability over a few decades. For instance, the Convention for the Conservation of Antarctic Marine Living Resources (CCAMLR) implements, among others, the following decision rule for the Patagonian toothfish fishery : “*establish the constant level of catch, such that the median toothfish escapement in the spawning biomass over a 35-year period is 50% of the pre-exploitation median level*”.

There is increasing awareness that climate change, as a threat to biodiversity, needs to be accounted for in management strategies, however this is often not translated into action. Very few existing marine protected areas have included climate change adaptation strategies (Tittensor et al., 2019) and fisheries management also lacks climate change consideration (Sumby et al., 2021; Goldsworthy and Brennan, 2021). At the European level, Rilov et al. (2019) show that climate change is rarely considered operationally in European Marine Spatial Plans.

A major hindrance to operationalisation is the scale of action. Climate change is often studied through large-scale processes and is considered, rightly so, as a global issue, whereas ecological processes are studied at much finer scales and solutions to the biodiversity crisis are investigated at a more local scale (Wilson et al., 2020). Besides, the uncertainties associated with climate change impacts on ecosystems at the scale of management units are considered to be major hindrances to action, among other obstacles such as political will and institutional inertia (Sumby et al., 2021; Wilson et al., 2020). To adapt to climate change and ensure efficient conservation and management in the future, better understanding of how ecosystems may be impacted by environmental changes, including the spatial heterogeneity and timescales of those impacts, is crucial.

The discussion on the need to account for climate change in biodiversity management is not new and recommendations have already been formulated in the past (e.g. Johnson and Welch (2009); McLeod et al. (2009); Magris et al. (2014)). Those recommendations have insisted on the need for improved regional institutional coordination, expanding spatial and temporal perspectives, or including climate change scenarios in

policy-making (Heller and Zavaleta, 2009). However, many recommendations in the scientific literature were found to lack sufficient specificity to make them directly applicable by policy-makers, thus remaining mostly theoretical (Heller and Zavaleta, 2009). Efforts from the scientific community have been ongoing to provide assessments on the current management adaptation strategies and recommendations based on worldwide case studies (e.g. Tittensor et al. (2019)). Indeed, there is still a need for concrete strategies and some of them may need to be region-specific.

1.1.4.2 The case of the Southern Indian Ocean

The Southern Indian Ocean (20-120°E, 70-30°S) is one of the regions in the world with the largest heat content increase over the last decades (Figure 1.7; Llovel and Terray (2016); Garcia-Soto et al. (2021)). This region also hosts a rich biodiversity, among the largest population of megafauna (Delord et al., 2014). This richness arises both from the confluence of different water masses and from the presence of major topographic features such as the Kerguelen Plateau and subantarctic islands. The Southern Indian Ocean is a transition area between subtropical, subantarctic and antarctic waters. In particular, the Kerguelen Plateau area is a major confluence where tropical and subtropical surface waters meet and interact with waters of subantarctic and antarctic origins (Park et al., 2014).

This richness has led to important conservation efforts but also to the development of economically important fisheries such as the Patagonian toothfish (*Dissostichus eleginoides*) fishery. As the fishing pressure is less strong than in other part of the world (Figure 1.8), this region can constitute a “natural laboratory” to study the effect of climate change on pelagic ecosystems.

Pelagic conservation

To protect the rich biodiversity of the Southern Indian Ocean, conservation measures have been implemented both in the exclusive economic zones (EEZs) of the subantarctic islands and in the areas under the jurisdiction of the Commission for the Conservation of Antarctic Marine Living Resources (CCAMLR, Box 1.1.4), mostly south of 45°S. Part of EEZs of the following territories, Prince Edward, Crozet, Kerguelen, Saint-Paul and Amsterdam and Heard and McDonald’s islands, are managed through Marine Protected

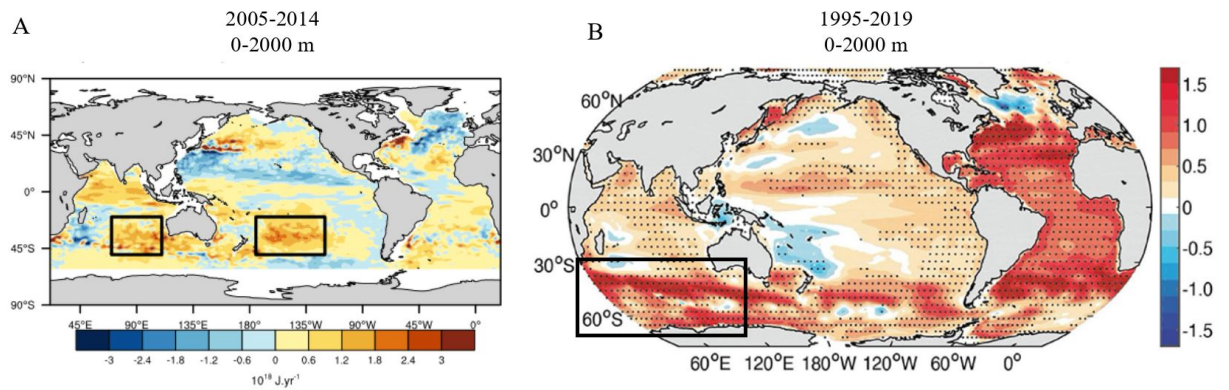


FIGURE 1.7: **Observed trends in ocean heat content over 0-2000 m**, between 2005-2014 (A, from [Llovel and Terray \(2016\)](#)) and 1995-2019 (B, from [Garcia-Soto et al. \(2021\)](#)).

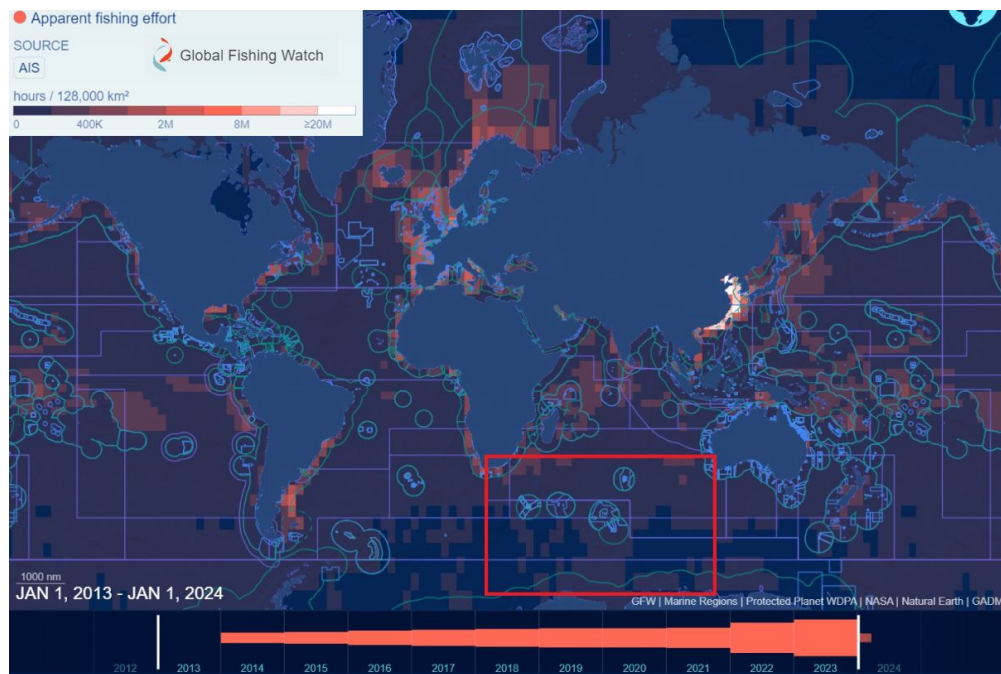


FIGURE 1.8: **Apparent fishing effort based on Automatic Identification System (AIS) data from the Global Fishing Watch between 2013 and 2024.** Exclusive Economic Zones are shown in green and Regional Fisheries management boundaries in purple and protected marine areas in blue. The Southern Indian Ocean is identified by the red box.

Areas (MPAs). The French national natural reserve at Crozet, Kerguelen and Saint-Paul and Amsterdam EEZ was created in 2006 and extended in 2016. This extension notably included the implementation of no-take reserves east of Kerguelen and over Skiff bank based on further ecoregionalisation work highlighting the high ecological significance of these areas ([Koubbi et al., 2016](#)). Around Heard and McDonald Islands, a MPA was created directly as a no-take marine reserve in 2002 and has been extended in 2014 ([Welsford et al., 2011](#)). This reserve has benefited from collaborations with the

fishing industry and has been considered as successful in supporting sustainable fishing activities while contributing to the recovery of some migratory seabirds populations such as king penguin (*Aptenodytes patagonicus*) and light-mantled sooty albatross (*Phoebastria palpebrata*; Brooks et al. (2019)). Similarly, the South African MPA around Prince Edward Islands has been officially implemented in 2013 as part of a representative system of MPAs, and notably to be used as a scientific reference for future management plans, to foster the recovery of Patagonian toothfish populations and to reduce the bycatch of toothfish fishery on marine seabirds.

Box. 1.1.4: Commission for the Conservation of Antarctic Marine Living Resources (CCAMLR)

The Commission for the Conservation of Antarctic Marine Living Resources (CCAMLR) is a Regional Seas Convention focused on the Southern Ocean, mostly south of 45°S but its northernmost boundaries vary between basins. It is part of the Antarctic Treaty System. It has been established in 1982 by an international convention and gathers today 27 members. The aim of this convention is mostly the conservation of Antarctic marine life. Conservation measures within CCAMLR includes the establishment of marine protected areas but also the sustainable management of exploratory and non-exploratory fisheries (e.g. krill, toothfish). A Scientific Committee, meeting every year, advises the Commission to ensure the use of the best available science.

The primary goal of the CCAMLR is the “*conservation of Antarctic marine living resources*” (Article II, Convention of CCAMLR). In the Indian ocean divisions of the CCAMLR, there are currently no marine protected areas, but there are conservation measures in place, notably to regulate fisheries, and there are two MPAs proposed in the Antarctic region. This convention explicitly indicates that any harvesting activity in the jurisdiction of the Convention must follow the conservation principles developed in the Article II of the Convention notably concerning the harvested population but also “*ecological relationships*” and the “*prevention of changes or minimisation of the risk of changes in the marine ecosystem which are not potentially reversible over two or three decades*” (Article II, Convention CCAMLR). This latter principle reflects the importance of a long-term perspective when implementing conservation measures.

Despite national efforts and CCAMLR principles, gaps remain in the Southern ocean conservation. In total, 5.8 % of the Southern Indian Ocean is covered by MPAs and only within EEZs. The current marine protected areas in the Southern Ocean are still not representative of the full range of benthic and pelagic ecoregions (Brooks et al., 2020). To fill this gap, work on pelagic ecoregionalisation in the Southern Indian Ocean is ongoing (Makhado et al., 2023). A workshop held in 2019 organized by the CCAMLR Scientific Committee developed a scientific work program for pelagic spatial planning in the eastern subantarctic region to investigate the relevance of adding new subantarctic spatial conservation tools in the High Seas of the CCAMLR area (Makhado et al., 2019). Indeed, the open ocean, extending beyond the EEZ, also called the “High Seas”, is a new frontier for conservation (Della Penna et al., 2017). The adoptions of the global target to protect 30 % of the ocean by 2030 by the Convention on Biological Diversity and of the treaty for the protection and sustainable use of marine biodiversity in areas beyond national jurisdiction (the so-called “BBNJ” treaty), provide a favorable international context to further develop conservation in the Southern Ocean.

Conservation is mainly based on a scientific understanding of ecologically significant areas, for different types of ecosystems. Indicators have been developed to integrate various knowledge and help the prioritization process. Some indicators focus on a particular group of species such as the Important Marine Mammals Area (IMMA) initiative created in 2013 by the International Committee on Marine Mammal Protected Areas and the International Union for Conservation of Nature’s (IUCN). Other indicators cover a wide range of species and ecosystems. For instance, the Convention on Biological Diversity adopted in 2008 a set of criteria to identify “ecologically and biologically significant areas” (EBSAs). Uniqueness, biological diversity or vulnerability are some of the criteria that can be used to define EBSAs. The IUCN also developed a global standard for the identification of “key biodiversity areas” (KBAs; IUCN (2016a)). Such areas have been identified in the Southern Indian Ocean, mostly in areas of higher primary productivity, notably around subtropical and subantarctic islands (Figure 1.9). In the Southern Indian Ocean, the identification of important areas is often based on the foraging zones of top predators (tracked through bio-logging technologies), since those top predators can be considered as “sentinel species”, both of the richness of the trophic web and of environmental changes (Carpenter-Kling et al., 2019; Hindell et al., 2020).

Throughout this PhD thesis, the acquired knowledge on climate change trends in the

Southern Indian Ocean will be discussed in relation to conservation objectives. In particular, Chapter 3 will provide a mapped overview of climate change threats that can be compared with protected and ecologically important areas and Chapter 4 will focus on how extreme events and long-term global warming can impact a physical feature characterising top predators foraging zones.

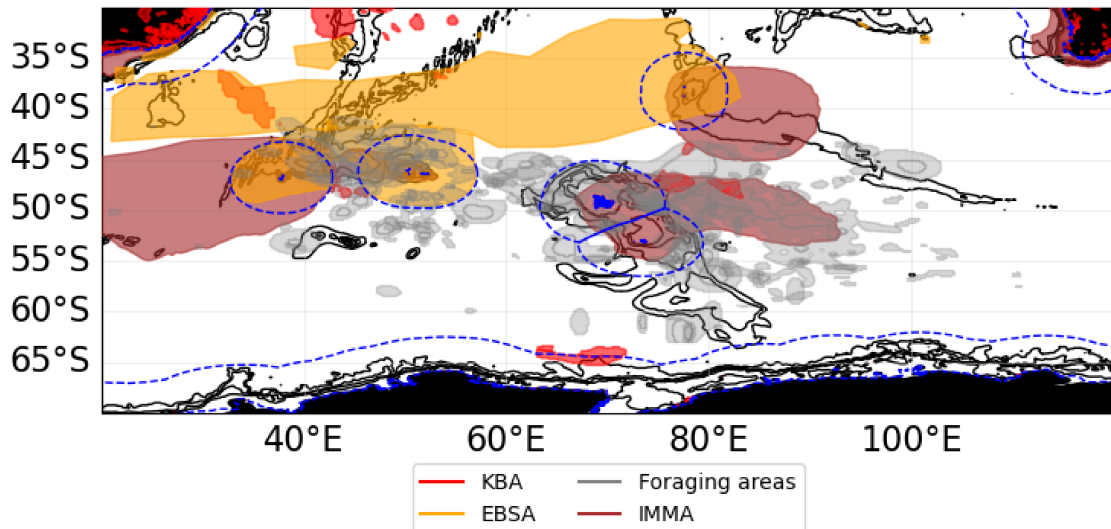


FIGURE 1.9: Map of the current key biodiversity areas (KBA, red; BirdLife International (2022)), important marine mammals areas (IMMA, brown; IUCN MMPATF (2023)) and ecologically and biologically significant areas (EBSA, orange; obtained from the clearing-house mechanism of the Convention on Biological Diversity <https://chm.cbd.int/database/>) in the Southern Indian Ocean. The exclusive economic zones are shown in dashed blue and examples of different top predators foraging areas are shown in gray (data provided by Malcolm O’Toole).

The Patagonian toothfish fishery

In the Southern Indian Ocean at subantarctic latitudes, the main anthropogenic activity is the Patagonian toothfish fishery. The Patagonian toothfish (*Dissostichus eleginoides*) is a demersal notothenoid fish endemic to the southern hemisphere and mostly found around subantarctic islands (Collins et al., 2010). The first recorded catch dates from 1977 under CCAMLR zone 48 and catches have then largely increased in 1984 (Figure 1.10). This fishery started around the Kerguelen Plateau in the late 1980s and has been a highly profitable activity ever since (Grilly et al., 2015). Today, the Patagonian fisheries is of importance to the French economy as it is La Reunion’s second largest exporting sector. Since the beginning of the century catches have stabilised at around 2000 tonnes per year ¹.

¹<https://www.ccamlr.org/en/fisheries/toothfish-fisheries>

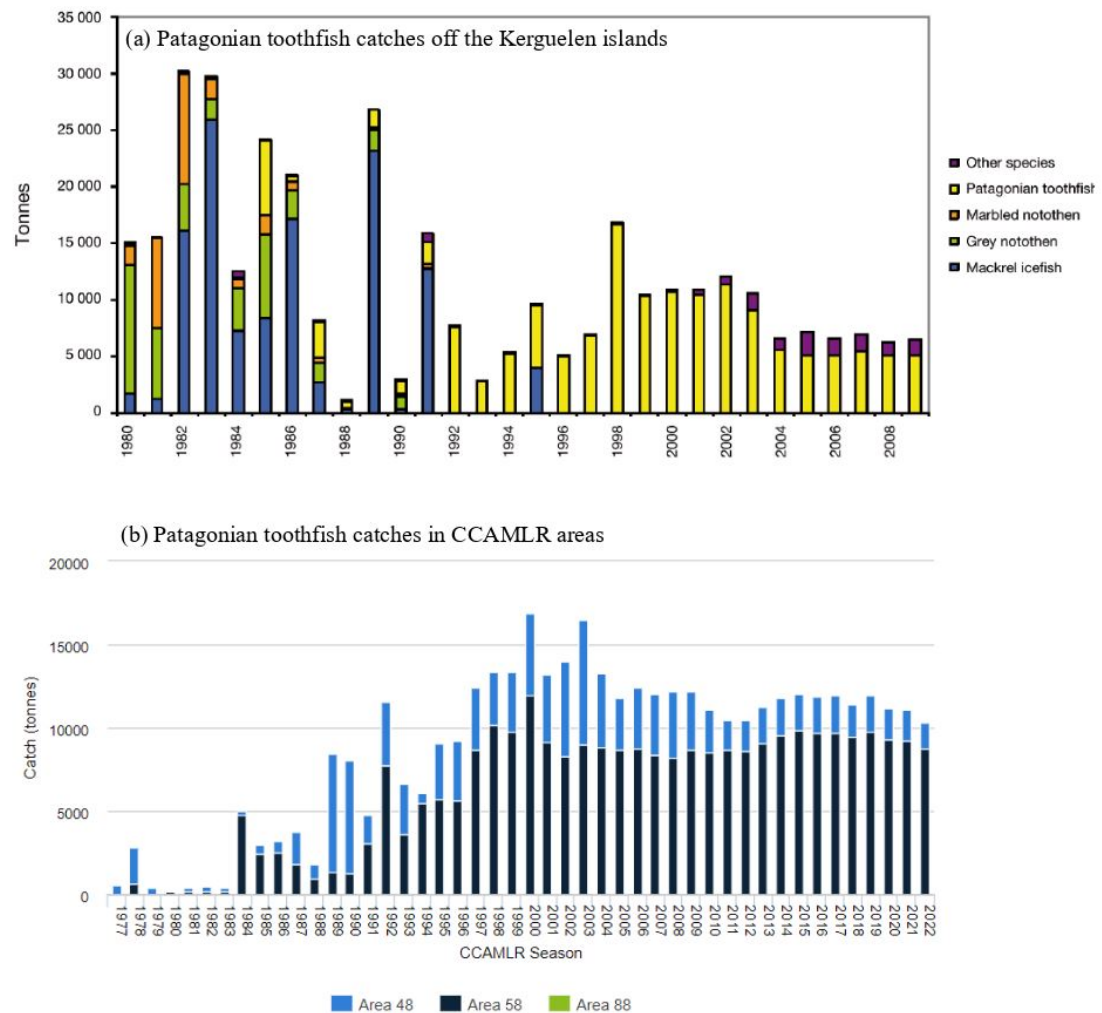


FIGURE 1.10: **Patagonian toothfish catches off the Kerguelen islands and in CCAMLR areas.** (A) Historical fishery catches from trawl and longline, off the Kerguelen Islands from [Duhamel et al. \(2011\)](#). (B) Catches of Patagonian toothfish throughout time for the different CCAMLR areas: the South Atlantic (Area 48), the South Indian (Area 58) and the South Pacific (Area 88); Source: <https://www.ccamlr.org/en/fisheries/toothfish-fisheries>

The Patagonian toothfish is a long-lived species (around 50-75 years; [Collins et al. \(2010\)](#)) with a complex life-cycle. Patagonian toothfish spawn at depth in winter; then the eggs rise to the surface and drift along the currents for around 3 months. Eggs become larvae that are still subjected to the local circulation. Juveniles fish are then mostly recruited (i.e. entry in the fish stock) over shallow bathymetries and as they mature they live deeper and further away from the shallow areas ([Collins et al. \(2010\)](#); [Péron et al. \(2016\)](#); Figure 1.11). Patagonian toothfish recruitment has shown to be highly variable ([Laptikhovsky and Brickle, 2005](#); [Collins et al., 2007](#); [Belchier and Collins, 2008](#); [Collins et al., 2010](#)).

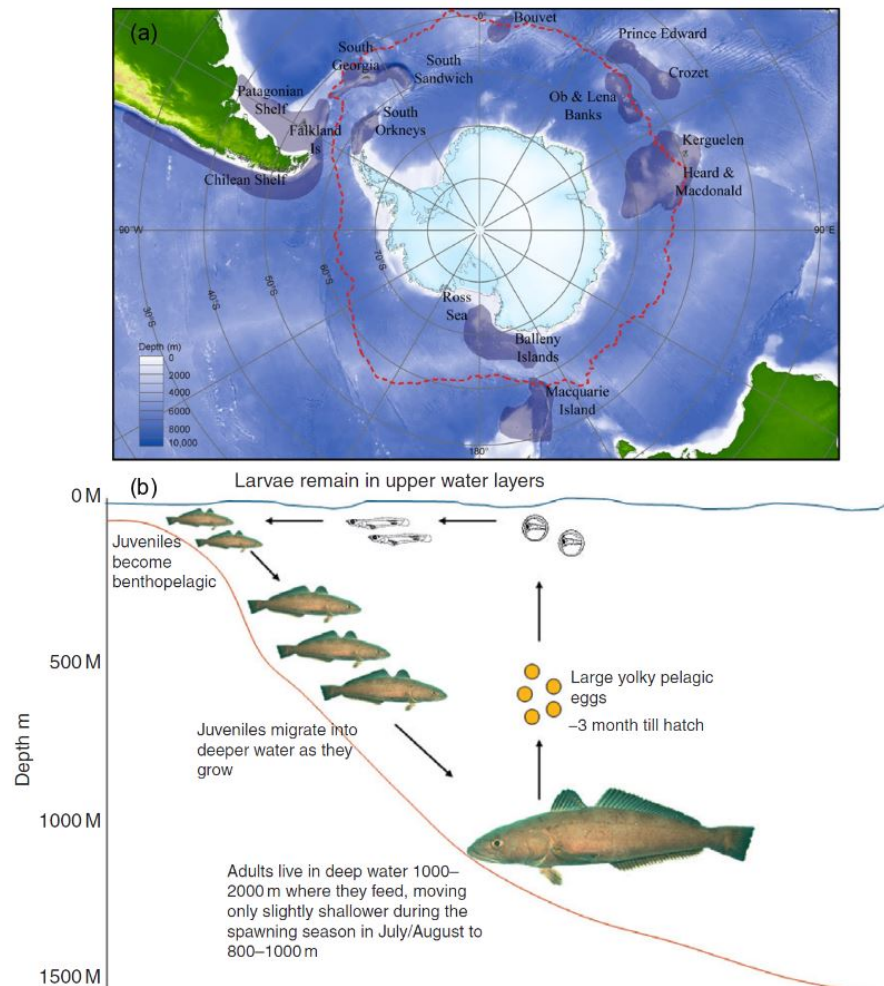


FIGURE 1.11: **Spatial distribution and life cycle of the Patagonian toothfish (*Dissostichus eleginoides*).** (A) Known circumpolar distribution of Patagonian toothfish, the red dotted line marks the Polar Front. (B) Schematic describing the Patagonian toothfish life cycle over various depths. Both figures are from [Collins et al. \(2010\)](#)

Recent stock assessments support decreasing trends in most Patagonian toothfish stocks managed (stock assessment reports to the CCAMLR for 2022 for CCAMLR zones 48.3, 48.4, Heard and McDonald, as well as Falkland islands, Kerguelen and Crozet; [Patterson and Tuyenman \(2022\)](#)). These observed trends have been associated with years of lower recruitment. However, whether decreased recruitment is due to natural variability or to a long-term change in environmental conditions is uncertain. Such event of low recruitment might be temporary but could also become more frequent in the future or reflect a long-term trend.

Consequently there are growing concerns on climate change impacts on the Patagonian toothfish. Although lower recruitment has been associated with warmer temperature

during spawning in South Georgia (Belchier and Collins, 2008), the impact of warmer temperatures on the stock remains uncertain. Low toothfish catch rates at the Australian stock of Heard and McDonald islands co-occurred with a marine heatwave in 2016 (Su et al., 2021) but no mechanistic understanding of the potential impacts of extreme events on toothfish catchability have yet been established. Scientists within CCAMLR have started to work to identify knowledge gaps and climate change management adaptation options (McDonald et al., 2023). During the CCAMLR workshop focused on climate change in September 2023, participants have highlighted key points such as “*the importance of incorporating climate change into management and regulatory frameworks, as well as stock assessments*” but also “*the need to move from motherhood statements on climate adaptation to tangible operational action*” (McDonald et al., 2023).

Despite the uncertainties on climate change impacts, current knowledge, by analogy with other fish species, points out that early-life stages (i.e. pelagic phases of eggs and larvae) may be more sensitive to environmental conditions, notably temperature and local currents (Pankhurst and Munday, 2011). In this thesis, Chapter 5 will investigate potential changes of the circulation and thus connectivity over the Kerguelen Plateau that might impact Patagonian toothfish early-life stages, to also reflect on how climate change could be accounted for in a remote and data-limited fishery.

Key point

Despite increasing awareness on the need to account for climate change in both marine conservation and fisheries management, such awareness has not yet been operationalized. The development of concrete strategies can arise from region-specific case studies and a better understanding of climate change impacts on ecosystems. The Southern Indian Ocean is an interesting case of a remote and data-limited area with important stakes of conservation and fisheries management.

1.1.5 Towards a more mechanistic understanding of climate change impacts on pelagic ecosystems at subantarctic latitudes

Not only to inform conservation and management efforts but also to tackle this research question in its own right, the scientific community is increasingly investigating

the impacts of climate change on biodiversity at different levels. The two most common approaches are (i) investigating ecosystems or species response to perturbations through *in situ* or experimental studies, and (ii) ecosystem modelling or species distribution modelling and projections.

The first approach is to study ecosystems or species response to perturbation through *in situ* or in laboratory studies and the results can be extrapolated using climate projections. For instance, [Faulkner et al. \(2014\)](#) determine the upper thermal range response to warming for crustaceans. Given that climate models are used to project future temperatures, the response of crustaceans to climate change can be anticipated. Experimental settings can also be used to simulate different emission scenarios, as was done to investigate the combined effects of acidification and warming on the embryonic physiology of an Antarctic dragonfish (*Gymnodraco acuticeps*; [Flynn et al. \(2015\)](#)). To account for the complexity of the biological system, mesocosms experiments can also be helpful ([Stewart et al., 2013](#)). A main advantage of these approaches is to be able to disentangle the effects of physical variables changes (e.g. temperature, pH) and analyse the complexity of the biological response. However, these approaches often do not account for the physical complexity and dynamic nature of the marine environment (e.g. ocean circulation) and cannot be deployed systematically, especially for open ocean ecosystems, thus limiting the interpretation of those results at scales relevant for conservation.

The second approach consists in determining the past and current habitat conditions for species or communities to project their future distributions. An important difficulty resides in the number of parameters to account for to determine fundamental niches (i.e. set of conditions in which a species can survive and reproduce) and realised niches (i.e. set of conditions actually used by the species after accounting for biotic interactions). Those methodologies mostly rely on statistical modelling, with an increasing interest for machine learning approaches ([Geary et al., 2020](#); [Melo-Merino et al., 2020](#); [López-Farrán et al., 2021](#); [Sillero et al., 2021](#)). Substantial efforts have been made to improve and develop those methods, further considering biotic interactions and expanding modelling from the species level to the community or bioregion levels (e.g. [McCormack et al. \(2021\)](#)). Those methodologies can allow to capture the complex and often non-linear relations between environmental and biological/ecological variables and can be used to directly advise management ([Howell et al., 2021](#)). However, this approach is challenging for data-limited ecosystems, as it should be based on a good representation of the current

niche, all the more so for pelagic ecosystems which requires a 3D understanding of their habitat. This is reflected by the geographical bias identified in a recent review: 48% of studies using ecological niche models or species distribution models for marine ecosystems were at local scales with a hotspot in the North Atlantic (Melo-Merino et al., 2020). Projections can be sensitive to the choice of biogeochemical models especially for pelagic species and many uncertainties remain at higher latitudes (Bryndum-Buchholz et al., 2019; Fernandes et al., 2020). This approach also assumes that the conditions favored historically remain favored in the future, then deducing impacts on ecosystems from large-scale changes of those factors. This approach thus generally focuses on large scale processes and longer timescales while assuming an homogeneity in the biological response. This approach can therefore be more limited at scales relevant for conservation and management in remote or data-limited regions (Fernandes et al., 2020).

Although these approaches are very useful to study climate change impacts on ecosystems, the focus has mostly been on the complexity of the biological response and of the relation between ecosystems and their environment (Figure 1.12 A). The physical drivers of change are often reduced to state variable changes, overlooking potentially important physical spatio-temporal complexity (Figures 1.12 and 1.13). At least two major elements can be considered as contributing to the complexity of physical changes in the pelagic realm and are today major hindrances to better understanding climate change impacts on pelagic ecosystems : i) one related to climate change impacting environmental conditions differently at depth compared to the surface and ii) a second one related to the complexity of linking climate change large-scale signals (> 100 km) to finer-scale physical features (between 1 and 100 km) that play a major ecological role.

1.1.5.1 The importance of accounting for a 3D habitat

The first hindrance, related to a changing 3D environment, is increasingly considered in modelling approaches (e.g. Brodie et al. (2018)) but remains challenging, notably due to a lack of *in situ* observations in some regions. In the Southern Indian Ocean, biological programs have greatly contributed to filling this gap (e.g. MEOP, Roquet et al. (2014)), in addition to the global effort to improve the spatial coverage of *in situ* observations (e.g. Argo floats, Argo (2000)). The development of long-term programs such

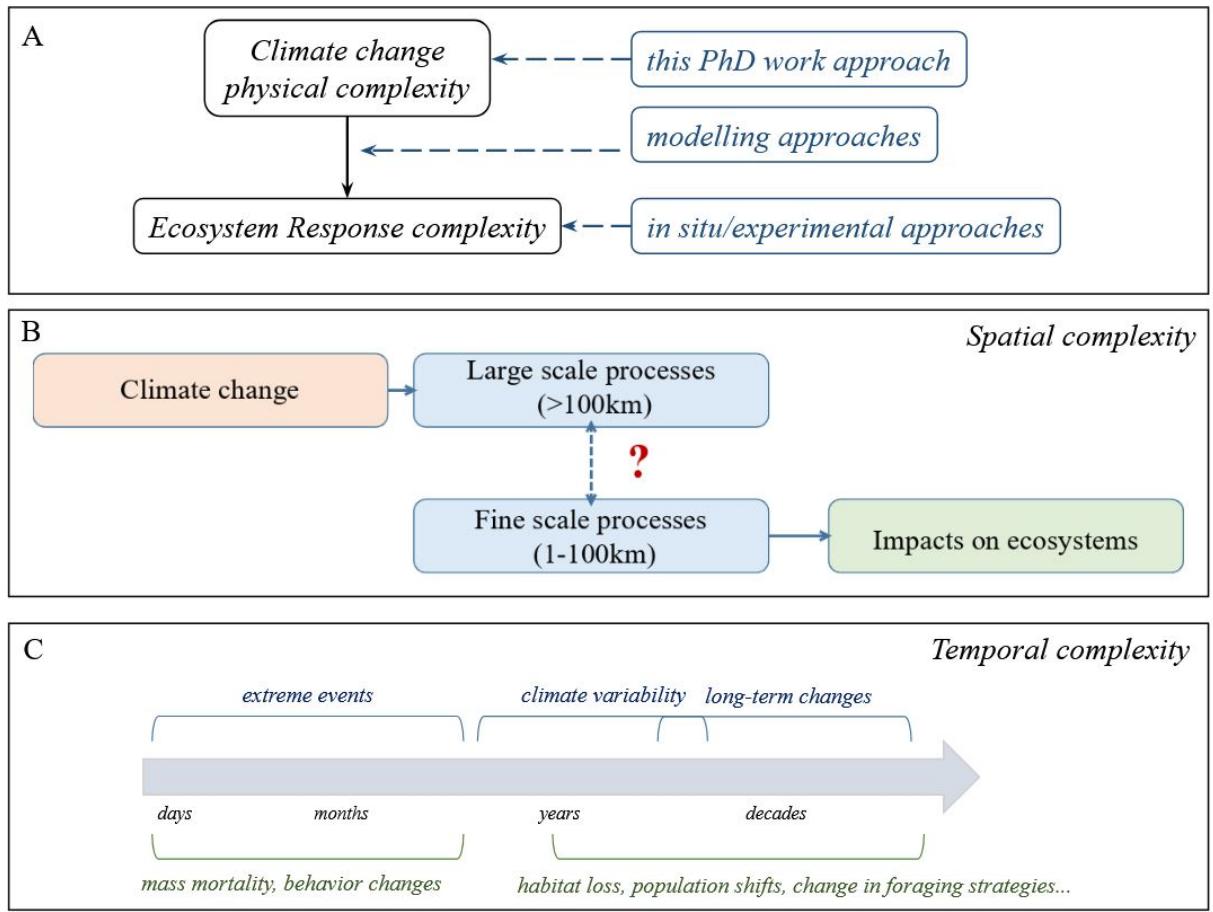


FIGURE 1.12: **Schematic illustrating the current knowledge gap regarding the complexity of the physical disturbances under climate change** that are important to study climate change impacts on ecosystems (A) and the importance of a multi-scale approach both spatially (B) and temporally (C).

as the “Toward Hydroacoustics and Ecology of Mid-trophic levels in Indian and Southern Ocean” (THEMISTO) program, to assess diversity and abundance of mesopelagic communities at different depth ranges across contrasted regions, are also key to unravel 3D ecological processes.

Those monitoring efforts have contributed to shed light on the vertical structuring of mesopelagic communities, in relation to hydrographic and ecological processes (McMahon et al., 2019; Cotté et al., 2022). Over the Kerguelen Plateau, a three-layer system has been identified between 12 m and 800 m, with distinct scattering layers between 10 and 200 m, 200 and 500 m and 500 to 800 m, but the composition of the communities vary depending on the level of primary productivity (Cotté et al., 2022). Crustaceans are abundant over the Plateau, mostly between 0 and 500 m, while mesopelagic fish

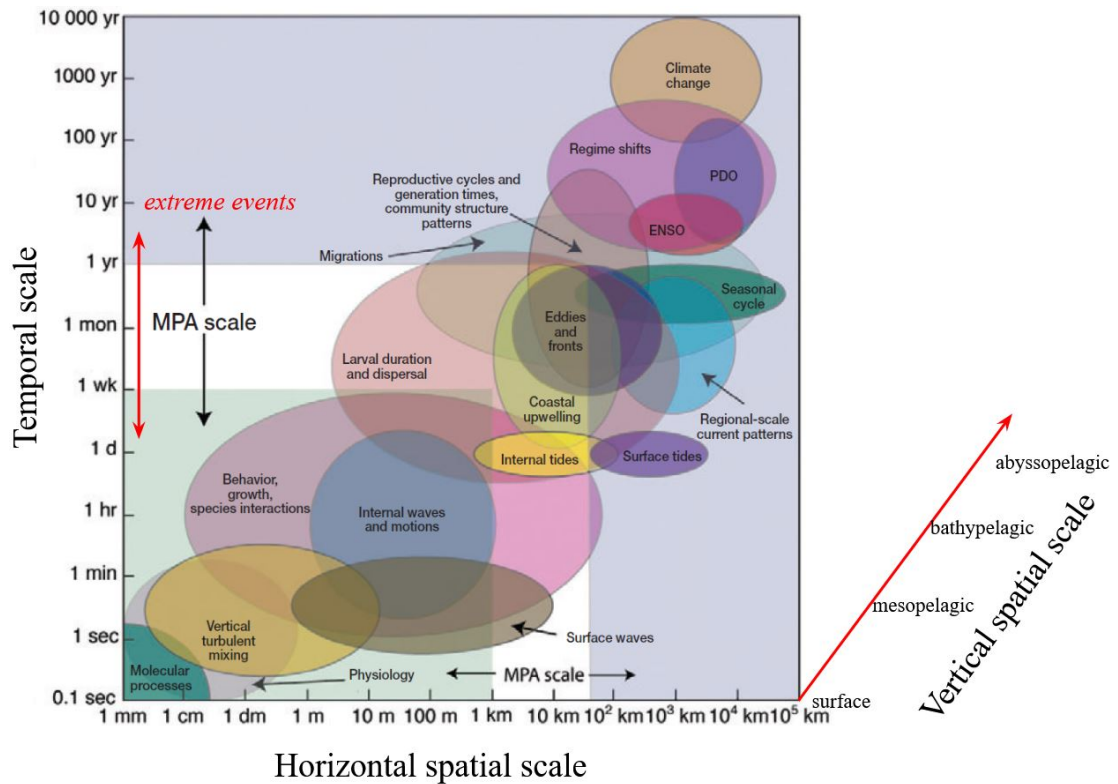


FIGURE 1.13: **Spatial and temporal scales of oceanographic and ecosystem processes from Carr et al. (2011)**, adding the temporal scale of extreme events and the importance of considering the vertical scale for pelagic ecosystems.

are mostly found below 400 m (Cotté et al., 2022). Latitudinal changes in acoustic responses across the ACC frontal system have also been observed. From the subantarctic to the subtropical zones, denser acoustic responses at the surface (0-100m) are observed along with the occurrence of an intense deep scattering layer between 400 and 600 m responding at 38 kHz, that could be explained by a shift in the assemblages and their acoustic characteristics across the frontal system (Izard et al., 2024).

The vertical distribution of mesopelagic prey plays an important role for top predators foraging strategies, to optimize the energy constraints associated with foraging distances and depths. Top predators such as elephant seals were found to target specific water masses, such as the Circumpolar Deep Water (CDW; Biuw et al. (2007); Hindell et al. (2016)). As such water mass shoals, the prey field is brought closer to the surface, which can increase aggregation and prey accessibility to predators (McMahon et al., 2019). Foraging strategies also differ between male and female elephant seals, with females mostly targeting the warmer part of the CDW and Antarctic Surface Water (AASW) while males favor the coldest part of AASW (Labrousse et al., 2015). The

vertical structure of the water column is particularly crucial for top predators with a physiologically-limited diving capacity such as king penguins (*Aptenodytes patagonicus*; Figure 1.14). The king penguins population of Crozet was found to mostly target the Polar Front to feed on oceanic species of lanternfish, their main prey, which is mostly associated with water masses around 4°C and 5°C (Guinet et al., 1997). The Polar Front is the edge of the presence of winter waters (water mass characterized by a subsurface minimum of temperature and formed from the AASW; Park et al. (1998)), and as the cold water masses sink at depth, going northward, the prey field above appears to be less available for top predators (Pakhomov et al., 1994; Charrassin and Bost, 2001; Scheffer et al., 2012). The characteristics of the winter water layer can thus be an important predictor of the prey capture attempts in a dive for king penguins (Brisson-Curadeau et al., 2023).

Anthropogenic pressures can affect those subsurface and deeper ocean layers. New activities might develop deeper, given the fishing industry's interest for mesopelagic fishes (Fjeld et al., 2023) or the discussions on deep sea mining (Hallgren and Hansson, 2021). Climate change is already inducing changes throughout the water column, at different rates, being a supplementary threat on species usually evolving in a relatively more stable environment than the surface layers (Game et al., 2009). This is of particular relevance in the Southern Ocean as an early emergence (i.e. trend larger than than the amplitude of natural or internal variations) of climate change signal in temperature has been found in climate models quite early in this region in the ocean interior (around 1980s-1990s), while it is found to emerge later for the ocean surface (Silvy et al., 2020). Besides, extreme events can be longer and more intense at depth, especially in the subsurface ocean (50 - 200 m; Fragkopoulou et al. (2023)). Transition areas, such as the Southern Indian Ocean, are associated with frequent and intense MHWs that can extend at depth, especially near boundary currents and fronts (Fragkopoulou et al., 2023). Such extreme events could thus strongly impact biodiversity in the ocean interior (Smale et al., 2019; Smith et al., 2023; Fragkopoulou et al., 2023).

All these elements suggest that only focusing on surface changes could tend to underestimate climate change pressure on pelagic ecosystems. Recent studies have suggested the incorporation of this third dimension of the ocean to inform the prioritization of conservation actions (Levin, 2018; Venegas-Li et al., 2018; Brito-Morales et al., 2022; Doxa et al., 2022), allowing for the determination of priorities which could contribute towards

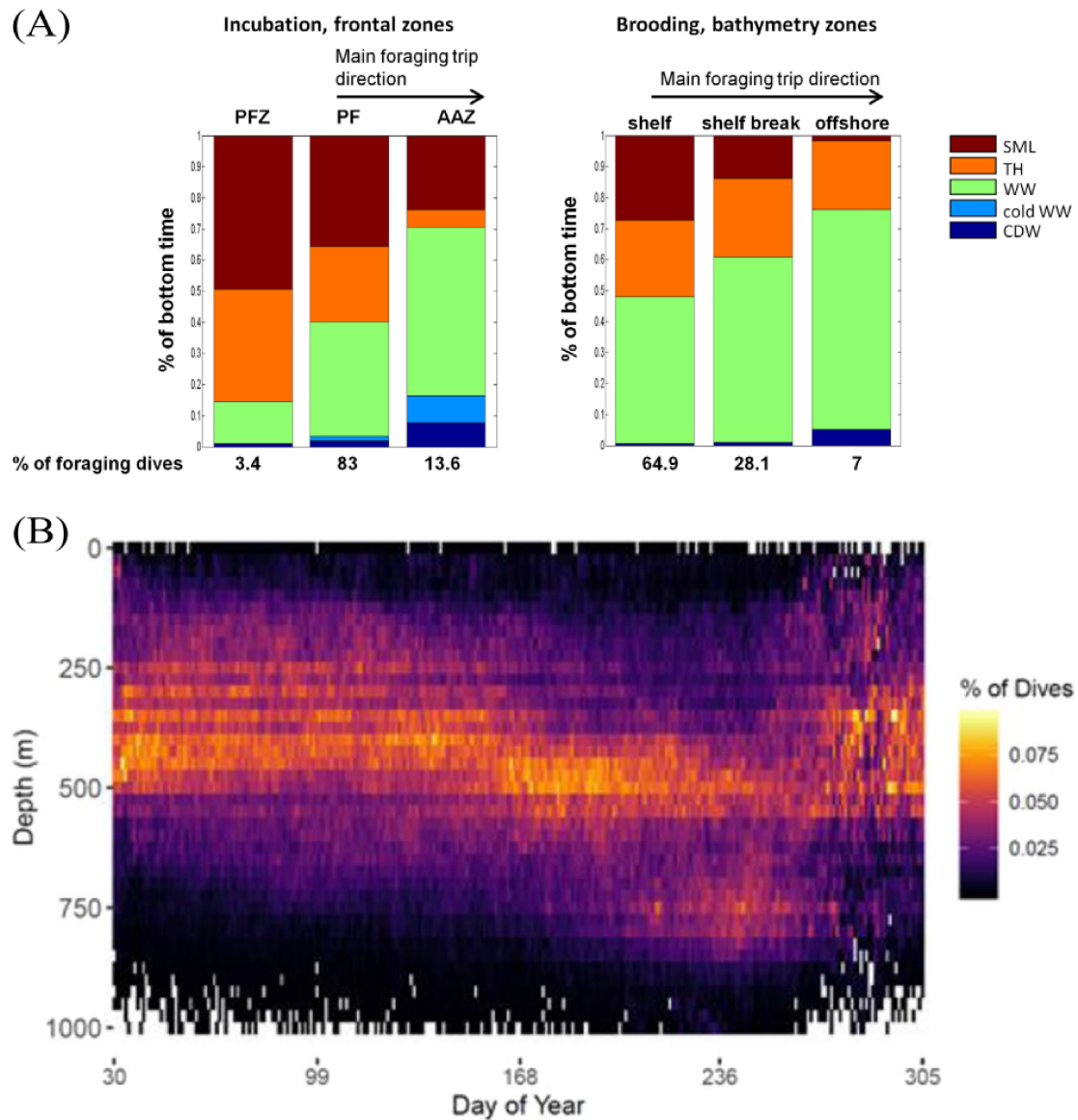


FIGURE 1.14: **Examples of top predators targeting subsurface and mesopelagic layers to forage.** (A) Water masses targeted by King penguins (*Aptenodytes patagonicus*) along their foraging trip. Abbreviations of the water masses are SML (Surface Mixed Layer), TH (Thermocline), WW (Winter Water), WWcold (cold Winter Water $>0.5^{\circ}\text{C}$), CDW (Circumpolar Deep Water). Figure from [Scheffer et al. \(2016\)](#). (B) Proportion of daily of dives at each depth for each day of the year during the post-moult period (February–October) for female elephant seal (*Mirounga leonina*); from [McMahon et al. \(2019\)](#).

efficient use of conservation resources within highly heterogeneous marine ecosystems. [Brito-Morales et al. \(2022\)](#) highlight the importance of vertically coherent marine protected areas across depth domains, to also protect climate refugia while pointing out the difficulty of this task due to disparate effects of climate change across depths.

In this PhD thesis, we account for this vertical dimension when possible, investigating whether it could buffer (e.g. vertical refuge) or enhance (e.g. additional pressures linked

to a 3D dynamic environment) climate change impacts on pelagic ecosystems. Chapter 4 notably focuses on the potential impacts of marine heatwaves and long-term warming on winter waters.

1.1.5.2 The importance of accounting for finer scale processes

Box. 1.1.5: Oceanic fronts

Oceanic fronts have multiple definitions. Fronts are commonly defined as areas of strong horizontal gradients of physical (e.g. temperature, salinity), chemical (e.g. nutrients) and/or biological (e.g. chlorophyll) properties (Johannessen, 1975; Belkin, 2003). There are different types of fronts associated with various physical processes but there are characteristics that can be used to identify them. For instance, fronts are often associated with strong jets. Fronts can also be defined as the separation between different water masses. Fronts can extend at depth, down to 2000 m or more. Fronts can be short-lived, seasonal or permanent depending on the regions and on the definition used. They play a key role in ocean-atmosphere interactions but also for primary production and the development of rich ecosystems.

The second hindrance, related to finer scale processes, is often not accounted for in the commonly used approaches to investigate climate change impacts on ecosystems. However, fine scale processes can play a major ecological role for pelagic ecosystems (Lévy et al., 2018; Della Penna and Gaube, 2020). From phytoplankton to top predators, features such as fronts, eddies, retention zones or filaments are key to understand the spatial and temporal distribution of ecosystems (Figure 1.15; Box 1.1.5).

These fine scale processes are shaping biodiversity distribution at different trophic levels, in addition to the latitudinal gradients of biodiversity observed for plankton (Koubbi et al., 2011), fish larval assemblages (Koubbi et al., 1991; Koubbi, 1993) or pelagic fishes (Duhamel, 1998; Duhamel et al., 2014). Frontal zones are often areas of increased vertical velocity which contribute to bringing nutrient-rich waters to the surface and triggering and/or fostering phytoplankton blooms and thus the trophic interactions associated. Phytoplankton blooms have been observed near fronts (Comiso et al., 1993; Moore and Abbott, 2000) and in waters masses that have flowed over shelves, seamounts or near

islands, which are often enriched in important nutrients for the bloom development such as iron (Ardyna et al., 2019; Sergi et al., 2020). Front position can also modulate zooplankton communities distribution (Figure 1.15). The variability of the subantarctic front position modulates the abundance of euphausiids, copepods and pelagic foraminifera (Meilland et al., 2016). The presence of the subsurface winter waters, whose northernmost extension marks the Polar Front, also plays a structuring role for the vertical distribution and relative abundance of mesopelagic organisms (Béhagle et al., 2017; McMahon et al., 2019; Hunt and Swadling, 2021).

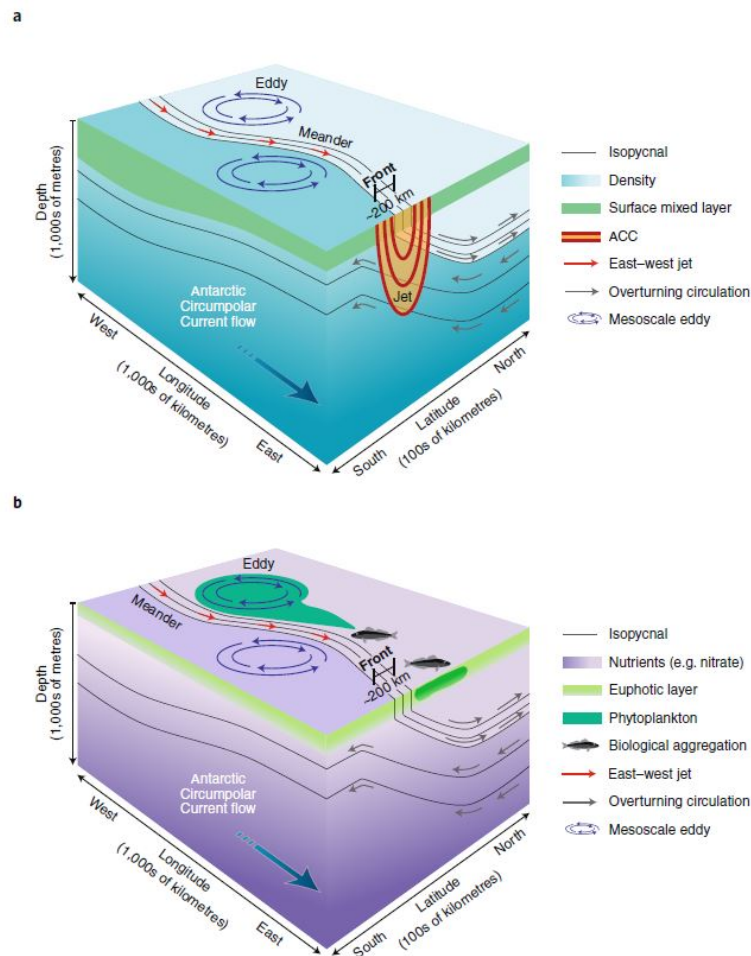


FIGURE 1.15: **Schematics of Antarctic Circumpolar Current fronts**, illustrating the (a) physical and (b) biogeochemical characteristics of an idealized ACC front. Credit: Christopher Chapman/Louise Bell; from Chapman et al. (2020).

Since the distributions of epipelagic and mesopelagic preys are driven by mesoscale features, front position and water masses presence, so are top predators foraging hotspots. Hotspots of biodiversity have been identified in relation to the Polar Front position (e.g. king penguins, *Aptenodytes patagonicus* foraging hotspots; Kooyman et al. (1982, 1992); Bost et al. (2015)), notably east of Kerguelen around the Polar Front meander (Thiers

et al. (2017); Figure 1.16 B). It has also been observed that elephant seals target long-lived cyclonic eddies or the edges of anticyclonic eddies for foraging where mesopelagic prey is expected to be more abundant (Dragon et al. (2010); Cotté et al. (2015); Figure 1.16 C) . Indeed, fishes tend to concentrate within such mesoscale features (Baudena et al., 2021). Mesoscale eddies themselves thus constitute unique habitats that are transported by local currents (Della Penna et al., 2022).

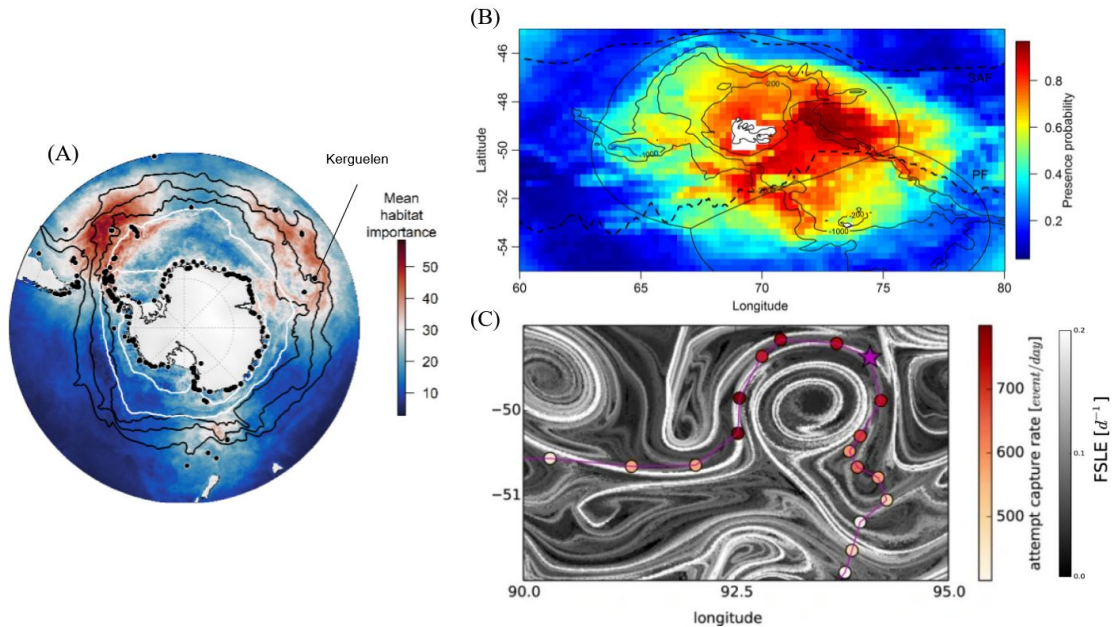


FIGURE 1.16: **Examples of studies highlighting spatial patterns of ecologically important areas**, zooming from a circumpolar scale to an eddy-scale. (A) Mean habitat importance based on 17 top predators tracking data, from Reisinger et al. (2022). (B) Sum of the predicted probabilities for four top predators; dashed lines mark the position of the Polar Front and the Sub-Antarctic Front, from Thiers et al. (2017). (C) Fronts as Finite Size Lyapunov Exponent (FSLE) ridges (gray scale) on 02/12/2011 and elephant seal (*Mirounga leonina*) attempt capture rate along its trajectory, from Della Penna et al. (2015).

Recent studies highlight climate change potential impacts on fine scale structures. In particular, mesoscale activity is projected to intensify in the Southern Ocean (Martinez-Moreno et al., 2021). However, those studies are often conducted to answer strictly physical questions about the ocean circulation and heat or carbon uptake, and not necessarily being related to potential ecological impacts. This importance of considering finer scales covers two challenges : a computing or technical challenge (fine scale resolution) and a scientific one (the interaction between scales, Figure 1.12 B). Indeed, climate models, which are key tools in climate studies, are most often too coarse to accurately represent such structures (Hewitt et al., 2022).

Spatial finer scales are also associated with shorter temporal scales (Figure 1.13). As such they could play an important role in modulating extreme events. Extreme events can span from days to months but can also generate long-term impacts. The abruptness and magnitude of an extreme can punctually increase species mortality or cause drastic behavior changes; but the frequency of such extremes can also lead to long-term alterations at the population or ecosystem levels (e.g. habitat shift, genetic selection; Gruber et al. (2021)). Accounting for this temporal complexity of climate change is thus crucial to understand the range of pressures exerted on ecosystems (Figure 1.12 C).

This PhD thesis is based on a multi-scale approach with a focus on scales relevant for conservation. Linking interannual variability and extreme events over the last decades and decadal projections from climate models is used to discuss potential ecological impacts. In particular, Chapter 5 aims at linking large-scale drivers and finer scale dynamic features that are ecologically significant, such as connectivity and retention.

Key point

An important gap in the research on climate change impacts on pelagic ecosystems is the study of the complexity of the physical changes resulting from climate change that might drive a biological/ecological response. Addressing this gap is at the core of this PhD work. More precisely, two main elements that need to be increasingly accounted for are i) the vertical dimension of the pelagic realm and ii) finer scale structures driving marine biodiversity distribution.

1.2 Objectives and structure of the thesis

The main objective of this thesis is to investigate climate change trends on ecologically significant variables and features, linking observed variability or trends to projected changes in climate models on a specific region: the Southern Indian Ocean (20-120°E, 70-30°S). As presented in the introduction, strong climate change impacts across the water column are expected, notably due to the important increase in ocean heat content observed at subantarctic latitudes these last decades, in a biodiversity-rich region with important conservation and fisheries issues. The following questions are investigated:

- How is climate change going to impact physical characteristics of ecological importance for pelagic ecosystems in the Southern Indian Ocean?
- How can we include this knowledge to guide conservation and fisheries management in the region?

The first question is addressed throughout Chapters 3, 4 and 5. In Chapter 3, we investigate what are the current and projected trends in warming and marine heatwaves in the Southern Indian Ocean. This chapter provides an overview of current knowledge on this region's warming trends and marine heatwaves characteristics, while confronting observations and climate models, allowing for a first characterisation of the spatial heterogeneity of climate change signal in this region. In Chapter 4, we then more specifically focus on the impacts of marine heatwaves and long-term global warming on an ecologically structuring water mass: the winter waters. The northernmost extent of the winter waters marks the position of the Polar Front, an important foraging hotspot for top predators. In Chapter 5, we investigate whether climate change could impact the local circulation, zooming over and around the Kerguelen Plateau where oceanic currents play an ecological role for Patagonian toothfish early-life stages transport and for the connectivity between stocks managed separately by France and Australia. Scientific perspectives are provided in Chapter 6 to further investigate the complexity of drivers of changes in the pelagic realm.

The second question is also addressed throughout the Chapters as all the studies were motivated to provide relevant information to policy-makers and through further "science and society" discussion points. Chapter 6 also addresses this question through a complementary work undertaken on the implications of climate change for the Patagonian toothfish fisheries management in the Southern Indian Ocean and through further reflection on the current hindrances to operationalize climate change awareness in biodiversity management.

Chapter 2

Data and methods

“Now is no time to think of what you do not have. Think of what you can do with what there is.”

Ernest Hemingway, The Old Man and the Sea

The study of the physical complexity of climate change impact-drivers requires a multi-data and multi-scale approach. The analyses are conducted using multiple datasets to explore the range of spatial and temporal scales that we can observe or model today. We consider different timescales to investigate different types of impacts and potential connections between extreme events on short timescales (days, weeks, months) and long-term trends (decades). Observations are useful to investigate both past variability and emerging trends, while climate models provide decadal trends in the future through projections under different scenario (Figure 2.1).

This chapter briefly introduces the different datasets used, from satellite and *in situ* observations to climate models. Further description of the products and of the specific analyses conducted are detailed in the material and method section of each main study.

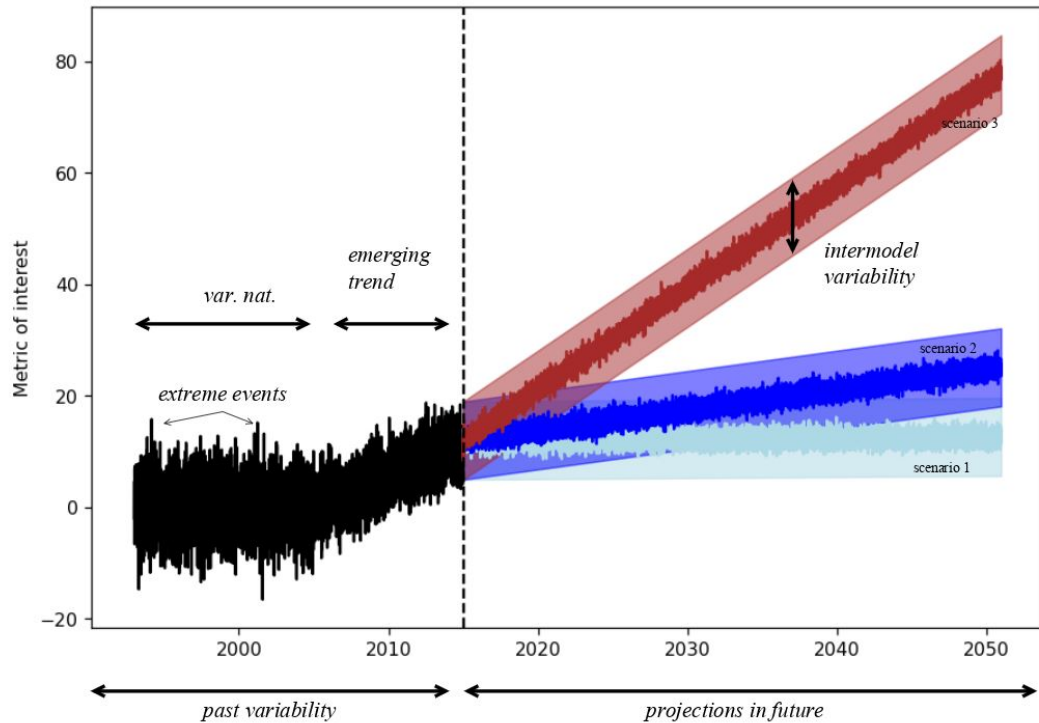


FIGURE 2.1: Schematic of our multi-scale approach, investigating both last decades variability and emerging trends and future projections under different emission scenarios.

2.1 Data

2.1.1 Satellite observations

Box. 2.1.1: Satellite observations

Satellite remote sensing relies on various technologies depending on the metric studied.

- Sea surface temperature is obtained from passive remote sensing using satellite infrared or microwave radiometers.
- Altimetry is active remote sensing based on the emission of radio waves and the time for the radar signal to reach the Earth and return to the satellite to estimate sea surface height.
- Satellite measures of chlorophyll concentrations are based on remote sensing reflectance (i.e. the ratio between water-leaving radiance and downwelling irradiance).

In each cases, multiple satellites and different interpolation algorithms are used to construct gridded products of those metrics, with finer resolutions over the years. Note that those products provide information on different parts of the water column. Altimetry-derived SSH is an equivalent depth-integrated value, responding to deep-reaching structures from below the mixed layer, whereas sea surface temperature and chlorophyll values derived from ocean colour are from the surface of the mixed layer only. Besides, because infrared and ocean colour measurements are affected by the presence of clouds, gridded products based on those data may have variable effective resolution over space and time.

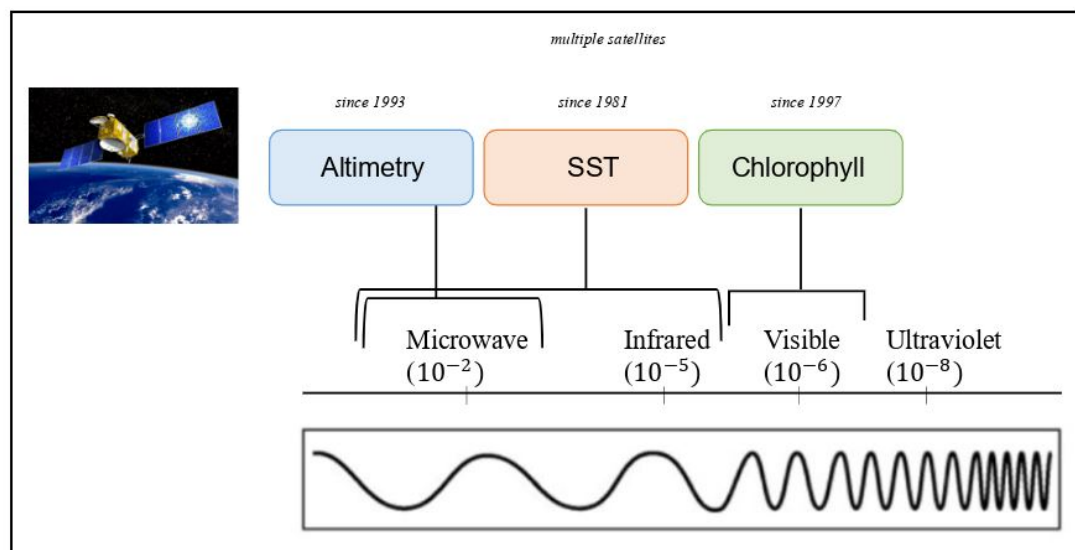


FIGURE 2.2: **Satellite observations relies on different technologies, targeting different wavelength depending on the metric studied.** A picture of [Jason-3](#) satellite used for altimetry is shown.

2.1.1.1 Altimetry

Altimetry is the method used to estimate the sea surface height from satellite emissions of a radar signal. Depending on the reference used to calculate the height, different metrics can be deduced, such as sea surface height or absolute dynamic topography. Geostrophic velocities can then be deduced from sea surface height by solving the geostrophic equations balancing the Coriolis and horizontal pressure gradient forces (Figure 2.3).

Altimetry-derived geostrophic velocities are computed by CLS/AVISO (Collecte Localisation Satellites/Archiving, Validation, and Interpretation of Satellite Oceanographic

data) and distributed by Copernicus Marine Environment Monitoring Service (CMEMS) as a gridded product on a $0.25^\circ \times 0.25^\circ$ horizontal grid resolution between 1993 and 2020 (<https://doi.org/10.48670/moi-00148>).

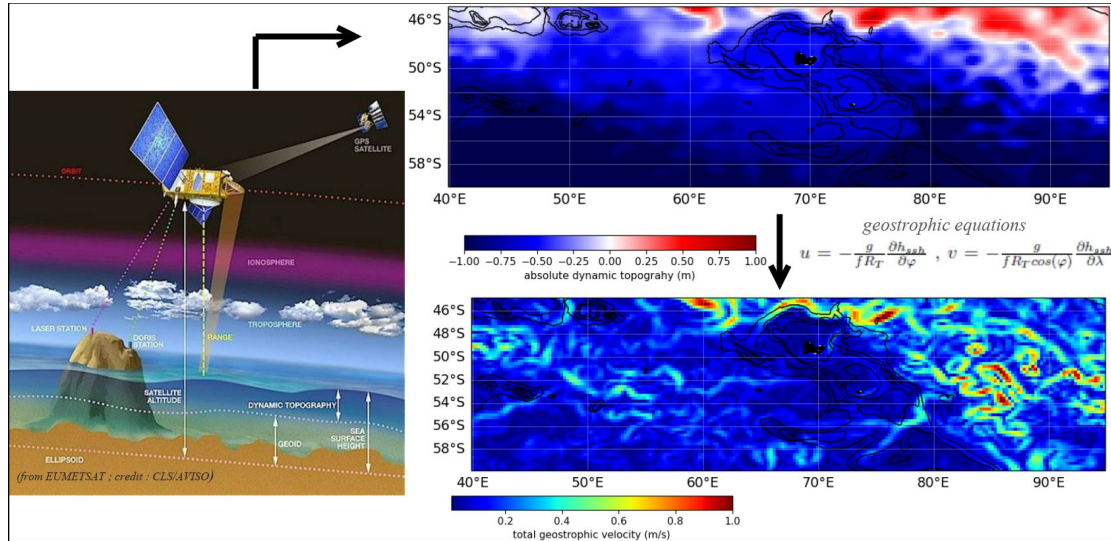


FIGURE 2.3: Different products are derived from satellite altimetry, for instance absolute dynamic topography, resulting from satellite sea surface height measurements, and geostrophic velocities derived from it (Picture on the left from EUMETSAT; credit CLS/AVISO; maps on the right are computed using AVISO products as illustrations).

2.1.1.2 Sea surface temperature

Multiple sea surface temperature products derived from satellite observations are available. Many products now integrate both satellite and *in situ* observations to improve the spatial resolution and accuracy of the products.

- **The Operational Sea Surface Temperature and Ice Analysis (OSTIA)** system run by the UK's Met Office (Good et al., 2020) provides daily sea surface temperature free of diurnal variability, also called the foundation sea surface temperature, at a $0.05^\circ \times 0.05^\circ$ horizontal grid resolution between 1982 and 2019. This product combines satellite measurements (L4 level) from both infrared and microwave radiometers with *in situ* measures from ships, drifting and moored buoys.
- **NOAA Daily Optimal Interpolation SST (OISST) v2.1** dataset provides SST with a resolution of $0.25^\circ \times 0.25^\circ$ from 1981 to present. It also consists in a combination of *in situ* and satellite observations. Satellite observations include

data from NOAA/AVHRR and MEtOp/AVHRR, while *in situ* observations consists in ICOADS dataset mostly to correct residual satellite SST biases (Reynolds et al., 2002, 2007; Banzon et al., 2016).

- **Hadley Centre Global Sea Ice and Sea Surface Temperature (HadISST)** dataset provides fields of SST with a resolution of $1^\circ \times 1^\circ$ from 1871 to present (Rayner et al., 2003). This dataset uses interpolation methods applied to SST data from the Marine Data Bank and ICOADS until 1981 and then a combination of satellite and *in situ* data from 1982 to present. However, this dataset can be limited in polar regions due to limited data inputs.

Differences between those SST products have been observed at high latitudes and may be due to several factors such as the interpolation methodology or which products are integrated (Yang et al., 2021).

2.1.1.3 Chlorophyll

Satellite observations of surface chlorophyll-a concentrations are provided by ACRI-ST company and based on the Copernicus-GlobColour processor (Level 4, <https://doi.org/10.48670/moi-00281>). The daily and monthly products are the combinations of outputs from SeaWiFS, MODIS, MERIS, VIIRS-SNPP and JPSS1 and OLCI-S3A and S3B sensors (Garnesson et al., 2019). The spatial resolution is 4 km and data is available from 1997 to present.

Chlorophyll satellite observations rely on reflectance measures in the visible spectrum which is sensitive to cloud coverage. Due to the high cloud coverage at high latitudes, especially over the Southern ocean in winter, chlorophyll data over this season is less reliable.

2.1.2 *In situ* data

- **Argo hydrographic profiles**

The Argo program, which is part of the Global Climate Observing System and the Global Ocean Observing System OceanView (GCOS, GOOS), provides local *in situ* temperature and salinity data through autonomous floats spread across

the globe (Argo, 2000). The Argo program was created in 1999 and is today the dominant source of subsurface data globally. Argo floats work based on 10-day cycle, where they repeatedly dive down to 1000 m and 2000 m before rising up to the surface to transmit the collected data to satellites.

We download 170 352 profiles over the area 20-120°E 70-30°S between 2001 and 2019. Among those profiles, 78 407 are complete between 5 and 900 m and are used in Chapter 4 to analyze marine heatwaves subsurface signal.

- **Elephant seal hydrographic profiles**

The Marine Mammals Exploring the Oceans Pole to Pole or MEOP consortium gathers the data collected from various national programs to produce a public quality-controlled database of 3D oceanographic data obtained from biologging in Polar regions (Treasure et al., 2017; Roquet et al., 2014).

MEOP-CTD database gathers temperature and salinity profiles since 2004, notably through elephant seals biologging in the Southern Ocean. These predators can dive down to 1000 m deep which provide information over the whole water column. We download 140 436 of those profiles available between 2004 and 2017 over 20-120°E 70:30°S Among those profiles, 9 484 are complete between 5 and 900 m and are used in Chapter 4 to analyze marine heatwaves subsurface signal, complementing the use of Argo data.

The spatial coverage of these two datasets are complementary. Indeed, Argo floats have global large-scale coverage and are nominally separated by 300 km while elephant seals only observe along their pathways, but at fine scales with ultra-high spatial and temporal resolution (multiple profiles per day separated by a few km). In addition, Argo floats are widely spread over the Southern Indian Ocean but less over the Kerguelen Plateau due to its shallow bathymetry. On the contrary, elephant seals sample largely over the Plateau (Figure 2.4 A and B). We also note that, for both datasets, the number of profiles varies over the years (Figure 2.4 C and D). Sampling through MEOP dataset is also higher after elephant seals moulting season (January-August), which could be linked to the animals' accessibility for researchers (Figures 2.4 E). No seasonal bias is observed in the Argo data available.

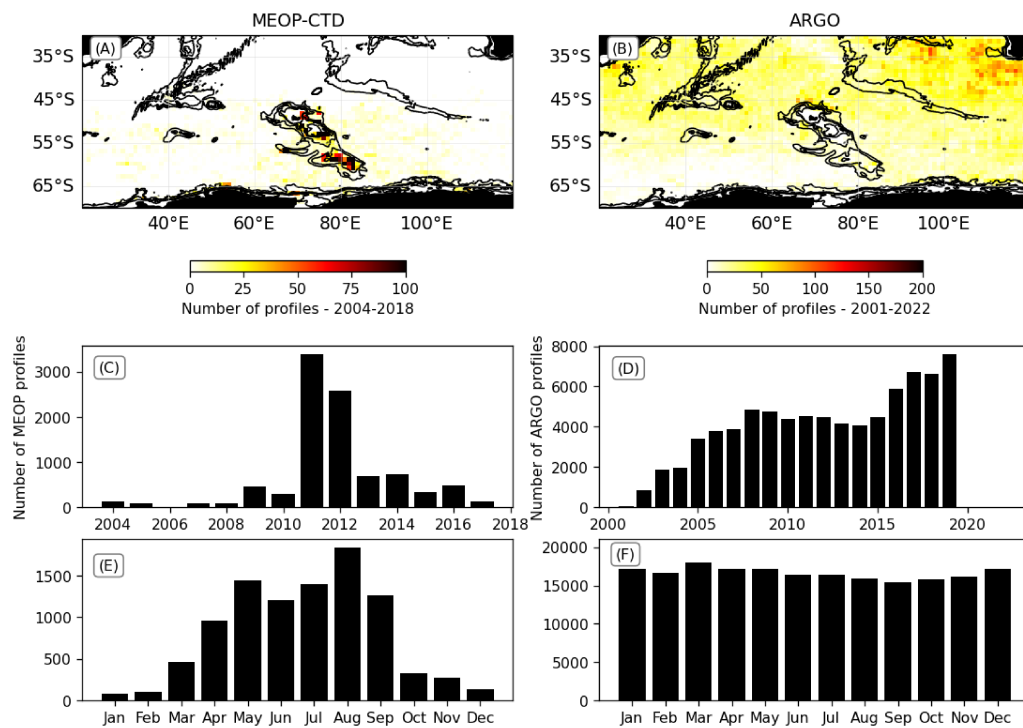


FIGURE 2.4: **Spatial (A-B) and temporal distributions of MEOP-CTD (left panels) and Argo (right panels) hydrographic profiles complete down to 900 m in the Southern Indian Ocean. Number of hydrographic profiles in this region per year (C-D) and per month (E-F) are shown.**

2.1.3 Reanalyses products

- **GLORYS12V1** product is the CMEMS global ocean eddy-resolving reanalysis, also referred as MERCATOR reanalysis. This product provides daily and monthly mean temperature over 50 vertical levels and with $1/12^\circ$ horizontal resolution between 1993 and 2019.

Evaluations of this reanalysis indicate a realistic mesoscale representation, with the global pattern of regional trends of sea surface height being in good agreement with altimetric data (Lellouche et al., 2018a,b) but also with encouraging results for monitoring the regional variability of the Antarctic Circumpolar Current (Artana et al., 2021), as well as regarding sea ice concentration budget (Nie et al., 2022). This product is used in Chapter 4 to provide a monthly climatology for the vertical temperature profiles and to determine the impact of marine heatwaves (MHWs) on winter waters (WWs).

- **ERA5** combines model data with worldwide observations being consistent with the laws of physics and provides hourly and monthly data from 1940 to 5 days behind real time, with a horizontal grid of $0.25^\circ \times 0.25^\circ$ for the atmosphere and $0.5^\circ \times 0.5^\circ$ for ocean waves (Hersbach et al., 2023). To produce outputs on surface wind characteristics, ERA5 integrates different satellite scatterometer data such as AMI (ERS1 and ERS2), ASCAT (MetOp-A/B), OSCAT (OCEANSAT-2), and SeaWinds (QuikSCAT). This product is used in Chapter 5 to compute total wind stress τ between 1993 and 2019 from the mean eastward and northward turbulent surface stress :

$$\tau = \sqrt{\tau_x^2 + \tau_y^2} \quad (2.1)$$

where τ_x and τ_y are respectively the mean eastward and northward turbulent surface stress in $N.m^{-2}$, calculated by the ECMWF Integrated Forecasting System's turbulent diffusion and turbulent orographic form drag schemes.

Note that the effective resolution of these reanalysis products are 6 to 7 times the grid resolution.

2.1.4 CMIP 6 models

The Coupled Model Intercomparison Project 6 (CMIP6) is the most recent phase of a global effort to improve global climate modelling, for the past and historical periods as well as for projections. The CMIP allows to investigate natural or anthropogenic changes using a multi-model approach.

Box. 2.1.2: Climate models

A coupled climate model simulates the atmosphere, the ocean, the cryosphere, the land surface, the vegetation on land and the ocean biogeochemistry (Figure 2.5 A). It computes the solution to differential equations of fluid motion and thermodynamics for each grid cells of its components to estimate time and space dependent values of key variables such as temperature or wind. An Earth System Model (ESM) is a coupled climate model that also explicitly models the movement of carbon through the earth system, closing the carbon cycle.

Different models exist, making different hypotheses to simulate those various and complex components. Around 49 climate modelling groups in the world provide

simulations from climate models. The Coupled Model Intercomparison Project (CMIP) was started in 1995 under the supervision of Working Group on Coupled Modelling (WGCM). This coordinated effort was used to develop common experiments and sets of scenarios to compare the different models outputs and projected changes.

Historical and projection simulations from the ScenarioMIP experiments are used in this PhD work. Historical simulations cover the period 1850–2014 and use historical forcing, mostly based on observations, that includes among others greenhouse gas, aerosol concentrations and solar forcing (Eyring et al., 2016). Projection simulations from the ScenarioMIP experiments extend over 2015–2100 and have been conducted under multiple emission trajectories, described through so-called Shared Socioeconomic Pathways (SSPs).

Different SSPs are considered throughout this PhD work. SSPs have been introduced in the CMIP6 exercise to outline various development trajectories based on distinct economic and political strategies (O’Neill et al. (2016) ; Figure 2.5 B), and subsequent forcing levels similar to the ones used in CMIP5, that are the Representative Concentration Pathways (RCPs). The SSP 1-2.6 represents a scenario in which the world shifts to a more sustainable path leading to an estimated warming of 1.8 °C by the end of the century (strong mitigation scenario). SSP 2-4.5 represents a path in which socioeconomic trends do not shift significantly from the historical patterns, with an estimated warming of 2.7 °C by the end of the century (modest mitigation scenario). SSP5-8.5 describes a world with no mitigation policies, leading to an estimated warming of 4.4°C by the end of the century (no mitigation scenario; Lee et al. (2021)). Through the examination of distinct scenarios, we can assess and compare potential future outcomes that will be contingent upon the commitment of countries to decrease their greenhouse gas emissions (Hausfather and Peters, 2020). Scenarios can also be used to test hypotheses, for instance on the reversibility of changes using “overshoot” scenarios. SSP5-3.4OS is considered as an “overshoot” scenario since the emission trajectory followed is the same as SSP5-8.5 from 2015 up to 2040 and then very strong mitigation is undertaken to rapidly reduce emissions to zero by around 2070 (O’Neill et al., 2016).

Across this PhD thesis, multiple models are used. Each model output is regridded to

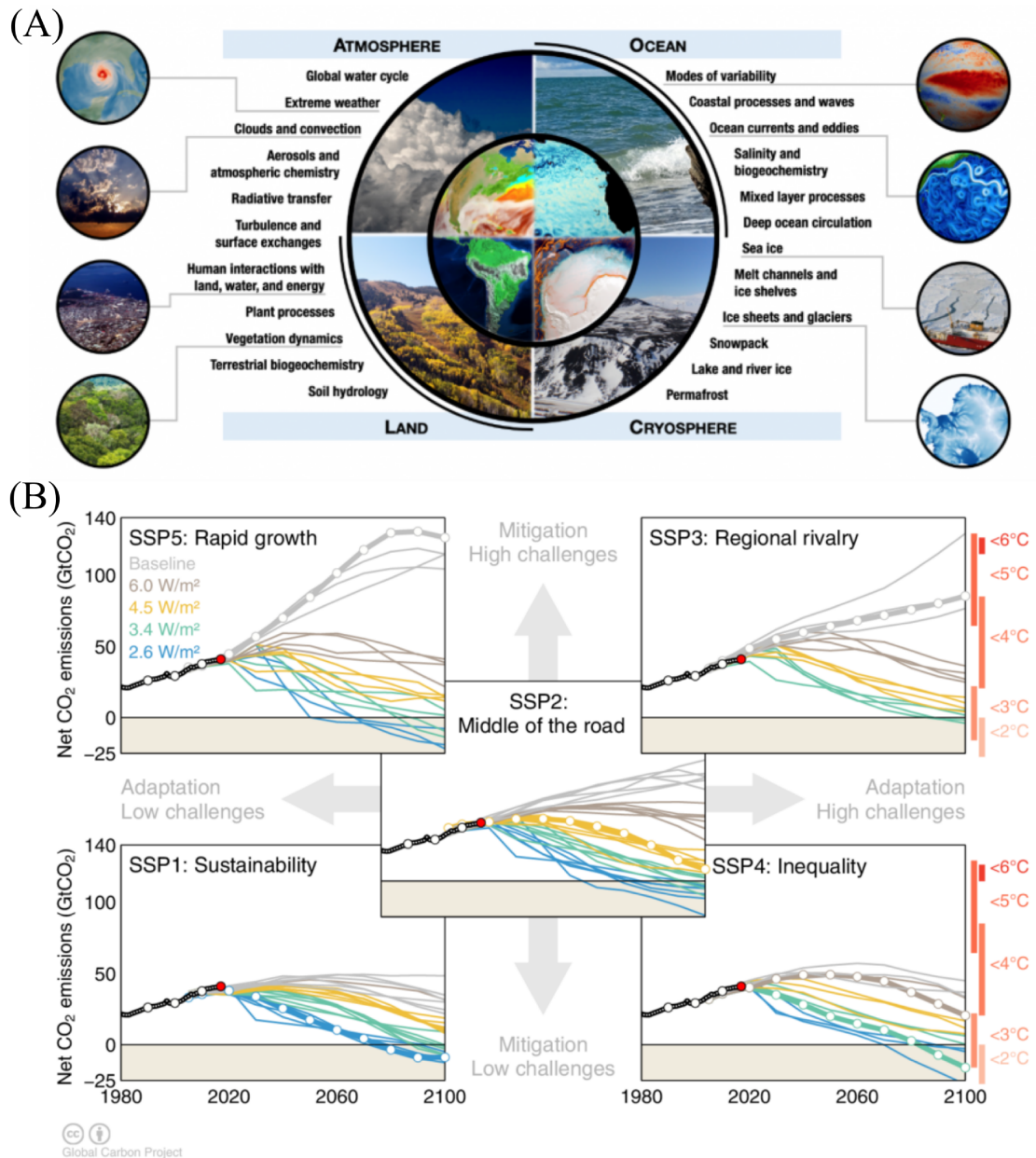


FIGURE 2.5: **Schematic of climate models components and Shared-Socioeconomic Pathways.** (A) Climate models components (Image courtesy of Paul Ullrich, University of California, Davis) (B) Global CO₂ emissions (GtCO₂) for various integrated assessment models runs in the Shared-Socioeconomic Pathways (SSP) database for each SSP. Chart via Glen Peters and Robbie Andrews and the Global Carbon Project.

the same regular $1^{\circ} \times 1^{\circ}$ horizontal grid using distance weighted average remapping (climate data operators; remapdis) as in Kwiatkowski et al. (2020). Each model output is also, when relevant, regridded vertically following the World Ocean Atlas standard (33 standardised vertical intervals from the surface (0 m) to the abyssal seafloor (5500 m)). Throughout this PhD work, different variables have been investigated, notably : *thetao* (sea temperature across different depth levels), *tos* (sea surface temperature at

the surface for the detection of marine heatwaves, as only *tos* was available daily), and *tauu* and *tauv* (the longitudinal and latitudinal components of the wind stress).

There are several ways to combine the results from multiple models. The traditional approach used by the IPCC, which is the main method used here, is to use a model ensemble mean, all models being weighted equally, and then to study the projections for fixed future periods (Figure 2.6 A). Future periods of 20 years are considered: the near term (2021–2040), the mid term (2041–2060) and the long term (2081–2100) as in the IPCC Assessment Report 6 (Chen et al., 2021). An alternative method is also considered to further support the projected trends obtained with the traditional method: the “time-shift approach” (Herger et al. (2015); Chen et al. (2021); Lee et al. (2021); Figure 2.6 B). Instead of specifying a fixed time period, this approach specifies a fixed global warming value compared to pre-industrial, typically 1.5°C, 2°C and 3°C (hereafter referred to as global warming levels or GWL 1.5°C, 2°C and 3°C, respectively). These GWLs are in general reached at different time periods depending on the models and on the scenarios. This method allows to account for the different climate sensitivities of the models and facilitates the comparison between global warming and regional spatial patterns. For each model and under each SSP, warming levels are defined as 20-year running means of globally averaged atmospheric surface temperature anomaly compared to the pre-industrial period (1850–1900). Then the change in a given metric is estimated using a climatology of 20 years centred on the first year for which the warming level exceeded a given threshold (e.g., 1.5°C), relative to the 1850–1900 reference value. These results are then averaged over the model ensemble and over the SSPs considered, all simulations being weighted equally.

Key point

The datasets used in this thesis provide complementary insights on the ocean variability and trends through different temporal and spatial sampling resolutions and methodologies: from coarse resolution models to precise but punctual *in situ* observations (Figure 2.7 A). Observations and model reanalyses are now available over a few decades, allowing for the analyses of climate trends (Figure 2.7 B). Climate models can be used to investigate different possible futures.

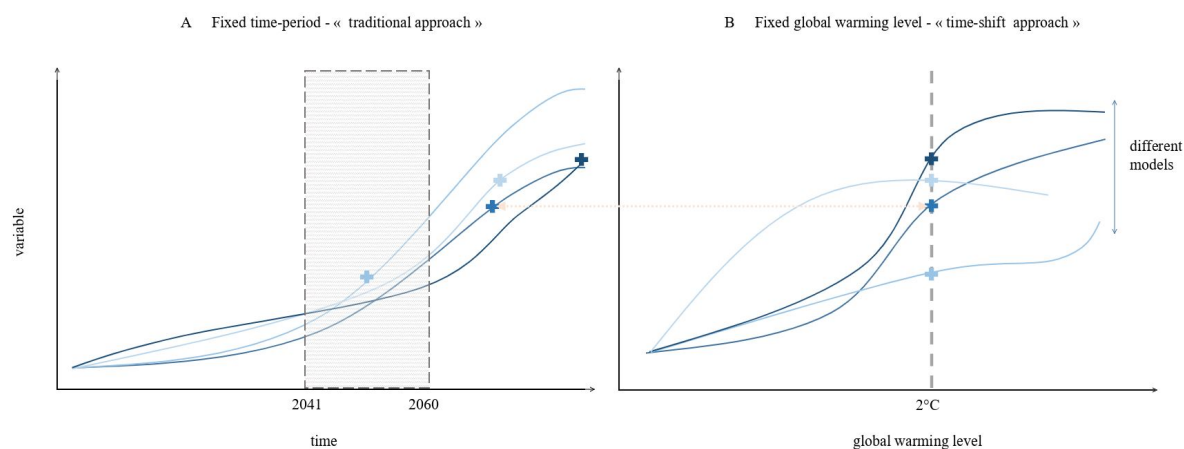


FIGURE 2.6: **Schematic of the different approaches to combine climate models' outputs**, illustrating (A) the “traditional approach”, averaging multiple models over a fixed period of time (e.g. 2041-2060) and (B) the “time-shift approach”, averaging multiple models over a given global warming threshold reached (e.g. 2°C). The crosses highlight that the values of the variable of interest for a given global warming level can correspond to different time periods across the models, as models reach global warming levels at different rates.

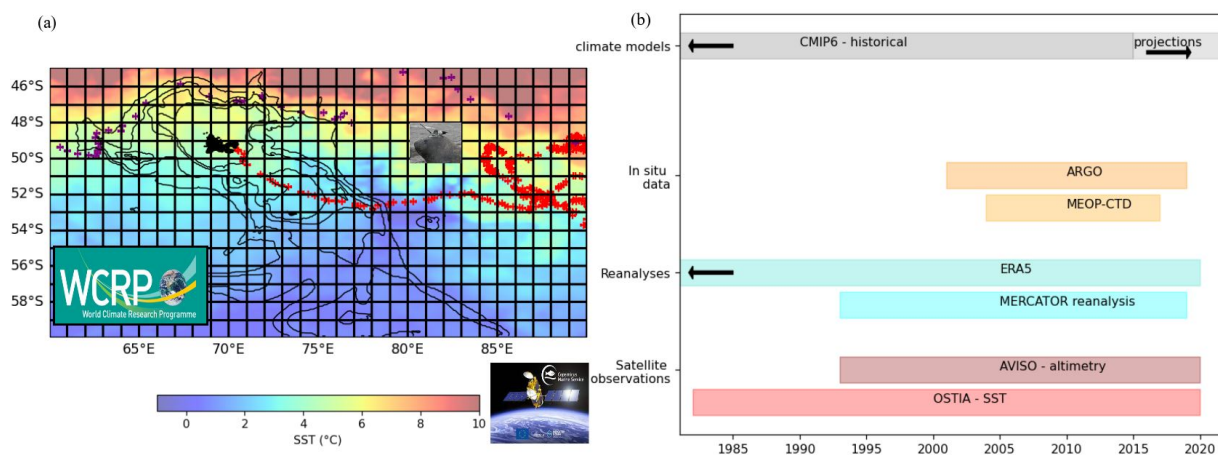


FIGURE 2.7: **Spatial and temporal complementarity of the datasets used in this PhD thesis.** (a) Schematic illustrating different datasets spatial resolution: sea surface temperature from OSTIA dataset at $0.05^\circ \times 0.05^\circ$ (colormap), climate models grid of $1^\circ \times 1^\circ$ (black grid) and punctual in situ observations from Argo (purple crosses) or MEOP (red crosses) datasets. The elephant seal picture was taken from the [MEOP website](#). (b) Temporal extent/availability of the different datasets used in this PhD work. Arrows indicate that the temporal extent of some datasets is larger than shown here. Climate models extend from 1850 to 2100 and ERA5 reanalysis starts in 1940.

Box. 2.1.3: Data availability

All the data used in this PhD work is publicly available. OSTIA, Copernicus-GlobColour, AVISO and MERCATOR reanalysis products are distributed by Copernicus Marine Service and therefore available at <https://marine>.

copernicus.eu/. NOAA OI SST V2 High Resolution dataset provided by the NOAA PSL is available from their website at <https://psl.noaa.gov>. Argo data is available at https://www.usgodae.org/cgi-bin/argo_select.pl and MEOP dataset is available at <http://www.meop.net>. ERA5 outputs are available at <https://cds.climate.copernicus.eu/cdsapp#!/dataset/reanalysis-era5-single-levels?tab=form>. CMIP6 models outputs are available at: <https://esgf-node.llnl.gov/projects/cmip6/>.

2.2 Methods

2.2.1 Computing climate velocity

Climate velocity is defined as the ratio between the temporal trend and the local spatial gradient of a variable (Loarie et al., 2009). In this study we focus on temperature (T) and therefore define the intensity of the horizontal climate velocity v as:

$$v = -\frac{\frac{\partial T}{\partial t}}{\|\nabla T\|^2} \quad (2.2)$$

By convention, v is positive in case of a warming and negative in case of a cooling. The climate velocity vector \vec{v} is then defined as:

$$\vec{v} = -\frac{\partial T}{\partial t} \left[\frac{\frac{\partial T}{\partial x}}{\|\nabla T\|^2} \cdot \vec{u}_x + \frac{\frac{\partial T}{\partial y}}{\|\nabla T\|^2} \cdot \vec{u}_y \right] \quad (2.3)$$

By convention, \vec{u}_x is positive eastward and \vec{u}_y is positive northward. \vec{v} points the direction to follow to remain in the same temperature conditions.

For all types of data, yearly means are used to estimate the warming rate and the spatial gradient is estimated using the mean data over the whole period of interest, with the assumption that the latitudinal pattern will not dramatically change in order to smooth potential spatial patterns due to inter-annual variability.

For CMIP6 outputs, climate velocity is estimated over the historical period (1850-2009) and then over future periods according to different scenarios (in between 2015 and 2100). Climate velocity is estimated for different depth layers : surface (0-200 m) and

mesopelagic (200-1000 m). We use the weighted average of the outputs over the depth layer to calculate a horizontal climate velocity. The climate velocities obtained from each model are then averaged, using an equal weighting for all models.

2.2.2 Detecting marine heatwaves

2.2.2.1 Definition

The definition of Hobday et al., 2016 of marine heatwaves (MHWs) as “discrete prolonged anomalously warm water event” is used (Hobday et al., 2016) to allow for comparison with other studies increasingly adopting this standardised definition. A MHW occurs when the temperature is above a threshold during at least 5 days (Figure 2.8 A). This threshold is defined as the 90th percentile of the data distribution. The climatology and threshold are estimated for each grid point of the region of interest and for each day of the year with an 11-day window and the threshold is also smoothed by applying a 31-day moving average. The climatology is estimated over at least 30 years of data, allowing to take into account low frequency climate mode of variability (e.g. ENSO, AMO) which can impact the development of MHWs (Scannell et al., 2016). These events can then be described by different metrics. The annual number of days affected by MHW and the mean intensity or cumulative intensity of events are particularly relevant to then estimate the ecosystems’ exposure to these extreme events.

2.2.2.2 Marine heatwaves subsurface characteristics

Although marine ecosystems can depend on environmental conditions at depth, MHWs are usually studied at the surface. This shortcoming may be explained by the lack of *in situ* daily data at depth, but it is important to consider MHWs over the whole water column to fully understand their impacts on pelagic and even benthic communities (Smale et al., 2017, 2019). For instance, the Patagonian toothfish, which represents important economic value for the French fisheries, can live at various depths at the different steps of its life cycle and juvenile recruitment may be sensitive to spawning temperature conditions (Belchier and Collins, 2008). There is therefore an increasing interest to study marine heatwaves penetration in subsurface waters at a regional scale

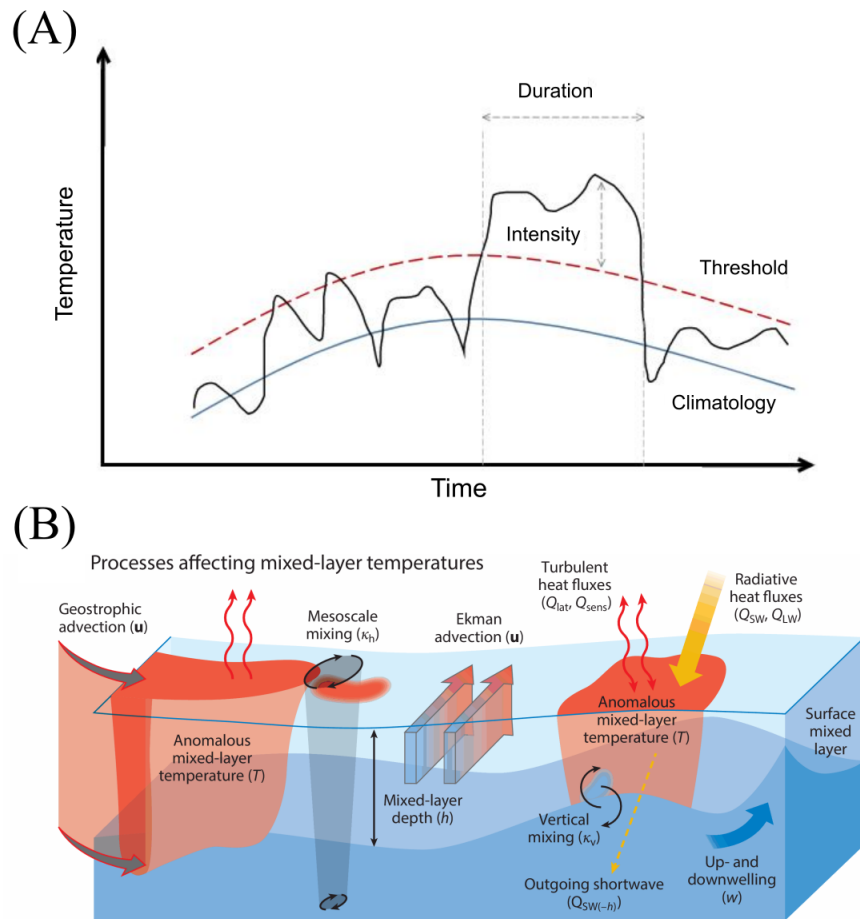


FIGURE 2.8: **Marine heatwaves (MHW) definition and associated physical processes.** (A) Schematic illustrating the definition of marine heatwaves and the main metrics used in this PhD work: mean MHW intensity and duration. (B) Figure from [Oliver et al. \(2021\)](#) illustrating the relevant physical processes in a mixed-layer temperature budget that could be associated with a MHW.

(e.g. [Schaeffer and Roughan \(2017\)](#); [Elzahaby and Schaeffer \(2019\)](#); [Darmaraki et al. \(2019\)](#); [Hu et al. \(2021\)](#); [Miyama et al. \(2021\)](#); [Su et al. \(2021\)](#); [Juza et al. \(2022\)](#)).

In this PhD thesis, metrics to investigate MHWs subsurface characteristics are estimated, such as the cumulative temperature anomaly (CTa) and the temperature anomaly depth (also called “MHW depth” in [Elzahaby and Schaeffer \(2019\)](#)). These metrics require the computation of an anomaly profile between an *in situ* temperature profile (e.g. Argo or MEOP hydrographic profile) and a reference (e.g. MERCATOR reanalysis, example on [Figure 2.9](#)). The use of MERCATOR reanalysis as a reference (for more details on the methodology see [Chapter 4 Section 4.2](#)) is based on the product quality over the Southern Ocean ([Section 2.1.3](#)), validation against reference estimated using Argo or MEOP data where possible and because the final aim of the analyses here is a relative and not absolute comparison of the metrics between MHW and non-MHW cases. CTa is

the sum of temperature anomalies down to the depth at which the temperature anomaly is no longer positive (Z_n ; Figure 2.9). CTa is then used to calculate the temperature anomaly depth:

$$TA_{depth} = \text{Max}(z(CTa(z) \leq 0.95 \times CTa(Z_n))) \quad (2.4)$$

This metric is calculated both for hydrographic profiles in a MHW and outside a MHW, to distinguish the part of the anomaly which is indeed due to the MHW and the part that may be either due to a bias in the reference (here MERCATOR reanalysis), compared to *in situ* observations, or due to a surface temperature anomaly that did not last more than five days (MHW definition).

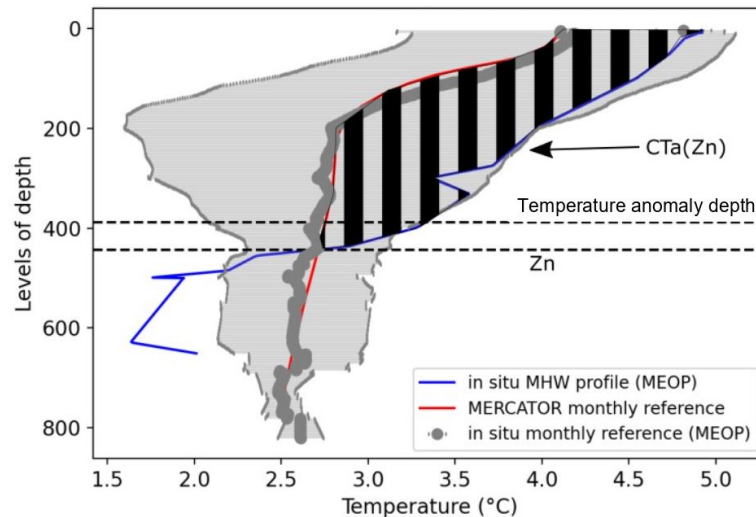


FIGURE 2.9: **Definition of temperature anomaly depth and cumulative temperature anomaly**, applied to an example at 88°E 52°S on 2016/12/05. $CTa(Z_n)$ is the sum of temperature anomalies down to the depth at which the temperature anomaly is no longer positive (Z_n) and is represented here by the hatched area (black bands) between the reference profiles and the *in situ* profile in blue. The temperature anomaly depth as defined by equation 2.4 is also indicated.

2.2.3 Lagrangian analyses

The Lagrangian approach consists in studying individuals particles along their trajectory in contrast to studying physical characteristics at a fixed point (Eulerian approach). To generate water parcels trajectories, the 2D geostrophic velocity fields derived from satellite altimetry are linearly interpolated in time (step of 4h) and space (resolution of 0.05°). The integration in time of the velocity field is conducted using a Runge-Kutta

integrator of order four (Press and Teukolsky, 1992). Trajectories of water parcels can be reconstructed forward or backward in time. Those analyses are conducted using the Lagrangian Manifolds Tracking Algorithm (LAMTA) python code developed with support from LOCEAN-IPSL and CNES (Rousselet et al., in preparation).

Trajectories are then used to compute other metrics depending on the research question (Figure 2.10). In Chapter 4, we aim at determining the origin of water masses associated with MHWs. The latitudinal advection of water parcels 15 days backward in time (around the average duration of a MHW) is estimated. A monthly climatology of latitudinal displacement is then determined over multiple years (1993-2020). Pearson correlations between anomalies of latitudinal displacement and the presence/absence of MHW are evaluated using the complete time series (1993-2020). To assess the significance of the Pearson correlation coefficients obtained, the associated p-value is calculated (significant if p-value < 0.05). In addition, to assess the robustness of the pattern and the coefficients obtained, the same analysis is conducted using randomly associated maps of anomalies of latitudinal displacement and maps of MHW presence/absence (so-called bootstrap approach).

In Chapter 5, a Lagrangian approach is used to investigate physical connectivity over the Kerguelen Plateau. This analysis is based on the Kerguelen Plateau's division in sub-areas. We compute the forward trajectories of water parcels, as described above, and we estimate the probability of transport from one sub-area to another (connectivity) or the probability to remain in the same sub-area (retention). This study is motivated by the ocean circulation role in Patagonian toothfish early-life stages transport, that is why forward advections are conducted over 91 days (around 3 months which is the duration of the egg phase), for each day between June 1st and October 31st (Patagonian toothfish spawning period; Collins et al. (2010)), each year between 1993 and 2019.

A complementary analysis is also conducted using backward advections from the sub-area east of Kerguelen, to investigate whether a similar interannual variability is observed accounting for all the trajectories (and not just the initial and final positions). Backward advections are conducted over 91 days, for each day between the 31st of August to the 30th of January, each year between 1993 and 2019 using the same equations as the forward advections described above. We define a particle density for each grid cell as the number of crossings of water parcels over a grid cell, here on a $0.25^\circ \times 0.25^\circ$ grid,

accounting for all the 91-days backward in time trajectories from a given day, to identify main transport pathways (similar notion as the “crossroadness” introduced in [Baudena et al. \(2019\)](#)). The average particle density for each year is then used to investigate the interannual variability of the transport pathways arriving to the east of Kerguelen. The interannual variability is only studied here for grid cells where the mean particle density is higher than 50% of the overall mean value, in order to focus the interpretation on the main pathways.

There are some limitations to the method used here. First, this approach neglects the integrated effect of vertical velocities, assuming that it is not strong enough to shift the trajectory below the mixed layer ([Sulman et al., 2013](#)). Second, the velocity field used is derived from altimetry observations which are also associated with approximations. Altimetry is mostly based on nadir along-track observations which are interpolated in space and time ([Traon et al., 1998](#); [Pascual et al., 2006](#)) which tends to make mesoscale structures rounder and smoother than they might be in reality or even smooth out mesoscale structures smaller than 70 km ([Xu and Fu, 2012](#)). Ageostrophic currents and Ekman transport are also neglected with this approach. However, this method has already been tested in the Kerguelen Plateau area. Lagrangian physical structures using geostrophic velocities have been successfully compared to the distribution of biogeochemical tracers (e.g. iron, chlorophyll; [d’Ovidio et al. \(2015\)](#); [Della Penna et al. \(2018\)](#)). Besides, it has been shown, using a $1/80^\circ$ model, that the vertical transport does not play an important role in driving tracers over the Kerguelen Plateau ([Rosso et al., 2014](#)).

2.2.4 Detecting winter waters and the Polar Front position

In the Southern Ocean, the Antarctic Circumpolar Current (ACC) is associated to a system of fronts ([Box 1.1.1](#)). Fronts commonly refers to boundaries between different water masses, but fronts can have multiple definitions ([Chapman et al. \(2020\)](#); [Box 1.1.5](#)). Commonly used definitions are based on gradient thresholds, for instance using sea surface temperature (SST) or sea surface height (SSH) gradients ; other definitions are based on a specific value of SST or SSH. The climatological position of the ACC fronts based on contours of the mean dynamic topography of Centre National d’Etudes Spatiales-Collect Localisation Satellites 2018 (CNES-CLS18) can be useful to provide a description of the region ([Park and Durand, 2019](#)).

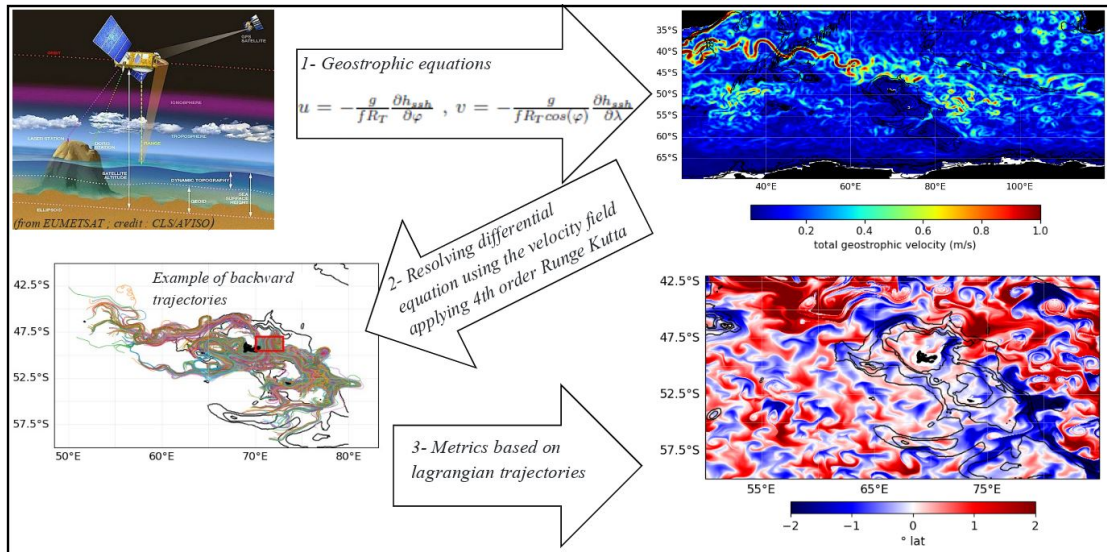


FIGURE 2.10: **Schematic illustrating the use of altimetry data to conduct Lagrangian analyses.** First, geostrophic velocities are derived from altimetry observations (computation by CLS/AVISO). Second, Lagrangian trajectories are computed from the geostrophic velocity field applying a Runge-Kutta integrator of order four. Third, from these trajectories, several metrics can be computed such as the latitudinal advection shown here on the bottom right panel. On this latter panel, the latitudinal advection over the last 15 days is shown for a given day as an example. The latitudinal advection is here negative if the water parcel was further south 15 days backward in time.

It has been shown that jets and hydrographic fronts are often collocated (Sokolov and Rintoul, 2002). However, this observation is not consistently confirmed and has resulted in varying interpretations regarding a possible shift of the ACC fronts (Meredith et al., 2019). Indeed, different definitions may not always align and therefore the definition used will depend on the scientific question (Chapman et al., 2020). In addition, in the context of climate change, the definitions based on temperature values for instance may no longer be relevant as the ocean warms but physical characteristics of fronts may persist.

The Polar Front plays a key role for the foraging ecology of top predators, notably as it marks the northernmost extension of the WWs which facilitate prey access (Pakhomov et al., 1994; Charrassin and Bost, 2001; Scheffer et al., 2012; McMahon et al., 2019). We therefore focus on this water mass based definition of the Polar Front to investigate climate change impacts on its characteristics.

2.2.4.1 Winter waters detection

WWs are detected through the presence of a subsurface temperature minimum between 100 and 400 m (Figure 2.11). GLORYS12V1 product is used to compute a daily and spatially continuous detection of WWs according to this definition, which enables the computation of the WWs probability of presence between 1993 and 2019. This probability is estimated by detecting, for each day between 1993 and 2019 and for each grid cell, whether the minimum temperature between 100 and 400 m is found at a depth less than 350 m, and then averaging the results (0 for absence of a temperature minimum in this interval, 1 for presence) over time. WWs are also characterized by the temperature at the minimum (also named WW temperature) and the depth of this minimum (also named WW depth), as in Sabu et al. (2020) (Figure 2.11). The same definition is applied to investigate projected changes in WWs characteristics in CMIP6 models in Chapter 4.

Other methods to detect WWs were considered. One of the approaches was based on a mechanistic understanding of WWs formation, by first identifying, for each grid point, the pycnocline for the deepest winter mixed layer and then determining the depth of this mixed layer in summer, as in Giddy et al. (2023). However, this definition appears to be less robust near the Polar Front (Giddy et al., 2023), which is the area of interest for our study. In addition, the shape of vertical profiles can be used to estimate the distance of *in situ* hydrographic profiles locations to the Polar Front, which is described in the following sub-section.

2.2.4.2 Decomposition of the thermohaline structure

Directly detecting WWs presence/absence, as described above, using *in situ* profiles is challenging due to the signal noise. To categorize the vertical structure of the temperature and salinity profiles with space and time as sampling dimensions, the method used here is similar to the one introduced by Pauthenet et al. (2017) for decomposing the thermohaline structure using a functional principal component analysis approach (R code available here: <https://github.com/EPauthenet/fda.oce> from Pauthenet et al. (2017); in this study the same approach is done in python).

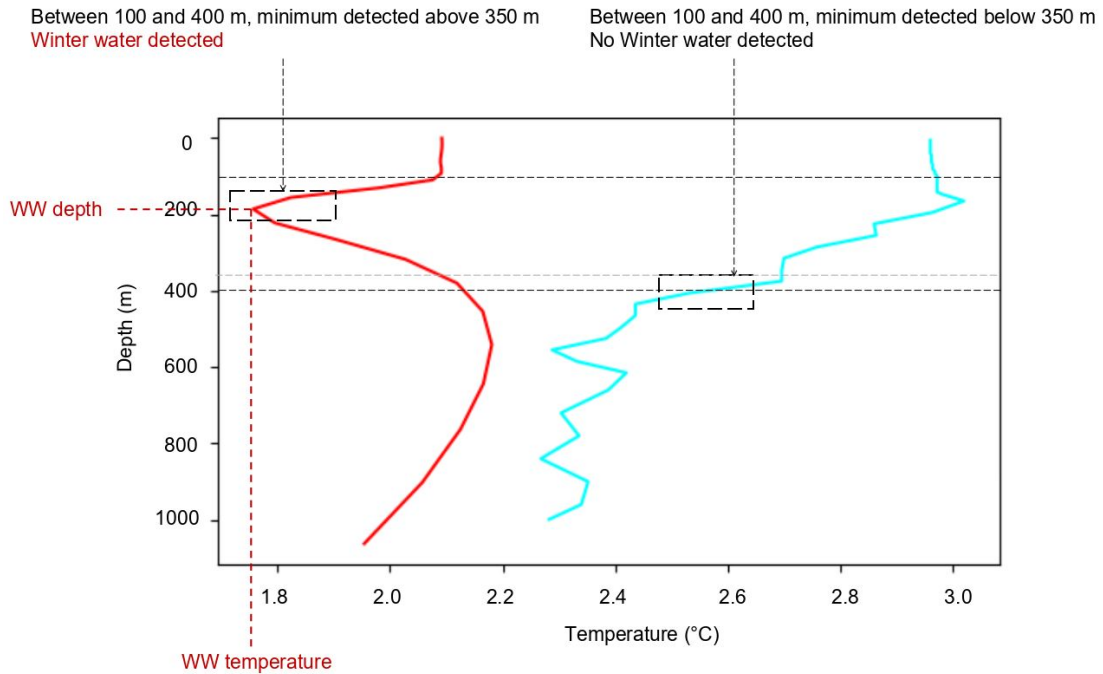


FIGURE 2.11: **Winter water (WW) detection based on temperature profiles.** Two cases are shown: in red where winter water occurrence is detected - in that case the winter water depth and temperature can be defined - and in cyan where it is not.

This analysis is conducted in Chapter 4 as supplementary material (Appendix B), using 30192 MEOP-CTD profiles and 18848 Argo profiles that are complete down to 400 m deep over 20-120°E and 58-40°S. In both datasets, around 8% of the profiles are found during a MHW.

First, the hydrographic profiles are transformed using B-splines functions. Elephant seals' hydrographic profiles have already been interpolated to fit a vertical grid of 1000 m deep with 1 m interval, but not all profiles contain data down to 1000 m. To use the maximum of profiles and because WWs signal is generally defined as a temperature minimum around 200 m, we chose to focus the analysis on profiles down to 400 m. For consistency, we interpolate Argo profiles to a vertical grid of 1000 m deep and also focus the analysis on profiles down to 400 m. Since B-splines are polynomial segments, the choice of the number of segments controls how much the profiles are smoothed. We choose $K=20$ since the focus is on the first 400 m and it was sufficient to capture the winter water signal. The profiles can be projected on the B-spline basis

Then, a functional principal component analysis (FPCA) is conducted on the profiles projections on the B spline basis. The aim of a FPCA is to determine the dominant modes of variation of functional data. Because we investigate temperature and salinity

variations simultaneously, we use a table with twice the 20 coefficients for each observation, and ensure that the same functional transformation is conducted on temperature and salinity profiles. The FPCA is equivalent to solving this eigenvalue problem:

$$V \times W \times M \times b_i = \lambda_i \times b_i \quad (2.5)$$

with i between 0 and $2K$, V is the crossed covariance matrix of the matrix containing the mean observations, W is the metric equivalence between the functions and the discrete observations, M is a weighting matrix to account for the different units of the variables and λ_i and b_i are respectively the eigenvalue and the eigenvector to solve the dimension reduction problem. With the obtained eigenvectors, we can then determine the eigenfunctions or vertical modes, accounting for both temperature and salinity variations.

For the elephant seals' hydrographic profiles, the first principal components (PCs) obtained can be associated with the presence-absence of WWs. This is checked by looking at the associated hydrographic profile signatures and the latitudinal distribution of the PC. However, this is not the case for the Argo profiles. For this data, we define the separation in the PC space that corresponds to the northernmost position of a subsurface minimum of temperature as in [Pauthenet et al. \(2018\)](#). This separation corresponds to a plane in the $PC1/PC2/PC3$ space such that the norm of the vertical temperature gradient between 100 and 400 m is minimized. The norm of the vertical temperature gradient is considered as a cost which is weighted by the density of the data in the PC space. The minimization is then conducted using the quasi-Newton method of Broyden, Fletcher, Goldfarb, and Shanno (BFGS; [Nocedal and Wright \(2006\)](#)) through the python function `optimize.minimize` of the `scipy` package. The optimal plan is characterized by the following equation :

$$a \times y_1 + b \times y_2 + c \times y_3 + d = 0 \quad (2.6)$$

where y_1 , y_2 and y_3 are coordinates along respectively PC1, PC2 and PC3. Each profiles can thus be attributed a CPF value where

$$CPF = a \times y_1 + b \times y_2 + c \times y_3 + d \quad (2.7)$$

characterizing its distance to the northernmost position of a subsurface minimum and such that $CPF > 0$ south of the Polar Front and $CPF < 0$ north of the Polar Front.

Chapter 3

Current and projected warming and marine heatwaves patterns in the Southern Indian Ocean

“Science is made up of so many things that appear obvious after they are explained.”

Frank Herbert, Dune

3.1 Context

The general aim of this Chapter is to provide a systematic description of observed and future changes over the Southern Indian Ocean, concerning both long-term changes and extreme events, to better grasp the spatial heterogeneity of climate change impacts and to inform conservation planning.

The focus is here on temperature, as it is a major driver of species distribution. Indeed, the Southern Indian Ocean is a transition area between subtropical and antarctic conditions. There is a general latitudinal distribution of the biodiversity along the latitudinal gradient of temperature and the system of fronts associated with the Antarctic Circumpolar Current. Temperature has physiological implications, as it can modulate

metabolic rates and energetic needs of some species (Boscolo-Galazzo et al., 2018), and can also be a key driver of habitats and trophic interactions, notably of foraging strategies (Constable et al., 2014; Reisinger et al., 2018; Hindell et al., 2020).

A first important point to elucidate is whether climate change signal can already be observed at the regional scale. The concept of “emergence” has been developed to identify when observed trends stand out from the background variability. Climate models indicate that the climate change signal in the subpolar Southern Ocean emerges quite early (1980s-1990s) throughout the water column but the model spread is quite high (Silvy et al., 2020). Besides, emergence from interannual variability can differ depending on the water masses (Auger et al., 2021).

Then, climate models and satellite observations are both needed to characterise climate change spatial heterogeneity, that is to understand where changes are occurring today and where they might intensify or weaken in the future. Better understanding this spatial heterogeneity, for both extreme events and long-term trends, is key for conservation planning, to identify the most threatened regions and the potential refugia. Climate velocities (i.e. the speed and direction at which isotherms drift under climate change Loarie et al. (2009)) can be useful to provide a complementary perspective on warming trends and on their implications for biodiversity redistribution (García Molinos et al., 2016; Brito-Morales et al., 2020).

In this chapter, the characterisation of current and projected warming and marine heatwaves (MHWs) patterns in the Southern Indian Ocean thus aims at:

- Studying the spatial distribution of the observed warming signal over these last decades and its robustness ;
- Comparing observations and CMIP6 models outputs in terms of warming trends and MHWs characteristics over the Southern Indian Ocean ;
- Spatializing temperature-related climate change threats in the region, notably through the identification of the areas projected to be the most exposed to ocean warming and MHWs under different emission scenarios and through the analysis of projected climate velocities at the surface (0 - 200 m) and in the mesopelagic area (200 - 1000 m).

3.2 Key results

This study highlights the spatial heterogeneity of warming and MHWs patterns in the Southern Ocean.

First, **natural variability still dominates temperature changes west of the Southern Indian Ocean but significant warming is observed east of the Kerguelen Plateau (east of 80°E)** and in the subtropical part of the Southern Indian Ocean, east of 60°E (between 0.1 and 0.3°C/decade). This pattern of natural variability is not well represented by models. However, a multiple-member analysis suggests a convergence of trends under climate change, meaning that in the long term, spatial patterns of warming are mostly driven by anthropogenic radiative forcing and are less modulated by natural variability.

Second, the comparison between MHWs characteristics in climate models and using satellite observations show that **MHWs intensity are underestimated in climate models**, probably due to coarse model resolution, although spatial patterns are similar. Indeed, both observations and multi-model mean indicate more intense MHWs north of 50°S, in particular between 45°S and 40°S west of the Kerguelen Plateau near the Agulhas Return Current. However, the striking pattern of high MHW intensity downstream of the Kerguelen Plateau between 55°S and 45°S (in a highly energetic area) is not well represented by the multi-model mean.

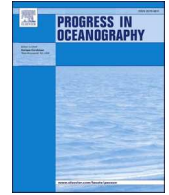
Third, **CMIP6 projections indicate an intensification of warming and marine heatwaves at subantarctic latitudes** (between 40°S and 55°S). Projected patterns of temperature change and MHW intensity are similar. MHWs in CMIP6 models are more linked to warming trends than to change in variability between 50° and 55°S. This subantarctic intensification is consistent with the current knowledge on heat transport in the Southern Ocean, notably the process of increased heat uptake in subpolar region, transported northward by wind-induced Ekman transport leading to heat accumulation at subantarctic latitudes (Frölicher et al., 2015; Armour et al., 2016; Sallée, 2018).

Through the estimation of projected climate velocities, a potentially neglected threat on pelagic ecosystems has been identified. Projected climate velocities at the end of the century both under a high mitigation scenario (SSP1-2.6) and a modest mitigation scenario (SSP2-4.5) are most often faster in the mesopelagic compared to the surface,

consistent with Brito-Morales et al. (2020). This can be explained by the lower temperature spatial gradient at depth compared to the surface, which increases the climate velocity. Organisms would need to shift faster at depth than at the surface to follow similar temperature conditions. Thermal niches may not shift at the same rate at depth and at the surface which could therefore shear pelagic habitats. **Not accounting for habitat shearing could lead to an underestimation of habitat shifts.** We further develop the use of climate velocity as a conservation tool in Section 3.4.

3.3 Main study

The main study presented in this Chapter has been published in “Progress in Oceanography” (Azarian et al., 2023). The associated Supplementary Material can be found in Appendix A.



Current and projected patterns of warming and marine heatwaves in the Southern Indian Ocean

Clara Azarian^{a,b,*}, Laurent Bopp^c, Alice Pietri^d, Jean-Baptiste Sallée^a, Francesco d'Ovidio^a

^a Sorbonne Université, CNRS, IRD, MNHN, Laboratoire d'Océanographie et du Climat: Expérimentations et Approches Numériques (LOCEAN-IPSL), Paris, France

^b Ecole Nationale des Ponts et Chaussées (ENPC), Champs-sur-Marne, France

^c Ecole Normale Supérieure/Université PSL, CNRS, Ecole Polytechnique, Sorbonne Université, Paris, Laboratoire de Météorologie Dynamique (LMD-IPSL) Paris, France

^d Instituto del Mar del Peru (IMARPE), Callao, Peru

ARTICLE INFO

Keywords:

Global climate models
Ocean warming
Ocean extremes
Southern Indian Ocean

ABSTRACT

The Southern Indian Ocean (20–120°E, 70–30°S) hosts an exceptional biodiversity that contributed to the inscription of the French and Australian natural reserves on the UNESCO World Heritage List. This region is a “hot spot” for ocean heat uptake and already experiences intense marine heat waves (MHW), as evidenced in 2011/2012 over the Kerguelen Plateau. In the coming decades, this region is also expected to face supplemental anthropogenic warming, depending on future greenhouse gas emissions, with unknown consequences for its marine ecosystems. Here, we present a regional analysis of ocean warming and MHW based on the analyses of historical observations and Coupled Model Intercomparison Project Phase 6 (CMIP6) climate projections. Consistent with observations over the last decades, we find an intensification through the 21st century of surface warming and MHW over a band located between 40°S and 55°S within the Antarctic Circumpolar Current region. CMIP6 models also project much faster climate velocities (i.e. the speed and direction at which isotherms drift in the wake of climate change) in the mesopelagic (200–1000 m) than at the surface (0–200 m). Lastly, a comparison between the two Shared Socioeconomic Pathways (SSP1-2.6 and SSP2-4.5) analysed in this study shows much larger changes in the second half of the 21st century for the higher emission scenario. These results suggest that the subantarctic islands will probably be mostly affected by warming and MHW under both scenarios, although committing to SSP1-2.6 could substantially alleviate the pressure on ecosystems in the long term. This study also highlights the need to consider a tri-dimensional environment that may evolve at different paces when designing efficient conservation measures.

1. Introduction

Ocean circulation. The Southern Indian Ocean (20–120°E, 70–30°S) is characterized by dynamic jets and a system of fronts associated with the Antarctic Circumpolar Current (ACC). The ACC is a strong eastward current (Donohue et al., 2016), driven by strong westerly winds (Rintoul and Naveira Garabato, 2013). As the ACC encounters the Kerguelen Plateau, it divides in several branches, with most of the ACC transport passing north of the Plateau (Park et al., 1991, 1993, 2009). A strong jet is also observed through the Fawn Trough, a deep passage across the Plateau at 56°S (Park et al., 2008; Roquet et al., 2009; Van Wijk et al., 2010; Vivier et al., 2015; Fig. 1). Northwest of the Southern Indian Ocean, the Agulhas Current, a western boundary

current, flows southward along the east coast of Africa. At around 40°S, this flow is split with the Agulhas Return Current transporting water eastward (Lutjeharms, 2006) and the Agulhas leakage transporting water to the South Atlantic (Schmidt et al., 2021). Generally, the frontal system and the circulation in the Southern Indian Ocean is an important biogeographical driver of phytoplankton and zooplankton communities which are at the basis of rich ecosystems (Hunt et al., 2001; Matsuno et al., 2020; Mishra et al., 2020; Venkataramana et al., 2020; Cotté et al., 2022).

Conservation efforts to protect a rich biodiversity. The Southern Indian Ocean region hosts several endemic species, including large populations of megafauna of high patrimonial and economical value like king penguins, yellow-nosed albatrosses, southern elephant seals, krill,

* Corresponding author at: Sorbonne Université, CNRS, IRD, MNHN, Laboratoire d'Océanographie et du Climat: Expérimentations et Approches Numériques (LOCEAN-IPSL), Paris, France.

E-mail address: clara.azarian@locean.ipsl.fr (C. Azarian).

<https://doi.org/10.1016/j.pocean.2023.103036>

Received 20 September 2022; Received in revised form 28 April 2023; Accepted 5 May 2023

Available online 13 May 2023

0079-6611/© 2023 Published by Elsevier Ltd.

toothfish, and many others (Delord et al., 2014). To protect the rich biodiversity of the Southern Indian Ocean, conservation measures have been implemented both in the exclusive economic zones (EEZs) of the subantarctic islands and in the areas under the Commission for the Conservation of Antarctic Marine Living Resources (CCAMLR). Part of EEZs of the following territories, Prince Edward, Crozet, Kerguelen and Heard and McDonald's islands, are managed through Marine Protected Areas (MPAs). The French national natural reserve (i.e. managed area with zones under strong or integral protection) within Crozet, Kerguelen and Saint-Paul and Amsterdam EEZ was created in 2006 and extended in 2016. The South African MPA around Prince Edward Islands have been officially implemented in 2013 and according to CCAMLR it contributes to a representative system of MPAs, to be used as a scientific reference for future management plans, to foster the recovery of Patagonian toothfish populations and to reduce the bycatch of toothfish fishery on marine seabirds. The Australian MPA around Heard and McDonald Islands was created in 2002 and has been extended in 2014. In total, 5.8 % of the Southern Indian Ocean is covered by MPAs and only within EEZs. The new frontier for conservation is now the vast open ocean region that extends beyond EEZs (Della Penna et al., 2017), known as the "High Seas". A workshop held in 2019 organized by the CCAMLR Scientific Committee developed a scientific work program for pelagic spatial planning in the eastern subantarctic region to investigate the relevance of adding new subantarctic spatial conservation tools in the High Seas of the CCAMLR area (Makhado et al., 2019).

Conservation and climate change. One key step in the design of a conservation plan is the evaluation of threats, including climate change (Meredith et al., 2019). The sector directly northward and within the Antarctic Circumpolar Current (ACC), corresponding to the latitudinal band 30°–50°S, in the Southern Indian Ocean is one of the regions of the world that has experienced the largest increase in ocean heat content in recent decades (Llovel and Terray, 2016; Roemmich et al., 2015; Sallée, 2018; Fox-Kemper et al., 2021). This large heat content increase has been explained by an increased heat uptake in the subpolar region transported northward by Ekman transport and subducted within and north of the ACC (Armour et al., 2016; Frölicher et al., 2015; Morrison et al., 2016; Sallée, 2018). In addition to large-scale processes (greater than 100 km), finer scale processes (1–100 km), which are key for the Southern Indian Ocean circulation (Kostianoy et al., 2004) and can be expected to intensify (Martinez-Moreno et al., 2019; Martinez-Moreno et al., 2021), could also potentially modulate climate change signal locally, maybe inducing important spatial heterogeneity in the temperature trends (e.g. anomalous vertical heat transport driven by submesoscale fronts altering oceanic heat uptake, Siegelman et al., 2020).

In the Southern Indian Ocean, species distributions are strongly shaped by the large meridional temperature gradient characterizing the region, which covers a transition zone from the subtropic to the Antarctic. Some species are even living close to their thermal tolerance limit (e.g., icefish, Kock and Everson, 2003; Collins et al., 2010) and it has been observed that warming could have a negative impact on the abundance of subantarctic krill, flagellates and Notothenioid fish (Constable et al., 2014) or even potentially on the juvenile recruitment of Patagonian toothfish (Belchier and Collins, 2008). Climate velocity, that is, the speed and direction at which isotherms drift in the wake of climate change (Loarie et al., 2009), can be a useful tool to study biodiversity redistributions due to climate change (García Molinos et al., 2016). Although there is no specific studies on the Southern Ocean using this tool, there are global studies that tend to show that the Southern Ocean may be a generally « slow-moving » basin compared to other regions (Burrows et al., 2014) but also that there may be an important spatial heterogeneity of this indicator (Brito-Morales et al., 2020).

Given the rich biodiversity and the observed and projected warming trends in the Southern Indian Ocean (Fox-Kemper et al., 2021), there is an urgent need to integrate climate change in biodiversity conservation and management. However, if climate change is increasingly presented as one of the threats on biodiversity in conservation plans, such a threat is rarely quantified and no associated actions are indicated. This issue will also likely be raised in line with the momentum fostered by the negotiations of a treaty on the conservation and sustainable use of marine biodiversity in areas beyond national jurisdiction (BBNJ), notably for the development of MPAs in the High Seas (Ban et al., 2014; Maxwell et al., 2020; Crespo et al., 2020). Despite an increasing awareness that climate change might hinder conservation measures efficiency and despite increasing literature on the need to develop new dynamical tools (Tittensor et al., 2019; Crespo et al., 2020), conservation policies seem to remain only focused on managing direct anthropogenic pressures as long as policy-makers have no concrete and operational courses of action to take into account the impacts of climate change (Wilson et al., 2020).

Current lack of relevant knowledge on climate change for policy-makers. Levers for potential action remain today unclear at the regional level and require a better understanding of climate change related hazards at relevant spatial and temporal scales for conservation (Wiens and Bachelet, 2010; Carr et al., 2011; Butt et al., 2016; Jones et al., 2016). Today, a gap remains in a systematic description of local observed and future changes over the entire Southern Indian Ocean.

In this study, we aim at addressing this shortcoming, by presenting a regional analysis of past and future ocean warming based on historical

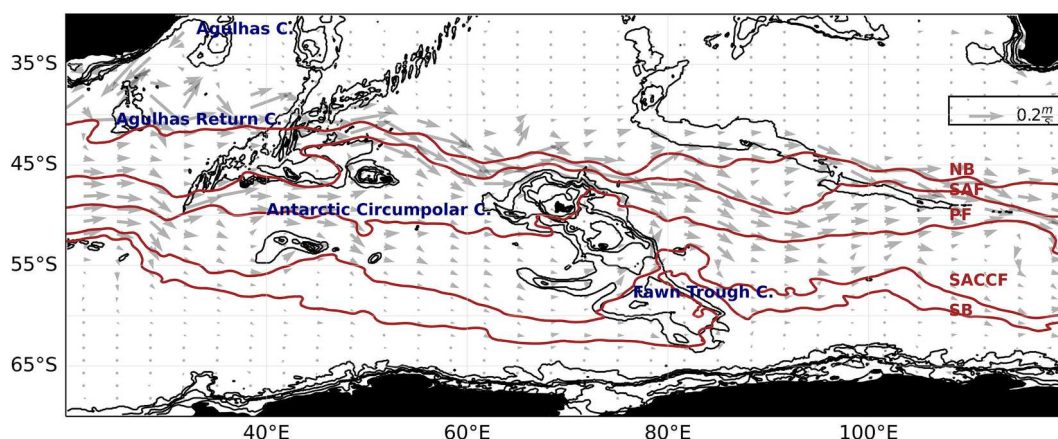


Fig. 1. Ocean circulation in the Southern Indian Ocean. The mean geostrophic velocity between 1993 and 2020 using AVISO product (<https://doi.org/10.48670/moi-00148>) is shown (grey arrows). Some specific currents are indicated in blue and the Antarctic Circumpolar Current (ACC) fronts, the Northern Boundary (NB), Subantarctic Front (SAF), Polar Front (PF), Southern ACC front (SACCF) and the Southern Boundary (SB) are shown in brown (constructed from mean dynamic topography, Source: Park and Durand, 2019, Park et al., 2019).

observations and climate projections under different scenarios. Here, we use a combination of decadal observations and CMIP6 simulations over the entire Southern Indian Ocean to estimate current trends and analyse projections to help identifying areas that are most likely to undergo significant temperature changes under two future emission scenarios: Shared Socioeconomic Pathways (SSPs) 1-2.6 (high mitigation scenario) and 2-4.5 (modest mitigation scenario; projected to lead to a global warming in 2100 similar to modelled pathways assuming continuation of policies implemented by the end of 2020; IPCC, 2022). We estimate the average temperature trends and extreme events, both listed as “climatic impact-drivers” of marine ecosystems according to the IPCC Assessment Report 6 (Chen et al., 2021; Cooley et al., 2022). We document average temperature trends in terms of warming patterns (°C/decade) as well as climate velocities (km/decade). This analysis is performed for the ocean surface (0–200 m) and for the mesopelagic (200–1000 m) regions. Extreme events are characterized in terms of marine heatwaves (MHW, Hobday et al., 2016; Frölicher et al., 2018). Su et al. (2021) characterized MHW but focusing only on the northern part of the Kerguelen Plateau. Our study extends the MHW analysis to the Southern Indian Ocean and uses CMIP6 models to project the evolution of MHW throughout the 21st century.

2. Material and methods

2.1. Data

2.1.1. Observations

The Operational Sea Surface Temperature and Ice Analysis (OSTIA) system run by the UK's Met Office (Good et al., 2020) provides daily sea surface temperature free of diurnal variability at a 0.05 deg. × 0.05 deg. horizontal grid resolution between 1982 and 2019 (available at <https://marine.copernicus.eu/>). This product combines satellite measurements from both infrared and microwave radiometers with in-situ measures from ships, and drifting and moored buoys.

The National Oceanic and Atmospheric Administration Daily Optimum Interpolation Sea Surface Temperature (NOAA OI SST V2 High Resolution) dataset, provided by the NOAA PSL (available from their website at <https://psl.noaa.gov>), combines sea surface temperature observations (SST at 0.2 m) from different platforms (satellites, ships, buoys and Argo floats) with a 0.25 deg × 0.25 deg horizontal grid resolution between 1982 and 2019 (Reynolds et al., 2007; Banzon et al., 2016). Contrary to OSTIA dataset, OISST does not include satellite measurements from microwave radiometers as SST inputs (Yang et al., 2021).

2.1.2. Global climate models – CMIP6

Models from the Coupled Model Intercomparison Project 6 (CMIP6; Eyring et al., 2016) are used in this study (Table 1). These are coupled ocean–atmosphere models developed by 49 different climate modelling groups¹ that have been used to carry out historical and projection simulations notably to investigate how the Earth system responds to forcing (Eyring et al., 2016).

Historical and projection simulations from the ScenarioMIP experiments are used. Historical simulations cover the period 1850–2014 and use historical forcing, mostly based on observations, that includes among others greenhouse gas, aerosol concentrations and solar forcing (Eyring et al., 2016). Projection simulations from the ScenarioMIP experiments cover 2015–2100 and over multiple emission trajectories, described through so-called Shared Socioeconomic Pathways (SSPs). More specifically, SSPs describe development pathways according to different economic and political strategies (O'Neill et al., 2017), and subsequent forcing levels similar to the ones used in CMIP5, that are the Representative Concentration Pathways (RCPs). However, SSPs

Table 1

CMIP6 models used, using yearly data over multiple depths and daily data at the surface and scenarios associated. CMIP6 models outputs are available at: <https://esgf-node.llnl.gov/projects/cmip6/>.

	Yearly data – multiple depth levels	Daily data - surface	Ocean horizontal resolution (before interpolation)	References
ACCESS-CM2	Historical, ssp126, ssp245	Historical, ssp126, ssp245	1°	Bi et al., 2020
ACCESS-ESM1-5	Historical, ssp126, ssp245	Historical, ssp126, ssp245	1°	Ziehn et al., 2020
BCC-CSM2-MR	Historical, ssp126, ssp245	Historical, ssp126, ssp245	1°	Wu et al., 2019
CAMS-CSM1-0	Historical, ssp126, ssp245	/	1°	Rong et al., 2019
CanESM5	Historical, ssp126, ssp245	Historical, ssp126, ssp245	1°	Swart et al., 2019; Christian et al., 2021
CanESM5-CanOE	Historical, ssp126, ssp245	/	1°	Swart et al., 2019; Christian et al., 2021
CESM2	Historical, ssp126, ssp245	Historical, ssp126, ssp245	1°	Danabasoglu et al., 2020
CESM2-WACCM	Historical, ssp126, ssp245	Historical, ssp126, ssp245	1°	Danabasoglu et al., 2020
CMCC-CM2-SR5	Historical, ssp126, ssp245	Historical, ssp126, ssp245	1°	Cherchi et al., 2019
CMCC-ESM2	Historical, ssp126, ssp245	Historical, ssp126, ssp245	1°	Lovato et al., 2022
CNRM-CM6-1	Historical, ssp126, ssp245	Historical, ssp126, ssp245	1°	Voltaire et al., 2019
CNRM-CM6-1-HR	/	Historical, ssp126, ssp245	0.25°	Voltaire et al., 2019
CNRM-ESM2-1	Historical, ssp126, ssp245	Historical, ssp126, ssp245	1°	Séférian et al., 2019
GFDL-CM4	Historical, ssp245	Historical, ssp245	0.25°	Held et al., 2019; Dunne et al., 2020
GFDL-ESM4	Historical, ssp126, ssp245	/	0.5°	Dunne et al., 2020
HadGEM3-GC31-LL	Historical, ssp126, ssp245	/	1°	Kuhlbrodt et al., 2018; Andrews et al., 2020
EC-Earth3	/	Historical, ssp126, ssp245	1°	Döscher et al., 2022
EC-Earth3-CC	Historical, ssp245	/	1°	Döscher et al., 2022
EC-Earth3-Veg	Historical, ssp126, ssp245	/	1°	Döscher et al., 2022
IPSL-CM6A-LR	Historical, ssp126, ssp245	Historical, ssp126, ssp245	1°	Boucher et al., 2020
MIROC-6	/	Historical, ssp126, ssp245	1°	Tatebe et al., 2019
MIROC-ES2L	Historical, ssp126, ssp245	/	1°	Hajima et al., 2020

(continued on next page)

¹ https://wcrp-cmip.github.io/CMIP6_CVs/docs/CMIP6_institution_id.html.

Table 1 (continued)

	Yearly data – multiple depth levels	Daily data – surface	Ocean horizontal resolution (before interpolation)	References
MPI-ESM1-2-HR	Historical, ssp126, ssp245	Historical, ssp126, ssp245	0.4°	Müller et al., 2018; Mauritsen et al., 2019
MPI-ESM1-2-LR	Historical, ssp126, ssp245	Historical, ssp126, ssp245	1.5°	Mauritsen et al., 2019
MRI-ESM2-0	Historical, ssp126, ssp245	Historical, ssp126, ssp245	1°x0.5°	Yukimoto et al., 2019
NESM3	Historical, ssp126, ssp245	Historical, ssp126, ssp245	1°	Cao et al., 2021
UKESM1-0-LL	Historical, ssp126, ssp245	/	1°	Sellar et al., 2019

represent an improvement in the sense that those scenarios include updated data on recent emission trends (O'Neill et al., 2016) and allow to explore the implication of different climate change mitigation policies (Riahi et al., 2017). In this study, for all analyses, two projection scenarios are considered: the SSPs 1-2.6 and 2-4.5. The SSP1-2.6 describes a world that shifts to a more sustainable path leading to an estimated warming of 1.8 °C by the end of the century (as compared to pre-industrial) whereas SSP2-4.5 represents a path in which socio-economic trends do not shift significantly from the historical patterns, with an estimated warming of 2.7 °C by the end of the century. The focus on those two scenarios allows the comparison between two possible futures whose occurrence will depend on countries' commitments to reduce their net greenhouse gas emissions (Hausfather and Peters, 2020).

Depending on the analysis, the variable considered is either *thetao* (sea temperature across different depth levels) or *tos* (sea surface temperature) as only *tos* was available daily. Each model output is regridded to the same regular 1°-1° horizontal grid using distance weighted average remapping (using climate data operators « cdo » remapdis) as in Kwiatkowski et al., 2020. Each model output is also regridded vertically following the World Ocean Atlas standard discretization (33 vertical intervals from the surface (0 m) to the abyssal seafloor (5500 m)).

There are several ways to combine the results from multiple models. The traditional approach used by the IPCC, which is the main method used here, is to use a model ensemble mean, all models being weighted equally, and then to study the projections for fixed future periods. For changes in temperature and projected MHW characteristics, future periods of 20 years are considered: the near term (2021–2040), the mid term (2041–2060) and the long term (2081–2100) as in the IPCC Assessment Report 6 (Chen et al., 2021). An alternative method is also considered to further support the projected trends obtained with the traditional method: the time-shift approach (Heger et al., 2015; Chen et al., 2021; Lee et al., 2021). Instead of specifying a fixed time period, this approach specifies a fixed global warming value compared to pre-industrial, typically 1.5 °C, 2 °C and 3 °C (hereafter referred to as « global warming levels » or GWL 1.5 °C, 2 °C and 3 °C, respectively). These GWLs are in general reached at different time periods depending on the models and on the scenarios. This method allows to account for the different climate sensitivities of the models and facilitates the comparison between global warming and regional spatial patterns. For each model and under each SSP, warming levels are defined as 20-year running means of globally averaged atmospheric surface temperature anomaly compared to the pre-industrial period (1850–1900). Then the change in a given metric (temperature, MHW indicator) is estimated using a climatology of 20 years centred on the first year for which the

warming level exceeded a given threshold (e.g., 1.5 °C), relative to the 1850–1900 reference value. These results are then averaged over the model ensemble and over the SSPs considered, all simulations being weighted equally. This method is applied to estimate the spatial patterns in warming and in MHW intensity for GWL 1.5 °C, GWL 2 °C and GWL 3 °C. To be able to investigate GWL 3 °C, given that not all models for SSP1-2.6 and SSP2-4.5 may reach this threshold, outputs from SSP5-8.5 are also used (Supplementary Fig. S1).

Models are also confronted with observations over the historical period for evaluation purposes. More precisely, we evaluate how well the spatial patterns and mean trends are reproduced by the models and compared to observations. This comparison is used as an indicator of what processes affecting trends may be or may not be reproduced by the model ensemble. Such information contributes to the interpretation of projections and uncertainties. Models and observations warming rates and MHW mean intensity are compared respectively over 1982–2019 (to account for natural interannual variability) and 1984–2014 (MHW analysis requiring 30 years of data). CMIP6 historical outputs are thus completed with SSP2-4.5 outputs until 2019, since SSP2-4.5 is most representative of today's emission pathway (Fricko et al., 2017; Hausfather and Peters, 2020). The temperature trends significance is determined using the coefficient of determination (R^2) of the linear regression as well as a signal-to-noise ratio (SNR) comparing the trend to the interannual variability of the anomaly between the expected (from the linear regression) and observed temperature, as defined in Auger et al., 2021.

To quantify the impact of natural variability on the projected trends, we also exploit additional simulations using the IPSL-CM6A-LR model, which exhibits an important centennial climate variability (Bonnet et al., 2021), through the analysis of the temperature trends of 11 members (r1i1p1f1, r2i1p1f1, r3i1p1f1, r4i1p1f1, r5i1p1f1, r6i1p1f1, r10i1p1f1, r11i1p1f1, r14i1p1f1, r22i1p1f1, r25i1p1f1). These members were all initialized in 1850, but with distinct initial conditions, mostly covering different states regarding the initial trend of the Atlantic Meridional Overturning Circulation (Bonnet et al., 2021). First, the temperature trends over the historical period (1975–2015) of the different members are compared. Second, projected changes in surface temperature for the near, mid and long term periods are compared. Finally, Pearson correlation coefficients between spatial patterns of changes in surface temperature for each member simulation relative to the r1i1p1f1 simulation over each year between 2015 and 2100 in SSP2-4.5 are estimated. The aim is to determine whether the initial conditions of the simulations and natural variability still play an important role in determining the regional characteristics of the projected trends compared to the radiative forcing.

2.2. Climate velocity

For climate velocity we use the classical definition as the ratio between the warming rate and the local spatial gradient of a variable as in Loarie et al., 2009 and Brito-Morales et al., 2018. The intensity of horizontal climate velocity v for temperature (T) is thus here defined as

$$v = \frac{\frac{\partial T}{\partial t}}{\|\nabla T\|}$$

By convention, v is positive in case of a warming ($\frac{\partial T}{\partial t} > 0$) and negative in case of a cooling.

The climate velocity vector \vec{v} is then defined as

$$\vec{v} = \frac{-\partial T}{\partial t} \left[\frac{\frac{\partial T}{\partial x}}{\|\nabla T\|^2} \vec{u}_x + \frac{\frac{\partial T}{\partial y}}{\|\nabla T\|^2} \vec{u}_y \right]$$

By convention, \vec{u}_x (longitudinal unit vector) is positive eastward and \vec{u}_y (latitudinal unit vector) is positive northward. \vec{v} points to the di-

rection to follow to remain at the same temperature.

For CMIP6 outputs, climate velocity is estimated over different historical periods of 50 years (1850–1900, 1950–2000, 1955–2005 and 1965–2015) to check the sensitivity of the pre-industrial or historical climate velocity that could be used as a baseline for comparison with the projected climate velocities. Then climate velocity is estimated over 2015–2065 and 2050–2100 for SSP1-2.6 and SSP2-4.5, respectively. Climate velocity is estimated for different depth zones: surface (0–200 m) and mesopelagic (200–1000 m). The average temperature weighted by the thickness of each standard depth layer is used to calculate a horizontal climate velocity. The climate velocities obtained from each model are then averaged to get the mean-ensemble results.

2.3. Marine heatwaves

The definition of a marine heatwave (MHW) as a “discrete prolonged anomalously warm water event” was introduced in Hobday et al., 2016 to allow for comparison with other studies increasingly adopting this standardized definition. In this work, a MHW is detected when the temperature is above a given threshold for at least 5 days. This threshold is defined as the 90th (for model evaluation) or the 99th percentile (for projections, to focus on the most intense events) of the data distribution. The climatology and threshold are estimated for each grid point of the region of interest and for each day of the year using an 11-day window. The threshold is also smoothed by applying a 30-day moving average. The climatology is estimated over at least 30 years of data, in order to smooth out climate mode of variability (e.g., ENSO, AMO; Scannell et al., 2016).

MHW can be quantified by different metrics. The definition of MHW intensity varies and can be determined relative to the seasonal climatology or to a chosen threshold (Hobday et al., 2016). Here we define MHW intensity relative to the threshold (90th percentile for model evaluation, 99th percentile for projections) and the mean intensity is weighted by the number of days affected. In addition, the mean number of days affected by MHW per year, also called mean annual MHW days, has been found strongly correlated to some observed ecological performance in the marine environment (e.g., seagrass density, Smale et al., 2019). The two metrics, mean MHW intensity and mean MHW annual days, are therefore used here to characterize MHW as potential climatic impact-drivers of marine ecosystems.

3. Results

3.1. Historical warming trends and marine heatwaves

3.1.1. Warming trends

The mean warming rate observed over the Southern Indian Ocean (20°–120°E, 70°–30°S) between 1982 and 2019 is 0.03 °C/decade (± 0.08 °C/decade, spatial standard deviation), as estimated by a linear regression of observation-based sea surface temperature from the OSTIA product, and 0.07 °C/decade (± 0.09 °C/decade) using OISST dataset (See Section 2.1.1). Such regional averaged temperature trend hides important east/west contrasts (Fig. 2, also for OISST as shown in Supplementary Fig. S2) with warming trends north of the area and east of the Kerguelen Plateau between 0.1 and 0.3 °C/decade that are found significant (R^2 between 0.4 and 0.5, SNR > 1). The cooling pattern west of the Kerguelen Plateau is not found significant, but has also been obtained on different observational datasets (Yang et al., 2021), suggesting high temporal variability in this area.

In comparison, the 24-single-member-CMIP6-models produces an ensemble mean warming rate from 1982 to 2019 close to the one obtained with OISST dataset (0.085 ± 0.053 °C/decade, spatial standard deviation). A majority of CMIP6 models (17 over 24) simulate higher mean warming rates than the observed one with OISST dataset but none shows an averaged cooling in the region (Fig. 2, Supplementary Fig. S3). The simulated spatial patterns of temperature trends are quite different

between different model simulations, but also between different ensemble members of the same model (IPSL-CM6A-LR, Supplementary Fig. S5A). The initial conditions of the simulations as well as decadal and/or multidecadal variability might thus play an important role in the regionalisation of temperature trends over the historical period.

Historical warming rates from the multimodel ensemble are more homogeneous than from any individual models or observations, despite greater warming rates being found between 40° and 50°S north and west of Prince Edward, Marion and Crozet islands (Fig. 2). The multimodel ensemble mean underestimates warming trends north of the ACC and east of the Kerguelen Plateau. It shows a general warming throughout the area. A lower signal and/or lower agreement between models is found south of the Kerguelen Plateau near the Antarctic shelves.

3.1.2. Climate velocity

The mean climate velocity over the Southern Indian Ocean is 4.9 km/decade (± 27 km/decade, spatial standard deviation) using OSTIA dataset and 10.64 km/decade (± 34 km/decade) using OISST dataset between 1982 and 2019 (see Sections 2.1.1 and 2.2). An east/west contrast is observed similar to what is found in Section 3.1.1. East of the Southern Indian Ocean (70°–120°E, 70°–30°S), the mean climate velocity is around 12 km/decade using OSTIA dataset and around 18 km/decade using OISST dataset.

3.1.3. MHW intensity

The regional mean MHW intensity observed over the Southern Indian Ocean between 1984 and 2014 is 0.35 °C above the 90th percentile of the local temperature distribution using the OSTIA dataset (Fig. 3). Detection of MHW from the OSTIA dataset highlights a pattern of greater MHW intensity north of the Kerguelen Plateau, in the region of influence of the ACC (Fig. 3, pattern also identified in Su et al., 2021). The 19-model ensemble, reproduced the spatial pattern with greater mean MHW intensity north of the Plateau, notably over the Crozet Plateau, and the less intense MHW west of the Kerguelen Plateau (Fig. 3, Supplementary Fig. S4).

However, the multimodel mean underestimates the intensity of MHW north of the ACC compared to observations. The mean MHW intensity between 40°S and 30°S obtained from the multimodel mean is 26 % lower than the one obtained from observations.

3.2. Projected warming trends and marine heatwaves

3.2.1. The impact of natural variability on the projected temperature trends

To quantify the impact of natural variability on the projected temperature trends, we first focus our analysis on one model (IPSL-CM6A-LR), for which we use an ensemble of simulations and investigate the similarity between members of the simulated patterns for historical and projected warming (see Section 2.1.2).

The mean warming rate over the Southern Indian Ocean varies from 0.031 °C/decade to 0.11 °C/decade over 1975–2015 between the 11 members of IPSL-CM6A-LR (Supplementary Fig. S5). Important differences regarding the spatial patterns are found, with members producing a general warming throughout the region (e.g. r6i1p1f1), others showing a cooling north of the area (e.g. r3i1p1f1, r4i1p1f1, r22i1p1f1) or a cooling east of the Kerguelen Plateau (e.g. r2i1p1f1, r14i1p1f1, r25i1p1f1).

Across the ensemble members, the mean change in surface temperature over the Southern Indian Ocean in SSP2-4.5 ranges from 0.15 °C to 0.44 °C in the near term (2021–2040), from 0.43 to 0.66 °C in the mid term (2041–2060) and from 0.83 °C to 1.06 °C in the long term (2081–2100), as compared to the historical period (1995–2014, Supplementary Fig. S5B). The timeseries of Pearson correlation coefficient relative to r1i1p1f1 member pinpoints the increased similarity between the members' patterns, notably from 2050 onward (correlation coefficient mainly over 0.5, Supplementary Fig. S5C). It could be that the remaining differences between the members' projections is to be

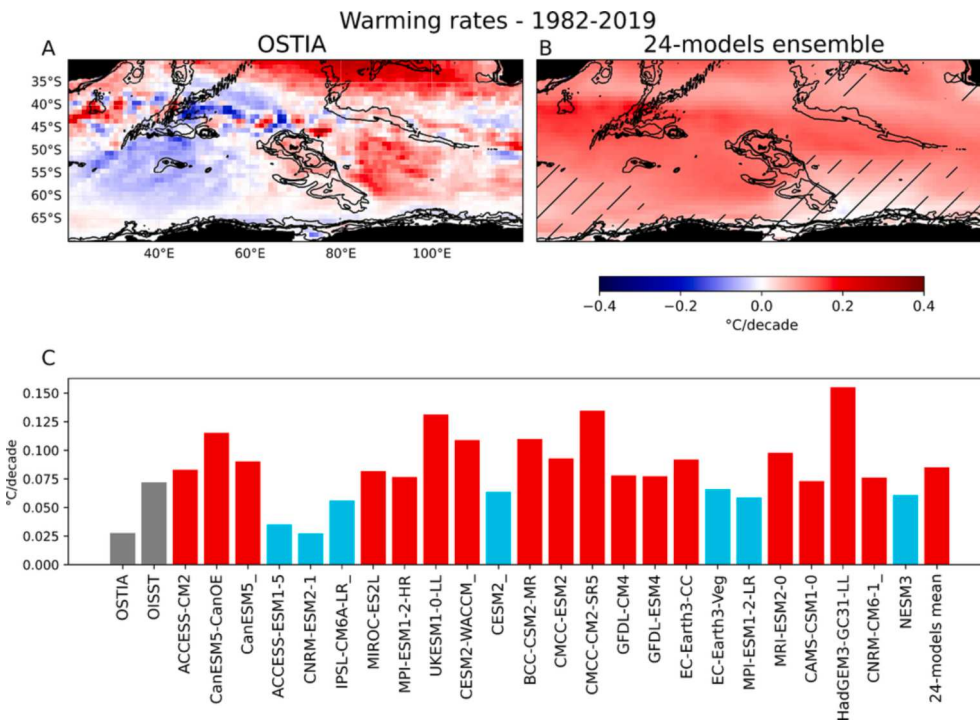


Fig. 2. Warming rates between 1982 and 2019 in the Southern Indian Ocean, using linear regression on surface temperature, using OSTIA observations (A) and a 24-single-member-CMIP6-model ensemble (B). Hatching indicates areas where the intermodel standard deviation of the warming rate is greater than the mean value, suggesting a low change or a low robustness of the output. For each model and for the 24-model ensemble, the mean warming rate over the area is also calculated and compared to the mean warming rates estimated from the OSTIA and OISST datasets (C). Bars colored in red indicate a higher warming rate than the one derived from OISST (gray bar) and in blue if it is a lower rate.

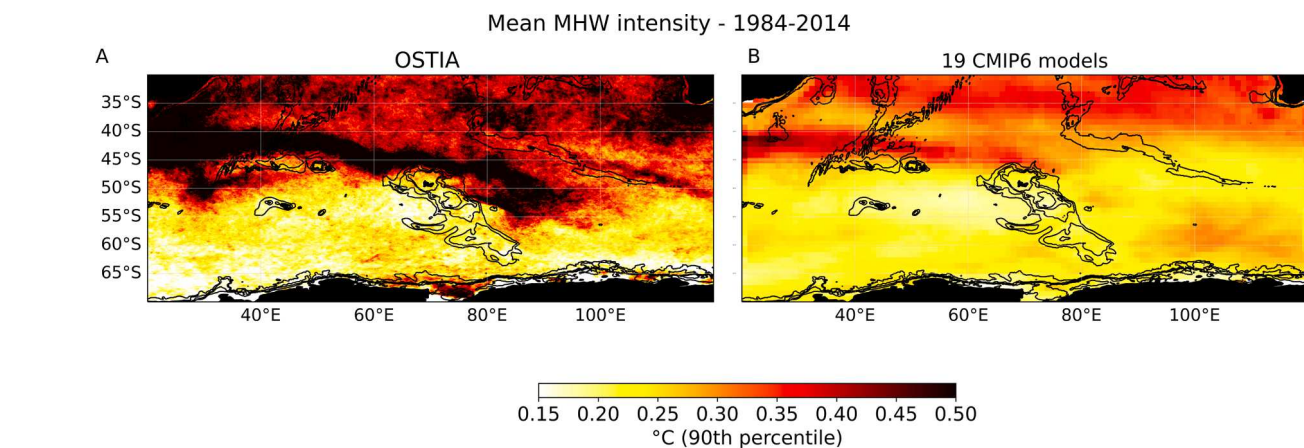


Fig. 3. Mean Marine Heatwaves (MHW) intensity as defined by the anomaly above the threshold (90th percentile) between 1984 and 2014 in the Southern Indian Ocean using OSTIA observations (A) and a 19-single-member-CMIP6-model ensemble (B). Hatching indicates areas where the intermodel standard deviation of the MHW intensity is greater than the mean value, suggesting a low robustness of the output.

attributed to a non-deterministic component in ocean response, notably intrinsic ocean variability (Dijkstra, 2016).

This suggests that over the historical period the natural variability is strong and drives a large spread of temperature trends between ensemble members. With increasing radiative forcing, this spread decreases, suggesting that the projected long term spatial patterns are not dependent on natural variability.

3.2.2. Projected warming

Over the Southern Indian Ocean and for SSP2-4.5, the projected warming is 0.29 °C (±0.06 °C, intermodel variability) in the near term (2021–2040), 0.58 °C (±0.09 °C) in the mid term (2041–2060) and 1.05 °C (±0.15 °C) in the long term (2081–2100), compared to the historical period (1995–2014). While the mean surface temperature change is similar in both scenarios in the near term, it is 1.2 and 1.7 times higher for SSP2-4.5 than for SSP1-2.6, in the mid and long term, respectively (Fig. 7).

Using the 24-model ensemble, a larger warming is simulated between 40°S and 50°S and up to 55°S, thus in regions including the Indian Ocean subantarctic Exclusive Economic Zones (EEZs, see Fig. 4). This latitudinal band of large warming is located in the ACC and expands southward with time and in SSP2-4.5.

Between 35° and 40°S, warming is lower than in the latitudinal band encompassing the subantarctic island’s EEZs (warming of 0.3–0.4 °C in SSP2-4.5 mid term). South of 55°S, surface temperature changes remain below 1 °C even in the long term in SSP2-4.5. The region south of the ACC has been shown to experience lower warming due to the local circulation and stratification change (Armour et al., 2016; Haumann et al., 2020).

3.2.3. Projected climate velocity

For the Southern Indian and in SSP2-4.5, the average climate velocities over 2015–2065 is 38.53 southward (±5.8, intermodel variability) and 47.43 (±8.1) km/decade at the surface and in the

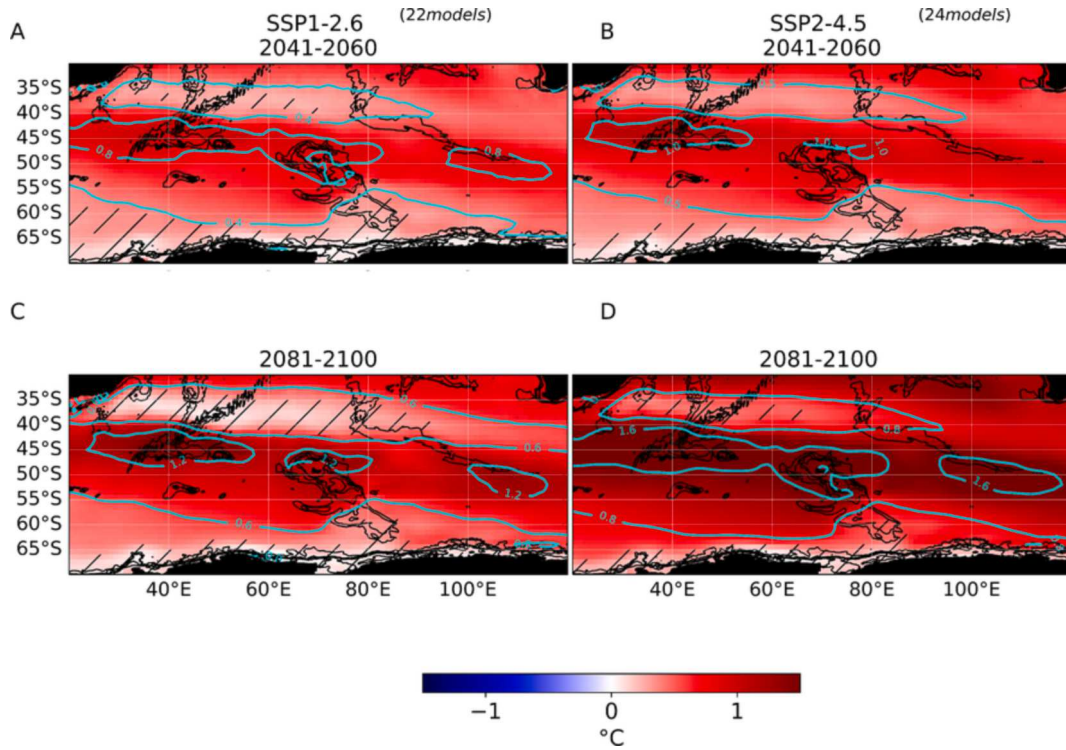


Fig. 4. Surface temperature change from the historical period (1995–2014) for the mid-term (A and B) and long term (C and D) projected periods under SSP1-2.6 (A and C) and SSP2-4.5 (B and D) using CMIP6 multimodel mean. Contour lines of similar temperature change are indicated in cyan. Hatched areas indicate where the intermodel standard deviation of the temperature change is higher than the mean value, suggesting a less robust output.

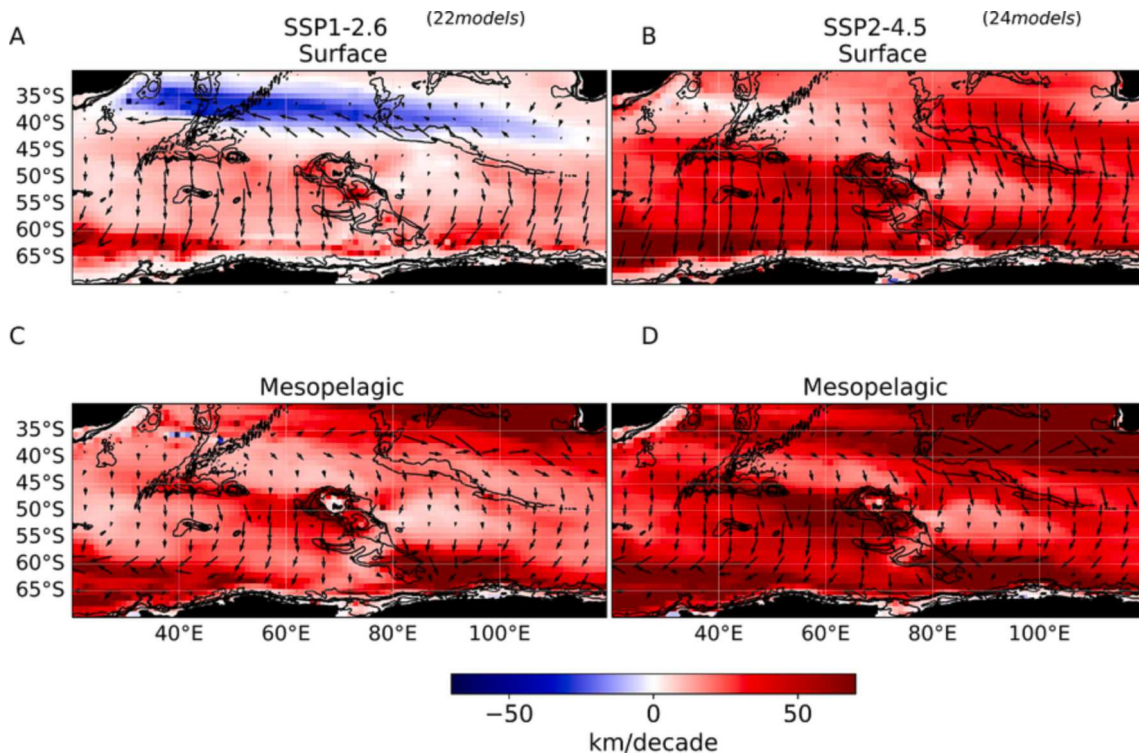


Fig. 5. Surface (0–200 m, A and B) and mesopelagic (200–1000 m, C and D) climate velocities, defined as the ratio between the warming rate and the temperature spatial gradient between 2050 and 2100 using multimodel means under SSP1-2.6 (A and C) and SSP2-4.5 (B and D). It can be interpreted as the velocity an individual should adopt to remain at the same temperature. By convention, positive climate velocities correspond to warming trends and negative ones to cooling trends. Black arrows indicate the direction of the climate velocity.

mesopelagic, respectively. When averaged over 2050–2100, it is 31.62 (± 5.6) and 57.46 (± 9.8) km/decade, at the surface and in the mesopelagic, respectively. At the end of the century, surface (mesopelagic) climate velocities are expected to be 5.3 times (1.8 times) faster in SSP2-4.5 as compared to SSP1-2.6 (Fig. 7). Mesopelagic climate velocities under both scenarios are also about 5 times faster for the period 2015–2065 compared to the historical period 1955–2005.

Negative surface climate velocities (i.e. northward) over 2050–2100, are found around 35°S in SSP1-2.6 (Fig. 5), meaning that this area is expected to cool towards the end of the 21st century. This cooling is only found at the surface and not at depth under SSP1-2.6, and is not projected under SSP2-4.5.

Important differences are found between surface and mesopelagic climate velocities. Mesopelagic conditions might undergo faster climate velocities than at the surface and that, already over 2015–2050 (Fig. 7). For the two projected periods and for both scenarios, mesopelagic climate velocities averaged over the Southern Indian Ocean are between one and four times faster than surface climate velocities. In contrast, for different periods of 50 years between 1850 and 2015, surface climate velocities are found between 1.5 and 3.1 faster than mesopelagic climate velocities. Those differences between climate velocities in the mesopelagic and at the surface are accentuated in some areas. Those differences can reach up to 160 km/decade southwest of Australia, 120 km/decade west of Kerguelen Plateau or vary between 40 and 70 km/decade north of Crozet Plateau in SSP2-4.5. Faster climate velocities in the mesopelagic compared to the surface for a same location (Fig. 5) can be due to the weaker spatial temperature gradients at depth as it is for instance the case west of the Australian coast.

3.2.4. Projected marine heatwaves

In the Southern Indian Ocean, the projected mean MHW intensity is 0.28 °C (above 99th percentile threshold) in the near term for both scenarios and 0.39 °C or 0.63 °C in the long term, respectively in SSP1-

2.6 or SSP2-4.5. The areas most affected by this intensification in the long term are located between 40°S and 55°S and in particular over Prince Edward, Marion, Crozet, Kerguelen and Heard and McDonald Islands (Fig. 6). The spatial pattern of mean MHW intensity in SSP2-4.5 for the near term is similar to the historical pattern (Fig. 3). North of the ACC, mean MHW intensity, for this scenario and time horizon, varies between 0.3 and 0.4 °C. In the long term under SSP2-4.5, a maximum MHW intensity of 0.97 °C is found over Crozet Plateau and the zonal maximum MHW intensity is found to be 0.81 °C at 48°S. The pattern obtained is similar to the pattern of surface temperature change (Fig. 4), suggesting that the detected MHW might be caused by a mean shift of the temperature distribution rather than a change in the spread of the temperature distribution (as in Oliver et al., 2019).

Additional analyses, investigating the daily temperature distribution shift in SSP2-4.5 relative to the historical period, show that the relative shift in the mean of the temperature distribution south of 50°S is much larger than the changes in the spread of the distribution, whereas north of 50°S similar orders of magnitude of relative change are found in terms of increased mean temperatures and increased distributions spread (Supplementary Fig. S6). In particular, the area between 35° and 40°S shows a larger relative change in the spread of the distribution than in the mean of the distribution, with increases of respectively 9.98 % and 7.60 % in the long term compared to the historical period.

In the Southern Indian Ocean, the projected mean annual MHW days is 46.1 days/year in the near term and 119.3 days/year in the long term in SSP1-2.6. These values increase to 42.8 days/year and 206 days/year respectively in SSP2-4.5 (Fig. 6). Annual MHW days under both scenarios are similar in the near term but it is 23 % higher in the mid term and 73 % higher in the long term in SSP2-4.5 compared to SSP1-2.6 (Fig. 7). Similar as for MHW intensity, the most impacted area is generally the latitudinal zone between 40°S and 55°S in the ACC region. In SSP2-4.5, in the near term, the zonal number of annual MHW days is maximum between 40°S and 55°S varying between 44.5 and 62.9 days,

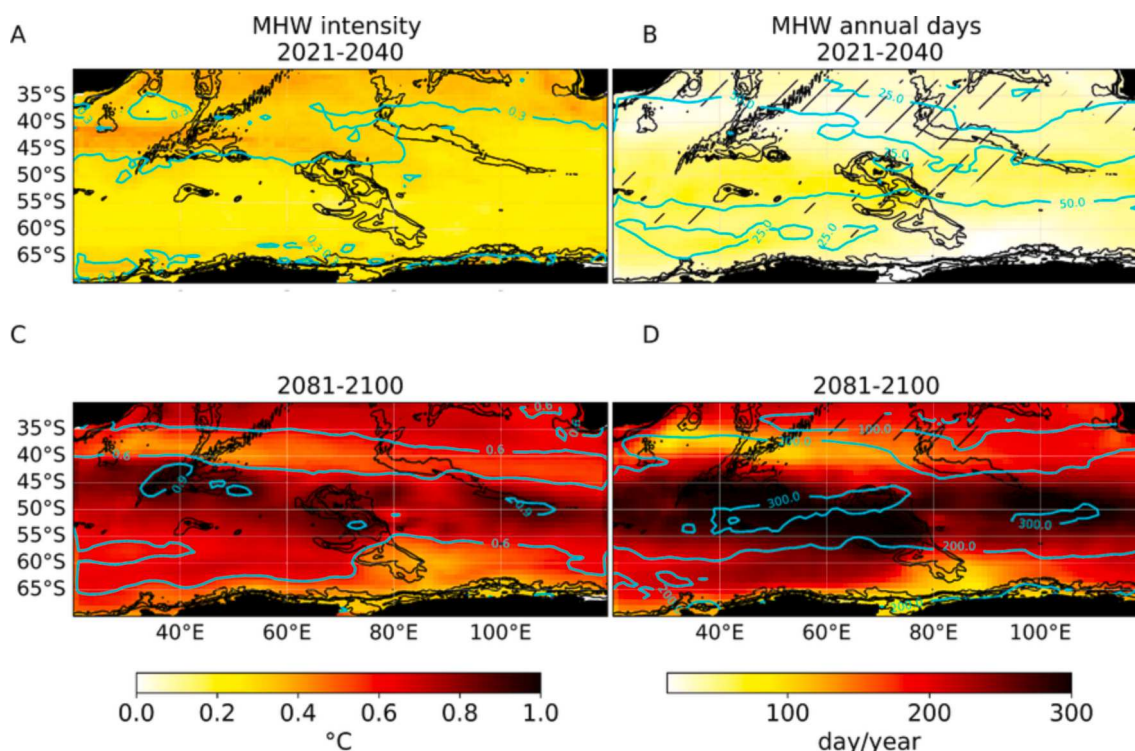


Fig. 6. Projected mean MHW intensity (as defined by the anomaly above the threshold of 99th percentile relatively, A and C) and projected mean number of days per year affected by MHW (B and D) under SSP2-4.5 using a 19-single-member-CMIP6-model ensemble for both 2021–2040 (A and B) and 2081–2100 (C and D). MHW were detected relative to a historical seasonally-varying climatology (1984–2014). Contour lines of similar metric are indicated in cyan. Hatching indicates areas where the intermodel standard deviation of the metric is greater than the mean value, suggesting a low robustness of the output.

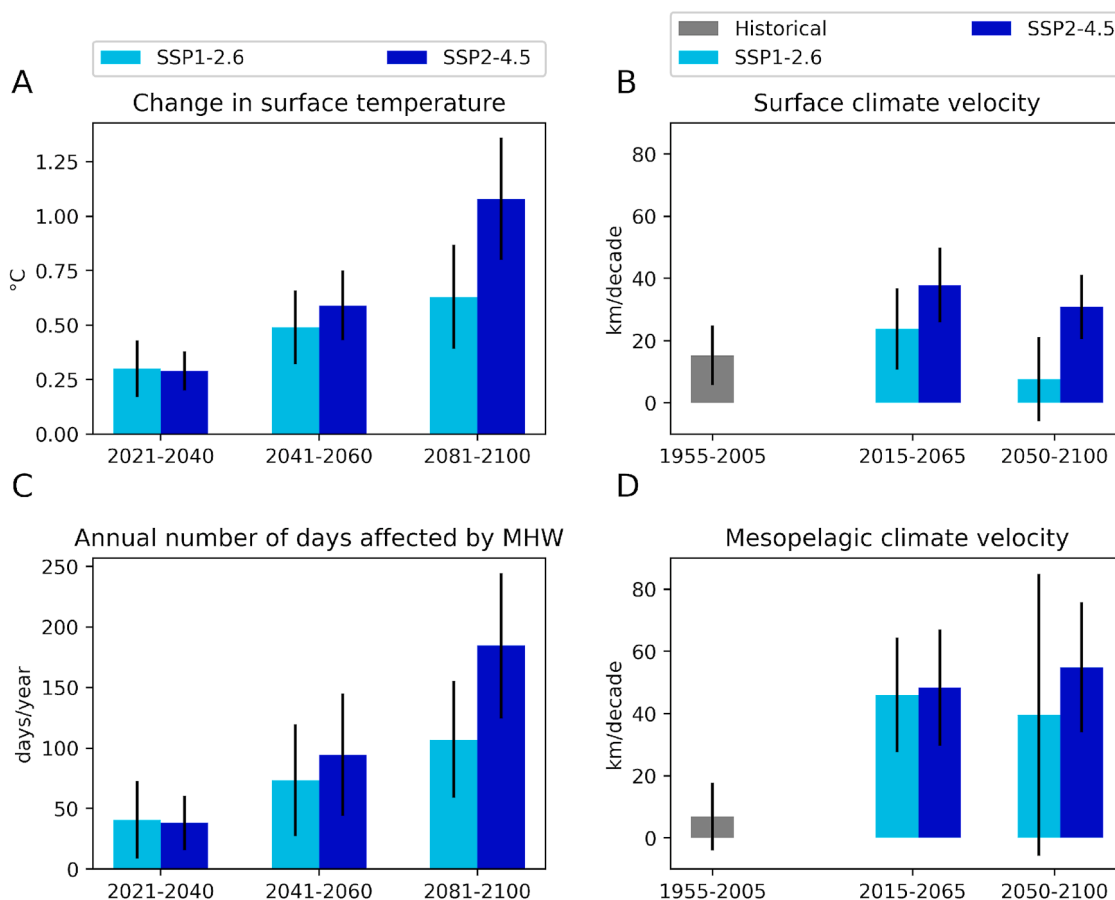


Fig. 7. Synthesis of the different climate impact drivers metrics over the Southern Indian Ocean (20°–120°E 70°–30°S): change in surface temperature (A, relative to 1995–2014); the annual number of day affected by MHW as defined using the 99th percentile threshold (C); average surface (B) and mesopelagic (D) climate velocities. The error bars correspond to the intermodel standard deviation for each metric.

the maximum being reached at 50°S. In the long term, the zonal number of annual MHW days is maximum between 40°S and 57°S varying between 194 and 290 days, the maximum being reached at 51°S. A permanent state of MHW is almost reached over the Kerguelen Plateau (312 days west of the Plateau). When considering the relationship between changes in surface temperatures and MHW annual days for the three projected time periods, it appears that over the whole area a permanent state of MHW could be reached for a 2 °C regional mean surface temperature change relative to the historical period (Supplementary Fig. S7).

3.3. Patterns of warming-related climatic impact-drivers for GWL 1.5 °C, 2 °C and 3 °C

Patterns of warming-related climatic impact-drivers are also investigated using a timeshift approach (see Section 2.1.2). Not only is this method used to confirm the robustness of the spatial patterns obtained through the traditional approach, but this method also contributes to describing future changes in accordance with targets defined in the Paris Agreement,² regardless of the mitigation pathway (Chen et al., 2021).

The mean sea surface temperature change over the Southern Indian Ocean is 0.6 °C (± 0.2 °C, intermodel variability), 0.7 °C (± 0.2 °C) and 1.1 °C (± 0.3 °C) greater than in 1850–1900 for global warming levels (GWLs, see Section 2.1.2) of 1.5 °C, 2 °C and 3 °C, respectively, as computed from the CMIP6 model ensemble (Fig. 8; we remind that GWLs are defined in respect to pre-industrial temperatures and not in

respect to the present). In the three cases, the patterns are similar, only the amplitude increases with increasing global warming. Surface temperature changes are warmer than 0.8 °C between 40° and 50°S for GWLs 1.5 °C and 2 °C and warmer than 1.2 °C for GWL 3 °C at the same latitudes. Surface temperature changes stay below 0.4 °C and 0.6 °C near the Antarctic, respectively for GWLs 2 °C and 3 °C.

The mean MHW intensity is 0.37 °C (± 0.037 °C, intermodel variability), 0.43 °C (± 0.050 °C) and 0.43 °C (± 0.050 °C), for GWLs 1.5 °C, 2 °C and 3 °C, respectively (Fig. 8). For GWL 1.5 °C, the most intense MHW are found in the subtropical region and north of the ACC (40°–45°S, 20°–90°E) varying between 0.5 °C and 0.6 °C. For GWLs 2 °C and 3 °C, mean MHW intensity between 40° and 50°S can be warmer than respectively 0.5 °C and 0.8 °C. For both warming trends and MHW characteristics, the patterns obtained here using GWLs are similar to the ones obtained using projections on fixed future periods (Section 3.2).

4. Discussion

4.1. Regional characteristics of temperature-related climatic impact-drivers

This study presents a regional analysis of current and projected trends of temperature-related climatic impact-drivers in the Southern Indian Ocean: temperature change, temperature-driven climate velocities and marine heatwaves (MHW). Our main findings can be summarized as follows.

Warming patterns are spatially heterogeneous in the region. Global ocean surface warming rates have been estimated at around 0.08 °C/decade between 1880 and 2022 (NOAA, 2023) and the IPCC

² https://unfccc.int/sites/default/files/english_paris_agreement.pdf.

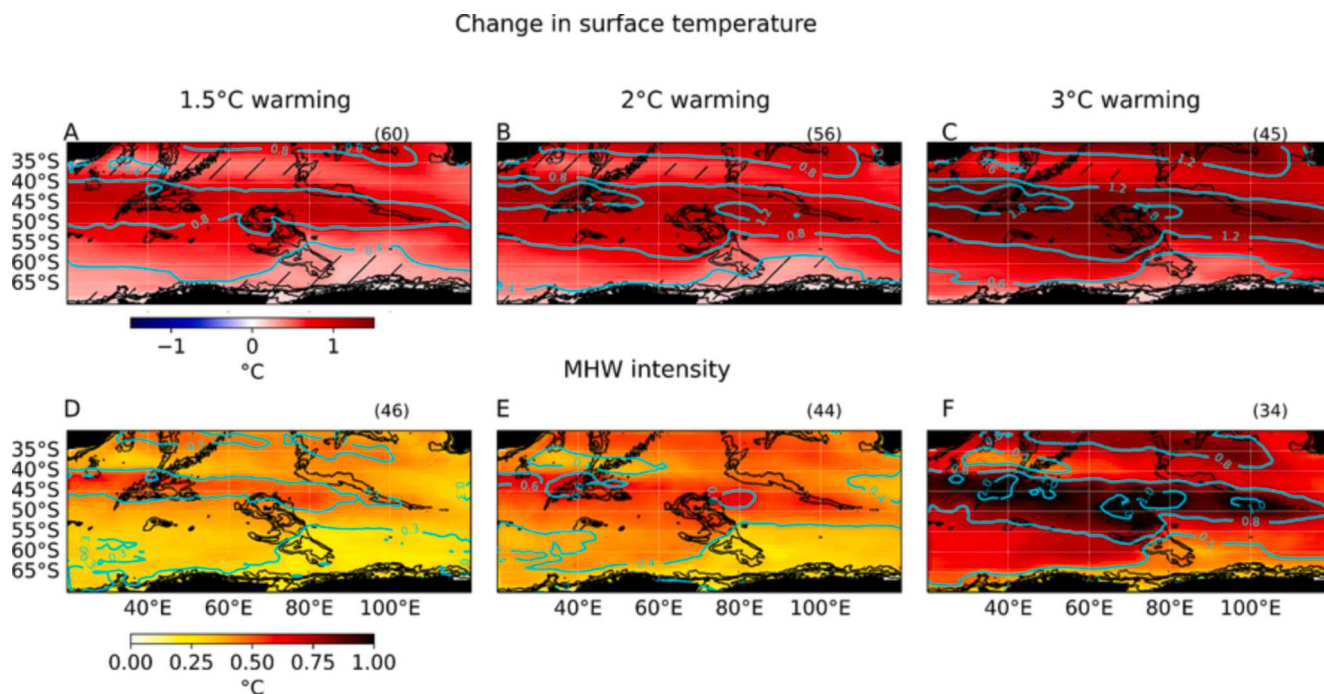


Fig. 8. Change in surface temperature for global warming levels (GWLs) 1.5 °C (A), 2 °C (B) and 3 °C (C) and mean MHW intensity for GWLs 1.5 °C (D), 2 °C (E) and 3 °C (F) warming world relative to the pre-industrial period (1850–1900) using a time-shift approach and CMIP6 mean ensembles. The number of simulations used (using SSP1-2.6, SSP2-4.5 and SSP5-8.5) in each case is indicated in parentheses. Contour lines of similar temperature change or MHW intensity are indicated in cyan. Stippling indicates areas where the intermodel standard deviation is higher than the mean value, suggesting a less robust output.

Assessment Report 6 has indicated a 0.60 °C increase in global SST from 1980 to 2020 (Fox-Kemper et al., 2021). In the Southern Indian Ocean, a greater warming north of the Antarctic Circumpolar Current (ACC) of around 0.11 °C/decade has been observed between 1950 and 2012, while cooling patterns have been observed near the Antarctic (Armour et al., 2016; Sallée, 2018). The mean warming trend here in the Southern Indian Ocean between 1982 and 2019 is lower, between 0.03 °C/decade and 0.07 °C/decade (Fig. 2, Supplementary Fig. S2). Observed warming trends are significant in the northern part of the region and east of Kerguelen Plateau and could vary between 0.1 and 0.3 °C/decade.

Climate velocities are faster over Kerguelen Plateau as compared to global ocean averages. The global ocean median climate velocity has been estimated around 13 km/decade over 1900–2010 (Sen Gupta et al., 2015) or 12 km/decade over 1955–2005 (Brito-Morales et al., 2020) at the surface and around 6.3 km/decade in the mesopelagic layer over 1955–2005 (200–1000 m). The mean surface climate velocity over the Southern Indian Ocean is found between 4.9 and 10.6 km/decade between 1982 and 2019 using OSTIA and OISST datasets. In particular, surface climate velocities are particularly fast over Heard and McDonalds Islands EEZ (20.3 km/decade, using OSTIA dataset; 44.0 km/decade, using OISST dataset), Saint-Paul and Amsterdam EEZ (12.9 km/decade; 24.4 km/decade) and Kerguelen EEZ (11.8 km/decade; 27.4 km/decade) while they are slower than global estimates or more variable over Crozet EEZ (-2.6 km/decade; 18.2 km/decade) and Prince Edward Islands EEZ (-5.8 km/decade; 5.9). Crozet and Prince Edward Islands EEZ are located in the area which seems to undergo a local cooling that could be associated with high temporal variability (Fig. 2, Supplementary Fig. S2). However, the analyses using IPSL-CM6A-LR members (see Sections 2.1.2 and 3.2.1) suggest that in the long term, radiative forcing will likely dominate warming trends compared to internal variability, and an important warming as well as fast climate velocities are projected over the Crozet Plateau (Section 3.2).

MHW events are particularly intense at the ACC northern boundary between 20°E and 95°E (north of the Kerguelen Plateau). The patterns of MHW mean intensity between 1984 and 2014 obtained

with the OSTIA dataset (Fig. 3) are consistent with past estimates (Su et al., 2021). However, zooming out from the northern part of the Kerguelen Plateau shows not only that the MHW are more intense at the northern boundary of the ACC, but also that MHW are generally more intense northward up to the subtropical zone. The global ocean mean intensity of MHW estimated from NOAA observations and defined as the anomaly of temperature compared to the 90th percentile threshold is around 0.35 °C (Plecha and Soares, 2020) when it can reach 1.2 °C north of Crozet EEZ.

Over the historical period, no significant spatial contrasts in mean annual MHW days are observed in the Southern Indian Ocean north of 60°S. The global ocean mean annual number of days affected by MHW has been estimated from around 30 days/year in 1900 to around 60 days/year in 2020 (Holbrook et al., 2020, using observations and models). Between 1984 and 2014 using OSTIA dataset, a mean number of around 24 days per year affected by MHW (90th percentile) is observed north of 60°S, with in average 23 annual MHW days over Kerguelen and Crozet EEZ (data not shown). South of 60°S, the mean annual MHW days is lower (16 days/year).

Five contrasted zones emerge. When comparing the projected regional characteristics of both warming and MHW characteristics (climatic impact-drivers), five zones (from the subtropics to the Antarctic continent) associated with specific dynamical features stand out relative to the level of change expected to occur (Fig. 9). The first (north of 35°S, subtropical region) and fourth (between 50°S and 55°S, southern part of the ACC) zones are affected by intermediate amplitudes of warming-related climatic impact-drivers. The second (between 35°S and 40°S, under the influence of the Agulhas Return Current) and fifth (south of 55°S, Antarctic colder water) zones have weaker warming and weaker changes in mean MHW intensity and in mean annual MHW days. Finally, the third zone (north of the ACC and covering subantarctic islands) is the one with the most important magnitudes of warming-related climatic impact-drivers, especially over topographic features: the Crozet Plateau, Kerguelen and the Southeastern ridge.

The projected mean MHW intensity might be underestimated in

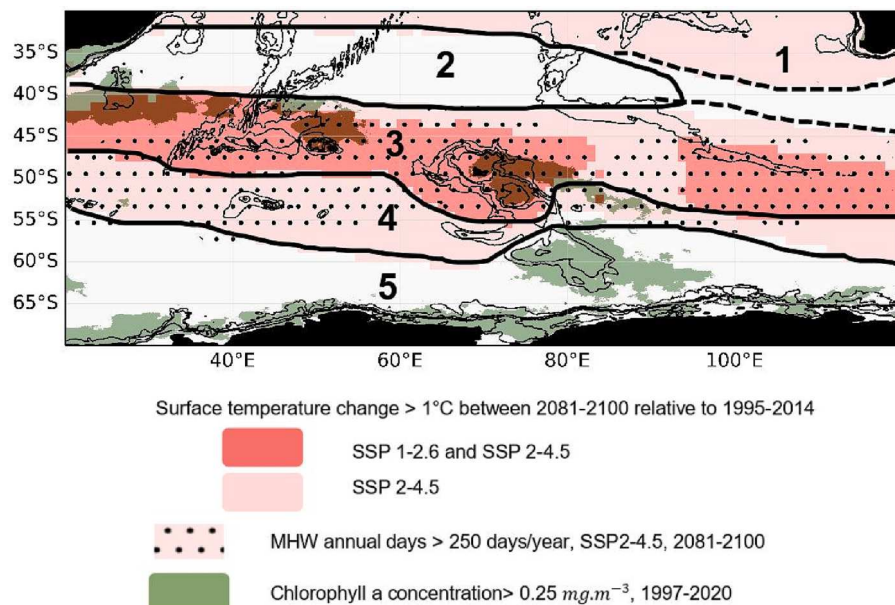


Fig. 9. Representation of the 5 zones identified in this study in terms of climatic impact-drivers' trends (warming and marine heatwaves) along with the identification of areas for which surface temperature increases by more than 1 °C at the end of the century relative to 1995–2014 under SSP1-2.6 and SSP2-4.5; and areas for which mean MHW annual days are higher than 250 day/year at the end of the century under SSP2-4.5 using CMIP6 models. Areas of chlorophyll *a* concentration greater than 0.25 mg.m⁻³ (using Copernicus-GlobColour product provided by ACRI-ST company, between 1997 and 2020) are identified in green to allow for comparison between spatialised climate trends and spatialised biological characteristics.

CMIP6. It can be noted that the projected mean MHW intensity might be underestimated, as it was found over the historical period relative to observations (Fig. 3) and in global studies using CMIP6 models (Pilo et al., 2019; Plecha and Soares, 2020). Since the observations suggest that the most intense MHW are related to mesoscale activity and that this mesoscale activity is not always well reproduced by climate models (Pilo et al., 2019; Su et al., 2021), but could be expected to intensify (Hogg et al., 2015; Patara et al., 2016; Martinez-Moreno et al., 2019; Martinez-Moreno et al., 2021), projections in terms of MHW intensity may be underestimated.

4.2. Implications of climate mitigation

This study also shows how regional patterns of temperature change and marine heatwaves can differ between SSP1-2.6 and SSP2-4.5. Not only can the magnitude of changes be mitigated in SSP1-2.6 but some patterns may be reversed at the end of the century, for instance through the surface cooling obtained around 35°S. However, the major differences between SSP1-2.6 and SSP2-4.5 mainly occurred in the long term.

The consequences of following one SSP instead of another can also be identified at the EEZ scale, both in terms of emerging trends and of magnitude of change. The projected changes in surface temperature over Saint-Paul and Amsterdam EEZ in SSP1-2.6 remain in the range of the observed interannual variability at that location, even in the long term, which is not the case for the other EEZs. Already in the mid term in SSP1-2.6 Crozet, Heard and McDonalds Islands, Kerguelen and Prince Edward Islands EEZ changes in surface temperature are found to be respectively 2.6, 2.5, 2.8 and 3.1 times higher than the observed (using OSTIA) interannual variability in sea surface temperature (Fig. 10). This indicates that emerging warming trends will also occur in a high mitigation scenario (SSP1-2.6) for subantarctic islands.

At the EEZ level, major differences between the two SSPs used in this study mainly occur in the long term. In the long term, the change in surface temperature is 0.62 °C, 0.49 °C, 0.58 °C, 0.65 °C and 0.43 °C warmer in SSP2-4.5 compared to SSP1-2.6 for Crozet, Heard and McDonalds Islands, Kerguelen, Prince Edward Islands and Saint-Paul and Amsterdam EEZ, respectively. In the long term, mean MHW intensity is 0.39 °C, 0.33 °C, 0.40 °C, 0.40 °C and 0.23 °C warmer in SSP2-4.5 compared to SSP1-2.6 for respectively Crozet, Heard and McDonalds Islands, Kerguelen, Prince Edward Islands and Saint-Paul and Amsterdam EEZ (Fig. 10).

This study therefore shows that the choice of a mitigation strategy and socio-economic development pathway can have direct regional consequences on climate change patterns in the long term, even at the scale of EEZs.

4.3. Coherence with known physical mechanisms and remaining questions

The aim here is to better understand the projected intensities and patterns of warming and marine heatwaves in the Southern Indian Ocean. This requires an evaluation of the models and a mechanistic understanding of the potential heat uptake and redistribution processes.

It can be firstly noted that CMIP6 models have improved compared to CMIP5 models for some key metrics in the Southern Ocean, such as the Antarctic Circumpolar Current (ACC) strength or the representation of differences in density across latitudes of the ACC (Beadling et al., 2020). In addition, the spatial patterns and interannual variability of MHW are better represented in CMIP6 compared to CMIP5 models, and more generally tend to be better represented in higher resolution climate models (Qiu et al., 2021).

There are at least three ways to evaluate a climate model: 1) to compare the model outputs to observation-based products, 2) to verify the agreement between multiple models and/or models' versions (this is done here by using an ensemble of models) and 3) to confront the projections to known physical mechanisms (Baumberger et al., 2017). Given the important role of natural variability for shaping the spatial patterns of historical warming trends, it is difficult to evaluate the quality of the CMIP6 ensemble in simulating warming trends in the Southern Indian Ocean by simply comparing them to past observations (Räaisaänen, 2007; Baumberger et al., 2017; Gopika et al., 2020). We therefore focus here on determining whether the projected patterns of warming and marine heatwaves are coherent with known or potential heat redistribution processes.

The intensity of the Southern Indian Ocean warming is not directly correlated to the intensity of global warming. The models used in our study have a wide range of Equilibrium Climate Sensitivities (ECS; defined as the long term global warming obtained after a doubling of the atmospheric CO₂ above its pre-industrial concentration; Charney et al., 1979; Forster et al., 2021). The ECS of the model ensemble we used in this study vary from 2.29 to 5.62 °C (Forster et al., 2021). However, no correlation was found between the mean ocean warming in the region and the model ECS, that is, models displaying greater warming are not

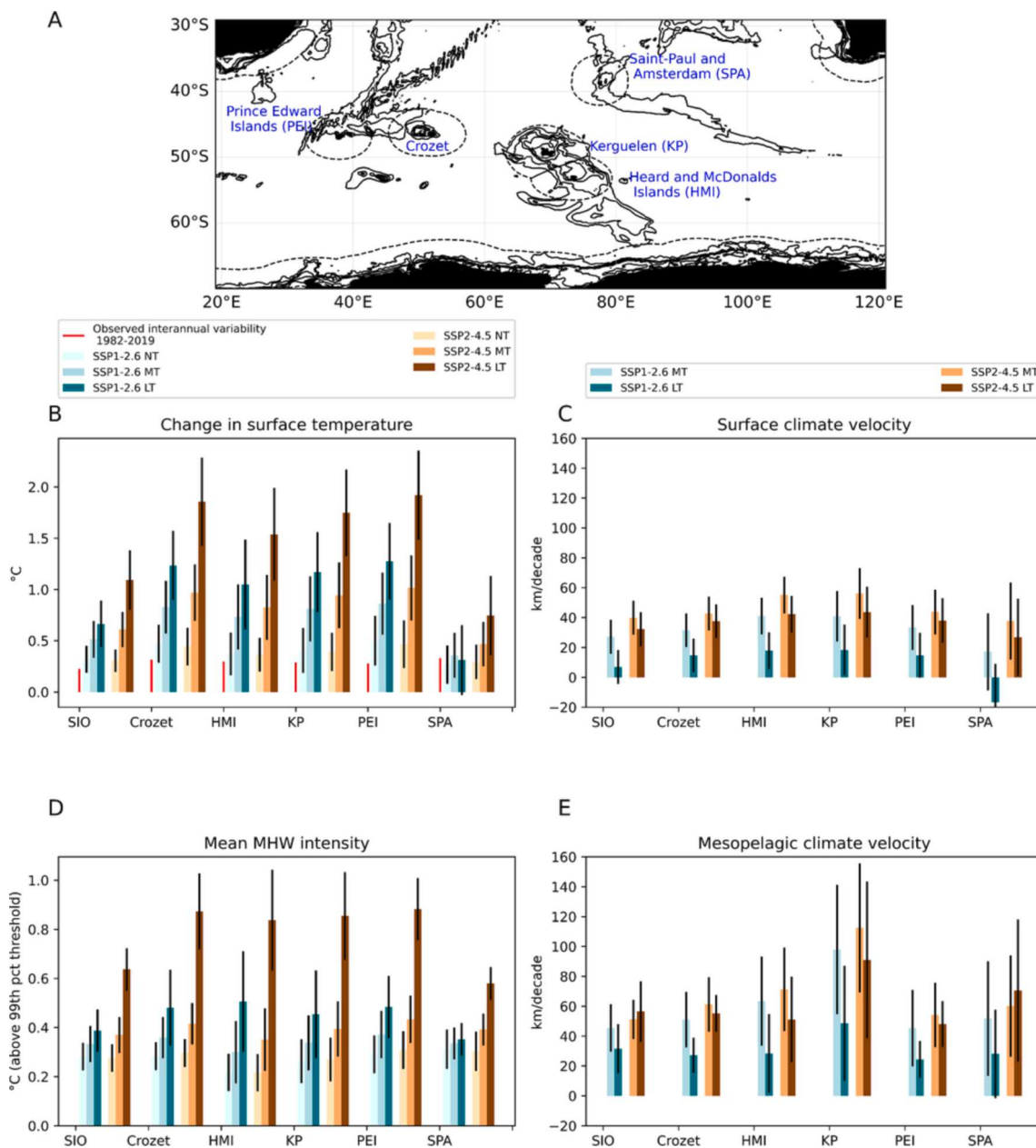


Fig. 10. Map of subtropical and subantarctic islands’ exclusive economic zones (EEZs) in the Southern Indian Ocean (A). Change in surface temperature relative to 1995–2014 (B), mean MHW intensity (D) and surface (C) and mesopelagic (E) climate velocities averaged over the Southern Indian Ocean (SIO) and different EEZs: Crozet, Heard and Mc Donalds Islands (HMI), Kerguelen (KP), Prince Edward Islands (PEI) and Saint-Paul and Amsterdam (SPA), for SSP1-2.6 and SSP2-4.5. Changes in surface temperature and mean MHW intensity are estimated over 2021–2040 (NT), 2041–2060 (MT) and 2081–2100 (LT). Climate velocities were estimated over 2015–2065 (MT) and 2050–2100 (LT). Change in surface temperature results are compared to the observed interannual variability in sea surface temperature in each location calculated from the OSTIA dataset between 1982 and 2019.

necessarily the ones with greater ECS (data not shown), suggesting that the regional warming in the Southern Indian Ocean is sensitive to local processes, reproduced differently in different models. It is therefore particularly important to investigate whether the projected warming and marine heatwaves patterns in the Southern Indian Ocean can be explained by known physical processes active in the region.

The coherence of the projected patterns of warming-related climatic impact-drivers with known or potential heat redistribution processes is discussed here to both assess the adequacy of the models (Baumberger et al., 2017) and understand their main physical drivers.

4.3.1. The impact of winds and local circulation on warming-related climatic impact-drivers’ patterns

CMIP6 projections, either through the traditional or the time-shift approaches (i.e. using GWLs, see Section 2.1.2), suggest an intensification of MHW and warming mostly in the region of influence of the ACC, in the subantarctic latitudinal band between 40° and 55°S. Such result is consistent with the observed increased heat uptake in the subpolar region transported northward by Ekman transport and subducted within and north of the ACC (Armour et al., 2016; Frölicher et al., 2015; Morrison et al., 2016; Sallée, 2018; Huguenin et al., 2022). The strength of this northward Ekman transport is modulated by the position and strength of the westerlies which is particularly strong over the Indian sector of the Southern Ocean (Lin et al., 2018). The westerlies are

expected to intensify and to shift poleward (Lee et al., 2021) and thus the associated northward transport of heat content anomaly (anomaly caused by warming) may be strengthened, accumulating heat over the subantarctic (Swart et al., 2019; Fox-Kemper et al., 2021; Silvy et al., 2022). In addition, southward heat transport also occur through eddy advection, partly compensating the Ekman northward heat transport (Farneti et al., 2010; Saenko et al., 2018), but there are still uncertainties on the degree of this compensation (Fox-Kemper et al., 2021).

Another pattern that stands out in this study is the lesser intensification of warming and marine heatwaves between 35° and 40°S. This latitudinal band is mostly under the influence of the Agulhas Current system, which consists in the Agulhas Current, a western boundary current flowing southward along the African coast, which brings warm waters into the Indian Ocean at around 40°S through the Agulhas Return Current up to 70°E (Lutjeharms, 2006). The remaining waters are transported to the South Atlantic between 32°S and 42°S and this westward inflow of relatively warm and salty water exiting the Indian sector is called the Agulhas leakage (Schmidt et al., 2021). Projections from global climate models suggest an increase in Agulhas leakage (Rouault et al., 2009; Backeberg et al., 2012; Biastoch and Böning, 2013), and a decrease of Agulhas Current transport by 11–23 % at the end of the century (Stellema et al., 2019; Ma et al., 2020; Sen Gupta et al., 2021). If we assume that the decreasing Agulhas Current feeds both the increasing Agulhas leakage and the Agulhas Return Current, and that the Agulhas Current is the main source of water for the Agulhas Return Current, then the Agulhas Return Current would have to decrease. A decreasing Agulhas Return Current would slow down a large heat transport source in the northern part of the Southern Indian Ocean, which could potentially explain the lesser warming projected in this area.

The Agulhas Current system transport is also modulated by the position and strength of the westerlies. Indeed, an equatorward shift of the westerlies (as observed in summer in SSP1-2.6, Bracegirdle et al., 2020) can be associated with an increase of the Agulhas leakage (Durgadoo et al., 2013).

Latitudinal differences in projected warming trends and climate velocities seem therefore consistent with known mechanisms in the region. In particular, the position and strength of the westerlies can have a different effect on a specific zone, depending on how westerlies impact the local circulation.

4.3.2. Remaining questions: On the role of unresolved spatial scales and modes of variability

The projected trends in warming and marine heatwaves therefore seem consistent with potential mechanisms of heat uptake and transport but some key questions remain. Uncertainties remain concerning the role of the ocean mesoscale circulation and the role of the decadal and longer variability.

Finer scale processes (meso- and submesoscale) have the potential to impact warming trends. Eddies can play a significant role in meridional heat transport (Morrison et al., 2016) and can for instance contribute to modulate heat uptake through submesoscale ventilation (Dove et al., 2021). Increased upward heat transport at submesoscale fronts can also alter surface heat uptake capacity (Siegelman et al., 2020) but the impact of such a process on warming trends locally is yet to be studied. In a changing climate with intensifying winds, it is expected that mesoscale activity might change (Martinez-Moreno et al., 2019; Martinez-Moreno et al., 2021). However, it remains unclear how such changes might also impact the projected warming trends. To investigate whether resolution could play a role in determining the patterns of projected temperature changes, we focus on two models, GFDL-CM4 and MPI-ESM1-2-HR with a resolution of 0.25° and 0.4° respectively. As for the model ensemble, a pattern of greater surface warming over the subantarctic is observed (Supplementary Fig. S8). This suggests that the influence of smaller scale processes on the warming patterns may remain limited, at least for the larger eddies represented in higher

resolution CMIP6 models. The net impact of eddies on the heat budget and how it will evolve under climate change remain an active field of research (Hewitt et al., 2022).

Internal variability is not negligible in the Southern Indian ocean between 1982 and 2019 but it is challenging to evaluate whether the representation of decadal and multidecadal variability modes and their interaction with the local circulation in the models is accurate. The Southern Indian Ocean is indeed under the influence of various modes of natural variability but depending on the time scale of interest, for instance for policy-makers, different modes of natural variability are to be considered. The Indian Ocean Subtropical Dipole (IOSD) and the El-Niño-Southern Oscillation (ENSO) can influence patterns of SST anomaly (Behera and Yamagata, 2001; Huang and Shukla, 2008; Morioka et al., 2010) on decadal timescales and the Southern Annular Mode (SAM) on even shorter timescales (Sallée et al., 2010). As the above-mentioned climatic modes of variability may not be in the same phase in reality and in the climate models, this increases the uncertainty on near-term climate projections (Hurrell et al., 2010; Chen et al., 2021).

Multidecadal variability may also not be negligible in the Southern Indian Ocean and could potentially impact projected trends on longer timescales (Zhang et al., 2018). Indeed, the natural variability observed in this study is important over a 37-year period. The east/west contrast obtained in the observations (Section 3.1.1) could result from the response to the positive-to-negative phase transition of the Atlantic Multidecadal Variability (AMV) but the teleconnection processes associated may not be well represented in climate models (Chung et al., 2022). There are therefore uncertainties on how natural modes of variability and their interactions with the local circulation will evolve, and whether they will enhance, buffer or mask the projected changes.

4.4. Potential impacts on ecosystems

Using the warming-related climatic impact-drivers regional characteristics, it is then important to make the link with the regional ecological characteristics. Here, based on the observed and projected trends in warming and MHW and based on knowledge on the ecology of the Southern Indian Ocean, examples of potential impacts are discussed.

Climate change might induce a shift in habitats for various species, thus potentially affecting the distribution of species with conservation and/or economic values (Reisinger et al., 2022). The region studied here covers three biogeochemical provinces (i.e. oceanographically and ecologically relatively homogeneous regions) as defined by Reygondeau et al., 2020, distributed latitudinally from north to south: the South Subtropical convergence, the Subantarctic water ring and the Antarctic (Reygondeau et al., 2020). Our results suggest that, as far as temperature interactions are concerned, a poleward shift of these provinces is expected and this shift is shown to be faster for the mesopelagic layer compared to the surface with potential ecological impacts for species living across multiple depth layers throughout their life cycle. Such shift between surface and mesopelagic conditions is particularly relevant for the Saint-Paul and Amsterdam region which is currently located at the transition between different bioregions: the South subtropical convergence in the north and the Subantarctic water ring in the south. By the end of the century, the temperature conditions south of Saint-Paul and Amsterdam EEZ will probably be similar to the ones in the south subtropical convergence province. For the north of the EEZ, the mesopelagic layer temperature conditions will shift faster and could be similar to the ones in the Indian South Subtropical Gyre province. Our study helps identifying other areas that could be undergoing an important shift between surface and mesopelagic conditions and therefore where long term biophysical monitoring could be of special interest: the north-western side of Kerguelen Plateau, slightly up to the southern part of the Crozet Plateau which has been identified as a foraging zone for top predators (e.g. Pütz, 2002).

The consequences of the long term shift of thermal conditions in top predators' foraging zones are anticipated by extreme events in the near

term (or in the past). The 1997 MHW that occurred in the northern part of the Southern Indian Ocean has been associated with a southward shift of the Polar Front south of the Crozet Plateau where king penguins (*Aptenodytes patagonicus*) from Crozet islands usually forage. The temperature anomaly was so intense and associated with such a major shift of the foraging zones that these zones were barely accessible to the penguins leading to important mortality of those populations (Bost et al., 2015). Over the whole region, the mean MHW intensity of this event remained greater than 0.5 °C for 36 days (obtained using OSTIA dataset). Given models projections it appears that such a drastic event may no longer be an extreme phenomenon and if associated with a significant shift in the Polar Front position, it could lead to systematic mass mortality events for top predators.

Intermediate levels of the food webs can also be affected by warming and MHW. Indeed, some populations of fish are already living at the edge of their thermal tolerance. Low-antarctic (i.e. just south of the Antarctic Polar Front) species can live in conditions above their upper optimal range of temperature (1 °C–1.5 °C) but further increases in temperature may become too physiologically demanding, especially as the intensification projected appears to occur over their distribution areas (Kock and Everson, 2003).

Besides, a whole range of MHW potential impacts in the Southern Indian Ocean has not yet been covered. Such impacts could include primary production changes (Hayashida et al., 2020), changes in species growth and abundance (Oliver, 2019; Smale and Wernberg, 2013), changes in population structure (Smale et al., 2017), behavioral changes, notably for reproduction and foraging (Fromant et al., 2021), changes in geographic distributions of species (Cure et al., 2017; Smale and Wernberg, 2013) or even genetic changes (e.g., Coleman et al., 2020). These impacts are yet to be studied in the Southern Indian Ocean.

4.5. Climate change and conservation

A regionalisation of temperature-related climatic impact-drivers, associated with further research on climate change impacts on ecosystems, should contribute to the further consideration of climate change impacts in conservation design and management. Increasing literature aims at addressing this issue and suggests management tools to help integrate climate resilience into MPA design (Tittensor et al., 2019; Crespo et al., 2020). However, efforts are needed to identify the risks posed by climate change at the regional scale. Our study of warming-related climatic impact-drivers mostly addresses the hazards dimension of a risk assessment (which would also include an analysis of the vulnerability and exposure of ecosystems, Chen et al., 2021) and points out the need to include the vertical analysis in the eco regionalisation process, since different layer depths may be impacted differently. In particular, this study shows that the relative difference between mesopelagic and surface climate velocity (a « climatic vertical shear ») is highest over Kerguelen Plateau and Saint-Paul and Amsterdam EEZ under both scenarios while it is the lowest over Heard and McDonalds Islands and Prince Edward Islands EEZ (Fig. 10). Yet, mesopelagic climate velocities over Heard and McDonalds Islands and Prince Edward Islands EEZ are still between 20 and 30 % faster than surface climate velocities in SSP2-4.5; and respectively between 50 % and 60 % and between 35 % and 66 % faster in SSP1-2.6 (Fig. 10).

The 3D information provided by climate velocity could be further used to project potential changes in marine biodiversity distribution and help inform conservation management (Arafah-Dalmau et al., 2021). Through this type of methodology, other concepts related to climate velocity can be used to understand the impact of climate change on species distribution, notably i) climate residence time (Loarie et al., 2009) and ii) climate refugia (Burrows et al., 2014; Brito-Morales et al., 2018). Indeed, it can be useful to know not only if certain environmental conditions will be found and where but also how long these conditions will last in a specific area (climate residence time, Loarie et al., 2009). The concept of climate refugia aims to identify areas that are relatively

less impacted by climate change, meaning low climate velocity and/or long climate residence time (Brito-Morales et al., 2018), but it can also be based on the time of emergence of the climate change signal to identify temporary refugia (Bruno et al., 2018). This concept could guide the development of surveillance programs to follow the evolution of environmental conditions on specific zones that are particularly affected by climatic impact-drivers. Climate velocity could also be used to anticipate future expansions of species and to check if current MPA networks cover these expansions (Arafah-Dalmau et al., 2021). Note that, to be even more biologically meaningful, climate velocity should be combined with other constraints of dispersion such as habitat permeability or connectivity (Brito-Morales et al., 2018). It may also be important to consider multiple variables such as pH (acidification), primary production or zooplankton abundance, since the interaction between multiple variables changes can result in multi-directional distribution shifts (e.g., VanDerWal et al., 2013).

From the characterisation of warming and marine heatwaves patterns presented here, it is difficult to identify potential climate refugia. However, this study pinpoints areas that are scientifically interesting to further study the impacts of climate change on ecosystems, for instance the area south of Crozet near the Antarctic Polar Front and Saint-Paul and Amsterdam EEZ. Indeed, the area south of Crozet, in the main zone of intensification identified in this study, is an important foraging zone for top predators (e.g. Pütz, 2002) and is expected to undergo intense warming and increases in MHW intensity and duration but it is also an area that can be subject to important natural variability (as seen on Fig. 2). It can therefore be very interesting to study whether this variability in the long term will be enough to counteract warming trends and whether ecosystems in this area compared to similar ecosystems east of the Kerguelen Plateau (at the same latitudes) will develop different features as a response to different changing conditions. The Saint-Paul and Amsterdam area can also be interesting to protect for further scientific investigation on how the difference between surface and mesopelagic temperature changes might affect endemic ecosystems.

5. Conclusion

The aim of this work is to provide a systematic description of observed and future temperature changes and marine heatwaves over the entire Southern Indian Ocean and to compare the projections over this region under two scenarios that reflect two possible socio-economic pathways.

This analysis shows the spatial heterogeneity of temperature trends and marine heatwaves characteristics at the regional scale, highlighting also some limits. The projected warming trends appear to be consistent with warming mechanisms identified in the literature, notably related to the dynamic of the ACC and the intensification and shifts of westerly winds. Concerning MHW intensity pattern, a better spatial fit between the observations and the models was obtained, although intensities may be underestimated in the models, mainly because of resolution limits, and current spatial patterns of MHW intensity are expected to intensify.

This intensification of both warming and marine heatwaves characteristics is expected to occur mostly over the subantarctic islands, with consequences on endemic species and ecosystems that are still to be further studied. It can be noted that the difference between SSP1-2.6 and SSP2-4.5 projections are mostly significant in the long term, with changes in both scenarios that could be important for ecosystems already in the near and mid term, highlighting the need to anticipate adaptation measures. Such measures would need to also consider that surface and deeper conditions may evolve at different pace.

Through a regional example, this study also reaffirms the need to globally commit to strong mitigation strategies and to follow a sustainable socio-economic development pathway to alleviate the potential impacts of warming and MHW.

Declaration of Competing Interest

The authors declare that they have no known competing financial interests or personal relationships that could have appeared to influence the work reported in this paper.

Data availability

This study used already publicly available data (see references in text).

Acknowledgements

We acknowledge the World Climate Research Programme's Working Group on Coupled Modelling, that is responsible for CMIP. The authors also thank the IPSL modelling group for the software infrastructure, which facilitated CMIP analysis. We acknowledge funding support from CNES, France and from the program LEFE led by CNRS-INSU, France (projects KERTREND and KERTREND-SAT). C.A. was financially supported by the French Ministry of Ecological Transition. A.P. acknowledges the financial support of the Project Concytec - World Bank "Characterization and forecast of extreme events in the Peruvian sea using an operational system of oceanic information", through its executing unit Fondo Nacional de Desarrollo Científico, Tecnológico y de Innovación Tecnológica (Fondecyt). L.B. acknowledges funding from the European Union's Horizon 2020 research and innovation program under grant agreement no. 820989 (project COMFORT).

Appendix A. Supplementary material

Supplementary data to this article can be found online at <https://doi.org/10.1016/j.pocan.2023.103036>.

References

- Andrews, M.B., Ridley, J.K., Wood, R.A., Andrews, T., Blockley, E.W., Booth, B., Burke, E., Dittus, A.J., Florek, P., Gray, L.J., Haddad, S., Hardiman, S.C., Hermanson, L., Hodson, D., Hogan, E., Jones, G.S., Knight, J.R., Kuhlbrodt, T., Misios, S., Mizieliński, M.S., Ringer, M.A., Robson, J., Sutton, R.T., 2020. Historical simulations with HadGEM3-GC3.1 for CMIP6 e2019MS001995. *J. Adv. Model. Earth Syst.* 12 (6) <https://doi.org/10.1029/2019MS001995>.
- Arafteh-Dalmau, N., Brito-Morales, I., Schoeman, D.S., Possingham, H.P., Klein, C.J., Richardson, A.J., 2021. Incorporating climate velocity into the design of climate-smart networks of marine protected areas. In: *Methods in Ecology and Evolution*. <https://doi.org/10.1111/2041-210X.13675>.
- Armour, K.C., Marshall, J., Scott, J.R., Donohoe, A., Newsom, E.R., 2016. Southern Ocean warming delayed by circumpolar upwelling and equatorward transport. *Nat. Geosci.* 9 (7), 549–554. <https://doi.org/10.1038/ngeo2731>.
- Auger, M., Morrow, R., Kesteven, E., Sallée, J.-B., Cowley, R., 2021. Southern Ocean in situ temperature trends over 25 years emerge from interannual variability. *Nat. Commun.* 12 (1), 514. <https://doi.org/10.1038/s41467-020-20781-1>.
- Backeberg, B., Penven, P., Rouault, M., 2012. Impact of intensified Indian Ocean winds on mesoscale variability in the Agulhas system. *Nat. Clim. Chang.* 2, 608–612. <https://doi.org/10.1038/nclimate1587>.
- Ban, N.C., Maxwell, S.M., Dunn, D.C., Hobday, A.J., Bax, N.J., Ardron, J., Gjerde, K.M., Game, E.T., Devillers, R., Kaplan, D.M., Dunstan, P.K., Halpin, P.N., Pressey, R.L., 2014. Better integration of sectoral planning and management approaches for the interlinked ecology of the open oceans. *Mar. Policy* 49, 127–136. <https://doi.org/10.1016/j.marpol.2013.11.024>.
- Banzon, V., Smith, T.M., Chin, T.M., Liu, C., Hankins, W., 2016. A long-term record of blended satellite and in situ sea-surface temperature for climate monitoring, modeling and environmental studies. *Earth Syst. Sci. Data* 8 (1), 165–176. <https://doi.org/10.5194/essd-8-165-2016>.
- Baumberger, C., Knutti, R., Hirsch Hadorn, G., 2017. Building confidence in climate model projections: an analysis of inferences from fit. *WIREs Clim. Change* 8 (3), e454.
- Beadling, R.L., Russell, J.L., Stouffer, R.J., Mazloff, M., Talley, L.D., Goodman, P.J., Sallée, J.B., Hewitt, H.T., Hyder, P., Pandde, A., 2020. Representation of southern ocean properties across coupled model intercomparison project generations: CMIP3 to CMIP6. *J. Clim.* 33 (15), 6555–6581. <https://doi.org/10.1175/JCLI-D-19-0970.1>.
- Behera, S.K., Yamagata, T., 2001. Subtropical SST dipole events in the southern Indian Ocean. *Geophys. Res. Lett.* 28 (2), 327–330. <https://doi.org/10.1029/2000GL011451>.
- Belchier, M., Collins, M.A., 2008. Recruitment and body size in relation to temperature in juvenile Patagonian toothfish (*Dissostichus eleginoides*) at South Georgia. *Mar. Biol.* 155, 493–503. <https://doi.org/10.1007/s00227-008-1047-3>.
- Bi, D., Dix, M., Marsland, S., O'Farrell, S., Sullivan, A., Bodman, R., Law, R., Harman, I., Sribnovsky, J., Rashid, H.A., Dobrohotoff, P., Mackallah, C., Yan, H., Hirst, A., Savita, A., Dias, F.B., Woodhouse, M., Fiedler, R., Heerdegen, A., 2020. Configuration and spin-up of ACCESS-CM2, the new generation Australian Community Climate and Earth System Simulator Coupled Model. *J. Southern Hemisphere Earth Syst. Sci.* 70 (1), 225–251. <https://doi.org/10.1071/ES19040>.
- Biaostoch, A., Böning, C.W., 2013. Anthropogenic impact on Agulhas leakage. *Geophys. Res. Lett.* 40, 1138–1143. <https://doi.org/10.1002/grl.50243>.
- Bonnet, R., Boucher, O., Deshayes, J., Gastineau, G., Hourdin, F., Mignot, J., Servonnat, J., Swingedouw, D., 2021. Presentation and evaluation of the IPSL-CM6A-LR ensemble of extended historical simulations. *J. Adv. Model. Earth Syst.* 13, e2021MS002565 <https://doi.org/10.1029/2021MS002565>.
- Bost, C.A., Cotté, C., Terray, P., Barbraud, C., Bon, C., Delord, K., Gimenez, O., Handrich, Y., Naito, Y., Guinet, C., Weimerskirch, H., 2015. Large-scale climatic anomalies affect marine predator foraging behaviour and demography. *Nat. Commun.* 6 (1), 8220. <https://doi.org/10.1038/ncomms9220>.
- Boucher, O., Servonnat, J., Albright, A.L., Aumont, O., Balkanski, Y., Bastrikov, V., Bekki, S., Bonnet, R., Bony, S., Bopp, L., Braconnot, P., Brockmann, P., Cadule, P., Caubel, A., Cheruy, F., Codron, F., Cozic, A., Cugnet, D., D'Andrea, F., Davini, P., de Lavergne, C., Denvil, S., Deshayes, J., Devillers, M., Ducharne, A., Dufresne, J.-L., Dupont, E., Éthé, C., Fairhead, L., Falletti, L., Flavoni, S., Foujols, M.-A., Gardoll, S., Gastineau, G., Ghattas, J., Grandpeix, J.-Y., Guenet, B., Guez, L.E., Guilyardi, E., Guimberteau, M., Hauglustaine, D., Hourdin, F., Idelkadi, A., Joussaume, S., Kageyama, M., Khodri, M., Krinner, G., Lebas, N., Levassasseur, G., Lévy, C., Li, L., Lott, F., Lurton, T., Luyssaert, S., Madec, G., Madeleine, J.-B., Maignan, F., Marchand, M., Marti, O., Mellul, L., Meurdesoif, Y., Mignot, J., Musat, I., Ottlé, C., Peylin, P., Planton, Y., Polcher, J., Rio, C., Rochetin, N., Rousset, C., Sepulchre, P., Sima, A., Swingedouw, D., Thiéblemont, R., Traore, A.K., Vancoppenolle, M., Vial, J., Vialard, J., Viovy, N., Vuichard, N., 2020. Presentation and evaluation of the IPSL-CM6A-LR climate model e2019MS002010. *J. Adv. Model. Earth Syst.* 12 (7) <https://doi.org/10.1029/2019MS002010>.
- Bracegirdle, T.J., Krinner, G., Tonelli, M., Haumann, F.A., Naughten, K.A., Rackow, T., Roach, L.A., Wainer, I., 2020. Twenty first century changes in Antarctic and Southern Ocean surface climate in CMIP6. *Atmos. Sci. Lett.* 21, e984.
- Brito-Morales, I., García Molinos, J., Schoeman, D.S., Burrows, M.T., Poloczanska, E.S., Brown, C.J., Ferrier, S., Harwood, T.D., Klein, C.J., McDonald-Madden, E., Moore, P. J., Pandolfi, J.M., Watson, J.E.M., Wenger, A.S., Richardson, A.J., 2018. Climate velocity can inform conservation in a warming world. *Trends Ecol. Evol.* 33 (6), 441–457. <https://doi.org/10.1016/j.tree.2018.03.009>.
- Brito-Morales, I., Schoeman, D.S., Molinos, J.G., Burrows, M.T., Klein, C.J., Arafteh-Dalmau, N., Kaschner, K., Garilao, C., Kesner-Reyes, K., Richardson, A.J., 2020. Climate velocity reveals increasing exposure of deep-ocean biodiversity to future warming. *Nat. Clim. Chang.* 10 (6), 576–581. <https://doi.org/10.1038/s41558-020-0773-5>.
- Bruno, J.F., Bates, A.E., Cacciapaglia, C., Pike, E.P., Amstrup, S.C., van Hooi donk, R., Henson, S.A., Aronson, R.B., 2018. Climate change threatens the world's marine protected areas. *Nat. Clim. Chang.* 8 (6), 499–503. <https://doi.org/10.1038/s41558-018-0149-2>.
- Burrows, M.T., Schoeman, D.S., Richardson, A.J., Molinos, J.G., Hoffmann, A., Buckley, L.B., Moore, P.J., Brown, C.J., Bruno, J.F., Duarte, C.M., Halpern, B.S., Hoegh-Guldberg, O., Kappel, C.V., Kiessling, W., O'Connor, M.I., Pandolfi, J.M., Parmesan, C., Sydeman, W.J., Ferrier, S., Williams, K.J., Poloczanska, E.S., 2014. Geographical limits to species-range shifts are suggested by climate velocity. *Nature* 507 (7493), 492–495. <https://doi.org/10.1038/nature12976>.
- Butt, N., Possingham, H.P., De Los Rios, C., Maggini, R., Fuller, R.A., Maxwell, S.L., Watson, J.E.M., 2016. Challenges in assessing the vulnerability of species to climate change to inform conservation actions. *Biol. Conserv.* 199, 10–15. <https://doi.org/10.1016/j.biocon.2016.04.020>.
- Cao, J., Ma, L., Liu, F., Chai, J., Zhao, H., He, Q., Wang, B., Bao, Y., Li, J., Yang, Y., Deng, H., Wang, B., 2021. NUIST ESM v3 data submission to CMIP6. *Adv. Atmos. Sci.* 38 (2), 268–284. <https://doi.org/10.1007/s00376-020-0173-9>.
- Carr, M.H., Woodson, C.B., Cheriton, O.M., Malone, D., McManus, M.A., Raimondi, P.T., 2011. Knowledge through partnerships: integrating marine protected area monitoring and ocean observing systems. *Front. Ecol. Environ.* 9 (6), 342–350. <https://doi.org/10.1890/0909096>.
- Charney, J.G., Arakawa, A., Baker, D.J., Bolin, B., Dickinson, R.E., Goody, R.M., Leith, C. E., Stommel, H.M., Wunsch, C.I., 1979. Carbon dioxide and climate: a scientific assessment. *Climate Res. Board* 13.
- Chen, D., Rojas, M., Samset, B.H., Cobb, K., Diongue Niang, A., Edwards, P., Emori, S., Faria, S.H., Hawkins, E., Hope, P., Huybrechts, P., Meinshausen, M., Mustafa, S.K., Plattner, G.-K., Tréguier, A.-M., 2021. Framing, context, and methods. In: Masson-Delmotte, V., Zhai, P., Pirani, A., Connors, S.L., Péan, C., Berger, S., Caud, N., Chen, Y., Goldfarb, L., Gomis, M.I., Huang, M., Leitzell, K., Lonnoy, E., Matthews, J.B.R., Maycock, T.K., Waterfield, T., Yelekçi, O., Yu, R., Zhou, B. (Eds.), *Climate Change 2021: The Physical Science Basis. Contribution of Working Group I to the Sixth Assessment Report of the Intergovernmental Panel on Climate Change*. Cambridge University Press, Cambridge, United Kingdom and New York, NY, USA, pp. 147–286. doi: 10.1017/9781009157896.003.
- Cherchi, A., Fogli, P.G., Lovato, T., Peano, D., Iovino, D., Gualdi, S., Masina, S., Scoccimarro, E., Materia, S., Bellucci, A., Navarra, A., 2019. Global mean climate and main patterns of variability in the CMCC-CM2 coupled model. *J. Adv. Model. Earth Syst.* 11 (1), 185–209. <https://doi.org/10.1029/2018MS001369>.

- Christian, J.R., Denman, K.L., Hayashida, H., Holdsworth, A.M., Lee, W.G., Riche, O.G.J., Shao, A.E., Steiner, N., Swart, N.C., 2021. Ocean biogeochemistry in the Canadian Earth System Model version 5.0.3: CanESM5 and CanESM5-CanOE. *Geoscientific Model Development Discussions*, 1–68. doi: 10.5194/gmd-2021-327.
- Chung, E.-S., Kim, S.-J., Timmermann, A., Ha, K.-J., Lee, S.-K., Stuecker, M.F., Rodgers, K.B., Lee, S.-S., Huang, L., 2022. Antarctic sea-ice expansion and Southern Ocean cooling linked to tropical variability. *Nat. Clim. Chang.* 12 (5), 461–468. <https://doi.org/10.1038/s41558-022-01339-z>.
- Coleman, M.A., Minne, A.J.P., Vranken, S., Wernberg, T., 2020. Genetic tropicalisation following a marine heatwave. *Sci. Rep.* 10 (1), 12726. <https://doi.org/10.1038/s41598-020-69665-w>.
- Collins, M.A., Brickley, P., Brown, J., Belchier, M., 2010. Chapter four - the Patagonian toothfish: biology, ecology and fishery. In: Lesser, M. (Ed.), *Advances in Marine Biology*, Vol. 58, pp. 227–300. Academic Press. doi: 10.1016/B978-0-12-381015-1.00004-6.
- Constable, A.J., Melbourne-Thomas, J., Corney, S.P., Arrigo, K.R., Barbraud, C., Barnes, D.K.A., Bindoff, N.L., Boyd, P.W., Brandt, A., Costa, D.P., Davidson, A.T., Ducklow, H.W., Emmerson, L., Fukuchi, M., Gutt, J., Hindell, M.A., Hofmann, E.E., Hosie, G.W., Iida, T., Jacob, S., Johnston, N.M., Kawaguchi, S., Kokubun, N., Koubbi, P., Lea, M.-A., Makhado, A., Massom, R.A., Meiners, K., Meredith, M.P., Murphy, E.J., Nicol, S., Reid, K., Richerson, K., Riddle, M.J., Rintoul, S.R., Smith Jr., W.O., Southwell, C., Stark, J.S., Sumner, M., Swadling, K.M., Takahashi, K. T., Trathan, P.N., Welsford, D.C., Weimerskirch, H., Westwood, K.J., Wienecke, B.C., Wolf-Gladrow, D., Wright, S.W., Xavier, J.C., Ziegler, P., 2014. Climate change and Southern Ocean ecosystems I: How changes in physical habitats directly affect marine biota. *Glob. Chang. Biol.* 20 (10), 3004–3025. <https://doi.org/10.1111/gcb.12623>.
- Cooley, S., Schoeman, D., Bopp, L., Boyd, P., Donner, S., Ghebrehiwet, D.Y., Ito, S.-I., Kiessling, W., Martinetto, P., Ojea, E., Racault, M.-F., Rost, B., Skern-Mauritzen, M., 2022. Oceans and coastal ecosystems and their services. In: Pörtner, H.-O., Roberts, D.C., Tignor, M., Poloczanska, E.S., Mintenbeck, K., Alegría, A., Craig, M., Langsdorf, S., Löschke, S., Möller, V., Okem, A., Rama, B. (Eds.), *Climate Change 2022: Impacts, Adaptation and Vulnerability. Contribution of Working Group II to the Sixth Assessment Report of the Intergovernmental Panel on Climate Change*. Cambridge University Press, Cambridge, UK and New York, NY, USA, pp. 379–550. doi: 10.1017/9781009325844.005.
- Cotté, C., Ariza, A., Berne, A., Habasque, J., Lebourges-Dhaussy, A., Roudaut, G., Espinasse, B., Hunt, B.P.V., Pakhomov, E.A., Henschke, N., Péron, C., Conchon, A., Koedooder, C., Izard, L., Chérel, Y., 2022. Macrozooplankton and micronekton diversity and associated carbon vertical patterns and fluxes under distinct productive conditions around the Kerguelen Islands. *J. Mar. Syst.* 226, 471–492. <https://doi.org/10.1016/B978-0-12-391851-2.00018-0>.
- Crespo, G.O., Mossop, J., Dunn, D., Gjerde, K., Hazen, E., Reygondeau, G., Warner, R., Tittensor, D., Halpin, 2020. Beyond static spatial management: Scientific and legal considerations for dynamic management in the high seas. *Mar. Policy* 122, 104102. <https://doi.org/10.1016/j.marpol.2020.104102>.
- Cure, K., Hobbs, J.-P.-A., Langlois, T.J., Abdo, D.A., Bennett, S., Harvey, E.S., 2017. Distributional responses to marine heat waves: insights from length frequencies across the geographic range of the endemic reef fish *Chaerodon rubescens*. *Mar. Biol.* 165 (1), 1. <https://doi.org/10.1007/s00227-017-3259-x>.
- Danabasoglu, G., Lamarque, J.-F., Bacmeister, J., Bailey, D.A., DuVivier, A.K., Edwards, J., Emmons, L.K., Fasullo, J., Garcia, R., Gettelman, A., Hannay, C., Holland, M.M., Large, W.G., Lauritzen, P.H., Lawrence, D.M., Lenaerts, J.T.M., Lindsay, K., Lipscomb, W.H., Mills, M.J., Neale, R., Oleson, K.W., Otto-Bliessen, B., Phillips, A.S., Sacks, W., Tilmes, S., van Kampenhou, L., Versteijn, M., Bertini, A., Dennis, J., Deser, C., Fischer, C., Fox-Kemper, B., Kay, J.E., Kinnison, D., Kushner, P. J., Larson, V.E., Long, M.C., Mickelson, S., Moore, J.K., Nienhouse, E., Polvani, L., Rasch, P.J., Strand, W.G., 2020. The Community Earth System Model Version 2 (CESM2) e2019MS001916. *J. Adv. Model. Earth Syst.* 12 (2) <https://doi.org/10.1029/2019MS001916>.
- Della Penna, A., Koubbi, P., Cotté, C., Bon, C., Bost, C.-A., d'Ovidio, F., 2017. Lagrangian analysis of multi-satellite data in support of open ocean Marine Protected Area design. *Fut. Oceanic Anim. Changing Ocean* 140, 212–221. <https://doi.org/10.1016/j.dsr2.2016.12.014>.
- Delord, K., Barbraud, C., Bost, C.-A., Chérel, Y., Guinet, C., Weimerskirch, H., 2014. Atlas of top predators from French Southern Territories in the Southern Indian Ocean (p. http://www.cebc.cnrs.fr/ecommm/Fr_ecomm/ecommm_ecor_OI1.html) [Research Report]. CNRS. doi: 10.15474/AtlasTopPredatorsOI.CEBC.CNRS_FrenchSouthernTerritories.
- Dijkstra, H., 2016. A normal mode perspective of intrinsic ocean-climate variability. *Annu. Rev. Fluid Mech.* 48 (1), 341–363. <https://doi.org/10.1146/annurev-fluid-122414-034506>.
- Donohue, K.A., Tracey, K.L., Watts, D.R., Chidichimo, M.P., Chereskin, T.K., 2016. Mean antarctic circumpolar current transport measured in Drake Passage. *Geophys. Res. Lett.* 43, 11760–11767. <https://doi.org/10.1002/2016GL070319>.
- Döscher, R., Acosta, M., Alessandri, A., Anthoni, P., Arsouze, T., Bergman, T., Bernardello, R., Boussetta, S., Caron, L.-P., Carver, G., Castrillo, M., Catalano, F., Cvijanovic, I., Davini, P., Dekker, E., Doblas-Reyes, F. J., Docquier, D., Echevarria, P., Fladrich, U., Fuentes-Franco, R., Gröger, M., v. Hardenberg, J., Hieronymus, J., Karami, M. P., Keskinen, J.-P., Koenigk, T., Makkonen, R., Massonnet, F., Ménégot, M., Miller, P. A., Moreno-Chamorro, E., Nieradzki, L., van Noije, T., Nolan, P., O'Donnell, D., Ollinaho, P., van den Oord, G., Ortega, P., Prims, O. T., Ramos, A., Reerink, T., Roussot, C., Ruprich-Robert, Y., Le Sager, P., Schmitt, T., Schröder, R., Serva, F., Sicardi, V., Sloth Madsen, M., Smith, B., Tian, T., Tourigny, E., Uotila, P., Vancoppenolle, M., Wang, S., Wärlind, D., Willén, U., Wyser, K., Yang, S., Yepes-Arbós, X., Zhang, Q., 2022. The EC-Earth3 Earth system model for the Coupled Model Intercomparison Project 6. *Geosci. Model Dev.* 15, 2973–3020. <https://doi.org/10.5194/gmd-15-2973-2022>.
- Dove, L.A., Thompson, A.F., Balwada, D., Gray, A.R., 2021. Observational evidence of ventilation hotspots in the Southern Ocean. *e2021JC017178 J. Geophys. Res. Oceans* 126 (7). <https://doi.org/10.1029/2021JC017178>.
- Dunne, J.P., Horowitz, L.W., Adcroft, A.J., Ginoux, P., Held, I.M., John, J.G., Krasting, J. P., Malyshev, S., Naik, V., Paulot, F., Shevliakova, E., Stock, C.A., Zadeh, N., Balaji, V., Blanton, C., Dunne, K.A., Dupuis, C., Durachta, J., Dussin, R., Gauthier, P. P.G., Griffies, S.M., Guo, H., Hallberg, R.W., Harrison, M., He, J., Hurlin, W., McHugh, C., Menzel, R., Milly, P.C.D., Nikonov, S., Paynter, D.J., Ploshay, J., Radhakrishnan, A., Rand, K., Reichl, B.G., Robinson, T., Schwarzkopf, D.M., Sentman, L.T., Underwood, S., Vahlenkamp, H., Winton, M., Wittenberg, A.T., Wyman, B., Zeng, Y., Zhao, M., 2020. The GFDL Earth System Model Version 4.1 (GFDL-ESM 4.1): overall coupled model description and simulation characteristics e2019MS002015. *J. Adv. Model. Earth Syst.* 12 (11) <https://doi.org/10.1029/2019MS002015>.
- Durgadoo, J.V., Loveday, B.R., Reason, C.J.C., Penven, P., Biastoch, A., 2013. Agulhas leakage predominantly responds to the southern hemisphere westerlies. *J. Phys. Oceanogr.* 43 (10), 2113–2131. <https://doi.org/10.1175/JPO-D-13-047.1>.
- Eyring, V., Bony, S., Meehl, G.A., Senior, C.A., Stevens, B., Stouffer, R.J., Taylor, K.E., 2016. Overview of the Coupled Model Intercomparison Project Phase 6 (CMIP6) experimental design and organization. *Geosci. Model Dev.* 9 (5), 1937–1958. <https://doi.org/10.5194/gmd-9-1937-2016>.
- Farneti, R., Delworth, T.L., Rosati, A.J., Griffies, S.M., Zeng, F., 2010. The role of mesoscale eddies in the rectification of the southern ocean response to climate change. *J. Phys. Oceanogr.* 40 (7), 1539–1557. <https://doi.org/10.1175/2010JPO4353.1>.
- Forster, P., Storelvmo, T., Armour, K., Collins, W., Dufresne, J.-L., Frame, D., Lunt, D.J., Mauritsen, T., Palmer, M.D., Watanabe, M., Wild, M., Zhang, H., 2021. The Earth's Energy Budget, Climate Feedbacks, and Climate Sensitivity. In: Masson-Delmotte, V., Zhai, P., Pirani, A., Connors, S.L., Péan, C., Berger, S., Caud, N., Chen, Y., Goldfarb, L., Gomis, M.I., Huang, M., Leitzell, K., Lonnoy, E., Matthews, J.B.R., Maycock, T.K., Waterfield, T., Yelekçi, O., Yu, R., Zhou, B. (Eds.), *Climate Change 2021: The Physical Science Basis. Contribution of Working Group I to the Sixth Assessment Report of the Intergovernmental Panel on Climate Change*. Cambridge University Press, Cambridge, United Kingdom and New York, NY, USA, pp. 923–1054. doi: 10.1017/9781009157896.009.
- Fox-Kemper, B., Hewitt, H.T., Xiao, C., Aalgeirsdóttir, G., Drijfhout, S.S., Edwards, T.L., Golledge, N.R., Hemer, M., Kopp, R.E., Krinner, G., Mix, A., Notz, D., Nowicki, S., Nurhati, I.S., Ruiz, L., Sallée, J.-B., Slangen, A.B.A., Yu, Y., 2021. Ocean, cryosphere and sea level change. In: Masson-Delmotte, V., Zhai, P., Pirani, A., Connors, S.L., Péan, C., Berger, S., Caud, N., Chen, Y., Goldfarb, L., Gomis, M.I., Huang, M., Leitzell, K., Lonnoy, E., Matthews, J.B.R., Maycock, T.K., Waterfield, T., Yelekçi, O., Yu, R., Zhou, B. (Eds.), *Climate Change 2021: The Physical Science Basis. Contribution of Working Group I to the Sixth Assessment Report of the Intergovernmental Panel on Climate Change*. Cambridge University Press, Cambridge, United Kingdom and New York, NY, USA, pp. 1211–1362. doi: 10.1017/9781009157896.011.
- Fricko, O., Havlik, P., Rogelj, J., Klimont, Z., Gusti, M., Johnson, N., Kolp, P., Strubegger, M., Valin, H., Amann, M., Ermolova, T., Forsell, N., Herrero, M., Heyes, C., Kindermann, G., Krey, V., McCollum, D.L., Obersteiner, M., Pachauri, S., Rao, S., Schmid, E., Schoepp, W., Riahi, K., 2017. The marker quantification of the Shared Socioeconomic Pathway 2: A middle-of-the-road scenario for the 21st century. *Global Environ. Chang.* 42, 251–267. <https://doi.org/10.1016/j.gloenvcha.2016.06.004>.
- Frölicher, T.L., Sarmiento, J.L., Paynter, D.J., Dunne, J.P., Krasting, J.P., Winton, M., 2015. Dominance of the southern ocean in anthropogenic carbon and heat uptake in CMIP5 models. *J. Clim.* 28 (2), 862–886. <https://doi.org/10.1175/JCLI-D-14-00117.1>.
- Frölicher, T.L., Fischer, E.M., Gruber, N., 2018. Marine heatwaves under global warming. *Nature* 560 (7718), 360–364. <https://doi.org/10.1038/s41586-018-0383-9>.
- Fromant, A., Delord, K., Bost, C.-A., Eizenberg, Y. H., Botha, J. A., Chérel, Y., Bustamante, P., Gardner, B. R., Braut-Favrou, M., Lec'hvien, A., Arnould, J.P.Y., 2021. Impact of extreme environmental conditions: foraging behaviour and trophic ecology responses of a diving seabird, the common diving petrel. *Prog. Oceanogr.* 198, 102676. doi: 10.1016/j.poccean.2021.102676.
- García Molinos, J., Halpern, B., Schoeman, D., Brown, C.J., Kiessling, W., Moore, P.J., Pandolfi, J.M., Poloczanska, E.S., Richardson, A.J., Burrows, M.T., 2016. Climate velocity and the future global redistribution of marine biodiversity. *Nat. Clim. Chang.* 6, 83–88. <https://doi.org/10.1038/nclimate2769>.
- Good, S., Fiedler, E., Mao, C., Martin, M.J., Maycock, A., Reid, R., Roberts-Jones, J., Searle, T., Waters, J., While, J., Worsfold, M., 2020. The current configuration of the OSTIA system for operational production of foundation sea surface temperature and ice concentration analyses. *Remote Sens. (Basel)* 12 (4), 720. <https://doi.org/10.3390/rs12040720>.
- Gopika, S., Izumo, T., Vialard, J., Lengaigne, M., Suresh, I., Kumar, M.R.R., 2020. Aliasing of the Indian Ocean externally-forced warming spatial pattern by internal climate variability. *Clim. Dyn.* 54 (1–2), 1093–1111. <https://doi.org/10.1007/s00382-019-05049-9>.
- Hajima, T., Watanabe, M., Yamamoto, A., Tatebe, H., Noguchi, M.A., Abe, M., Ohgaito, R., Ito, A., Yamazaki, D., Okajima, H., Ito, A., Takata, K., Ogochi, K., Watanabe, S., Kawamiya, M., 2020. Development of the MIROC-ES2L Earth system model and the evaluation of biogeochemical processes and feedbacks. *Geosci. Model Dev.* 13 (5), 2197–2244. <https://doi.org/10.5194/gmd-13-2197-2020>.
- Haumann, F.A., Gruber, N., Münnich, M., 2020. Sea-ice induced southern ocean subsurface warming and surface cooling in a warming climate. *AGU Adv.* 1 (2), e2019AV000132 <https://doi.org/10.1029/2019AV000132>.

- Hausfather, Z., Peters, G.P., 2020. Emissions – the ‘business as usual’ story is misleading. *Nature* 577 (7792), 618–620. <https://doi.org/10.1038/d41586-020-00177-3>.
- Hayashida, H., Matar, R.J., Strutton, P.G., Zhang, X., 2020. Insights into projected changes in marine heatwaves from a high-resolution ocean circulation model. *Nat. Commun.* 11 (1), 4352. <https://doi.org/10.1038/s41467-020-18241-x>.
- Held, I.M., Guo, H., Adcroft, A., Dunne, J.P., Horowitz, L.W., Krasting, J., Shevliakova, E., Winton, M., Zhao, M., Bushuk, M., Wittenberg, A.T., Wyman, B., Xiang, B., Zhang, R., Anderson, W., Balaji, V., Donner, L., Dunne, K., Durachta, J., Gauthier, P.P.G., Ginoux, P., Golaz, J.-C., Griffies, S.M., Hallberg, R., Harris, L., Harrison, M., Hurlin, W., John, J., Lin, P., Lin, S.-J., Malyshev, S., Menzel, R., Milly, P.C.D., Ming, Y., Naik, V., Paynter, D., Paulot, F., Ramaswamy, V., Reichl, B., Robinson, T., Rosati, A., Seman, C., Silvers, L.G., Underwood, S., Zadeh, N., 2019. Structure and performance of GFDL’s CM4.0 climate model. *J. Adv. Model. Earth Syst.* 11 (11), 3691–3727. <https://doi.org/10.1029/2019MS001829>.
- Heger, N., Sanderson, B.M., Knutti, R., 2015. Improved pattern scaling approaches for the use in climate impact studies. *Geophys. Res. Lett.* 42, 3486–3494. <https://doi.org/10.1002/2015GL063569>.
- Hewitt, H., Fox-Kemper, B., Pearson, B., Roberts, M., Klocke, D., 2022. The small scales of the ocean may hold the key to surprises. *Nat. Clim. Chang.* 12, 496–499. <https://doi.org/10.1038/s41558-022-01386-6>.
- Hobday, A.J., Alexander, L.V., Perkins, S.E., Smale, D.A., Straub, S.C., Oliver, E.C.J., Benthuyssen, J.A., Burrows, M.T., Donat, M.G., Feng, M., Holbrook, N.J., Moore, P.J., Scannell, H.A., Sen Gupta, A., Wernberg, T., 2016. A hierarchical approach to defining marine heatwaves. *Prog. Oceanogr.* 141, 227–238. <https://doi.org/10.1016/j.pocean.2015.12.014>.
- Hogg, A.M., Meredith, M.P., Chambers, D.P., Abrahamson, E.P., Hughes, C.W., Morrison, A.K., 2015. Recent trends in the Southern Ocean eddy field. *J. Geophys. Res. Oceans* 120 (1), 257–267. <https://doi.org/10.1002/2014JC010470>.
- Holbrook, N.J., Sen Gupta, A., Oliver, E.C.J., Hobday, A.J., Benthuyssen, J.A., Scannell, H.A., Smale, D.A., Wernberg, T., 2020. Keeping pace with marine heatwaves. *Nat. Rev. Earth Environ.* 1 (9), 482–493. <https://doi.org/10.1038/s43017-020-0068-4>.
- Huang, B., Shukla, J., 2008. Interannual variability of the South Indian Ocean in observations and a coupled model. *Indian J. Mar. Sci.* 37 (1), 23.
- Huguenin, M.F., Holmes, R.M., England, M.H., 2022. Drivers and distribution of global ocean heat uptake over the last half century. *Nat. Commun.* 13, 4921. <https://doi.org/10.1038/s41467-022-32540-5>.
- Hunt, B.P.V., Pakhomov, E.A., McQuaid, C.D., 2001. Short-term variation and long-term changes in the oceanographic environment and zooplankton community in the vicinity of a sub-Antarctic archipelago. *Mar. Biol.* 138, 369–381. <https://doi.org/10.1007/s002270000467>.
- Hurrell, J.W., Delworth, T., Danabasoglu, G., Drange, H., Griffies, S., Holbrook, N., Kirtman, B., Keenlyside, N., Latif, M., Marotzke, J., Meehl, G.A., 2010. Decadal climate prediction: opportunities and challenges. *OceanObs’09. Sustained Ocean Observations and Information for Society* 521–533.
- IPCC, 2022. Summary for policymakers. In: Shukla, P.R., Skea, J., Slade, R., Al Khourdajie, A., van Diemen, R., McCollum, D., Pathak, M., Some, S., Vyas, P., Fradera, R., Belkacemi, M., Hasija, A., Lisboa, G., Luz, S., Malley, J. (Eds.), *Climate Change 2022: Mitigation of Climate Change. Contribution of Working Group III to the Sixth Assessment Report of the Intergovernmental Panel on Climate Change*. Cambridge University Press, Cambridge, UK and New York, NY, USA. doi: 10.1017/9781009157926.001.
- Jones, K.R., Watson, J.E.M., Possingham, H.P., Klein, C.J., 2016. Incorporating climate change into spatial conservation prioritisation: a review. *Biol. Conserv.* 194, 121–130. <https://doi.org/10.1016/j.biocon.2015.12.008>.
- Kock, K.-H., Everson, I., 2003. Shedding new light on the life cycle of mackerel icefish in the Southern Ocean. *J. Fish Biol.* 63 (1), 1–21. <https://doi.org/10.1046/j.1095-8649.2003.00150.x>.
- Kostianoy, A.G., Ginzburg, A.I., Frankignoulle, M., Delille, B., 2004. Fronts in the Southern Indian Ocean as inferred from satellite sea surface temperature data. *J. Mar. Syst.* 45 (1), 55–73. <https://doi.org/10.1016/j.jmarsys.2003.09.004>.
- Kuhlbrodt, T., Jones, C.G., Sellar, A., Storkey, D., Blockley, E., Stringer, M., Hill, R., Graham, T., Ridley, J., Blaker, A., Calvert, D., Copsey, D., Ellis, R., Hewitt, H., Hyder, P., Ineson, S., Mulcahy, J., Sahaan, A., Walton, J., 2018. The low-resolution version of HadGEM3 GC3.1: development and evaluation for global climate. *J. Adv. Model. Earth Syst.* 10 (11), 2865–2888. <https://doi.org/10.1029/2018MS001370>.
- Kwiatkowski, L., Torres, O., Bopp, L., Aumont, O., Chamberlain, M., Christian, J.R., Dunne, J.P., Gehlen, M., Ilyina, T., John, J.G., Lenton, A., Li, H., Lovenduski, N.S., Orr, J.C., Palmieri, J., Santana-Falcón, Y., Schwingler, J., Séférian, R., Stock, C.A., Tagliabue, A., Takano, Y., Tjiputra, J., Toyama, K., Tsujino, H., Watanabe, M., Yamamoto, A., Yool, A., Ziehn, T., 2020. Twenty-first century ocean warming, acidification, deoxygenation, and upper-ocean nutrient and primary production decline from CMIP6 model projections. *Biogeosciences* 17 (13), 3439–3470. <https://doi.org/10.5194/bg-17-3439-2020>.
- Lee, J.-Y., Marotzke, J., Bala, G., Cao, L., Corti, S., Dunne, J.P., Engelbrecht, F., Fischer, E., Fyfe, J.C., Jones, C., Maycock, A., Mutemi, J., Ndiaye, O., Panickal, S., Zhou, T., 2021. Future global climate: scenario-based projections and near-term information. In: Masson-Delmotte, V., Zhai, P., Pirani, A., Connors, S.L., Péan, C., Berger, S., Caud, N., Chen, Y., Goldfarb, L., Gomis, M.I., Huang, M., Leitzell, K., Lonnoy, E., Matthews, J.B.R., Maycock, T.K., Waterfield, T., Yelekçi, O., Yu, R., Zhou, B. (Eds.), *Climate Change 2021: The Physical Science Basis. Contribution of Working Group I to the Sixth Assessment Report of the Intergovernmental Panel on Climate Change*. Cambridge University Press, Cambridge, United Kingdom and New York, NY, USA, pp. 553–672. doi: 10.1017/9781009157896.006.
- Lin, X., Zhai, X., Wang, Z., Munday, D.R., 2018. Mean, variability, and trend of southern ocean wind stress: role of wind fluctuations. *J. Clim.* 31 (9), 3557–3573. <https://doi.org/10.1175/JCLI-D-17-0481.1>.
- Llavel, W., Terray, L., 2016. Observed southern upper-ocean warming over 2005–2014 and associated mechanisms. *Environ. Res. Lett.* 11 (12), 124023. <https://doi.org/10.1088/1748-9326/11/12/124023>.
- Loarie, S.R., Duffy, P.B., Hamilton, H., Asner, G.P., Field, C.B., Ackerly, D.D., 2009. The velocity of climate change. *Nature* 462 (7276), 1052–1055. <https://doi.org/10.1038/nature08649>.
- Lovato, T., Peano, D., Butenschön, M., Matera, S., Iovino, D., Scoccimarro, E., Fogli, P. G., Cherchi, A., Bellucci, A., Gualdi, S., Masina, S., Navarra, A., 2022. CMIP6 simulations with the CMCC earth system model (CMCC-ESM2). e2021MS002814 *J. Adv. Model. Earth Syst.* 14 (3). <https://doi.org/10.1029/2021MS002814>.
- Lutjeharms, J.R.E. (Ed.), 2006. The Agulhas return flow. In: *The Agulhas Current*, pp. 209–231. Springer. doi: 10.1007/3-540-37212-1-7.
- Ma, J., Feng, M., Lan, J., Hu, D., 2020. Projected future changes of meridional heat transport and heat balance of the Indian Ocean. *Geophys. Res. Lett.* 47 (4), e2019GL086803.
- Makhado, A.B., Lowther, A., Koubbi, P., Ansoerg, I., Brooks, C., Cotté, C., Crawford, R., Dlusia, S., d’Ovidio, F., Fawcett, S., Freeman, D., Grant, S., Huggett, J., Hindell, M., Hulley, P.A., Kirkman, S., Lamont, T., Lombard, M., Masothla, M.J., Lea, M.-A., Oosthuizen, W.C., Orgeret, F., Reisinger, R., Samaai, T., Sergi, S., Swadling, K., Somhlaba, S., Van de Putte, A., Von de Meden, C., Yemane, D., 2019. Expert Workshop on Pelagic Spatial Planning for the eastern subantarctic region (Domains 4, 5 and 6). SC-CAMLR-38/BG/29.
- Martínez-Moreno, J., Hogg, A.M., Kiss, A.E., Constantinou, N.C., Morrison, A.K., 2019. Kinetic energy of eddy-like features from sea surface altimetry. *J. Adv. Model. Earth Syst.* 11 (10), 3090–3105. <https://doi.org/10.1029/2019MS001769>.
- Martínez-Moreno, J., Hogg, A.M., England, M.H., Constantinou, N.C., Kiss, A.E., Morrison, A.K., 2021. Global changes in oceanic mesoscale currents over the satellite altimetry record. *Nat. Clim. Chang.* 11 (5), 397–403. <https://doi.org/10.1038/s41558-021-01006-9>.
- Matsuno, K., Wallis, J.R., Kawaguchi, S., Bestley, S., Swadling, K.M., 2020. Zooplankton community structure and dominant copepod population structure on the southern Kerguelen Plateau during summer 2016. *Deep-Sea Res. II* 174, 104788. <https://doi.org/10.1016/j.dsr2.2020.104788>.
- Mauritsen, T., Bader, J., Becker, T., Behrens, J., Bittner, M., Brokopf, R., Brovkin, V., Claussen, M., Crueger, T., Esch, M., Fast, I., Fiedler, S., Fläschner, D., Gayler, V., Giorgetta, M., Goll, D.S., Haak, H., Hagemann, S., Hedemann, C., Hohenegger, G., Ilyina, T., Jahns, T., Jimenez-de-la-Cuesta, D., Jungclaus, J., Kleinen, T., Kloster, S., Kracher, D., Kinne, S., Kleberg, D., Lasslop, G., Kornblueh, L., Marotzke, J., Matei, D., Meraner, K., Mikolajewicz, U., Modali, K., Möbis, B., Müller, W.A., Nabel, J.E.M.S., Nam, C.C.W., Notz, D., Nyawira, S.-S., Paulsen, H., Peters, K., Pincus, R., Pohlmann, H., Pongratz, J., Popp, M., Raddatz, T.J., Rast, S., Redler, R., Reick, C.H., Rohrschneider, T., Schemann, V., Schmidt, H., Schnur, R., Schulzweida, U., Six, K.D., Stein, L., Stemmler, I., Stevens, B., von Storch, J.-S., Tian, F., Voigt, A., Vrese, P., Wieners, K.-H., Wilkenskeld, S., Winkler, A., Roeckner, E., 2019. Developments in the MPI-ESM Earth System Model version 1.2 (MPI-ESM1.2) and Its Response to Increasing CO₂. *J. Adv. Model. Earth Syst.* 11 (4), 998–1038. <https://doi.org/10.1029/2018MS001400>.
- Maxwell, S.M., Gjerde, K.M., Connors, M.G., Crowder, L.B., 2020. Mobile protected areas for biodiversity on the high seas. *Science* 367 (6475), 252–254. <https://doi.org/10.1126/science.aaz9327>.
- Meredith, M., Sommerkorn, M., Cassotta, S., Derksen, C., Ekaykin, A., Hollowed, A., Kofinas, G., Mackintosh, A., Melbourne-Thomas, J., Muelbert, M.M.C., Ottersen, G., Pritchard, H., Schuur, E.A.G., 2019. Polar regions. In: Pörtner, H.-O., Roberts, D.C., Masson-Delmotte, V., Zhai, P., Tignor, M., Poloczanska, E., Mintenbeck, K., Alegría, A., Nicolai, M., Okem, A., Petzold, J., Rama, B., Weyer, N.M. (Eds.), *IPCC Special Report on the Ocean and Cryosphere in a Changing Climate*. Cambridge University Press, Cambridge, UK and New York, NY, USA, pp. 203–320. doi: 10.1017/9781009157964.005.
- Mishra, R.K., Naik, R.K., Venkataramana, V., Jena, B., Anilkumar, N., Soares, M.A., Sarkar, A., Singh, A., 2020. Phytoplankton biomass and community composition in the front zones of Southern Ocean. *Deep-Sea Res. II* 178, 104799. <https://doi.org/10.1016/j.dsr2.2020.104799>.
- Morioka, Y., Tozuka, T., Yamagata, T., 2010. Climate variability in the southern Indian Ocean as revealed by self-organizing maps. *Clim. Dyn.* 35, 1059–1072. <https://doi.org/10.1007/s00382-010-0843-x>.
- Morrison, A.K., Griffies, S.M., Winton, M., Anderson, W.G., Sarmiento, J.L., 2016. Mechanisms of southern ocean heat uptake and transport in a global eddy climate model. *J. Clim.* 29 (6), 2059–2075. <https://doi.org/10.1175/JCLI-D-15-0579.1>.
- Müller, W.A., Jungclaus, J.H., Mauritsen, T., Baehr, J., Bittner, M., Budich, R., Bunzel, F., Esch, M., Ghosh, R., Haak, H., Ilyina, T., Kleinen, T., Kornblueh, L., Li, H., Modali, K., Notz, D., Pohlmann, H., Roeckner, E., Stemmler, I., Tian, F., Marotzke, J., 2018. A higher-resolution version of the Max Planck Institute earth system model (MPI-ESM1.2-HR). *J. Adv. Model. Earth Syst.* 10 (7), 1383–1413. <https://doi.org/10.1029/2017MS001217>.
- NOAA National Centers for Environmental Information, 2023. State of the Climate: Global Climate Report for 2022. Accessed January 18, 2023, from <https://www.ncei.noaa.gov/access/monitoring/monthly-report/global/202213>.
- O’Neill, B.C., Tebaldi, C., van Vuuren, D.P., Eyring, V., Friedlingstein, P., Hurtt, G., Knutti, R., Kriegler, E., Lamarque, J.-F., Lowe, J., Meehl, G.A., Moss, R., Riahi, K., Sanderson, B.M., 2016. The scenario model intercomparison project (ScenarioMIP) for CMIP6. *Geosci. Model Dev.* 9 (9), 3461–3482. <https://doi.org/10.5194/gmd-9-3461-2016>.
- O’Neill, B.C., Kriegler, E., Ebi, K.L., Kemp-Benedict, E., Riahi, K., Rothman, D.S., van Ruijven, B.J., van Vuuren, D.P., Birkmann, J., Kok, K., Levy, M., Solecki, W., 2017. The roads ahead: narratives for shared socioeconomic pathways describing world

- Venkataramana, V., Anilkumar, N., Swadling, K., Mishra, R.K., Tripathy, S.C., Sarkar, A., Augusta, S.M., Sabu, P., Pillai, H., 2020. Distribution of zooplankton in the Indian sector of the Southern Ocean. *Antarct. Sci.* 32 (3), 168–179. <https://doi.org/10.1017/S0954102019000579>.
- Vivier, F., Park, Y.-H., Sekma, H., Le Sommer, J., 2015. Variability of the Antarctic Circumpolar Current transport through the Fawn Trough, Kerguelen Plateau. *Deep-Sea Res. II* 114, 12–26. <https://doi.org/10.1016/j.dsr2.2014.01.017>.
- Voldoire, A., Saint-Martin, D., Sénési, S., Decharme, B., Alias, A., Chevallier, M., Colin, J., Guérémy, J.-F., Michou, M., Moine, M.-P., Nabat, P., Roehrig, R., Salas y Méliá, D., Séférian, R., Valcke, S., Beau, I., Belamari, S., Berthet, S., Cassou, C., Cattiaux, J., Deshayes, J., Douville, H., Ethé, C., Franchistéguy, L., Geoffroy, O., Lévy, C., Madec, G., Meurdesoif, Y., Msadek, R., Ribes, A., Sanchez-Gomez, E., Terray, L., Waldman, R., 2019. Evaluation of CMIP6 DECK Experiments With CNRM-CM6-1. *J. Adv. Model. Earth Syst.* 11 (7), 2177–2213. <https://doi.org/10.1029/2019MS001683>.
- Wiens, J.A., Bachelet, D., 2010. Matching the multiple scales of conservation with the multiple scales of climate change. *Conserv. Biol.* 24 (1), 51–62. <https://doi.org/10.1111/j.1523-1739.2009.01409.x>.
- Wilson, K.L., Tittensor, D.P., Worm, B., Lotze, H.K., 2020. Incorporating climate change adaptation into marine protected area planning. *Glob. Chang. Biol.* 26 (6), 3251–3267. <https://doi.org/10.1111/gcb.15094>.
- Wu, T., Lu, Y., Fang, Y., Xin, X., Li, L., Li, W., Jie, W., Zhang, J., Liu, Y., Zhang, L., Zhang, F., Zhang, Y., Wu, F., Li, J., Chu, M., Wang, Z., Shi, X., Liu, X., Wei, M., Huang, A., Zhang, Y., Liu, X., 2019. The Beijing Climate Center Climate System Model (BCC-CSM): The main progress from CMIP5 to CMIP6. *Geosci. Model Dev.* 12 (4), 1573–1600. <https://doi.org/10.5194/gmd-12-1573-2019>.
- Yang, C., Leonelli, F.E., Marullo, S., Artale, V., Beggs, H., Nardelli, B.B., Chin, T.M., Toma, V.D., Good, S., Huang, B., Merchant, C.J., Sakurai, T., Santoleri, R., Vazquez-Cuervo, J., Zhang, H.-M., Pisano, A., 2021. Sea surface temperature intercomparison in the framework of the Copernicus Climate Change Service (C3S). *J. Clim.* 34 (13), 5257–5283. <https://doi.org/10.1175/JCLI-D-20-0793.1>.
- Yukimoto, S., Kawai, H., Koshiro, T., Oshima, N., Yoshida, K., Urakawa, S., Tsujino, H., Deushi, M., Tanaka, T., Hosaka, M., Yabu, S., Yoshimura, H., Shindo, E., Mizuta, R., Obata, A., Adachi, Y., Ishii, M., 2019. The Meteorological Research Institute Earth System Model version 2.0, MRI-ESM2.0: Description and basic evaluation of the physical component. *J. Meteorol. Soc. Jpn* 97, 931–965. <https://doi.org/10.2151/jmsj.2019-051>.
- Zhang, Y., Feng, M., Du, Y., Phillips, H.E., Bindoff, N.L., McPhaden, M.J., 2018. Strengthened Indonesian throughflow drives decadal warming in the Southern Indian Ocean. *Geophys. Res. Lett.* 45 (12), 6167–6175. <https://doi.org/10.1029/2018GL078265>.
- Ziehn, T., Chamberlain, M.A., Law, R.M., Lenton, A., Bodman, R.W., Dix, M., Stevens, L., Wang, Y.-P., Srbinovsky, J., Ziehn, T., Chamberlain, M.A., Law, R.M., Lenton, A., Bodman, R.W., Dix, M., Stevens, L., Wang, Y.-P., Srbinovsky, J., 2020. The Australian Earth System Model: ACCESS-ESM1.5. *Journal of Southern Hemisphere Earth. Syst. Sci.* 70 (1), 193–214. <https://doi.org/10.1071/ES19035>.

3.4 Science and society : Climate velocities are useful tools to inform conservation in the Southern Indian Ocean

Climate velocities are computed in the previous section (Azarian et al., 2023) to provide a complementary perspective on climate change spatial heterogeneity, especially given their common use as a proxy of the shift in temperature-driven marine species' distributions (Pinsky et al., 2013; Sunday et al., 2015). Climate velocity has also been highlighted as a useful tool for conservation, notably in relation to protected marine areas, to project species habitat shifts but also through notions such as climate refugia or climate connectivity (Brito-Morales et al., 2018). In this section, we aim at exploring the various applications of climate velocity to guide management in the Southern Indian Ocean.

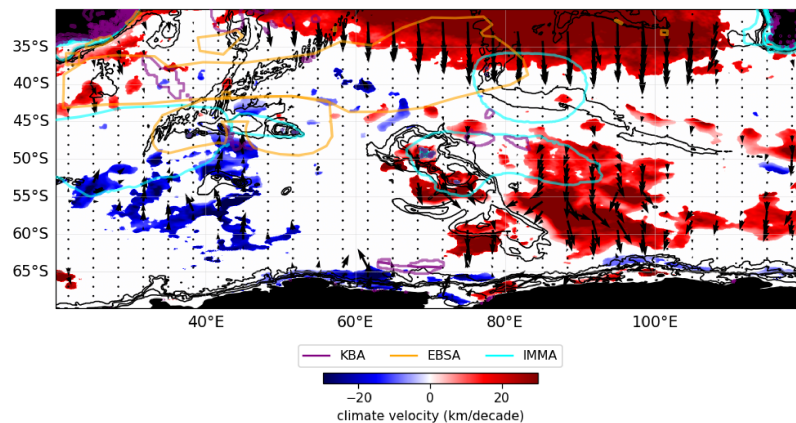


FIGURE 3.1: Climate velocity as calculated in Azarian et al. (2023), masked by SST signal-to-noise ratio as defined in Auger et al. (2021), both using OSTIA dataset between 1982 and 2019. Areas of conservation interest such as Key Biodiversity Areas (KBA, purple; BirdLife International (2022)), Ecologically and Biologically Significant Areas (EBSA, orange; obtained from the clearing-house mechanism of the Convention on Biological Diversity, <https://chm.cbd.int/database/>) and Important Marine Mammals Areas (IMMA, cyan; IUCN MMPATF (2023)) are also shown.

First, climate velocities can complete the interpretation of current warming trends. We note that, by definition, climate velocity requires that a significant trend has emerged. (Azarian et al., 2023) show that interannual variability may still dominate the western part of the Southern Indian Ocean. The interpretation of climate velocity over the last decades is a bit more complex as the climate change signal has not emerged throughout

the area. As a complementary analysis, we mask climate velocity norm by the signal-to-noise ratio S defined in [Auger et al. \(2021\)](#). On [Figure 3.1](#), climate velocity is only shown where the temperature trend dominates the interannual variability ($S > 1$). Most ecologically important areas, notably EBSAs and IMMAs, are large enough not to be entirely subjected to significant climate velocities. Contrary to the eastern side of the Kerguelen Plateau, the western side of the Plateau north of the Fawn Trough is currently experiencing southward/southeastward climate velocities of around 27 km/decade. The impacts of such contrast on spatially segregated species according to their size and sex like the Patagonian toothfish could be worth investigating. Interesting information can also be derived from the direction of change. While climate velocities are strictly directed southward from the subtropical region, there is a divergence of climate velocities around 86°E-55.5°S that could be related to the influence of western boundary currents at the southern part of the Plateau.

Second, climate velocity can be useful to identify timescales of relevance for area-based conservation measures. From climate velocities, other metrics such as climate residence time (i.e. time when the conditions protected initially will no longer be under the protection of current area-based measures, introduced in [Loarie et al. \(2009\)](#) and [Brito-Morales et al. \(2018\)](#)) can be computed. Providing such timescale can be informative as to how long fixed area-based measures may be relevant. Area-based measures, such as marine protected areas, are often based on regionalisation works which determine physical and/or biogeochemical and/or ecological coherent zones. A new regionalisation method to account for the vertical structure of the ocean has been recently introduced in [Merland et al. \(under review\)](#), using a functional principal component analysis as in [Pauthenet et al. \(2017\)](#). The identified epipelagic (0 - 200 m) and mesopelagic (200 - 1000 m) regions are defined based on the vertical temperature, salinity and oxygen concentrations of the last decades and are found to mostly have a latitudinal distribution (L). Consequently, we can use the climate velocities (CV) computed in [Azarian et al. \(2023\)](#), to compute the associated climate residence time (CRT) for each of these identified regions ¹ ([Figure 3.2](#)):

$$CRT = \frac{L}{CV} \quad (3.1)$$

¹The CRT introduced in [Loarie et al. \(2009\)](#) and [Brito-Morales et al. \(2018\)](#) is estimated as the ratio between the diameter of an area divided by the mean CV of that area, the equation is here adapted for regions that are mostly latitudinal bands.

In the mesopelagic, all regions have a CRT shorter than a century, except one antarctic and one subtropical mesopelagic region that have a relatively wide latitudinal extent (Merland et al. (under review); Figure 3.2). Indeed, this metric emphasizes the vulnerability of transition areas, both at the surface and at depth, which have a narrower latitudinal range and thus often shorter CRT. This is an important information to consider when designing a network of marine protected areas, as different areas contributing to the network's representativity may have different CRT.

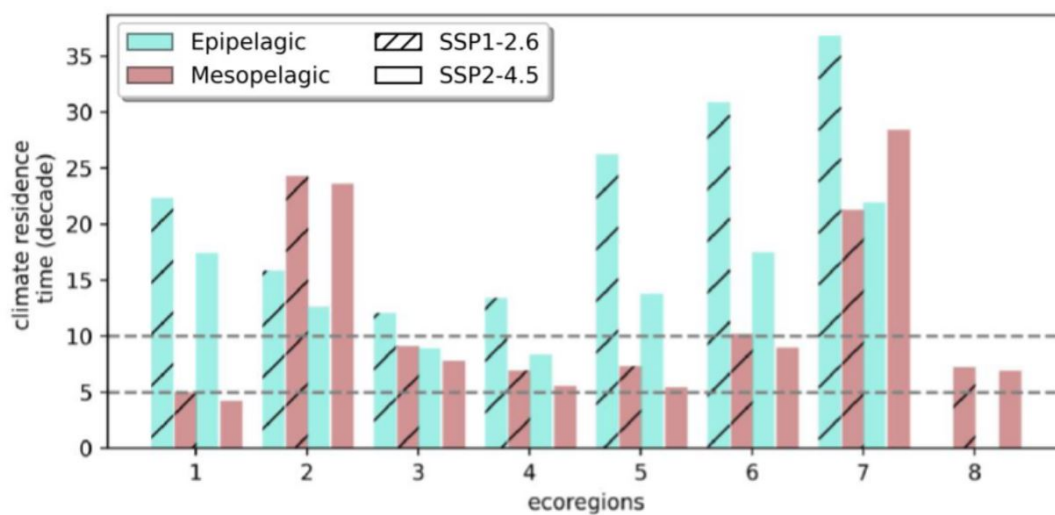


FIGURE 3.2: **Climate residence time over each epipelagic (blue) and mesopelagic (brown) regions determined with the regionalisation approach using a functional principal analysis in Merland et al. (under review), using climate models over 20°E-120°E 60°S-30°S as in Azarian et al. (2023), under SSP1-2.6 (hatched) and SSP2-4.5 (not hatched). Horizontal lines at 50 years and 100 years have been added to facilitate the reading of the chart. This figure is part of my specific contribution to Merland et al. (under review).**

Third, the analysis of climate velocities enables the investigation of other threats: not only habitat shift but also habitat continuity. Another climate change pressure has been identified in Azarian et al. (2023) : habitat shearing, which occurs when climate velocities at the surface and at depth differ while ecosystems evolve throughout the water column. Again, such threat is spatially heterogeneous with antarctic and subtropical areas being more impacted than subantarctic areas at the end of the century under SSP2-4.5 (Figure 3.3). Under SSP2-4.5, it appears that such habitat shearing may be stronger north and south of the ACC, as well as around Kerguelen, between the Polar Front and the subantarctic front (Figure 3.3).

Overlapping information on the ratio between climate velocity in the mesopelagic and at the surface and changes as described in Azarian et al. (2023) shows that areas that

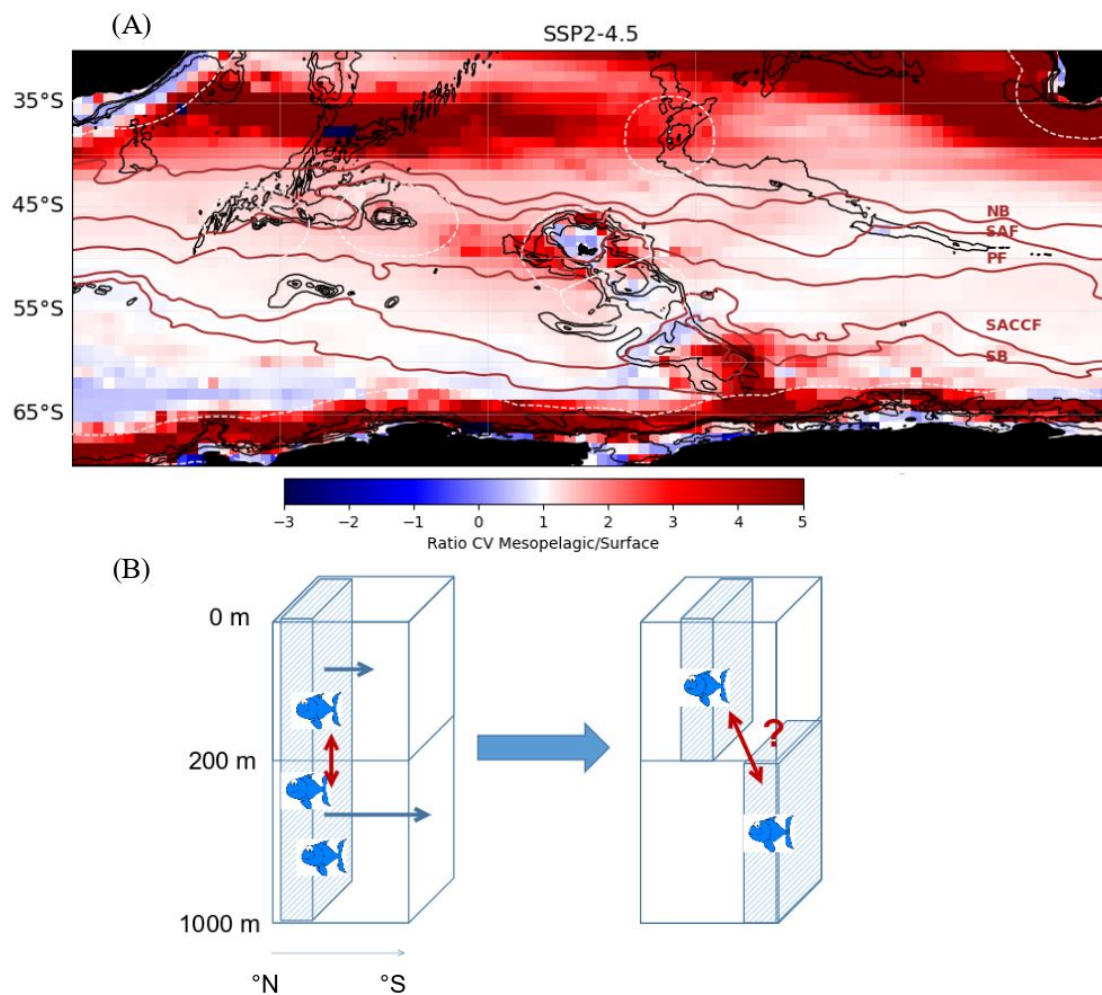


FIGURE 3.3: **Identification of the habitat shearing threat.** (A) Ratio between climate velocity in the mesopelagic and at the surface under SSP2-4.5 at the end of the century using the same CMIP6 models as in Azarian et al. (2023). (B) Schematic illustrating the concept of habitat shearing, suggesting a potential impact for pelagic ecosystems living at different depths.

are initially thought to be less impacted by climate change, due to weaker patterns of change, may still be exposed to other pressures such as habitat shearing (Figure 3.4). In particular, the area 2 identified in Azarian et al. (2023) (between 35°S and 40°S, under the influence of the Agulhas Return Current) is characterised by weaker warming and weaker changes in mean MHW intensity and in mean annual MHW days, but mesopelagic climate velocities are projected to be, in this area, more than 3 times faster than surface climate velocities under SSP2-4.5 at the end of the century (Figure 3.3). This area has been defined as an Ecologically and Biologically Significant Area (EBSA), referred to as [the Agulhas Front EBSA](#), notably due to the high productivity supporting rich ecosystems and important feeding areas for a large number of seabirds. Criteria such as “uniqueness and rarity”, “special importance of life history stages of

species”, “importance for threatened, endangered or declining species and/or habitats” and “biological productivity” are considered high for this area. Whether habitat shearing will threaten those characteristics remain to be studied. This will probably depend on how pelagic communities are driven by the vertical structure of environmental conditions which is still today an active field of research. Still, the overview presented on Figure 3.4 suggests caution when indicating that an area may be more or less exposed to climate change.

This additional threat of habitat shearing points out the need to consider climate change impacts on vertical structures of ecological importance (e.g. habitats, foraging hotspots). While this Chapter provides an overview on the spatial heterogeneity and magnitude of temperature-related changes, the link to potential ecological impacts can remain difficult to establish. Focusing on a vertical structure known to be key for pelagic ecosystems can contribute to a more mechanistic understanding of climate change impacts.

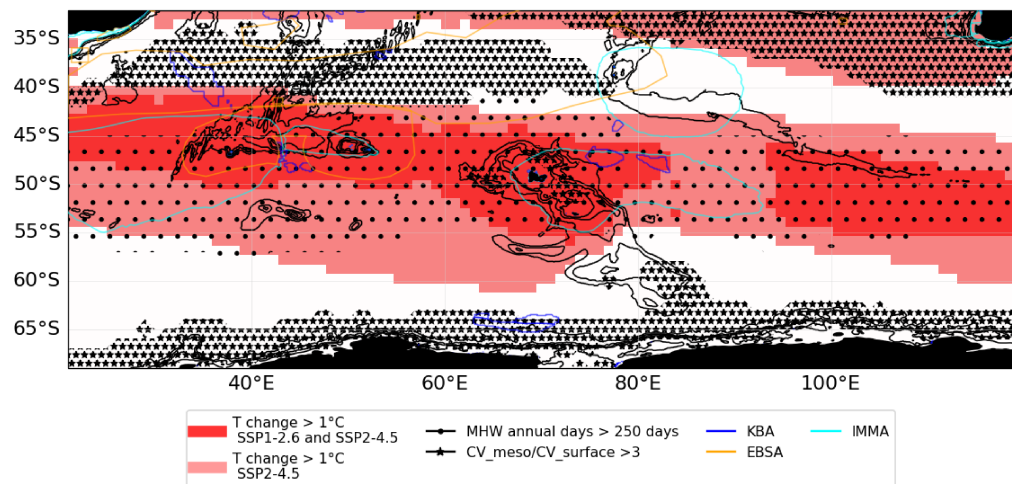


FIGURE 3.4: Overview of the main projected temperature-related changes under climate change in the Southern Indian Ocean determined in Chapter 3. Areas where surface temperature increases by more than 1°C at the end of the century relative to 1995–2014 under SSP1-2.6 and SSP2-4.5 (red colors) and where the MHW occur in average more than 250 days/year at the end of the century under SSP2-4.5 using CMIP6 models (dotted hatching), from Azarian et al. (2023). The habitat shearing threat is identified here as a ratio between mesopelagic and surface climate velocities greater than 3 (stars hatching). Contours of key biodiversity areas (blue; BirdLife International (2022)), important marine mammals areas (cyan; IUCN MMPATF (2023)) and ecologically and biologically significant areas (orange; obtained from the clearing-house mechanism of the Convention on Biological Diversity, <https://chm.cbd.int/database/>) are included.

Conclusion

This Chapter highlights the spatial and temporal variability of temperature-related climatic impact drivers, also confirming the important role of the Southern Ocean circulation in the spatial heterogeneity of warming patterns. It therefore sheds light on different types of areas that would be interesting to monitor more specifically :

- Areas where the warming signal due to climate change is not yet significant : south of Crozet near the Polar Front ;
- Areas where the most intense changes are projected : subantarctic latitudes (55-40°S) ;
- Areas with weaker warming and MHW intensity change but important habitat shearing: around the Agulhas Return Current.

Such spatial information can help guide future conservation planning, especially in the pelagic subantarctic ([Makhado et al., 2023](#)).

Three potential uses of climate velocity to inform conservation have also been illustrated in this Chapter:

- To map the current direction of change ;
- To identify timescales of relevance for potential area-based conservation measures ;
- To characterize threats on habitat continuity.

Indeed, habitat shearing is a potential threat for pelagic ecosystems that arises from this study and that, to our knowledge, had not been identified before. It raises the importance of considering climate change impacts on vertical structures that may condition ecological processes. In the next Chapter, we therefore investigate MHWs and global warming impacts on winter waters, a subsurface water mass playing a key role for top predators foraging ecology.

Chapter 4

Marine heatwaves and global warming impacts on winter waters in the Southern Indian Ocean

“We can only sense that in the deep and turbulent recesses of the sea are hidden mysteries far greater than any we have solved.”

R. Carson, The Sea Around Us

4.1 Context

In the Southern Ocean, winter waters (WWs) refer to a subsurface water mass characterized by a minimum of temperature which plays an important ecological role, especially by facilitating prey access for top predators (Figure 4.1). Indeed, WWs have a known structuring effect on subantarctic ecosystems, conditioning the composition, abundance and vertical distribution of mesopelagic organisms (Béhagle et al., 2017; McMahan et al., 2019; Hunt and Swadling, 2021). As ocean is warming and marine heatwaves (MHWs) are going to intensify, especially at subantarctic latitude (Chapter 3), we investigate the

potential impacts of different levels of warming on the presence, depth and temperature minimum associated with this important subsurface water mass in the Southern Indian Ocean.

To that purpose, we focus on two timescales. First, we study how WWs are impacted by surface MHWs on short timescales (days, weeks), using SST satellite observations for MHWs detection, hydrographic profiles from Argo floats and from the MEOP program as well as Mercator reanalysis product. Second, we analyse the long-term (decadal) change in presence, depth and temperature of WWs under different global warming levels, using 12 CMIP6 models outputs from scenarios SSP1-2.6, SSP2-4.5 and SSP5-8.5.

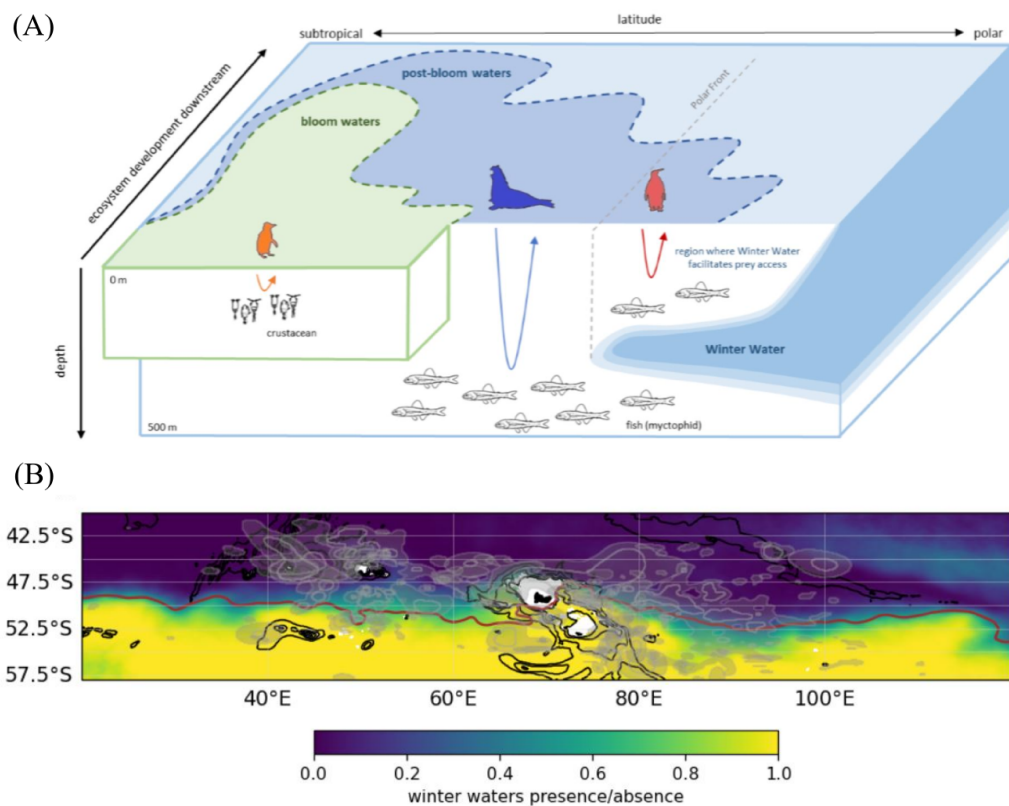


FIGURE 4.1: Winter waters ecological role and mean probability of presence in the Southern Indian Ocean. (A) Ecological role played by winter waters for top predators foraging strategies (Credit: Malcolm O’Toole). (B) Mean winter waters probability of presence over 1993-2019 (using definition detailed in Chapter 2 Section 2.2.4.1 with Mercator reanalysis product), overlapped with the Polar Front mean position from Park and Durand (2019) and examples of foraging areas identified for various top predators (e.g. king penguins, wandering albatross...) in different monitoring campaigns (data provided by Malcolm O’Toole).

4.2 Key results

This study highlights how climate change may impact the presence and characteristics of WWs on different timescales.

This study first provides a better understanding of MHWs in the subantarctic and confirms **the strong link between MHWs and the ocean circulation**. MHWs anomaly extends at depth and is linked to changes in WWs characteristics in areas where they are usually present. This study shows that **WWs are shifted southward locally or are being warmer and deeper when a MHW occurs at the surface**.

Climate projections indicate a southward shift of WWs, and thus the Polar Front, (as defined as the northernmost extension of WWs), under global warming. However, this southward shift is **asymmetric between the west and the east of the Kerguelen Plateau**. We estimate that the WWs position is relatively stable east of the Plateau up to 2.6°C global warming.

Those impacts of short-term extreme events and long-term changes on WWs distribution and characteristics bring out ecological concerns. In the short term, the impacts of MHWs on WWs are localised. Comparing MHW characteristics at depth with both randomly distributed Argo floats and data collected by elephant seals reveals that elephant seals tend to sample shallower and less intense MHWs and thus may tend to avoid the most intense MHWs. Despite the localised impact of one MHW, multiple events or even their scale (extent, duration) could have an impact on top predators' foraging strategy and behaviour. This was observed for the particularly spread and long-lasting MHW event of 1997 associated with a southward shift of the Polar Front and mass mortality in king penguins (*Aptenodytes patagonicus*) populations from Crozet (Bost et al., 2015).

Investigating both short and long timescales in this study provides a useful understanding of the potential impacts of global warming on ecosystems in the long term. **In the decades to come, such extreme changes could become average states**, even though different physical drivers may be at play on longer timescales. The ecological impacts of the 1997 MHW could thus be repeated more frequently in the long term, having long lasting impacts on those species even under 1.5°C global warming.

The asymmetry in the WWs shift on either side of the Plateau suggests that top predators populations might be impacted differently by climate change depending on their

spatial distributions. The area east of Kerguelen could thus be considered as a “climate refugium”, at least up to 2.6°C global warming. We further develop this concept of refugium and how this knowledge can be useful for conservation in Section 4.4.

4.3 Main study

The main study presented in this Chapter has been published in “Journal of Marine Systems” (Azarian et al., 2024). The associated Supplementary Material can be found in Appendix B.



Marine heatwaves and global warming impacts on winter waters in the Southern Indian Ocean

Clara Azarian^{a,b,*}, Laurent Bopp^c, Jean-Baptiste Sallée^a, Sebastiaan Swart^d,
Christophe Guinet^e, Francesco d'Ovidio^a

^a Sorbonne Université, CNRS, IRD, MNHN, Laboratoire d'Océanographie et du Climat: Expérimentations et Approches Numériques (LOCEAN-IPSL), Paris, France

^b Ecole Nationale des Ponts et Chaussées (ENPC), Champs-sur-Marne, France

^c Ecole Normale Supérieure/Université PSL, CNRS, Ecole Polytechnique, Sorbonne Université, Laboratoire de Météorologie Dynamique (LMD-IPSL), Paris, France

^d University of Gothenburg, Gothenburg, Sweden

^e Centre d'Etudes Biologiques de Chizé, UMR7372 CNRS-La Rochelle Université, Villiers en Bois, France

ARTICLE INFO

Keywords:

Southern Indian Ocean
Winter waters
Marine heatwaves
Global warming

ABSTRACT

In the Southern Ocean, the term “winter waters” (WWs) refers to a water mass characterized by a subsurface layer of minimum temperature that plays an important ecological role for marine ecosystems, and in particular for top predators. Given that the Southern Ocean is experiencing warming and intense marine heatwaves (MHWs), particularly at subantarctic latitudes, we investigate here how different levels of warming might impact the presence, depth and minimum temperature of WWs in the Indian sector of the Southern Ocean. In particular, we assess how WWs are impacted by surface MHWs using *in situ* Argo hydrographic observations and logging data. The results indicate that WWs are substantially reduced, deeper and warmer during the presence of MHWs. Using the most recent climate projections, we find a significant, but scenario-dependent, southward shift of WWs under global warming. Potential impacts of such WW shifts on pelagic ecosystems, at different timescales (from daily to decadal), are discussed.

1. Introduction

“Winter waters” (WWs) is a term used to qualify the subsurface minimum temperature layer present in the Southern Ocean. The Polar Front, one of the most prominent hydrographic features in this basin, is often defined as its northernmost extension (Gordon and Huber, 1984; Park et al., 1998; Pauthenet et al., 2018). WWs are formed from the freezing cold surface waters of the winter mixed layer of the subpolar Southern Ocean, and are then capped by a warmer and fresher surface layer in spring-summer as sea-ice melts and air temperature warms. This seasonal cycle leaves behind a cold water mass in the subsurface between about 100 and 400 m, which is stably stratified by the vertical salinity profile (Sharma and Mathew, 1985; Park and Gamberoni, 1993; Belkin and Gordon, 1996). WWs temperature typically ranges between $-2\text{ }^{\circ}\text{C}$ and $3\text{ }^{\circ}\text{C}$ (Gordon, 1975; Park and Gamberoni, 1993; Sabu et al., 2020).

The distributions and characteristics of WWs depend on large-scale drivers such as wind stress or sea-ice extent (Gordon and Huber,

1984), which are expected to change under global warming (Lee et al., 2021). Water masses of the Southern Ocean are overall observed and projected to continue to warm in the future (Sallée et al., 2013; Sallée, 2018; Auger et al., 2021). The observed temperature change across the Southern Ocean is actually heterogeneous. Cooling is observed in the southern end of the Southern Ocean, while warming occurs at depth and also within and north of the Antarctic Circumpolar Current (ACC; Armour et al., 2016; Llovel and Terray, 2016; Morrison et al., 2016; Sallée, 2018; Auger et al., 2021; Fox-Kemper et al., 2021). No warming trends have yet been reported for the WWs and their future evolution remains uncertain.

In this paper, we aim at shedding light on the impact of a warming climate on WWs. As WWs are characterized by a minimum of temperature, their distribution and characteristics can be expected to be affected by a warming climate. Our main motivation in this endeavor is underpinned by the demonstrated importance of this water mass for Southern Ocean ecosystems. WWs have been shown to play a structuring role for pelagic ecosystems and for the vertical distribution and relative

* Corresponding author at: Sorbonne Université, CNRS, IRD, MNHN, Laboratoire d'Océanographie et du Climat: Expérimentations et Approches Numériques (LOCEAN-IPSL), Paris, France.

E-mail address: clara.azarian@locean.ipsl.fr (C. Azarian).

<https://doi.org/10.1016/j.jmarsys.2023.103962>

Received 7 June 2023; Received in revised form 30 November 2023; Accepted 21 December 2023

Available online 28 December 2023

0924-7963/© 2023 Published by Elsevier B.V.

abundance of mesopelagic organisms (Béghagle et al., 2017; McMahon et al., 2019; Hunt and Swadling, 2021). WWs in particular are associated with mesopelagic organisms being more concentrated towards the surface and thus easily accessible prey for top predators (e.g. king penguins, *Aptenodytes patagonicus*, Kooyman et al., 1982; Kooyman et al., 1992).

There are two main ways climate change could impact WWs characteristics. First, changes in large-scale circulation patterns may alter the distribution of WWs, and in particular the southward shift of the Polar Front or the increase of eddy shedding southward from the Polar Front may push WWs southward and change their distribution. Second, local surface warming occurring at the time of WWs formation in winter, or penetrating downward in spring-summer by diffusion or vertical mixing, could warm WWs, or eventually erode the temperature minimum entirely. Here, we first use observation-based datasets to test the hypothesis that anomalously warm surface conditions affect WWs distribution and characteristics through one or a combination of these two processes. Second, we use climate models to investigate how these processes unfold into a net change in WWs distribution and characteristics under a diverse range of global warming levels.

Anomalously warm surface conditions are commonly referred to as marine heatwaves (MHWs; Hobday et al., 2016; Frölicher et al., 2018; Oliver et al., 2021). There is increasing evidence that MHWs detected at the surface can penetrate to depth (Elzahaby and Schaeffer, 2019; Darmaraki et al., 2019; Hu et al., 2021; Miyama et al., 2021; Grobelindemann et al., 2022), with the potential to locally modify subsurface water masses characteristics such as WWs. In addition, it was shown that MHWs in the southern Indian basin can be associated with a southward shift of the Polar Front, which in 1997 led to a mass mortality of Crozet king penguins as their foraging zones were shifted too far south from their breeding island (Bost et al., 2015). We see here the importance of better understanding the impact of warm surface conditions on WWs, which can have dramatic consequences for ecosystems. Such extreme events can be seen as a snapshot into the future under a warmer climate. However, dominant processes at short and long timescales can differ, so that a proper analysis of future projections must also be carried out before any conclusions are drawn.

We focus our study on the Indian sector of the Southern Ocean because this is one of the regions of the world that has experienced the largest increase in ocean heat content in recent decades (Roemmich et al., 2015; Lovel and Terray, 2016; Sallée, 2018; Fox-Kemper et al., 2021). It has also been shown that the position of the Polar Front can be highly variable west of the Kerguelen Plateau (Pauthenet et al., 2018). Since this region also hosts a rich biodiversity and notably top predators whose behavior and foraging success has been related to physical properties of water masses (McIntyre et al., 2011; Guinet et al., 2014), the Southern Indian Ocean is of particular interest to study how warming can impact WWs and, in turn, pelagic ecosystems.

The paper is organized as follows. First, we investigate the relationship between WWs and surface extreme temperature anomalies, combining *in situ* data with multisatellite observations and a 1/12° ocean reanalysis product. This is motivated by the findings that the pattern of intense MHWs at the northern boundary of the ACC might be associated with mesoscale eddies (Su et al., 2021) and that, consequently, advective processes could shift the position of WWs locally. This first part shows that both advective and local diffusion processes related to surface warming can contribute to reducing WWs extent or signal. We also highlight potential biases in the MHWs characteristics sampled by elephant seals compared to random sampling by Argo floats. Second, we investigate how these impacts on WWs are intensified under global warming, leading to a reduced extent of WWs, using CMIP6 models. Finally, we discuss the potential mechanisms driving MHWs and global warming impacts on WWs distribution, the contrast between observed trends, projections and paleoceanographic studies and the potential ecological implications of a southward shift of the WWs.

2. Material and methods

2.1. Observations and Mercator reanalysis

Temperature *in situ* profiles are collected from Argo float data between 2001 and 2019 over the area 20–120°E 70–30°S (Argo, 2000). We download 170,352 profiles, among which 78,407 are complete between 5 and 900 m. Temperature *in situ* profiles are also collected between 2004 and 2017 from biologging in the Southern Indian Ocean and gathered by the Marine Mammals Exploring the Oceans Pole to Pole or MEOP consortium (Treasure et al., 2017; Roquet et al., 2014). We download 140,436 profiles, among which 9484 are complete between 5 and 900 m.

The GLORYS12V1 product is the Copernicus Marine Environment Monitoring Service (CMEMS) global ocean eddy-resolving reanalysis delivered by Mercator Ocean, thereafter referred to as MERCATOR reanalysis. This product provides daily and monthly mean temperature over 50 vertical levels and with 1/12° horizontal resolution between 1993 and 2019. This product is used in this paper to provide a monthly climatology for the vertical temperature profiles. The GLORYS12V1 product is also used to determine the probability of presence of WWs between 1993 and 2019. This probability is estimated by detecting, for each day between 1993 and 2019 and for each grid cell, whether the minimum temperature between 100 and 400 m is found at a depth <350 m, and then averaging the results (0 for absence of a temperature minimum in this interval, 1 for presence) over time. WWs are also characterized by the temperature at the minimum (also named WWs temperature) and the depth of this minimum (also named WWs depth), as in Sabu et al. (2020).

The Operational Sea Surface Temperature and Ice Analysis (OSTIA) system run by the UK's Met Office (Good et al., 2020) provides daily sea surface temperature free of diurnal variability, also called the foundation sea surface temperature, at a 0.05° x 0.05° horizontal grid resolution between 1982 and 2019. This product combines satellite measurements (L4 level) from both infrared and microwave radiometers with *in-situ* measures from ships, drifting and moored buoys. This dataset was used for surface MHW detection.

2.2. Marine heatwaves detection and characteristics

A MHW is identified as an event of at least 5 days for which the sea surface temperature (SST) is above the 90th percentile of a data distribution using a seasonally-varying climatology for each grid point and for each day of the year using an 11-day window (Hobday et al., 2016). The threshold is also smoothed by applying a 30-day moving average. An average of 24 days/year under MHW is estimated between 1993 and 2019 over the area 20–120°E, 58–40°S.

The temperature anomaly depth, also called “MHW depth” in Elzahaby and Schaeffer (2019), is calculated to investigate whether surface MHWs are associated with deeper temperature anomalies (see Supplementary Methods). To do so, temperature anomaly profiles are obtained using the combination of information from different datasets:

- OSTIA dataset: for the detection of surface MHW using Hobday et al. (2016) definition (90th percentile)
- Argo float data: daily hydrographic profiles
- MERCATOR reanalysis: provide for each grid cell a monthly climatology profile

From each Argo hydrographic profile, we compute the vertical cumulative temperature anomaly, and the depth where 95% of the cumulative temperature anomaly is reached, also named “temperature anomaly depth”. Temperature anomalies are defined as a departure from a seasonal climatological mean produced from an ocean reanalysis (MERCATOR). Using satellite SST, we then group each of these profiles as within a MHW or outside. The Argo profile is said to be in a MHW

according to the surface detection of a MHW using sea surface temperature observations (OSTIA). A bootstrap approach with 10,000 iterations is used to obtain the mean values of the two metrics, as the sample sizes (in and out MHW) differ.

2.3. Altimetry analysis

Altimetry-derived geostrophic velocities are computed by CLS/AVISO (Collecte Localisation Satellites/Archiving, Validation, and Interpretation of Satellite Oceanographic data) and distributed by Copernicus Marine Environment Monitoring Service (CMEMS) as a gridded product on a $0.25^\circ \times 0.25^\circ$ horizontal grid resolution between 1993 and 2020 (doi: [10.48670/moi-00148](https://doi.org/10.48670/moi-00148)).

Using AVISO geostrophic velocities, the latitudinal advection of water parcels over 15 days backward in time is estimated. The latitudinal displacement is positive when the water parcel has moved southward over the last 15 days. The duration of 15 days for the advection is chosen as this is the typical timescale for MHW durations (Oliver et al., 2018). A monthly climatology of latitudinal displacement is determined over multiple years (1993–2020). Correlations between anomalies of latitudinal displacement and the presence/absence of MHW are evaluated to investigate the co-occurrence between MHW and an anomalous southward displacement of surface warmer water.

2.4. CMIP6 models

Coupled models from the Coupled Model Intercomparison Project 6 (CMIP6) have been used to conduct historical and projection simulations notably to investigate how the Earth system responds to forcing (Eyring

et al., 2016). The 12 models used here (described in Supplementary Material S1) are selected among 26 CMIP6 models as they provide a realistic representation of the circumpolar mean position of WWs between 1995 and 2014 using their historical simulations (Supplementary Methods and Supplementary Material S2). Historical (1850–2014) and projection (2015–2100) simulations from CMIP6 are used here. Three emission trajectories, also called Shared Socioeconomic Pathways (SSPs), are considered: the SSPs 1–2.6, 2–4.5 and 5–8.5 (Lee et al., 2021). The variable considered here is monthly θ_{sea} (sea water potential temperature across different depth levels in $^\circ\text{C}$). WWs are detected through the presence of a temperature minimum between 100 and 400 m at a depth <350 m. The outputs of the 12 models under the three SSPs are combined following the so-called ‘time-shift approach’, which consists in averaging the models outputs over a period that, for each model, corresponds to a given global warming level (GWL; Herger et al., 2015; Chen et al., 2021; Lee et al., 2021; see Supplementary Methods).

3. Results

3.1. Winter waters distribution and modulation by marine heatwaves

Based on the MERCATOR reanalysis product presented above, we describe the typical characteristics of WWs in the Southern Indian Ocean ($20^\circ\text{--}120^\circ\text{E}$, $70^\circ\text{--}30^\circ\text{S}$). On average between 1993 and 2019, their northernmost extension is estimated to be between 52°S and 46°S , and it can be noted that at their northern edge, WWs presence is no longer continuous as illustrated on Fig. 1A. WWs mean temperature is 1.3°C but varies between -0.55°C and 3°C depending on the latitude/

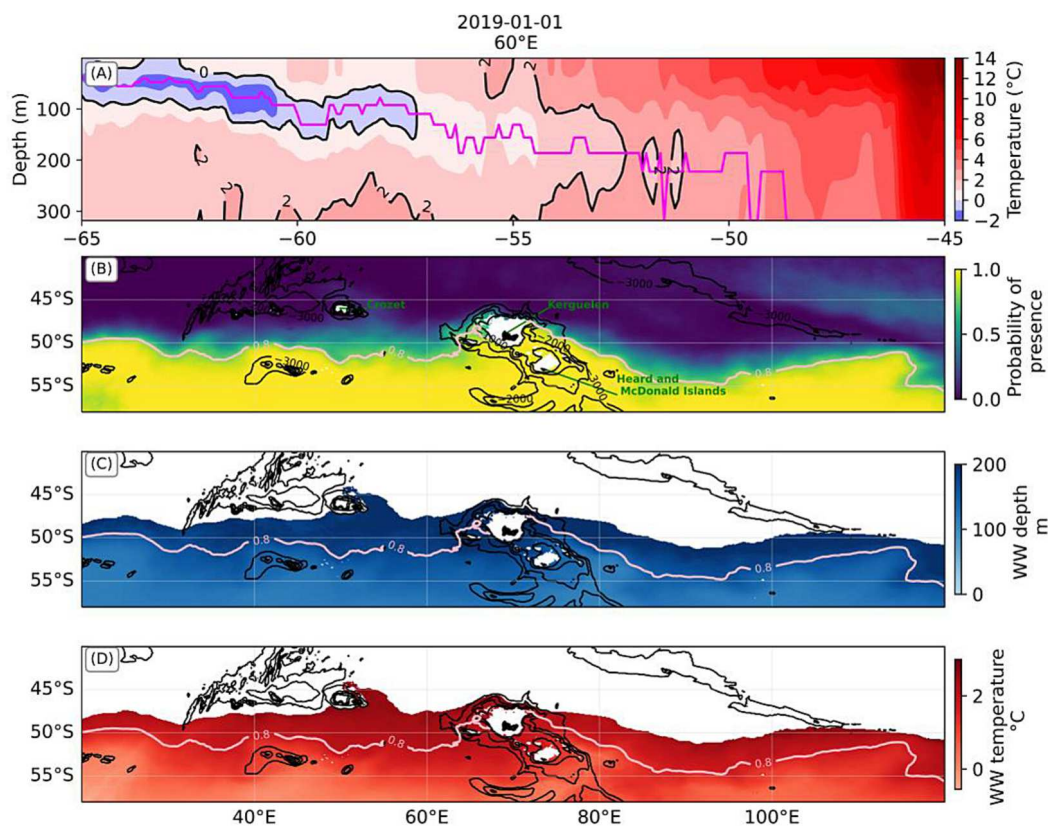


Fig. 1. Winter waters climatological description and characteristics using MERCATOR reanalysis product between 1993 and 2019. (A) Example of the vertical signature of winter waters (minimum temperature between 100 and 400 m) at 60°E on the 1st of January 2019. The position of the minimum temperature along the cross section is indicated in magenta. The characteristics of the winter waters studied here are the probability of presence of winter water (B, presence is 1, absence is 0), the depth of the minimum temperature (C) and the temperature minimum value (D). A mask to only select grid cells where on average the minimum temperature is below 3°C was used on C and D. The contour of the 80% probability of presence of winter waters is shown in pink on B, C and D. (For interpretation of the references to colour in this figure legend, the reader is referred to the web version of this article.)

longitude (Fig. 1D; note that we use a maximum historical WWs temperature at 3 °C; see Supplementary Methods) and WWs mean depth is 155 m and varies between 110 and 280 m (Fig. 1C). By definition, the water mass north of the WWs is not characterized by a minimum temperature between 100 and 400 m and is warmer than the water masses south of the Polar Front throughout the upper 400 m (e.g. Fig. 1A). We now focus on the variability of presence, temperature, and depth of WWs and seek to determine what is the influence on its variability of warm surface events, such as marine heatwaves.

3.1.1. Southward shift of winter waters distribution under marine heatwaves

We first seek to determine whether MHWs are deep reaching in the Indian sector of the Southern Ocean. In MHWs, the temperature anomaly depth is 3 times deeper than outside MHWs (Fig. 2B), highlighting that MHWs are not limited to the surface layer but extend at depth. We note that outside MHWs the mean temperature anomaly depth is by construction much shallower because many profiles associated with null or negative vertical temperature anomalies would be associated with a depth of 0. Consistent with the estimated difference in temperature anomaly depth, in MHWs, the typical cumulative temperature anomaly is much larger than outside, almost 5 times larger, with a mean cumulative temperature anomaly estimated at 549 °C.m (± 8 °C.

m; Fig. 2C).

As MHWs are associated with deeper and intense temperature anomalies (Fig. 2), we investigate whether this is due to a replacement of water masses through the southward advection of warmer waters. Positive correlations are found across the Indian sector of the Southern Ocean between an anomalous southward latitudinal displacement of water parcels over 15 days (typical MHW duration; the convention used here is that the latitudinal displacement is positive when the water parcel has moved southward), and the presence of MHW, estimated using OSTIA dataset, between 1993 and 2020 (mean correlation coefficient over the area of 0.2, Fig. 3A). These correlations are higher in the area where the most intense MHWs have previously been found (see Fig. 3A in Azarian et al., 2023), north of the Southern ACC Front between 20°E and 40°E and between the Subantarctic Front and the Northern boundary between 40°E and 70°E (correlation coefficient of >0.3 and up to 0.87; Fig. 3A). MHWs are therefore associated with the southward advection of water. If this occurs across the Polar Front, within mesoscale eddies or front meanders, it would imply that northern and warmer water masses are advected southward, effectively pushing WWs southward, and generating a deep positive temperature anomaly (e.g. Fig. 2B). Indeed, the water mass north of the northernmost extension of WWs often have transitional properties between Antarctic Surface Waters and Subantarctic Surface Waters (the latter dominates north

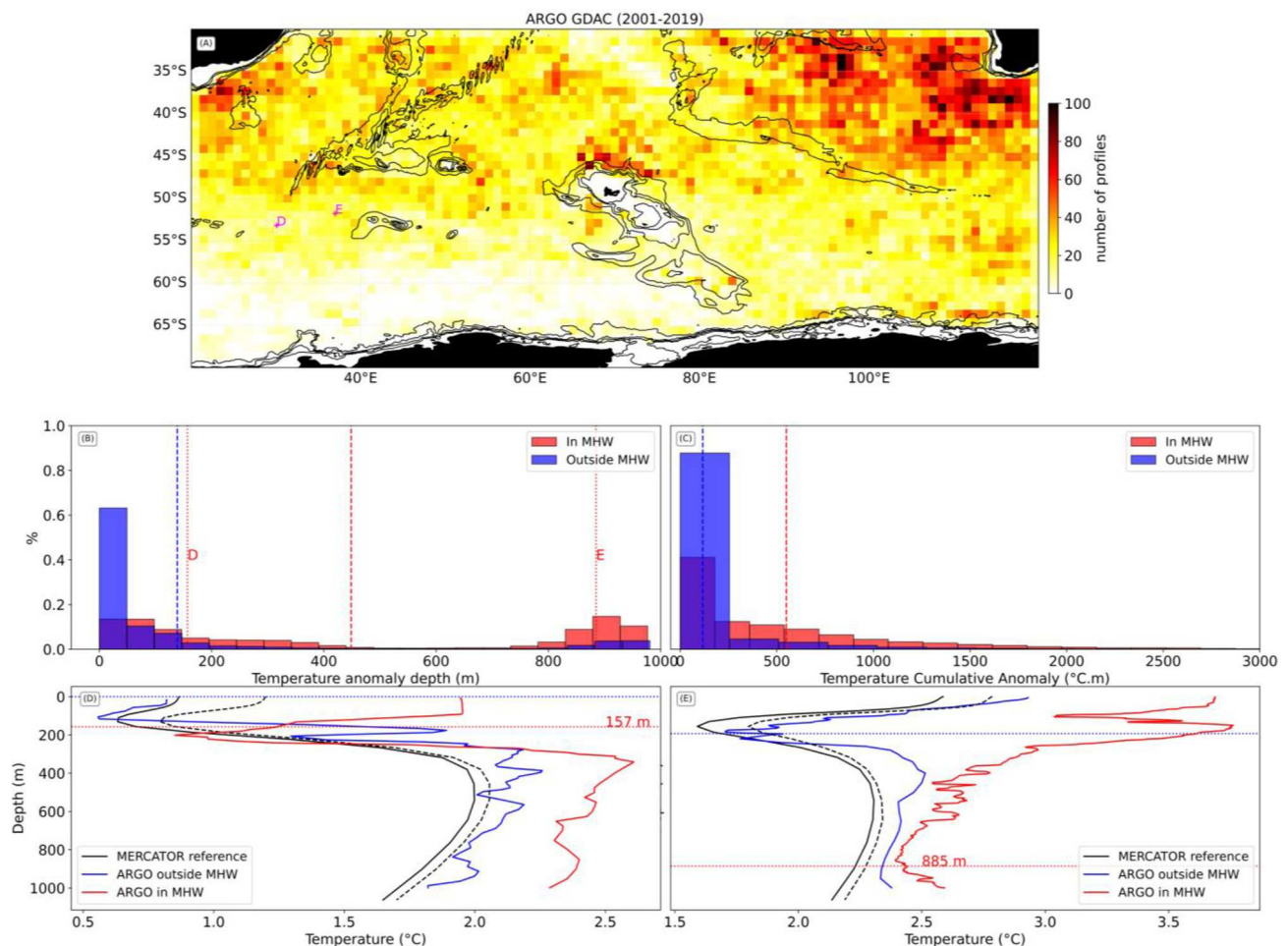


Fig. 2. (A) Spatial distribution of 78,407 Argo hydrographic profiles that are complete up to 900 m between 2001 and 2019. Mean MHW depth (B) and mean cumulative temperature anomaly (C) calculated from the anomaly profiles between Argo profiles and a monthly reference obtained with MERCATOR reanalysis over the area 20–120°E, 70–30°S. The mean values of the two metrics, in and out of a MHW, are shown (dashed vertical lines). Examples of Argo profiles in a MHW (red; 30.1°E/53.2°S on 20/11/2019 (D); 37°E/51.8°S on 10/12/2015 (E)) and outside a MHW (blue; 30.1°E/54°S on 20/11/2013 (D); 37.9°E/52°S on 08/12/2014 (E)); together with associated monthly reference from MERCATOR reanalysis (black solid for reference to Argo observation out a MHW; black dashed for reference to Argo observation in a MHW). The temperature anomaly depths associated with these profiles are shown directly on (D) and (E) and reported on (B) for the MHW cases (dotted lines). (For interpretation of the references to colour in this figure legend, the reader is referred to the web version of this article.)

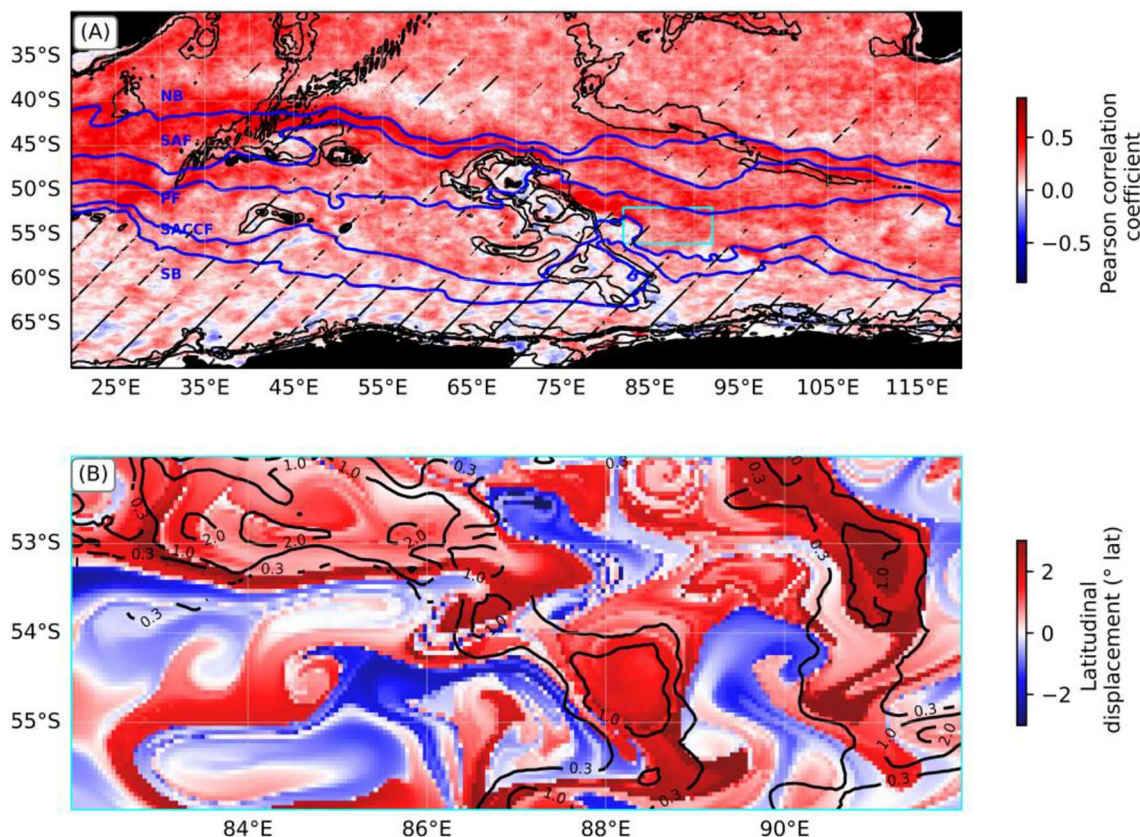


Fig. 3. (A) Correlation between the latitudinal displacement anomaly (using AVISO geostrophic velocities) and the presence/absence of marine heatwaves (MHWs, using OSTIA daily data and [Hobday et al., 2016](#) definition, 90th percentile) using monthly averages over multiple years between 1993 and 2020. The Antarctic Circumpolar Current (ACC) fronts such as the Subantarctic Front (SAF), the Polar Front (PF) and the Southern ACC front (SACCF), as well as the Northern (NB) and the Southern (SB) boundaries are shown in blue (from [Park and Durand, 2019](#)). Hatched areas indicate where the results are not significant ($p > 0.01$). (B) Example of the overlap between marine heatwaves intensity and the latitudinal displacement over 15 days on the 27th of december 2017 over the area 82–92°E 56–52°S (area shown in cyan in A). The black contours correspond to MHW intensity of 0.3 °C, 1 °C and 2 °C. (For interpretation of the references to colour in this figure legend, the reader is referred to the web version of this article.)

of the Subantarctic Front), with temperatures typically ranging between 3° and 8 °C, though their properties mostly depend on mixing ([Carter et al., 2008](#)). Consistently, we find that the presence of MHW significantly decreases the probability of presence of WWs, using MERCATOR ocean reanalysis between 1993 and 2019 ([Fig. 4A](#)). This southward shift of WWs in presence of MHWs is also consistent with *in situ* observations analysis (Supplementary Materials S3).

The impact of warm ocean surface conditions on WWs can therefore come from a southward water transport that would cause both a local MHW and a displacement of WWs further southward. This is illustrated by the example on [Fig. 2E](#): there is no longer a minimum temperature on the Argo profile during the MHW and the profile is warmer than the MERCATOR reference at the same location throughout the water column, suggesting the presence of a different water mass. However, remaining WWs temperature and depth can also be directly affected: either because their distribution is shifted or because of vertical heat diffusion. This is illustrated by the example on [Fig. 2D](#): the temperature anomaly during the MHW is the most intense at the surface and there is still a minimum temperature, although this minimum is deeper and slightly warmer than the MERCATOR reference at the same location. Indeed, WWs in MHWs are deeper and warmer than WWs that are not in a MHW ([Fig. 4B and C](#)). The mean difference between the mean WWs depth anomaly in and out MHWs is around 17 m (± 25 m, spatial standard deviation). The mean difference between the mean WWs temperature anomaly in and out MHW is around 0.33 °C (± 0.45 °C, spatial standard deviation).

We note that the spatial patterns of warming and deepening during

MHWs tend to follow mean dynamic topography contours, which represent the general circulation ([Fig. 4](#)). In particular, changes are weaker in areas of northward cold water mass intrusion such as around Conrad Rise (20–26°E), the Fawn Trough (74–83°E) or east of the Southeast Indian ridge (110–116°E). Hotspots of deepening and warming of WWs under MHWs are found west of Crozet Plateau (25–34°E) and east of Kerguelen Plateau (76–102°E), which are standing meanders and areas of high eddy kinetic energy ([Fig. 4](#); [Siegelman et al., 2019](#); [Dove et al., 2022](#)). The differences between WWs temperature anomalies (and depth anomalies) in MHWs compared to outside MHWs are two to three times warmer (and deeper) in these two locations compared to the regional mean of those differences. These two locations also correspond to the areas where the difference between the probability of presence of WWs given a MHW and the probability of presence of WWs given no MHW is the strongest. The probabilities of WWs presence given a MHW are 71% lower (than those given no MHW) on average in these two locations and up to 100% lower. A 100% decrease means that no WW is detected during a MHW in a grid cell where WW can be detected when there is no MHW.

3.1.2. Shallow and cold bias in marine heatwaves sampled by elephant seals

Elephant seals often forage near the Polar Front and can rely on oceanographic conditions to adapt their foraging strategy ([McIntyre et al., 2011](#); [Guinet et al., 2014](#)). MEOP-CTD dataset (see [Section 2.1](#)) provides elephant seals hydrographic profiles that can be used to evaluate the temperature anomaly depth during extreme events, as

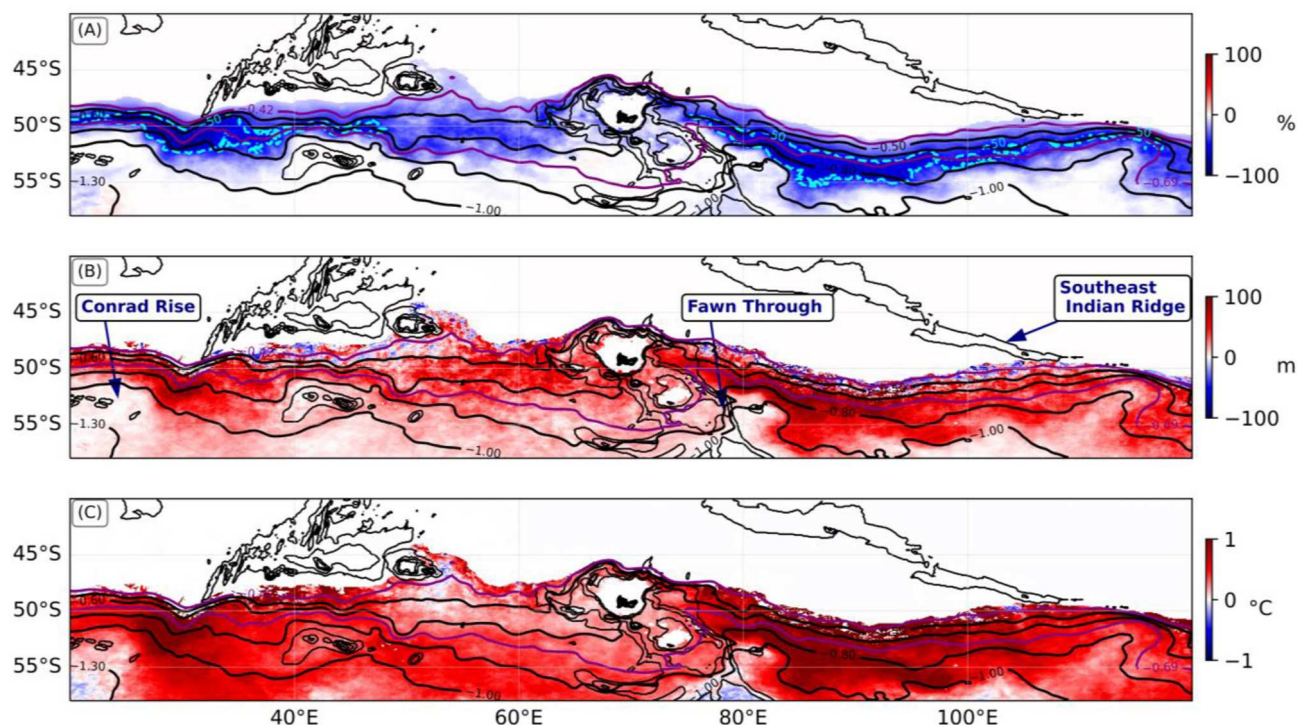


Fig. 4. Impacts of marine heatwaves (MHWs) on winter waters (WWs) using MERCATOR reanalysis product between 1993 and 2019, through (A) the difference between the probability of presence of WWs given that there is a MHW and the probability of presence of WWs given that there is not a MHW (contour of 50% difference in cyan; negative values indicate that the probability of presence of WWs is lower when there is a MHW); (B) the difference between the WW depth anomaly (relative to a monthly climatology, 1993–2019) in and out of a MHW; and (C) the difference between the WWs temperature anomaly (relative to a monthly climatology, 1993–2019) in and out of a MHW. A mask to only select grid cells where a minimum temperature between 100 and 400 m $< 3^{\circ}\text{C}$ is observed on average over 1993–2019 is applied on these figures. Mean dynamic topography contours (mean between 1993 and 2012, HYBRID-CNES-CLS18-CMEMS2020, Mulet et al., 2021) are shown in black, with the -0.69 and -0.42 m contours, which have been respectively associated with the southern and northern branches of the Polar Front (Chapman, 2017), that are shown in purple on these figures. (For interpretation of the references to colour in this figure legend, the reader is referred to the web version of this article.)

previously done with Argo float data. The aim here is to identify possible biases in the water masses properties sampled by elephant seals in respect to Argo estimates.

We investigate in particular the depth of temperature anomalies during MHWs sampled by elephant seals near the Polar Front east of the Kerguelen Plateau (80°E – 100°E , 55°S – 45°S), which is an important foraging area (Bost et al., 2009; Dragon et al., 2010; Cotté et al., 2015; Allegue et al., 2022), and as such represents a region where both elephant seal and Argo data are available (Figs. 2A and 5A). We use 467 MEOP-CTD profiles available between 2004 and 2017 (Fig. 5A) and 4101 Argo profiles between 2001 and 2019. The mean temperature anomaly depth is 7% shallower and the mean cumulative temperature anomaly is 21% less intense using elephant seals data compared to Argo data, although those same metrics outside a MHW are similar for both datasets (Fig. 5B, C). These results suggest that elephant seals do not sample (i.e., avoid) deeper and more intense marine heatwaves. While MEOP-CTD dataset is complementary to Argo data, using elephant seal data to study MHWs can therefore introduce a bias towards shallower and less intense MHWs possibly due to animal preference to avoid higher-than-normal temperatures.

3.2. Winter waters in the future for different warming levels

In the previous section, we show that in the past decades transient warm ocean surface events are associated with anomalies in WWs characteristics, as WWs can shift southward or be warmed and deepened, due to advective processes or local diffusion. In this section, we now seek to determine if in a globally warmer climate, WWs would be affected durably in similar ways.

Consistently with a southward water mass displacement, as global warming levels increase, the northernmost position of WWs (defined as the 80% probability of presence; referred to as Polar Front) shifts southward in CMIP6 models. The mean southward shift is 1.6° ($\pm 0.9^{\circ}$, along longitudes standard deviation), 2.1° ($\pm 1.3^{\circ}$), 3.1° ($\pm 1.4^{\circ}$) and 5.2° latitude ($\pm 1.5^{\circ}$ latitude) when averaged from 20°E to 120°E , for GWL 1.5°C , 2°C , 3°C and 4.5°C respectively (Fig. 6).

There is an important asymmetry in the WWs southward shift between east and west of the Kerguelen Plateau. West of the Kerguelen Plateau (20°E – 70°E), WWs shift southward by around 2.2° , 2.8° , 3.9° and 5.9° latitude for GWLs 1.5°C , 2°C , 3°C and 4.5°C , respectively. East of the Kerguelen Plateau (70°E – 120°E), the WWs shift southward by around 1° , 1.4° , 2.3° and 4.6° latitude for GWLs 1.5°C , 2°C , 3°C and 4.5°C , respectively (Fig. 6). Compared to the western side of the plateau (65°E – 70°E), on the eastern side of the Kerguelen Plateau (75°E – 80°E), the Polar Front is relatively stable for low warming levels before shifting southward (Fig. 7). This relative stability of the Polar Front east of the Kerguelen Plateau is however very dependent on the chosen models. For each model and each scenario, we determine the global warming level for which the Polar Front position anomaly in absolute starts to be permanently $> 0.4^{\circ}$ latitude (that is twice the mean natural variability of the Polar Front position between 75° and 80°E across models and scenarios). East of the Kerguelen Plateau, this mean threshold is 2.6°C ($\pm 0.6^{\circ}\text{C}$, intermodel and inter scenarios standard deviation; Fig. 7C).

We next investigate how the remaining WWs shifted southward are affected by local warming under the different global warming levels. Under all future warming levels, WWs are projected to warm (Fig. 8). When averaged over the area 20°E – 120°E , 70°S – 30°S , the mean change of temperature (relative to 1850–1900) for the multimodel mean is 0.6°C

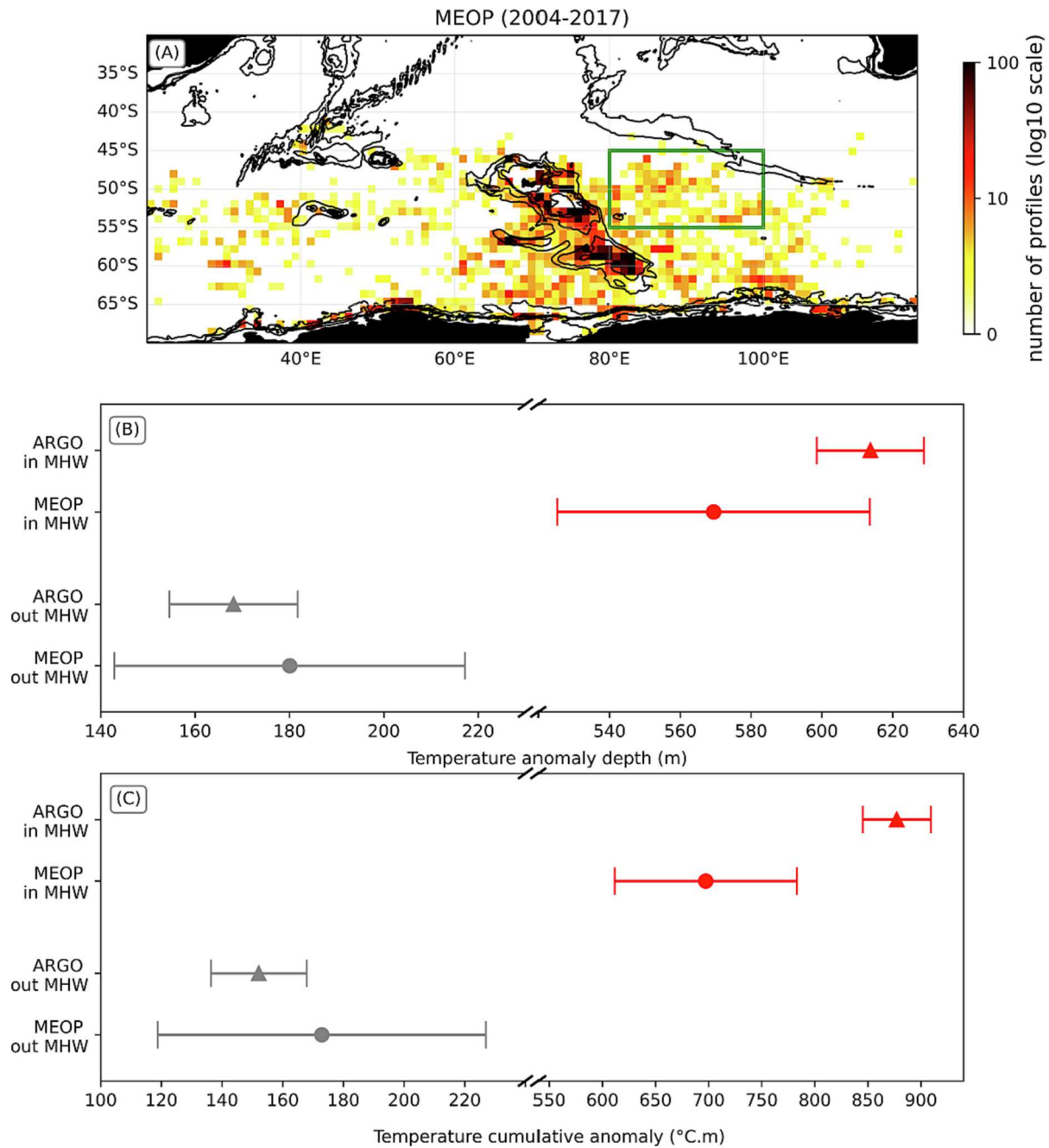


Fig. 5. Spatial distribution of 9484 hydrographic profiles that are complete up to 900 m, from MEOP-CTD dataset between 2004 and 2017 (A). Mean temperature anomaly depth (in m, B) and mean cumulative temperature anomaly ($^{\circ}\text{C}\cdot\text{m}$, C) calculated from the anomaly profiles between elephant seals profiles (round marker) or Argo profiles (triangles) and a monthly reference obtained with MERCATOR reanalysis. These calculations are done both for profiles found in (red) and out (gray) a MHW respectively over the area 80–100°E 55–45°S (green rectangle on A). The mean values and errorbars are estimated using a bootstrap approach, as presented in Section 2.2. (For interpretation of the references to colour in this figure legend, the reader is referred to the web version of this article.)

($\pm 0.3^{\circ}\text{C}$, regional mean intermodal standard deviation), 0.8°C ($\pm 0.4^{\circ}\text{C}$), 1.1°C ($\pm 0.5^{\circ}\text{C}$), 1.4°C ($\pm 0.6^{\circ}\text{C}$) for respectively GWLs 1.5°C , 2°C , 3°C and 4.5°C (Fig. 8). Compared to the warming, the overall projected deepening of WWs under global warming is relatively weak and not significant for a large proportion of our region of interest, especially east of the Kerguelen Plateau (Supplementary Material S4). The area-average deepening ranges from 5 to 9 m between GWL 1.5°C and 4.5°C but changes in WWs depth vary widely spatially within a single model and between models (Supplementary Material S4).

4. Discussion

4.1. Rapid winter waters variability associated with marine heatwaves

Our study shows that MHWs can be associated either with a replacement of WWs or with warmer and deeper WWs (see Section 3.1).

Our findings suggest that MHWs in the Southern Indian Ocean can be related to the regional mesoscale activity. Surface mean MHW intensity patterns show that the most intense MHWs are located along the northern boundary of the ACC (as defined in Park et al., 2019) in areas of high SST variability but also east of the Kerguelen Plateau in high eddy kinetic energy areas (Su et al., 2021; Azarian et al., 2023). Consistently,

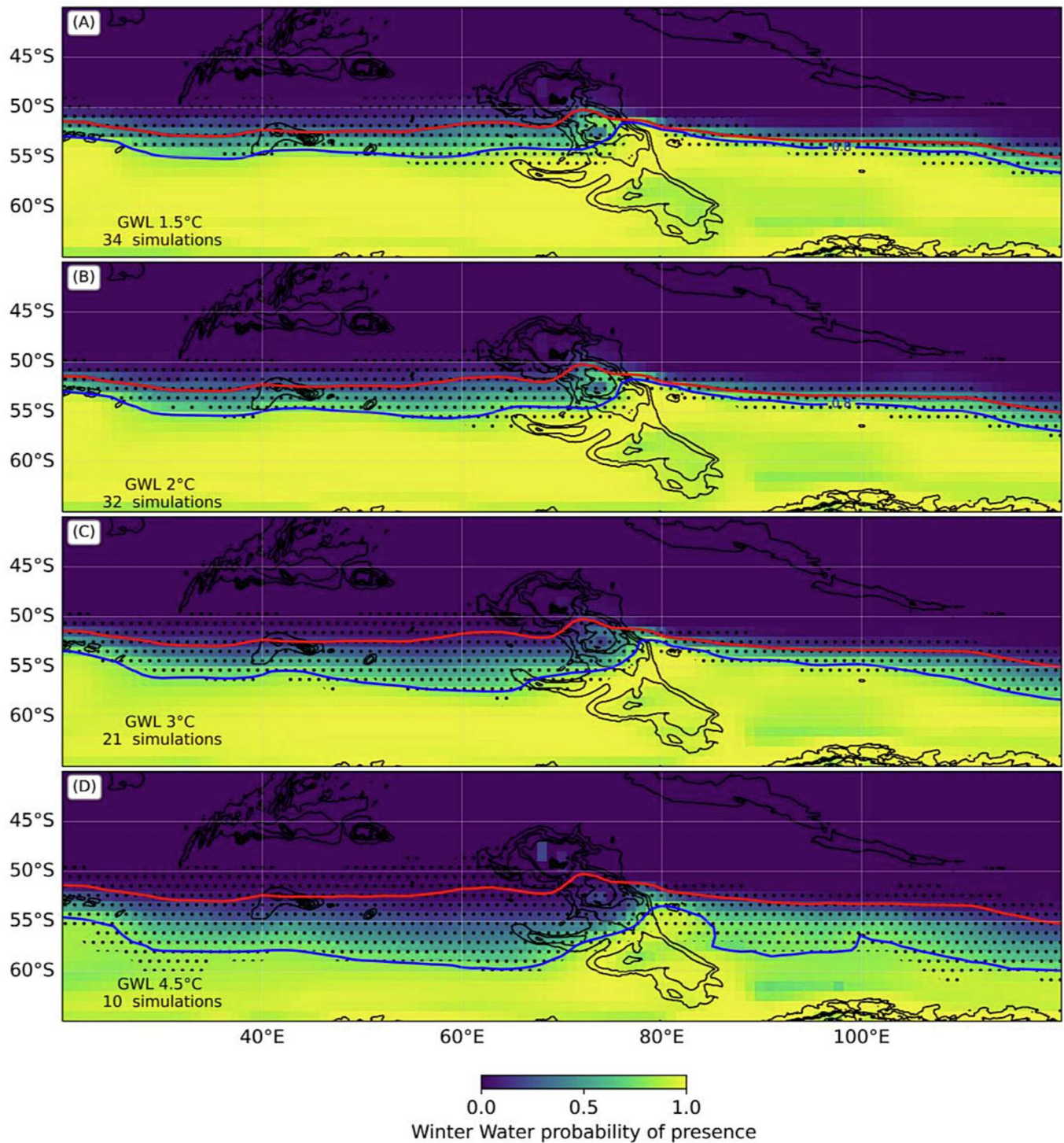


Fig. 6. Winter waters probability of presence for a global warming level of 1.5 °C (A), 2 °C (B), 3 °C (C) and 4.5 °C (D) relative to 1850–1900 using 12 CMIP6 models and SSP1–2.6, SSP2–4.5 and SSP5–8.5. The blue contours indicate the northernmost limit of 80% probability of presence of winter waters for each global warming level. The red contours indicate the northernmost limit of 80% probability of presence of winter waters for the preindustrial period (1850–1900) for the same number of simulations in each case. Dotted areas indicate where at least 80% of the simulations agree with the sign of the change of presence/absence of winter waters relative to 1850–1900. (For interpretation of the references to colour in this figure legend, the reader is referred to the web version of this article.)

Su et al., 2021 show, using an eddy-resolving model and NOAA-OI observations, the similarity between patterns of surface temperature anomalies and of sea level variability, used as a proxy for eddy activity, east of the Kerguelen Plateau. East of the Kerguelen Plateau (80–100°E; 55–45°S), we observe that MHWs sampled by elephant seal are shallower and less intense (Fig. 5). This area east of Kerguelen is a major foraging zone for elephant seals females and juveniles (*Mirounga leonina*)

whose behavior is related to mesoscale activity near the Polar Front (Baillieu et al., 2010; Dragon et al., 2010; Cotté et al., 2015; Cox et al., 2020). Elephant seals were found to avoid the interior of anticyclonic structures for capturing prey (Dragon et al., 2010). The observed bias of subsurface MHWs characteristics with MEOP-CTD datasets compared to Argo floats data (Fig. 5) is thus consistent with MHWs being strongly associated with anticyclonic eddies. Also, Argo-derived MHW presence

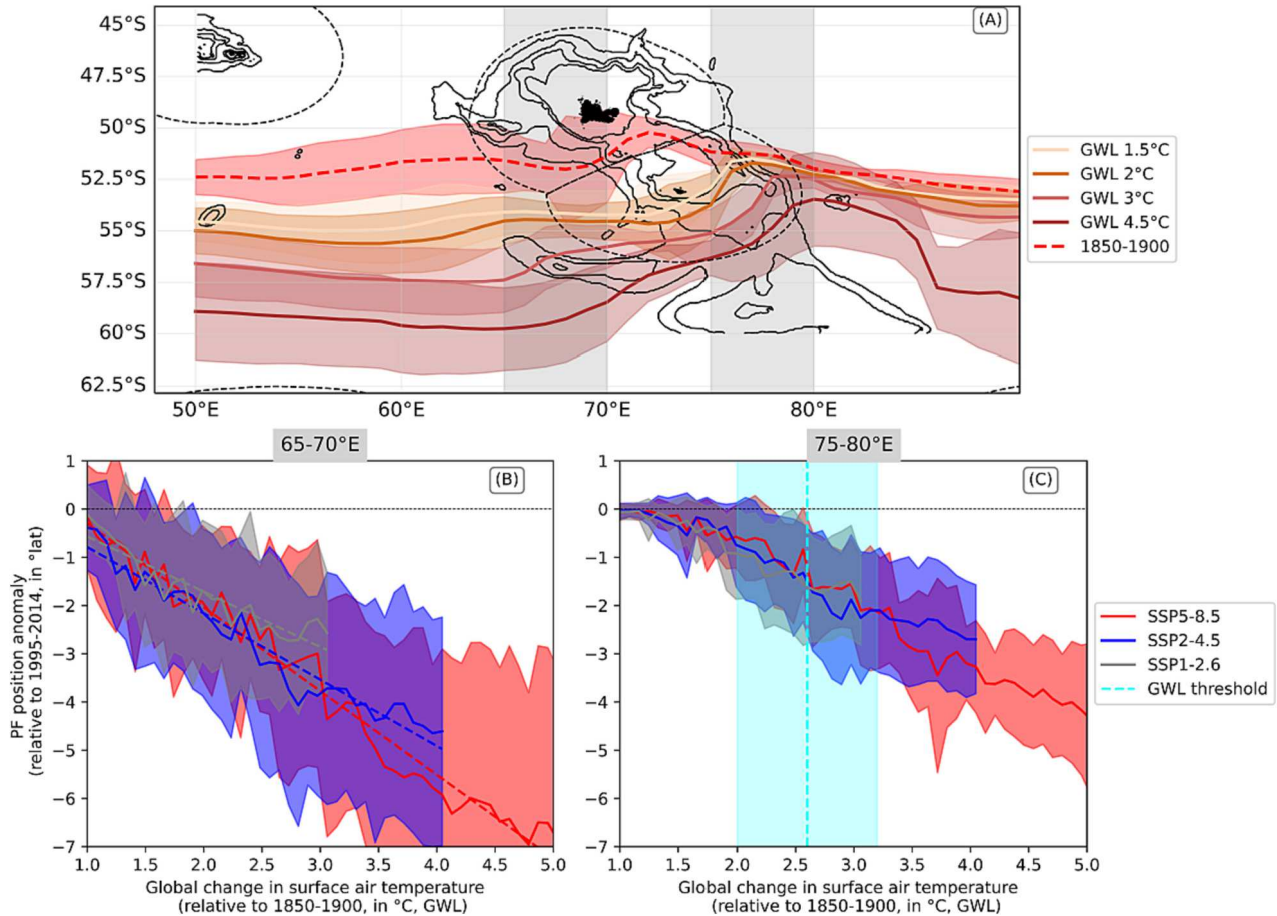


Fig. 7. Northernmost limit of 80% probability of presence of winter waters (similar to Fig. 6) for global warming levels (GWLs, global change in surface air temperature) 1.5 °C, 2 °C, 3 °C and 4.5 °C, as well as for the preindustrial period (1850–1900, dashed red line) between 50° and 90°E (A). The colored areas on (A) correspond to the intermodel standard deviation. Polar Front (PF) position anomaly (relative to 1995–2014) for the average of 12 CMIP6 models under SSP1–2.6 (gray), SSP2–4.5 (blue) and SSP5–8.5 (red), averaged over 65–70°E (B) and 75–80°E (C) for different GWLs (relative to 1850–1900). The two areas studied are shown in gray on panel A. The solid lines correspond to the multimodal mean value and the colored areas represent the intermodel standard deviation. On panel B, the dashed lines represent the linear regression of the PF position anomaly (over 65–70°E) with global warming for the different scenarios. On panel C, the vertical dashed line indicates the mean value, across the different models and scenarios, of the global warming threshold for which the absolute anomaly in the latitude of the PF is permanently >0.4° latitude (that is twice the natural variability of the PF position east of the Kerguelen Plateau; referred to as GWL threshold). (For interpretation of the references to colour in this figure legend, the reader is referred to the web version of this article.)

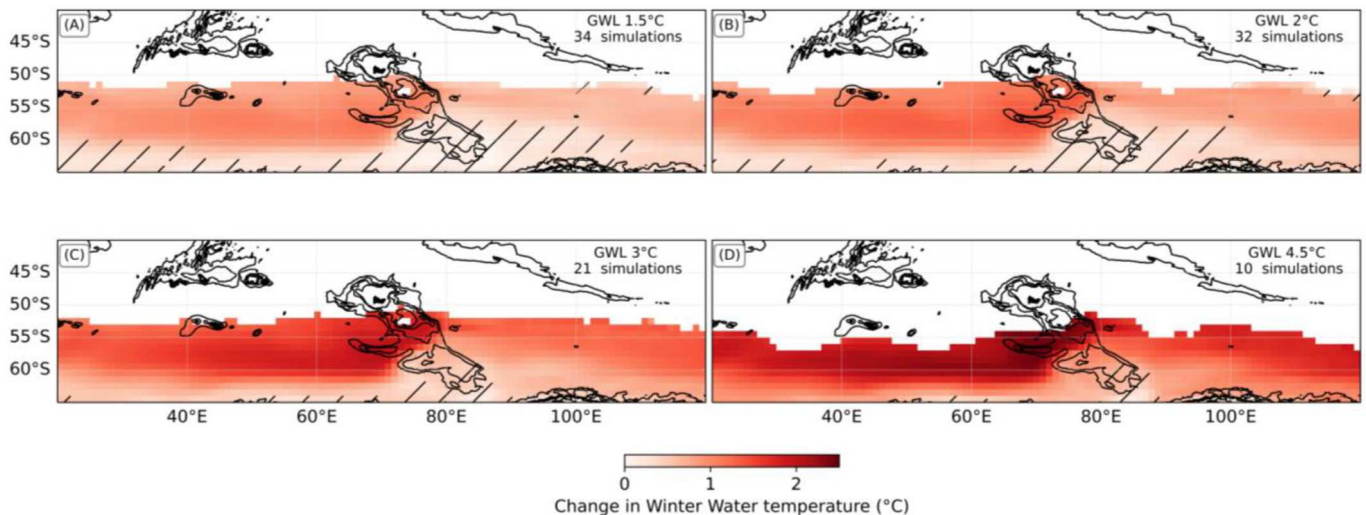


Fig. 8. Change in winter waters' temperature for a global warming level of 1.5 °C, 2 °C, 3 °C and 4.5 °C relative to 1850–1900 using 12 CMIP6 models and SSP1–2.6, SSP2–4.5 and SSP5–8.5. Only mean values obtained from >80% of the simulations are shown (as winter waters shift differently depending on models). Hatching indicates areas where the intermodel standard deviation is superior to the multimodel mean.

is found consistently in locations with higher eddy kinetic energy compared with profiles outside MHWs, especially in winter (Kolmogorov-Smirnov statistic-test = 0.12, p -value = $2.4 \cdot 10^{-22}$; Supplementary Material S5).

In this study, we show that MHW occurrence is positively correlated to a southward advection of water, especially at the northern boundary of the ACC (correlation coefficient up to 0.87; Fig. 3). The advection of water parcels showed that MHW are associated with southward latitudinal displacements that, on timescales of the order of a MHW duration (15 days), can be >110 km further than usual (Fig. 3B). This observation highlights the role of advective processes on MHWs.

The link described above between the mesoscale circulation and the presence of MHWs may also explain MHWs' subsurface signal. Surface temperature anomalies can be advected southward by eddies and penetrate deeper in the water column. Eddies can also trap and advect northern water masses southward, forming an anticyclonic meander in the Polar Front, and eventually generating a temperature anomaly across the water column. MHWs could be triggered by the southward advection of water masses across the Polar Front, e.g. within mesoscale eddies or front meanders, which would essentially drive WWs distribution further southward. This study shows that indeed MHWs are associated with a lower probability of presence of WWs (Fig. 4A). WWs northernmost extension (at least 80% of probability of presence) is shifted southward by around 1.4° latitude on average during MHWs in the Southern Indian Ocean. MHWs can therefore be associated with the variability of the Polar Front position, if the definition is taken of the Polar Front as the northernmost boundary of WWs. Such relation between MHWs and front shifts has already been observed in other regions (e.g. East Asian Marginal Seas, Choi et al., 2022, or the Kuroshio-Oyashio system, Du et al., 2022). The observed warming and deepening of WWs, also across all longitudes (Fig. 4 B and C), is not contradictory with advective processes, as the southward shift of WWs distribution can lead to deeper and warmer WWs replacing shallower and colder WWs.

In addition to advective processes, locally enhanced mixing could contribute to extending temperature anomalies at depth, especially in highly energetic regions such as east of the Kerguelen Plateau (Dove et al., 2022). The observed warming of WWs (Fig. 4C) can also be due to vertical mixing of the cold subsurface water mass with warmer surface water (Giddy et al., 2023). Giddy et al., (2023) show that a warming trend of 0.2°C over 28 days in the WW layer was driven by a convergence of heat flux from both above and below the WW layer; since in our study we find WWs temperature anomalies of 0.33°C during MHWs (Fig. 4C), diffusive processes may not be negligible.

4.2. Projected southward shift and warming of WWs in CMIP6 models

Intensity, duration, and extension of MHWs are expected to increase in the future both globally and in the Southern Indian Ocean. At the global scale, the average global number of MHW days is projected to increase by a factor of 16 even in a 1.5°C warming world (Frölicher et al., 2018). In addition, MHWs are projected to be more intense and to last longer, mostly due to ocean warming, especially in the subantarctic Indian Ocean (Azarian et al., 2023). An almost permanent state of MHW, relative to the historical period (1984–2014), is almost reached west of the Kerguelen Plateau (311.8 annual MHW days) at the end of the century using CMIP6 models under SSP2–4.5 (Azarian et al., 2023). Here we discuss the potential shift and warming of WWs under global warming on decadal timescales in both observations and CMIP6 analysis.

4.2.1. Comparing CMIP6 projections to past observations and paleoceanographic reconstructions

Our study shows a southward shift of WWs under global warming and thus of the Polar Front if this front is defined as the northernmost extension of WWs, using WWs probability of presence as an indicator

(see Section 3.2). The amplitude of this shift varies depending on the models but it can already be observed for a GWL 1.5°C . In a 1.5°C warming world, a maximum shift of around 4° latitude southward is found at 72°E (i.e. over the Kerguelen Plateau; compared to its pre-industrial position; Fig. 7).

This climate change signal may not have emerged yet in the observations. Different results have been found regarding actual trends in Polar Front shift depending on the front detection method used (Chapman et al., 2020). There is a consensus today that there is no evidence of a southward shift of the mean ACC position from observations (Gille, 2014; Chambers, 2018; Pauthenet et al., 2018; Meredith et al., 2019). Over the past decades the Polar Front may have remained within its natural range of latitude. This is also what is observed with the MERCATOR product using the definition of the Polar Front applied in our study (i.e. northernmost boundary of WW). In particular, although an increase in MHW occurrence is observed east of the Kerguelen Plateau over the period 1993–2019, using OSTIA dataset, there is no significant increase in MHWs that are associated with a southward shift of WWs (Supplementary Material S6). In this study, we also find no significant southward shift of WWs, using MERCATOR reanalysis between 1993 and 2019 (Supplementary Materials S6). Instead, we do observe a northward shift of around 2° latitude of the Polar Front west of the Kerguelen Plateau between 47° and 65°E (Supplementary Materials S6). However, also in this area, no causal relation between Polar Front shift and occurrence of MHWs can be identified, because no significant trend in MHWs is observed using the OSTIA dataset. We thus conclude that, over the last 30 years, the position of the Polar Front and the SST may still be dominated by natural variability (Azarian et al., 2023).

However, a shift of the Polar Front, and thus of WWs, in the Southern Indian Ocean might have already occurred in a warmer world in the past (Civel-Mazens et al., 2021). During peak-Interglacials, the Polar Front was found to pass through the Fawn Trough instead of nearby Kerguelen Islands; in our study, this regime shift of the Polar Front is also found at the end of the century in some models and for high GWLs (e.g. 4.5°C ; Fig. 6D).

Such projected shift could be due to changes in air-sea interactions, advection and sea ice dynamics which all drive WWs characteristics (Gordon and Huber, 1984; Sharma and Mathew, 1985; Toole, 1981; Evans et al., 2018; Pauthenet et al., 2018). In particular, changes in freshwater fluxes, notably due to Antarctic sea ice melting and change in sea-ice transport, could be an important driver of WWs mass transformation (Abernathey et al., 2016; Haumann et al., 2016). Sea ice melting and meltwater advection in summer contributes to making WWs colder than subantarctic summer surface water (Park et al., 1998; Anilkumar et al., 2015). If sea ice volume decreases, so might the supply of WWs and possibly their extension.

We remind that different metrics can be used to define the Polar Front (Chapman et al., 2020). Therefore, whether the Polar Front may shift in the future might vary depending on the region studied and the definition used. For instance, a water mass based definition of a front, or a surface temperature contour, might not always be well suited to follow future change of the jet position, at least regionally (Meijers et al., 2019). Jets and fronts of the Southern Indian Ocean could be controlled by different dynamical and non dynamical processes, thus generating a decorrelation between the jets and the fronts position under global warming but this would require further investigation.

4.2.2. Ecological implications of a projected asymmetrical southward shift of winter waters

In the long term, a drastic change in the WWs extension, and thus of the Polar Front, could have a significant impact on the composition and spatial distribution of the ecosystems. The changes caused by extreme events will tend to become average states depending on the GWL (WWs southward shift and warming; Figs. 6 and 8), except for potential effects on WWs depth which are more uncertain (see Section 3.2; Supplementary Material S4).

The asymmetry of the WWs southward shift in the CMIP6 models between the western side and the eastern side of the Kerguelen Plateau (Fig. 7) indicates that eastern ecosystems may be somehow shielded from climate change. This buffering effect against climate change observed on the eastern side of the Plateau could provide a “refuge” to some species of the Kerguelen Plateau. The concept of “climate refugia” has been introduced to identify local areas undergoing limited or slower changes in climate, and are typically potential candidates for protection (Burrows et al., 2014; Brito-Morales et al., 2018). In this study, the spatial differentiation of climate change impacts observed in CMIP6 models could be useful to guide conservation measures implemented in the French Southern Lands.

This contrast between the west and the east of Kerguelen Plateau also echoes the differences in vulnerability to a warming ocean observed between Crozet and Kerguelen king penguins' populations (*Aptenodytes patagonicus*, Bost et al., 2015; Brisson-Curadeau et al., 2022). It was found that, over the last 25 years, king penguins from Crozet were more sensitive to prey distance to the colony, associated with the fluctuations of the Polar Front position, than king penguins from Kerguelen. It was suggested that this latter population can be positively impacted by a warming ocean, through an increase in prey abundance and growth rates, as foraging areas east of Kerguelen are more stable (Bost et al., 2015; Brisson-Curadeau et al., 2022). However, these studies did not take into account that there may be a warming threshold (around 2.6 °C, see Section 3.2; Fig. 7C) when the Polar Front might no longer be stable east of the Kerguelen Plateau. An ocean warmer than 2.6 °C could then have dire consequences on the Kerguelen king penguins and on other predators that rely on WWs in the vicinity of their colonies. Note that this warming threshold is higher than the 1.5 °C target of the Paris

Agreement, which illustrates how committing to strong mitigation policies could significantly alleviate climate change pressure on biodiversity.

5. Conclusion

Winter Waters (WWs) refers to a subsurface water mass, characterized by a temperature minimum between 100 m and 400 m. This water mass plays an important ecological role in the Southern Indian Ocean, often constraining the foraging areas of several predator species. In the context of climate change, the aim of this study is to shed light on the impact of a warming climate on WWs. We found that WWs presence, temperature and depth can strongly be impacted by warming at different timescales (Fig. 9). In the recent decades (most recent 30 years), extreme local warming events (MHWs) are found to be related to changes in the distribution of WWs: their northernmost extension (at least 80% of probability of presence) is shifted southward by around 1.4° latitude during MHWs. Under global warming, this southward shift of WWs could be increased and maintained in the long term. In particular, WWs northernmost extension is projected to shift southward by around 2.5° latitude under a 2 °C warming world between 50° and 90°E using 12 CMIP6 models.

If MHWs ecological impacts can generally be limited in time and space, major extreme events such as the 1997 MHW (Bost et al., 2015) have been associated with dramatic consequences on land-based marine top predators. Impacts during such extreme events may foreshadow long-term changes for ecosystems in the future. WWs response to warming, however, is not homogeneous in our study area. CMIP6 projections suggest that the position of WWs east of the Kerguelen Plateau is

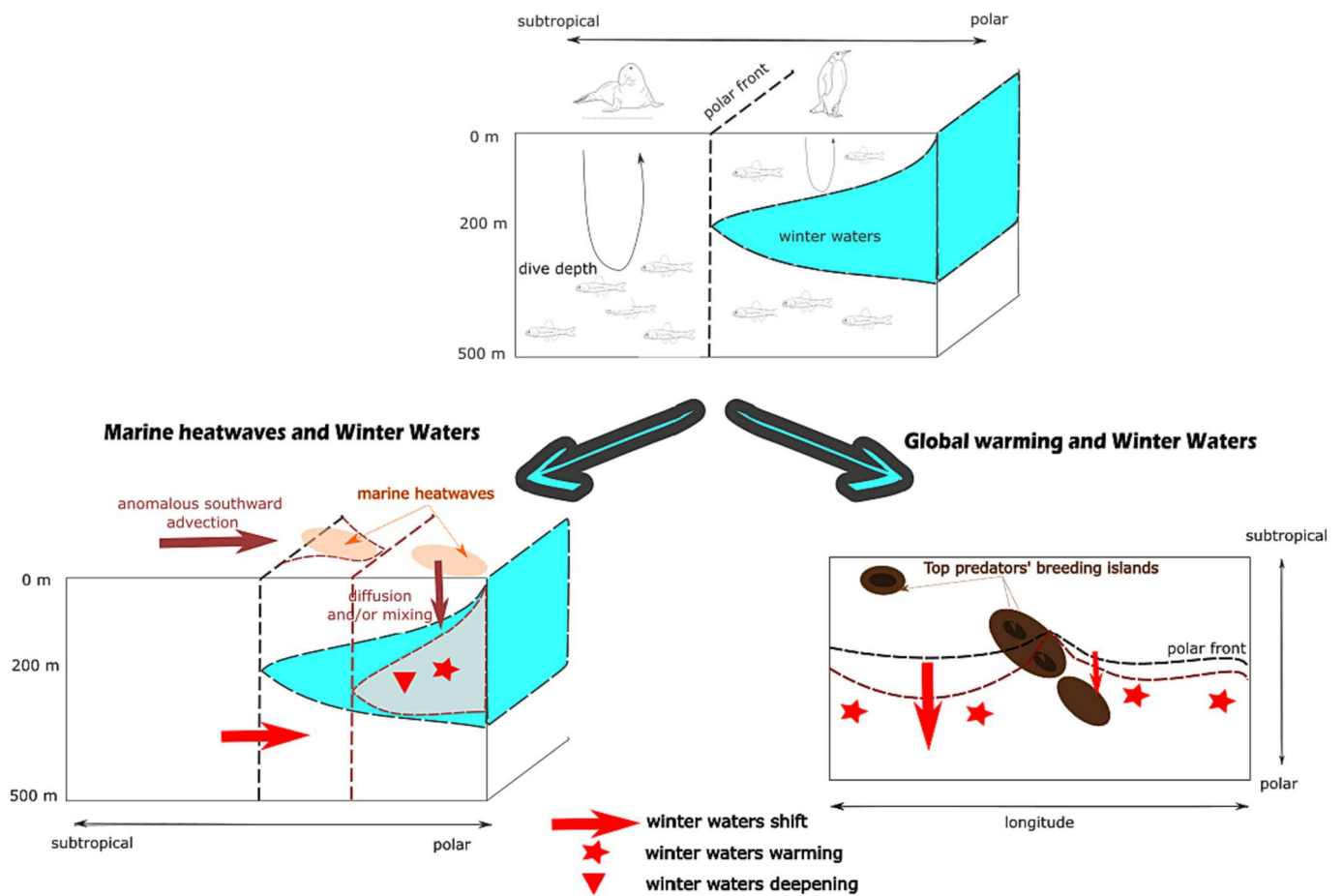


Fig. 9. Summary of the impacts of marine heatwaves and long-term global warming on winter waters, whose presence and characteristics play an important ecological role, notably for Southern Indian Ocean land-based top predators.

relatively more stable, at least up to 2.6 °C global warming. The presence of WWs nearby Kerguelen's colonies of top predators could therefore be preserved under a Paris Agreement scenario.

This study therefore points out how warming can affect ecologically significant subsurface physical features which are crucial for pelagic ecosystems. Understanding how such features might change spatially and at different timescales could be useful for policy-makers to account for climate change impacts in conservation and for mitigation strategies.

CRedit authorship contribution statement

Clara Azarian: Conceptualization, Formal analysis, Visualization, Writing – original draft, Writing – review & editing. **Laurent Bopp:** Conceptualization, Supervision, Writing – original draft, Writing – review & editing, Funding acquisition. **Jean-Baptiste Sallée:** Conceptualization, Writing – original draft, Writing – review & editing. **Sebastiaan Swart:** Conceptualization, Writing – original draft, Writing – review & editing. **Christophe Guinet:** Conceptualization, Writing – original draft, Writing – review & editing. **Francesco d'Ovidio:** Conceptualization, Supervision, Writing – original draft, Writing – review & editing, Funding acquisition.

Declaration of Competing Interest

The authors declare that they have no known competing financial interests or personal relationships that could have appeared to influence the work reported in this paper.

Data availability

This study used already publicly available data (see references in text and Supplementary Materials).

Acknowledgements

Publicly available datasets were analyzed in this study. The OSTIA, AVISO and Mercator reanalysis products were downloaded from copernicus marine service (<https://marine.copernicus.eu/>). The Argo data were downloaded from Argo GDAC Data Browser (https://www.usgodaes.org/cgi-bin/argo_select.pl), and these data are collected and made freely available by the International Argo Program and the national programs that contribute to it (<https://argo.ucsd.edu>, <https://www.ocean-ops.org>). The Argo Program is part of the Global Ocean Observing System. The elephant seal data are collected and made freely available by the International MEOP Consortium and the national programs that contribute to it (<http://www.meop.net>). Both French and Australian MEOP data were used. The Australian seal tracking data are collected by the Integrated Marine Observing System (IMOS). IMOS is a national collaborative research infrastructure, supported by the Australian Government. It is operated by a consortium of institutions as an unincorporated joint venture, with the University of Tasmania as Lead Agent. CMIP6 models outputs are publicly available here: <http://esgf-node.llnl.gov/projects/cmip6/>.

We acknowledge the World Climate Research Programme's Working Group on Coupled Modeling, that is responsible for CMIP. The authors also thank the IPSL modeling group for the software infrastructure, which facilitated CMIP analysis. We acknowledge funding support from the program LEFE led by CNRS-INSU, France and from the program TOSCA led by CNES, France (projects KERTREND and KERTREND-SAT). C.A. was financially supported by the French Ministry of Ecological Transition. L.B. acknowledges funding from the European Union's Horizon 2020 research and innovation program under grant agreement no. 820989 (project COMFORT). S.S. and J-B-S received funding from the European Union's Horizon 2020 research and innovation program under Grant Agreement 821001 (SO-CHIC). S.S. is also supported by a Wallenberg Academy Fellowship (WAF 2015.0186) and the Swedish

Research Council (VR 2019-04400).

Appendix A. Supplementary data

Supplementary data to this article can be found online at <https://doi.org/10.1016/j.jmarsys.2023.103962>.

References

- Abernathy, R.P., Cerovecki, I., Holland, P.R., Newsom, E., Mazloff, M., Talley, L.D., 2016. Water-mass transformation by sea-ice in the upper branch of the Southern Ocean overturning. *Nat. Geosci.* 9, 596–601. <https://doi.org/10.1038/ngeo2749>.
- Allegue, H., Guinet, C., Patrick, S.C., Hindell, M.A., McMahon, C.R., Réale, D., 2022. Sex, body size, and boldness shape the seasonal foraging habitat selection in southern elephant seals. *Ecol. Evol.* 12, e8457 <https://doi.org/10.1002/ece3.8457>.
- Anilkumar, N., George, J., Chacko, R., Nuncio, N., Sabu, P., 2015. Variability of fronts, fresh water input and chlorophyll in the Indian Ocean sector of the Southern Ocean. *N. Z. J. Mar. Freshw. Res.* 49 (1), 20–40. <https://doi.org/10.1080/00288330.2014.924972>.
- Argo, 2000. Argo Float Data and Metadata from Global Data Assembly Centre (Argo GDAC). SEANO. <https://doi.org/10.17882/42182>.
- Armour, K.C., Marshall, J., Scott, J.R., Donohoe, A., Newsom, E.R., 2016. Southern Ocean warming delayed by circumpolar upwelling and equatorward transport. *Nat. Geosci.* 9, 549–554.
- Auger, M., Morrow, R., Kestenare, E., Sallée, J.-B., Cowley, R., 2021. Southern Ocean in-situ temperature trends over 25 years emerge from interannual variability. *Nat. Commun.* 12, 514. <https://doi.org/10.1038/s41467-020-20781-1>.
- Azarian, C., Bopp, L., Pietri, A., Sallée, J.B., d'Ovidio, F., 2023. Current and projected patterns of warming and marine heatwaves in the Southern Indian Ocean. *Prog. Oceanogr.* 103036 <https://doi.org/10.1016/j.pocean.2023.103036>.
- Bailleul, F., Cotté, C., Guinet, C., 2010. Mesoscale eddies as foraging area of a deep-diving predator, the southern elephant seal. *Mar. Ecol. Prog. Ser.* 408, 251–264. <https://doi.org/10.3354/meps08560>.
- Béhagle, N., Cotté, C., Lebourges-Dhaussy, A., Roudaut, G., Duhamel, G., Brehmer, P., Josse, E., Cherel, Y., 2017. Acoustic distribution of discriminated micronektonic organisms from a bi-frequency processing : the case study of eastern Kerguelen oceanic waters. *Prog. Oceanogr.* 156, 276–289. <https://doi.org/10.1016/j.pocean.2017.06.004>.
- Belkin, I.M., Gordon, A.L., 1996. Southern Ocean fronts from the Greenwich meridian. *J. Geophys. Res.* 101 (2), 3675–3696.
- Bost, C.A., Cotté, C., Bailleul, F., Cherel, Y., Charrassin, J.B., Guinet, C., Ainley, D.G., Weimerskirch, H., 2009. The importance of oceanographic fronts to marine birds and mammals of the southern oceans. *J. Mar. Syst.* 78 (3), 363–376. <https://doi.org/10.1016/j.jmarsys.2008.11.022>.
- Bost, C.A., Cotté, C., Terray, P., Barbraud, C., Bon, C., Delord, K., Gimenez, O., Handrich, Y., Naito, Y., Guinet, C., Weimerskirch, H., 2015. Large-scale climatic anomalies affect marine predator foraging behaviour and demography. *Nat. Commun.* 6 (1), 8220. <https://doi.org/10.1038/ncomms9220>.
- Brisson-Curadeau, É., Elliott, K., Bost, C.-A., 2022. Contrasting bottom-up effects of warming ocean on two king penguin populations. *Glob. Chang. Biol.* <https://doi.org/10.1111/gcb.16519>.
- Brito-Morales, I., García Molinos, J., Schoeman, D.S., Burrows, M.T., Poloczanska, E.S., Brown, C.J., Ferrier, S., Harwood, T.D., Klein, C.J., McDonald-Madden, E., Moore, P. J., Pandolfi, J.M., Watson, J.E.M., Wenger, A.S., Richardson, A.J., 2018. Climate velocity can inform conservation in a warming world. *Trends Ecol. Evol.* 33 (6), 441–457. <https://doi.org/10.1016/j.tree.2018.03.009>.
- Burrows, M.T., Schoeman, D.S., Richardson, A.J., Molinos, J.G., Hoffmann, A., Buckley, L.B., Moore, P.J., Brown, C.J., Bruno, J.F., Duarte, C.M., Halpern, B.S., Hoegh-Guldberg, O., Kappel, C.V., Kiessling, W., O'Connor, M.I., Pandolfi, J.M., Parmesan, C., Sydeman, W.J., Ferrier, S., Williams, K.J., Poloczanska, E.S., 2014. Geographical limits to species-range shifts are suggested by climate velocity. *Nature* 507 (7493), 492–495. <https://doi.org/10.1038/nature12976>.
- Carter, L., McCave, I.N., Williams, M.J.M., 2008. Circulation and water masses of the Southern Ocean: A review. In: Florindou, F., Siebert, M. (Eds.), *Developments in Earth & Environmental Sciences*, Vol. 8. Elsevier, Amsterdam, pp. 85–113. [https://doi.org/10.1016/S1571-9197\(08\)00004-9](https://doi.org/10.1016/S1571-9197(08)00004-9).
- Chambers, D.P., 2018. Using kinetic energy measurements from altimetry to detect shifts in the positions of fronts in the Southern Ocean. *Ocean Sci.* 14, 105–116. <https://doi.org/10.5194/os-14-105-2018>.
- Chapman, C.C., 2017. New perspectives on frontal variability in the Southern Ocean. *J. Phys. Oceanogr.* 47, 1151–1168. <https://doi.org/10.1175/JPO-D-16-0222.1>.
- Chapman, C.C., Lea, M.-A., Meyer, A., Sallée, J.-B., Hindell, M., 2020. Defining Southern Ocean fronts and their influence on biological and physical processes in a changing climate. *Nat. Clim. Chang.* 10 (3), 209–219. <https://doi.org/10.1038/s41558-020-0705-4>.
- Chen, D., Rojas, M., Samset, B.H., Cobb, K., Niang, A., Diongue, Edwards, P., Emori, S., Faria, S.H., Hawkins, E., Hope, P., Huybrechts, P., Meinshausen, M., Mustafa, S.K., Plattner, G.-K., Tréguier, A.-M., 2021. Framing, context, and methods. In: Masson-Delmotte, V., Zhai, P., Pirani, A., Connors, S.L., Péan, C., Berger, S., Caud, N., Chen, Y., Goldfarb, L., Gomis, M.I., Huang, M., Leitzell, K., Lonnoy, E., Matthews, J. B.R., Maycock, T.K., Waterfield, T., Yelekçi, O., Yu, R., Zhou, B. (Eds.), *Climate Change 2021: The Physical Science Basis. Contribution of Working Group I to the Sixth Assessment Report of the Intergovernmental Panel on Climate Change*.

- Cambridge University Press, Cambridge, United Kingdom and New York, NY, USA, pp. 147–286. <https://doi.org/10.1017/9781009157896.003>.
- Choi, W., Bang, M., Joh, Y., Ham, Y.-G., Kang, N., Jang, C.J., 2022. Characteristics and mechanisms of marine heatwaves in the east Asian marginal seas: regional and seasonal differences. *Remote Sens.* 14, 3522. <https://doi.org/10.3390/rs14153522>.
- Civel-Mazens, M., Crosta, X., Cortese, G., Michel, E., Mazaud, A., Ther, O., Ikehara, M., Itaki, T., 2021. Antarctic Polar Front migrations in the Kerguelen Plateau region, Southern Ocean, over the past 360 kyrs. *Glob. Planet. Chang.* 202, 103526 <https://doi.org/10.1016/j.gloplacha.2021.103526>.
- Cotté, C., d'Ovidio, F., Dragon, A.-C., Guinet, C., Lévy, M., 2015. Flexible preference of southern elephant seals for distinct mesoscale features within the Antarctic Circumpolar Current. *Prog. Oceanogr.* 131, 46–58. <https://doi.org/10.1016/j.pocean.2014.11.011>.
- Cox, S.L., Authier, M., Orgeret, F., Weimerskirch, H., Guinet, C., 2020. High mortality rates in a juvenile free-ranging marine predator and links to dive and forage ability. *Ecol. Evol.* 10, 410–430. <https://doi.org/10.1002/ece3.5905>.
- Darmaraki, S., Somot, S., Sevault, F., Nabat, P., 2019. Past variability of Mediterranean Sea marine heatwaves. *Geophys. Res. Lett.* 46 (16), 9813–9823. <https://doi.org/10.1029/2019GL082933>.
- Dove, L.A., Balwada, D., Thompson, A.F., Gray, A.R., 2022. Enhanced ventilation in energetic regions of the Antarctic circumpolar current. *Geophys. Res. Lett.* <https://doi.org/10.1029/2021GL097574>.
- Dragon, A.-C., Monestiez, P., Bar-Hen, A., Guinet, C., 2010. Linking foraging behaviour to physical oceanographic structures : Southern elephant seals and mesoscale eddies east of Kerguelen Islands. In: 3rd GLOBEC OSM: From Ecosystem Function to Ecosystem Prediction, pp. 61–71. <https://doi.org/10.1016/j.pocean.2010.09.025>, 87(1).
- Du, Y., Feng, M., Xu, Z., Yin, B., Hobday, A.J., 2022. Summer Marine heatwaves in the Kuroshio-Oyashio extension region. *Remote Sens.* 14 <https://doi.org/10.3390/rs141329> (13:2980).
- Elzahaby, Y., Schaeffer, A., 2019. Observational insight into the subsurface anomalies of marine heatwaves. *Front. Mar. Sci.* 6, 745. <https://doi.org/10.3389/fmars.2019.00745>.
- Evans, D.G., Zika, J.D., Naveira Garabato, A.C., Nurser, A.J.G., 2018. The cold transit of Southern Ocean upwelling. *Geophys. Res. Lett.* 45, 13386–13395. <https://doi.org/10.1029/2018GL079986>.
- Eyring, V., Bony, S., Meehl, G.A., Senior, C.A., Stevens, B., Stouffer, R.J., Taylor, K.E., 2016. Overview of the Coupled Model Intercomparison Project Phase 6 (CMIP6) experimental design and organization. *Geosci. Model Dev.* 9 (5), 1937–1958. <https://doi.org/10.5194/gmd-9-1937-2016>.
- Fox-Kemper, B., Hewitt, H.T., Xiao, C., Aðalgeirsdóttir, G., Drijfhout, S.S., Edwards, T.L., Gollidge, N.R., Hemer, M., Kopp, R.E., Krinner, G., Mix, A., Notz, D., Nowicki, S., Nurhati, I.S., Ruiz, L., Sallée, J.-B., Slangen, A.B.A., Yu, Y., 2021. Ocean, cryosphere and sea level change. In: Masson-Delmotte, V., Zhai, P., Pirani, A., Connors, S.L., Péan, C., Berger, S., Caud, N., Chen, Y., Goldfarb, L., Gomis, M.I., Huang, M., Leitzell, K., Lonnoy, E., Matthews, J.B.R., Maycock, T.K., Waterfield, T., Yelekçi, O., Yu, R., Zhou, B. (Eds.), *Climate Change, 2021. The Physical Science Basis. Contribution of Working Group I to the Sixth Assessment Report of the Intergovernmental Panel on Climate Change*. Cambridge University Press, Cambridge, United Kingdom and New York, NY, USA, pp. 1211–1362. <https://doi.org/10.1017/9781009157896.011>.
- Frölicher, T.L., Fischer, E.M., Gruber, N., 2018. Marine heatwaves under global warming. *Nature* 560 (7718), 360–364. <https://doi.org/10.1038/s41586-018-0383-9>.
- Giddy, I.S., Fer, I., Swart, S., Nicholson, S.-A., 2023. Vertical convergence of turbulent and double-diffusive heat flux drives warming and erosion of Antarctic Winter Water in summer. *J. Phys. Oceanogr.* 53, 1941–1958. <https://doi.org/10.1175/JPO-D-22-0259.1>.
- Gille, S.T., 2014. Meridional displacement of the Antarctic Circumpolar Current. *Phil. Trans. R. Soc. A* 372, 20130273. <https://doi.org/10.1098/rsta.2013.0273>.
- Good, S., Fiedler, E., Mao, C., Martin, M.J., Maycock, A., Reid, R., Roberts-Jones, J., Searle, T., Waters, J., While, J., Worsfold, M., 2020. The current configuration of the OSTIA system for operational production of Foundation Sea surface temperature and ice concentration analyses. *Remote Sens.* 12 (4), 720. <https://doi.org/10.3390/rs12040720>.
- Gordon, A.L., 1975. An Antarctic oceanographic section along 170°E. *Deep-Sea Res.* 33, 357–377. [https://doi.org/10.1016/0011-7471\(75\)90060-1](https://doi.org/10.1016/0011-7471(75)90060-1).
- Gordon, A.L., Huber, B.A., 1984. Thermohaline stratification below the Southern Ocean sea ice. *J. Geophys. Res. Oceans* 89 (C1), 641–648. <https://doi.org/10.1029/JC089iC01p00641>.
- Großelindemann, H., Ryan, S., Ummenhofer, C.C., Martin, T., Biastoch, A., 2022. Marine heatwaves and their depth structures on the northeast U.S. Continental Shelf. *Front. Clim.* 4, 857937 <https://doi.org/10.3389/fclim.2022.857937>.
- Guinet, C., Vacqué-García, J., Picard, B., Bessigneul, G., Lebras, Y., Dragon, A.C., Viviant, M., Arnould, J.P.Y., Bailleul, F., 2014. Southern elephant seal foraging success in relation to temperature and light conditions: insight into prey distribution. *Mar. Ecol. Prog. Ser.* 499, 285–301.
- Haumann, F.A., Gruber, N., Münnich, M., Frenger, I., Kern, S., 2016. Sea-ice transport driving Southern Ocean salinity and its recent trends. *Nature* 537, 89–92. <https://doi.org/10.1038/nature19101>.
- Herger, N., Sanderson, B.M., Knutti, R., 2015. Improved pattern scaling approaches for the use in climate impact studies. *Geophys. Res. Lett.* 42 (9), 9. <https://doi.org/10.1002/2015GL063569>.
- Hobday, A.J., Alexander, L.V., Perkins, S.E., Smale, D.A., Straub, S.C., Oliver, E.C.J., Benthuyens, J.A., Burrows, M.T., Donat, M.G., Feng, M., Holbrook, N.J., Moore, P.J., Scannell, H.A., Sen Gupta, A., Wernberg, T., 2016. A hierarchical approach to defining marine heatwaves. *Prog. Oceanogr.* 141, 227–238. <https://doi.org/10.1016/j.pocean.2015.12.014>.
- Hu, S., Li, S., Zhang, Y., Guan, C., Du, Y., Feng, M., Ando, K., Wang, F., Schiller, A., Hu, D., 2021. Observed strong subsurface marine heatwaves in the tropical western Pacific Ocean. *Environ. Res. Lett.* 16 (10), 104024 <https://doi.org/10.1088/1748-9326/ac26f2>.
- Hunt, B.P.V., Swadlow, K.M., 2021. Macrozooplankton and micronekton community structure and diel vertical migration in the Heard Island Region, Central Kerguelen Plateau. *J. Mar. Syst.* 221, 103575 <https://doi.org/10.1016/j.jmarsys.2021.103575>.
- Kooyman, G.L., Davis, R.W., Croxall, J.P., Costa, D.P., 1982. Diving depths and energy requirements of king penguins. *Science* 217, 726–727.
- Kooyman, G.L., Cherel, Y., Maho, Y.L., Croxall, J.P., Thorson, P.H., Ridoux, V., Kooyman, C.A., 1992. Diving behavior and energetics during foraging cycles in king penguins. *Ecol. Monogr.* 62, 143–163. <https://doi.org/10.2307/2937173>.
- Lee, J.-Y., Marotzke, J., Bala, G., Cao, L., Corti, S., Dunne, J.P., Engelbrecht, F., Fischer, E., Fyfe, J.C., Jones, C., Maycock, A., Mutemi, J., Ndiaye, O., Panickal, S., Zhou, T., 2021. Future global climate: 1291 Scenario-Based Projections and Near-Term Information. In: Masson-Delmotte, V., Zhai, P., Pirani, A., Connors, S.L., Péan, C., Berger, S., Caud, N., Chen, Y., Goldfarb, L., Gomis, M.I., Huang, M., Leitzell, K., Lonnoy, E., Matthews, J.B.R., Maycock, T.K., Waterfield, T., Yelekçi, O., Yu, R., Zhou, B. (Eds.), *Climate Change 2021: The Physical Science Basis. Contribution of Working Group I to the Sixth Assessment Report of the Intergovernmental Panel 1293 on Climate Change*. Cambridge University Press, Cambridge, United Kingdom and New York, NY, USA, pp. 553–672. <https://doi.org/10.1017/9781009157896.006>.
- Lovel, W., Terray, L., 2016. Observed southern upper-ocean warming over 2005–2014 and associated mechanisms. *Environ. Res. Lett.* 11, 124023.
- McIntyre, T., Anson, I.J., Bornemann, H., Plötz, J., Tosh, C.A., Bester, M.N., 2011. Elephant seal dive behaviour is influenced by ocean temperature: implications for climate change impacts on an ocean predator. *Mar. Ecol. Prog. Ser.* 441, 257–272. <https://doi.org/10.3354/MEPS09383>.
- McMahon, C.R., Hindell, M.A., Charrassin, J.-B., Corney, S., Guinet, C., Harcourt, R., Jonsen, I., Trebilco, R., Williams, G., Bestley, S., 2019. Finding mesopelagic prey in a changing Southern Ocean. *Sci. Rep.* 9, 19013. <https://doi.org/10.1038/s41598-019-55152-4>.
- Meijers, A.J.S., Meredith, M.P., Murphy, E.J., Chambers, D.P., Belchier, M., Young, E.F., 2019. The role of ocean dynamics in king penguin range estimation. *Nat. Clim. Chang.* 9, 120–121. <https://doi.org/10.1038/s41558-018-0388-2>.
- Polar regions. In: Meredith, M., Sommerkorn, M., Cassotta, S., Derksen, C., Ekaykin, A., Hollowed, A., Kofinas, G., Mackintosh, A., Melbourne-Thomas, J., Muelbert, M.M.C., Ottersen, G., Pritchard, H., Schuur, E.A.G., Pörtner, H.-O., Roberts, D.C., Masson-Delmotte, V., Zhai, P., Tignor, M., Poloczanska, E., Mintenbeck, K., Alegría, A., Nicolai, M., Okem, A., Petzold, J., Rama, B., Weyer, N.M. (Eds.), 2019. *IPCC Special Report on the Ocean and Cryosphere in a Changing Climate*. Cambridge University Press, Cambridge, UK and New York, NY, USA, pp. 203–320. <https://doi.org/10.1017/9781009157964.005>.
- Miyama, T., Minobe, S., Goto, H., 2021. Marine heatwave of sea surface temperature of the Oyashio region in summer in 2010–2016. *Front. Mar. Sci.* 7, 1150. <https://doi.org/10.3389/fmars.2020.576240>.
- Morrison, A.K., Griffies, S.M., Winton, M., Anderson, W.G., Sarmiento, J.L., 2016. Mechanisms of Southern Ocean heat uptake and transport in a global eddying climate model. *J. Clim.* 29, 2059–2075. <https://doi.org/10.1175/JCLI-D-15-0579.1>.
- Mulet, S., Rio, M.H., Etienne, H., Artana, C., Cancet, M., Dibarboure, G., Feng, H., Husson, R., Picot, N., Provost, C., Strub, P.T., 2021. The new CNES-CLS18 global mean dynamic topography. *Ocean Sci.* 17 (3), 789–808. <https://doi.org/10.5194/os-17-789-2021>.
- Oliver, E.C.J., Donat, M.G., Burrows, M.T., Moore, P.G., Smale, D.A., Alexander, L.V., Benthuyens, J.A., Feng, M., Sen Gupta, A., Hobday, A.J., Holbrook, N.J., Perkins-Kirkpatrick, S.E., Scannell, H.A., Straub, S.C., Wernberg, T., 2018. Longer and more frequent marine heatwaves over the past century. *Nat. Commun.* 9, 1324. <https://doi.org/10.1038/s41467-018-03732-9>.
- Oliver, E.C.J., Benthuyens, J.A., Darmaraki, S., Donat, M.G., Hobday, A.J., Holbrook, N.J., Schlegel, R.W., Sen Gupta, A., 2021. Marine heatwaves. *Annu. Rev. Mar. Sci.* 13 (1), 313–342. <https://doi.org/10.1146/annurev-marine-032720-095144>.
- Park, Y.-H., Durand, I., 2019. Altimetry-Derived Antarctic Circumpolar Current Fronts. *SEANOE*. <https://doi.org/10.17882/59800>.
- Park, Y.-H., Gamberoni, L., 1993. Frontal structure, waters masses and circulation in the Crozet Basin. *J. Geophys. Res.* 98 (7), 12361–12385.
- Park, Y.-H., Charriaud, E., Feix, M., 1998. Thermohaline structure of the Antarctic surface water/winter water in the Indian sector of the Southern Ocean. *J. Mar. Syst.* 17 (1), 5–23. [https://doi.org/10.1016/S0924-7963\(98\)00026-8](https://doi.org/10.1016/S0924-7963(98)00026-8).
- Park, Y.-H., Park, T., Kim, T.-W., Lee, S.-H., Hong, C.-S., Lee, J.-H., Rio, M.-H., Pujol, M.-I., Ballarotta, M., Durand, I., Provost, C., 2019. Observations of the Antarctic circumpolar current over the Udintsev Fracture Zone, the narrowest choke point in the Southern Ocean. *J. Geophys. Res. Oceans* 124, 4511–4528. <https://doi.org/10.1029/2019JC015024>.
- Pathenhet, E., Roquet, F., Madec, G., Guinet, C., Hindell, M., McMahon, C.R., Harcourt, R., Nerini, D., 2018. Seasonal meandering of the polar front upstream of the Kerguelen plateau. *Geophys. Res. Lett.* 45 (18), 9774–9781. <https://doi.org/10.1029/2018GL079614>.
- Roemmich, D., Church, J., Gilson, J., Monselesan, D., Sutton, P., Wijffels, S., 2015. Unabated planetary warming and its ocean structure since 2006. *Nat. Clim. Chang.* 5, 240–245. <https://doi.org/10.1038/nclimate2513>.
- Roquet, F., Williams, G., Hindell, M.A., Harcourt, R., McMahon, C., Guinet, C., Charrassin, J.-B., Reverdin, G., Boehme, L., Lovell, P., Fedak, M., 2014. A southern

- Indian Ocean database of hydrographic profiles obtained with instrumented elephant seals. *Sci. Data* 1 (1), 140028. <https://doi.org/10.1038/sdata.2014.28>.
- Sabu, P., Libera, S.A., Chacko, R., Anilkumar, N., Subeesh, M.P., Thomas, A.P., 2020. Winter water variability in the Indian Ocean sector of Southern Ocean during austral summer. Understanding the link between atmospheric, physical and biogeochemical processes in the Indian sector of the Southern Ocean Deep-Sea Res. II Top. Stud. *Oceanogr.* 178, 104852. <https://doi.org/10.1016/j.dsr2.2020.104852>.
- Sallée, J.-B., 2018. Southern ocean warming. *Oceanography* 31 (2), 52–62.
- Sallée, J.-B., Shuckburgh, E., Bruneau, N., Meijers, A.J.S., Bracegirdle, T.J., Wang, Z., 2013. Assessment of Southern Ocean mixed-layer depths in CMIP5 models : historical bias and forcing response. *J. Geophys. Res. Oceans* 118 (4), 1845–1862. <https://doi.org/10.1002/jgrc.20157>.
- Sharma, G.S., Mathew, B., 1985. Hydrography and circulation off the Antarctic in the Indian Ocean region. *Proc. Indian Acad. Sci* 94 (1), 13–27.
- Siegelman, L., O’Toole, M., Flexas, M., Rivière, P., Klein, P., 2019. Submesoscale Ocean fronts act as biological hotspot for southern elephant seal. *Sci. Rep.* 9, 5588.
- Su, Z., Pilo, G.S., Corney, S., Holbrook, N.J., Mori, M., Ziegler, P., 2021. Characterizing marine heatwaves in the Kerguelen plateau region. *Front. Mar. Sci.* 7, 1119. <https://doi.org/10.3389/fmars.2020.531297>.
- Toole, J.M., 1981. Sea ice, winter convection and temperature minimum layer in the Southern Ocean. *J. Geophys. Res.* 86, 8037–8047.
- Treasure, A.M., Roquet, F., Ansoorge, I.J., Bester, M.N., Boehme, L., Bornemann, H., Charrassin, J.-B., Chevallier, D., Costa, D.P., Fedak, M.A., Guinet, C., Hammill, M.O., Harcourt, R.G., Hindell, M.A., Kovacs, K.M., Lea, M.-A., Lovell, P., Lowther, A.D., Lydersen, C., McIntyre, T., McMahon, C.R., Muelbert, M.M.C., Nicholls, K., Picard, B., Reverdin, G., Trites, A.W., Williams, G.D., de Bruyn, P.J.N., 2017. Marine mammals exploring the oceans pole to pole : a review of the MEOP consortium. *Oceanography* 30 (2), 132–138.

4.4 Science and society: Characterizing temporary refugia

From the study on MHWs and global warming impacts on WWs emerges the identification of a potential refugium east of Kerguelen. Climate refugia are commonly defined as regions that are less affected by climate change than their surroundings. These areas may therefore foster ecosystems' resilience. A key point is that we here identify a refugium based on the stability of a dynamic feature of ecological significance: the Polar Front position as defined by the northernmost extension of the WWs. Yet, we also determine a global warming threshold above which the Polar Front starts to significantly shift southward, suggesting that this potential refugium is temporary, with a lifetime depending on the emission scenario. The existence of this temporary refugium triggers two questions with underlying management implications:

- What are the physical mechanisms leading to such a refugium?
- Is the southward shift of the Polar Front reversible?

Topographic constraints might generate temporary refugia

The stability of the Polar Front position east of the Kerguelen Plateau and, by contrast, the high variability of its position west of the Plateau have already been observed on a seasonal and interannual timescale (Pauthenet et al., 2018). This contrast supports that topography can play a key role in constraining the flow and the positions of fronts. This is consistent with theoretical frameworks such as the barotropic vorticity balance (Waldman and Giordani, 2023). The barotropic vorticity balance is derived from the conservation of momentum and the hypothesis of a depth-independent circulation. Such balance can be written as follows:

$$\beta V = J(p_b, H) + k \cdot \nabla \times \tau + k \cdot \nabla \times A \quad (4.1)$$

where V is the time-mean integrated meridional velocity, β is the meridional gradient of the Coriolis parameter, $J(p_b, H)$ is the bottom pressure torque which depends on the pressure at the bottom and the bathymetry, $k \cdot \nabla \times \tau$ the wind stress curl and $k \cdot \nabla \times A$ the non-linear advection term. As the current flows from deep to shallow topography,

the water column is squashed which generates vorticity and is balanced by increased meridional transport with the flow being deviated equatorward (Rintoul, 2018).

Our analysis in the previous sections has focused on the Southern Indian Ocean and the Kerguelen Plateau. To support whether topography indeed plays a role in the projected changes of the Polar Front position (still defined as the northernmost extension of the WWs), we conduct a complementary analysis at a circumpolar scale, using the same CMIP6 models as in Azarian et al. (2024).

Over the historical period (1995-2014), the Polar Front is indeed deviated north at North Scotia Ridge, at the South Atlantic Ridge, at the Kerguelen Plateau, at the Southeast Indian Ridge and the Pacific Antarctic Ridge (Figure 4.2 A). We note that the stronger latitudinal shifts of the Polar Front under SSP2-4.5 at the end of the century also occur at these topographic features. As the flow crosses the topography, the front's deviation is either reduced or slightly shifted, resulting in large anomalies of the Polar Front position. At the Pacific Antarctic Ridge, the South Atlantic Ridge and the Southeast Indian Ridge, there is a starker shift of the mean Polar Front over 2081-2100 compared to 2041-2060 (Figure 4.2 B), which could be linked to the existence of global warming thresholds in these areas as well. After crossing the identified topographic features, the Polar Front shift most often weakens, especially after the Kerguelen Plateau and the Southeast Indian Ridge. We also note a limited shift around the Drake Passage, even under the strong emission scenario at the end of the century. Overall, this complementary analysis highlights the importance of topographic features in the local response of the Polar Front (defined as WWs northernmost extension) to climate change. Although, the complexity and differences in topographic shapes could modulate the differences in response of the Polar Front position upstream and downstream of those features, such impact suggests that topographic features can be associated with temporary climate refugia (up to a to-be-determined threshold).

Is the southward shift of the Polar Front reversible?

The presence of the Kerguelen Plateau constrains the position of the Polar Front east and thus seems to buffer climate change impact. While the Polar Front shifts southward linearly with global warming west of Kerguelen, the Polar Front east of Kerguelen starts to significantly shift southward after a global warming threshold estimated at around

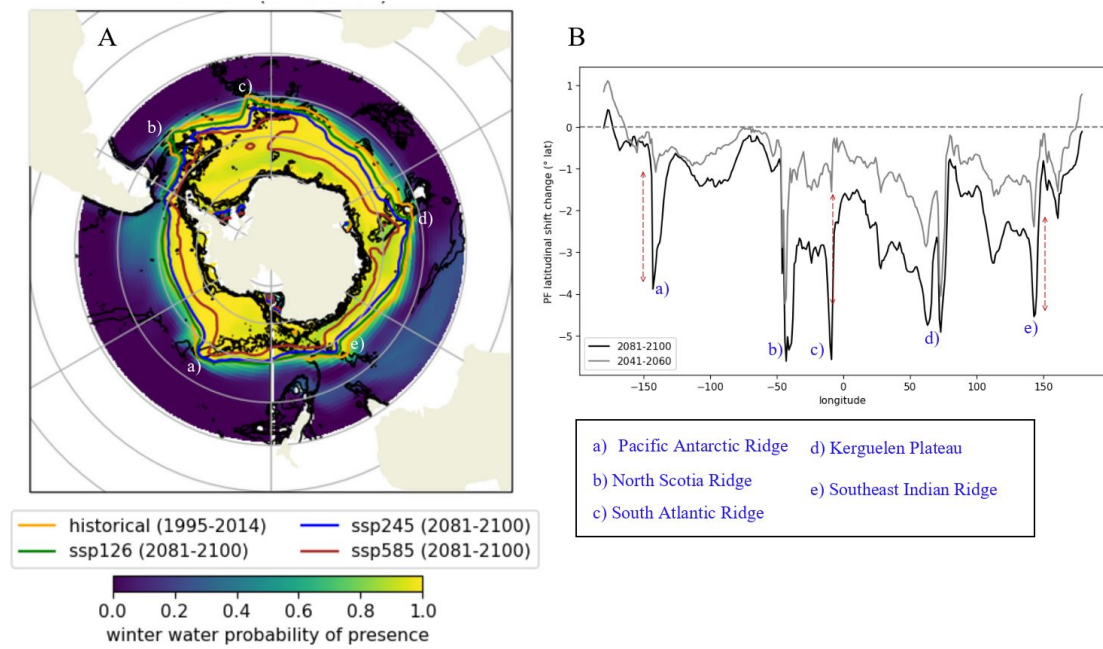


FIGURE 4.2: **Changes in the Polar Front position, as defined as the northernmost extension of the winter waters, at the circumpolar scale.** (A) Mean winter water probability of presence in 11 CMIP6 models between 1995 and 2014 overlapped with the position of the Polar Front (northernmost 80% probability of presence of winter waters) historically (orange), under SSP1-2.6 (green), SSP2-4.5 (blue) and SSP5-8.5 (brown) at the end of the century. (B) Change in the Polar Front position under SSP2-4.5 relative to 1995-2014 over 2041-2060 (gray) and 2081-2100 (black). Key topographic features are indicated in blue on Panel B and white on Panel A.

2.6°C is reached (Azarian et al., 2024). Does that mean that a tipping point has been crossed?

A tipping point is defined by the IPCC as “a critical threshold beyond which a system reorganises, often abruptly and/or irreversibly” (IPCC, 2023). Tipping points have been increasingly considered, notably in the media, to communicate on the urgency to mitigate climate change (Heinze et al., 2021; McKay et al., 2022). This is also an important notion to warn management of potentially abrupt changes in ecosystems that might occur after the crossing of such tipping point and to identify the important indicators to monitor accordingly (Lenton et al., 2008; Hewitt and Thrush, 2019). A crucial element of defining a tipping point is the concept of reversibility, which is inherently related to a defined timescale. In that case, is the southward shift of the Polar Front reversible on decadal timescales?

To investigate this question, we use overshoot simulations (SSP5-3.4OS) from the five out of the 12 CMIP6 models used previously (Azarian et al., 2024) for which such simulations are available. The scenario used is SSP5-8.5 from 2015 up to 2040 and

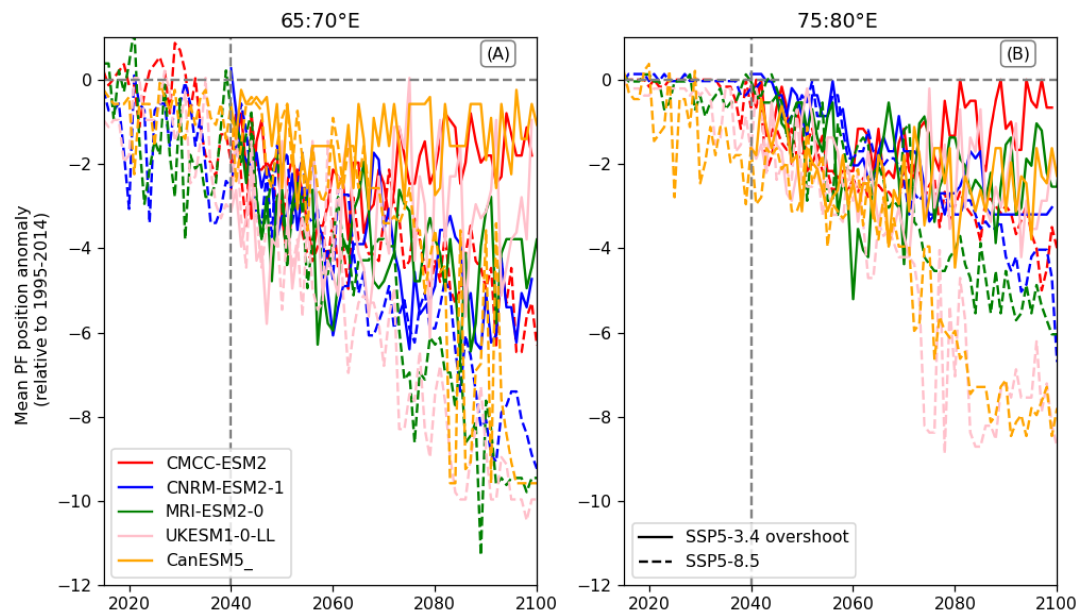


FIGURE 4.3: **Evolution of the mean Polar Front position under a strong emission scenario and an overshoot scenario.** Mean Polar Front (definition based on winter waters northernmost extension) latitude anomaly under SSP5-3.4 overshoot (solid lines) and SSP5-8.5 (dashed lines) relative to 1995-2014 over 65°-70°E (A) and 75°-80°E (B) for 5 CMIP6 models.

then very strong mitigation is undertaken to rapidly reduce emissions to zero by around 2070 (O'Neill et al., 2016). Depending on the models, the Polar Front, still defined by the northernmost extension of the WWs, is projected to shift back a bit further north and/or to stabilise around 20 years after the start of the drastic emission reduction both east and west of the Kerguelen Plateau (Figure 4.3). The shift of the Polar Front is not projected to be irreversible over a few decades and appears strongly linked to the global warming level. Whether, the ecological consequences of such shift are reversible would require further investigation.

To conclude on the tipping point nature of the projected Polar front shift, further analyses would be required to quantify the abruptness of this shift. This notion might vary depending on the area studied, as illustrated for one climate model on Figure 4.4. Figure 4.4 panels B and D show that for one fixed area a brutal change from WWs presence to absence can occur at the end of the century while the probability of presence decreases more linearly for the areas of panels C and E. We note that differences in timeseries behavior can also arise from the size of the area considered. Further analyses could, for instance, focus on king penguins foraging areas to investigate how abruptly those foraging areas might change. Figure 4.4 also illustrates that increased variability in the WWs

distribution can occur before a more permanent WWs shift, which could also impact top predators foraging strategy and which emphasizes even more the temporary nature of the identified refugium east of Kerguelen.

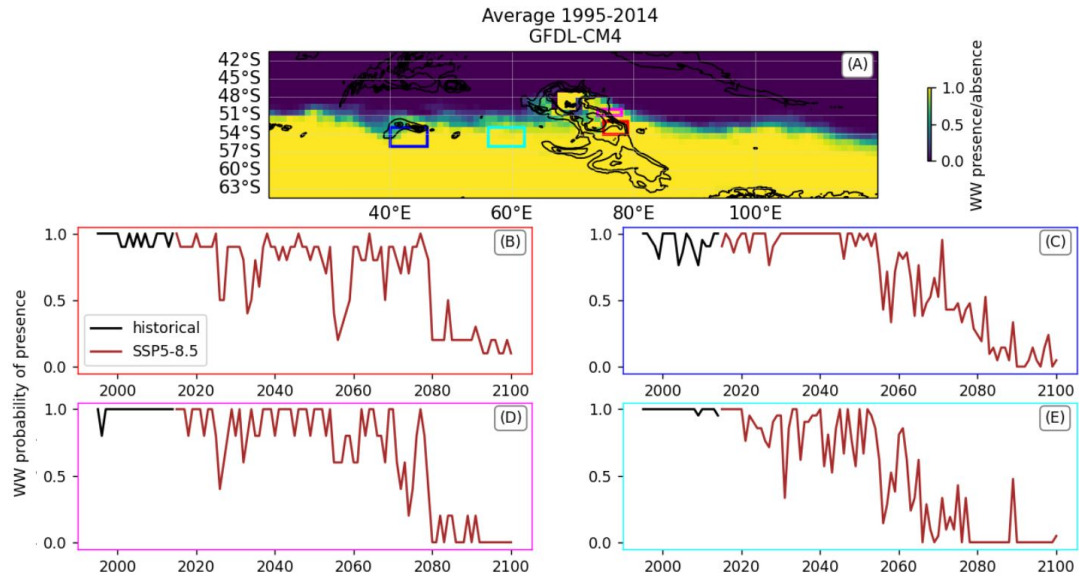


FIGURE 4.4: Examples using the climate model GFDL-CM4 of the evolution of winter water probability of presence, in small areas near the Kerguelen Plateau, under a strong emission scenario. (A) Mean winter water probability of presence in February over 1995-2014 for the climate model GFDL-CM4. Evolution over time of the February winter water probability of presence in GFDL-CM4, over the historical period (1995-2014) and up to the end of the century under SSP5-8.5, for different smaller areas represented by colored rectangles on the panel A: (B, red) 75-79°E 54-52°S, (C, blue) 40-46°E 56-53°S, (D, magenta) 74-78°E 51-50°S, and (E, cyan) 56-62°E 56-53°S.

The southward shift of WWs, and thus of the Polar Front, east of Kerguelen may not be irreversible but could generate major ecological consequences. The relative stability of this front east of Kerguelen up to a certain warming threshold makes this area an interesting temporary refugium. This is particularly noteworthy for conservation due to the rich biodiversity and trophic interactions occurring east of Kerguelen (Koubbi et al., 2016; Thiers et al., 2017). This area may also be of ecological significance for the development of the Patagonian toothfish early-life stages. The Patagonian toothfish fishery is an important economic resource in the region. The future of the connectivity between spawning areas on the western side of the Kerguelen Plateau (Mori et al., 2016; Péron et al., 2016) and this potential refugium and recruitment area east of Kerguelen is thus of both ecological and societal importance. This is the focus of the next Chapter.

Conclusion

This Chapter studies how MHWs and global warming can impact a structuring subsurface water mass for pelagic ecosystems. WWs are shifted southward or being deeper and warmer during a surface MHW. These impacts are projected to become average states in the coming decades (except for WWs deepening). Conducting those analyses on two different timescales allows to :

- Pinpoint the temporal heterogeneity of climate change impacts on WWs
- Anticipate that the ecological impacts observed during extreme events might tend to become average states in the future

However, the interpretation of the comparison between the two timescales analyses must be done with caution as different physical drivers may be at play on longer timescales and future impacts may also depend on ecosystems' adaptive capacity. Remaining questions following this study include:

- What are the physical mechanisms driving the southward shift of the Polar Front in the Southern Indian Ocean in CMIP6 models?
- Could MHWs in the future be considered as precursors of the Polar Front southward shift?

Moreover, this Chapter further discusses the notion of climate refugia, also clarifying that the southward shift of the Polar Front east of Kerguelen is not irreversible in overshoot climate projections, although the associated ecological consequences could mark an ecological tipping point.

This climate refugium overlaps an area of ecological importance for the early-life stages of the Patagonian toothfish, an important economic resource. As both Chapters 3 and 4 indicate contrasted climate change impacts between either sides of the Kerguelen Plateau, we now aim at investigating the potential impact of climate change on the local circulation, over the Kerguelen Plateau, that may play a key role in connecting Patagonian toothfish spawning areas on the western side of the Plateau to this important area east of Kerguelen.

Chapter 5

Assessing the potential influence of climate change on life history connectivity of the Patagonian toothfish over and around the Northern Kerguelen Plateau

“Au-dessus de nous, l’espace ;
au-dessous, un miroir ; la surface des
eaux est pareille au regard de beaux
yeux ouverts ; on s’y perd sans
comprendre.”

*A. Conti, Le Carnet Viking: 70 jours
en mer de Barents*

5.1 Context

Previous Chapters have focused on temperature-related changes and their impacts on a structuring subsurface water mass. To further investigate climate change impacts on physical drivers of ecological processes, we now focus on the ocean circulation zooming

over the Kerguelen Plateau, where it plays an important role for the ecology of the Patagonian toothfish (*Dissostichus eleginoides*), a long-lived predatory fish and a key economic resource.

Climate change impacts on Patagonian toothfish are uncertain. A strong variability in recruitment (i.e. entry in the fish stock), probably due to environmental variability, is already observed (Collins et al., 2007, 2010; Laptikhovsky and Brickle, 2005), with significant consequences on stock assessments (Patterson and Tuynman, 2022; Péron et al., 2022). Different hypotheses have been developed to generally better understand recruitment variability, mostly based on early-life stages dependence on environmental conditions (Houde, 2008). The stable ocean hypothesis (Lasker, 1975, 1981), the environmental window hypothesis (Cury and Roy, 1989) and Bakun's triad (Bakun, 1996), all suggest a link between hydrodynamic processes and the presence and accessibility of productive areas (food availability) for advected early-life stages (Figure 5.1). Besides, it is expected that early-life stages might be more vulnerable to environmental conditions as they develop in the upper 200 m and are transported by local currents (Pankhurst and Munday, 2011), compared to the adult demersal and opportunistic stage of the life cycle (Collins et al., 2010). Although knowledge on Patagonian toothfish eggs and larvae is limited, understanding the variability of the local circulation through particle tracking studies can provide some insight on a potential driver of recruitment variability (Mori et al., 2022).

Considering the pathways of early-life stages transport is particularly important over the Kerguelen Plateau. Indeed, the main current crossing the Plateau is zonal flowing eastward (Park et al. (2008b); Figure 5.2), meaning that eggs spawned east of the Plateau have more chance to be transported far offshore of the Plateau toward unsuitable areas of recruitment, unless there are some retention processes; whereas eggs spawned west of the Plateau can be retained over shallow bathymetry as they are transported toward the eastern side of the Plateau. The connectivity over the Kerguelen Plateau due to local ocean currents can therefore play an important role in ensuring supply of larvae to the eastern side of the Kerguelen Plateau in case of an intensification of the zonal flow. This connectivity can have implications for the management of the stock as it then raises questions of competition between the Australian and French stocks. A modelling study highlighted that the potential competition effect between Kerguelen and Heard island

toothfish fisheries would depend on the connectivity between the stocks (Subramaniam et al., 2020).

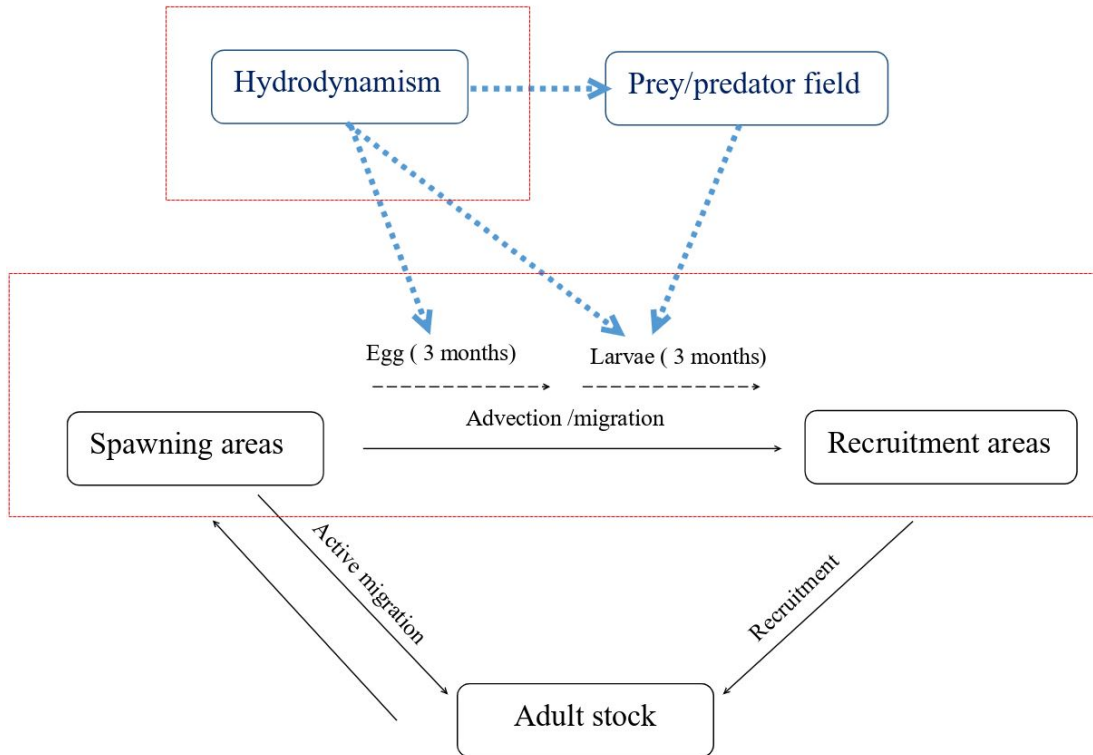


FIGURE 5.1: **Schematic of fish life cycle adapted from Harden-Jones (1968).** In the case of the Patagonian toothfish, the egg and larval phases have been estimated both at around 3 months (Collins et al., 2010) and are subjected to hydrodynamic processes. In addition, larvae have a limited swimming capacity and their survival are influenced by food availability and predatory pressure (blue dashed arrows). Red rectangles indicate the main processes that we focus on in this Chapter 5.

The aim of this Chapter is therefore to investigate whether the local circulation over and around the Kerguelen Plateau during Patagonian toothfish spawning season could be impacted by climate change. To do so, we :

- Estimate the interannual variability of the connectivity over the Kerguelen Plateau during the Patagonian toothfish spawning season, especially the connectivity between the western side of the Plateau and east of Kerguelen using a Lagrangian approach based on altimetry-derived geostrophic velocities ;
- Identify the main large-scale drivers of the connectivity variability, that can be supported by theoretical frameworks ;

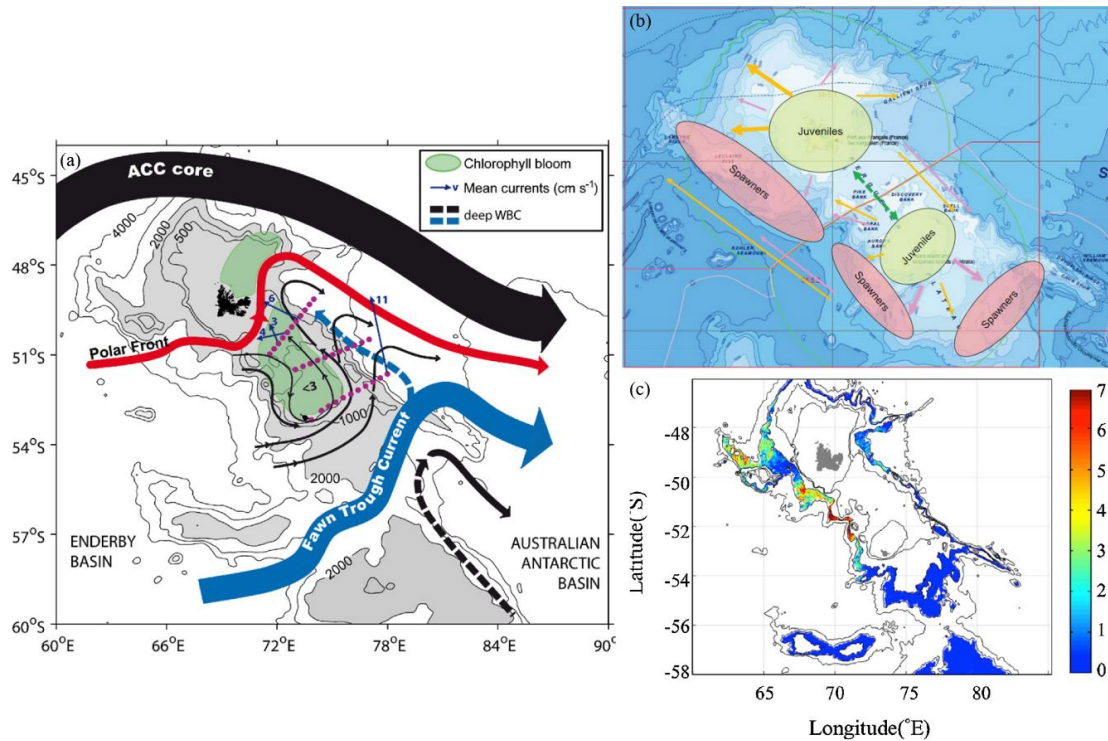


FIGURE 5.2: Current knowledge on the local circulation and the spatial distribution of the Patagonian toothfish over and around the Kerguelen Plateau. (A) Schematic of the geostrophic circulation over and around the Kerguelen Plateau from [Park et al. \(2008c\)](#). (B) Schematic of the distribution of the Patagonian toothfish population structure on the Kerguelen Plateau highlighting potential exchange of juveniles between areas (dark green arrows) as well as males (orange arrows) and females (pink arrows) movements into deeper waters as they grow. Boundaries of the Australian and French EEZ are shown in green lines and of the CCAMLR areas in red lines (Figure from [Ziegler and Welsford \(2019\)](#)). (C) Potential spawning locations that lead to consistent settlement success as defined in [Mori et al. \(2016\)](#) over 2000–2006, with simulations using the AVISO velocity field. The colorbar indicates the frequency of successful recruitment from a particular spawning location out of those seven years (Figure from [Mori et al. \(2016\)](#)).

- Study climate models projections of those main large-scale drivers under different emission scenario and discuss potential interpretations of their implications for connectivity.

There have been prior efforts to quantify the connectivity between Patagonian toothfish spawning and recruitment areas ([Mori et al. \(2016\)](#) ; Figure 5.2 C). The study presented here is complementary to this work as :

- It is based on longer timeseries of AVISO geostrophic velocities (27 years) ;
- It does not make assumptions about the spawning and recruitment areas bathymetry;

- It investigates the drivers of this interannual variability to enable the discussion on climate change potential impacts.

In this Chapter, we use the understanding of past variability and extremes to interpret future projections, searching for links between local and large-scale processes. As this study is motivated by the ecological importance of oceanic currents for Patagonian toothfish early-life stages transport (Figures 5.1, and 5.2), we also aim at reflecting on climate change implications for Patagonian toothfish fisheries management.

5.2 Key results

This study sheds light on the **high interannual variability of the connectivity probability between the west of Heard and the east of Kerguelen** during the Patagonian toothfish spawning season (winter). Over these last decades, this variability is found to be **mostly driven by the winter wind stress magnitude**, with high connectivity being associated with increased wind stress and low connectivity associated with decreased wind stress (and the occurrence of potentially blocking features). In climate models, **winter wind stress is projected to intensify** in the near term under different emission scenario but, in the long term, projections differ depending on the models and the scenario. A significant projected intensification of the winter wind stress at the end of the century is only found under a strong emission scenario (SSP5-8.5). However, the Polar Front east of Kerguelen, as defined by the northernmost extension of Winter Waters, is projected to shift southward for a global warming level higher than around 2.6°C (Chapter 4) which could be reached mid-century depending on the scenario. Such shift, especially if it is linked to a southward shift of the currently associated jet, could lead to a significant and unprecedented (at the scale of the last decades) reorganization of the circulation patterns over the Plateau.

Climate change could therefore have impacts on the local circulation at different timescales. A short-term increase in the connectivity between the west of Heard and the east of Kerguelen could occur in the coming decades due to the intensification of westerlies, with a potential increased dependence between the French and the Australian stocks. However, how crucial this connectivity is for the Patagonian toothfish French

stock and whether a potential future blocking due to a Polar Front shift could modify the population dynamics remain uncertain.

The connectivity between the west of Heard and the east of Kerguelen is found to negatively covary with the retention east of Kerguelen. As wind stress increases, retention east of Kerguelen could be impacted, notably around the Polar Front meander, potentially limiting Patagonian toothfish early-life stages concentration in those areas. If the core of the Polar Front meander could be an interesting area for larval survival following Bakun's triad hypothesis (high primary productivity, concentration of potential prey, retention processes, [Bakun \(1996\)](#)), its characteristics could be impacted under climate change. **Climate change, through both wind stress increases or through the Polar Front shift in the region, could impact retention patterns east of Kerguelen.**

The results from this study could be extended to other fish species spawning in winter with pelagic early-life stages (e.g. *Champscephalus gunnari*, *Notothenia rossii*; [Koubbi et al. \(2009\)](#)). Retention east of Kerguelen plays a major role not only for the Patagonian toothfish, but also for the broader ecosystem, notably as retentive areas tend to be hotspots of trophic interactions ([d'Ovidio et al., 2013](#); [Koubbi et al., 2016](#)). Although the area east of Kerguelen EEZ around the Polar Front meander is under strict protection ([Azam et al., 2019](#)), the associated biodiversity could be impacted by changed patterns of retentive processes under climate change.

5.3 Main study

The main study is presented here as an article manuscript soon to be submitted. The associated Supplementary Material can be found in Appendix C.

Assessing the Potential Influence of Climate Change on Life History Connectivity of the Patagonian Toothfish over and around the Northern Kerguelen Plateau

Clara Azarian 1 2, Laurent Bopp, 3, Félix Massiot-Granier 4, Louise Rousselet 1, Jilda Caccavo 1 5,
Philippe Koubbi 1, and Francesco d'Ovidio 1

1 Sorbonne Université, CNRS, IRD, MNHN, Laboratoire d'Océanographie et du Climat:
Expérimentations et Approches Numériques (LOCEAN-IPSL), Paris, France.

2 Ecole Nationale des Ponts et Chaussées (ENPC), Champs-sur-Marne, France.

3 Ecole Normale Supérieure / Université PSL, CNRS, Ecole Polytechnique, Sorbonne Université,
Laboratoire de Météorologie Dynamique (LMD-IPSL) Paris, France.

4 Laboratoire de Biologie des Organismes et Ecosystèmes Aquatiques (BOREA), MNHN, CNRS, UCN,
IRD, SU, UA, Paris, France

5 Laboratoire des Sciences du Climat et de l'Environnement, LSCE/IPSL, CEA-CNRS-UVSQ, Université
Paris-Saclay, Gif-sur-Yvette, France.

Corresponding author: C. Azarian; clara.azarian@locean.ipsl.fr

Abstract

The ocean circulation over the Northern Kerguelen Plateau transports early-life stages of the Patagonian toothfish (*Dissostichus eleginoides*), potentially playing an important role in connecting fish stocks that are managed by different countries. Growing concerns exist regarding the potential impact of climate change on this resource. However, the spatial resolution provided in current climate projections is too coarse to directly assess the effects of climate change on the circulation over the Northern Kerguelen Plateau. This study aims to address this gap by leveraging insights from past interannual variability. We first characterize the interannual variability of the connectivity between potential spawning and recruitment areas, notably between west of Heard Island and east of the Kerguelen plateau, using geostrophic velocities derived from satellite altimetry. Second, we investigate potential large-scale drivers of this variability. Third, we study the projected changes of the identified large-scale drivers using climate projections. Our findings reveal: i) significant interannual variability in connectivity between the west of Heard Island and east of the Kerguelen plateau, ii) primarily driven by wind stress, iii) and a projected intensification of these patterns under climate change scenarios throughout the 21st century to varying degrees depending on the emission scenario. The potential impacts of climate change on ecologically significant local features (connectivity, retention) and their implications for fisheries management and conservation are discussed.

1. Introduction

The Kerguelen Plateau is a major topographic feature in the Indian sector of the Southern Ocean that deflects the strong zonal flow of the Antarctic Circumpolar Current (ACC). The ACC transport is mostly divided between a strong flow (between 0.1 and 0.5 m/s on average) north of the Kerguelen Plateau and through the Fawn Trough (around 56°S; see Figure 1B and 2B; Park et al., 2008a, 2008c, 2009, van Wijk et al., 2010). Around 79°E, the Fawn Trough Current is divided in two branches: one that transports cold Antarctic Water northward along the eastern slope of the Plateau and can reach around 48°S while the other, the main flow, crosses the topography and meanders southeastward (Park et al., 2008c, Park et al., 2008a; Roquet et al., 2009; Park et al., 2014). The circulation between the Kerguelen and Heard shelves is

much slower (< 5 cm/s on average, Figure 1B) and anticyclonic, contributing to a northward transport between Heard and Kerguelen Islands (Park et al., 2014). The dominant water masses over the Heard shelf are Antarctic Surface Waters and Winter Waters respectively at the surface and subsurface. The northernmost extension of the Winter Waters marks the position of the Polar Front which passes south of Kerguelen islands flowing northward and then meanders southward due to topographic constraints (Park et al., 2014; Pauthenet et al., 2018).

The slow circulation between the Heard and Kerguelen Island shelves plays an important ecological role. The increased retention over shallow bathymetries, associated with iron inputs from the islands and their shelves, is favorable to increased productivity (Park et al., 2008b). This slower circulation also contributes to the transport of Patagonian toothfish (*Dissostichus eleginoides*) eggs and larvae, that mostly remain in the upper 200 m of the water column (North, 2002). Although aggregating spawning hotspots have not yet been identified over the Northern Kerguelen Plateau (Péron et al., 2016), the locations of Patagonian toothfish spawning areas in other regions have been associated with the influence of local oceanic circulation (Bridgen et al., 2017; Bamford et al., 2024), either through their influence on productivity (Young et al., 2011) or their enhancement of retention (Young et al., 2012). This potential influence of the local circulation is all the more relevant as spawning occurs in winter when off-shelf transportation is usually stronger (Young et al., 2014; Bamford et al., 2024). Over the Northern Kerguelen Plateau, spawning occurs between June and October, probably synchronized with the spring phytoplankton bloom that can provide food for early-life stages (Koubbi et al., 2009; Collins et al., 2010). Patagonian toothfish spawning locations that may be most likely to lead to successful recruitment (which refers to the number of fish surviving and entering a fishery) have been suggested and partly identified on the western side of the Northern Kerguelen Plateau (Duhamel, 1987; Lord et al., 2006; Duhamel et al., 2011; Welsford et al., 2012; Mori et al., 2016). Such localisation seems consistent with local circulation patterns, since the main oceanic current is flowing eastward, meaning that eggs spawned east of the Plateau are more likely to be transported far offshore toward unsuitable areas of recruitment, unless there are some retention processes ; whereas eggs spawned west of the Plateau can be retained over shallow bathymetries.

Important recruitment areas appear to be located east of the Kerguelen Islands (Figure 1; Lord et al., 2006; Duhamel and Hautecoeur, 2009). Suitable recruitment areas can be characterized by increased productivity

to provide food to larvae as well as retention processes to avoid larval drift far offshore (Bakun, 1996; Houde, 2008). The northeastern shelf off Baleiniers Gulf in particular has been identified as a possible retention zone for pelagic organisms (Koubbi et al., 2000; Koubbi et al., 2016). In addition, high concentrations of myctophid fish larvae (potential prey for Patagonian toothfish larvae and juveniles; Collins et al., 2010) have been observed in the area of the Polar Front meander east of Kerguelen (Koubbi et al., 2009), which has also been identified as a possible retention area (Koubbi et al., 2016). This area is ecologically significant as the increased retention can favor the development of higher trophic levels locally (d'Ovidio et al., 2015), thus being a favored foraging area for land-based marine predators (Thiers et al., 2017), a central motivation for the no-take zones designated within the Kerguelen natural reserve (Figure 1A). Circulation patterns in the area support the prediction that early-life stages spawned east of Kerguelen should disperse downstream, away from the Plateau. Consequently, understanding how the area east of the Kerguelen Islands is connected to western areas of the Northern Kerguelen Plateau is essential to understanding recruitment success.

The potential effect of climate change on this local circulation and on the associated connectivity between the west of the Plateau and the east of Kerguelen remains unknown. Projections from climate models indicate an intensification of warming and marine heatwaves (i.e. extreme events of surface temperature) especially between 40°S and 50°S in the Indian sector of the Southern Ocean (Azarian et al., 2023) as well as a southward shift of the Polar Front over the Northern Kerguelen Plateau under global warming (Azarian et al., 2024). However, the resolution of climate models remains too coarse to adequately represent fine scale circulation over complex topography, such as the Plateau, and thus to directly address this question of climate change impact on local connectivity.

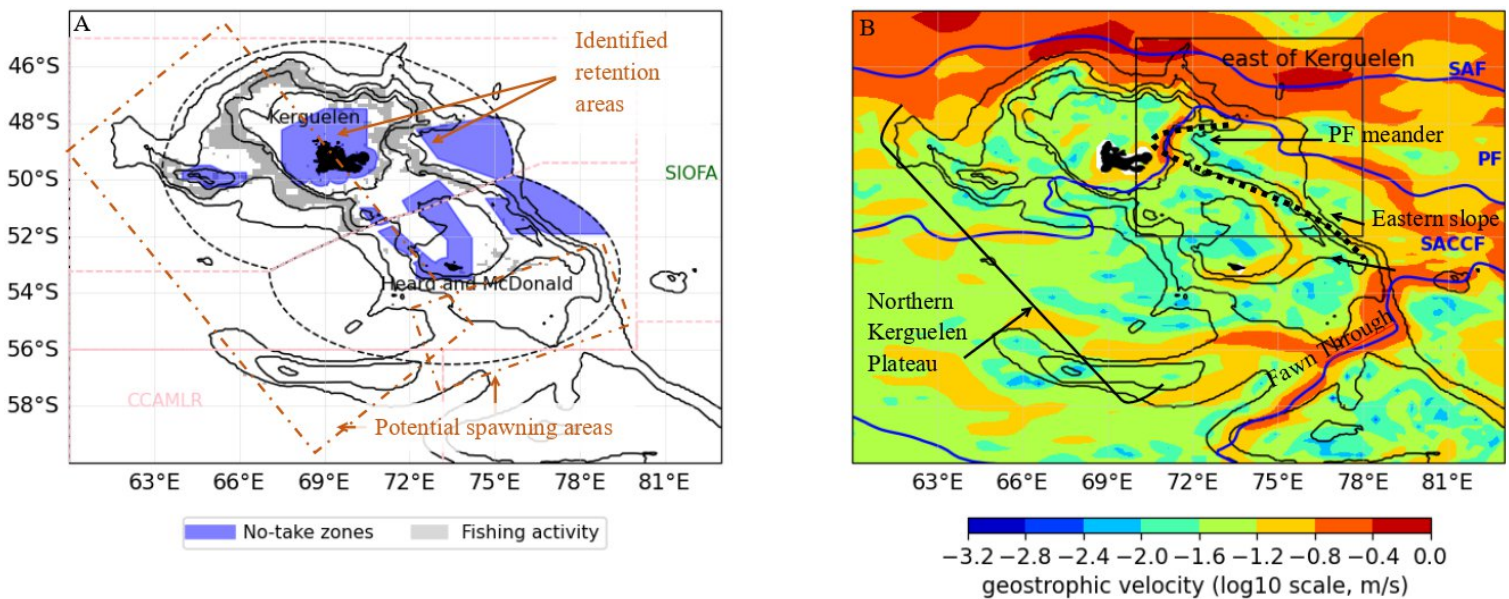
Understanding the impact of climate change on connectivity between potential spawning areas west of the Northern Kerguelen Plateau and potential recruitment areas east of Kerguelen can provide useful information to manage the highly profitable toothfish fisheries present in this region (Duhamel et al., 2011; Grilly et al., 2015). Although the Patagonian toothfish population in this region is genetically connected and can be considered as one metapopulation (Appleyard et al, 2002, 2003; Ziegler and Welsford, 2019), it is managed by different organizations, both at the national and international level, as shown in Figure 1. Adult toothfish can migrate occasionally over large distances (e.g. Burch et al., 2019), but are mostly

considered sedentary (Appleyard et al., 2002 ; Marlow et al., 2003 ; Williams and Lamb, 2002), meaning that the transport of early life-stages can play an important role in connecting different stocks.

The objective of this study is to address the following question: will the local geostrophic circulation, connecting areas west of the Northern Kerguelen Plateau to the east of Kerguelen, be modified, enhanced or weakened, under climate change ? To that aim, we follow three steps.

- First, we characterize the interannual variability of the circulation connectivity using satellite altimetry-derived geostrophic velocities.
- Second, we investigate the potential large-scale drivers of this variability.
- Third, we study the projected patterns of change in the large-scale drivers identified using Coupled Model Intercomparison Project Phase 6 (CMIP6) climate models.

Finally, we discuss this understanding of the connectivity with regard to its current and future implications



for the Patagonian toothfish fisheries stock and management.

Figure 1: (A) Areas of fishing activity between 2016 and 2019 (gray, data from the Global Fish Watch) and management boundaries: Commission for the Conservation of Antarctic Marine Living Resources (CCAMLR, pink contours), Kerguelen and Heard and McDonald exclusive economic zones (EEZs, gray contours) and the Southern Indian Ocean Fisheries Agreement (SIOFA noted in green, SIOFA's

jurisdiction is to the east/north of the CCAMLR pink boundaries). No-take zones within EEZs marine protected areas are shown in blue (data from: Protected Planet, UNEP-WCMC and IUCN, 2023). Potential spawning areas are qualitatively located within the dashed brown rectangles (as in Ziegler and Welsford, 2019) and identified retention areas are indicated by two brown arrows. (B) Mean geostrophic velocity over 1993-2019 from AVISO product in log10 scale. The Subantarctic Front (SAF), the Polar Front (PF) and the Southern ACC Front (SACCF) are shown in blue (from Park and Durand, 2019). The different geographical regions considered in this study are indicated in black. The zone referred to as the “east of Kerguelen” throughout this study covers the area within the black rectangle. The black dotted line marks what is referred to as the “eastern slope”.

2. Material and Methods

2.1. Investigating the interannual variability of the connectivity over the Northern Kerguelen Plateau

Altimetry-derived geostrophic currents and Absolute Dynamics Topography (ADT) are computed by CLS/AVISO (Collecte Localisation Satellites/Archiving, Validation, and Interpretation of Satellite Oceanographic data) and distributed by Copernicus Marine Environment Monitoring Service (CMEMS) as a gridded product on a $0.25^\circ \times 0.25^\circ$ horizontal grid resolution between 1993 and 2019 (<https://doi.org/10.48670/moi-00148>). Geostrophic currents are calculated using satellite altimetry, by solving the equation for geostrophic equilibrium, the balance between the horizontal pressure gradient force and the Coriolis force.

We investigate the connectivity between different parts of the Northern Kerguelen Plateau using forward advection of water parcels based on altimetry-derived 2D geostrophic velocities. We use geostrophic velocities since the circulation over the Northern Kerguelen Plateau is mostly barotropic (Killworth and Hughes, 2002; Park et al., 2008c; Vivier et al., 2015) and the geostrophic velocity field was found relevant to capture the advection of biogeochemical tracers such as iron or chlorophyll in this region (d’Ovidio et al., 2015; Della Penna et al., 2018). In addition, Patagonian toothfish eggs are pelagic and have only been found in the upper 200 m, though direct observations of Patagonian toothfish eggs remain limited (Evseenko et al., 1995; North et al., 2002). We define 7 areas (Figure 2A) to investigate the probability of

going from one area to another (« connectivity »), the probability of going from one area to the same one (« retention ») and the probability of going from one area to none of the defined areas (« loss »). Although the definition of the 7 areas is inspired from the methodology in Mori et al., 2016, it is adapted to fit bathymetric features (e.g. Elan Bank, Chun Spur), and dynamic processes (e.g. the zone east of Kerguelen is extended to include the retroflexion of the flow as seen on Figure 2B). The forward advection of water parcels from the different areas was conducted using the Lagrangian Manifolds Tracking Algorithm (LAMTA) Python code developed with support from LOCEAN-IPSL and CNES (Rousselet et al. in preparation). To generate water parcels trajectories, the 2D geostrophic velocity fields derived from satellite altimetry (from the AVISO product) are linearly interpolated in time (step of 4h) and space (resolution of 0.05°). The integration in time of the velocity field is conducted using a Runge-Kutta integrator of order four (Press et al., 1992). Forward advectons are conducted over 91 days (around 3 months, which is the duration of the egg phase), for each grid point of the defined boxes (with a 0.05° resolution), for each day between June 1st and October 31st (Patagonian toothfish spawning period; Lord et al., 2006; Collins et al., 2010) each year between 1993 and 2019. A complementary analysis is conducted using backward advectons from the east of Kerguelen, to investigate whether a similar interannual variability is observed accounting for all the trajectories (and not just the initial and final positions). Backward advectons are conducted over 91 days, for each grid point over the east of Kerguelen area (KE on Figure 2A), for each day between the 31st of August to the 30th of January, each year between 1993 and 2019 using the same equations as the forward advectons described above.

We define “particle density” for each grid cell as the number of crossings of water parcels over such a grid cell, here on a $0.25^\circ \times 0.25^\circ$ grid, accounting for all the 91-days backward in time trajectories from a given day to identify main transport pathways (similar to the notion of “crossroadness” introduced in Baudena et al. 2019). The average particle density for each year is then used to investigate the interannual variability of the transport pathways arriving to the east of Kerguelen (KE on Figure 2). The interannual variability is only studied here for grid cells where the mean particle density is higher than 50% of the overall mean value, in order to focus the interpretation on the main transport pathways.

In this study, our focus is primarily on the Patagonian toothfish egg phase as it is the life stage with the greatest dispersal potential (Harden-Jones, 1968), but we note that retention is also key for the larval phase

(Bakun, 1998), which is still subject to currents, despite larvae's potential to vertically adjust their position (Young, 2020). To further characterize the observed retention east of Kerguelen, we also compute the distance between the initial and final location of the 91-days backward trajectories arriving east of Kerguelen.

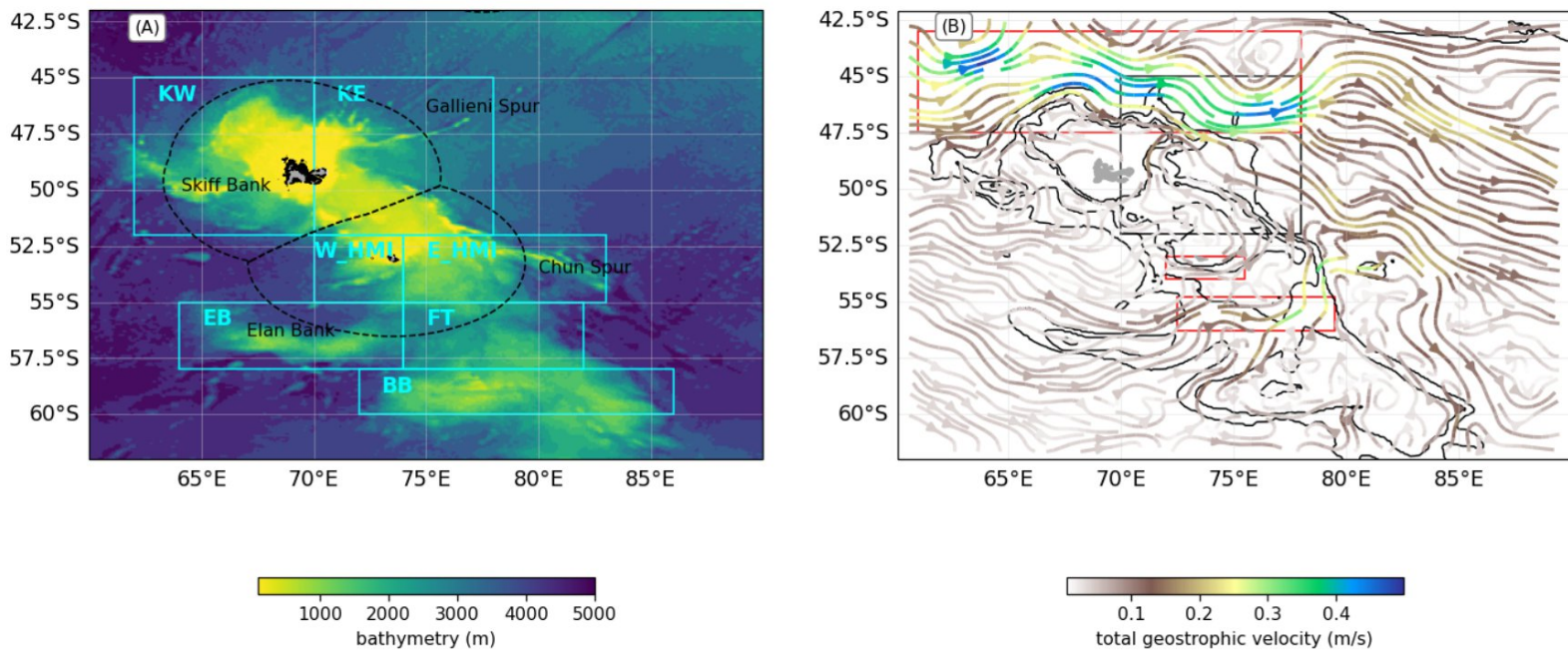


Figure 2 : (A) Bathymetry and delimitation of areas for advection analyses. (B) Streamlines of geostrophic velocities (averaged between June and October, 1993 to 2019, from AVISO product) colored by the norm of the geostrophic velocity. The red rectangles indicate the areas used to estimate the intensity of the currents, from north to south: north of the Kerguelen Plateau, south of Heard Island, through the Fawn Trough.

2.2. Investigating large-scale drivers of the connectivity variability

Different large-scale drivers can modulate the surface circulation over the Northern Kerguelen Plateau, notably wind forcing and the strength and position of the main ACC branches (Vivier et al., 2015). First, the effect of wind forcing is considered through the wind stress magnitude, the wind stress curl and the latitude of the maximum wind stress magnitude. These variables are estimated using the mean eastward

and northward turbulent surface stress from ERA5 reanalysis, which is a product combining model data with worldwide observations being consistent with the laws of physics, between 1993 and 2019 (Hersbach et al., 2023). Second, the effects of the ACC strength and position are investigated, notably estimating the zonal velocities north of the Plateau and through the Fawn Trough (red rectangles on Figure 2B), using AVISO geostrophic velocities between 1993 and 2019. As a correlation was found in a previous study between the meridional transport over the Northern Kerguelen Plateau and the position of the Polar Front between 60°E and 70°E (Pauthenet et al., 2018), we also consider the Polar Front position west of the Plateau between 60°E and 70°E in our analysis. This metric is calculated based on the northernmost extension of a subsurface water mass called the “winter waters” characterized by a subsurface temperature minimum (Park et al., 1998), using the GLORYS12V1 product (i.e. CMEMS global ocean eddy-resolving reanalysis delivered by Mercator Ocean), as in Azarian et al. (2024). We also use another definition of the Polar Front, the -0.30 m absolute dynamic topography contour distributed by AVISO + (<https://doi.org/10.24400/527896/a01-2023.004>; Sallée et al., 2008). In addition, other variables that could be associated with changes in the circulation, such as sea surface temperature (using satellite observations OSTIA, doi:10.48670/moi-00165, Good et al., 2020) and sea ice extent (observations reprocessing from MET Norway distributed by CMEMS) have been considered (Supplementary Material S1). We study the link between connectivity and these large-scale drivers by investigating correlations and composite averages of these large-scale drivers based on months with the highest or the lowest connectivity.

2.3. CMIP6 models

We use 36 models from the Coupled Model Intercomparison Project 6 (CMIP6; Supplementary Material S2), which are climate models principally used to study the Earth system response to natural or anthropogenic radiative forcing (Eyring et al., 2016). We use historical and projection simulations from the ScenarioMIP experiments, using three emission trajectories, also called Shared Socioeconomic Pathways (SSPs): SSP1-2.6, SSP2-4.5 and SSP5-8.5, that can be considered as strong, modest and no mitigation scenarios respectively, leading to an estimated global warming of 1.8°C, 2.7°C and 4.4°C at the end of the century respectively (O’Neill et al., 2016; Lee et al., 2021). Based on the results of the two first steps (sections 2.1 and 2.2), we identify that wind stress magnitude is an important driver of the connectivity

variability; we therefore investigate the projected changes in wind stress magnitude in the CMIP6 models using the variables τ_{uu} and τ_{uv} . Each model output is regridded to the same regular 1° - 1° horizontal grid using distance weighted average remapping (using climate data operators « cdo » remapdis) as in Kwiatkowski et al. (2020).

3. Results

3.1. Interannual variability of the connectivity over the Northern Kerguelen Plateau

3.1.1. High interannual variability of the connectivity between the western side of the Northern Kerguelen Plateau and the east of Kerguelen

We first quantify the connectivity between western areas - the west of Kerguelen (KW on Figure 2), the west of Heard island (W_HMI) and Elan Bank (EB) - and the east of Kerguelen (KE; Figure 3, Supplementary Material S3). The probabilities of water parcels arriving east of Kerguelen are: 1) 29% (\pm 5%) after leaving from the west of Heard Island; 2) 19% (\pm 1.3%), after leaving from the west of Kerguelen; and 3) only 2.2% (\pm 1.4%) after leaving from Elan Bank (Figure 3A). The connectivity between the west of Heard and the east of Kerguelen ranges between 19% and 39%, thus indicating a higher interannual variability than the connectivity between the west and east of Kerguelen, which ranges between 16% and 22%.

The highest losses (i.e. water parcels leaving from one area to arrive in none of the predefined zones on Figure 2A) are observed for the eastern areas (KE, E_HMI). This loss is estimated at around 64% (\pm 3.4%, interannual variability) and 56% (\pm 3.6%) for the east of the Kerguelen and the east of Heard Island respectively (Figure 3B).

Retention east of Kerguelen (i.e. trajectories of water parcels starting in KE and arriving in KE) is estimated at 33% (\pm 3%, interannual variability) and can reach up to 40%. This high probability of retention can be due to spatially heterogeneous retentive processes such as slower circulation or retentive eddies. The orthodromic distance (i.e., shortest path) between the initial and final locations of the 91-days backward trajectories from the east of Kerguelen is also computed as another metric to characterize retention. The

retention east of Kerguelen is negatively correlated to this « distance metric » along the eastern slope of the Plateau, suggesting that high retention here is mostly driven by weakened flow along this pathway (Supplementary Material S4).

3.1.2. Recirculation zone

The retention east of Kerguelen is also negatively correlated to the connectivity between southwestern areas (W_HMI and EB) and the east of Kerguelen (KE, p values $\sim 10^{-5}$) while it is positively correlated to the zonal connectivity between the west and the east of Heard (W_HMI and E_HMI; p value=0.03 ; Figure 4A).

When averaging months with the highest retention east of Kerguelen, closed contours of ADT around 50°S are observed between 72.5°E and 78.4°E (Figure 4B) as well as negative anomalies of absolute dynamic topography (ADT) over the Northern Kerguelen Plateau (Supplementary S5A). On the contrary, such closed features are not observed when averaging over months with the lowest retention east of Kerguelen and positive ADT anomalies are observed over the Northern Kerguelen Plateau (Figure 4C, Supplementary S5B). We refer to this feature, observed during high retention months, as a “recirculation zone”. It is associated with a positive ADT anomaly and southward intrusion of waters on the eastern edges of the zone (Supplementary S5 C, D). Indeed, a positive anomaly in latitudinal advection, as shown in Supplementary S5C, indicates that the water parcels on the eastern edges of the zone were further north 15 days backward in time and have consequently moved southward since then. In addition, a positive sea surface temperature gradient anomaly is observed at the southern edge of the recirculation zone, crossing the eastern slope of the Plateau (Supplementary Material S5 E, F), highlighting that this recirculation zone could block the northwestward flow along this eastern slope.

The eastern slope of the Plateau is an important pathway to the east of Kerguelen but the circulation in this region is also highly variable on an interannual timescale (Figure 5). Particle densities, using 91-days backward in time trajectories from the east of Kerguelen (see definition section 2.1), are higher than 50% of the mean value north of the Plateau and over the Plateau north of 55°S. This indicator is also the most

variable along steep slopes on the western side of the Kerguelen shelf near the 1000 m bathymetry contour between 49.5°S and 52.8°S as well as slightly east of the eastern slope between 48.3°S and 53.4°S, notably in the area where recirculation is observed (Figure 5).

Summarizing this first section, we highlight the high interannual variability of the connectivity between the west of Heard and the east of Kerguelen. We also show that lower connectivity between southwestern areas (west of Heard and Elan Bank) and the east of Kerguelen, which will now be referred to as the “southwest-northeast connectivity” for brevity, is associated with higher retention east of Kerguelen, and the occurrence of a recirculation zone over the eastern slope of the Plateau. In the second section, we investigate the large-scale drivers of this observed variability.

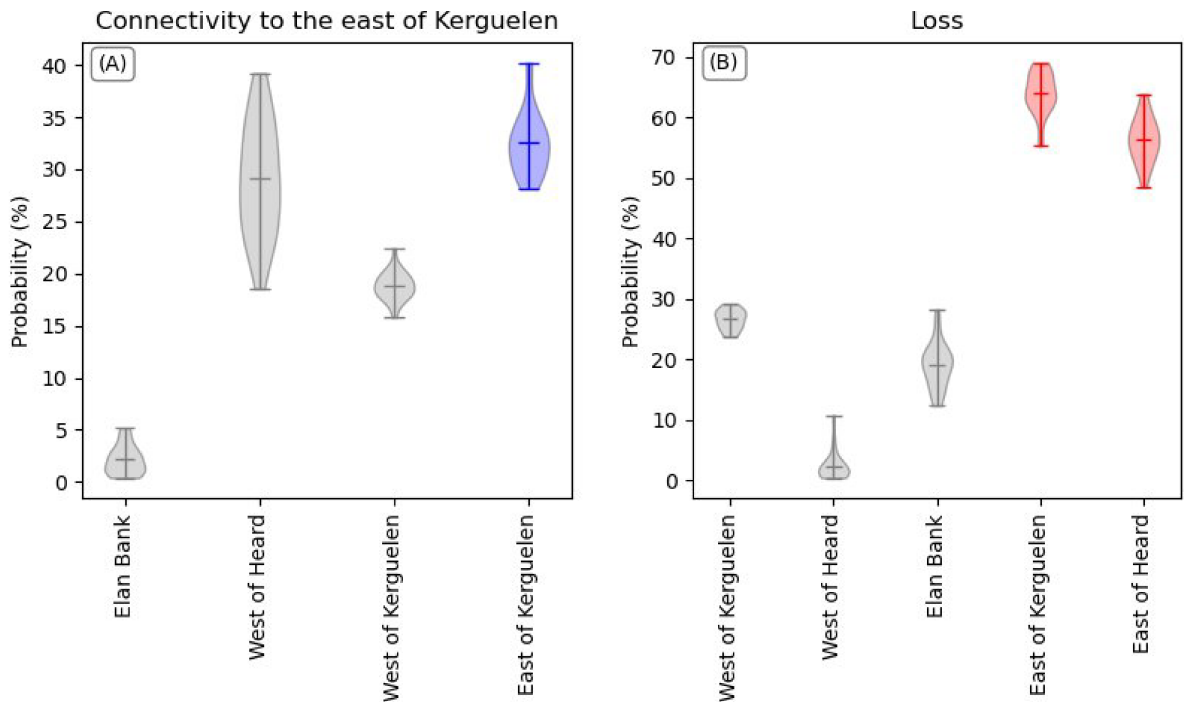


Figure 3 : (A) Probability of a water parcel leaving from one area to arrive east of Kerguelen (‘connectivity’) after 91 days (areas as defined on Figure 2). (B) Probability of a water parcel leaving from one area to arrive in none of the predefined areas on Figure 2 after 91 days (‘loss’), using AVISO geostrophic velocities between June and October and between 1993 and 2019. The error bars indicate the interannual variability of those metrics.

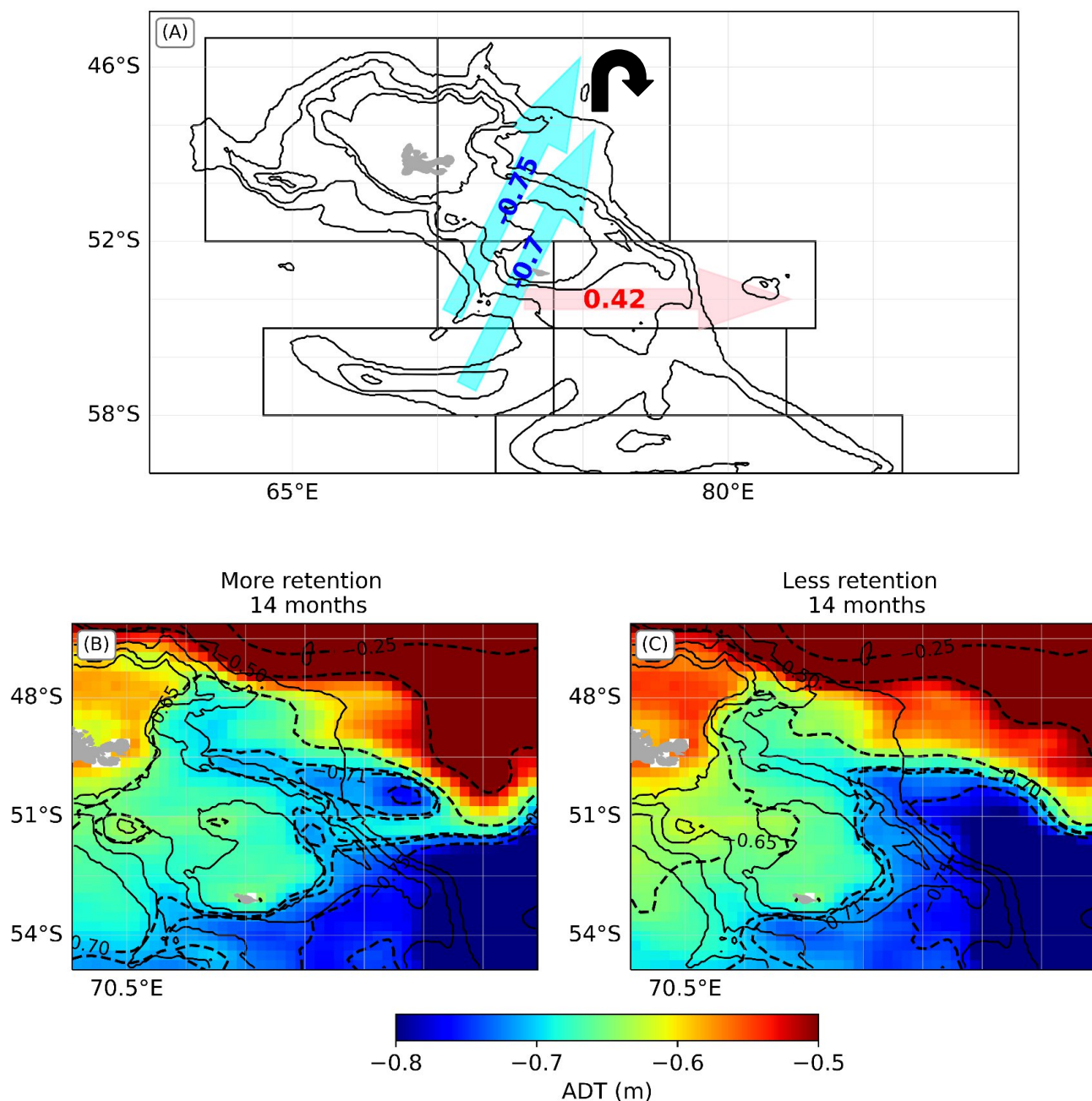


Figure 4 : (A) Correlations between the retention east of Kerguelen (black arrow) and other connectivity indexes: blue arrows indicate a negative correlation (and the red one a positive correlation) between the connectivity represented by the colored arrow and the retention east of Kerguelen. For instance, higher connectivity between the west of Heard and the east of Kerguelen is associated with less retention east of Kerguelen. Composites based on the retention values east of Kerguelen on absolute dynamic topography (contours and colormap) for the months with the highest retention values (B) and the lowest retention values (C).

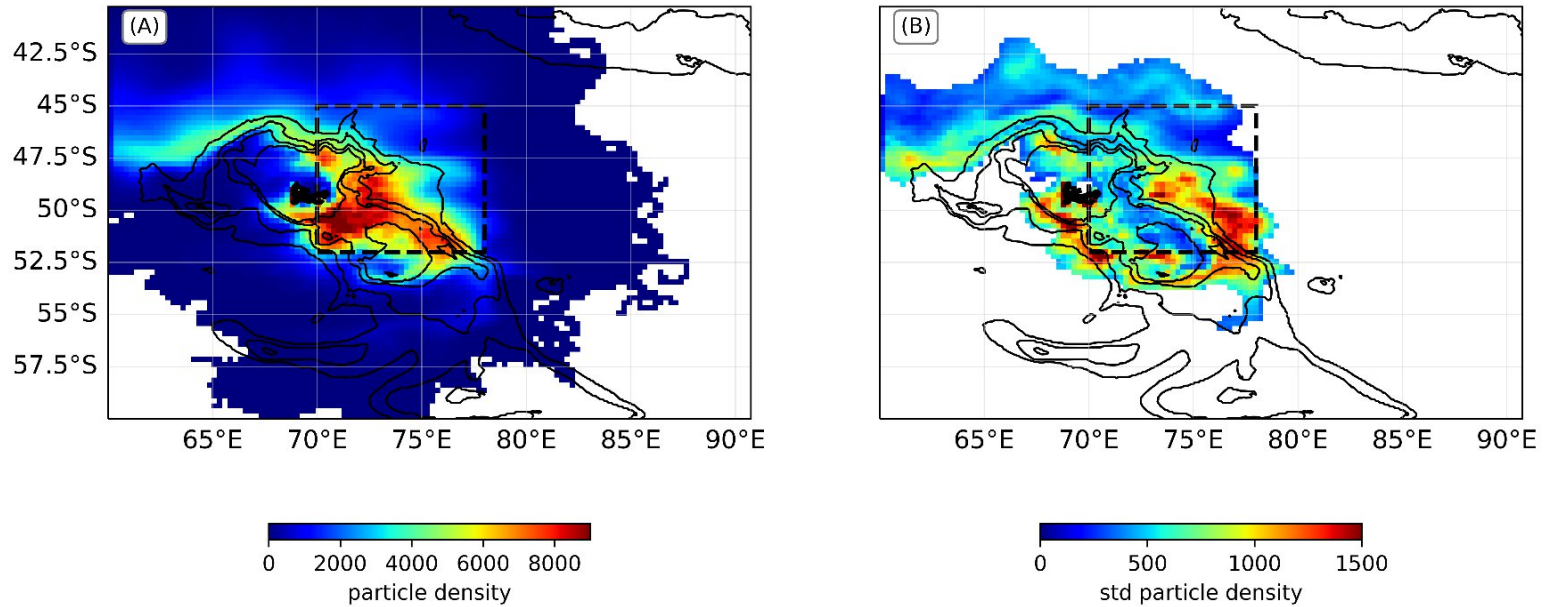


Figure 5: Number of water parcels that go through or arrive in a grid cell (‘particle density’, A) and its associated interannual standard deviation (B) using the 91-days backward advections between August and January 1993 to 2019 using AVISO geostrophic velocities. The black dotted rectangle indicates the area of the initial positions for the backward trajectories. The interannual variability on Panel B is only shown here for grid cells where the mean particle density is higher than 50% of the overall mean value.

3.2. Wind stress magnitude: a major driver of the interannual variability in connectivity

We investigated correlations between the retention and connectivity indexes and several large-scale drivers (Table 1, Supplementary Material S6). Wind stress magnitude is negatively correlated to the retention east of Kerguelen (p value=0.00076), and positively correlated to the connectivity between the west of Heard (p value=0.00059) or Elan Bank (p value=0.019) and the east of Kerguelen (southwest-northeast connectivity). A strengthening of the westerlies is thus associated with increased southwest-northeast connectivity and weakened retention. We also note that wind stress is positively correlated to the distance

metric (used to characterize more finely retentive processes) along the eastern slope in the east of Kerguelen area (mean correlation of 0.49 where p value < 0.05 ; Supplementary Material S4).

The link between wind stress and southwest-northeast connectivity is also supported by the composite analysis shown in Figure 6. High retention east of Kerguelen and low connectivity between the west of Heard and the east of Kerguelen are associated with weaker wind stress, -0.02 Pa (± 0.007 Pa, spatial variability) and -0.04 Pa (± 0.01 Pa) respectively, over areas where the composite anomaly is significant (Figure 6). In these cases, we also note a northward shift of the maximum wind stress, by 1.3° lat ($\pm 0.6^\circ$ lat, spatial variability) and 3.0° lat ($\pm 0.8^\circ$ lat), for high retention and low connectivity composites respectively (Figure 6). High connectivity between the west of Heard and the east of the Kerguelen Plateau is associated with stronger wind stress south of the wind stress maximum and a southward shift of the wind stress maximum of around 1.3° lat ($\pm 0.4^\circ$ lat). In addition, high retention east of Kerguelen is associated with a local decrease in the wind stress curl magnitude over the Fawn Trough (around 55° S, Supplementary Material S7).

A significant negative correlation is found between the latitude of the Polar Front west of Kerguelen (60 - 70° E) and the connectivity between the west of Heard and the east of Kerguelen using both the winter water-based definition (p value = 0.030) and the ADT-based definition (p value = 0.0017) of the Polar Front (Table 1). There is also a significant positive correlation between the retention east of Kerguelen and the position of the Polar Front west of Kerguelen using the ADT-based definition (p value = $3e-3$), meaning that higher retention is associated with ADT contours located further north.

Table 1: Pearson correlation on detrended time series of annual values averaged between June and October from 1993 to 2019 between connectivity or retention indexes and potential drivers (as presented in Methods). ** indicate p values < 0.001 and * indicate p values < 0.05 .

	Retention east of Kerguelen	West of Heard to east of Kerguelen	Elan Bank to east of Kerguelen
Total wind stress (60-90°E, 60-45°S)	-0.61**	0.62**	0.45*
Latitude of the maximum wind stress	0.39*	-0.54*	-0.18
Polar Front position 60-70°E (Winter water based definition)	0.30	-0.41*	-0.18
Polar Front position 60-70°E (ADT based definition)	0.54*	-0.57*	-0.29
Zonal velocity through the Fawn Trough	0.28	-0.15	-0.10
Zonal velocity North of the Kerguelen Plateau	0.25	-0.41*	-0.020

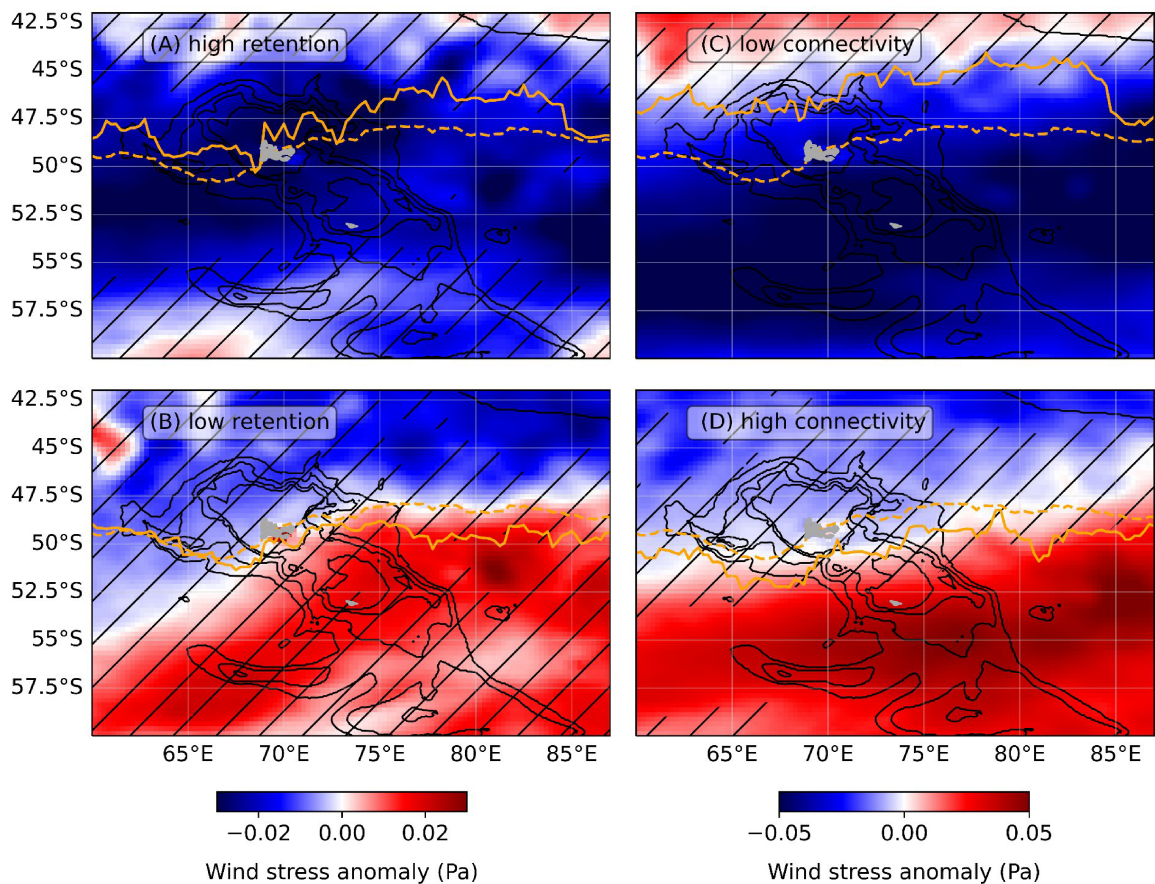


Figure 6: Wind stress anomaly, estimated from ERA 5 reanalysis, averaged over the 14 months of highest (A) and lowest (B) retention east of Kerguelen, and of lowest (C) and highest (D) connectivity between the west of Heard and the east of Kerguelen. Hatched areas indicate where the average wind stress anomaly is

lower than the standard deviation of randomly sampled 14-month averages. The orange solid line marks the latitude of the maximum wind stress for the associated composite and the orange dashed line marks the mean latitude of the maximum wind stress over 1993-2019.

3.3 Scenario-dependent strengthening of the wind stress under climate change

In the second section, we highlighted the link between the southwest-northeast connectivity and wind stress over 60-90°E, 60-45°S. In this third and final section, we investigate the projected changes in wind stress under climate change over this same region. The position of the Polar Front has also been found to be correlated, to some extent, with connectivity. The projected changes in the Polar Front position over the Kerguelen Plateau, as defined by the northernmost extension of the winter waters, were investigated in Azarian et al., 2024, showing a southward shift of this front west of the Plateau under global warming.

In the Indian sector of the Southern Ocean, the maximum wind stress is located at around 50.25°S using ERA5 (Figure 7). CMIP6 multi-model mean reproduces a similar maximum wind stress (around 0.26 Pa), although the maximum wind stress is further north (around 48.5°S; Figure 7).

The multi-model mean at the end of the century (2081-2100) shows an intensification of westerlies between 40°S and 65°S under SSP1-2.6, SSP2-4.5 and SSP5-8.5. However, there is a high heterogeneity in the modeled response, with 9 out of 36 models and 11 out of 34 models indicating a weakening of westerlies over the Kerguelen Plateau (60-90°E, 60-45°S) under SSP2-4.5 and SSP1-2.6 respectively. The pattern of westerlies strengthening is more robust under SSP5-8.5 as more than 80% of the models agree on the sign of change (relative to 1995-2014; Figure 8D).

Wind stress increases over the Northern Kerguelen Plateau (64-90°E, 60-45°S) with a similar trend during the first half of the century regardless of the scenario. A linear increase of the wind stress anomaly (relative to 1995-2014), using the multi-model mean, is found until 2045 under SSP1-2.6, until 2057 for SSP2-4.5 and until the end of the century under SSP5-8.5 (Figure 8A). Mean wind stress anomaly and the latitude of the maximum wind stress anomaly are negatively correlated, for all SSPs (Figure 8B), meaning that increased wind stress is associated with a southward shift of the wind stress maximum. This relationship

remains consistent regardless of whether the first or the last half of the century is considered, under both SSP1-2.6 and SSP2-4.5 (data not shown).

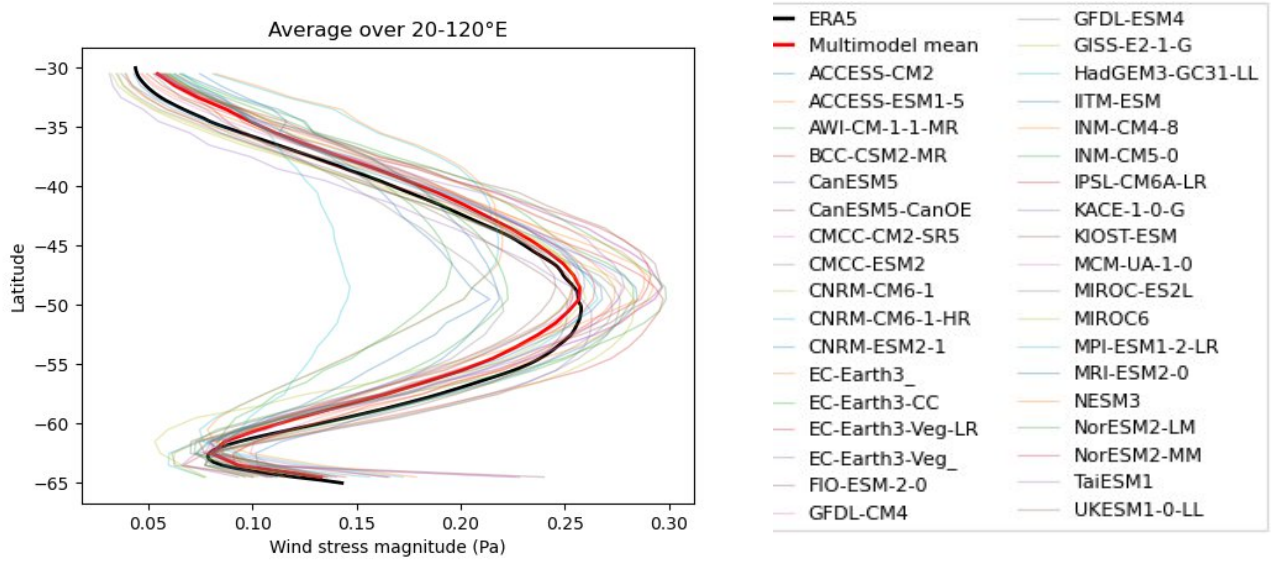


Figure 7: Winter wind stress magnitude averaged over 20-120°E from ERA 5 (black thick line), 36 CMIP6 models (colored thin lines) and their ensemble mean (red thick line) between 1995-2014.

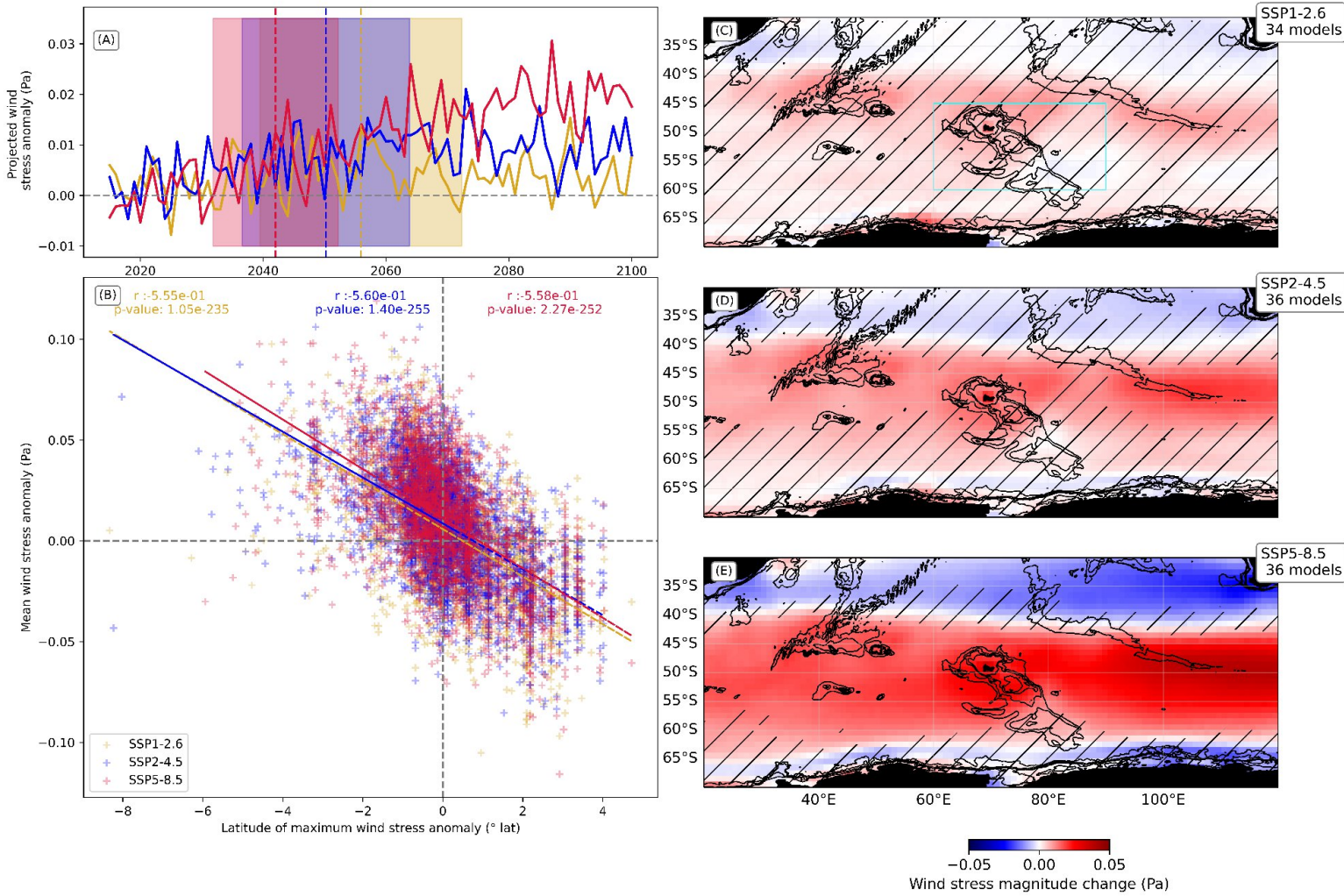


Figure 8: Projected change in winter wind stress anomaly relative to 1995-2014 (A) over the 21st century averaged over 60-90°E and 60-45°S (blue rectangle in C). Vertical dashed lines indicate for each scenario the mean year when models reach 2.6°C global warming (the associated colored bands represent the inter-model variability), the warming threshold identified in Azarian et al., 2024, around which the Polar Front east of Kerguelen abruptly shifts significantly southward (the legend for the colors is the same as indicated on panel B). (B) The relationship between the mean winter wind stress anomaly and the latitude of maximum winter wind stress anomaly using all the models and years between 2015 and 2100 for the three Shared-Socioeconomic Pathways (SSPs). Projected change in winter wind stress anomaly relative to 1995-2014 over 2081-2100 using multi-model means under SSP1-2.6 (C), SSP2-4.5 (D) and SSP5-8.5 (E). Hatched areas indicate where <80% of the models agree on the sign of change.

4. Discussion

This study highlights high interannual variability in connectivity probabilities between the west of Heard and the east of Kerguelen (section 3.1), which in turn exhibit a significant correlation with wind stress magnitude (section 3.2). Projections indicate a strengthening of wind stress already starting during the first half of the century across all climate change scenarios, and throughout the entirety of the 21st century under the most severe emission scenario (section 3.3). While the relationship between wind stress and the southwest-northeast connectivity may not be entirely linear, and other local processes could potentially influence connectivity patterns, our findings suggest an increased southwest-northeast connectivity under climate change. This interpretation is tempered by the projected detachment of the Polar Front east of Kerguelen above a global warming threshold of 2°C to 3°C (Azarian et al., 2024). Above this threshold the local circulation is projected to undergo an unprecedented change (Azarian et al. 2024), potentially blocking the northward flow along the eastern slope of the Plateau and thus having the opposite effect of weakening the southwest-northeast connectivity across the Plateau.

Consequently, an increased linkage between the Australian and French stocks, currently managed separately, may only occur for the first half of the century (i.e., up to a global warming level between 2°C and 3°C). Increased collaboration between the two countries may be required to ensure consistency between conservation measures (e.g. type of gear, fishing depths), to maximize successful recruitment. Whether a short-term increase followed by a potential long-term decline in connectivity might change the characteristics of the stock and impact the population dynamics remains an open question.

4.1. Interannual variability of the transport pathways over the Kerguelen Plateau

This study sheds light on the southwest-northeast connectivity over the Northern Kerguelen Plateau. While ocean circulation can link Elan Bank and the east of Kerguelen, the likelihood of reaching the east of Kerguelen from Elan Bank over a three-month period is relatively low (approximately 5%, as depicted in Figure 3A). This low probability could explain why such connectivity was not observed in Mori et al.,

2016, particularly given that their methodology involved simulating larval transport with assumptions on the bathymetry for the spawning locations and for the successful recruitment areas for juveniles. In contrast, our study differs in that we refrain from making assumptions on the bathymetry. Instead, we focus on surface processes impacting toothfish eggs once they have reached the upper 200 m of the water column shortly after spawning, by investigating the geostrophic circulation variability and its potential alterations under climate change - a novel context in which the reproductive behavior and early-life ecology of the Patagonian toothfish, which remains an area of active research, may potentially evolve.

The connectivity between the west of Heard and the east of Kerguelen was previously observed in Mori et al., 2016 and is corroborated in this study as well (Figure 3A). We find that the associated probability is on average 29% between 1993 and 2019, whereas it remains below 10% between 2000 and 2006 in Mori et al., 2016, which, as indicated previously, could be attributed to methodological differences. In addition to connectivity, this study highlights the variability of the retention east of Kerguelen, which appears to be associated with a recirculation zone (Figure 4B). Such a recirculation zone could potentially hinder the northward circulation along the eastern slope of the Plateau. However, reduced northward transport could also facilitate the formation of such a recirculation zone. This feature is consistent with previously identified retentive mesoscale recirculation structures in 2011/2012 by d'Ovidio et al., 2015. The retention east of Kerguelen, as defined in this study, appears mostly driven by the strength of the flow along the eastern slope, meaning that weakened retention east of Kerguelen does not necessarily mean an absence of retentive hotspots but may reflect a change in the spatial distribution of retention areas (Supplementary Material S4).

4.2. Wind stress can modulate connectivity

In this study, we show a correlation between the southwest-northeast connectivity and wind stress magnitude (Table 1, Figure 6). Composite analyses also support that higher (lower) retention is associated with weaker (stronger) wind stress (Figures 6 A and C) and weaker (stronger) absolute wind stress curl over the Fawn Trough (Supplementary Material S7). The “distance metric”, used as a complementary metric to characterize retention, is associated with stronger wind stress along the eastern slope of the Northern Kerguelen Plateau (Supplementary Material S4).

This result is consistent with existing theoretical frameworks, such as the topographic Sverdrup balance (Roquet, 2009). This framework describes the balance between the integrated meridional transport due to the Coriolis force, the wind stress curl and the bottom pressure torque, the latter resulting from the interaction between the flow and the topography (Hughes and DeCuevas, 2001; Jackson et al., 2006). As the flow crosses isobaths from deep to shallow bathymetry, the bottom pressure torque deflects the flow equatorward (Rintoul et al., 2018). If the interaction with the topography is constant, then increased wind stress curl magnitude can lead to increased northward transport. Topography plays a major role over the Kerguelen Plateau as it controls the overlying flow through potential vorticity constraints (Rintoul, 2018). Conservation of the potential vorticity means that the flow tends to follow f/H contours, where f is the planetary vorticity and H the bathymetry. Model experiments have shown that greater wind forcing contributes to increasing the influence of those contours and thus to deflecting currents northward due to increased interaction with the ocean bottom (Jackson et al., 2006). On the contrary, when wind stress weakens, it can lead to increased stratification (Pellichero et al., 2020) which can isolate surface waters from deeper forces (Olbers and Eden, 2003). Such conditions could facilitate crossing the eastern slope of the Plateau in winter, which is consistent with the observation that higher retention east of Kerguelen, associated with weaker winds (section 3.2), is positively correlated with the zonal connectivity between the west and the east of Heard, and also with the loss from the west of Heard (corr=0.69, p value=5.8e-5) and from the east of Heard (corr=0.55, p value=2.7e-3; Figure 4A).

High connectivity or low retention is also associated with southward shifts in ADT contours and positive ADT anomalies (Table 1, Figure 4 B and C, Supplementary S5 A,B), which could also be due to changes in wind stress. Such a link, associated with the Southern Annular Mode (SAM), has been observed as particularly strong in the Indian sector of the Southern Ocean (Armitage et al., 2018). The correlations observed between connectivity and the Polar Front as defined by an ADT contour can therefore be due to wind forcing as well. However, wind forcing does not completely explain the southwest-northeast connectivity variability, which may also be modulated by local processes. In particular, the position of the Polar Front defined by a subsurface signal, which is more variable west of the Plateau (Pauthenet et al., 2018), could contribute to modulating the connectivity between west of Heard and east of Kerguelen (Table 1).

4.3. The projected intensification of wind stress under climate change depends on the emission scenario

As wind stress stands out as the main large-scale driver modulating the southwest-northeast connectivity, we investigate its projected changes under different emission scenarios. The wind stress is projected to intensify over the Indian sector of the Southern Ocean, which is consistent with previous studies (Bracegirdle et al., 2020; Goyal et al., 2021; Deng et al., 2022). A mean strengthening of around 0.02 Pa between 62°S and 40°S, and up to 0.05 Pa (relative to 1995-2014), is projected under the strongest emission scenario SSP5-8.5 (Figure 8), which is similar to the circumpolar wind strength anomaly (relative to 1979-2010) obtained using CMIP5 models under RCP8.5 (Swart et al., 2012). We note that recent studies using CMIP6 models focus on the wind speed, showing increased circumpolar wind speeds under both SSP5-8.5 and SSP2-4.5, but this trend is reversed at the end of the century under SSP1-2.6 (Deng et al., 2022). Indeed, depending on the emission scenario, the pattern of wind stress change is uncertain at the end of the century (Figure 8 C, D and E).

The evolution of the Southern Ocean westerlies depends on multiple factors. The latitude of the westerlies is primarily influenced by the meridional temperature gradient (Ceppi et al., 2012). Consequently, the variability in wind stress change patterns among models and scenarios may stem from the uneven distribution of surface warming in the Southern Hemisphere (Deng et al., 2022). The characteristics of the westerlies are also influenced by changes in atmospheric circulation both in polar and tropical regions (Mindlin et al., 2020; Yang et al., 2020) whose representations can differ depending on climate models and scenarios.

However, climate change can also lead to unprecedented disruptions such as the southward shift of the Polar Front east of Kerguelen (Azarian et al., 2024). Uncertainties remain on the impacts of such a shift on circulation, since it is projected using a water mass-based definition of this front that could no longer be aligned with the dynamic definition of the Polar Front as a jet (Chapman et al., 2020). Theoretically, such a shift could impede the northward flow along the eastern slope, consequently reducing the southwest-

northeast connectivity. A global warming threshold, where the Polar Front starts to significantly shift southward east of Kerguelen has been estimated at around 2.6°C (Azarian et al, 2024). This threshold could be reached by the middle of the century depending on the climate change scenario (Figure 8A).

4.4. Perspectives on potential climate change impacts for the Patagonian toothfish fishery

The potential for increased connectivity driven by wind stress must be considered within the broader context of a warming ocean, at various depths, which has the potential to modify or shift the habitat of adult toothfish. A decrease in maximum catch potential is projected under climate change over the Kerguelen and Heard EEZs, though the amplitude of the change depends on the scenario and the ecological modeling approach (Cheung et al., 2018). Niche modeling based on the current distribution of Patagonian toothfish has also been used to project habitat range under climate change, notably at mid-century under a strong emission scenario (RCP8.5) using one climate model, i.e. MPIM-ESM-R (Kaschner et al., 2007; Scarponi et al., 2018; AquaMaps, 2019). It shows that the Patagonian toothfish distribution may extend further south, near the Antarctic, but also that the probability of occurrence south of Heard island and around Elan Bank might be reduced (AquaMaps, 2019). Although the methodology used has its limitations, the maps provided by AquaMaps highlight the possibility that changes in Patagonian toothfish habitat could be heterogeneous and more complex than a linear southward shift. Early-life stages could still be transported to the east of Kerguelen under climate change, but both spawning and suitable recruitment areas might change in the long term.

In addition, the southwest-northeast connectivity is negatively correlated to retention east of Kerguelen (Figure 4A), with a link observed between retention and wind stress (Table 1, Figure 6A and C ; Supplementary Material S4). Along with increased connectivity under climate change, retention east of Kerguelen could be impacted, particularly around the Polar Front meander, potentially limiting the settlement of Patagonian toothfish early-life stages in these offshore areas. While assessing the impact of increased connectivity and reduced retention on recruitment is outside the scope of this study, such work will be critical to understanding downstream impacts on the stock biomass. Still, retentive processes east of Kerguelen play a major role for the broader ecosystem, notably as retentive areas tend to be hotspots for

trophic interactions (d'Ovidio et al., 2013; Koubbi et al., 2016). The region east of Kerguelen delineated here is quite large and a decreased retention can be linked to different processes. Nonetheless, it is important to emphasize the role that we identify here of increased flow along the Plateau eastern slope in reducing retention east of Kerguelen. Although the area east of Kerguelen EEZ around the Polar Front meander is under strict protection (Azam et al., 2019), the associated biodiversity remains vulnerable to changing patterns of retentive processes under climate change.

5. Conclusion

This study highlights the high interannual variability of the southwest-northeast connectivity, which appears to be mostly driven by the wind stress. Consequently, such connectivity may be temporarily enhanced in the future due to increased wind stress over the first half of the 21st century, regardless of the emission scenario. On the contrary, retention east of Kerguelen, which contributes to localized biodiversity hotspots favorable to fish early-life stages, could be impacted by changes in circulation patterns under a strong emission scenario. As a shift of the Polar Front east of Kerguelen is also projected to occur by mid-century in a 2.6°C global warming world, oceanic circulation might be greatly disrupted, with the potential to impede connectivity and the emergence of new circulation patterns. Such changes would not only have strong implications for the Patagonian toothfish fishery management, but also for the role of the eastern no-take zone within the Kerguelen marine reserve, whose rich biodiversity relies in part on retentive processes.

References

- Appleyard, S., Ward, R., and Williams, R. (2002). Population structure of the Patagonian toothfish around Heard, McDonald and Macquarie Islands. *Antarctic Science*, 14(4), 364-373. doi:10.1017/S0954102002000238
- Appleyard, S., Williams, R. and Ward, R. (2003). Fine scale genetic investigation into Patagonian toothfish structure within the west indian ocean sector of the southern ocean. WG-FSA-03/66
- AquaMaps (2019, October). Computer generated distribution maps for *Dissostichus eleginoides* (Patagonian toothfish), with modeled year 2050 native range map based on IPCC RCP8.5 emissions scenario. Retrieved from <https://www.aquamaps.org>.
- Armitage, T. W. K., Kwok, R., Thompson, A. F., & Cunningham, G. (2018). Dynamic topography and sea level anomalies of the Southern Ocean: Variability and teleconnections. *Journal of Geophysical Research: Oceans*, 123, 613–630. <https://doi.org/10.1002/2017JC013534>
- Azam C-S., Thellier T., Verdier A-G., and Marteau C. (2019). The French Southern Lands marine protected area: genesis of one the largest marine protected areas in the world. In *The Kerguelen Plateau: Marine Ecosystem and Fisheries. Proceedings of the Second Symposium*. Welsford D., Dell J., Duhamel G. (Eds). The Department of the Environment and Energy, Australian Antarctic Division, Kingston
- Azarian, C., Bopp, L., Pietri, A., Sallée, J.B. and d'Ovidio, F., (2023). Current and projected patterns of warming and marine heatwaves in the Southern Indian Ocean. *Progress in Oceanography*, p.103036. doi.10.1016/j.pocean.2023.103036.
- Azarian, C., Bopp, L., Sallée, J. B., Swart, S., Guinet, C., and d'Ovidio, F. (2024). Marine heatwaves and global warming impacts on winter waters in the Southern Indian Ocean. *Journal of Marine Systems*, 243, 103962.
- Bamford, C. C. G., Hollyman, P. R., Abreu, J., Darby, C., and Collins, M. A. (2024). Spatial, temporal, and demographic variability in patagonian toothfish (*Dissostichus eleginoides*) spawning from twenty-five years of fishery data at South Georgia. *Deep Sea Research Part I: Oceanographic Research Papers*, 203, 104199.
- Bakun, A. (1996) Patterns in the Ocean: Ocean Processes and Marine Population Dynamics. University of California Sea Grant, in Cooperation with Centro de Investigaciones Biológicas del Noroeste, La Paz, p.323
- Bakun, A., 1998. Ocean triads and radical interdecadal variation: bane and boon to scientific fisheries management. In *Reinventing fisheries management* (pp. 331-358). Dordrecht: Springer Netherlands.
- Baudena, A., Ser-Giacomi, E., López, C., Hernández-García, E. and d'Ovidio, F. (2019). Crossroads of the mesoscale circulation. *Journal of Marine Systems*, 192, 1-14. doi.10.1016/j.jmarsys.2018.12.005.
- Bost, C. A., Cotté, C., Bailleul, F., Cherel, Y., Charrassin, J. B., Guinet, C., Ainley, D. G., and Weimerskirch, H. (2009). The importance of oceanographic fronts to marine birds and mammals of the southern oceans. *Journal of Marine Systems*, 78(3), 363-376. <https://doi.org/10.1016/j.jmarsys.2008.11.022>
- Bracegirdle, T.J., Krinner, G., Tonelli, M., et al. (2020). Twenty first century changes in Antarctic and Southern Ocean surface climate in CMIP6. *Atmos Sci Lett*. 21:e984. <https://doi.org/10.1002/asl.984>

Burch, P., Péron, C., Potts, J., Ziegler, P., Welsford, D., Dell, J., & Duhamel, G. (2019). Estimating Patagonian toothfish (*Dissostichus eleginoides*) movement on the Kerguelen Plateau: reflections on 20 years of tagging at heard island and mcdonald islands. In *The Kerguelen Plateau: Marine Ecosystem and Fisheries. Proceedings of the Second Symposium* (pp. 237-245). Kingston: The Department of the Environment and Energy, Australian Antarctic Division.

Cai, W., T. Cowan, S. Godfrey, and S. Wijffels, 2010: Simulations of Processes Associated with the Fast Warming Rate of the Southern Midlatitude Ocean. *J. Climate*, **23**, 197–206, <https://doi.org/10.1175/2009JCLI3081.1>.

Ceppi, P., Hwang, Y.T., Frierson, D.M. and Hartmann, D.L. (2012). Southern Hemisphere jet latitude biases in CMIP5 models linked to shortwave cloud forcing. *Geophysical Research Letters*, *39*(19).

Cheung WWL, Bruggeman J, Butenschön M (2018) Projected changes in global and national potential marine fisheries catch under climate change scenarios in the twenty-first century. In: Barange M, Bahri T, Beveridge MCM et al (eds) *Impacts of climate change on fisheries and aquaculture: synthesis of current knowledge, adaptation and mitigation options*. FAO Fisheries and Aquaculture Tech. Paper 627, pp 63–85. Rome, FAO.

Collins, M. A., Brickle, P., Brown, J., and Belchier, M. (2010). The Patagonian toothfish: biology, ecology and fishery. *Advances in marine biology*, *58*, 227-300.

Della Penna, A., Trull, T. W., Wotherspoon, S., De Monte, S., Johnson, C. R., & d’Ovidio, F. (2018). Mesoscale variability of conditions favoring an iron-induced diatom bloom downstream of the Kerguelen Plateau. *Journal of Geophysical Research: Oceans*, *123*, 3355–3367. <https://doi.org/10.1029/2018JC013884>

Deng, K., Azorin-Molina, C., Yang, S., Hu, C., Zhang, G., Minola, L., & Chen, D. (2022). Changes of Southern Hemisphere westerlies in the future warming climate. *Atmospheric Research*, *270*, 106040.

d’Ovidio, F., De Monte, S., Della Penna, A., Cotté, C. and Guinet, C. (2013). Ecological implications of eddy retention in the open ocean: a Lagrangian approach. *Journal of Physics A: Mathematical and Theoretical*, *46*(25), p.254023.

d’Ovidio, F., Della Penna, A., Trull, T. W., Nencioli, F., Pujol, M.-I., Rio, M.-H., Park, Y.-H., Cotté, C., Zhou, M., and Blain, S. (2015). The biogeochemical structuring role of horizontal stirring: Lagrangian perspectives on iron delivery downstream of the Kerguelen Plateau, *Biogeosciences*, *12*, 5567–5581, <https://doi.org/10.5194/bg-12-5567-2015>.

Duhamel, G. (1987). Reproduction des Nototheniidae et Channichthyidae des îles Kerguelen. *CNFRA*, *57* : 91-107.

Duhamel, G., and Hautecoeur, M. (2009). Biomass, abundance and distribution of fish in the Kerguelen Islands EEZ (CCAMLR Statistical Division 58.5.1). *CCAMLR Science*, Vol. 16: 1-32.

Duhamel, G., Pruvost, P., Bertignac, M., Gasco, N., & Hautecoeur, M. (2011). Major fishery events in Kerguelen Islands: *Notothenia rossi*, *Champscephalus gunnari*, *Dissostichus eleginoides*-Current distribution and status of stocks. *The Kerguelen Plateau: marine ecosystem and fisheries. Société française d’ichtyologie, Paris*, *35*, 275-286.

Evseenko SA, Kock K-H, Nevinsky MM. Early life history of the Patagonian toothfish, *Dissostichus*

eleginoides Smitt, 1898 in the Atlantic sector of the Southern Ocean. *Antarctic Science*. 1995;7(3):221-226. doi:10.1017/S0954102095000319

Eyring, V., Bony, S., Meehl, G. A., Senior, C. A., Stevens, B., Stouffer, R. J., and Taylor, K. E. (2016). Overview of the Coupled Model Intercomparison Project Phase 6 (CMIP6) experimental design and organization. *Geoscientific Model Development*, 9(5), 1937-1958. <https://doi.org/10.5194/gmd-9-1937-2016>

Good, S., Fiedler, E., Mao, C., Martin, M.J., Maycock, A., Reid, R., Roberts-Jones, J., Searle, T., Waters, J., While, J. and Worsfold, M. (2020). The current configuration of the OSTIA system for operational production of foundation sea surface temperature and ice concentration analyses. *Remote Sens. (Basel)* 12 (4), 720. <https://doi.org/10.3390/rs12040720>.

Goyal, R., Gupta, A. S., Jucker, M., & England, M. H. (2021). Historical and projected changes in the Southern Hemisphere surface westerlies. *Geophysical Research Letters*, 48, e2020GL090849. <https://doi.org/10.1029/2020GL090849>

Grilly, E., Reid, K., Lenel, S., & Jabour, J. (2015). The price of fish: A global trade analysis of Patagonian (*Dissostichus eleginoides*) and Antarctic toothfish (*Dissostichus mawsoni*) ☆. *Marine Policy*, 60, 186-196.

Harden-Jones, F.R. (1968). *Fish migration*. London (Edward Arnold). 325 p.

Hersbach, H., Bell, B., Berrisford, P., Biavati, G., Horányi, A., Muñoz Sabater, J., Nicolas, J., Peubey, C., Radu, R., Rozum, I., Schepers, D., Simmons, A., Soci, C., Dee, D., Thépaut, J-N. (2023): ERA5 hourly data on single levels from 1940 to present. Copernicus Climate Change Service (C3S) Climate Data Store (CDS), DOI: 10.24381/cds.adbb2d47 (Accessed on 26-10-2023)

Houde, E.D., 2008. Emerging from Hjort's shadow. *Journal of Northwest Atlantic Fishery Science*, 41.

Hughes, C. W., and B. A. de Cuevas, 2001: Why Western Boundary Currents in Realistic Oceans are Inviscid: A Link between Form Stress and Bottom Pressure Torques. *J. Phys. Oceanogr.*, **31**, 2871–2885, [https://doi.org/10.1175/1520-0485\(2001\)031<2871:WWBCIR>2.0.CO;2](https://doi.org/10.1175/1520-0485(2001)031<2871:WWBCIR>2.0.CO;2).

Jackson, L., C. W. Hughes, and R. G. Williams (2006). Topographic Control of Basin and Channel Flows: The Role of Bottom Pressure Torques and Friction. *J. Phys. Oceanogr.*, **36**, 1786–1805, <https://doi.org/10.1175/JPO2936.1>.

Kaschner, K., Ready, J., Agbayani, E., Eastwood, P., Rees, T., Reyes, K., Rius, J., Froese, R. (2007). About aquamaps: creating standardized range maps of marine species.

Killworth, P.D. and Hughes, C.W., 2002. The Antarctic Circumpolar Current as a free equivalent-barotropic jet. *Journal of marine research*, 60(1), pp.19-45.

Koubbi, P., Duhamel, G. and Hebert, C. (2000). Role of bay, fjord and seamount on the early life history of *Lepidonotothen squamifrons* from the Kerguelen Islands. *Polar Biol* **23**, 459–465. <https://doi.org/10.1007/s003009900106>

Koubbi, P., Duhamel, G., Hecq, J-H., et al (2009). Ichthyoplankton in the neritic and coastal zone of Antarctica and Subantarctic islands: A review. *J Mar Syst* 78:547–556. doi: 206 10.1016/j.jmarsys.2008.12.024

Koubbi, P., Guinet, C., Alloncle, N., Ameziane, N., Azam, C. S., Baudena, A., Bost, C., Romain, C., Chazeau, C., Coste, G., Cotte, C., d'Ovidio, F., Karine, D., Duhamel, G., Forget, A., Gasco, N., Hauteceur,

M., Lehodey, P., Lo Monaco, C., and Weimerskirch, H. (2016). Ecoregionalisation of the Kerguelen and Crozet islands oceanic zone. Part I: Introduction and Kerguelen oceanic zone. CCAMLR Document WG-EMM-16/43.

Kwiatkowski, L., Torres, O., Bopp, L., Aumont, O., Chamberlain, M., Christian, J.R., Dunne, J.P., Gehlen, M., Ilyina, T., John, J.G., Lenton, A., Li, H., Lovenduski, N.S., Orr, J.C., Palmieri, J., Santana-Falc'ón, Y., Schwinger, J., S'ef'erian, R., Stock, C.A., Tagliabue, A., Takano, Y., Tjiputra, J., Toyama, K., Tsujino, H., Watanabe, M., Yamamoto, A., Yool, A., Ziehn, T., 2020. Twenty-first century ocean warming, acidification, deoxygenation, and upper-ocean nutrient and primary production decline from CMIP6 model projections. *Biogeosciences* 17 (13), 3439–3470. <https://doi.org/10.5194/bg-17-3439-2020>.

Lee, J.-Y., J. Marotzke, G. Bala, L. Cao, S. Corti, J.P. Dunne, F. Engelbrecht, E. Fischer, J.C. Fyfe, C. Jones, A. Maycock, J. Mutemi, O. Ndiaye, S. Panickal, and T. Zhou (2021). Future Global Climate: Scenario-Based Projections and Near-Term Information. In *Climate Change 2021: The Physical Science Basis. Contribution of Working Group I to the Sixth Assessment Report of the Intergovernmental Panel on Climate Change* [Masson-Delmotte, V., P. Zhai, A. Pirani, S.L. Connors, C. Péan, S. Berger, N. Caud, Y. Chen, L. Goldfarb, M.I. Gomis, M. Huang, K. Leitzell, E. Lonnoy, J.B.R. Matthews, T.K. Maycock, T. Waterfield, O. Yelekçi, R. Yu, and B. Zhou (eds.)]. Cambridge University Press, Cambridge, United Kingdom and New York, NY, USA, pp. 553–672, doi:10.1017/9781009157896.006.

Lord, C., Duhamel, G., and Pruvost, P. (2006). The patagonian toothfish (*Dissostichus eleginoides*) fishery in the Kerguelen Islands (Indian Ocean sector of the Southern Ocean). *CCAMLR Science*, 13, 1-25.

Marlow, T. R., Agnew, D. J., Purves, M. G., and Everson, I. (2003). Movement and growth of tagged *Dissostichus eleginoides* around South Georgia and Shag Rocks (Subarea 48.3). *CCAMLR Sci.* 10, 101–111.

Mindlin, J., Shepherd, T.G., Vera, C.S., Osman, M., Zappa, G., Lee, R.W. and Hodges, K.I., 2020. Storyline description of Southern Hemisphere midlatitude circulation and precipitation response to greenhouse gas forcing. *Climate Dynamics*, 54, pp.4399-4421.

Mori, M., Corney, S., Melbourne-Thomas, J., Welsford, D., Klocker, A., and Ziegler, P. (2016). Using satellite altimetry to inform hypotheses of transport of early life stage of Patagonian toothfish on the Kerguelen Plateau. *Ecological Modelling*. 340. 45-56. [10.1016/j.ecolmodel.2016.08.013](https://doi.org/10.1016/j.ecolmodel.2016.08.013)

North AW (2002). Larval and juvenile distribution and growth of Patagonian toothfish around South Georgia. *Antarctic Science*, 14(1):25-31. doi:10.1017/S0954102002000548

Olbers, D. and Eden, C. (2003). A simplified general circulation model for a baroclinic ocean with topography. Part I: Theory, waves, and wind-driven circulations. *Journal of Physical Oceanography*, 33(12), pp.2719-2737.

O'Neill, B.C., Tebaldi, C., Van Vuuren, D.P., Eyring, V., Friedlingstein, P., Hurtt, G., Knutti, R., Kriegler, E., Lamarque, J.F., Lowe, J. and Meehl, G.A. (2016). The scenario model intercomparison project (ScenarioMIP) for CMIP6. *Geoscientific Model Development*, 9(9), pp.3461-3482.

Park, Y.-H., Charriaud, E., and Fieux, M. (1998). Thermohaline structure of the Antarctic Surface Water/Winter Water in the Indian sector of the Southern Ocean. *Journal of Marine Systems*, 17(1), 5-23. [https://doi.org/10.1016/S0924-7963\(98\)00026-8](https://doi.org/10.1016/S0924-7963(98)00026-8)

Park, Y.-H., Gasco, N. and Duhamel, G. (2008a). Slope currents around the Kerguelen Islands from demersal longline fishing records. *Geophysical Research Letters*, 35 (L09604). doi:10.1029/2008GL033660.

- Park, Y.-H., Fuda, J.-L., Durand, I. and Naveira Garabato, A.C. (2008b). Internal tides and vertical mixing over the Kerguelen Plateau. *Deep-Sea Research II*, 55, 582–593. doi:10.1016/j.dsr2.2007.12.027
- Park, Y.-H., F. Roquet, I. Durand, and J.-L. Fuda (2008c). Large-scale circulation over and around the northern Kerguelen Plateau, *Deep Sea Res. Part II*, 55, 566–581, doi:10.1016/j.dsr2.2007.12.030.
- Park, Y.-H., F. Vivier, F. Roquet, and E. Kestenare (2009). Direct observations of the ACC transport across the Kerguelen Plateau, *Geophys. Res. Lett.*, 36, L18603, doi:10.1029/2009GL039617.
- Park, Y.-H., I. Durand, E. Kestenare, G. Rougier, M. Zhou, F. d’Ovidio, C. Cotte, and J.-H. Lee (2014), Polar Front around the Kerguelen Islands: An upto-date determination and associated circulation of surface/subsurface waters, *J. Geophys. Res. Oceans*, 119, 6575–6592, doi:10.1002/2014JC010061
- Park, Y.-H., Durand, I., 2019. Altimetry-derived antarctic circumpolar current fronts. SEANOE. <https://doi.org/10.17882/59800>.
- Pascual, A., Faugère, Y., Larnicol, G., and Le Traon, P. Y. (2006). Improved description of the ocean mesoscale variability by combining four satellite altimeters. *Geophys. Res. Lett.* 33:L02611. doi: 10.1029/2005GL024633
- Pauthenet, E., Roquet, F., Madec, G., Guinet, C., Hindell, M., McMahon, C. R., Harcourt, R., and Nerini, D. (2018). Seasonal Meandering of the Polar Front Upstream of the Kerguelen Plateau. *Geophysical Research Letters*, 45(18), 9774-9781. <https://doi.org/10.1029/2018GL079614>
- Pellichero, V., Boutin, J., Claustre, H., Merlivat, L., Sallée, J.-B., and Blain, S. (2020). Relaxation of wind stress drives the abrupt onset of biological carbon uptake in the Kerguelen bloom: A multisensor approach. *Geophysical Research Letters*, 47, e2019GL085992. <https://doi.org/10.1029/2019GL085992>
- Péron, C., Welsford, D. C., Ziegler, P., Lamb, T. D., Gasco, N., Chazeau, C., Sinègre, R. And Duhamel, G. (2016). Modelling spatial distribution of Patagonian toothfish through life-stages and sex and its implications for the fishery on the Kerguelen Plateau. *Progress in Oceanography*, 141, 81-95.
- Press, W. H., and Teukolsky, S. A. (1992). Adaptive stepsize Runge-Kutta integration. *Computers in Physics*, 6(2), 188-191.
- Rintoul, S.R. (2018) The global influence of localized dynamics in the Southern Ocean. *Nature* 558, 209–218. <https://doi.org/10.1038/s41586-018-0182-3>
- Roquet, F. (2009). La circulation océanique autour du plateau de Kerguelen : de l’observation à la modélisation. Océan, Atmosphère. Université Pierre et Marie Curie - Paris VI. Français. NNT : 2009PA066680ff. [ffitel-00814528f](https://tel.archives-ouvertes.fr/tel-00814528f)
- Roquet, F., Y.-H. Park, C. Guinet, F. Bailleul, and J.-B. Charrassin. (2009). Observations of the Fawn Trough Current over the Kerguelen Plateau from instrumented elephant seals. *Journal of Marine Systems* 78:377–393, <https://doi.org/10.1016/j.jmarsys.2008.11.017>.
- Rosso, I., A. M. Hogg, P. G. Strutton, A. E. Kiss, R. Matear, A. Klocker, and E. van Sebille(2014). Vertical transport in the ocean due to sub-mesoscale structures: Impacts in the Kerguelen region. *Ocean Modell.*, 80, 10–23, <https://doi.org/10.1016/j.ocemod.2014.05.001>.
- Rousselet L., d’Ovidio F., Izard L., Della Penna A., Petrenko A., Barrillon S., Nencioli F., Doglioli A., (submitted), A Software Package for an Adaptive Satellite-based Sampling for Oceanographic cruises

(SPASSOv2.0): tracking fine scale features for physical and biogeochemical studies. *Journal of Atmospheric and Oceanic Technology*.

Sallée, J. B., K. Speer, and R. Morrow, (2008). Response of the Antarctic Circumpolar Current to Atmospheric Variability. *J. Climate*, **21**, 3020–3039, <https://doi.org/10.1175/2007JCLI1702.1>.

Scarponi, P., G. Coro, and P. Pagano. A collection of Aquamaps native layers in NetCDF format. *Data in brief* 17 (2018) : 292-296.

Son, S.-W., Tandon, N. F., Polvani, L. M., and Waugh, D. W. (2009), Ozone hole and Southern Hemisphere climate change, *Geophys. Res. Lett.*, **36**, L15705, doi:10.1029/2009GL038671.

Son, S.-W., et al. (2010), Impact of stratospheric ozone on Southern Hemisphere circulation change: A multimodel assessment, *J. Geophys. Res.*, **115**, D00M07, doi:10.1029/2010JD014271.

Sumby, J., Haward, M., Fulton, E. A., and Pecl, G. T. (2021). Hot fish: The response to climate change by regional fisheries bodies. *Marine Policy*, **123**, 104284. <https://doi.org/10.1016/j.marpol.2020.104284>

Swart, N. C., and Fyfe, J. C. (2012), Observed and simulated changes in the Southern Hemisphere surface westerly wind-stress, *Geophys. Res. Lett.*, **39**, L16711, doi:10.1029/2012GL052810.

Thiers, L., Delord, K., Bost, CA., Guinet, C., Weimerskirch, H. (2017) Important marine sectors for the top predator community around Kerguelen Archipelago. *Polar Biol* **40**, 365–378. <https://doi.org/10.1007/s00300-016-1964-4>

UNEP-WCMC and IUCN (2023), Protected Planet: The World Database on Protected Areas (WDPA) and World Database on Other Effective Area-based Conservation Measures (WD-OECM) [Online], November 2023, Cambridge, UK: UNEP-WCMC and IUCN. Available at: www.protectedplanet.net

Van Wijk, E.M., Rintoul, S.R., Ronai, B.M., Williams, G.D., 2010. Regional circulation around Heard and McDonald Islands and through the Fawn Trough, central Kerguelen Plateau. *Deep-Sea Research I* **57**, 653–669. <http://dx.doi.org/10.1016/j.dsr.2010.03.001>.

Vivier, F., Park, Y. H., Sekma, H., and Le Sommer, J. (2015). Variability of the antarctic circumpolar current transport through the fawn trough, kerguelen plateau. *Deep Sea Research Part II: Topical Studies in Oceanography*, **114**, 12-26.

Welsford, D., Nowara, G., McIvor, J. and Candy, S. (2012). The spawning dynamics of Patagonian toothfish in the Australian EEZ at Heard Island and the McDonald Islands and their importance to spawning activity across the Kerguelen Plateau.

Williams R., Lamb T. (2002). Behaviour of *Dissostichus eleginoides* fitted with archival tags at Heard Island: preliminary results. CCAMLR WG-FSA 02/60.

Yang, D., Arblaster, J.M., Meehl, G.A., England, M.H., Lim, E.P., Bates, S. and Rosenbloom, N. (2020). Role of tropical variability in driving decadal shifts in the Southern Hemisphere summertime eddy-driven jet. *Journal of Climate*, **33**(13), pp.5445-5463.

Young, E. F., Meredith, M. P., Murphy, E. J., and Carvalho, G. R. (2011). High-resolution modelling of the shelf and open ocean adjacent to South Georgia, Southern Ocean. *Deep Sea Research Part II: Topical Studies in Oceanography*, **58**(13-16), 1540-1552.

Young, E. F., Rock, J., Meredith, M. P., Belchier, M., Murphy, E. J., and Carvalho, G. R. (2012). Physical and behavioural influences on larval fish retention: contrasting patterns in two Antarctic fishes. *Marine Ecology Progress Series*, 465, 201-215.

Young, E. F., Thorpe, S. E., Banglawala, N., and Murphy, E. J. (2014). Variability in transport pathways on and around the South Georgia shelf, Southern Ocean: Implications for recruitment and retention. *Journal of Geophysical Research: Oceans*, 119(1), 241-252.

Young, C.M., 2020. Behavior and locomotion during the dispersal phase of larval life. *Ecology of marine invertebrate larvae*, pp.249-277

Ziegler, P., and Welsford, D. (2019). “The Patagonian toothfish (*Dissostichus eleginoides*) fishery at Heard Island and McDonald Islands (HIMI) – population structure and history of the fishery stock assessment,” in *The Kerguelen Plateau: Marine Ecosystem and Fisheries*, eds G. Duhamel and D. Welsford (Kingston, TAS: Société française d’ichtyologie).

5.4 Science and society: Identifying ecologically important areas to maximize Patagonian toothfish stock resilience.

The previous study focuses on the southwest-northeast physical connectivity over and around the Kerguelen Plateau, thus between potential spawning areas and potential recruitment areas for Patagonian toothfish, to investigate how climate change could impact such ecologically important physical feature. Few assumptions are made on the characteristics of the spawning and recruitment sites since no reproductive hotspots have today been identified (Péron et al., 2016; Yates et al., 2018). When investigating how climate change may impact the southwest-northeast connectivity, we find that uncertainties remain too large to provide a precise answer but that changes in this connectivity might not be linear under global warming with potentially unprecedented changes due to the projected southward shift of winter waters east of the Kerguelen Plateau. This study concludes on the variable connectivity between Australian and French stocks with a potential short-term increase and long-term decline.

In the face of uncertain climate change impacts on Patagonian toothfish, improved knowledge on potentially vulnerable early-life stages is key. The identification of recruitment areas could be a major step to develop management strategies to maximize stock resilience and ensure fisheries sustainability:

- By developing campaigns in the field to observe and study *in situ* Patagonian toothfish early-life stages. Improved understanding of Patagonian toothfish early life ecology can help refine the definition of the stock status and its sustainability. Indeed, sustainability today is mostly based on the spawning biomass while recruitment could be impacted by changing environmental conditions regardless of the number and weight of reproductive adults.
- By identifying ecologically important areas and whether they are already under adapted conservation measures or not.

In the main study of this Chapter, we hypothesize that the retentive zones in Kerguelen eastern coastal waters and at the Polar Front meander could be important recruitment areas for Patagonian toothfish early-life stages. As complementary analyses, we further

investigate what are the potential recruitment areas connected to realistic hypothetical spawning areas. We focus on whether hotspots of arrival points after 3 months (egg phase) and 6 months (egg and larval phases) advections can be observed and whether these hotspots vary interannually.

We consider two potential spawning areas: one west of Kerguelen, including Skiff bank (then referred to as the Skiff area to distinguish it from the “west of Kerguelen” area in the main study) and one west of Heard, which is similar as the “west of Heard” area defined in the main study (blue rectangles on Figure 5.3). Ongoing research at the French National Museum of Natural History aims at identifying reproduction hotspots and associated phenology based on catch per unit effort (CPUE) data on reproductive stages over the last decade (biometry data on captured toothfish collected onboard by fisheries inspectors). Preliminary investigations suggest Skiff Bank and the west of Kerguelen islands as a potentially important reproductive area in July (personal communication from Fanny Ouzoulias). As in the previous study, we compute forward advections from these potential spawning areas, this time over both 3 months (eggs phase) and 6 months (egg and larvae phase) starting in July from the Skiff area and in June from the west of Heard area (Yates et al., 2018) to focus on possible spawning peaks. We then calculate the number of arrival points over a $0.1^\circ \times 0.1^\circ$ grid, which is here called the “arrival points density” presented in log10 scale to better highlight spatial contrasts (Figure 5.3).

Those two hypothetical spawning areas are connected to different arrival hotspots. Figure 5.3 shows that high arrival points densities from the Skiff area are found both within the initial zone (blue rectangle on Figure 5.3 A) and over Kerguelen shelf, especially north of Kerguelen islands, even over 6-month advections. High arrival points densities from the west of Heard area are mostly found over Heard shelf, extending northward up to the position of the Polar Front meander for 6-month advections. We note that high arrival points densities are found over Pike and Discovery banks (located north of the Heard shelf) after 6-month advections.

There is a high spatial heterogeneity in the interannual variability of the arrival points densities from both hypothetical spawning areas. High interannual variability of the arrival points density from the Skiff area are found around northwestern coast of Kerguelen (data not shown). Computing the ratio of the standard deviation over the mean

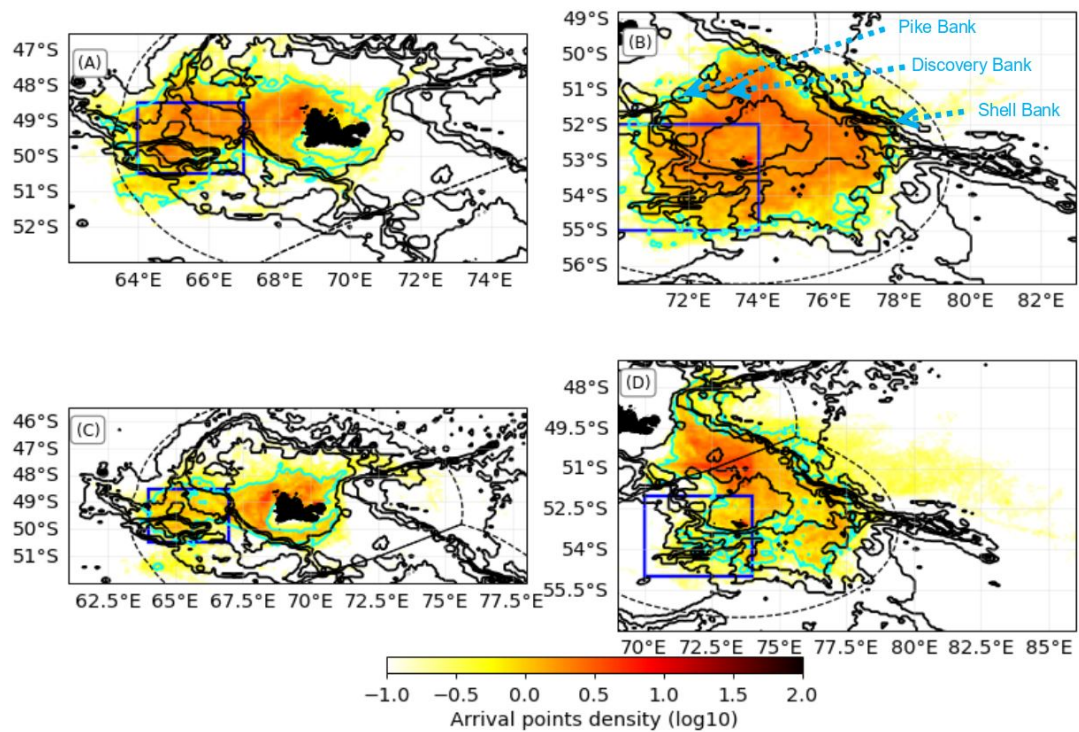


FIGURE 5.3: **Arrival points density in log₁₀ scale after 3 months (A,B) or 6 months (C,D) advections from potential spawning areas either from the Skiff area (A,C) or the west of Heard (B,D) as indicated by the blue rectangles, following the same methodology as in the main study of this Chapter regarding particle density but here only considering the trajectories' final locations. Contours of the 99.9th percentile of the arrival density are shown in cyan. Note that we use here a finer bathymetry product (used for Mercator reanalysis and provided by CMEMS) to locate small banks such as Pike, Discovery and Shell banks.**

arrival points density can be useful to pinpoint arrival hotspots that are relatively stable between years. For advections from the Skiff area, such ratio remain close to one or higher where the mean arrival points density is high (Figure 5.4 A and C). However, we need to interpret the results in Kerguelen coastal waters with caution as we reach here the limits of traditional altimetry in coastal areas (Cipollini et al., 2014). High interannual variability of the arrival points density from the west of Heard are mostly found north of Heard shelf around 72.5°-74.2°E and 51.8°-50.3°S (data not shown). This latter area is at the frontier between the two exclusive economic zones and includes Discovery Bank. The interannual variability of arrival points density is lower than the mean density value over Heard shelf and at Shell Bank (Figure 5.4 B and D).

If we consider that potential recruitment areas could be defined by high probability of connectivity with hypothetical spawning areas and low interannual variability of such connectivity, we point out:

- In relation to the Skiff bank area : potential recruitment areas remain mostly west of Kerguelen or in Kerguelen coastal waters, although finer hotspots of arrivals within these areas appear to greatly vary between years.
- In relation to the west of Heard area : potential recruitment areas are found over Heard shelf and east up to Shell Bank.

We note that the Polar Front meander does not stand out as a major arrival hotspot, despite the existing connectivity with both studied spawning areas. In these analyses, we focus on areas that are the most connected to the hypothetical spawning areas but those analyses are complementary to the results of the main study of this Chapter. Overall, it is important to consider both highly and lowly connected areas to spawning areas to better understand the big picture of eggs and larvae dispersion phase.

We can then compare the potentially ecologically important areas identified to the localisation of current protected marine areas where fishing activities are strongly restricted. Important areas such as Skiff bank, Discovery bank, Shell bank, the core of the Polar Front meander and Kerguelen coastal waters are already included in no-take zones (Welsford et al., 2011; UNEP-WCMC and IUCN, 2023), while the area north of Skiff bank or the shelf break east of Kerguelen shelf fall outside these delineations (Figure 5.5). It has been observed that fishing pressure could be increased at the edges of no-takes zones but such effect could be regulated through the implementation of buffer zones with intermediate fishing restrictions (Ohayon et al., 2021). Whether such buffer zones could be needed to avoid disturbances in potential Patagonian toothfish recruitment areas could be worth investigating. Another strategy could be to further protect spawning areas that are most likely to contribute to successful recruitment (e.g. area north of Skiff bank or west of Heard; Figure 5.5).

Note that these analyses are preliminary and do not constitute finalized recommendations but there are used here as illustrations of how scientific knowledge can be used to inform management and guide the identification of key areas that could help maximize Patagonian toothfish stock resilience to climate change.

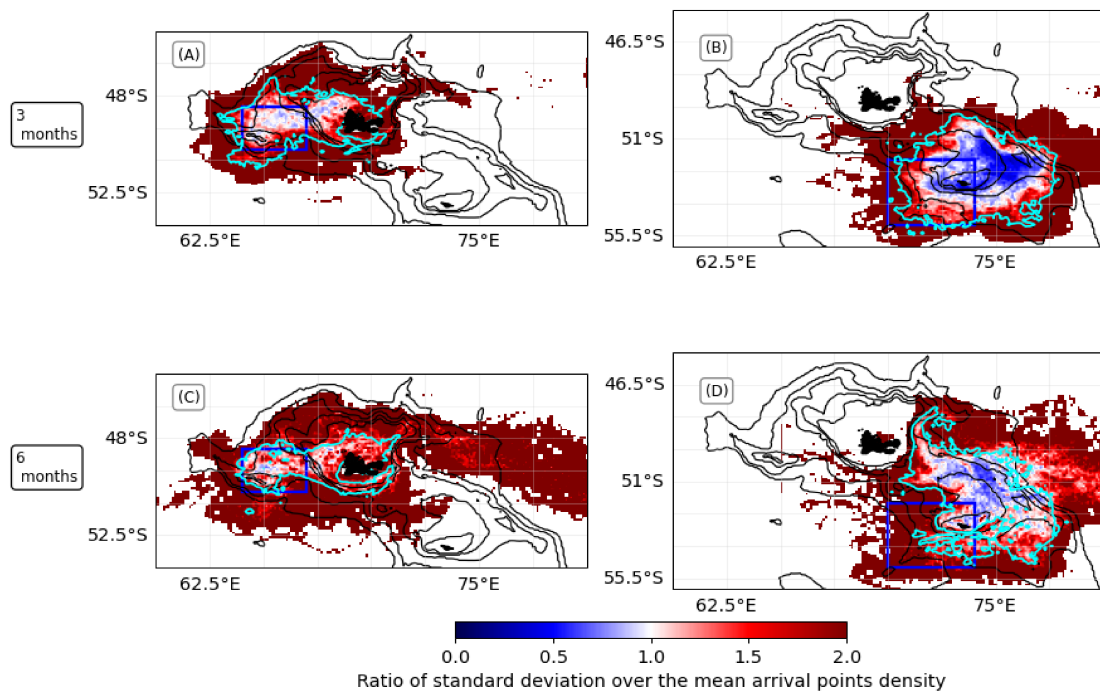


FIGURE 5.4: Ratio of the standard deviation over the mean of arrival points density after 3 months (A,B) or 6 months (C,D) advections from potential spawning areas either from the Skiff area (A,C) or the west of Heard (B,D) as indicated by the blue rectangles, following the same methodology as in the main study of this Chapter regarding particle density but here only considering the trajectories' final locations. Contours of the 99.9th percentile of the arrival points density are shown in cyan.

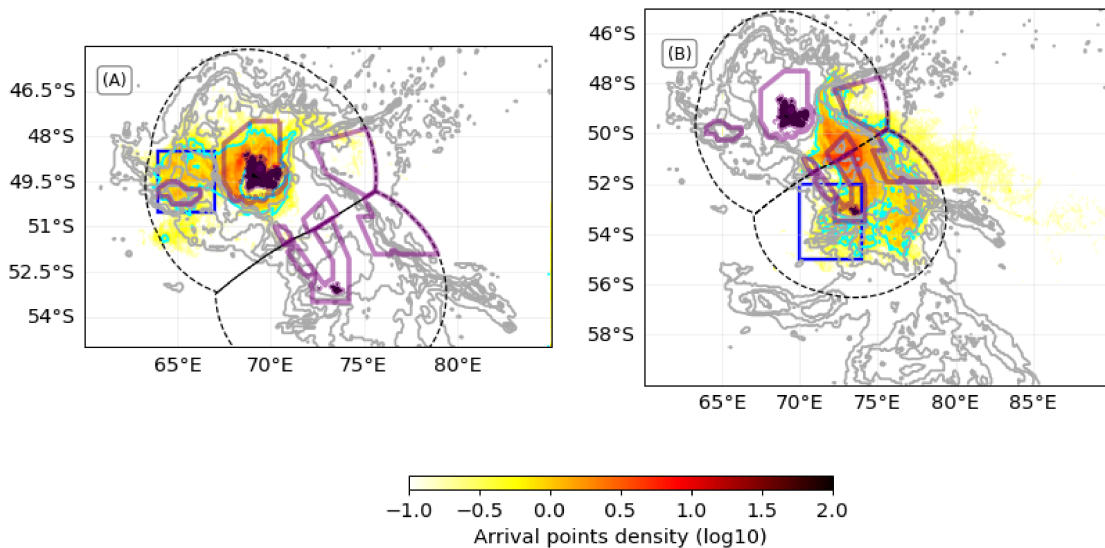


FIGURE 5.5: Arrival points density in log10 scale after 6 months advections from potential spawning areas either from the Skiff area (A) or west of Heard (B) as indicated by the blue rectangles, following the same methodology as in the main study of this Chapter regarding particle density but here only considering the trajectories' final locations. Contours of the 99.9th percentile of the arrival density are shown in cyan, bathymetry contours in darkgray and no-takes zones in purple (data from UNEP-WCMC and IUCN (2023)).

Conclusion

This Chapter studies climate change potential impacts on the circulation over and around the Kerguelen Plateau, which plays an important ecological role for Patagonian toothfish early-life stages by physically connecting western areas of the Plateau (i.e. potential spawning sites) and the east of Kerguelen (i.e. potential recruitment site). When investigating climate change impacts on fishes, it is important to account for their complex life cycles, especially given that recruitment is highly variable interannually and that larval connectivity is often a major unknown (Petitgas et al., 2013).

This study highlights the high interannual variability of the connectivity between the west of Heard and the east of Kerguelen, which appears mostly driven by winter wind stress, although other local processes can modulate it. Given that the winter wind stress is projected to intensify in climate models, this connectivity could be expected to intensify, at least in the coming decades. However, uncertainties remain on winter westerlies intensification in the long term depending on climate change scenarios. Besides, Chapter 4 has shown that the Polar Front east of the Plateau could significantly shift southward in a global warming world above 2°C, an unprecedented change over the last decades, which could modify the local circulation patterns.

Despite the remaining uncertainties on the future circulation over the Kerguelen Plateau, the life history connectivity between French and Australian stocks is here highlighted. Besides, Lagrangian tools can be useful to reflect on potentially ecologically significant areas for Patagonian toothfish early-life stages that could guide the development of management strategies, notably to maximize Patagonian toothfish stock resilience.

Chapter 6

Conclusions, limits and perspectives

“There is perhaps no better demonstration of the folly of human conceits than this distant image of our tiny world. To me, it underscores our responsibility to deal more kindly with one another, and to preserve and cherish the pale blue dot, the only home we’ve ever known.”

Carl Sagan, The Pale Blue Dot

6.1 Main findings

There is today abundant evidence that significant physical changes have been occurring in the Southern Ocean these last decades, yet evaluating climate change impacts on pelagic ecosystems remains a challenge. Ecological long-term monitoring efforts reveal mixed trends, that vary depending on the region and the species and that often integrate the effects of multiple stressors. Such uncertainty can hinder the development of climate-adapted strategies for conservation and fisheries management at a time where climate change has been officially qualified as a major threat for biodiversity ([IPBES, 2019](#)).

The issue of climate change impacts on pelagic ecosystems is inherently complex and interdisciplinary. Methodologies have been developed to investigate the complexity of ecological responses to environmental changes and to better model the interactions between ecosystems and their environment. However those approaches often overlook the complexity of the physical drivers of change. The aim of this thesis is to address this gap by focusing on climate change impacts on ecologically significant physical features, considering both their spatial and temporal complexity, in the case of the Southern Indian Ocean. In particular, the study of marine heatwaves (MHWs) in Chapters 3 and 4 enable us to investigate physical disturbances on shorter timescales (i.e. days, months) that may foreshadow future long-term impacts (i.e. decadal changes). Chapter 4 specifically focuses on winter waters (WWs), since this subsurface water mass structures pelagic communities, making prey more accessible to top predators. Chapter 5 is centered on the geostrophic circulation over and around the Kerguelen Plateau, which plays a key role for the transport and thus connectivity of Patagonian toothfish early-life stages.

A first question is raised: *How is climate change going to impact physical characteristics of ecological importance for pelagic ecosystems in the Southern Indian Ocean?*

Climate change can impact temperature conditions in the Southern Indian Ocean through both extreme events and long-term trends which are projected to intensify over the subantarctic latitudes (Chapter 3). Those temperature changes can impact WWs presence and characteristics at those different timescales, thus impacting major foraging hotspots for top predators (Chapter 4). Over the Kerguelen Plateau, the current southwest-northeast circulation, connecting key areas for the ecology of the Patagonian toothfish, might be intensified in the short term due to westerlies strengthening (Chapter 5). However, long-term climate change impacts on this connectivity are uncertain as the Polar Front east of Kerguelen (defined as the northernmost extension of the WWs) is projected to significantly shift southward, for a global warming level of around 2.6°C (Chapter 4), which could completely modify connectivity and retention processes over the Plateau.

Chapters 3, 4 and 5 therefore all highlight the spatial and temporal heterogeneity of climate change impacts, through focusing on temperature trends and extremes, WWs and the ocean circulation over Kerguelen Plateau (Figure 6.1). Strong contrasts of climate change impacts are found between the eastern and the western parts of the

Southern Indian Ocean. Temperature trends are not yet significant south of Crozet near the Polar Front while a warming hotspot is observed east of 80°E (Chapter 3). Larger shifts of the Polar Front are projected west of the Kerguelen Plateau, compared to the east where the Polar Front remains relatively stable up to a global warming threshold of around 2.6°C (Chapter 4).

The ocean circulation and the topography are highlighted as drivers of the spatial and temporal heterogeneity of climate change impacts. Ocean circulation can enhance exposure to extreme events: the Agulhas Return Current is an area of high MHW intensity and wind-induced northward Ekman transport might contribute to the projected intensification of warming and MHWs intensity at subantarctic latitudes (Chapter 3). Ocean circulation can also buffer changes: spatial patterns of warming and deepening of WWs during MHWs are also linked to the ocean circulation, with weaker changes in areas of northward cold water mass intrusion (Chapter 4). The topography of the Kerguelen Plateau constrains the flow, thus potentially buffering and delaying climate change impacts on WWs distribution east of the Plateau (Chapter 4).

Throughout Chapters 3, 4 and 5, the use of CMIP6 models under different scenarios enables us to showcase differences in magnitude, and in some cases in direction, of change depending on socio-economic strategies. For instance, a cooling is projected in the Agulhas Return Current region at the end of the century under a strong mitigation scenario (SSP1-2.6) while other scenarios project warming throughout the Southern Indian Ocean (Chapter 3). There are also important uncertainties regarding the future changes in variables such as winter wind stress depending on the scenario and timescale considered (Chapter 5).

Overall, this PhD thesis provides insights regarding the two hindrances to better understanding climate change impacts on pelagic ecosystems identified in Chapter 1, which are i) the need to account for a 3D habitat and ii) the need to account for finer scale processes. This work further supports the importance of considering climate change impacts at depth: either through the identification of the “habitat shearing” threat (Chapter 3) or the impacts of MHWs and global warming on subsurface WWs (Chapter 4). The first example shows that changes at depth can have amplified consequences on pelagic ecosystems by impacting habitat continuity. The second example illustrates how warming at different timescales can affect ecologically significant subsurface physical features

which are crucial for pelagic ecosystems. This PhD work also contributes to reflecting on climate change physical impacts on a multiple spatial-temporal scale framework (Figure 6.1). Throughout this work, multiple timescales are considered, from short timescales extreme events to decadal timescales projections. Chapter 5 also more directly contributes to linking spatial fine scale processes, such as connectivity and retention, and larger-scale drivers, such as wind stress.

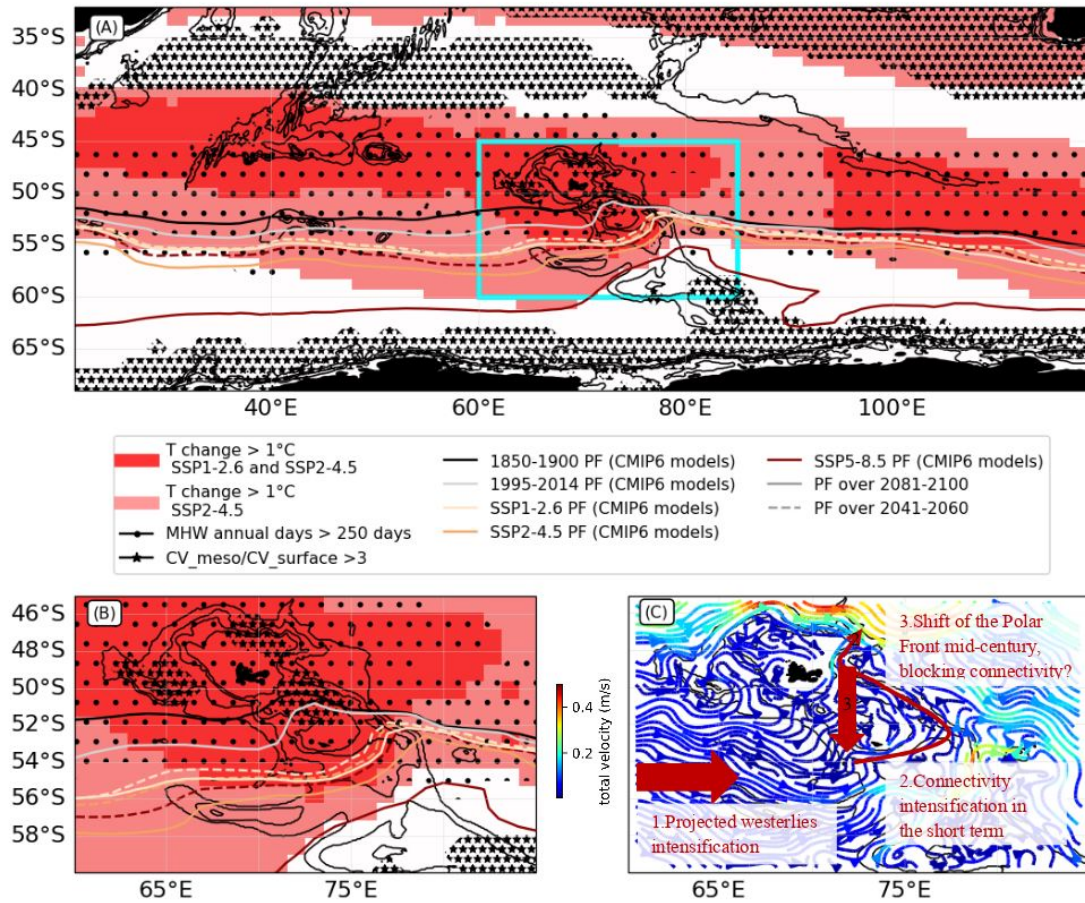


FIGURE 6.1: **Summary figure of the climate change impacts on physical features of ecological importance for pelagic ecosystems identified in Chapter 3, 4 and 5.** (A) Summary of projected changes in CMIP6 models in temperature (T change), MHW annual days (under SSP2-4.5), habitat shearing (adapted from [Azarian et al. \(2023\)](#) and Chapter 3) and Polar Front (PF) positions as defined as the northernmost extension of the winter waters depending on different scenarios (Chapter 4). Habitat shearing is here defined where the projected climate velocity in the mesopelagic (CV meso) is higher than 3 times the projected climate velocity at the surface (CV surface) under SSP2-4.5. (B-C) Zoom over the Kerguelen Plateau area (cyan rectangle on panel A), showing the same metrics as in Panel A (B) and showing the streamlines of mean winter total AVISO altimetry-derived geostrophic velocity over 1993-2020 (C) with also a summary of Chapter 5 main results.

A second question is raised: *How can we include this knowledge to guide conservation and fisheries management in the region?*

Developing further knowledge on climate change impacts in the Southern Indian Ocean also aims at providing relevant knowledge for conservation and fisheries management. Consequently, all Chapters have included discussions on the management implications associated with scientific results. Different tools have been illustrated, notably climate velocities and the notion of climate refugia which both enable to account for the spatial and temporal complexity of changes.

Throughout the Chapters, the area east of Kerguelen between the isobaths 2000 and 3000 m (Figure 6.2), emerges as a climate refugium for pelagic ecosystems, with both ocean circulation and topography that can act as buffers. The deviation of a warm and highly energetic flow by the topography north of the Kerguelen Plateau and/or the transport of cold WWs from the south of the Kerguelen Plateau could explain why the Polar Front meander appears to experience less frequent and less intense MHWs than nearby open ocean regions (Chapter 3; Figure 6.2 A,B). In this area, the WWs distribution, and thus the Polar Front, has also been more stable over the last decades than west of the Kerguelen Plateau (Chapters 4, 5; Figure 6.2 C). This offshore pelagic refugium may however be temporary, as CMIP6 models analysis reveals the existence of a threshold at which the Polar Front meander shifts further south (Chapter 4), which could also potentially block the physical connectivity over the Plateau (Chapter 5).

Identifying climate refugia is a key prospect and concrete strategy to integrate climate change in biodiversity management. Climate refugia are regions that are less affected by climate change than their surroundings, thus potentially increasing species' resilience within. As such, they may avoid the eradication of some species during extreme events or climate change overshoots. The identified refugium east of Kerguelen is already included in a no-take zone within the Kerguelen marine reserve and could play an important role for climate change adaptation in the region.

Chapter 5 raises the issue of connectivity toward this refugium which may be disturbed under climate change, with potential implications for the management of Patagonian toothfish stocks. Although many unknowns remain concerning climate change impacts on the stock biomass, Chapter 5 main study supports the relevance of increasing collaborations between French and Australian managers at the scale of the Kerguelen Plateau.

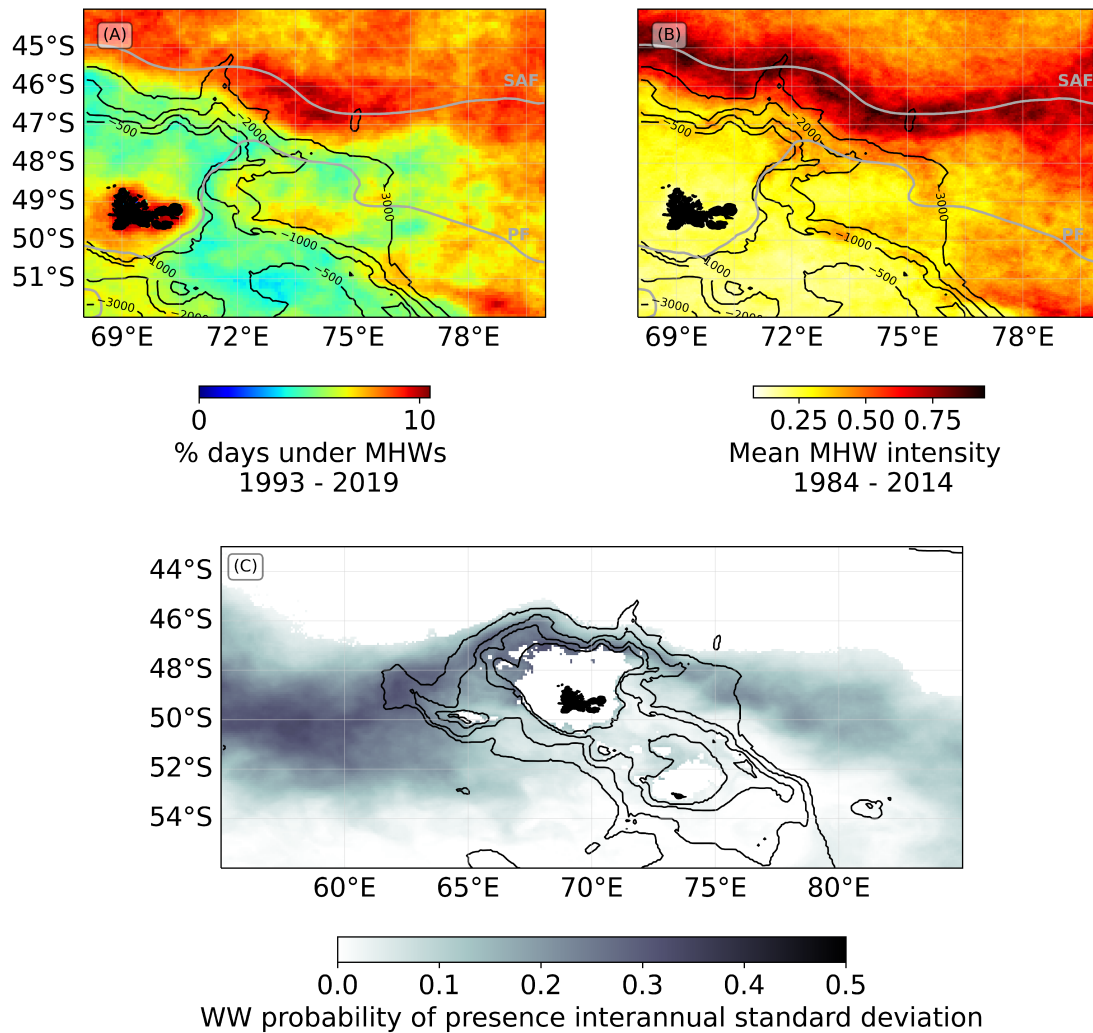


FIGURE 6.2: Identification of a pelagic climate refugium offshore east of Kerguelen shelf break, between the isobaths 2000 and 3000 m. (A) Percentage of days between 1993 and 2019 that are under MHW conditions and (B) mean MHW intensity between 1984 and 2014 (from Chapter 3) using OSTIA dataset as in Azarian et al. (2023). The Subantarctic Front (SAF) and Polar Front (PF) climatological position from Park and Durand (2019) are shown in grey. (C) Interannual variability of the winter waters probability of presence over 1993-2019 (as in Chapter 4).

6.2 Scientific perspectives

Scientific perspectives outline

This PhD thesis has focused on specific physical indicators that can be associated to different impacts on ecosystems. This “Scientific perspectives” section thus presents perspectives on better understanding both the drivers of changes and the potential impacts on pelagic ecosystems :

- On drivers of changes:
 - Improving the mechanistic understanding of physical drivers of change, notably frontal shifts and changes in ocean circulation (Section [6.2.1](#))
 - Toward (re)defining extreme events at depth (Section [6.2.2](#))
- On potential impacts on pelagic ecosystems (Section [6.2.3](#)):
 - Do elephant seals change or adapt their behaviors in response to extreme events? (Section [6.2.3.1](#))
 - Can the local circulation modulate the conditions of development for Patagonian toothfish early-life stages? (Section [6.2.3.2](#))

6.2.1 Improving the mechanistic understanding of physical drivers of change

This PhD thesis has focused on identifying climate change impacts on physical features of ecological significance but further analyses would be needed to provide a complete understanding of the physical mechanisms driving these impacts. Such understanding would be useful to further discuss or even narrow the uncertainties around climate models projected changes.

The ACC system is a structuring and dynamic physical feature which is key for most Southern Ocean ecosystems. Yet, whether the ACC will shift in the future remains an open question. In Chapter [4](#), we highlight the potential southward shift of the Polar Front using a water mass based definition in the Southern Indian Ocean, also pointing out the longitudinal heterogeneity of this shift and its dependence on global warming levels. It can be noted that the multi-model mean position of the Polar Front in

CMIP6 models historical simulations is a bit further south than the one observed using satellite altimetry or derived with Mercator reanalysis (Azarian et al., 2024). Still, the relative shifts projected over time and over different scenarios in climate models suggest that there is one or more mechanisms fostered by global warming that can lead to a contraction of the WWs distribution. Whether the magnitude of the shift is well represented by CMIP6 models might be debated but a paleo-oceanographic study points out that such magnitude of shift might have happened in the past (Civel-Mazens et al., 2021).

Better understanding the underlying mechanisms driving this shift can help determine potential enhancers or buffers (e.g. natural variability) of this change, that may be absent, parameterized or represented differently depending on the models. It would then allow to refine our estimate of the projected shift magnitude and also better characterize the abruptness of this shift. Identifying the physical mechanisms driving this shift in CMIP6 models is outside the scope of Chapter 4, but the hypothesis of WWs mass transformation through freshwater fluxes, notably due to Antarctic sea ice melting and change in sea-ice transport (Abernathy et al., 2016; Haumann et al., 2016) is discussed. Sea ice modelling is challenging and an active field of research. While the Antarctic sea ice seasonal cycle representation has improved from the CMIP5 to CMIP6 exercise, a large intermodel spread remains (Roach et al., 2020; Shu et al., 2020). Models with large sea ice extent over historical simulations tend to project greater losses in sea ice in the future, notably in summer (Holmes et al., 2022). Although this would require further investigation, we note that the models selected in Chapter 4 reflect a wide range of sea ice climatological properties (Figure 6.3), which suggests that the observed southward shift is not just due to a bias in the initial sea ice volume. Similarly, those models cover a wide range of ACC strength (Figure 6.3), that could correspond to different dynamical regimes. Although they were not studied in the scope of Chapter 4, the following questions could require further investigation:

- Is the volume of Antarctic sea ice driving the volume of WWs and potentially its northward extension? In that case, could the rate of decrease in Antarctic sea ice modulate the rate of the Polar Front southward shift?
- Are the dynamic (e.g. jet) and water mass based definitions of the Polar Front still aligned or decoupled in the future?

- Can a southward shift of the Polar Front, even locally, be associated with a shift of the other ACC fronts or can it shift within the range of the ACC that would remain stable over time?

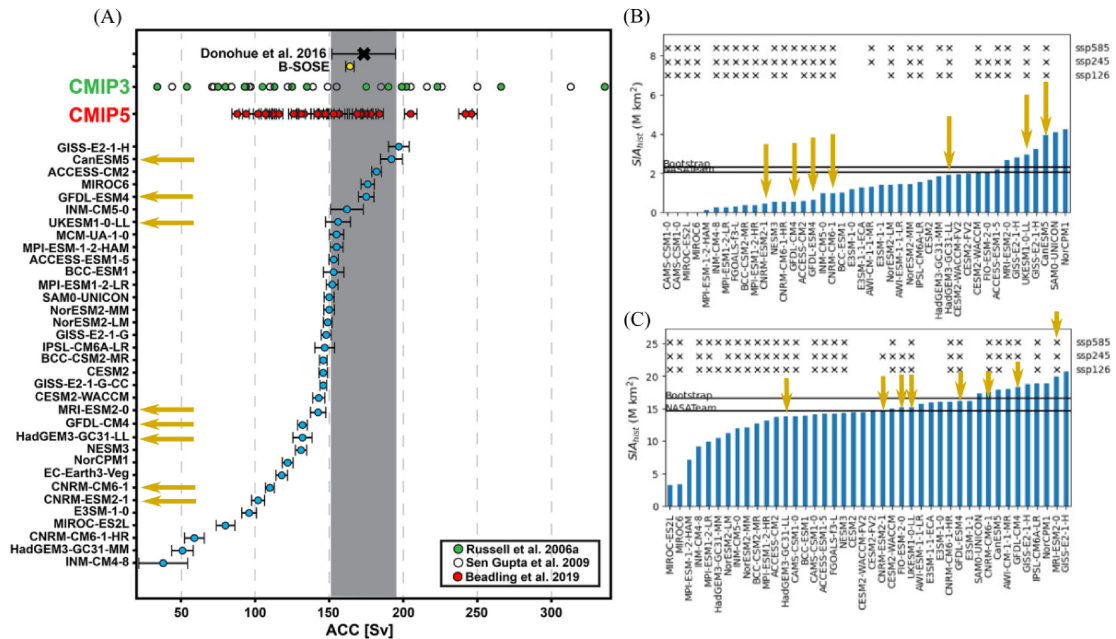


FIGURE 6.3: Spread in volume transport of the ACC through the Drake Passage and in the historical sea ice area across different CMIP6 models. (A) Volume transport of the ACC through the Drake Passage across different climate models (Figure from Beadling et al. (2020), with gray shading indicating the observational uncertainty estimated in Donohue et al. (2016)). (B-C) Historical climatology of sea ice area in February (B) and September (C) for different CMIP6 models (Figures from the supplementary materials of Holmes et al. (2022)). On all panels, the gold arrows point out the models used in Chapter 4, but note that not all the models used in Chapter 4 are shown on this graphs since they were not all considered in Beadling et al. (2020) and Holmes et al. (2022).

Addressing these questions could also be useful to better understand the future of the ocean circulation over and around the Kerguelen Plateau. Indeed, in Chapter 5, results interpretations are limited by the perspective of a potential shift of the Polar Front east of Kerguelen. Whether the dynamic definition of the Polar Front still aligns in the future with the water mass based definition used in this PhD thesis could condition the concrete impact of WWs shift on the connectivity. Does the jet east of Kerguelen shift in the future along with WW distribution or does it remain constrained by the topography? The main issue today to answer this question is still that, as indicated in Chapter 5, climate models are too coarse and do not necessarily account for the Kerguelen Plateau

topography correctly to adequately represent this fine scale feature. Dynamical down-scaling over the Kerguelen Plateau or the use of high resolution modelling of the ACC (e.g. PERIANT simulations) could be a way forward to investigate that question.

The underlying physical processes hypothesized in Chapter 5 would also be worth exploring. Indeed, our study is consistent with theoretical frameworks such as topographic steering (Gille, 2003) and the barotropic vorticity balance with a potentially important contribution of the bottom pressure torque in deviating the flow, which then connects the west of Heard island to the east of Kerguelen. High connectivity during Patagonian toothfish spawning season is associated with positive anomalies of absolute dynamic topography (Chapter 5), which are also positively correlated with ocean bottom pressure in the Southern Indian Ocean between 2003 and 2016 using Gravity Recovery and Climate Experiment (GRACE) satellite data (Niu et al., 2022). It was also shown that atmospheric forcing, notably through the Southern Annular Mode (SAM), can play an important role in the local ocean bottom pressure variability (Niu et al., 2022) which could then modulate the bottom pressure torque (Jackson et al., 2006) written as :

$$J(p_b, H) = \frac{\partial p_b}{\partial x} \frac{\partial H}{\partial y} - \frac{\partial p_b}{\partial y} \frac{\partial H}{\partial x} \quad (6.1)$$

with p_b the pressure at the sea floor and H the ocean depth. Here we assume that the flow is barotropic and that with increasing wind stress there is an increasing influence of the bottom pressure torque steering the flow. Comparing past variability to projected wind changes, it seems unlikely that wind stress will reach an unprecedented threshold where the effect would no longer be increased topographic steering but on the contrary crossing f/H contours (with f the planetary vorticity) before the shift of the Polar Front occurs. Yet, it would be interesting to investigate whether the barotropic assumption over the Plateau would still hold under climate change as the water column stratification increases (Li et al., 2020; Kwiatkowski et al., 2020; Sallée et al., 2021).

6.2.2 Towards (re)defining extreme events at depth

6.2.2.1 Further characterizing marine heatwaves impacts at depth

In Chapter 3, we indicate that marine heatwaves (MHWs) are to be more frequent and intense under global warming and, in Chapter 4, we find that the MHWs detected at the surface these last decades are associated with the southward advection of water parcels, thus impacting subsurface water masses, leading to local meanders in the Polar Front. A next step would be to continue investigating MHWs impact at depth, either on other ecologically important water masses, such as the Circumpolar Deep Waters which are also important for elephant seals foraging (Biuw et al., 2007; McMahon et al., 2019), or more generally on the vertical structure of the water column and pelagic habitat continuity.

MHWs impacts at depth is a global and active field of research. There are now multiple evidence, both through regional (Elzahaby and Schaeffer, 2019; Elzahaby et al., 2021; Hu et al., 2021) and global studies (Fragkopoulou et al., 2023), that MHWs at depth can be more intense than at the surface. This has been mostly evidenced for subsurface layers but also for bottom MHWs events, although the intensity and duration of bottom events were found to vary with ocean depth in North America Large Marine Ecosystems (Amaya et al., 2023a).

Different types of MHWs vertical structure have recently been identified (Zhang et al., 2023). It can be noted that MHWs in the Southern Indian Ocean can mostly be characterized as “subsurface-intensified” (i.e. maximum temperature anomaly in the subsurface) and “deep MHWs” (i.e. temperature anomalies decaying slowly with depth; Zhang et al. (2023); Figure 6.4 A-D). In particular, south of the ACC, upwelling and mixing disturbances can generate deep MHWs, which are then mostly modulated by vertical processes (Hu et al., 2021; Zhang et al., 2023).

The vertical structure of MHWs is strongly related to MHWs development and transport mechanisms. Indeed, MHWs are statistical indicators integrating various processes that may vary depending on the regions but also seasonally. Radiative processes will mostly impact the surface but advective processes can bring anomalously warmer water throughout the mixed layer depth (Oliver et al. (2021); Figure 2.8 B). In some regions the mixed layer depth (MLD) can play an important role in modulating the penetration

of temperature anomalies (Amaya et al., 2021; Elzahaby et al., 2022). A deep MLD can lead to more MHWs related to advection and less driven by air-sea heat flux for instance. Then advection-driven MHWs tend to be deeper, more intense at depth and to last longer than surface driven MHWs on average (Elzahaby et al., 2021).

Temperature anomalies formed at the surface can also penetrate in the water column and the penetration depth often depends on the level of stratification of the water column. Through vertical mixing, MHW can penetrate in the subsurface and can persist longer than at the surface (Elzahaby and Schaeffer, 2019; Scannell et al., 2020). In that sense, temperature anomalies formed in winter can also be trapped in the subsurface and re-emerge the next winter (Alexander et al., 1999; Byju et al., 2018). This may be another explanation as to why MHWs can last longer at depth (Elzahaby and Schaeffer, 2019). In this PhD work, complementary analyses in relation to Chapter 4 (Azarian et al., 2024) were conducted to further explore the seasonal characteristics of the MHWs sampled by Argo floats (Figure 6.5). Those analyses show that those MHWs are associated with increased eddy kinetic energy (as indicated in Chapter 4) but also reveal that summer MHWs tend to be shallower, less intense, shorter but spreading over larger areas, especially compared to winter MHWs. The processes at play to generate and transport MHWs might differ seasonally, consequently leading to potential variations in the impact of MHWs at different depths. However, although MLDs from the Argo profiles (using the definitions from Weller and Plueddemann (1996); de Boyer Montégut et al. (2004)) vary seasonally, there are no significant differences between the MLD in and outside a MHW (Figure 6.5) and no correlation was found between the mixed layer depth and the temperature anomaly depth (or MHW depth on Figure 6.5A ; data not shown). This could be due to the high variability of MLD in the Southern Ocean (Dong et al., 2008), which thus might not be the main driver of the MHWs vertical extent in the Southern Indian Ocean.

6.2.2.2 Can there be “hidden MHWs”?

This recent knowledge on MHW deeper extent reveals that the threat posed by MHWs on pelagic species could be higher than expected, since MHWs deeper extent can curtail their ability to avoid extreme events by migrating vertically. Another question also

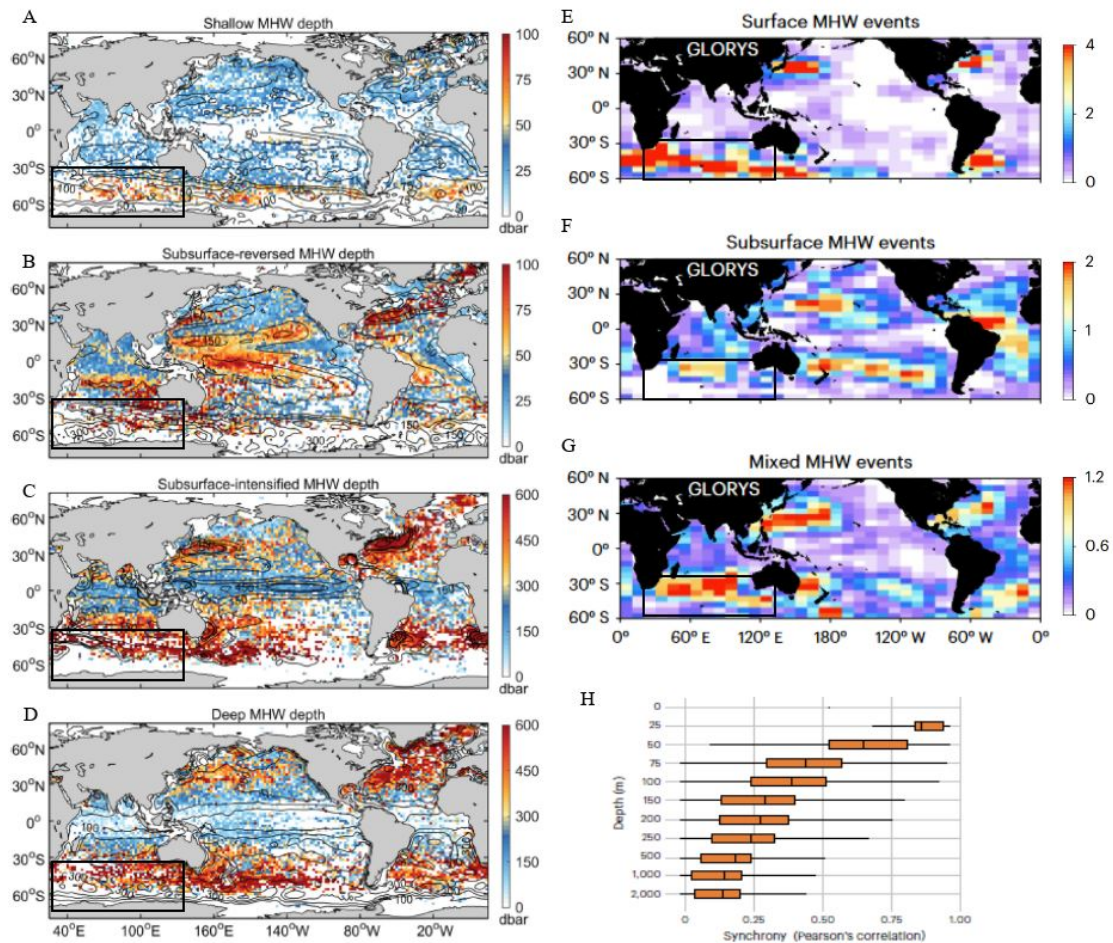


FIGURE 6.4: Figures extracted from recent peer-reviewed literature on MHWs extent at depth (Fragkopoulou et al., 2023; Sun et al., 2023; Zhang et al., 2023). (A-C) Spatial distributions of the mean MHWs depths depending on their vertical structure as defined by Zhang et al. (2023). Climatological mean number of (E) surface, (F) subsurface and (G) mixed MHWs events as defined by Sun et al. (2023) based on GLORYS12V1 reanalysis product. (H) Temporal correlation of temperature anomalies between surface and subsurface MHWs detected using GLORYS12V1 reanalysis product at the global level (Fragkopoulou et al., 2023). Black rectangles were added on (A-G) to spot the Southern Indian Ocean.

emerges: can there be important MHWs at depth, notably below the mixed layer, decoupled from a surface MHW signal?

A global study indicates that the co-occurrence of MHWs at depth and at the surface decreases with depth (Fragkopoulou et al. (2023); Figure 6.4 H). It has been suggested that increased stratification could tend to increase the decoupling between the surface and the subsurface, whereas weakened stratification, for instance due to wind-induced vertical mixing, could lead to an increased vertical extent of MHWs (Juza et al., 2022). This question is all the more relevant for the Southern Ocean, as it was shown that

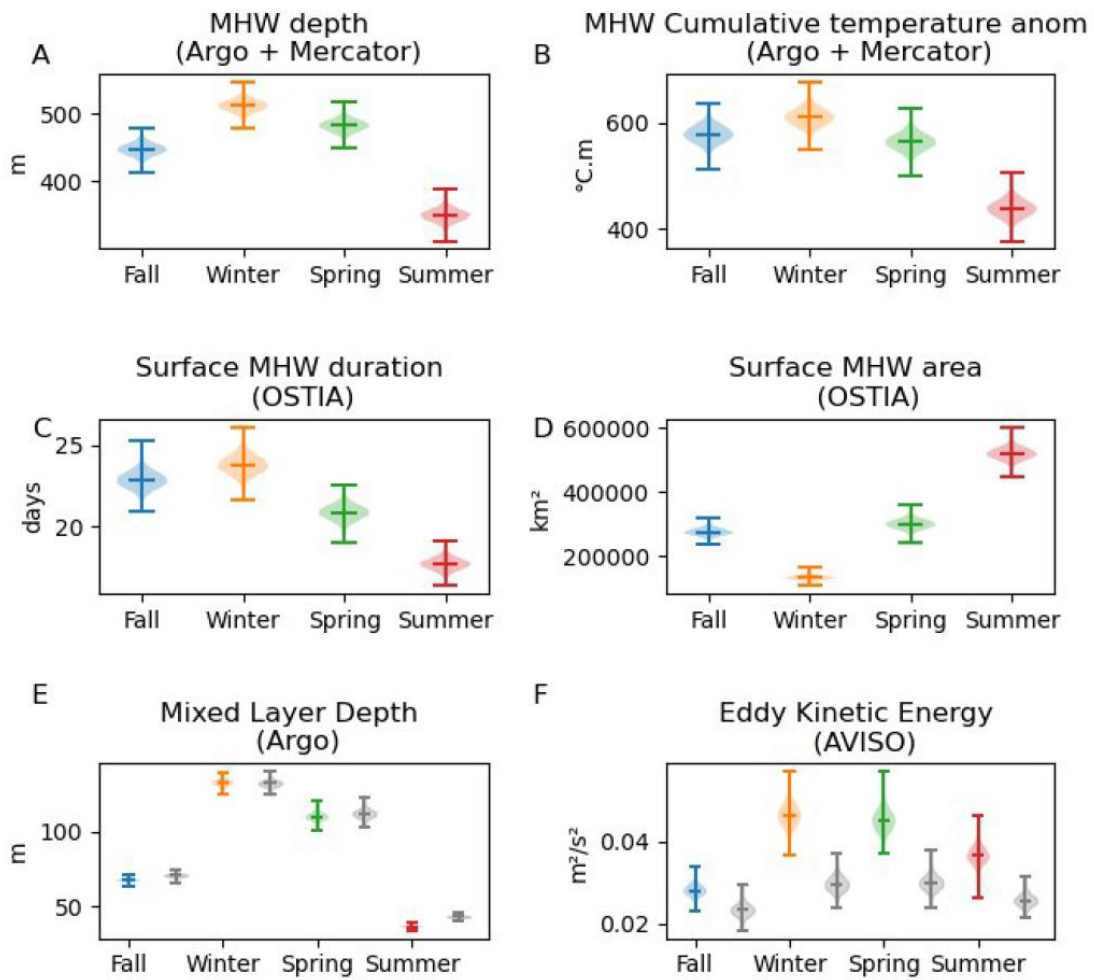


FIGURE 6.5: **Seasonal characteristics of marine heatwaves, detected with OSTIA dataset and sampled by Argo floats** as in Chapter 4. We calculated mean temperature anomaly depth (A) and cumulative temperature anomaly (B) using anomaly profiles comparing Argo profiles (complete down to 900 m at least) to a monthly reference obtained with MERCATOR reanalysis (1993-2019) as in [Elzahaby and Schaeffer \(2019\)](#). The duration (C) and area (D) of the MHW in which the Argo profiles are located, are estimated using OSTIA dataset. Comparison between the mixed layer depth of the Argo profiles in a MHW (color) and outside a MHW (grey) by season (E). Comparison between the mean eddy kinetic energy (compute from AVISO geostrophic velocities) in the location of the profile in MHW (color) and outside a MHW (grey) by season (F). The seasons are : fall (March, April, May), winter (June, July, August), spring (September, October, November) and summer (December, January, February).

climate change can lead to deeper summertime mixed layer but also increased stratification ([Sallée et al., 2021](#)), thus potentially modifying the MHWs vertical structures and the propagation of temperature anomalies.

The vertical extent of MHWs was not investigated in CMIP6 models in this PhD thesis as daily 3D outputs were not yet available. However, daily 3D temperature and salinity

outputs from the CNRM-ESM2-1 model were recently made available to us, through a collaboration with Yerray Santana-Falcon and Roland S  ferian (CNRM/Meteo-France). As a preliminary analysis to explore the vertical structure of MHWs in the Southern Indian Ocean, we apply the MHWs definition from (Hobday et al., 2016) on each of the 75 vertical levels of the r11i1p1f2 member of this model. We also compute the isothermal layer depth (ILD), also called the temperature-mixed layer depth, with the following definition:

$$ILD = z(\theta = \theta_{10m} \pm 0.2^{\circ}C) \quad (6.2)$$

with z , depth and θ , the potential temperature.

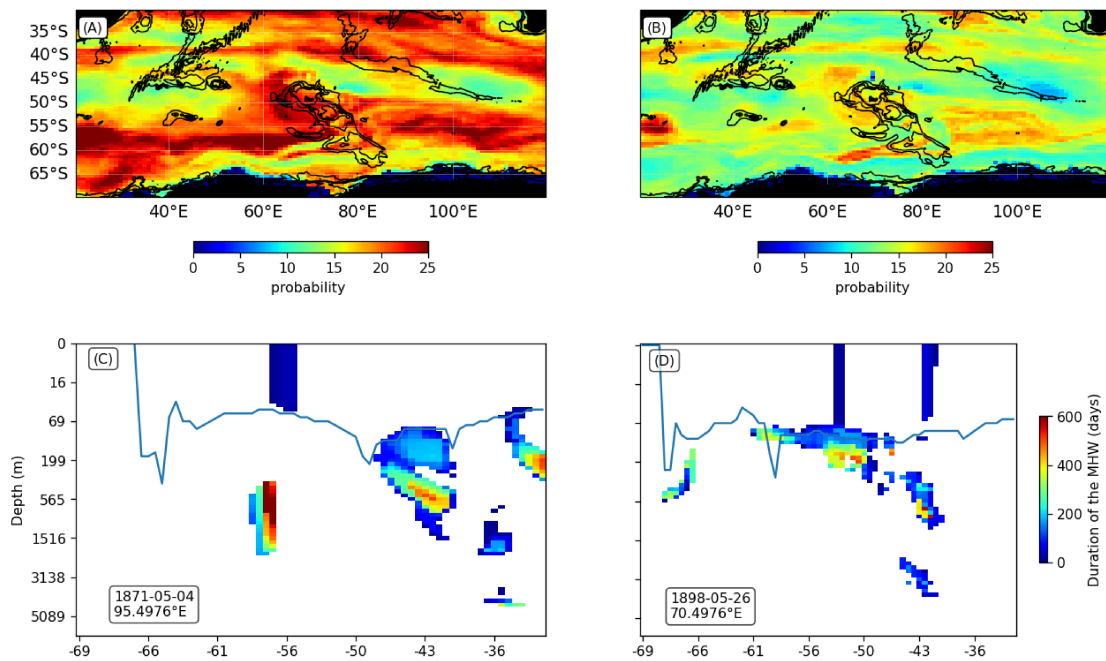


FIGURE 6.6: **Probability of “hidden” marine heatwaves (MHWs) and examples of MHWs detected at depth in CNRM-ESM2-1 under a historical simulation.** Probability (%) of detecting a MHW down to 100 m below the isothermal layer depth (ILD, A) and between 100 and 200 m below the ILD (B) given that no MHW is detected at the surface over 1870-1900 using historical simulations of the r11i1p1f2 member of CNRM-ESM2-1. Examples of MHWs detected at depth and their duration, at 95.5°E on 1871-05-04 (C) and at 70.5°E on 1898-05-28 (D). The ILD is also indicated by the blue line on panels C and D.

We can then define a “hidden MHW” as a MHW detected at depth below the ILD while there is no MHW signal at the surface. It means that the conditions are still extreme at depth but can no longer be observed with satellite observations. Probabilities of detecting a MHW 100 m below the ILD and between 100 and 200 m below the ILD given that no MHW is detected at the surface are shown on Figure 6.6 A and B, and

are estimated respectively at around 19 % ($\pm 4\%$, spatial standard deviation, and up to 32 %) and around 14 % ($\pm 3\%$, and up to 27 %) on average over 1870-1900.

Exploring some examples also reveals the occurrence of MHWs at depth, decoupled from a surface signal, that are modulated by the ILD (Figure 6.6 C and D). These examples also point out the limitations of applying Hobday et al. (2016) definition to different depth layers. On Figure 6.6 C, a deep MHW between around 500 and 1600 m is detected with a duration of around 700 days and with a low intensity (data not shown). Temperature at depth is often less variable than sea surface temperature which makes extreme values more easily reached at depth following Hobday et al. (2016) definition. These slight changes, which may not have ecological implications, can then be detected over long periods, which can lead to an overestimation of extreme events duration at depth.

Under climate change, water masses can be transformed and/or shifted which can then be detected as extreme events decoupled from the surface. Examples on Figure 6.7 show that there is an important projected shift of water masses in the upper 500 m leading to new conditions at these latitudes throughout the water column, and that high mean MHW intensities are found where this change is strong, that is at the surface and in the subsurface but much less below 1000 m.

The definition of MHWs at the surface can already be debated depending on the research question (Amaya et al., 2023b). At depth, this indicator might also integrate other processes at different timescales and intensities. Adjustments to MHW definition may be needed to adapt the methodology at depth (e.g. accounting for a depth layer for the threshold and not just one depth level, applying the statistical detection to density classes instead of z-levels). The definition itself of an extreme event at depth may require further discussion.

To summarize, MHWs impact at depth is a growing concern as numerous recent studies evidence their potentially larger impacts at depth (duration, intensity). Studying the impact of MHWs at depth on other ecologically significant water masses or on the pelagic habitat continuity would be in direction continuation with this PhD thesis. The possibility of “hidden MHWs” in the subsurface or below the mixed layer would mean that only focusing on surface extreme events can lead to an underestimation of the pressure exerted on pelagic ecosystems. Yet the definition of a MHW at depth should

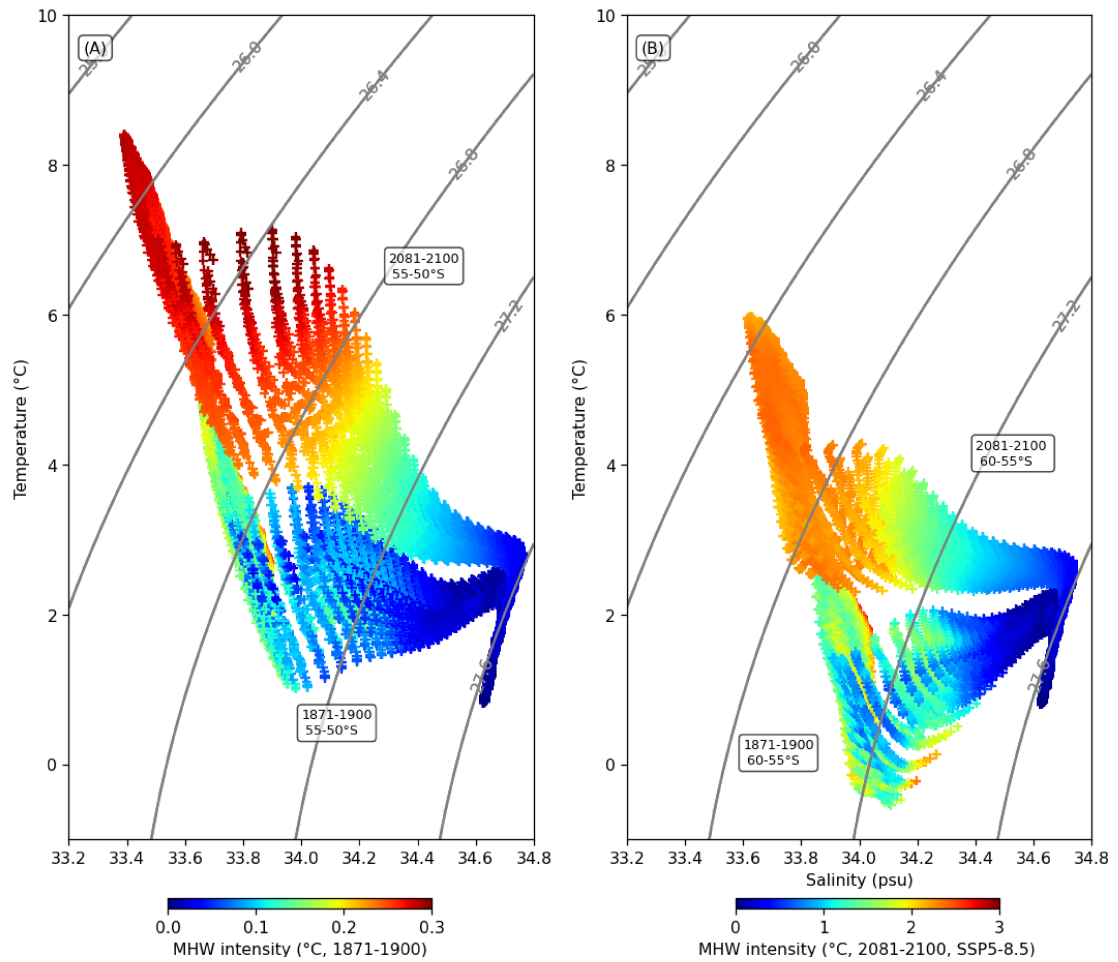


FIGURE 6.7: **Historical and projected MHW intensity on T/S diagrams using CNRM-ESM2-1.** T/S diagrams over 55-50°S (A) and 60-55°S (B) using historical (1870-1900) and SSP5-8.5 (2081-2100) simulations of the r11i1p1f2 member of CNRM-ESM2-1 and colored by mean marine heatwaves intensity. Note that the colorbars for the historical and projected simulations differ.

be treated with caution to focus on ecologically impactful events. Further work to understand and characterize extreme events at depth is therefore necessary and may lead to redefining what are extremes at depth. Further research could focus on addressing the following questions :

- How frequent and long are “hidden MHWs”? Are those characteristics going to change under climate change?
- Does the commonly used definition by Hobday et al., 2016 still holds at depth? How can we define MHWs at depth?

6.2.3 Further characterizing the potential ecological impacts

This PhD thesis unveils the multi-scale dimensions of climate change impacts on physical characteristics of ecological importance for pelagic ecosystems. A next step would be to further investigate the impacts on those ecosystems.

Although Chapters 4 and 5 were first motivated by specific ecological processes, respectively foraging hotspots for top predators and the connectivity for Patagonian toothfish early-life stages, they raise wider potential ecological impacts. On short timescales, (i.e. days to weeks), the alteration of WWs characteristics due to MHWs (Chapter 4) could lead to localized effects on zooplankton communities. For instance [Henschke et al. \(2021\)](#) suggest that southward intrusions of warmer water can foster salps blooms development over the Kerguelen Plateau. The changes caused by extreme events may tend to become average states affecting the whole ecosystems. In the long term (i.e. decades), a drastic change in the Polar Front position could have a significant impact on the composition and spatial distribution of planktonic communities, with bottom-up effects impacting the whole trophic web.

Increased collaborations with ecologists, biologists and biogeochemists would be required to pursue this work, further integrating biotic and biogeochemical changes (e.g. acidification) to assess climate change impacts on pelagic ecosystems. This topic is quite vast, we suggest here two specific research questions that arise from this PhD thesis and that would enable further linkages between climate change impacts on physical and ecological processes :

- Do elephant seals change or adapt their behaviors in response to extreme events?
- Can the local circulation modulate the conditions of development for Patagonian toothfish early-life stages?

6.2.3.1 Do elephant seals change or adapt their behaviors in response to extreme events?

The elephant seals (*Mirounga leonina*) example illustrates how a species relying on the thermohaline structure of the water column for foraging could be impacted by MHWs. In Chapter 4, we observe that using elephant seals data to characterize subsurface MHWs

tend to produce a bias toward shallower and less intense MHWs east of the Kerguelen Plateau (80°-100°E; 55°-45°S; Figure 5 on [Azarian et al. \(2024\)](#)). This area is a foraging zone for elephant seals whose behavior is related to mesoscale activity near the Polar Front ([Bailleul et al., 2010](#); [Dragon et al., 2010](#); [Cotté et al., 2015](#)), where mesopelagic prey are found to be more abundant ([Baudena et al., 2021](#)). Elephant seals were found to target cyclonic eddies or the edges of anticyclonic structures to capture prey ([Dragon et al., 2010](#)). This relationship was shown to be more important during the post-moulting period (January-August), which is probably due to the seasonal change in the prey field associated with the mesoscale eddies ([Cotté et al., 2015](#)). The observed bias of subsurface MHWs characteristics with MEOP-CTD datasets ([Azarian et al., 2024](#)) is consistent with MHWs being strongly associated with anticyclonic eddies and with elephant seals profiles being mostly collected in autumn. Although further ecological analyses would be needed to better understand elephant seals' behavior toward extreme events, the results presented in [Azarian et al. \(2024\)](#) suggest that elephant seals may tend to avoid more intense and deeper MHWs. Elephant seals may also dive deeper when encountering MHWs in order to access their prey. Female elephant seals were found to dive deeper and forage less efficiently when the temperature at 200 m was warmer, indicating a lower accessibility of prey under warmer conditions with direct consequences on their foraging efficiency ([Guinet et al., 2014](#)).

Further analyses would be needed to better determine elephant seals response to MHWs, both in terms of diving depth and foraging areas. An analysis of the trajectories could be conducted to identify how they may avoid MHWs (illustrative examples on Figure 6.8). It would be interesting to distinguish responses depending on the sex and size of the individuals as they have different foraging strategies ([Guinet et al., 2014](#); [Hindell et al., 2021](#)). A hypothesis would be that smaller females may have more energetic constraints and thus would tend to avoid MHWs more often than bigger females. Although elephant seals may be less sensitive to ocean warming and to the shift of WWs in the long term than king penguins by foraging further south ([Mestre et al., 2020](#)), the projected increase in MHWs occurrence and intensity could potentially lead to a shift in their foraging strategies and mean body conditions.

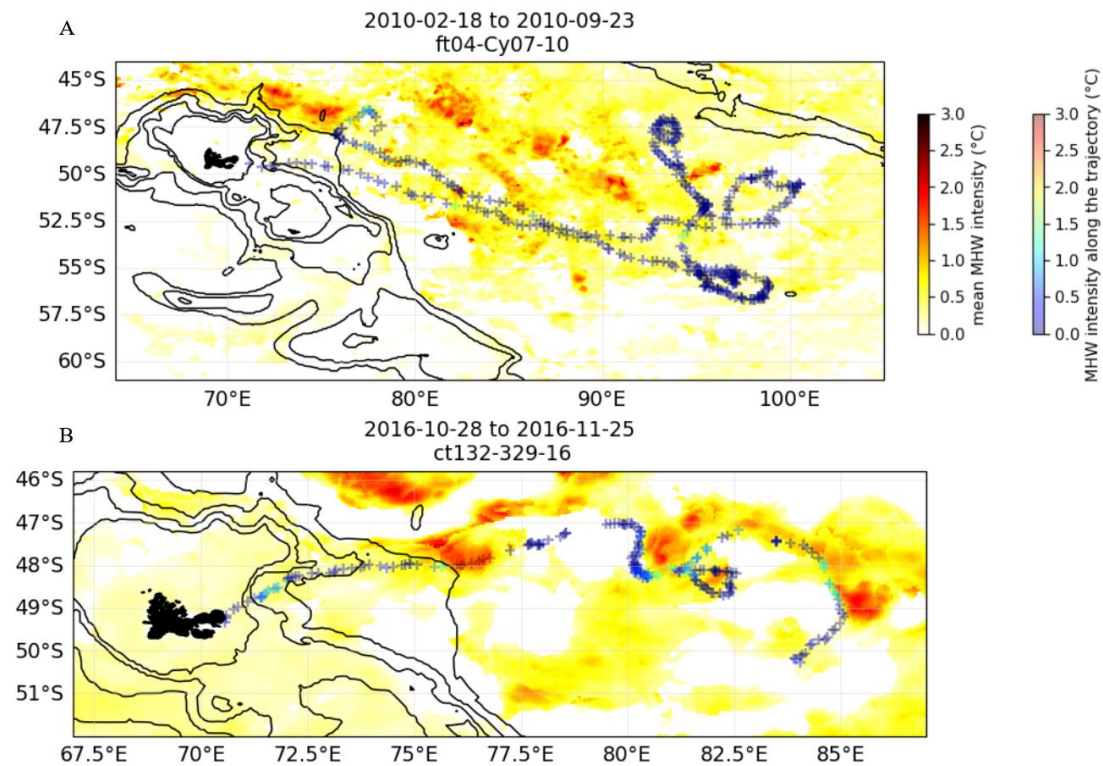


FIGURE 6.8: **Examples of elephant seals trajectory** (MEOP dataset, tag name indicated in subtitle) **overlapped with the mean MHW intensity over the period of the trajectory** (MHW detected using OSTIA dataset) in February to September 2010 (A) and October to November 2016 (B). The MHW intensity at the time and location of each elephant seal position is also indicated

6.2.3.2 Can the local circulation modulate the conditions of development for Patagonian toothfish early-life stages?

Chapter 5 focuses on the ocean circulation over and around the Kerguelen Plateau as a potential driver of Patagonian toothfish recruitment variability. In addition to transport, the biotic and abiotic conditions of development along transport pathways might also be key for successful recruitment (Bashevkin et al., 2020). As perspectives, we consider here three parameters that can be important in describing suitable conditions for recruitment: the phytoplankton bloom, the mesopelagic prey/predator field and temperature (Figure 6.9).

Could the variability of the circulation over the Kerguelen Plateau also modulate the characteristics (e.g. strength, phenology) of the phytoplankton bloom?

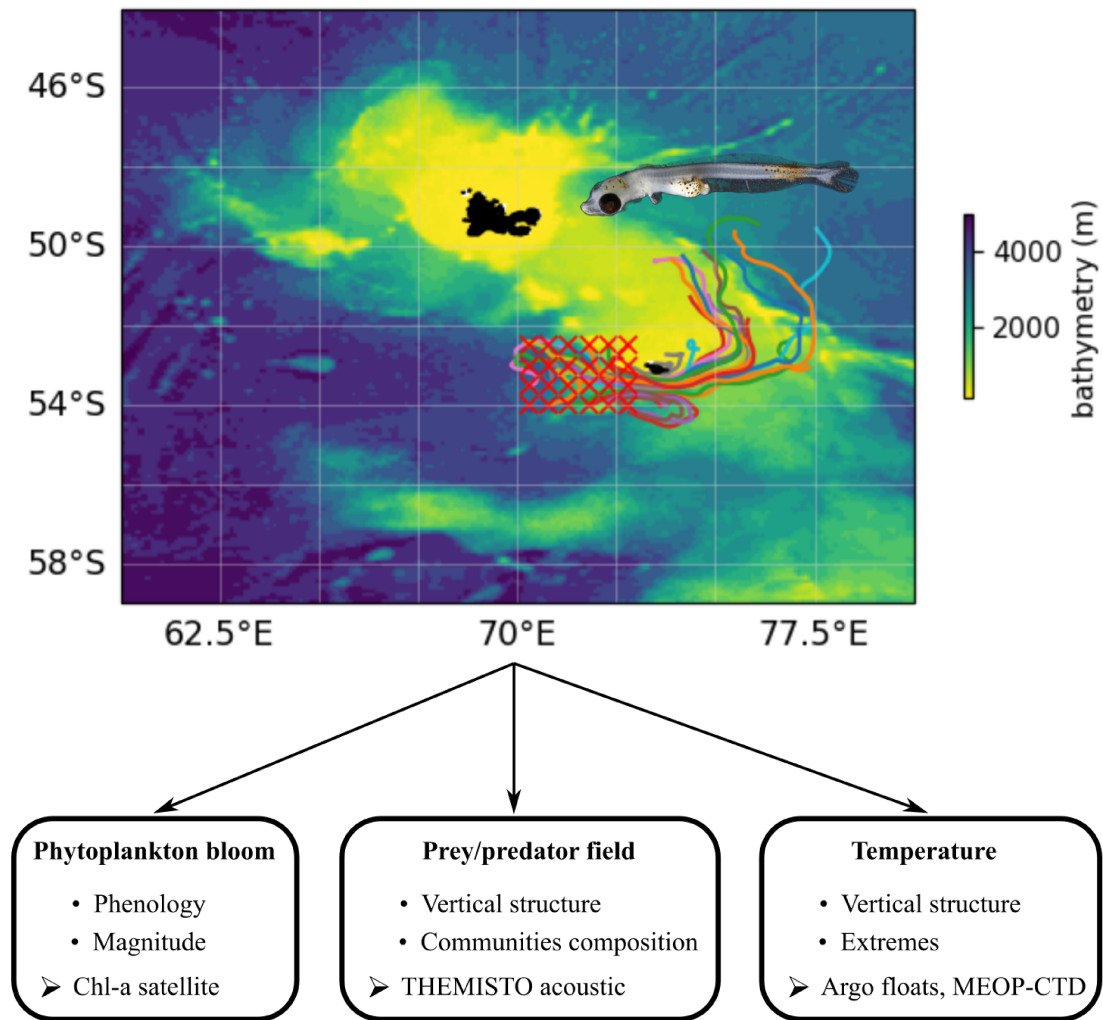


FIGURE 6.9: Schematic illustrating potential research leads associated with investigating the conditions of development for Patagonian toothfish larvae over the Kerguelen Plateau. The bathymetry product is the one used for Mercator reanalysis and distributed by CMEMS. Examples of 3-month forward trajectories from the red crosses starting on 2012-07-31 (using AVISO geostrophic velocities) are shown (colored lines). The picture of a 26 days post-hatching Patagonian toothfish larvae is from Mujica et al. (2016).

It has been hypothesised that Patagonian toothfish spawning season might be synchronised with the phytoplankton bloom over the Plateau to provide sufficient food for the larval stage (Koubbi et al., 2009; Collins et al., 2010). There are two blooms observed in the Kerguelen area: one east of the Kerguelen Plateau, with an intense plume that extends offshore, and one earlier and less intense that occurs over the Plateau itself (Blain et al., 2001; Mongin et al., 2008; Maraldi et al., 2009). Meridional transport over the shelf between Heard and Kerguelen islands could contribute to the northward advection of iron-rich waters from Heard (van Beek et al., 2008). Associated with enhanced vertical mixing bringing up iron to the mixed layer due to strong internal tides, this

could support the occurrence of the bloom over the Plateau (Blain et al., 2007; Park et al., 2008a). Interannual variations in phytoplankton spatial patterns have already been observed in relation to changes in the dominant water mass around Kerguelen islands (Ivanchenko, 1993) and the position of the Polar Front has also been associated with the spatial distribution of chlorophyll concentration over the Plateau (Charrassin et al., 2004; Park et al., 2008b; van Wijk et al., 2010).

Chapter 5 points out the variability of the flow along the eastern slope of the Kerguelen Plateau. As a complementary analysis to further investigate the spatial variability of the retentive patterns east of Kerguelen, we conduct an Empirical Orthogonal Function (EOF) analysis¹ on the “distance metric” introduced in Chapter 5, which is high when the retention is low. Although the variance explained by the first mode of variability is around 13.8%, the first mode of variability shows a contrast between retention along the eastern slope and at the core of the meander (between 73°E and 76°E at around 49°S; Figure 6.10 A). This first mode of variability is also positively correlated to the probability of retention east of Kerguelen as defined in Chapter 5 (Figure 6.10 C), further supporting that low retention east of Kerguelen is associated with a stronger flow along the Plateau eastern slope. When computing summer composites of satellite-observed chlorophyll-a concentrations depending on the level of retention east of Kerguelen, we observe higher summer chlorophyll-a concentrations along the eastern slope and at the core of the meander during low retention years (Figure 6.11). This suggests that the dynamics during low retention years (i.e. strong eastern slope flow and higher retention at the meander core) may shape the bloom spatial patterns.

Further study would be required to complete and confirm these preliminary analyses and to also investigate potential impacts of the local dynamics variability on the phenology of the bloom. Understanding these processes over the past variability could help reflect on the risk of future mismatch between the toothfish spawning season and the bloom occurrence or between recruitment areas and the bloom spatial patterns.

Could climate change impact Patagonian toothfish early-life stages prey/predator field?

¹An EOF analysis is a decomposition of the dataset in terms of orthogonal basis functions which are determined from the data. It aims at simplifying spatial-temporal data through transforming it to spatial patterns of variability (EOFs) and temporal projections of these patterns (principal components or PCs). Here EOFs and PCs are obtained by using the transform method of the `pea` object (python function `sklearn.decomposition.PCA()`).

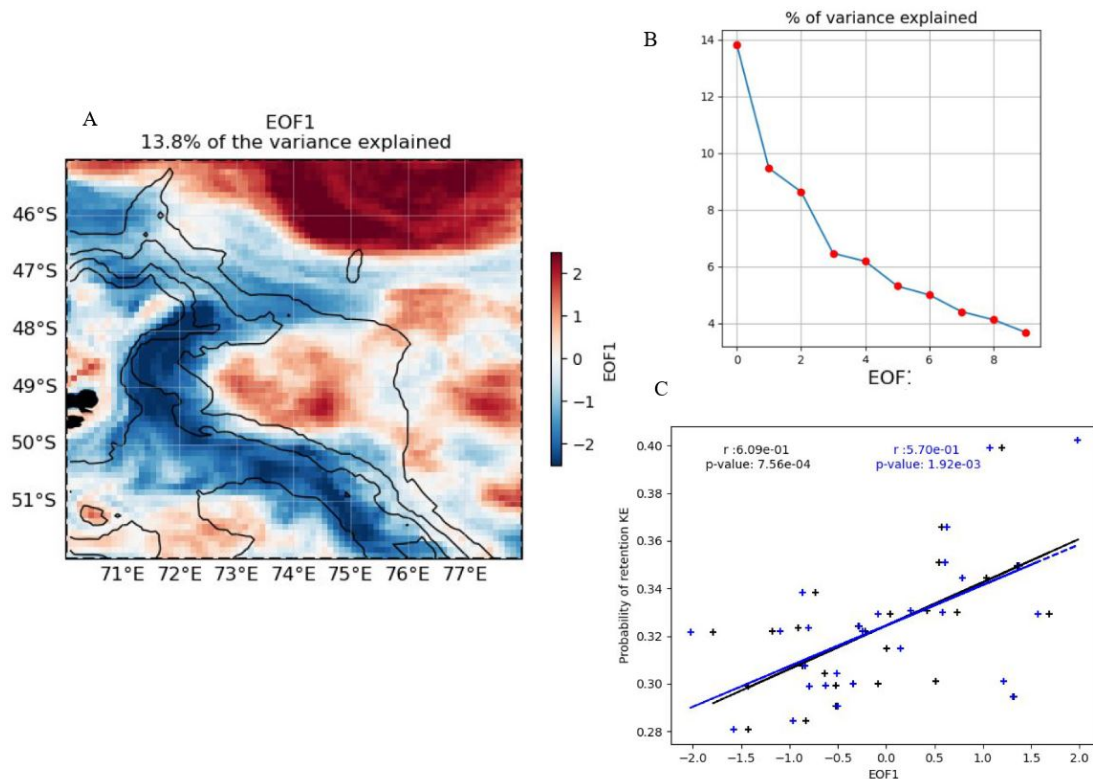


FIGURE 6.10: **Empirical Orthogonal Function (EOF) analysis on the “distance metric” as defined in Chapter 5.** (A) EOF1 spatial patterns (i.e. first mode of variability). (B) Percentage of variance explained by each EOF. (C) Correlation between EOF1 values and the probability of retention east of Kerguelen (KE) as defined in Chapter 5, using either an 0.1° grid (blue) or a 0.25° grid (black).

Starvation and predation are generally the main causes of mortality for fish larvae (Koubbi et al., 2009). Little is known about the ecology of Patagonian toothfish early-life stages, but eggs and larvae are part of the planktonic community and may be influenced by the composition of these communities through predatory pressure and food availability for the larvae. Notothenioids larvae have generally been found to be carnivorous, feeding importantly on tintinnids, small copepods or euphausiid early-life stages (Koubbi et al., 2009).

To address that question, acoustic data from the “Toward Hydroacoustics and Ecology of Mid-trophic levels in Indian and Southern Ocean” (THEMISTO) program could be useful. The interannual variability of the mesopelagic communities and their vertical structure over the Plateau could be investigated.

Could temperature changes affect larval development?

Chapter 5 illustrates the different origins of water parcels arriving east of Kerguelen

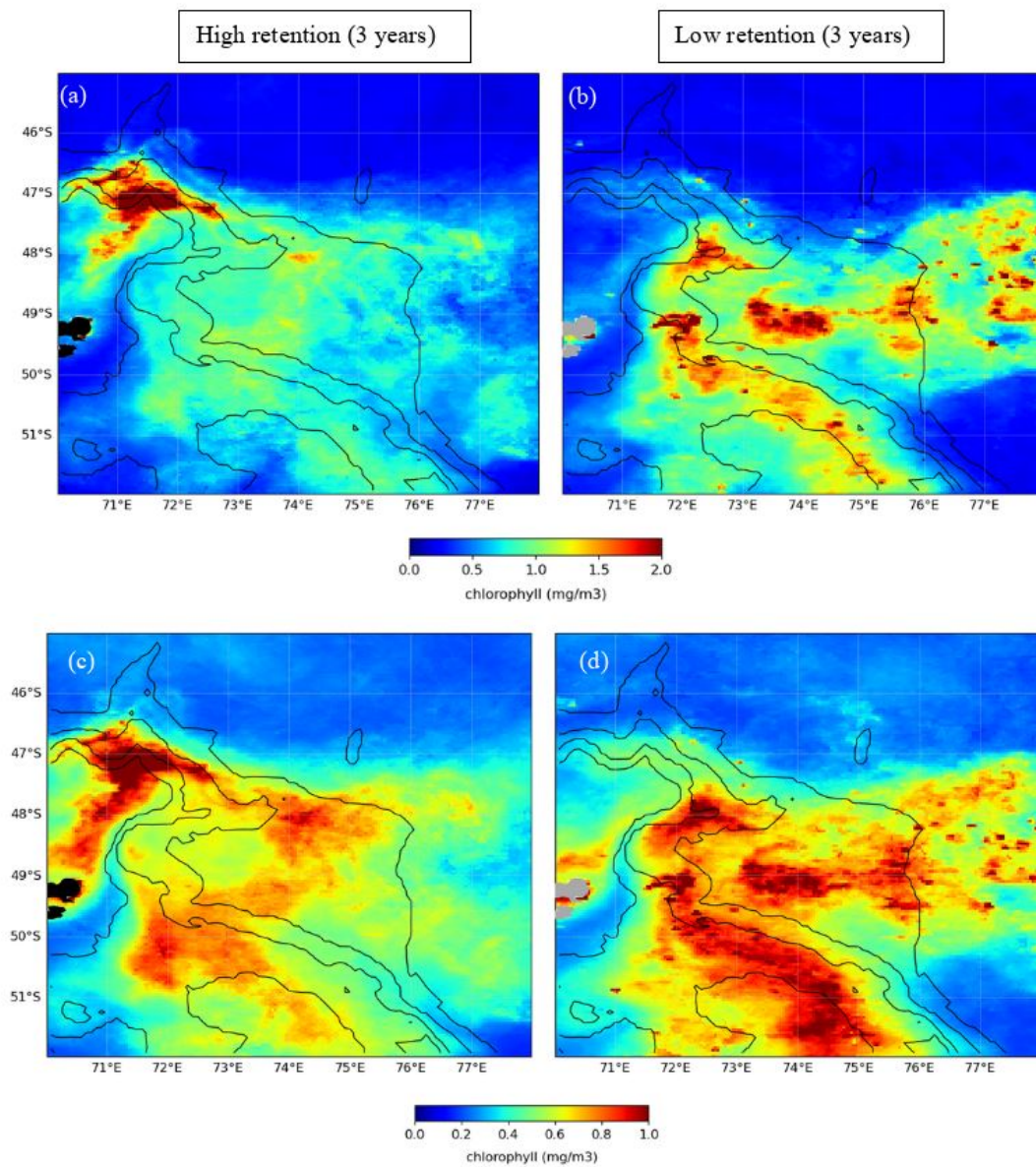


FIGURE 6.11: **Summer chlorophyll-a composites depending on the level of connectivity between the west of Heard and the east of Kerguelen.** December (a, b) and November-December-January (c, d) satellite chlorophyll-a composites (using the satellite chlorophyll product presented in section 2.1.1.3) over the years of high (a, c) and low (b, d) connectivity between the west of Heard and the east of Kerguelen as defined in Chapter 5.

which may thus experience different temperature conditions along the way and travel through areas that may be impacted differently by climate change. Temperature could influence early-life stages development through potential impacts on embryonic duration, egg survival, but also size at hatching, developmental rate or even pelagic larval duration and survival since higher temperature can induce higher metabolic rates and thus higher energetic demands (Rombough, 1997; Pankhurst and Munday, 2011). Combining

information on transport pathways, through Lagrangian trajectories, and the Dynamic Energy Budget (DEB) theory, which is a metabolic theory at the individual level (Kooijman, 2000), could provide further insights on the potential impacts of climate change on Patagonian toothfish recruitment and on the differences of climate change exposure depending on the spawning hotspots. We can already note a directional mismatch between climate velocities directed south (Chapter 3) and a short-term potential increase of the southwest-northeast connectivity over the Kerguelen Plateau (Chapter 5) which could exacerbate climate change risks on pelagic planktonic stages (García Molinos et al., 2017). In addition to temperature, it might be relevant to consider, if possible, the combined effect with ocean acidification on larval development (Pistevos et al., 2017).

More generally, the overview provided by this PhD thesis on climate change threats for pelagic ecosystems covers projected changes of state variables such as temperature (Chapter 3), but also projected changes in dynamic features such as water masses (Chapter 4) and transport pathways (Chapter 5). The dynamic of the ocean is often implicitly accounted for in the changes studied through an Eulerian approach (studying a spatially fixed point) as advection can play a key role in modulating heat transport and distribution. However, adopting a Lagrangian approach to study climate change impacts can be useful for pelagic ecosystems, especially for planktonic phases subjected to currents that may flow over differently impacted areas, thus integrating impacts along the way (Figure 6.12). Such a Lagrangian approach also has the benefits to be associated with an ecological process and hypothesis on the mechanism of impact (e.g. larval development).

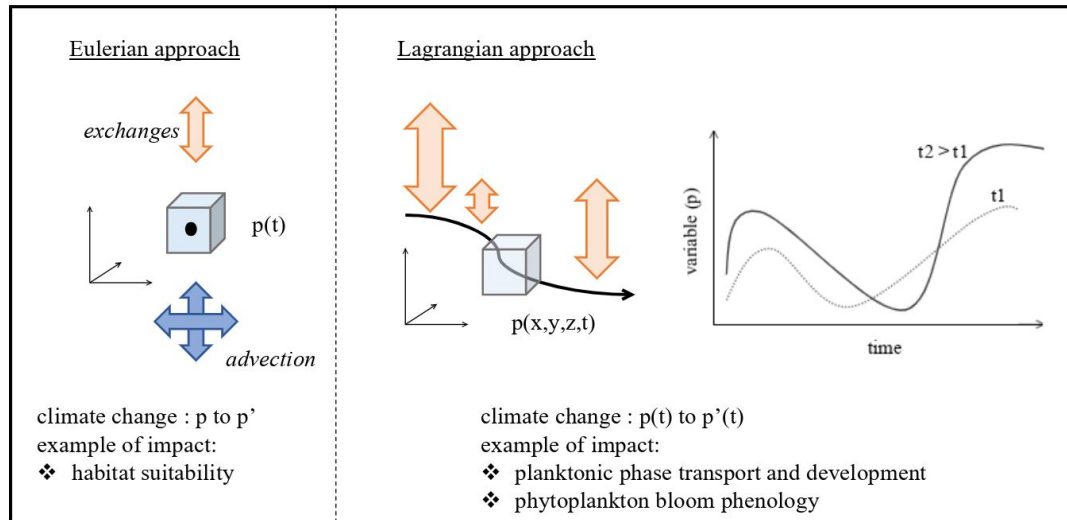


FIGURE 6.12: Schematic illustrating the differences between an Eulerian and a Lagrangian approach of climate change impacts on physical oceanographic features or variables leading to different types of ecological impacts. In the Eulerian approach, climate change signal at a given location is mostly driven by local exchanges (e.g. heat fluxes) and advective processes that modifies a state variable (e.g. from p to p'). In the Lagrangian approach, a water parcel can travel through areas undergoing different changes, the focus is then on the evolution of the variable as a function of space and time (from $p(x,y,z,t)$ to $p'(x,y,z,t)$) with integrated impacts along transport pathways.

Box. 6.2.1: Recent extremes

We note that during this PhD thesis, because of the multiple datasets used and the timing of this work, we focused our analyses up to 2019/2020. Recent years have been particularly warm, with 2023 the warmest year on record (WMO, 2024). Intense MHWs occurred in the Southern Indian Ocean in autumn-winter 2023 (Figure 6.13), with potential impacts on pelagic ecosystems that would be worth investigating. As time goes by, extreme events should become more intense and frequent (Chapter 3; Oliver et al. (2018)), with potentially unprecedented changes, which can also help refine our understanding of the physical processes at play and of MHWs impacts on pelagic ecosystems.

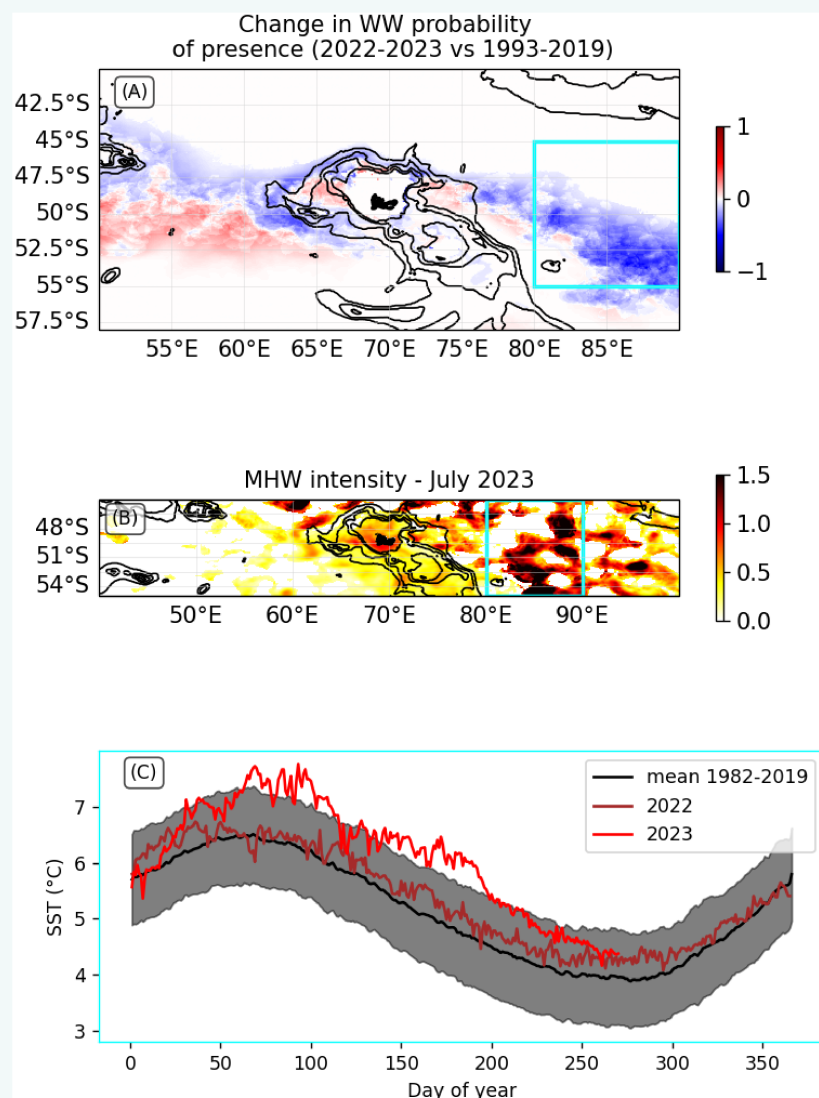


FIGURE 6.13: **Complementary analyses on recent years (2022-2023).** (A) Change in winter water probability of presence in 2022/2023 compared to 1993-2019 using MERCATOR reanalysis product. (B) Mean MHW intensity (above the 90th percentile) over July 2023 using OSTIA dataset (baseline over 1982-2019). (C) Mean sea surface temperature (SST) over 80°-90°E 55-45°S (cyan rectangle on Panels A and B) for each day of the year averaged over 1982-2019 (black line) as well as in 2022 (brown line) and 2023 (red line) using OSTIA dataset.

6.3 Societal perspectives

A main goal of this thesis is to reflect on the knowledge needed to guide conservation and fisheries management in the Southern Indian Ocean. Consequently, those results have also been communicated to policy-makers, notably in the context of the Commission for the Conservation of Antarctic Marine Living Resources (CCAMLR) working groups and workshops, as policy briefs. In particular, the CCAMLR workshop on climate change organized in September 2023 reflects this increasing interest to improve the integration of scientific knowledge on climate change potential impacts throughout CCAMLR's work program. CCAMLR is also ahead of most Regional Seas Conventions or Regional Fisheries Management Organizations regarding climate change considerations (Rayfuse, 2018; Wendebourg, 2020; Sumby et al., 2021) and could be a leading example for those other organizations. Climate change awareness has increased but concrete adaptation actions must now be designed, planned and implemented.

The two following subsections aim at reflecting on this link between science and policy-makers to lead to action through :

- a case study on the management implications of climate change on the Patagonian toothfish fishery (Section 6.3.1) ;
- further reflections on whether scientific uncertainty is a real barrier to the operational consideration of climate change in the management of marine biodiversity (Section 6.3.2).

6.3.1 Climate change management implications on the Patagonian toothfish fishery in the Southern Indian Ocean

6.3.1.1 Climate change: a rising issue on the agenda of intergovernmental fisheries management

The growing awareness, within Regional Fisheries Management Organisations, that climate change can be an additional pressure on fish stocks has led to this topic being increasingly put on the agenda. Although very little action has emerged from these initiatives so far (Sumby et al., 2021), concrete direct impacts of climate change on fisheries are now forcing policy-makers to consider new management strategies.

In the Southern Indian Ocean, the Patagonian toothfish (*Dissostichus eleginoides*) fishery represents an important economic interest, both at the national and international level (Chapter 1 Section 1.1.4.2). Growing concerns have recently been voiced at the CCAMLR concerning the sustainability of this fishery, notably in a context of environmental changes.

The work summarized here has been conducted in collaboration with the office for International and European affairs of the French Ministry of Agriculture, in charge of the Southern Indian Ocean Fisheries Agreement (SIOFA), part of the delegation of the CCAMLR and with an advisory role to the French Southern Lands for fisheries management. This work was also fueled by exchanges with biologists from the French National Museum of Natural History. During this work (15 days over May to July 2023), the aim was to:

- Provide a short review of the knowledge on Patagonian toothfish ecology and connectivity ;
- Synthetize and compare the Patagonian toothfish fishery management in SIOFA, the French Southern Lands and CCAMLR ;
- Discuss the potential impacts of climate change on the stock and whether the current management framework is relevant or could be (easily) adapted to face those new challenges.

Three documents were provided to the Ministry of Agriculture following this three-step work and can be find in Appendix D.

6.3.1.2 Leads for climate-adaptive management actions

The current fisheries management is schematically based on the following steps (Figure 6.14, Appendix D). First, a decision rule that encapsulates the management objectives is defined and agreed upon. In the CCAMLR, the decision rule for the Patagonian toothfish fishery is made of three parts:

- *“Establish the constant level of catch, such that the probability of the spawning biomass dropping below 20% of its pre-exploitation median level (B_0) over a 35-year harvesting period is 10% ;*

- *Establish the constant level of catch, such that the median toothfish escapement in the spawning biomass over a 35-year period is 50% of the pre-exploitation median level ;*
- *Select the lower of the two catches as the level for the toothfish catch limit”.*

The decision rule in the French Southern Lands is similar, except that in the second part, the threshold is set to 60% of the pre-exploitation median level of spawning biomass to follow a precautionary approach.

Second, scientists working within the CCAMLR framework or through a Convention with the French Southern Lands (e.g. National Museum of Natural History) run a stock assessment model (e.g. the population dynamic model CASAL 2 (C++ Algorithmic Stock Assessment Laboratory; Bull (2012))). This model is an age-class model that is statistically parameterized based on historical data (e.g. mark-recapture data, catch per unit effort, otoliths) and then projected over 35 years, investigating different Total Allowable Catches (TAC) options. Scientists then provide recommendations to policy-makers on a TAC that would respect the decision rule. Other recommendations may include best practices to limit the fisheries impact on different parts of the ecosystem. This stock assessment phase is done annually at CCAMLR and in the French Southern Lands.

Third, policy-makers establish conservation measures, including the final decision on the TAC, that will then be distributed through quotas to the different fishing vessels, but also measures on the type of fishing gears authorized or the fishing season for instance.

From the short scientific review on the Patagonian toothfish (Appendix D), and notably due to the bathymetric constraints in its life cycle, it appears unlikely that the Patagonian toothfish stocks would migrate far outside the Kerguelen Plateau area. However, there is already an observed decrease in the reproductive biomass in all managed Patagonian toothfish stocks (Appendix D). This decrease in biomass has mostly been associated with low recruitment years. However, the causes of this decline, to our knowledge, have not been clearly identified.

Whether the current decline is a result of environmental change or not, climate change could contribute to it and challenges many of the conventional assumptions that scientists rely on to assess stock status and estimate the TAC. In particular, the current

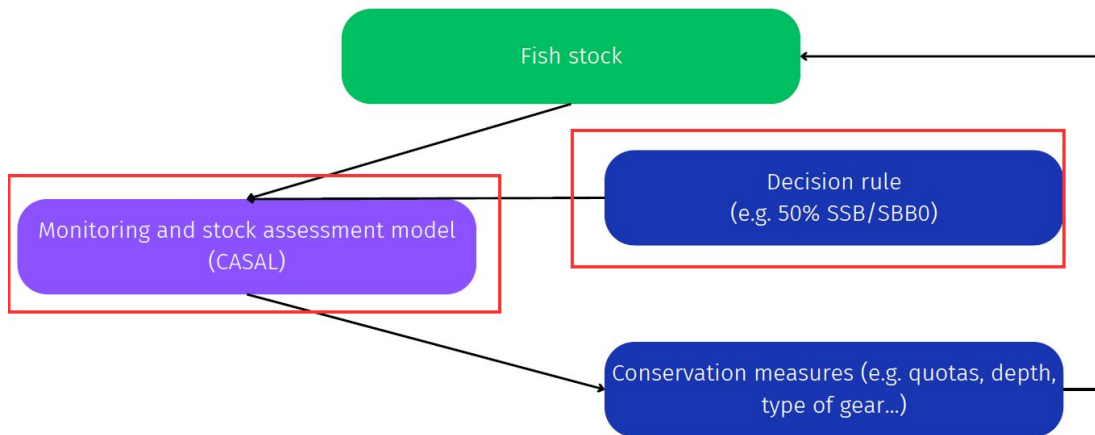


FIGURE 6.14: **Schematic of the key steps in Patagonian toothfish management.** The management object is the fish stock (in green). Scientists are in charge of conducting scientific assessment of the fish stocks (in purple) which is based on the adopted decision rule and will guide policy-makers in adopting future conservation measures (policy-makers role in blue). The scientific assessment and the decision rule are framed in red as they are major tools to integrate climate change impacts and to ensure sustainability in fisheries management.

fishery management is mostly based on a static view of the stock's characteristics, both in the decision rule and in the stock assessment model, and may not be adapted to a stock with changing properties over time. For instance, the decision rule is based on an estimate of the pre-exploitation spawning biomass, which corresponds to the equilibrium state of the stock without fishing, which may no longer be relevant. The stock assessment model also assumes fixed metabolic rates over time, with no relations to environmental variables. In addition, in this model, all past recruitment intensity indices are considered equally plausible in the future. Consequently, both the recent decline and the past high levels of recruitment are used to project the future population dynamic. This methodology could overestimate the future stock biomass if the recent decline actually marks a regime shift in the population.

Tools already exist that could contribute to a climate-adaptive management (e.g. the precautionary principle, ecosystem-based management), but transformative changes in management practices are also needed. Throughout this work, three potential lines of discussion have been identified:

- **Enhancing stocks resilience** : Maximize the stock reproductive capacity through the protection of key areas (e.g. spawning hotspots). Given that Patagonian toothfish reproductive capacity varies with size and age, it could also be beneficial to

determine the fishing selectivity pattern that would maximize the stock reproductive capacity. From this information, managers could then implement spatial and temporal limitations to adapt fishing effort accordingly.

- **Developing a stronger risk management approach** : Develop a scenario approach to better include climate risk in TAC estimations. Projections of stock biomass could be done under multiple recruitment scenarios before determining the TAC to better account for the uncertainty associated with recruitment and the models. Management responses could be anticipated, according to different scenarios : for instance, develop TAC adaptation measures in case of a major recruitment decline event.
- **Adapting the current methodology** : More structural questions need to be addressed: is the current management objective still robust in the context of climate change? Is focusing on the spawning biomass as a management target, when recruitment might be impacted by climate change regardless of reproductive capacity, enough to ensure the sustainability of the fisheries? Could additional indicators be necessary to more adequately follow the stock status (e.g. recruitment index)?

Although this case study on the Patagonian toothfish in the Southern Indian Ocean is quite specific, some of the identified implications of climate change for fisheries management can be generalized. In particular, the recruitment phase is a crucial step in the stock dynamic, which may be impacted by climate change and over which information are often less available. A decline in recruitment has been observed for many stocks: it is estimated that the average recruitment capacity of stocks worldwide has declined by about 3% of the historical maximum per decade ([Britten et al., 2016](#)). The issue of how models are used to monitor stock status and to validate fisheries sustainability is also not specific to toothfish fisheries management. In 2015, ecosystemic or environmental factors were included in the management of only about 2% of the world's fishing stocks ([Skern-Mauritzen et al., 2016](#)).

Around a third of the world fisheries are still not sustainably managed ([FAO, 2022](#)) and, globally, substantial challenges remain regarding wider ecological impacts and socio-economic issues ([Cochrane, 2021](#)). However, climate change should not be considered as just an additional topic to account for. Since climate change may disturb how ecosystems

are distributed and are functioning, it is a necessary dimension to integrate in the general efforts to make fisheries more sustainable.

6.3.2 Are scientific uncertainties a real barrier to the operational consideration of climate change in the management of marine biodiversity?

Context

The following section presents a structured summary of the reflections I have developed while working on the question of how to account for climate change in the management of marine biodiversity. It draws on my professional and personal reading as well as my experiences at the science-society interface. This is not an exhaustive essay on the subject, but rather some thoughts on particular obstacles to the operationalisation of climate change awareness, starting from the question of scientific uncertainty. I feel it is important to share these reflections, particularly in relation to the nature and role of scientific expertise. Although far from revolutionary, I hope that this sharing of ideas will raise the reader's interest and foster further investigation on these issues.

Climate change is a major threat to marine biodiversity in addition to other anthropogenic pressures. Yet today, climate change is rarely considered operationally as indicated in Chapter 1. The aim of the present discussion is to reflect on what is missing to operationalise climate change awareness and to investigate the validity of the common remarks addressed to scientists regarding climate change impacts uncertainty. The question is thus: are scientific uncertainties a real barrier to the operational consideration of climate change in the management of marine biodiversity?

First, as presented in Chapter 1, there are still major knowledge gaps limiting our understanding of the magnitude and timescales of the coming climate change impacts on marine ecosystems. The scientific expertise needed to inform policy-makers is changing and requires policy-makers' adaptation to a different scientific methodology. This scientific paradigm shift may be a stronger obstacle to operationalisation than the scientific uncertainties themselves. Second, scientific uncertainties should not lead to inaction as adaptation options already exist, although they might require a methodological shift,

this time, from management institutions. Finally, climate change calls into question not only current biodiversity management practices but also the underlying principles on which they are based. In this discussion, we consider both conservation and fisheries management, though acknowledging that each field has its specificities, also taking the perspective of data-limited and/or remote areas such as the Southern Indian Ocean (20°-120°E 70°-30°S).

A major methodological shift: scientists are no fortune tellers

There are still major uncertainties regarding climate change impacts on ecosystems at scales relevant for management. In this PhD thesis, we aimed at addressing this gap by delving into the complexity of the physical changes that could impact ecological processes. By doing so, our end-goal was to provide relevant information for policy-makers to adapt conservation and fisheries management in the Southern Indian Ocean. When presenting or discussing these results in a policy-oriented context, frequent questions mostly focused on the levels of uncertainty around those results. Those inquiries, while entirely valid, reflect a particular way of thinking, that might be influenced by the scientific advice commonly provided to these institutions.

Both conservation and fisheries management are based on a scientific understanding of the environment. Biodiversity management in the Southern Indian Ocean both at the national level within the French Southern Lands or at the international level within the Commission for the Conservation of Antarctic Marine Living Resources (CCMALT), for instance, strongly relies on scientific advice through diverse scientific committees, working groups and workshops. This maintained interaction between scientists and policy-makers has allowed the transmission of some scientific concepts such as population dynamics or the ecosystem approach. The scientific advice is based on sustained monitoring efforts and the current understanding of ecosystemic processes. In the Southern Indian Ocean, scientific advice has become a key element for decision-making. Managers strongly relies on ecoregionalisation studies and scientific expertise to identify conservation priorities. For fisheries management, scientists are running population dynamic models to estimate and advise on the total allowable catch (TAC) which establishes maximum fishing limits. Managers adopt the final decision but they mostly follow scientific advice, or at least, use it as a reference for their decision.

The science developed to provide this expertise differs from climate sciences on one main aspect: the former is based on studying what exists and what can be more or less directly observed, the latter involves studying projections and working on hypotheses that can only be verified as time passes. Or not. Because climate scientists also investigate different scenarios and thus different possible futures, based on our understanding of the Earth system, when only one will actually occur. This represents an important scientific methodological shift with important changes in the acceptable level of uncertainty.

The scientific expertise on such an interdisciplinary topic (climate change impacts on marine ecosystems) is quite vast and can be directed to different policy-makers at different scales as climate and biodiversity issues are often addressed separately. The scale of the scientific knowledge developed is generally adapted to the goal: alerting on a global threat can rely on a large-scale approach, while guiding management at the regional scale might require more tailored advice at finer scales, which can also introduce further uncertainties. The [FISH-MIP](#) exercise ([Tittensor et al., 2018](#)) is a striking example of the international scientific effort, since 2013, to link climate science and biodiversity management, as it aims at informing the projected state of marine biomass, notably for fisheries. However, it is mostly used to investigate large-scale trends and may not be adapted to be directly included in regional management policies. There is certainly a crucial need for science that may guide policy-makers in operationalising their climate change awareness, if such awareness is already present.

Dealing with uncertainties also means identifying the knowledge that requires high confidence. For many physical changes such as ocean warming, there is a growing consensus on the direction of change, which may be more important than estimating very precisely the magnitude of changes ([IUCN, 2016b](#)). Pinpointing current knowledge gaps and uncertainties should not mask the abundant scientific literature demonstrating the threat posed by climate change on marine biodiversity and the urgency of mitigating and adapting to climate change.

Although there are still knowledge gaps on climate change impacts on ecosystems, the methodological shift that goes with climate science expertise, in contrast with previous scientific expertise in those management institutions, notably relative to the acceptable level of uncertainty, could be a much stronger obstacle to climate adaptation in biodiversity management practices, than scientific uncertainties themselves.

There is no scientific excuse for inaction

Scientists' role is not only to advise but also to alert on burning issues. The alert on climate change impact on marine biodiversity and the need to account for it in marine biodiversity management has been ongoing these last decades. A frequent justification to delay climate change consideration in biodiversity management has been the request for further research to narrow down the great uncertainties regarding the concrete impacts of climate change on marine ecosystems. However, this argument neglects the fact that marine biodiversity is already being managed under high uncertainty. In the case of the Patagonian toothfish fishery, recruitment (i.e. juvenile entry in the stock), which is essential for the sustainability of the stock, is highly variable and the causes of this variability remain uncertain (Laptikhovsky and Brickle, 2005; Collins et al., 2007; Belchier and Collins, 2008; Collins et al., 2010). Many unknowns regarding this fish reproduction ecology and early-life stages also remain, due to limited access to *in situ* observations. In addition, the current Patagonian toothfish stock assessment model is based on several assumptions, not explicitly accounting for environmental variability, but is still used to directly provide precise numbers (e.g. TAC) that will be most often directly used by policy-makers (Section 6.3.1; Appendix D). Scientists estimate the acceptable level of uncertainty and all the while providing advise, they continue on improving their methodology.

There is enough knowledge to adapt current management practices. As previously mentioned, this topic is not new. McLeod et al. (2009) already pointed out the lack of climate change considerations in marine protected areas studies and design, providing some recommendations. Many reviews have gathered knowledge based on case studies to see how climate change is addressed and/or what could be best practices (e.g. Magris et al. (2014); Wilson et al. (2020); Chavez-Molina et al. (2023)). Most recommended practices for conservation rely on mapping climate change impacts, such as species shift, on developing dynamic conservation measures (e.g. Figure 6.15) or on incorporating vulnerability into spatial prioritisation processes to promote ecosystem resilience (McLeod et al., 2012; Tittensor et al., 2019). New strategies could also optimize marine protected areas planning based on multiple objectives, accounting for future benefits (Sala et al., 2021). Climate change adapted fisheries management strategies have also been suggested, notably based on existing tools to increase ecosystem resilience to climate

change (e.g. Cinner et al. (2009); Grafton (2010)) and through more flexible and adaptive management practices at different timescales (Pinsky and Mantua, 2014; Pentz et al., 2018).

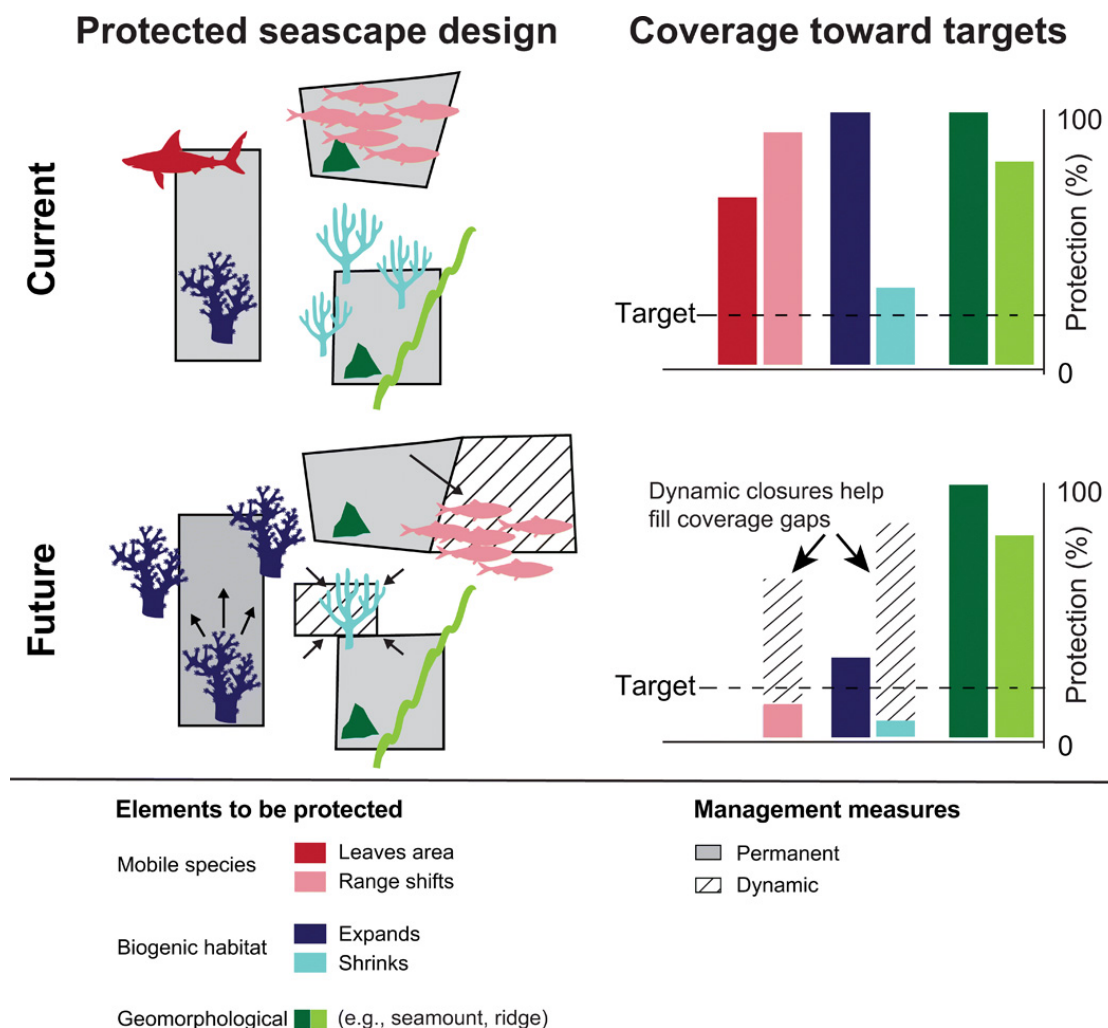


FIGURE 6.15: Schematic illustrating the need for climate-responsive management features. Figure from Tittensor et al. (2019).

However, some of the recommended approaches may not be adapted to data-limited regions (which are yet managed) and could lead to delaying climate adaptation there. A review by Jones et al. (2016) shows that the most common approach to study climate change impacts is to use niche, bioclimatic modelling or species distribution models as forecasts (e.g. Cheung et al. (2008); Lawson et al. (2023)). The forecasted distributions are then included in spatial prioritization softwares that allow for conservation priority sites selection. The limits of this approach have been widely discussed (Beaumont et al., 2005; Heikkinen et al., 2006; Koenigstein et al., 2016), with a recurrent reminder on the need for more mechanistic understanding of climate change impacts, despite the many

improvements of this methodology over the years (e.g. link to experimental work data, integration of dynamic subsurface variables, coupling with energetic models).

Besides, there are still geographical and species bias today on the topic of climate change in conservation. [Wilson et al. \(2020\)](#) review shows that 82% of real-world examples of climate change adaptation in marine protected area planning derive from tropical reefs. This bias also implies that many of our methodologies to incorporate climate change in conservation and fisheries management are based on case studies where we have important data availability, monitoring programs or strong modelling efforts. Other methodologies may be needed to account for climate change in remote or data limited areas.

Generally, accounting for climate change impacts should require a multi-scale approach in which both long-term plans and short-term adaptations are key. Indeed, adopting a more dynamic view in a climate change context means accounting for decadal changes in environmental parameters and probably ecosystem functioning but also preparing for more frequent and more intense extreme events. Developing a multi-scale risk management approach enable to account for uncertainties (also due to data limitations) at different timescales (Figure 6.16). In the long term, spatial planning and long-term objectives could be based on the assessment of different future scenarios (e.g. climate scenarios or different scenarios of possible climate change impacts; [Brooks et al. \(2001\)](#)). Management responses to extremes could also be anticipated with a long-term perspective, with concrete implications on short-term management through the regular monitoring of those extremes and the enforcement of planned response measures if needed ([Pinsky and Mantua, 2014](#)). There has been recent highlights on marine heatwaves, as their significant impacts on marine biodiversity, and thus also fisheries, have been documented ([Smale et al., 2019](#); [Smith et al., 2023](#)). Depending on the monitoring level and data availability, forecasting tools can be useful to help developing a risk assessment framework with associated response measures. Flexibility in management practices might be needed to adapt to extreme events, for instance through reduced captures, adapted fishing selectivity or temporary closures ([Mills et al., 2013](#); [Bris et al., 2018](#); [Caputi et al., 2019](#); [Smith et al., 2021](#)).

Another important paradigm shift is the transition from a static to a more dynamic view of the ocean. This shift has already started at the seasonal scale (e.g. temporary fishing

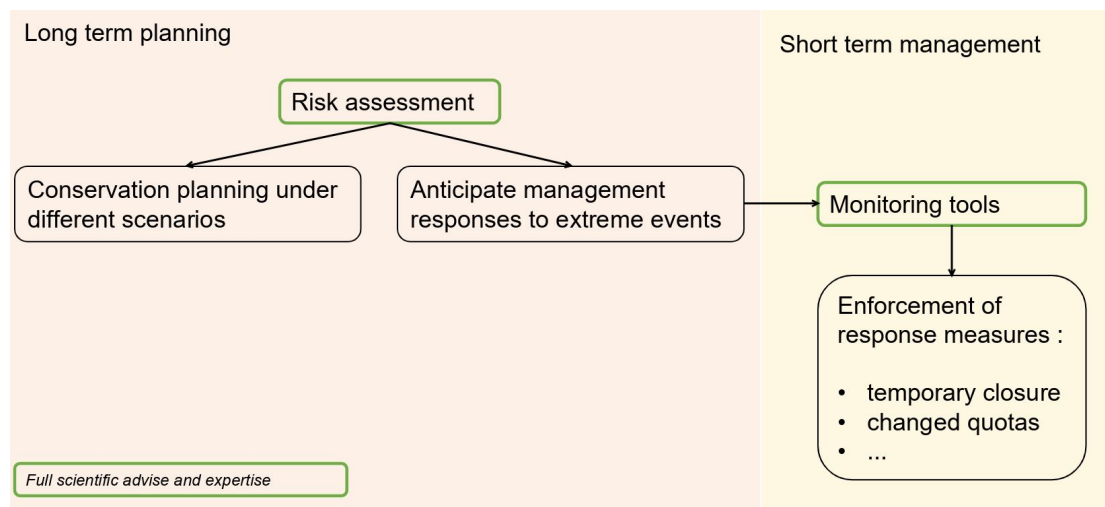


FIGURE 6.16: Schematic illustrating the two main timescales of a theoretical risk management approach to account for climate change impacts on ecosystems, incorporating scientific uncertainty in the management approach.

closures) to better manage fisheries (e.g. depending on the life cycle, [Beets and Manuel \(2007\)](#)) or to mitigate fishing impacts on seabirds (e.g. breeding seasons, [Constable and Welsford \(2011\)](#)). Yet, the consideration of this seasonal cycle is still anchored in the perspective that there is an ecosystemic equilibrium over time. In the context of climate change, a dynamic perspective means understanding that there might not be a well-defined ecosystem equilibrium in the long term.

Overall, climate change implies a stark methodological shift, not only for the scientific community, but also for policy-makers. This should be reflected in the collaboration between those two communities. Constructing science as an obligatory passage point toward policy formulation and decision-making can enable policy-makers to offload their responsibility and can lead to missed opportunities of co-construction efforts that would lead to operationalization ([Maas et al., 2022](#)). It should also be policy-makers role to be pro-active in the search of solutions based on the issues highlighted by the scientific community.

Reconsidering current practices and principles of biodiversity management

Although scientific uncertainty is a real issue, the current state of knowledge should be enough to trigger action; yet difficulties may arise from the significant methodological shifts required both from the scientific community and policy-makers. Those methodological shifts can be difficult to conduct because they may actually call into question some underlying principles of conservation and fishery management. As there might be

no equilibrium but changing ecosystems, the following questions arise: are we trying to desperately conserve what cannot be conserved? Are we trying to sustainably manage fisheries that cannot be sustainable? In this section, we might delve a bit deeper into almost philosophical considerations, with the aim to widen the horizon of biodiversity management.

Conservation and fishery management, despite their specificities, can be grouped under the term “biodiversity management” as they actually both emerge from a will to “manage” or “control” ecosystems to respond to the societal objectives of either preserving a heritage or regulating a resource. As developed by numerous philosophers, western societies’ relation to nature has largely been influenced by the will to control it (Descartes, 1637; de Beauvoir, 1949; Arvon, 1961; Hadot, 2004). Through their relationship with the world and with science, western societies have developed a form of metaphysical obsession with the immutable and the timeless. This desire to frame nature within laws that simplify it and make it more accessible to us, has contributed to placing man at a distance from, if not above, this nature. In addition, our biodiversity management practices tend to introduce a hierarchy between natural elements, whether in terms of the utility they appear to have for us, or even in our aesthetic relationship with the world (e.g. wilderness). Conservation, through a heritage approach, can also lead to a form of appropriation of this nature. Although this may also develop a sense of ownership that can lead to a sense of obligation and responsibility, it is still anchored in a static view that nature can be under control.

This perception of nature as a stable equilibrium also has political connotations. Nature’s beauty, balance and stability are celebrated as sources of inspiration for human societies (Egerton, 1973; N’Diaye, 2021) as well as related to moral values: “*A thing is right when it tends to preserve the integrity, stability and beauty of the biotic community. It is wrong when it tends otherwise.*” (Leopold, 1949). On the contrary, disorder, imbalance, change and even chaos are not considered sustainable modes of existence. As climate change calls into question this notion of equilibrium on management timescales, it raises the issue of adapting political ideals of justice and freedom to a changing, and more unpredictable world.

What’s more, climate change calls into question what can be considered natural in western societies, by blurring the culturally-established boundary between man and

nature. This dividing line loses its meaning as man influences the planet's climate and biodiversity (Uggla, 2010).

Faced with this challenge to the relationship with nature that underpins biodiversity management today, it may be necessary to define a new system of values that would fit in with a dynamic, changing world (Kricher, 2009), one that does not cling to the conditions of the past and present at all costs, but which, by respecting the present as much as possible, protects the conditions of viability for the future. The ecophenomenology movement, notably through the works of Erazim Kohák (*The Embers and the Stars*, 1984) or Neil Evernden (*The Natural Alien*, 1985), invites us to reflect on an ecological ethic that would go beyond simple behavioral mottos still anchored in technical views. In western societies, our ethics and metaphysical conceptions have given rise to the ecological crisis, can they really be useful to us in dealing with it?

A new ethic might be a way to regulate western societies predatory behavior toward natural resources : “ *Le Prométhée définitivement déchaîné, auquel la science confère des forces jamais encore connues et l'économie son impulsion effrénée, réclame une éthique qui, par des entraves librement consenties, empêche le pouvoir de l'homme de devenir une malédiction pour lui*” ² (Jonas, 1979). Ultimately, whether it's for conservation or fisheries management, policy-makers aim to regulate this appetite to exploit natural resources. When conservation establishes protective measures for specific areas, it effectively excludes other areas from these protections. Once again, the notions of stability and equilibrium play a crucial role in this approach, since they enable us to establish zones that are considered representative and sufficient to maintain the proper functioning of ecosystems. Doesn't this vision of spatial hierarchy reach its limits when faced with dynamic ecosystems? Wouldn't it be more appropriate to develop a genuine defense of nature's rights (Serres, 2020) and move towards greater sobriety in the exploitation of natural resources (Baudouin, 2019)? As far as fisheries management is concerned, we tend to enable fishing as much as possible as long as we consider that fish stocks will be able to renew itself, and that the activity is therefore sustainable. But shouldn't we base our use of natural resources on real needs for worldwide food security, rather than on economic gains?

² “*The definitively unleashed Prometheus, to whom science confers forces never before known and the economy its unbridled impetus, calls for an ethic which, through freely consented restraints, prevents man's power from becoming a curse for him.*”

This need for a potential total overhaul of our relationship with the natural world is a debate that extends far beyond scientific knowledge, and should be addressed in the public arena to generate transformative actions and to ensure the sustainability of fundamental democratic values in a changing world.

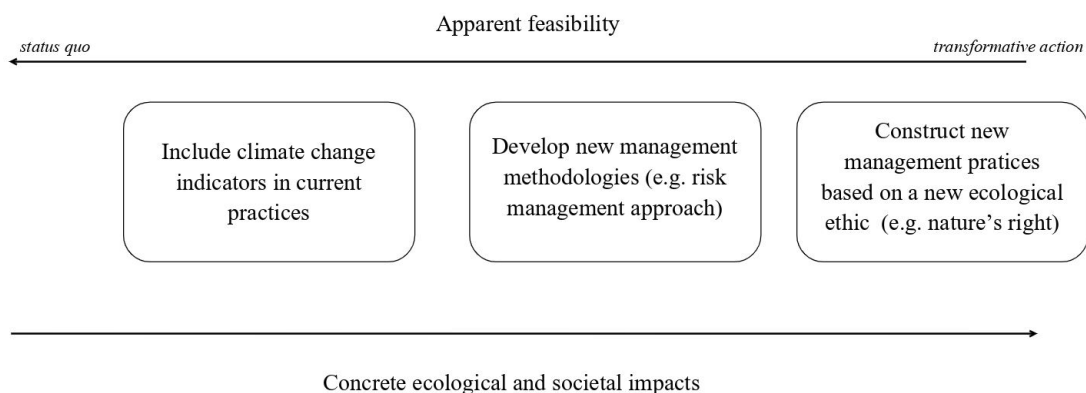


FIGURE 6.17: **Schematic providing a simplified overview of the different potential strategies to account for climate change in biodiversity management,** depending on the level of apparent feasibility (more or less efforts to implement) from a *status quo* situation to the different options presented that are ranked in order of increased transformative change.

Conclusion

In conclusion, scientific uncertainty is not a real barrier to effectively accounting for climate change in the management of marine biodiversity. It can, however, appear to be a barrier when we wish to maintain, at all costs, management practices that can be now outdated in a dynamic world. The scientific expertise provided to address this issue is based on new methodologies whose modes of validation and uncertainty levels contrast with previous expertise. And yet, even today, biodiversity management takes place in a context of great uncertainty, particularly in data-limited regions. Transformative management actions are possible, but also require a methodological shift from policy-makers and the development of a multi-scale approach to risk management. The complexity of making these transitions may stem from a more fundamental questioning of western societies' relationship with nature, and hence with the "management" of nature. Is the improvement of current practices by adopting ecosystem-based approaches with climate change considerations enough or could the development of a new ecological ethic be the ultimate way to effectively account for climate change in biodiversity protection and fisheries management and to halt biodiversity loss?

Concluding remarks

The aim of these concluding remarks is not to reiterate the conclusions of the scientific chapters, which have been highlighted at the end of each Chapter and at the beginning of this Chapter 6, but to offer a more general conclusion that also encompasses reflections from the previously developed scientific and societal perspectives (Figure 6.18).

	INDICATORS	IMPACTS	MANAGEMENT TOOLS
Focus of this PhD thesis	<ul style="list-style-type: none"> • Climate velocities • Marine heatwaves • Winter waters characteristics 	<ul style="list-style-type: none"> • Habitat shear • Reduced prey accessibility • Changes in fish stock connectivity 	Conservation <ul style="list-style-type: none"> • Climate residence time • Climate refugia Fisheries management <ul style="list-style-type: none"> • Stock connectivity • Maximizing stock resilience
Perspectives	<ul style="list-style-type: none"> • Improving mechanistic understanding of fronts shifts and local circulation variability • Further characterizing or (re)defining MHWs at depth 	<ul style="list-style-type: none"> • What is elephant seals behavioral response to extreme events ? • Can the local circulation modulate the conditions of development for Patagonian toothfish ? 	<ul style="list-style-type: none"> • Development of risk management approaches • How to better integrate and communicate scientific uncertainty to guide policy-making ? • Toward new ethics in biodiversity management ?

FIGURE 6.18: Summary of the focus of this PhD work and its scientific and societal perspectives.

This thesis has been an opportunity to reflect on how to study the impact of climate change on pelagic ecosystems. By motivating physical oceanographic analyses with ecological and management considerations, the idea was to broaden our vision of potential impacts and to characterize their temporal and spatial heterogeneity.

Through the development of this multi-scale picture - albeit an incomplete one, given our focus on specific physical characteristics - we can extract implications for management and discuss notions (e.g. refugia, resilience) that may support certain adaptation strategies. These may be more or less transformative, but this will also depend on the potential future changes in value systems regarding our relations to biodiversity and natural resources.

The provided overview of current and future threats to the pelagic ecosystems in the Southern Indian Ocean is not very optimistic, and accounting for climate change in biodiversity management is no silver bullet. The magnitude of the impacts and of the adaptation required will mostly depend on global warming levels. Yet, I think it is important to conclude on a hopeful note : there is no insoluble problem, but there are choices to be made, and we are in a position to make them. As Albert Camus wrote in his *Carnets* (1942-1951): “*La tragédie n’est pas une solution*”/“*Tragedy is not a solution*”.

Appendix A

**Supplementary Material Azarian
et al., 2023**

Appendix A: Supplementary Materials

Figure S1: List of models used for the timeshift approach analyses for both SSP 245 and SSP585.

For changes in temperature (yearly data) 22 models	For MHW intensity (daily data) 17 models
ACCESS-CM2 ACCESS-ESM1-5 BCC-CMS2-MR CAMS-CSM1-0 CanESM5 CanESM5-CanOE CESM2-WACCM CMCC-ESM2 CMCC-CM2-SR5 CNRM-CM6-1 GFDL-CM4 GFDL-ESM4 HadGEM3-GC31-LL EC-Earth3-CC EC-Earth3-Veg IPSL-CM6A-LR MIROC-ES2L MPI-ESM1-HR MPI-ESM1-LR MRI-ESM2-0 NESM3 UKESM1-0-LL	ACCESS-CM2 ACCESS-ESM1-5 BCC-CMS2-MR CanESM5 CESM2-WACCM CMCC-ESM2 CMCC-CM2-SR5 CNRM-CM6-1 CNRM-CM6-1-HR GFDL-CM4 EC-Earth3 IPSL-CM6A-LR MIROC6 MPI-ESM1-HR MPI-ESM1-LR MRI-ESM2-0 NESM3

Figure S2 : Temperature trends between 1982 and 2019 in the Southern Indian Ocean (top panel), using linear regression on sea surface temperature, using OISST (left) and OSTIA (right) datasets. Timeseries of sea surface temperature for two areas (bottom panel): one west of the Southern Indian Ocean, covering Prince Edward Islands and Crozet (orange) and one north of Saint-Paul and Amsterdam (green) using OISST (full) and OSTIA (dashed) datasets

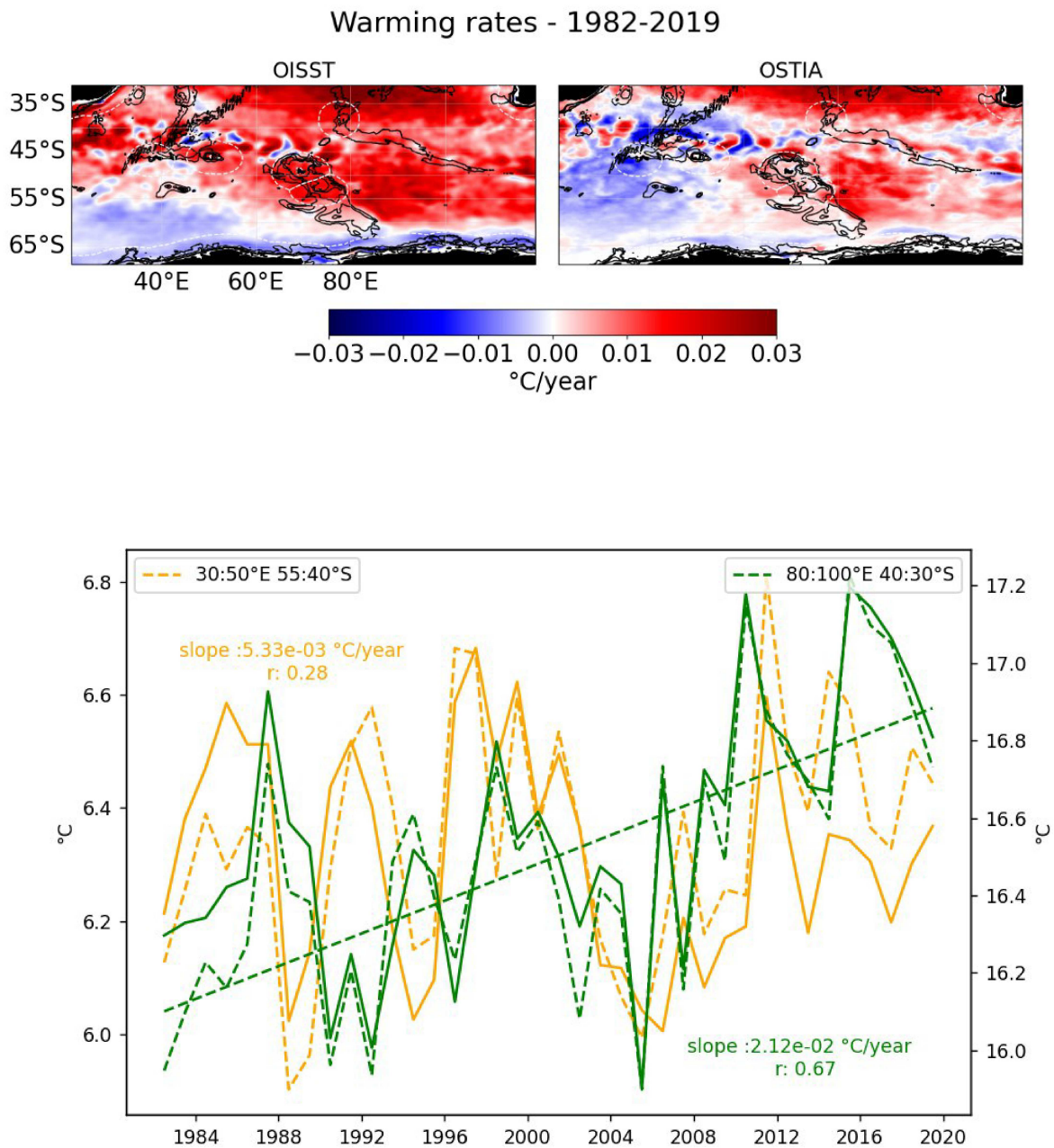


Figure S3: Warming rates between 1982-2019 for each of the 24 CMIP6 models studied.

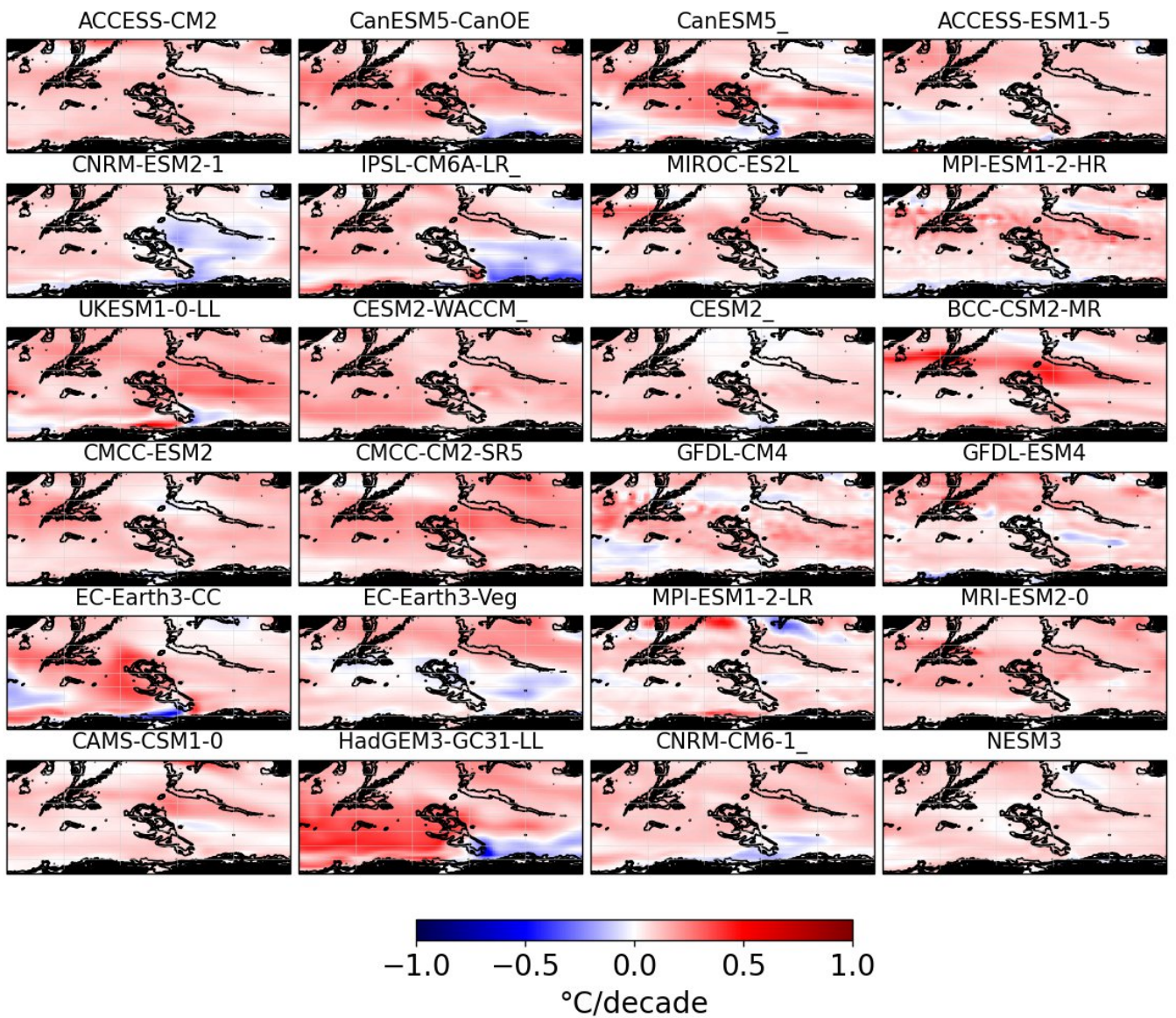


Figure S4: MHW intensity over 1984-2014 (90th percentile) for each of the 19 CMIP6 models studied.

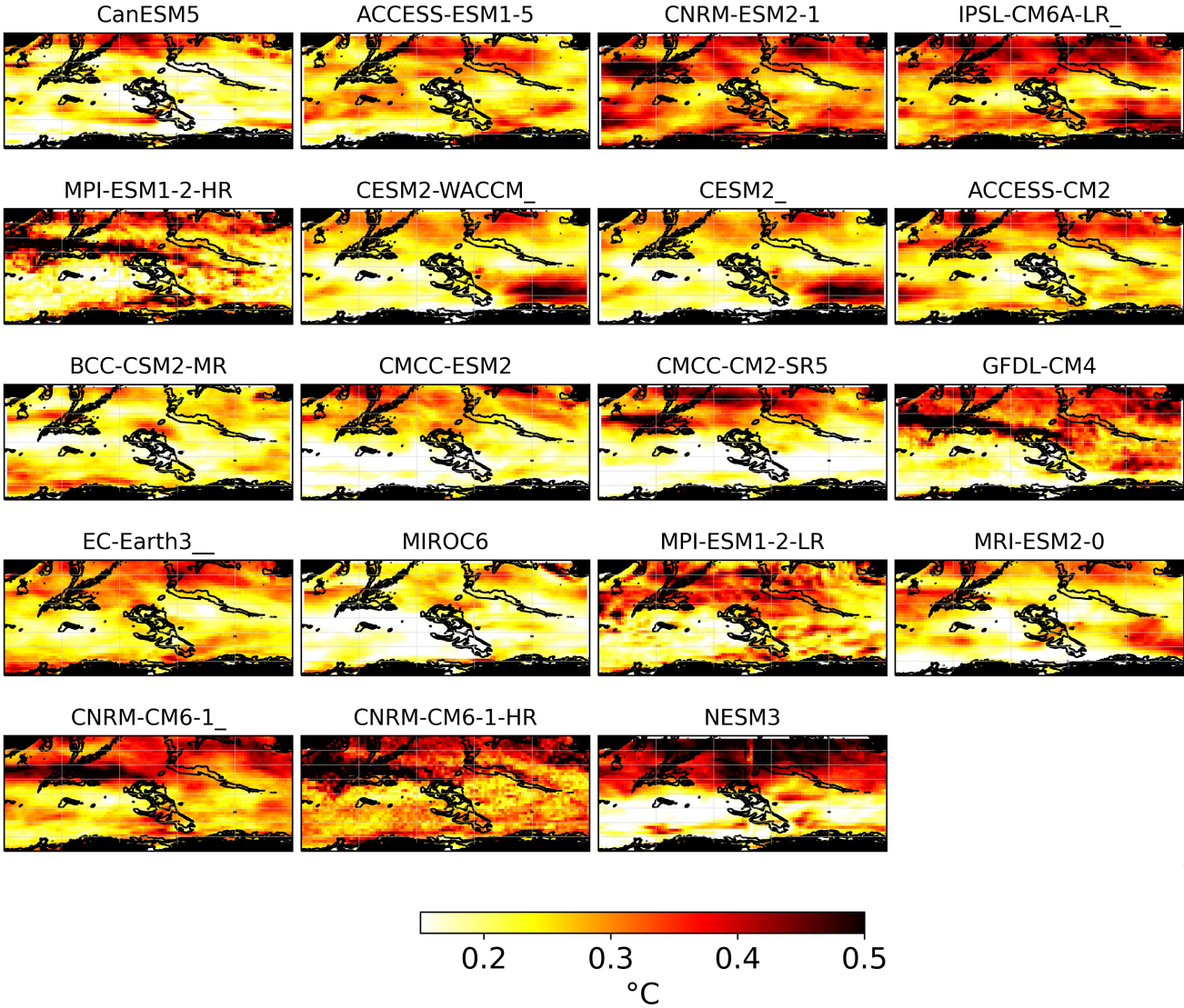


Figure S5 : (A) Warming trends between 1975 and 2015 of 10 IPSL-CM6A-LR members. (B) Change in surface temperature (2081-2100 minus 1995-2014) of the same 10 IPSL-CM6A-LR members under SSP2-4.5. (C) Time series of mean Pearson correlation coefficient, as an indicator of spatial similarity, for each 10 IPSL-CM6A-LR members relative to r1i1p1f1 member, under SSP2-4.5.

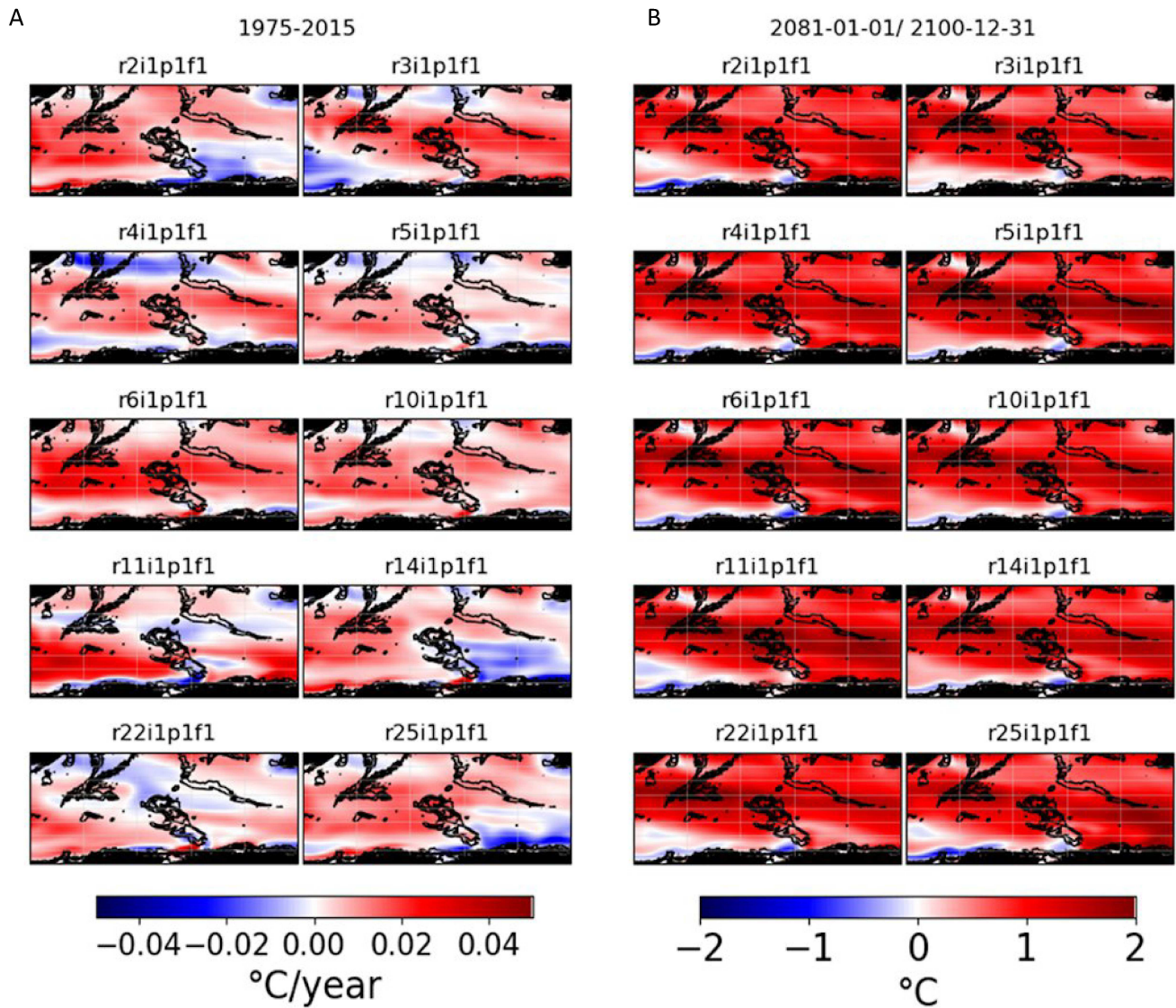


Figure S6: Relative increase in the mean (full) or spread (hatched) of the daily temperature distribution under SSP2-4.5 relative to historical period (1995-2014) from 19 CMIP6 models for 2021-2040 (near term, NT), 2041-2060 (mid term, MT) and 2081-2100 (long term, LT).

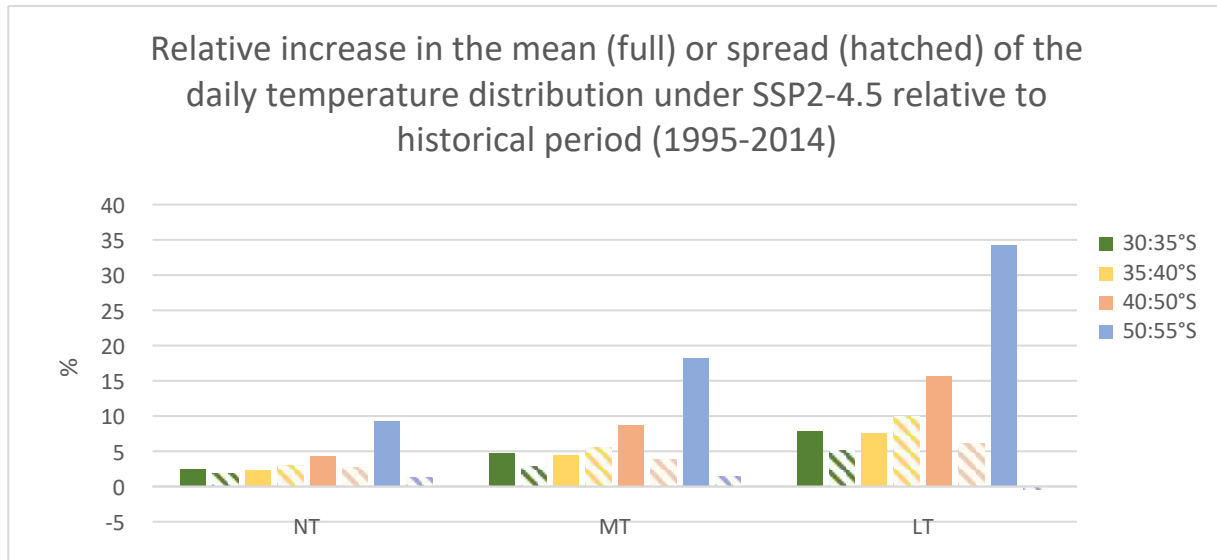


Figure S7: Relation between the change in surface temperature and MHW annual days for 20-year periods under SSP1-2.6 and SSP2-4.5 averaged over the area. Error bars correspond to intermodel variability.

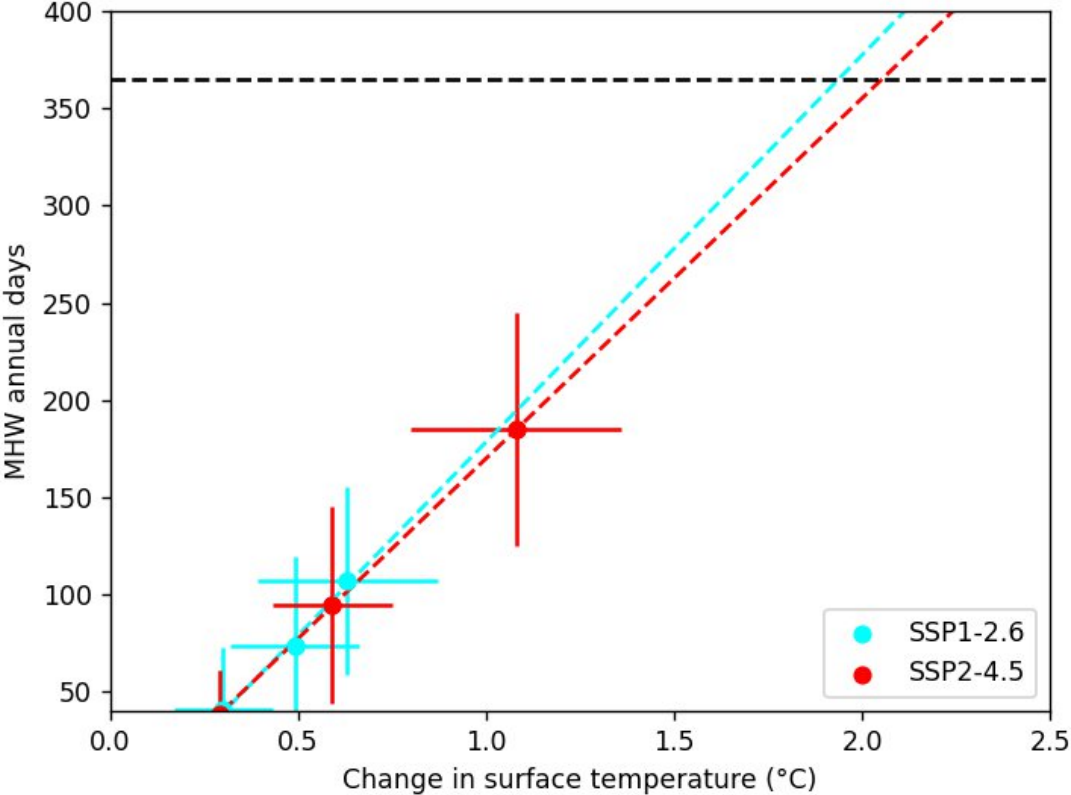
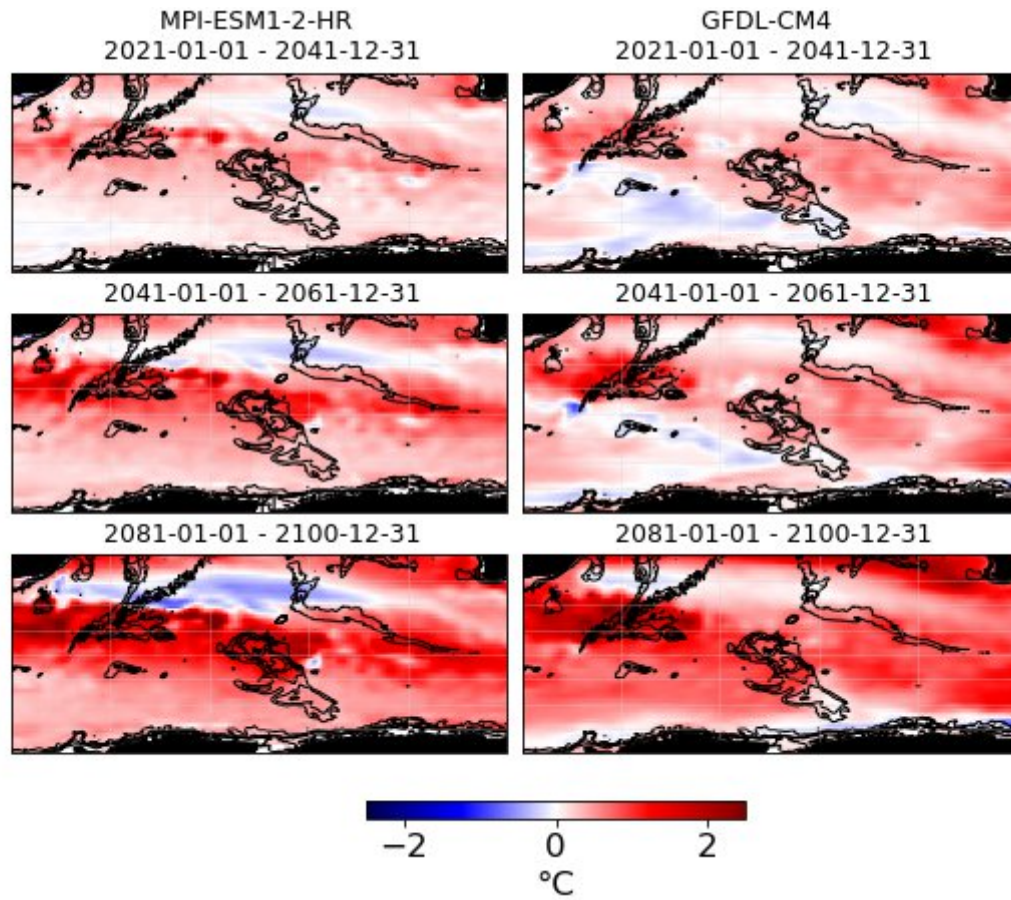


Figure S8: Change in surface temperature for the near-, mid- and long-terms under SSP2-4.5 for two high resolution models: MIP-ESM1-2-HR and GFDL-CM4.



Appendix B

Supplementary Material Azarian
et al., 2024

Supplementary Material

Supplementary Material and Methods:

The text below provides a more detailed description of the Material and Methods used in this study.

a. In situ observations

Temperature, salinity and pressure *in situ* profiles are collected from Argo float data between 2001 and 2019 over the area 20:120°E 70:30°S (Argo, 2000). In total, we download 170 352 profiles, among which 78 407 are complete between 5 and 900 m. This data is obtained from Argo GDAC Data Browser. These data were collected and made freely available by the International Argo Program and the national programs that contribute to it (<http://www.argo.ucsd.edu>, <http://argo.jcommops.org>). The Argo Program is part of the Global Ocean Observing System.

The Marine Mammals Exploring the Oceans Pole to Pole or MEOP consortium gathers the data collected from various national programs to produce a public quality-controlled database of 3D oceanographic data obtained from biologging in Polar regions (Treasure et al., 2017). Here the MEOP-CTD database is used, gathering temperature and salinity profiles between 2004 and 2017 notably through elephant seals in the Southern Indian Ocean (Roquet et al., 2014). In total, we download 140436 profiles, among which 9 484 are complete between 5 and 900 m.

To categorize ARGO or MEOP-CTD hydrographic profiles according to the presence or absence of winter waters (WWs), we use the method introduced by Pauthenet et al., 2017, using a functional principal component analysis approach (R code available here: <https://github.com/EPauthenet/fda.oce>; in this study the same approach is done in python and presented in Supplementary Materials S4).

b. Mercator reanalysis

The GLORYS12V1 product is the Copernicus Marine Environment Monitoring Service (CMEMS) global ocean eddy-resolving reanalysis covering the altimetry delivered by Mercator Ocean. This product provides daily and monthly mean temperature over 50 vertical levels and with 1/12° horizontal resolution between 1993 and 2019. Evaluations of this reanalysis indicate a realistic mesoscale representation, with the global pattern of regional trends of sea surface height being in good agreement with altimetric data (Lellouche et al., 2018) but also encouraging results for monitoring the regional variability of the Antarctic Circumpolar Current (Artana et al., 2021), as well as regarding sea ice

concentration budget (Nie et al., 2022). This product is used in this paper to provide a monthly climatology for the vertical temperature profiles.

The GLORYS12V1 product is also used to determine the probability of presence of WWs. This probability is estimated by detecting, for each day between 1993 and 2019 and for each grid cell, whether the minimum temperature between 100 and 400 m is found at a depth less than 350 m, and then averaging the results over time. The obtained result is confronted with background knowledge on the Antarctic Polar Front for validation (Park et al., 1998; Park et al., 2014; Pauthenet et al., 2018). WWs are also characterized by the temperature at the minimum (also named winter waters temperature) and the depth of this minimum (also named winter waters depth), as in (Sabu et al., 2020).

c. Satellite observations and surface marine heatwaves detection

The Operational Sea Surface Temperature and Ice Analysis (OSTIA) system run by the UK's Met Office (Good et al., 2020) provides daily sea surface temperature free of diurnal variability, also called the foundation sea surface temperature, at a $0.05^\circ \times 0.05^\circ$ horizontal grid resolution between 1982 and 2019. This product combines satellite measurements (L4 level) from both infrared and microwave radiometers with in-situ measures from ships, drifting and moored buoys. This dataset was used for surface marine heatwaves (MHW) detection.

A MHW is identified as an event of at least 5 days for which the sea surface temperature (SST) is above the 90th percentile of a data distribution using a seasonally-varying climatology for each grid point and for each day of the year using an 11-day window (Hobday et al., 2016). The threshold is also smoothed by applying a 30-day moving average. The intensity of the MHW at the surface is defined as the anomaly of temperature relative to the 90th percentile threshold.

d. MHW subsurface characteristics

The temperature anomaly depth, also called "MHW depth" in (Elzahaby and Schaeffer, 2019), is calculated to investigate whether surface MHWs are associated with deeper temperature anomalies. To do so, temperature anomaly profiles are obtained using the combination of information from different datasets:

- OSTIA dataset : for the detection of surface MHW using Hobday et al., (2016) definition (90th percentile)
- ARGO data : daily hydrographic profiles
- MERCATOR reanalysis : provide for each grid cell a monthly climatology profile

The metrics presented in Elzahaby and Schaeffer, (2019) to characterize MHW at depth are used here. In particular, the cumulative temperature anomaly (CTa) up to the depth at which the temperature anomaly is no longer positive (Z_n) is used to define the temperature anomaly depth:

$$\text{Temperature anomaly depth} = \text{Max} (z(\text{CTa}(z) \leq 0.95 * \text{CTa}(Z_n)))$$

This metric is calculated both for profiles (that extend up to 900 m at least) in a MHW and outside a MHW because the anomaly is here the difference between the *in situ* hydrographic profile and a monthly climatology profile from MERCATOR reanalysis. It is important to distinguish the part of the anomaly which is indeed due to the MHW and the part that may be either due to a bias in MERCATOR reanalysis compared to *in situ* observations or due to a surface temperature anomaly that did not last more than five days. As only 7% of the MEOP-CTD profiles are complete between 5 and 900 m, we conduct the analysis of temperature anomaly depth over the Southern Indian Ocean (20°:120°, 70°:30°S) using Argo dataset only.

From each Argo profiles, we compute their vertical cumulative temperature anomaly, and the depth where 95% of the cumulative temperature anomaly is reached, also named “temperature anomaly depth”. Temperature anomalies are defined as a departure from a seasonal climatological mean produced from an ocean reanalysis (MERCATOR). Using satellite SST, we then group each of these profiles as within a MHW or outside. The Argo profile is said to be in a MHW according to the surface detection of a MHW using sea surface temperature observations (OSTIA). A bootstrap approach with 10000 iterations is used to obtain the mean values of the two metrics, as the sample sizes (in and out MHW) differ.

e. Conditional probabilities of presence of winter waters

We test the hypothesis that MHWs are associated with a lower probability of presence of WWs. The detection of WWs (as described in section b) is conducted on daily 3D temperature profiles of MERCATOR reanalysis product between 1993 and 2019.

For each pixel, we calculate the probability of presence of the WWs given that there is a MHW (as detected using OSTIA dataset, over 1993-2019 using 1982-2019 climatology), also noted

$\mathbb{P}(WW|MHW)$ and the probability of presence of the WWs given that there is not a MHW $\mathbb{P}(WW|NO_MHW)$:

$$\mathbb{P}(WW|MHW) = \frac{\mathbb{P}(WW \cap MHW)}{\mathbb{P}(MHW)} = \frac{\sum_{t=1}^T x_{ww_t} \cdot x_{mhw_t}}{\sum_{t=1}^T x_{mhw_t}},$$

$$\mathbb{P}(WW|NO_MHW) = \frac{\mathbb{P}(WW \cap NO_MHW)}{\mathbb{P}(NO_MHW)} = \frac{\sum_{t=1}^T x_{ww_t} \cdot (1 - x_{mhw_t})}{\sum_{t=1}^T (1 - x_{mhw_t})},$$

where $x_{ww_t}, x_{mhw_t} \in [0,1]$. x_{ww_t} and x_{mhw_t} indicate the presence/absence of WWs and MHW respectively for a time t for a given pixel. These probabilities are calculated over the area $20^\circ:120^\circ E - 58^\circ:-40^\circ S$ and over the period 1993-2019. If MHW are associated with a shift of WWs, then we should obtain $\mathbb{P}(WW|MHW) < \mathbb{P}(WW|NO_MHW)$.

f. Altimetry analysis

Altimetry-derived geostrophic velocities are computed by CLS/AVISO (Collecte Localisation Satellites/Archiving, Validation, and Interpretation of Satellite Oceanographic data) and distributed by Copernicus Marine Environment Monitoring Service (CMEMS) as a gridded product on a $0.25^\circ \times 0.25^\circ$ horizontal grid resolution between 1993 and 2020 (<https://doi.org/10.48670/moi-00148>). Geostrophic currents are calculated using satellite altimetry, by solving the equation for geostrophic equilibrium, the balance between the horizontal pressure gradient force and the Coriolis force.

A Lagrangian approach is useful to investigate whether MHWs are related to advective processes. Using AVISO geostrophic velocities, the latitudinal advection of water parcels 15 days before (around the average duration of a MHW) could be estimated. A monthly climatology of latitudinal displacement is then determined over multiple years (1993-2020). Correlations between anomalies of latitudinal displacement and the presence/absence of MHW are evaluated using the complete time series (1993-2020). To assess the significance of the Pearson correlation coefficients obtained, the associated p -value is calculated. In addition, to assess the robustness of the pattern and the coefficients obtained, the same analysis is conducted using randomly associated maps of anomalies of latitudinal displacement and maps of MHW presence/absence.

g. CMIP6 models

Coupled ocean-atmosphere models from the Coupled Model Intercomparison Project 6 (CMIP6) are used in this study. These models have been used to conduct historical and projection simulations notably

to investigate how the Earth system responds to forcing (Eyring et al., 2016). The 12 models used here (described in Table S1) have been selected among 26 CMIP6 models as they provide a realistic representation of the circumpolar mean position of WWs between 1995-2014 using their historical simulations (Supplementary Material S2). Three qualitative criteria are used: i) the simulated WWs should not be too south (e.g. INM-CM5-0, INM-CM4-8, EC-Earth3, EC-Earth3-CC, EC-Earth3-Veg, MIROC-ES2L, CIESM, ACCESS-ESM1-5); ii) the simulated WWs should not be too north (e.g. CAMS-CSM1-0, BCC-CSM2-MR); iii) the detection of simulated WWs should not generate too much noise and not be observed in areas where WWs are not realistically present (e.g. NESM3, MPI-ESM1-2-LR, MPI-ESM1-2-HR, IPSL-CM6A-LR).

Historical (1850-2014) and projection (2015-2100) simulations from CMIP6 are used here. Historical simulations are constrained by historical forcing, mostly based on observations (Eyring et al., 2016). Different emission trajectories are used for the projections and are called Shared Socioeconomic Pathways (SSPs). In this study, three projection scenarios are considered: the SSPs 1-2.6, 2-4.5 and 5-8.5. The SSP1-2.6 describes a world with strong mitigation policies, leading to an estimated warming of 1.8 °C by the end of the century (as compared to pre-industrial; Lee et al., 2021). The SSP2-4.5 describes a world with socio-economic trends similar to the recent historical patterns, leading to an estimated warming of 2.7 °C by the end of the century. The SSP5-8.5 describes a world with no mitigation policies, leading to an estimated warming of 4.4°C by the end of the century (Lee et al., 2021).

The variable considered is monthly *thetao* (sea water potential temperature across different depth levels in °C). Each model output is regridded to the same regular 1°-1° horizontal grid using distance weighted average remapping (using climate data operators « cdo » remapdis) as in Kwiatkowski et al. 2020. Each model output is also regridded vertically following the World Ocean Atlas standard discretization (33 vertical intervals from the surface (0 m) to the abyssal seafloor (5500 m)). WWs are detected through the presence of a temperature minimum between 100 m and 400 m at a depth less than 350m.

Multiple models are used to investigate WWs future position and their results are combined following the so-called ‘time-shift approach’, which consists in averaging the models outputs over a period that, for each model, corresponds to a given global warming level (GWL ; Herger et al., 2015; Chen et al., 2021; Lee et al., 2021). GWLs are 20-year running means of globally averaged atmospheric surface temperature anomaly compared to the pre-industrial period (1850-1900) and are reached at different time periods for different models and different scenarios. For a given GWL, model outputs are averaged over 20 years centered around the year where the GWL is reached for each model and each SSP considered and then all simulations are averaged, being weighted equally.

As the shift in WWs may vary according to the models, we consider that the multimodel mean value of shift is significant if at least 80% of the simulations contribute to this mean value and agree on the sign of the change. Multimodel mean changes in WWs' temperature and depth are considered significant if at least 80% of the simulations contribute to the mean value and if the mean value is superior to intermodel standard deviation.

Note that in both MERCATOR reanalysis and CMIP6 models, WWs are detected through the presence of a minimum between 100 m and 400 m at a depth less than 350m. Using this definition over the Southern Indian Ocean, subsurface minimums are also detected in areas with no winter waters but that present a subsurface temperature inversion (Dong et al., 2008). To remove this noise in the signal, we apply a mask for the historical period based on the WWs temperature ($T < 3^{\circ}\text{C}$), as the WWs northernmost extension has been usually defined as the 2°C isotherm at the 100–300 m depth range but can also reach 3°C (Park et al., 1993; Belkin and Gordon, 1996).

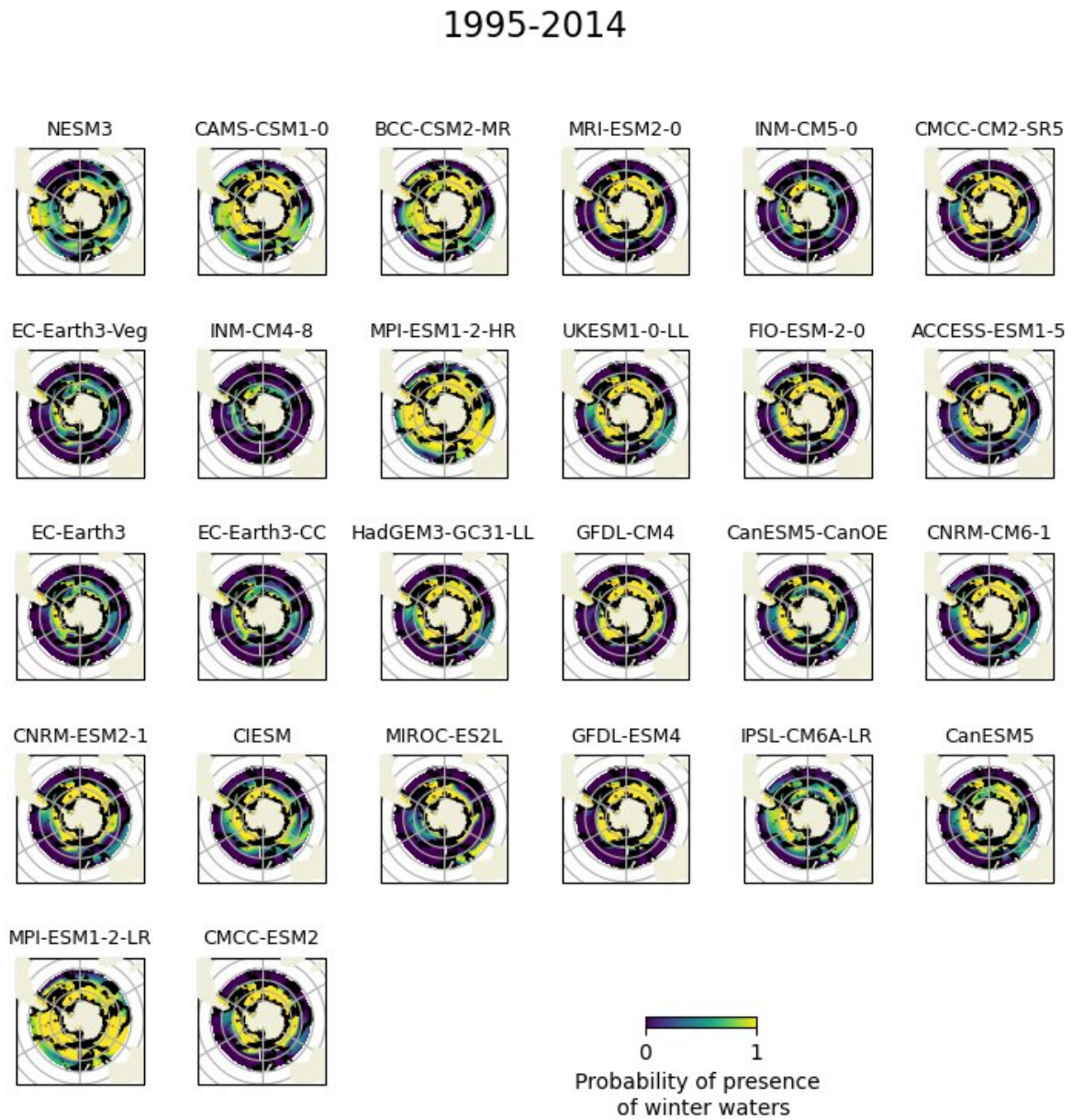
Supplementary Material S1 : Table of the CMIP6 models used

Table S1: CMIP6 models used and scenarios associated. CMIP6 models outputs are available at : <https://esgf-node.llnl.gov/projects/cmip6/>.

	Member	Experiment and/or scenario	Ocean horizontal resolution (before interpolation)	References
CanESM5	rlilp1fl	Historical, ssp126, ssp245, ssp585	1°	Swart et al., 2019; Christian et al., 2021
CanESM5-CanOE	rlilp2fl	Historical, ssp126, ssp245, ssp585	1°	Swart et al., 2019; Christian et al., 2021
CMCC-CM2-SR5	rlilp1fl	Historical, ssp126, ssp245, ssp585	1°	Cherchi et al., 2019
CMCC-ESM2	rlilp1fl	Historical, ssp126, ssp245, ssp585	1°	Lovato et al., 2022
CNRM-CM6-1	rlilp1f2	Historical, ssp126, ssp245, ssp585	1°	Voldoire et al., 2019
CNRM-ESM2-1	rlilp1f2	Historical, ssp126, ssp245, ssp585	1°	Séférian et al., 2019
FIO-ESM-2-0	rlilp1fl	Historical, ssp126, ssp245, ssp585	1.1° in longitude and 0.27–0.54° in latitude	Bao et al., 2020; Shu et al., 2022
GFDL-CM4	rlilp1fl	Historical, ssp245, ssp585	0.25°	Held et al., 2019; Dunne et al., 2020
GFDL-ESM4	rlilp1fl	Historical, ssp126, ssp245, ssp585	0.5°	Dunne et al., 2020
HadGEM3-GC31-LL	rlilp1f3	Historical, ssp126, ssp245, ssp585	1°	Kuhlbrodt et al., 2018; Andrews et al., 2020
MRI-ESM2-0	rlilp1fl	Historical, ssp126, ssp245, ssp585	1°x0.5°	Yukimoto et al., 2019
UKESM1-0-LL	rlilp1f2	Historical, ssp126, ssp245, ssp585	1°	Sellar et al., 2019

Supplementary Material S2: Selection of CMIP6 models

Figure S2: Probability of presence of winter waters for 26 CMIP6 models over the historical period (1995-2014).



Supplementary Material S3: Functional Principal Component Analysis on MEOP-CTD and Argo in situ observations to investigate the impact of MHWs on the shapes of the vertical profiles and position to the Polar Front.

S3.1. Approach

The aim is to categorize the elephant seals' and ARGO hydrographic profiles according to the presence or absence of certain water masses such as the winter waters (WWs) which are ecologically important for some species (ex. king penguins; Bost et al., 2015). However, directly detecting the presence/absence of WWs, as is done with the MERCATOR product, using *in situ* profiles is challenging due to the signal noise. Since we seek to categorize the vertical structure of the temperature and salinity profiles with space and time as sampling dimensions, the method used here is similar to the one introduced by Pauthenet et al., 2017 using a functional principal component analysis approach (R code available here: <https://github.com/EPauthenet/fda.occ>; in this study the same approach is done in python).

The following analysis is focused on the area 20:120°E and 58:40°S, with then 30192 MEOP-CTD profiles and 18848 ARGO profiles that are complete up to 400m deep. In both datasets, around 8% of the profiles are found during a MHW.

First, the hydrographic profiles are transformed using B-splines functions. Elephant seals' hydrographic profiles have already been interpolated to fit a vertical grid of 1000 m deep with 1 m interval, but not all profiles contain data up to 1000 m. To use the maximum of profiles and because WWs signal is generally defined as a temperature minimum around 200 m, we chose to focus the analysis on profiles up to 400 m. For consistency, we interpolate ARGO profiles to a vertical grid of 1000 m deep and also focus the analysis on profiles up to 400 m. Since B-splines are polynomial segments, the choice of the number of segments controls how much the profiles are smoothed. We choose $K=20$ since the focus is on the first 400 m and it was sufficient to capture the winter water signal. The profiles can be projected on the B-spline basis $\{\phi_1, \dots, \phi_K\}$, thus producing continuous curves $x_n^{\theta \text{ or } S}(z)$ with $n \in [0, N]$, N being the total number of observations.

Then, a functional principal component analysis (FPCA) is conducted on the profiles projections on the B-spline basis. The aim of a FPCA is to determine the dominant modes of variation of functional data. Because we investigate temperature and salinity variations simultaneously, we use a table with twice the 20 coefficients for each observation, and ensure that the same functional transformation is conducted on temperature and salinity profiles. The FPCA is equivalent to solving this eigenvalue problem: $VW M b_i = \lambda_i b_i$ with $i \in [0, 2.K]$, V is the crossed covariance matrix of the matrix containing the mean

observations, W is the metric equivalence between the functions and the discrete observations, M is a weighting matrix to account for the different units of the variables and λ_i and b_i are respectively the eigenvalue and the eigenvector to solve the dimension reduction problem. With the obtained eigenvector, we can then determine the eigenfunctions or vertical modes, accounting for both temperature and salinity variations.

For the elephant seals' hydrographic profiles, the first principal components (PC) obtained can be associated with the presence/absence of WWs. This is checked by looking at the associated hydrographic profile signatures and the latitudinal distribution of the PC. However, this is not the case for the ARGO profiles. For this data, we define the separation in the PC space that corresponds to the northernmost position of a subsurface minimum of temperature as in Pauthenet et al., 2018. This separation corresponds to a plane in the PC1/PC2/PC3 space such that the norm of the vertical temperature gradient between 100 and 400 m is minimized. The norm of the vertical temperature gradient is considered as a cost which is weighted by the density of the data in the PC space. The minimization is then conducted using the quasi-Newton method of Broyden, Fletcher, Goldfarb, and Shanno (BFGS) (Nocedal and Wright, 2006) through the python function *optimize.minimize* of the scipy package. The optimal plan is characterized by the following equation : $a.y_1+b.y_2+c.y_3+d=0$ where y_1, y_2 and y_3 are coordinates along respectively PC1, PC2 and PC3. Each profiles can thus be attributed a CPF value where $CPF=a.y_1+b.y_2+c.y_3+d$, characterizing its distance to the northernmost position of a subsurface minimum and such that $CPF>0$ south of the Polar Front and $CPF <0$ north of the Polar Front.

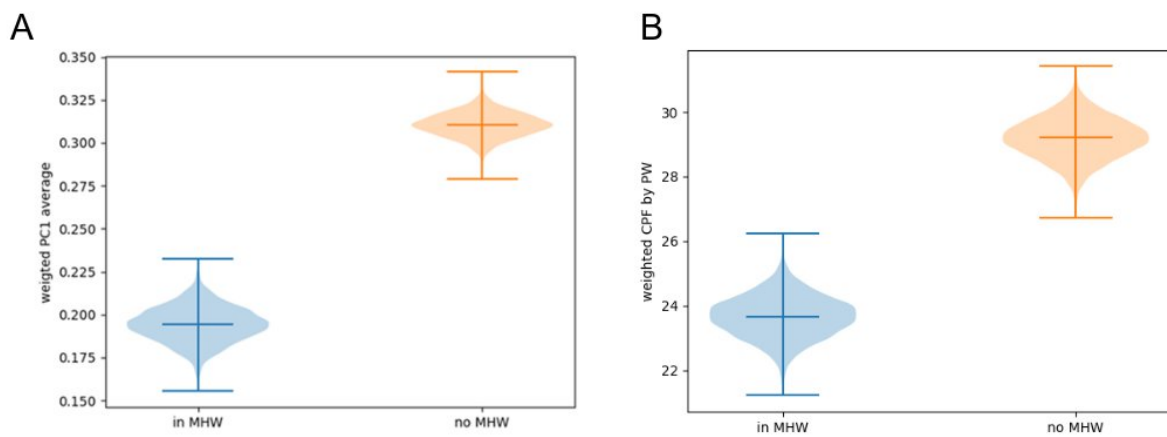
S3.2. Results

Using MEOP-CTD data, we find that the first two modes of variation are sufficient to explain 90% of the variance, with the first mode accounting for 50% of the variance with a major contribution from temperature (81%). A positive (negative) PC1 corresponds to a colder (warmer) and fresher (saltier) profile with a temperature minimum between 100 and 200 m. PC1 latitudinal distribution fits the pattern of presence/absence of WWs. The mean averages of PC1 values for profiles in and out of MHWs weighted by the probability of presence of the WWs, estimated from MERCATOR reanalysis are respectively 0.19 and 0.31 when considering the whole area (20:120°E 58:40°S, Figure S4A).

Using Argo profiles, we use the CPF metric (as described in the section above) to characterize the distance of a profile to the northernmost limit of the WWs, either from the north ($CPF<0$) or from the south ($CPF>0$). The mean averages of CPF values for profiles in a MHW weighted by the probability of presence of the WWs (estimated from MERCATOR reanalysis) is about 19% lower than the same metric for profiles outside a MHW (Figure S4B). This means that profiles in a MHW that are south of the Polar Front tend to be closer to the Polar Front during a MHW compared to outside a MHW.

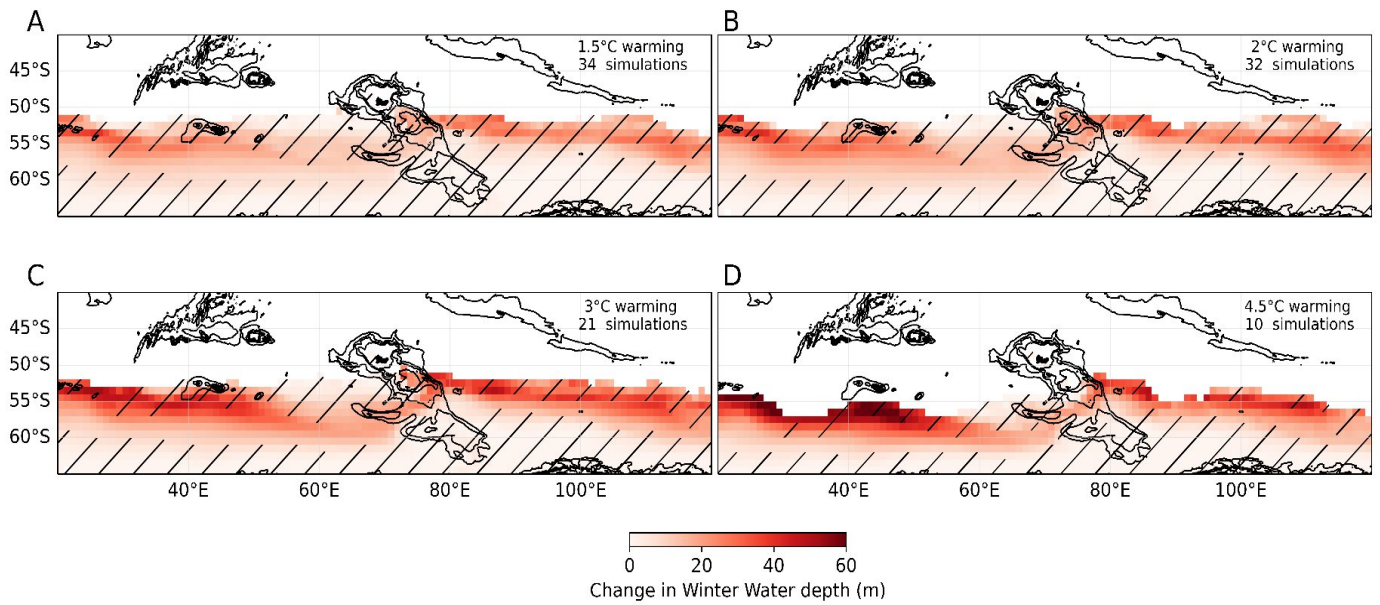
In both cases (using MEOP-CTD and Argo data), these results suggest that MHWs are associated with a localized southward shift of the winter waters.

Figure S3: (A) Distribution of the average PC1 obtained from the functional principal component analysis conducted on 30192 elephant seals profiles weighted by the probability of presence of winter waters over 1993-2019 (calculated from MERCATOR reanalysis) for profiles found in and out of a MHW (according to the detection conducted with the OSTIA daily SST). The distribution was obtained through 10000 random sampling of 2525 profiles over the area studied (20:120°E 58:40°S). (B) Distribution of the average CPF value obtained from the functional principal component analysis conducted on 18848 Argo profiles weighted by the probability of presence of winter waters over 1993-2019 for profiles found in and out of a MHW. The distribution was obtained through 10000 random sampling of 1504 profiles over the area studied (20:120°E 58:40°S).



Supplementary Material S4: Winter waters depth change at the end of the 21st century (2081-2100) relative to 1995-2014 for 12 CMIP6 models

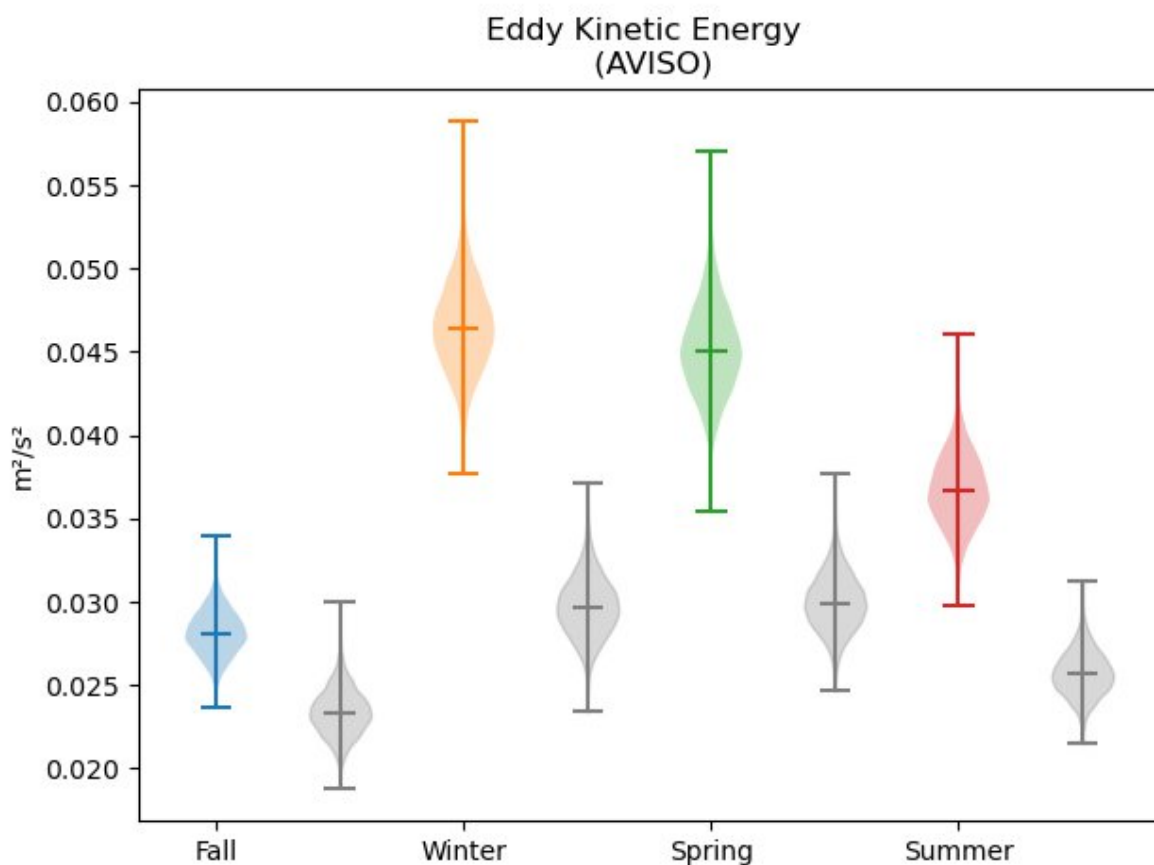
Figure S4: Change in winter waters' depth for a global warming level of 1.5°C, 2°C, 3°C and 4.5°C relative to 1850-1900 using 12 CMIP6 models and SSP1-2.6, SSP2-4.5 and SSP5-8.5. Only mean values obtained from more than 80% of the simulations are shown (as winter waters shift differently depending on models). Hatching indicates areas where the intermodel standard deviation is superior to the multimodel mean.



Supplementary Material S5: Seasonal characteristics of the marine heatwaves sampled with Argo floats

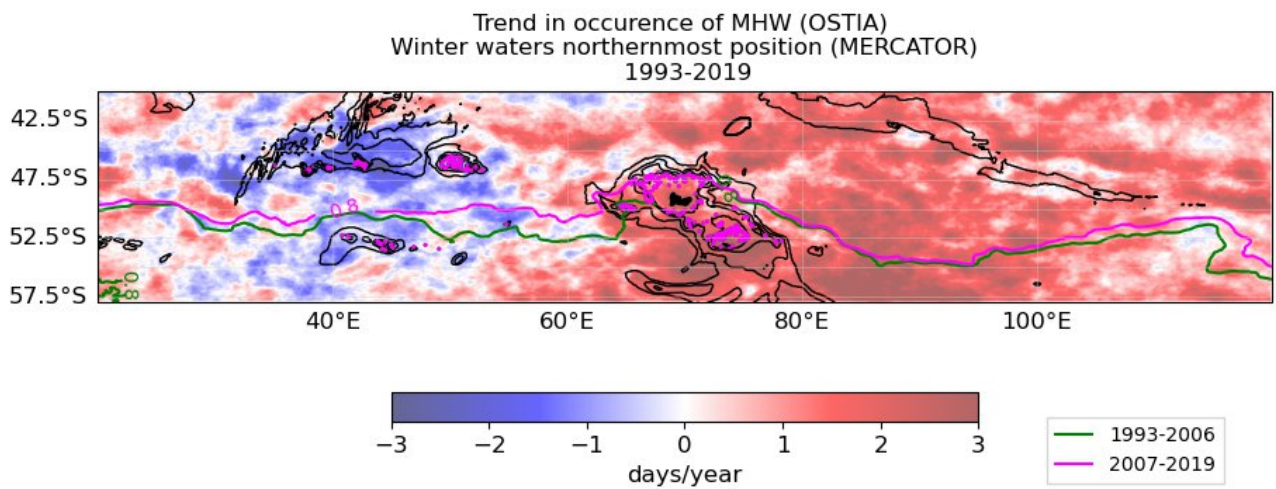
The eddy kinetic energy (EKE) at the location of each Argo profile is also estimated to better understand the link between mesoscale activity and MHW subsurface characteristics, using AVISO altimetry-derived geostrophic velocities : $EKE = \frac{1}{2} \cdot [(u - \underline{u})^2 + (v - \underline{v})^2]$ where u and v are the zonal and meridional geostrophic velocities respectively and \underline{u} and \underline{v} are their daily climatology (over 1993-2020).

Figure S5 : Comparison between the mean eddy kinetic energy in the location of the Argo profiles located in a marine heatwave (MHW; color) and outside a MHW (grey) by season. The seasons are : fall (March, April, May), winter (June, July, August), spring (September, October, November) and summer (December, January, February).



Supplementary Material S6: Decadal trends in MHWs and in the Polar Front position

Figure S6: Trend in the number of days affected by marine heatwaves per year using OSTIA sea surface temperatures between 1993 and 2019 and position of the northernmost limit of the 80% probability of presence of winter waters over 1993-2006 (green) and 2007-2019 (magenta), using MERCATOR reanalysis.



References used in Supplementary Materials

Andrews, M.B., Ridley, J.K., Wood, R.A., Andrews, T., Blockley, E.W., Booth, B., Burke, E., Dittus, A.J., Florek, P., Gray, L.J., Haddad, S., Hardiman, S.C., Hermanson, L., Hodson, D., Hogan, E., Jones, G.S., Knight, J.R., Kuhlbrodt, T., Misios, S., Mizielinski, M.S., Ringer, M.A., Robson, J., Sutton, R.T. (2020). Historical simulations with HadGEM3-GC3.1 for CMIP6 e2019MS001995. *J. Adv. Model. Earth Syst.* 12 (6) <https://doi.org/10.1029/2019MS001995>.

Artana, C., Ferrari, R., Bricaud, C., Lellouche, J.-M., Garric, G., Sennéchaël, N., Lee, J.-H., Park, Y.-H., & Provost, C. (2021). Twenty-five years of Mercator ocean reanalysis GLORYS12 at Drake Passage : Velocity assessment and total volume transport. *Advances in Space Research*, 68(2), 447-466. <https://doi.org/10.1016/j.asr.2019.11.033>

Argo (2000). Argo float data and metadata from Global Data Assembly Centre (Argo GDAC). SEANOE. <https://doi.org/10.17882/42182>

Bao, Y., Song, Z., and Qiao, F. (2020). FIO-ESM version 2.0: Model description and evaluation. *Journal of Geophysical Research: Oceans*, 125, e2019JC016036. <https://doi.org/10.1029/2019JC016036>

Belkin, I.M., and Gordon, A.L. (1996). Southern Ocean fronts from the Greenwich meridian. *Journal of Geophysical Research*, 101 (2), 3675-3696

Bost, C. A., Cotté, C., Terray, P., Barbraud, C., Bon, C., Delord, K., Gimenez, O., Handrich, Y., Naito, Y., Guinet, C., and Weimerskirch, H. (2015). Large-scale climatic anomalies affect marine predator foraging behaviour and demography. *Nature Communications*, 6(1), 8220. <https://doi.org/10.1038/ncomms9220>

Chen, D., M. Rojas, B.H. Samset, K. Cobb, A. Diongue Niang, P. Edwards, S. Emori, S.H. Faria, E. Hawkins, P. Hope, P. Huybrechts, M. Meinshausen, S.K. Mustafa, G.-K. Plattner, and A.-M. Tréguier, 2021: Framing, Context, and Methods. In *Climate Change 2021: The Physical Science Basis. Contribution of Working Group I to the Sixth Assessment Report of the Intergovernmental Panel on Climate Change* [Masson-Delmotte, V., P. Zhai, A. Pirani, S.L. Connors, C. Péan, S. Berger, N. Caud, Y. Chen, L. Goldfarb, M.I. Gomis, M. Huang, K. Leitzell, E. Lonnoy, J.B.R. Matthews, T.K. Maycock, T. Waterfield, O. Yelekçi, R. Yu, and B. Zhou (eds.)]. Cambridge University Press, Cambridge, United Kingdom and New York, NY, USA, pp. 147–286, doi:10.1017/9781009157896.003

Cherchi, A., Fogli, P.G., Lovato, T., Peano, D., Iovino, D., Gualdi, S., Masina, S., Scoccimarro, E., Materia, S., Bellucci, A., Navarra, A., (2019). Global mean climate and main patterns of variability in the CMCC-CM2 coupled model. *J. Adv. Model. Earth Syst.* 11 (1), 185–209. <https://doi.org/10.1029/2018MS001369>.

Christian, J.R., Denman, K.L., Hayashida, H., Holdsworth, A.M., Lee, W.G., Riche, O.G.J., Shao, A.E., Steiner, N., Swart, N.C. (2021). Ocean biogeochemistry in the Canadian Earth System Model version 5.0.3: CanESM5 and CanESM5-CanOE. *Geoscientific Model Development Discussions*, 1–68. doi: 10.5194/gmd-2021-327.

Dong, S., J. Sprintall, S. T. Gille, and L. Talley (2008), Southern Ocean mixed-layer depth from Argo float profiles. *J. Geophys. Res.*, 113, C06013, doi:10.1029/2006JC004051.

Dunne, J.P., Horowitz, L.W., Adcroft, A.J., Ginoux, P., Held, I.M., John, J.G., Krasting, J. P., Malyshev, S., Naik, V., Paulot, F., Shevliakova, E., Stock, C.A., Zadeh, N., Balaji, V., Blanton, C., Dunne, K.A., Dupuis, C., Durachta, J., Dussin, R., Gauthier, P. P.G., Griffies, S.M., Guo, H., Hallberg, R.W., Harrison, M., He, J., Hurlin, W., McHugh, C., Menzel, R., Milly, P.C.D., Nikonov, S., Paynter, D.J., Ploshay, J., Radhakrishnan, A., Rand, K., Reichl, B.G., Robinson, T., Schwarzkopf, D.M., Sentman, L.T., Underwood, S., Vahlenkamp, H., Winton, M., Wittenberg, A.T., Wyman, B., Zeng, Y., Zhao, M. (2020). The GFDL Earth System Model Version 4.1 (GFDL-ESM 4.1): overall coupled model description and simulation characteristics e2019MS002015. *J. Adv. Model. Earth Syst.* 12 (11) <https://doi.org/10.1029/2019MS002015>.

Elzahaby, Y., and Schaeffer, A. (2019). Observational Insight Into the Subsurface Anomalies of Marine Heatwaves. *Frontiers in Marine Science*, 6, 745. <https://doi.org/10.3389/fmars.2019.00745>

Eyring, V., Bony, S., Meehl, G. A., Senior, C. A., Stevens, B., Stouffer, R. J., and Taylor, K. E. (2016). Overview of the Coupled Model Intercomparison Project Phase 6 (CMIP6) experimental design and organization. *Geoscientific Model Development*, 9(5), 1937-1958. <https://doi.org/10.5194/gmd-9-1937-2016>

Good, S., Fiedler, E., Mao, C., Martin, M. J., Maycock, A., Reid, R., Roberts-Jones, J., Searle, T., Waters, J., While, J., and Worsfold, M. (2020). The Current Configuration of the OSTIA System for Operational Production of Foundation Sea Surface Temperature and Ice Concentration Analyses. *Remote Sensing*, 12(4), 720. <https://doi.org/10.3390/rs12040720>

Held, I.M., Guo, H., Adcroft, A., Dunne, J.P., Horowitz, L.W., Krasting, J., Shevliakova, E., Winton, M., Zhao, M., Bushuk, M., Wittenberg, A.T., Wyman, B., Xiang, B., Zhang, R., Anderson, W., Balaji, V., Donner, L., Dunne, K., Durachta, J., Gauthier, P.P.G., Ginoux, P., Golaz, J.-C., Griffies, S.M., Hallberg, R., Harris, L., Harrison, M., Hurlin, W., John, J., Lin, P., Lin, S.-J., Malyshev, S., Menzel, R., Milly, P.C.D., Ming, Y., Naik, V., Paynter, D., Paulot, F., Ramaswamy, V., Reichl, B., Robinson, T., Rosati, A., Seman, C., Silvers, L.G., Underwood, S., Zadeh, N. (2019). Structure and performance of GFDL's CM4.0 climate model. *J. Adv. Model. Earth Syst.* 11 (11), 3691–3727. <https://doi.org/10.1029/2019MS001829>.

Herger, N., Sanderson, B. M., and Knutti, R. (2015). Improved pattern scaling approaches for the use in climate impact studies. *Geophysical Research Letters*, 42(9), 9. <https://doi.org/10.1002/2015GL063569>

Hobday, A. J., Alexander, L. V., Perkins, S. E., Smale, D. A., Straub, S. C., Oliver, E. C. J., Benthuisen, J. A., Burrows, M. T., Donat, M. G., Feng, M., Holbrook, N. J., Moore, P. J., Scannell, H. A., Sen Gupta, A., and Wernberg, T. (2016). A hierarchical approach to defining marine heatwaves. *Progress in Oceanography*, 141, 227-238. <https://doi.org/10.1016/j.pocean.2015.12.014>

Kuhlbrodt, T., Jones, C.G., Sellar, A., Storkey, D., Blockley, E., Stringer, M., Hill, R., Graham, T., Ridley, J., Blaker, A., Calvert, D., Copsey, D., Ellis, R., Hewitt, H., Hyder, P., Ineson, S., Mulcahy, J., Siahann, A., Walton, J. (2018). The low-resolution version of HadGEM3 GC3.1: development and evaluation for global climate. *J. Adv. Model. Earth Syst.* 10 (11), 2865–2888. <https://doi.org/10.1029/2018MS001370>.

Kwiatkowski, L., Torres, O., Bopp, L., Aumont, O., Chamberlain, M., Christian, J. R., Dunne, J. P., Gehlen, M., Ilyina, T., John, J. G., Lenton, A., Li, H., Lovenduski, N. S., Orr, J. C., Palmieri, J., Santana-Falcón, Y., Schwinger, J., Séférian, R., Stock, C. A., ... Ziehn, T. (2020). Twenty-first century ocean warming, acidification, deoxygenation, and upper-ocean nutrient and primary production decline from CMIP6 model projections. *Biogeosciences*, 17(13), 3439-3470. <https://doi.org/10.5194/bg-17-3439-2020>

Lee, J.-Y., J. Marotzke, G. Bala, L. Cao, S. Corti, J.P. Dunne, F. Engelbrecht, E. Fischer, J.C. Fyfe, C. 1290 Jones, A. Maycock, J. Mutemi, O. Ndiaye, S. Panickal, and T. Zhou (2021). Future Global Climate: 1291 Scenario-Based Projections and NearTerm Information. In *Climate Change 2021: The Physical Science* 1292 Basis. Contribution of Working Group I to the Sixth Assessment Report of the Intergovernmental Panel 1293 on Climate Change [Masson-Delmotte, V., P. Zhai, A. Pirani, S.L. Connors, C. Péan, S. Berger, N. 1294 Caud, Y. Chen, L. Goldfarb, M.I. Gomis, M. Huang, K. Leitzell, E. Lonnoy, J.B.R. Matthews, T.K. 1295 Maycock, T. Waterfield, O. Yelekçi, R. Yu, and B. Zhou (eds.)]. Cambridge University Press, 1296 Cambridge, United Kingdom and New York, NY, USA, pp. 553–672, 1297 doi:10.1017/9781009157896.006

Lellouche, J.-M., Greiner, E., Le Galloudec, O., Garric, G., Regnier, C., Drevillon, M., Benkiran, M., Testut, C.-E., Bourdalle-Badie, R., Gasparin, F., Hernandez, O., Levier, B., Drillet, Y., Remy, E., & Le Traon, P.-Y. (2018). Recent updates to the Copernicus Marine Service global ocean monitoring and forecasting real-time 1/12° high-resolution system. *Ocean Science*, 14(5), 1093-1126. <https://doi.org/10.5194/os-14-1093-2018>

- Lovato, T., Peano, D., Butenschon, M., Materia, S., Iovino, D., Scoccimarro, E., Fogli, P. G., Cherchi, A., Bellucci, A., Gualdi, S., Masina, S., Navarra, A., (2022). CMIP6 simulations with the CMCC earth system model (CMCC-ESM2). e2021MS002814 *J. Adv. Model. Earth Syst.* 14 (3). <https://doi.org/10.1029/2021MS002814>
- Nie, Y., Uotila, P., Cheng, B., Massonnet, F., Kimura, N., Cipollone, A., & Lv, X. (2022). Southern Ocean sea ice concentration budgets of five ocean-sea ice reanalyses. *Climate Dynamics*. <https://doi.org/10.1007/s00382-022-06260-x>
- Nocedal, J., and Wright, S.J. (2006). Numerical Optimization. Springer New York.
- Park, Y.-H., and Gamberoni, L., (1993). Frontal Structure, Waters Masses and Circulation in the Crozet Basin. *Journal of Geophysical Research*, 98 (7), 12361-12385.
- Park, Y.-H., Charriaud, E., and Fieux, M. (1998). Thermohaline structure of the Antarctic Surface Water/Winter Water in the Indian sector of the Southern Ocean. *Journal of Marine Systems*, 17(1), 5-23. [https://doi.org/10.1016/S0924-7963\(98\)00026-8](https://doi.org/10.1016/S0924-7963(98)00026-8)
- Park, Y.-H., Durand, I., Kestenare, E., Rougier, G., Zhou, M., d'Ovidio, F., Cotté, C., and Lee, J.-H. (2014). Polar Front around the Kerguelen Islands: An up-to-date determination and associated circulation of surface/subsurface waters. *Journal of Geophysical Research: Oceans*, 119(10), 6575-6592. <https://doi.org/10.1002/2014JC010061>
- Pauthenet, E., Roquet, F., Madec, G., & Nerini, D. (2017). A Linear Decomposition of the Southern Ocean Thermohaline Structure. *Journal of Physical Oceanography*, 47(1), 29-47. <https://doi.org/10.1175/JPO-D-16-0083>.
- Pauthenet, E., Roquet, F., Madec, G., Guinet, C., Hindell, M., McMahon, C. R., Harcourt, R., and Nerini, D. (2018). Seasonal Meandering of the Polar Front Upstream of the Kerguelen Plateau. *Geophysical Research Letters*, 45(18), 9774-9781. <https://doi.org/10.1029/2018GL079614>
- Roquet, F., Williams, G., Hindell, M. A., Harcourt, R., McMahon, C., Guinet, C., Charrassin, J.-B., Reverdin, G., Boehme, L., Lovell, P., and Fedak, M. (2014). A Southern Indian Ocean database of hydrographic profiles obtained with instrumented elephant seals. *Scientific Data*, 1(1), 140028. <https://doi.org/10.1038/sdata.2014.28>
- Sabu, P., Libera, S. A., Chacko, R., Anilkumar, N., Subeesh, M. P., and Thomas, A. P. (2020). Winter water variability in the Indian Ocean sector of Southern Ocean during austral summer. *Understanding the link between atmospheric, physical and biogeochemical processes in the Indian sector of the Southern Ocean*, 178, 104852. <https://doi.org/10.1016/j.dsr2.2020.104852>

Séférian, R., Nabat, P., Michou, M., Saint-Martin, D., Voldoire, A., Colin, J., Decharme, B., Delire, C., Berthet, S., Chevallier, M., Sénési, S., Franchistéguy, L., Vial, J., Mallet, M., Joetzjer, E., Geoffroy, O., Gu'ér'emy, J.-F., Moine, M.-P., M'Sadek, R., Ribes, A., Rocher, M., Roehrig, R., Salas-y-M'elia, D., Sanchez, E., Terray, L., Valcke, S., Waldman, R., Aumont, O., Bopp, L., Deshayes, J., Ethé, C., and Madec, G. (2019). Evaluation of CNRM Earth System model, CNRM-ESM2-1: role of Earth system processes in present-day and future climate. *J. Adv. Model. Earth Syst.*, 11, 4182–4227. doi: 10.1029/2019MS001791.

Sellar, A. A., Jones, C. G., Mulcahy, J., Tang, Y., Yool, A., Wiltshire, A., O'connor, F. M., Stringer, M., Hill, R., Palmieri, J., Woodward, S., Mora, L., Kuhlbrodt, T., Rumbold, S., Kelley, D. I., Ellis, R., Johnson, C. E., Walton, J., Abraham, N. L., Andrews, M. B., Andrews, T., Archibald, A. T., Berthou, S., Burke, E., Blockley, E., Carslaw, K., Dalvi, M., Edwards, J., Folberth, G. A., Gedney, N., Griffiths, P.T., Harper, A. B., Hendry, M. A., Hewitt, A. J., Johnson, B., Jones, A., Jones, C. D., Keeble, J., Liddicoat, S., Morgenstern, O., Parker, R.J., Predoi, V., Robertson, E., Siahann, A., Smith, R. S., Swaminathan, R., Woodhouse, M.T., Zeng, G., Zerroukat, M. (2019). UKESM1: description and evaluation of the UK Earth System Model. *J. Adv. Model. Earth Syst.*, 11, 4513–4558. doi: 10.1029/2019MS001739.

Shu, Q., Song, Z., Bao, Y., Yang, X., Song, Y., Li, X., Wei, M. and Qiao, F. (2022). FIO-ESM v2.0 CORE2-forced experiment for the CMIP6 Ocean Model Intercomparison Project. *Acta Oceanol. Sin.* 41, 22–31. <https://doi.org/10.1007/s13131-022-2000-x>

Swart, N.C., Cole, J.N.S., Kharin, V.V., Lazare, M., Scinocca, J.F., Gillett, N.P., Anstey, J., Arora, V., Christian, J.R., Hanna, S., Jiao, Y., Lee, W.G., Majaess, F., Saenko, O.A., Seiler, C., Seinen, C., Shao, A., Sigmond, M., Solheim, L., von Salzen, K., Yang, D., Winter, B. (2019). The Canadian Earth System Model version 5 (CanESM5.0.3). *Geosci. Model Dev.* 12 (11), 4823–4873. <https://doi.org/10.5194/gmd-12-4823-2019>

Treasure, A. M., Roquet, F., Ansoorge, I. J., Bester, M. N., Boehme, L., Bornemann, H., Charrassin, J.-B., Chevallier, D., Costa, D. P., Fedak, M. A., Guinet, C., Hammill, M. O., Harcourt, R. G., Hindell, M. A., Kovacs, K. M., Lea, M.-A., Lovell, P., Lowther, A. D., Lydersen, C., McIntyre, T., McMahon, C.R., Muelbert, M.M.C., Nicholls, K., Picard, B., Reverdin, G., Trites, A.W., Williams, G.D., and de Bruyn, P. J. N. (2017). Marine Mammals Exploring the Oceans Pole to Pole : A Review of the MEOP Consortium. *Oceanography*, 30(2), 132-138.

Voltaire, A., Saint-Martin, D., S'eni, S., Decharme, B., Alias, A., Chevallier, M., Colin, J., Gu'ery, J.-F., Michou, M., Moine, M.-P., Nabat, P., Roehrig, R., Salas y M'elia, D., S'ef'rian, R., Valcke, S., Beau, I., Belamari, S., Berthet, S., Cassou, C., Cattiaux, J., Deshayes, J., Douville, H., Eth'e, C., Franchist'eguy, L., Geoffroy, O., L'evy, C., Madec, G., Meurdesoif, Y., Msadek, R., Ribes, A., Sanchez-Gomez, E., Terray, L., Waldman, R., (2019). Evaluation of CMIP6 DECK Experiments With CNRM-CM6-1. *J. Adv. Model. Earth Syst.* 11 (7), 2177–2213. <https://doi.org/10.1029/2019MS001683>.

Yukimoto, S., Kawai, H., Koshiro, T., Oshima, N., Yoshida, K., Urakawa, S., Tsujino, H., Deushi, M., Tanaka, T., Hosaka, M., Yabu, S., Yoshimura, H., Shindo, E., Mizuta, R., Obata, A., Adachi, Y., Ishii, M. (2019). The Meteorological Research Institute Earth System Model version 2.0, MRI-ESM2.0: Description and basic evaluation of the physical component. *J. Meteorol. Soc. Jpn* 97, 931–965. <https://doi.org/10.2151/jmsj.2019-051>.

Appendix C

**Supplementary Material Azarian
et al., in preparation**

Supplementary Material

Supplementary Material S1: Table of the variables considered as potential drivers of the circulation over the Kerguelen Plateau.

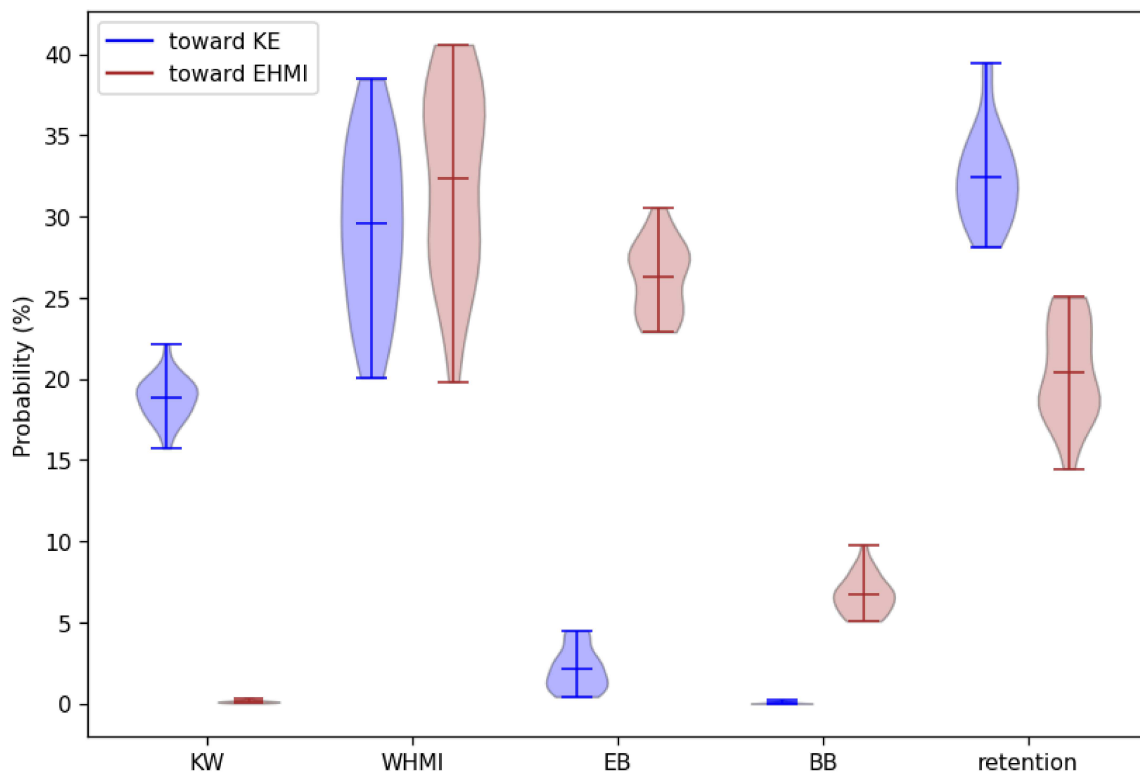
	Driver	Data
Wind action	<i>Total wind stress</i>	ERA5 reanalysis
	<i>Wind stress curl south of 52°S</i>	ERA5 reanalysis
	<i>Latitude of the maximum wind stress</i>	ERA5 reanalysis
	<i>Marshall's SAM index</i>	Station-based provided by NCAR
Polar Front Position	<i>Polar Front position west (winter waters definition)</i>	GLORYS12V1 MERCATOR reanalysis
	<i>Polar Front position east (winter waters definition)</i>	GLORYS12V1 MERCATOR reanalysis
	<i>Polar Front position west (-0.30 m absolute dynamic topography contour)</i>	Satellite observations (altimetry), product by CTOH and distributed by AVISO+
Antarctic Circumpolar Current Dynamics	<i>Zonal velocity through the Fawn Trough</i>	AVISO geostrophic velocities (altimetry)
	<i>Zonal velocity North of the Kerguelen Plateau</i>	AVISO geostrophic velocities (altimetry)
	Latitudinal position of the jet at the Fawn Trough	AVISO geostrophic velocities (altimetry)
	Latitudinal position of the jet North of the Kerguelen Plateau	AVISO geostrophic velocities (altimetry)
	Eddy kinetic energy	AVISO geostrophic velocities (altimetry)
Sea surface temperature	<i>Latitude of 2°C isotherm</i>	Observations (OSTIA)
	Sea surface temperature (SST)	Observations (OSTIA)
	<i>Previous summer SST</i>	Observations (OSTIA)
Sea ice dynamics	Sea ice extent	Satellite observations (from MET Norway)
Mixed layer depth	Mixed layer depth (MLD)	GLORYS12V1 MERCATOR reanalysis
	Previous summer MLD	GLORYS12V1 MERCATOR reanalysis

Supplementary Material S2: Table of the climate models used and scenarios associated. CMIP6 models outputs are available at : <https://esgf-node.llnl.gov/projects/cmip6/>.

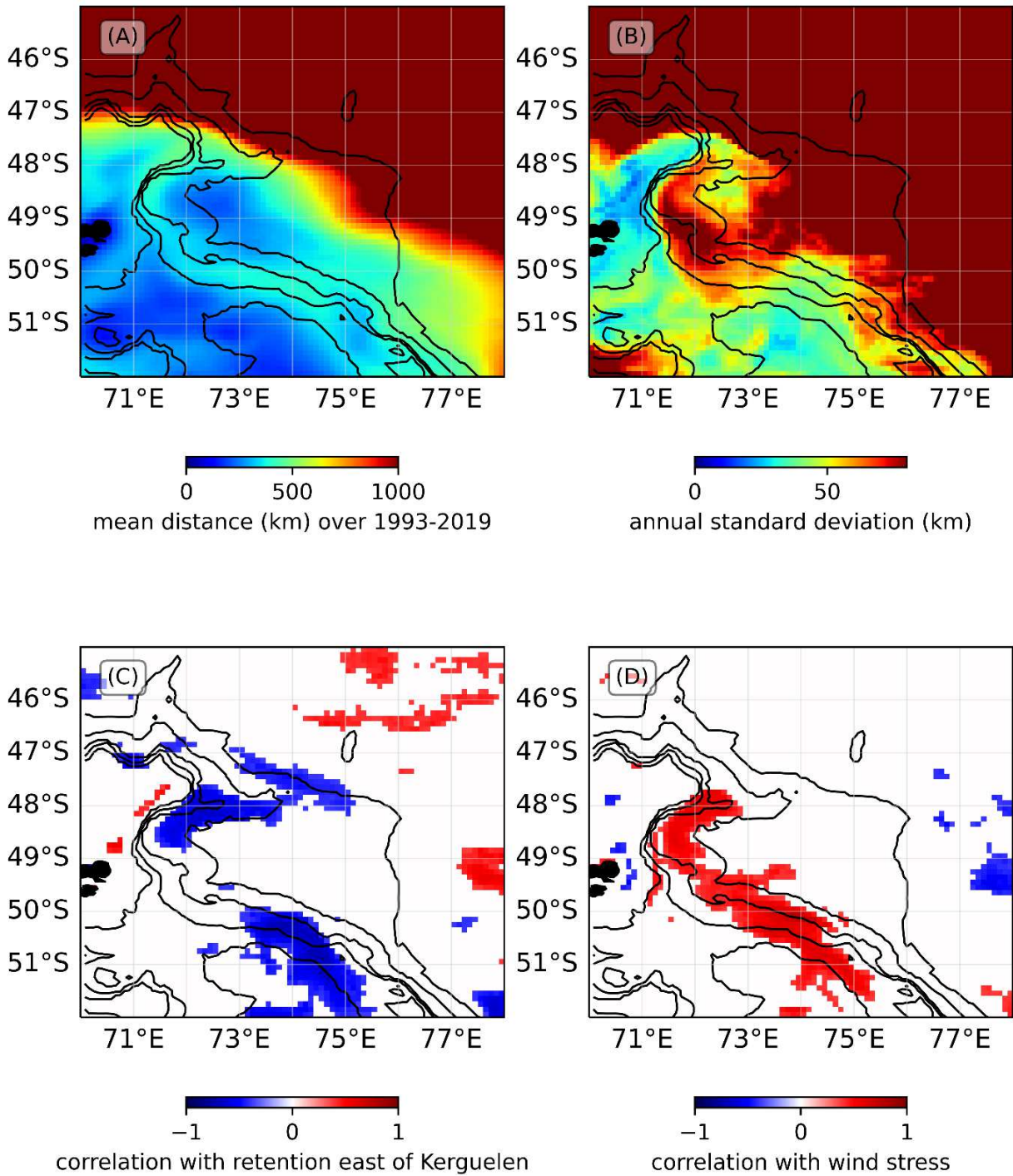
Models	Member	Experiment and/or scenario	References
ACCESS-CM2	rlilp1f1	Historical, ssp126, ssp245, ssp585	Bi et al 2020
ACCESS-ESM1-5	rlilp1f1	Historical, ssp126, ssp245, ssp585	Ziehn et al. (2019a, b) (Ziehn et al., 2020)
AWI-CM-1-1-MR	rlilp1f1	Historical, ssp126, ssp245, ssp585	Semmler et al., 2019
BCC-CSM2-MR	rlilp1f1	Historical, ssp126, ssp245, ssp585	Wu et al 2019
CanESM5	rlilp1f1	Historical, ssp126, ssp245, ssp585	Swart et al., 2019; Christian et al., 2021
CanESM5-CanOE	rlilp2f1	Historical, ssp126, ssp245, ssp585	Swart et al., 2019; Christian et al., 2021
CMCC-CM2-SR5	rlilp1f1	Historical, ssp126, ssp245, ssp585	Cherchi et al., 2019
CMCC-ESM2	rlilp1f1	Historical, ssp126, ssp245, ssp585	Lovato et al., 2022
CNRM-CM6-1	rlilp1f2	Historical, ssp126, ssp245, ssp585	Voltaire et al., 2019
CNRM-CM6-1-HR	rlilp1f2	Historical, ssp126, ssp245, ssp585	Voltaire et al., 2019
CNRM-ESM2-1	rlilp1f2	Historical, ssp126, ssp245, ssp585	Séférian et al., 2019
EC-Earth3	rlilp1f1	Historical, ssp126, ssp245, ssp585	Döscher et al., 2022
EC-Earth3-CC	rlilp1f1	Historical, ssp126, ssp245, ssp585	Döscher et al., 2022
EC-Earth3-Veg-LR	rlilp1f1	Historical, ssp126, ssp245, ssp585	Döscher et al., 2022
EC-Earth3-Veg	rlilp1f1	Historical, ssp126, ssp245, ssp585	Döscher et al., 2022
FIO-ESM-2-0	rlilp1f1	Historical, ssp126, ssp245, ssp585	Bao et al., 2020; Shu et al., 2022
GFDL-CM4	rlilp1f1	Historical, ssp245, ssp585	Held et al., 2019; Dunne et al., 2020
GFDL-ESM4	rlilp1f1	Historical, ssp126, ssp245, ssp585	Dunne et al., 2020
GISS-E2-1-G	rlilp1f2	Historical, ssp126, ssp245, ssp585	Kelley et al., 2020
HadGEM3-GC31-L	rlilp1f3	Historical, ssp126, ssp245, ssp585	Kuhlbrodt et al., 2018; Andrews et al., 2020
IITM-ESM	rlilp1f1	Historical, ssp126, ssp245, ssp585	Krishnan et al., 2019;2021
INM-CM5-0	rlilp1f1	Historical, ssp126, ssp245, ssp585	Volodin and Gritsun, 2020

IPSL-CM6A-LR	rlilp1f1	Historical, ssp126, ssp245, ssp585	(Boucher et al., 2020) Boucher et al. (2018, 2019)
KACE-1-0-G	rlilp1f1	Historical, ssp126, ssp245, ssp585	Byun et al., 2019
KIOST-ESM	rlilp1f1	Historical, ssp126, ssp245, ssp585	Kim et al., 2019
MCM-UA-1-0		Historical, ssp126, ssp245, ssp585	Stouffer et al., 2019
MIROC-E2SL	rlilp1f2	Historical, ssp126, ssp245, ssp585	(Hajima et al., 2020) Hajima et al. (2019); Tachiiri et al. (2019)
MIROC6	rlilp1f1	Historical, ssp126, ssp245, ssp585	Tatebe et al., 2019
MPI-ESM1-2-LR	rlilp1f1	Historical, ssp126, ssp245, ssp585	Mauritsen et al., 2019
MRI-ESM2-0	rlilp1f1	Historical, ssp126, ssp245, ssp585	Yukimoto et al., 2019
NESM3	rlilp1f1	Historical, ssp126, ssp245, ssp585	Cao et al., 2021
NorESM2-LM	rlilp1f1	Historical, ssp126, ssp245, ssp585	(Tjiputra et al., 2020) Seland et al. (2019a, b)
NorESM2-MM	rlilp1f1	Historical, ssp126, ssp245, ssp585	Seland et al., 2020
TaiESM1	rlilp1f1	Historical, ssp126, ssp245, ssp585	Lee et al., 2020 (Wang et al., 2021)
UKESM1-0-LL	rlilp1f2	Historical, ssp126, ssp245, ssp585	Sellar et al., 2019

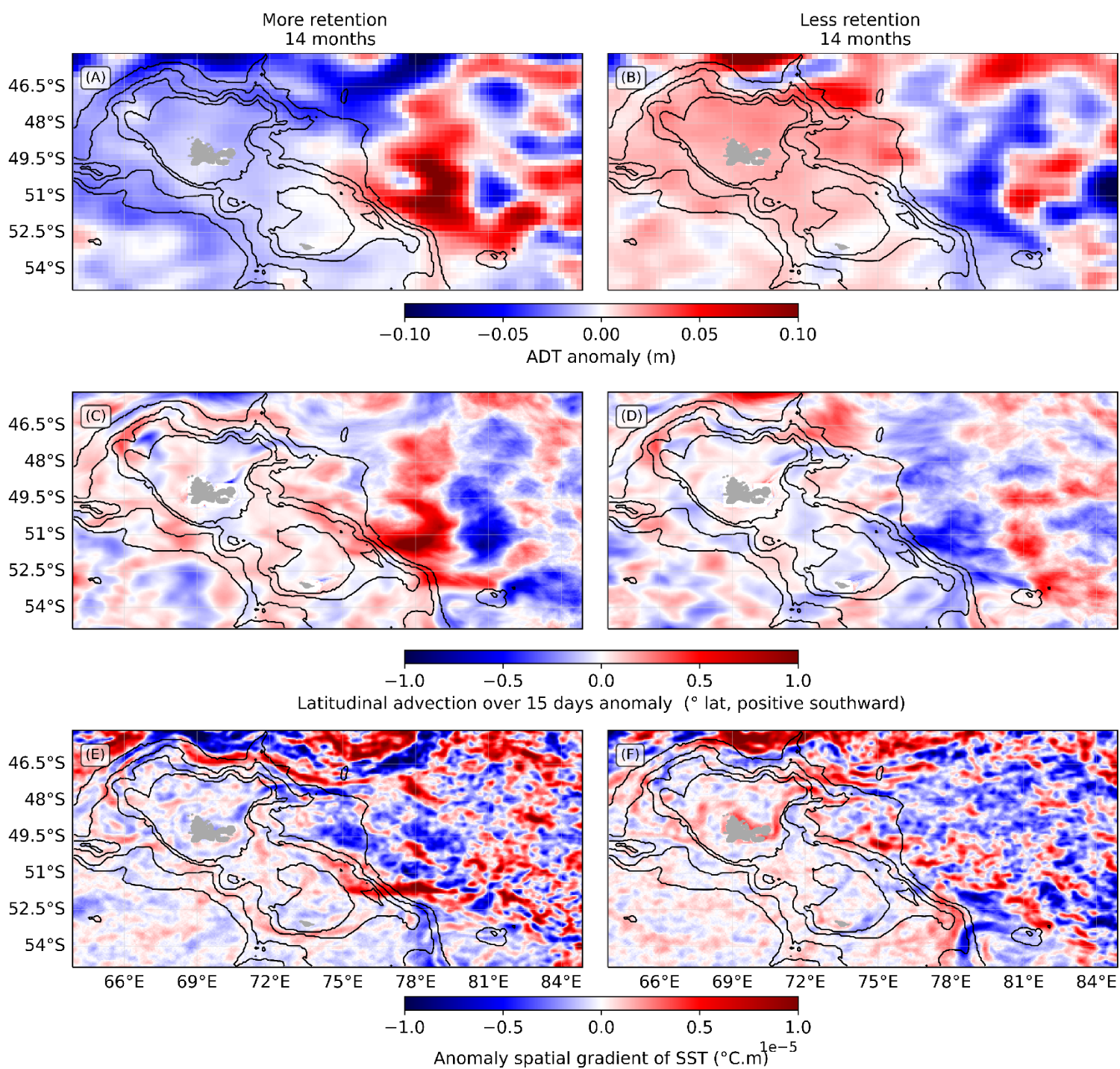
Supplementary Material S3: Probability of a water parcel leaving from one area - west of Kerguelen (KW), west of Heard (WHMI), Elan Bank (EB) or Banzarre Bank (BB) - to arrive east of Kerguelen (KE, blue) or to arrive east of Heard (EHMI, red; ‘connectivity’), or probability to remain in KE or EHMI (‘retention’) after 91 days (areas as defined on Figure 2).



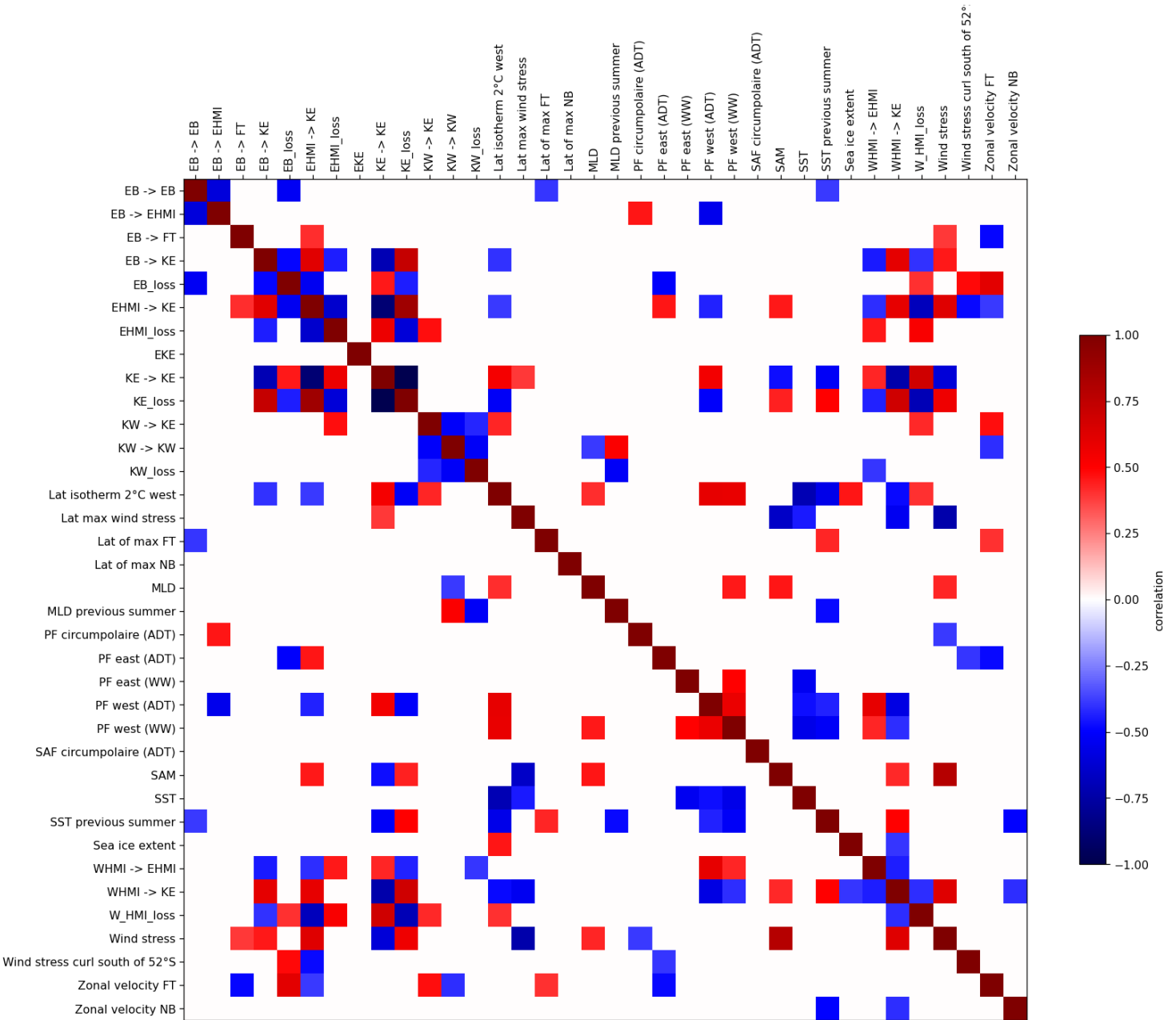
Supplementary Material S4: (A) Mean distance between initial and final positions based on 91-days backward trajectories over 1993 and 2019 and (B) its interannual variability. Pearson correlation between this distance metric and: the probability of remaining east of Kerguelen (KE_KE, see section 2.1; C) and wind stress (using ERA5 product; D) during the spawning period (June to October). Only correlations associated with a p-value<0.05 are shown on panels C and D.



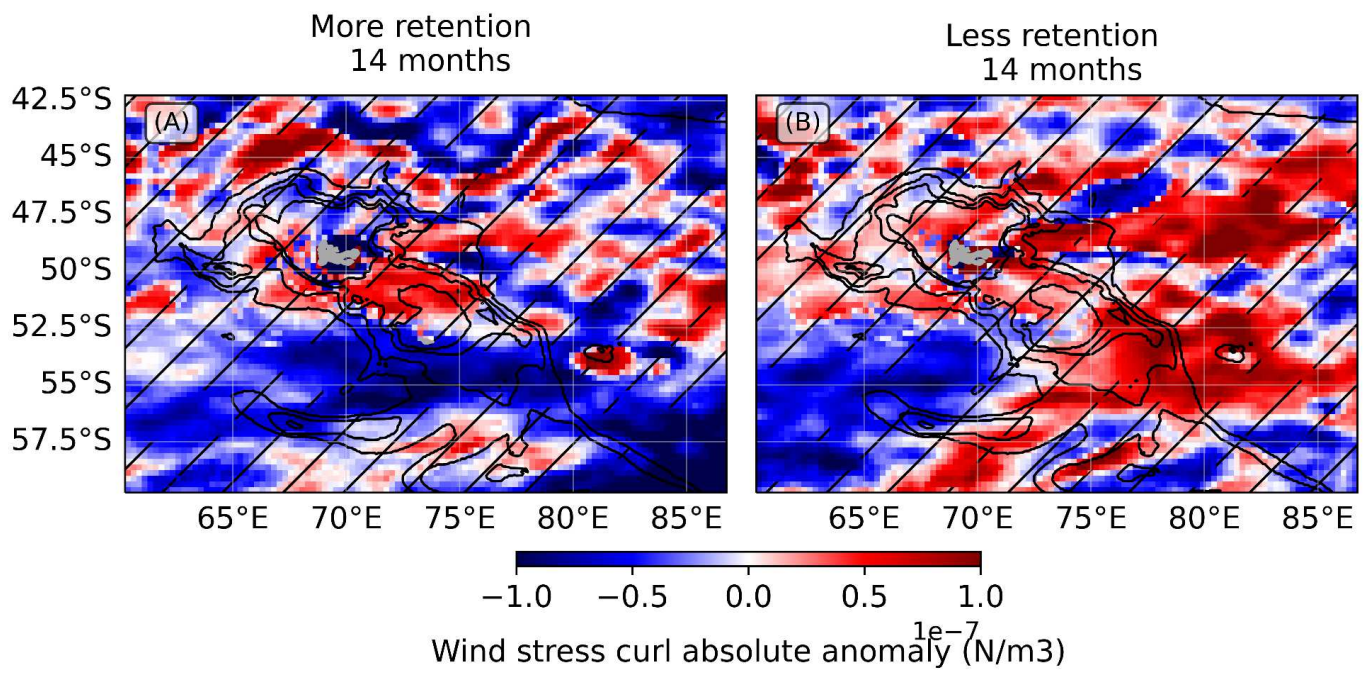
Supplementary Material S5: Composite anomaly of (A-B) absolute dynamic topography (ADT) anomaly from AVISO product, (C-D) latitudinal advection anomaly over 15 days using AVISO geostrophic velocities, and (E-F) SST spatial gradient norm anomaly based on the level of retention east of Kerguelen over 1993-2019. Composites during high (low) retention months are shown on left (right) panels.



Supplementary Material S6: Correlation matrix of detrended timeseries of connectivity, loss, retention indexes and the drivers introduced in Supplementary Material S1. Only Pearson correlations with a p-value<0.05 are shown.



Supplementary Material S7: Composite anomaly of the absolute wind stress curl (using ERA5 product) based on the level of retention east of Kerguelen (high retention A, low retention B). Hatched areas indicate where the average wind stress curl anomaly is lower than the standard deviation of randomly sampled 14-months averages.



Appendix D

**Syntheses on the implications of
climate change for the Patagonian
toothfish fishery management in
the Southern Indian Ocean**

Synthèse relative aux connaissances scientifiques sur la légine australe dans l'océan Indien Sud (*Dissostichus eleginoides*)

Par Clara Azarian, juillet 2023

Résumé

La légine australe (*Dissostichus eleginoides*) est un poisson démersal, c'est-à-dire vivant au fond de l'océan, parcourant diverses profondeurs au cours de son cycle de vie (200 – 2200 m) dans des conditions dites subantarctiques (**entre 2°C et 11°C**). La taille moyenne de la légine est de 70 cm et peut atteindre un peu plus de 2 m. C'est une **espèce à durée de vie longue** (35-50 ans). Le régime alimentaire de la légine australe est varié (ex. poissons, octopodes, calamars et crustacés). Cette espèce migre peu, bien que certains individus puissent se déplacer sur de grandes distances. De grandes incertitudes demeurent sur la biologie reproductive de cette espèce ce qui peut entraîner des biais dans l'évaluation de son stock. En outre, les impacts des variations de conditions environnementales sur cette espèce, notamment au début de son cycle de vie, restent incertains mais de nombreuses hypothèses peuvent être posées par analogie avec d'autres espèces.

I/ Cycle de vie

La légine australe est une **espèce à durée de vie longue** (35-50 ans, Nevinskii and Kozlov 2002) avec un cycle de vie parcourant diverses profondeurs.

Un poisson est dit mature lorsqu'il a la capacité de se reproduire, généralement à partir de 6 à 9 ans. La fécondité absolue de la légine australe est assez élevée comparée aux autres espèces de la famille des nototheniidés, allant de 48 000 à plus de 500 000 œufs par individu, en fonction de la taille de l'individu et de la localisation géographique (Collins et al., 2010). La ponte des larves s'effectue en profondeur (environ 1000 m) et en hiver **entre les mois de juin et d'octobre** sur le Plateau de Kerguelen (Agnew et al., 1999; Laptikhovskiy et al., 2006a; Lord et al., 2006; Arana, 2009). **Certains lieux de ponte importants ont été identifiés comme par exemple le banc Skiff ou le banc Elan** (Koubbi et al., 2016). Les œufs remontent alors à la surface (entre 0 et 200 m) et sont transportés par les courants marins locaux pendant 3 mois. Au bout de 3 mois les œufs éclosent, les larves résultantes continuent d'être soumises au courant, avec une mobilité relative, pendant encore 3 mois à l'issue desquels elles deviennent des juvéniles (Collins et al., 2010). Les larves et ensuite juvéniles évoluent dans des profondeurs inférieures à 300 m jusqu'à l'âge entre 6 et 7 ans puis, **avec l'âge, les individus vivent dans de plus en plus profondément dans l'océan** (Collins et al., 2010, Péron et al., 2016). Il est commun aux espèces démersales, vivant au fond de l'océan, que les premières phases du cycle de vie s'effectuent dans des eaux peu profondes pour des raisons de disponibilité de la nourriture, d'évitement de compétition ou de prédateurs ou même pour des raisons physiologiques (Macpherson and Duarte, 1991).

L'entrée des individus dans le stock ou « recrutement » constitue une étape cruciale dans l'évaluation des stocks car les premières étapes du cycle de vie de la légine sont associées à une plus forte sensibilité aux facteurs environnementaux et donc à une plus forte mortalité, ce qui peut significativement influencer l'état du stock. Le recrutement peut être très variable d'une année sur l'autre (Belchier et Collins, 2008). Toutefois, le début du cycle de vie de la légine est complexe à

étudier car il est encore difficile techniquement d'échantillonner des œufs ou des larves de cette espèce. Par comparaison avec d'autres espèces de poissons et notamment la légine antarctique, on peut supposer que **les larves dépendent fortement de leur environnement pour leur développement**, avec probablement une synchronisation entre le moment de leur ponte et les pics de productivité primaire aussi appelés « bloom de phytoplancton » (Koubbi et al., 2009; Young et al., 2014).

De nombreuses incertitudes demeurent sur la biologie reproductive de la légine. Des études menées aux îles Falkland montrent une **grande variabilité spatio-temporelle dans les cycles reproductifs de la légine** : tous les individus matures ne pondent pas nécessairement chaque année (Brown, 2011 ; Boucher et al., 2018). On observe que les jeunes individus matures peuvent ne pondre qu'un an sur deux et que la viabilité des œufs produits augmente avec l'âge et la taille de l'individu reproducteur. Ce phénomène de « saute » de la ponte (ou « skipping » en anglais) pourrait être lié à des conditions environnementales dégradées et/ou des difficultés à se nourrir (Rideout 2005 ; Brown, 2011 ; Rideout and Tomkiewicz, 2011) et n'est pas négligeable : **sur une année, une grande proportion de la population de légine peut ne pas se reproduire** (ex. aux îles Falkland, Boucher et al., 2018). Dans le cas des îles Falkland, cette variabilité pourrait être due à une plus grande variabilité des conditions environnementales à la limite nord de la distribution de légine australe (Brown, 2011). Cette irrégularité de la ponte n'est actuellement pas prise en compte dans l'estimation de la biomasse reproductrice, qui tend alors à être surestimée.

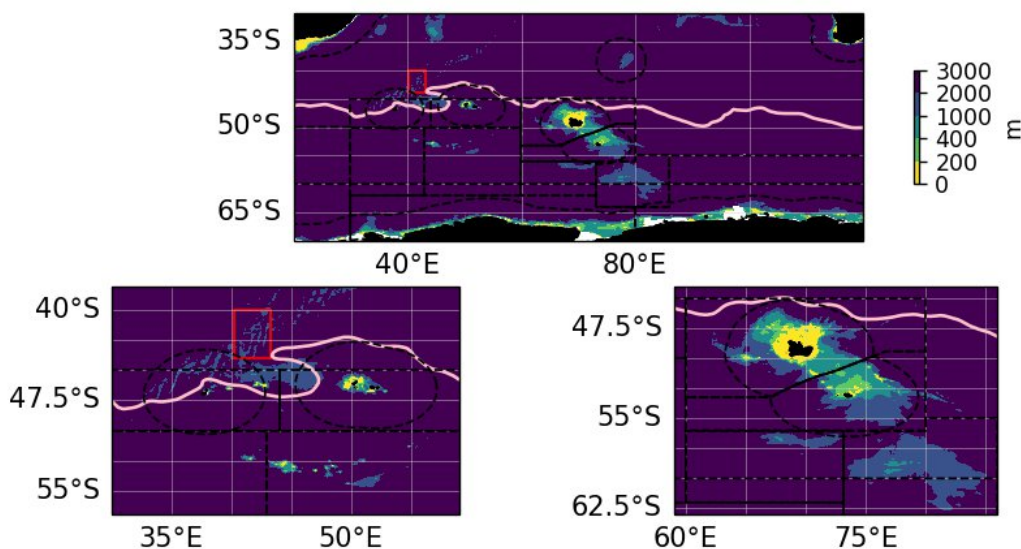


Figure 1: Bathymétrie de l'océan indien sud (panel haut) et zooms sur les régions de Crozet (panel gauche) et sur le Plateau de Kerguelen (panel droit ; source : produit de réanalyse MERCATOR mis à disposition par Copernicus Marine Service). Chaque étape du cycle de vie de la légine est associée à une plage de profondeur (ex. profondeurs inférieures à 300 m jusqu'à 6 à 7 ans). Le front subantarctique (SAF) est indiqué en rose (source : Park and Durand, 2019). La zone South Indian Ridge que l'APSOI souhaite réguler à l'avenir pour la pêche à la légine (en plus de Del Cano et Williams' Ridge) est indiquée en rouge.

II. Connectivité des stocks

Bien que la légine soit considérée comme un poisson **relativement sédentaire** (Appleyard et al., 2002 ; Marlow et al., 2003 ; Williams and Lamb, 2002), de larges déplacements d'adultes ont déjà pu être observés. En effet, les adultes évoluent en profondeur dans des conditions environnementales (ex. température) relativement stables, adoptant un régime alimentaire opportuniste mais ils peuvent migrer pour leur reproduction et ils ont la **capacité de migrer sur de grandes distances** (parfois plus de 2500 km, Welsford et al., 2007, 2011).

Les programmes de capture-marquage-recapture et les connaissances sur la circulation océanique dans la région (Figure 2) permettent de mettre en évidence la connectivité entre certaines zones. Certaines études génétiques montrent aussi l'existence d'échanges entre l'ensemble des stocks de l'Indien sud (Appleyard et al, 2002, 2003). Toutefois, la quantification précise des flux entre stocks (que ce soit par migration des adultes ou transport des larves) reste difficile à évaluer. Il n'est pas évident que ces flux soient suffisants pour compenser des pertes de biomasse d'un stock à l'autre.

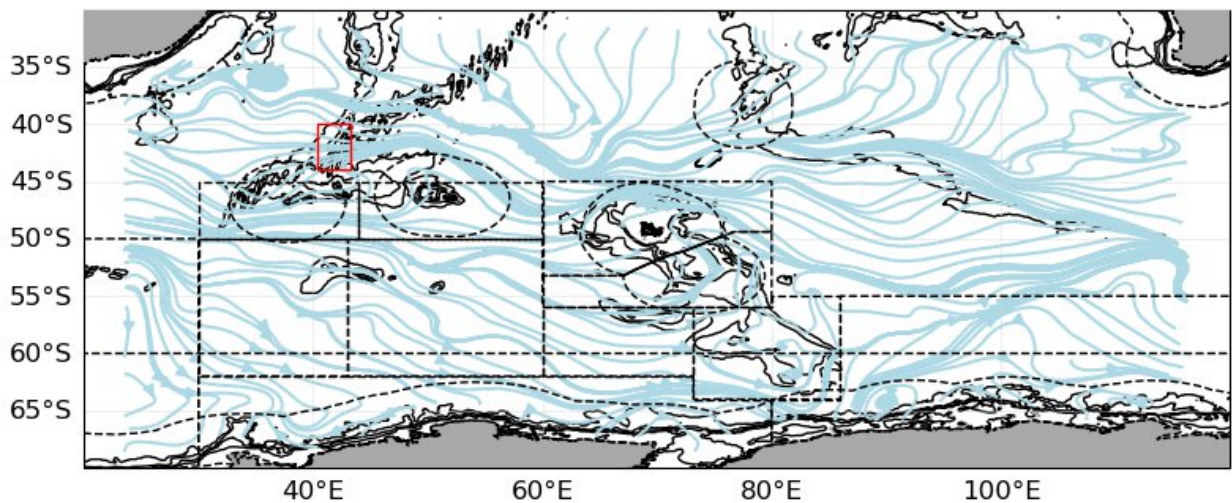


Figure 2 : Connectivité par les courants océaniques dans l'océan Indien sud. Les lignes bleues représentent les lignes de courant moyennes (principalement d'ouest en est) en utilisant les vitesses de courant déterminées à partir d'observations satellites (produit AVISO entre 1993 et 2019). Les contours des zones économiques exclusives et de la CCAMLR sont représentés en noir pointillé. La zone South Indian Ridge que l'APSOI souhaite réguler à l'avenir pour la pêche à la légine (en plus de Del Cano et Williams' Ridge) est indiquée en rouge.

Sur le Plateau de Kerguelen

Au niveau du Plateau de Kerguelen, les poissons marqués se déplacent principalement sur des courtes distances mais ils peuvent parfois sortir de la zone de gestion sur de plus grandes distances (e.g. Burch et al., 2019). Certains paramètres dans le modèle d'évaluation des stocks ont été adaptés pour corriger le biais qui peut être induit par de faibles flux migratoires, notamment entre les zones économiques exclusives (ZEEs) australiennes et françaises (cf. Burch et al., 2017).

Outre par l'éventuelle migration d'adultes, la connectivité entre les stocks peut aussi provenir du **transport des phases œufs et larvaires, déterminé par les courants océaniques locaux** (Figure 2). Le courant océanique principal dans la région, appelé Courant Circumpolaire Antarctique, est particulièrement fort et circule d'ouest en est.

D'autres courants, plus faibles, sur le Plateau de Kerguelen, induisent un transport du sud vers le nord du Plateau (Park et al., 2009). Les principales zones de ponte pour les stocks français et australiens du Plateau de Kerguelen se situent alors à l'ouest et au sud du Plateau (Figure 3), avec un **succès de recrutement plus élevé pour les zones de ponte à l'ouest** (Welsford et al., 2012 ; Mori et al., 2016 ; Yates et al., 2018).

A noter que le Courant Circumpolaire Antarctique permet aussi une connectivité entre les stocks de Crozet et Kerguelen (Figure 2 ; Zhu et al., 2021).

Entre les stocks en haute mer et les stocks français

Del Cano Rise est un relief topographique situé entre la zone 3b de l'Accord relatif aux Pêches de dans le Sud de l'Océan Indien (APSOI) et la ZEE de Crozet. Depuis 2019, l'APSOI réglemente la pêche à Del Cano Rise dans sa juridiction. Les caractéristiques de ce stock et de celui de Crozet devraient être similaires compte tenu de leur grande proximité géographique. **A noter que la bathymétrie dans la zone Del Cano Rise de l'APSOI est plus profonde que 1000 m et il est donc très peu probable que le stock soit renouvelé par un recrutement local. Il semble plus cohérent qu'il y ait une migration d'adultes de Crozet vers cette zone de l'APSOI.** Il pourrait y avoir théoriquement à Del Cano Rise des zones de ponte, les œufs et larves étant ensuite transportés par le courant vers le Plateau de Crozet mais ceci nécessiterait d'être confirmé par des observations sur le terrain.

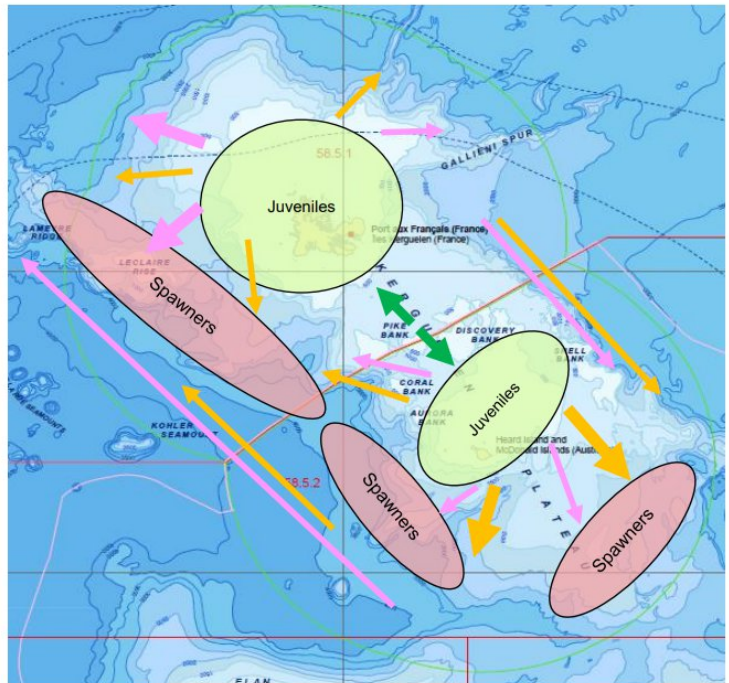
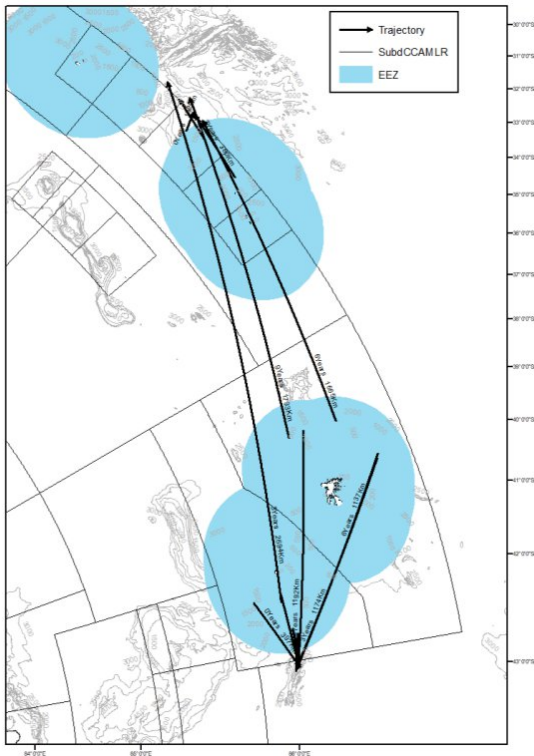


Figure 3: Distribution géographique des adultes reproducteurs ("spawners") et des juvéniles sur le Plateau de Kerguelen. Déplacements des mâles (flèches orange) et des femelles (flèches roses) et migrations des poissons sur le Plateau entre les stocks français et australien (flèches vertes ; source : Ziegler et al., 2019, SC-04-21).



Les stocks des bancs Ob et Lena peuvent aussi être connectés aux stocks de Crozet et de Kerguelen (cf. livret 6 rapport annuel de pêche australe 2022). Les rendements observés par les navires français et japonais aux bancs Ob et Lena sont faibles et ont entraîné l'arrêt du plan de recherche associé à cette zone.

Des déplacements entre des zones CCAMLR et APSOI ont aussi été observés sur quelques individus adultes (Figure 4) mais les facteurs explicatifs de telles migrations de longue distance ne sont pas entièrement connus à ce jour.

Figure 4: Exemples de trajectoires observées reliant des zones de la CCAMLR à des zones de l'APSOI en traversant les ZEE australiennes et françaises à partir de techniques de marquage-recapture (figures issues de WG-FSA-2019/45).

III. Comportements et position dans le réseau trophique

Comportements

La légine australe est un animal **relativement solitaire**, qui tend à éviter ses congénères et qui **migre peu**, probablement du fait de la faible quantité de muscle permettant aux poissons une nage lente et soutenue (Collins et al., 2010). Certains déplacements ont pu être observés, potentiellement en lien avec des comportements reproducteurs ou alimentaires (Boucher et al., 2018).

Proies

Le régime alimentaire de la légine australe est diversifié et varie en fonction de la localisation géographique et au cours du cycle de vie (Collins et al., 2010). Les juvéniles sont le plus souvent piscivores, ciblant les espèces les plus abondantes localement. Les adultes sont des carnivores opportunistes (ex. poissons, octopodes, calamars et crustacés). Certaines observations suggèrent que les adultes peuvent aussi montrer des comportements de charognards ou -de cannibalisme.

Prédateurs

A de faibles profondeurs, les légines juvéniles sont les proies des manchots (Brown and Klages, 1987; Goldsworthy et al., 2001), des otaries (Green et al., 1989; Reid and Arnould, 1996) et des éléphants de mer (Green et al., 1989; Reid and Nevitt, 1998; Slip, 1995). Toutefois, au fur et à mesure qu'ils croissent et vivent plus en profondeur, **le nombre de prédateurs potentiels diminue** (principalement des cachalots).

Parasites

Les légines peuvent également être infectées par des **communautés de parasites dont la composition et la distribution varient géographiquement et avec la profondeur**. La taille d'un individu de légine peut déterminer le type de parasite le plus probable de l'infecter (Brickle et al., 2005 ; Brickle et al., 2006).

IV. Potentiels impacts des conditions environnementales sur les stocks de légine

Les conditions environnementales peuvent impacter les stocks de légine à différents niveaux (habitat, croissance, mortalité, fécondité, comportement). Ces différents impacts sont liés aux différentes contraintes physiologiques de la légine en fonction de son âge et de sa taille. Les facteurs pouvant avoir un effet métabolique sur les poissons sont principalement : **la température et l'oxygène**.

Habitat

Contrairement à la légine antarctique, la légine australe ne dispose pas de protéines anti-gel lui permettant de vivre dans des conditions de température en-dessous des 2°C. Le domaine habitable par la légine pourrait alors potentiellement s'étendre plus au sud avec le réchauffement climatique. L'existence d'une limite maximale de température limitant l'extension au nord de la légine australe a été suggérée, cette limite pouvant être marquée par la présence du front subantarctique (López-Abellán, 2005 ; voir la limite du front subantarctique sur la Figure 1). **Il n'est donc pas évident de prévoir si la zone habitable pour la légine adulte va plutôt s'étendre, se déplacer ou se réduire** (à noter que la zone habitable pour les juvéniles est contrainte par la présence d'eaux peu profondes et est donc fortement liée à la présence de plateaux, voir Figure 1).

L'habitat de la légine australe peut aussi être contraint par la distribution de ses proies et prédateurs. Une étude utilisant les données des pêcheries françaises et australiennes sur le Plateau de Kerguelen entre 1997 et 2018 montre que les facteurs environnementaux (ex. intensité des vents, température) modulent fortement la dynamique du réseau trophique dans cette région (Subramaniam et al., 2020).

Impacts physiologiques

Des températures plus chaudes peuvent avoir différents impacts sur les individus et les stocks. Une corrélation entre des températures plus chaudes et un recrutement de juvéniles plus faible, ce qui se traduit par un stock réduit, a pu être observée en Géorgie du Sud (Belchier et Collins, 2008). Il n'est pas clair si cette corrélation est due à un effet des conditions environnementales sur les premiers stades biologiques ou s'il s'agit d'une conséquence de l'effet de la température sur la fécondité des adultes. Les changements de température peuvent en effet engendrer des contraintes métaboliques **affectant la croissance et la fécondité des individus matures**. La légine australe est une espèce ectotherme, c'est-à-dire dont la température peut moduler des processus métaboliques comme la

croissance et la fécondité, les deux processus pouvant être en compétition en termes d'allocation d'énergie. L'étude des tailles de légine en Géorgie du Sud et aux îles Sandwich suggère que la taille des individus augmente avec la latitude et sous des températures plus froides (Soeffker et al., 2022). Sous des conditions « froides », la maturité est retardée, laissant plus de temps aux individus pour croître ce qui permet une fécondité accrue. Au contraire, **sous des conditions plus chaudes, la croissance est plus rapide et la fécondité diminue** (Brown, 2011 ; Yates et al., 2019 pour la légine antarctique). La taille des œufs produits peut aussi être influencée par la température : les œufs sont le plus souvent plus gros (et donc plus résistants) dans des conditions plus froides, mais des œufs plus gros peuvent aussi résulter en une fécondité plus faible (Laptikhovsky et al., 2006b ; Brown, 2011).

La température pourrait aussi impacter les comportements de reproduction des adultes. Il est possible que certains adultes évitent de pondre lors d'années chaudes (Collins et al., 2010). Toutefois, de tels comportements observés dans diverses régions (Everson and Murray, 1999 ; Arana et al., 2009 ; Brown et al., 2013) **sont le plus souvent attribués à une alimentation déficiente et à un mauvais état nutritionnel** (Rideout, 2005 ; Rideout and Tomkiewicz, 2011). La température peut alors parfois servir de « proxy » de l'état de l'écosystème ; par exemple, dans le cas de l'étude en Géorgie du Sud de 2008, il a été suggéré que des températures plus froides étaient associées à un recrutement en krill plus élevé et donc la présence de proies de meilleures qualités permettant un succès reproducteur plus important (Murphy et al., 2007 ; Belchier et Collins, 2008)

Les processus métaboliques sont aussi sensibles à la quantité d'oxygène disponible. L'océan austral est un océan riche en oxygène mais cette quantité d'oxygène disponible diminue avec le changement climatique (près de 16 % de la perte mondiale d'oxygène au cours des 50 dernières années ; Levin et al., 2018). En outre, la légine australe est un poisson qui a évolué dans le contexte d'un environnement stable et qui **peut donc être sensible même à de faibles variations en oxygène** (Lee et al., 2021). Le potentiel impact de ces variations de quantité d'oxygène avec le changement climatique sur les individus de légine n'a pas encore été évalué.

A retenir

- La légine australe est une espèce évoluant à **toutes les profondeurs** au cours de son cycle de vie (surface à ~2200m).
- Le début du cycle de vie de la légine (œufs, larves, juvéniles) s'effectue dans des eaux peu profondes au niveau de Plateaux (**habitat contraint par la bathymétrie**).
- La phase de « **recrutement** » (i.e. entrée dans le stock), qui **peut varier fortement** dans le temps et dans l'espace sous l'effet des conditions environnementales, est cruciale pour assurer la pérennité du stock.
- La légine est une espèce qui **migre peu** (territoriale) mais qui est capable de se déplacer sur de longue distance si besoin (parfois plus de 2500 km).
- De nombreuses incertitudes demeurent sur la biologie reproductive de cette espèce : **cela peut conduire à une surestimation de la biomasse reproductrice** dans les modèles d'évaluation des stocks.

Références

- Appleward, S., Ward, R., and Williams, R. (2002). Population structure of the Patagonian toothfish around Heard, McDonald and Macquarie Islands. *Antarctic Science*, 14(4), 364-373. doi:10.1017/S0954102002000238
- Appleward, S., Williams, R. and Ward, R. (2003). Fine scale genetic investigation into Patagonian toothfish structure within the west indian ocean sector of the southern ocean. WG-FSA-03/66
- Agnew, D. J., Heaps, L., Jones, C., Watson, A., Berkietta, K. and Pearce, J. (1999). Depth distribution and spawning pattern of *Dissostichus eleginoides* at South Georgia. *CCAMLR Science* 6, 19– 36.
- Arana, P. (2009). Reproductive aspects of the Patagonian toothfish (*Dissostichus eleginoides*) off southern Chile. *Latin American Journal of Aquatic Research*, 37(3), 381-393.
- Belchier, M., and Collins, M. A. (2008). Recruitment and body size in relation to temperature in juvenile Patagonian toothfish (*Dissostichus eleginoides*) at South Georgia. *Marine Biology*, 155, 493-503.
- Boucher, E. M. (2018). Disentangling reproductive biology of the Patagonian toothfish *Dissostichus eleginoides*: skipped vs obligatory annual spawning, foraging migration vs residential life style. *Environmental Biology of Fishes*, 101(9), 1343-1356.
- Brickle, P., MacKenzie, K., and Pike, A. (2005). Parasites of the Patagonian toothfish, *Dissostichus eleginoides* Smitt 1898, in different parts of the sub-Antarctic. *Polar Biol.* 28, 663–671.
- Brickle, P., MacKenzie, K., and Pike, A. (2006). Variations in the parasite fauna of the Patagonian toothfish (*Dissostichus eleginoides* Smitt, 1898), with length, season, and depth of habitat around the Falkland Islands. *J. Parasitol.* 92, 282–291.
- Brown, C. R., and Klages, N. T. (1987). Seasonal and annual variation in diets of macaroni (*Eudyptes chrysolophus chrysolophus*) and southern rockhopper (*E. chrysocome chrysocome*) penguins at sub-Antarctic Marion Island. *J. Zool.* 212, 7–28.
- Brown, J. (2011). Ecology and life history of a deepwater notothenid, *Dissostichus eleginoides* Smitt 1989, around the Falkland Islands, SW Atlantic Ocean. PhD thesis from the University of Aberdeen. <https://ethos.bl.uk/OrderDetails.do?uin=uk.bl.ethos.540485>
- Brown, J., Brickle, P. and Scott, B. (2013). Investigating the movements and behaviour of Patagonian toothfish (*Dissostichus eleginoides* Smitt, 1898) around the Falkland Islands using satellite linked archival tags. *Journal of Experimental Marine Biology and Ecology.* 443. 65–74. 10.1016/j.jembe.2013.02.029.
- Burch P., Ziegler, P., Welsford, D. and Péron, C. (2017). Estimation and correction of migration-related bias in the tag-based stock assessment of Patagonian toothfish in Division 58.5.2. CCAMLR WGSAM-17/11
- Burch, P., Péron, C., Potts, J., Ziegler, P., and Welsford, D. (2019). Estimating Patagonian toothfish (*Dissostichus eleginoides*) movement on the Kerguelen Plateau: reflections on 20 years of tagging at Heard Island and McDonald Islands. *Second Kerguelen Plateau Symposium: marine ecosystem and fisheries: 237-245.*

- Collins, M. A., Brickle, P., Brown, J., and Belchier, M. (2010). The Patagonian toothfish: biology, ecology and fishery. *Advances in marine biology*, 58, 227-300.
- Everson, I., and Murray, A. W. A. (1999). Size at sexual maturity of Patagonian toothfish. *CCAMLR Sci.* 6, 37–46.
- Goldsworthy, S. D., He, X., Tuck, G. N., Lewis, M., and Williams, R. (2001). Trophic interactions between the Patagonian toothfish, its fishery, and seals and seabirds around Macquarie Island. *Mar. Ecol. Prog. Ser.* 218, 283–302.
- Green, K., Burton, H. R., and Williams, R. (1989). The diet of Antarctic fur seals *Arctocephalus gazella* (Peters) during the breeding season at Heard Island. *Antarct. Sci.* 1, 317–324.
- Koubbi, P., Duhamel, G., Hecq, J-H., et al (2009). Ichthyoplankton in the neritic and coastal zone of Antarctica and Subantarctic islands: A review. *J Mar Syst* 78:547–556. doi: 206 10.1016/j.jmarsys.2008.12.024
- Koubbi, P., Guinet, C., Alloncle, N., Amziane, N., Azam, C.-S., Baudena, A., Bost, C., Romain, C., Chazeau, C., Coste, G., Cotte, C., F, D., Karine, D., Duhamel, G., A, F., Gasco, N., Hautecoeur, M., Lehodey, P., Lo Monaco, C., and Weimerskirch, H. (2016). Ecoregionalisation of the Kerguelen and Crozet islands oceanic zone. Part I: Introduction and Kerguelen oceanic zone. *CCAMLR-WG-EMM-16/43*.
- Laptikhovskiy, V., Arkhipkin, A., and Brickle, P. (2006a). Distribution and reproduction of the Patagonian toothfish *Dissostichus eleginoides* Smitt around the Falkland Islands. *Journal of Fish Biology*, 68(3), 849-861.
- Laptikhovskiy, V. (2006b). Latitudinal and bathymetric trends in egg size variation: a new look at Thorson's and Rass's rules. *Marine Ecology*, 27: 7-14. <https://doi.org/10.1111/j.1439-0485.2006.00077.x>
- Lee, B., Arkhipkin, A., and Randhawa, H. S. (2021). Environmental drivers of Patagonian toothfish (*Dissostichus eleginoides*) spatial-temporal patterns during an ontogenetic migration on the Patagonian Shelf. *Estuarine, Coastal and Shelf Science*, 259, [107473]. <https://doi.org/10.1016/j.ecss.2021.107473>
- Levin, L. A. (2018). Manifestation, drivers, and emergence of open ocean deoxygenation. *Annu. Rev. Mar. Sci* 10, 229–260.
- López-Abellán, L. (2005). Patagonian toothfish in international waters of the southwest Indian Ocean (Statistical Area 51). *CCAMLR science journal of the Scientific Committee and the Commission for the Conservation of Antarctic Marine Living Resources*. 12. 207-214.
- Lord, C., Duhamel, G., and Pruvost, P. (2006). The patagonian toothfish (*Dissostichus eleginoides*) fishery in the Kerguelen Islands (Indian Ocean sector of the Southern Ocean). *CCAMLR Science*, 13, 1-25.
- Macpherson, E., and Duarte, C. M. (1991). Bathymetric trends in demersal fish size: is there a general relationship?. *Marine Ecology Progress Series*, 103-112.

- Marlow, T. R., Agnew, D. J., Purves, M. G., and Everson, I. (2003). Movement and growth of tagged *Dissostichus eleginoides* around South Georgia and Shag Rocks (Subarea 48.3). *CCAMLR Sci.* 10, 101–111.
- Mori, M., Corney, S., Melbourne-Thomas, J., Welsford, D., Klocker, A., and Ziegler, P. (2016). Using satellite altimetry to inform hypotheses of transport of early life stage of Patagonian toothfish on the Kerguelen Plateau. *Ecological Modelling.* 340. 45-56. 10.1016/j.ecolmodel.2016.08.013.
- Murphy, E.J., Watkins, J.L., Trathan, P.N., Reid, K., Meredith, M.P., Thorpe, S.E. et al (2007) Spatial and temporal operation of the Scotia Sea eco system: a review of large-scale links in a krill centred food web. *Philos Trans R Soc B* 362:113–148. doi:10.1098/rstb.2006.1957
- Nevinskii, M. M., and Kozlov, A. N. (2002). The fecundity of the patagonian toothfish *Dissostichus eleginoides* around South Georgia Island (South Atlantic). *Journal of Ichthyology*, 42(7), 548-550.
- Péron, C., Welsford, D. C., Ziegler, P., Lamb, T. D., Gasco, N., Chazeau, C., ... And Duhamel, G. (2016). Modelling spatial distribution of Patagonian toothfish through life-stages and sex and its implications for the fishery on the Kerguelen Plateau. *Progress in Oceanography*, 141, 81-95.
- Péron, C., Chazeau, C., Faure, J., Gasco, N., Martin, A., Massiot-Granier, F., Pruvost, P., Rajaonalison, F., and Selles, J. (2022). Rapport « Données statistiques de pêche des navires français et étrangers dans les zones économiques exclusives des îles Kerguelen, Crozet et Saint-Paul/Amsterdam et les eaux internationales CCAMLR et APSOI. Convention Ministère de l'Agriculture et de la Souveraineté Alimentaire (Direction générale des affaires maritimes, de la pêche et de l'aquaculture, DGAMPA) et Muséum National d'Histoire Naturelle.
- Reid, K., and Arnould, J. P. Y. (1996). The diet of Antarctic fur seals *Arctocephalus gazella* during the breeding season at South Georgia. *Polar Biol.* 16, 105–114.
- Reid, K., and Nevitt, G. A. (1998). Observation of southern elephant seal, *Mirounga leonina*, feeding at sea near South Georgia. *Mar. Mamm. Sci.* 14, 637–640.
- Rideout, R. M., Rose, G. A., and Burton, M. P. (2005). Skipped spawning in female iteroparous fishes. *Fish and Fisheries*, 6(1), 50-72.
- Rick M. Rideout and Jonna Tomkiewicz (2011) Skipped Spawning in Fishes: More Common than You Might Think, *Marine and Coastal Fisheries*, 3:1, 176-189, DOI: 10.1080/19425120.2011.556943
- Soeffker, M., Hollyman, P.R., Collins, M.A., Hogg, O.T., Riley, A., Laptikhovskiy, V., Earl, T., Roberts, J., MacLeod, J.E., Belchier, M., and Darby, C. (2022). Contrasting life-history traits of two toothfish (*Dissostichus* spp.) species at their range edge around the South Sandwich Islands, *Deep Sea Res. Part II*, 201,105098.
- Subramaniam, R. C., Melbourne-Thomas, J., Corney, S. P., Alexander, K., Péron, C., Ziegler, P., et al. (2020). Time-dynamic food web modeling to explore environmental drivers of ecosystem change on the Kerguelen Plateau. *Front. Mar. Sci.* 7:641. doi: 10.3389/fmars.2020.00641.
- Welsford, D., Lamb, T., and Nowara, G.B.,(2007). Overview and update of Australia's scientific tagging program in the Patagonian toothfish (*Dissostichus eleginoides*) fishery in the vicinity of Heard and McDonald Islands (Division 58.5.2). CCAMLR document WG-FSA-07/48. 9 p. Hobart: CCAMLR.

- Welsford, D., Candy, S., Lamb, T., Nowara, G., Constable, A., and Williams, R. (2011). Habitat use by Patagonian toothfish (*Dissostichus eleginoides* Smitt, 1898) on the Kerguelen Plateau around Heard Island and the McDonald Islands. *Cybium: international journal of ichthyology*. 35. 125-136. [10.26028/cybium/2011-35SP-013](https://doi.org/10.26028/cybium/2011-35SP-013).
- Welsford, D., Nowara, G., Mclvor, J. and Candy, S. (2012). The spawning dynamics of Patagonian toothfish in the Australian EEZ at Heard Island and the McDonald Islands and their importance to spawning activity across the Kerguelen Plateau.
- Williams, R. and Lamb, T. (2002). Behaviour of *dissostichus eleginoides* fitted with archival tags at Heard Island : preliminary results. WG-FSA-02/60.
- Yates, P., Ziegler, P., Welsford, D., Mclvor, J., Farmer, B. and Woodcock, E. (2018), Spatio-temporal dynamics in maturation and spawning of Patagonian toothfish *Dissostichus eleginoides* on the sub-Antarctic Kerguelen Plateau. *J Fish Biol*, 92: 34-54. <https://doi.org/10.1111/jfb.13479>
- Yates, P., Ziegler, P., Welsford, D., Wotherspoon, S., Burch, P., and Maschette, D. (2019). Distribution of Antarctic toothfish *Dissostichus mawsoni* along East Antarctica: environmental drivers and management implications. *Fish. Res.* 219:105338. doi: 10.1016/j.fishres.2019.105338
- Young, E. F., Thorpe, S. E., Banglawala, N., and Murphy, E. J. (2014), Variability in transport pathways on and around the South Georgia shelf, Southern Ocean: Implications for recruitment and retention, *J. Geophys. Res. Oceans*, 119, 241–252, doi:10.1002/2013JC009348.
- Zhu, G.P., Yang, D. and Wei, L. (2021). Comparing otolith shape of Patagonian toothfish (*Dissostichus eleginoides*) between the Kerguelen Islands and the Crozet Islands, East Antarctic. WG-FSA-2021/54

Synthèse relative aux réglementations et à la gestion de la légine australe

Par Clara Azarian, juillet 2023

Résumé

La pêche à la légine australe est gérée dans l'océan indien sud par différents acteurs : par les Terres Australes et Antarctiques Françaises (TAAF) dans les zones économiques exclusives (ZEEs) de Crozet et Kerguelen ; par la Commission pour la conservation de la faune et la flore marines de l'Antarctique (CCAMLR) dont les règles sont suivies également dans la ZEE australienne des îles Heard et McDonald ; et par l'Accord des Pêches du Sud de l'Océan Indien (APSOI) qui est une organisation régionale de gestion des pêches. Cette gestion initialement co-construite entre les TAAF et la CCAMLR est parmi les plus précautionneuses au monde, adoptant également des mesures de protection de l'écosystème. La gestion au sein de l'APSOI est plus récente et lacunaire mais elle est aussi en développement, avec de fortes influences de la CCAMLR pour la stratégie de gestion dans une optique d'harmonisation des pratiques. La gestion de la légine australe est précautionneuse avec certaines mesures démontrant déjà une certaine flexibilité des réglementations (ex. possibilité de fermetures temporaires). Toutefois la prise en compte du changement climatique comme une menace potentielle pour la durabilité du stock reste absente des cadres de gestion des TAAF et de l'APSOI. Des travaux sont en cours dans le cadre de la CCAMLR pour opérationnaliser cette prise de conscience et pourraient inspirer des évolutions des cadres réglementaires de la CCAMLR mais aussi des TAAF et de l'APSOI afin d'assurer la durabilité des pêcheries de légine australe dans un contexte de changement climatique.

Les objectifs de cette synthèse :

- Rappeler les principes de la gestion actuelle de la légine australe.
- Résumer et comparer les objectifs de gestion et les mesures adoptées par les différents gestionnaires.
- Évaluer la prise en compte du risque climatique dans la gestion de la légine australe.

I. Une gestion multi-acteurs des stocks de légine

La légine australe dans l'océan Indien Sud est gérée par des acteurs très différents en termes de statuts juridique, d'objectifs généraux et de parties prenantes. Les principaux gestionnaires considérés ici sont la préfecture des **Terres Australes et Antarctiques Françaises** sur les zones économiques exclusives (ZEE) de Crozet et Kerguelen, la **Commission pour la conservation de la faune et la flore marines de l'Antarctique** (CCAMLR) incluant en particulier ici pour la gestion de la légine australe la ZEE australienne de Heard et McDonald et l'**Accord des Pêches du Sud de l'Océan Indien** (APSOI) qui n'a pour le moment adopté des mesures de gestion pour la légine australe qu'en des zones spécifiques (et non pas à l'échelle de son zonage, en vert sur la Figure 1) : Del Cano Rise et William's Ridge (Figure 1).

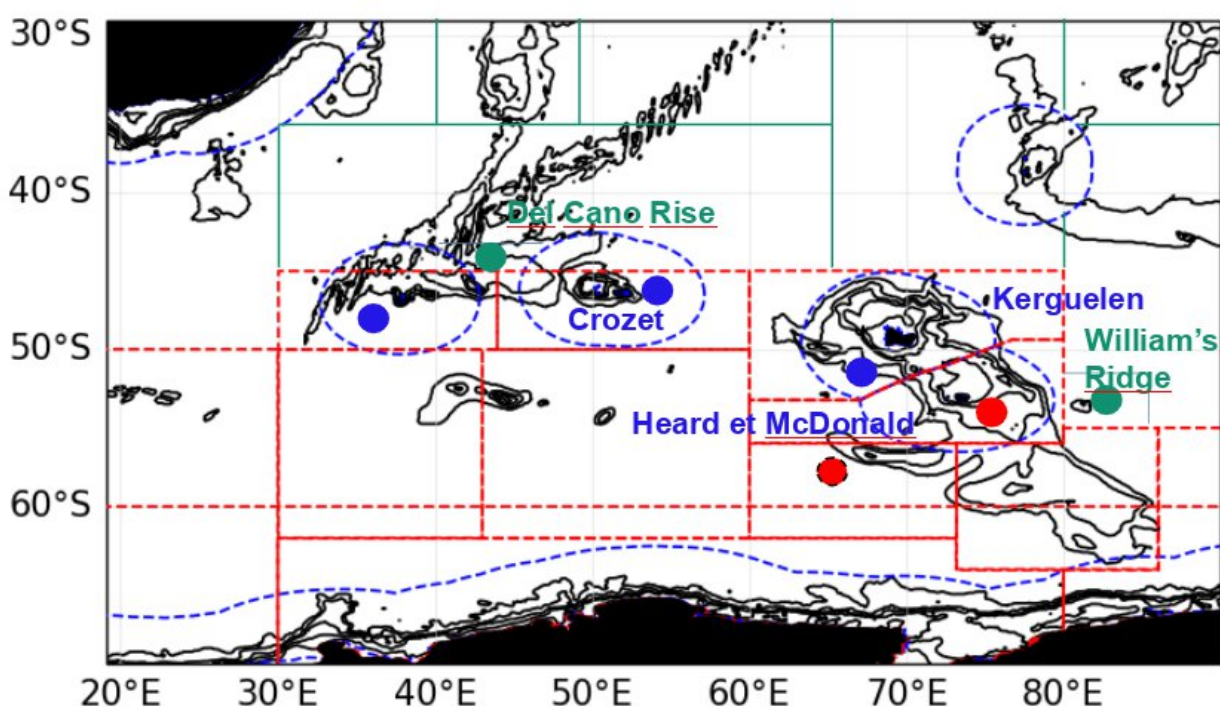


Figure 1: Frontières juridiques de gestion : zones économiques exclusives (en bleu), CCAMLR (en rouge) et APSOI (en vert). Les points de couleur marquent la présence de pêche à la légine régulée dans ces zones (bleu pour ZEE, rouge pour CCAMLR et vert pour APSOI), les pointillés autour d'un point marquent la présence d'une pêcherie exploratoire.

La légine australe est pêchée depuis la fin des années 1970 en zone CCAMLR (dont la Convention a été établie en 1982). La plus ancienne pêcherie à la légine australe dans le secteur indien de l'océan austral est celle de Kerguelen qui a débuté dans le **milieu des années 1980**, d'abord au chalut, puis à la palangre au début des années 1990 (Kock, 2000 ; Duhamel et al., 2006). De la pêche illícite, non déclarée et non réglementée (INN) se pratique dans la région depuis 1996 mais a été ensuite fortement réduite au niveau des TAAF et des zones CCAMLR grâce à des actions de surveillance accrue, l'appréhension des pêcheurs et des mesures économiques pour réduire la rentabilité de cette pêche INN. La mise en place de système de quotas a permis la stabilisation du niveau de capture (Figure 2)

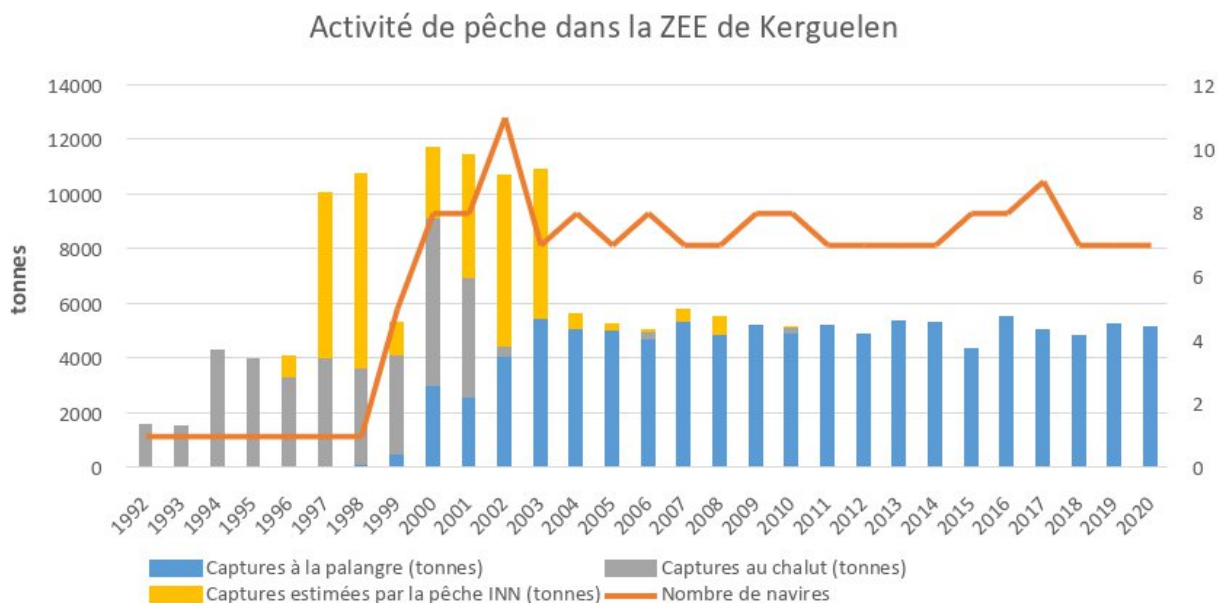


Figure 2: Captures de légine australe entre 1992 et 2020 dans la zone économique exclusive de Kerguelen (incluant des estimations de captures par la pêche INN) et nombre de navires de pêche. (données: https://fishdocs.ccamlr.org/FishRep_KI_TOP_2020.html)

Le développement des règles de gestion de la légine australe des TAAF et de la CCAMLR s'est effectué en parallèle avec des influences mutuelles entre les deux instances. Bien que la France soit membre de la CCAMLR et que le champ d'application de cette convention puisse couvrir les ZEE de Kerguelen et de Crozet, la France bénéficie d'un statut particulier qui lui confère pour ces ZEE le droit d'appliquer les mesures de conservation de la CCAMLR uniquement **sur une base volontaire** (Déclaration du Président). Par souci de transparence, la France communique à la CCAMLR ses évaluations de stocks de légine australe.

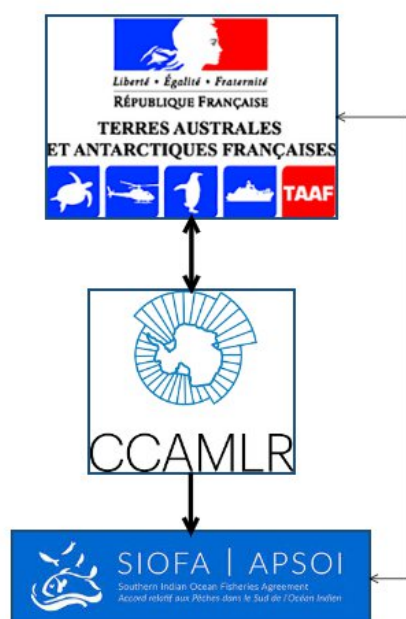
La gestion de la pêche à la légine australe par l'APSOI est plus récente (depuis 2019) et ses règles sont encore en construction, permettant ainsi une **forte influence des règles de la CCAMLR** sur cette organisation régionale de gestion des pêches. On note par exemple dans les recommandations du comité scientifique de l'APSOI d'adopter les mêmes objectifs de gestion pour la légine australe qu'à la CCAMLR. Ainsi, malgré la nature très différente de ces organismes de gestion (Tableau 1), **un effort d'harmonisation de certaines pratiques est mené**.

Cette harmonisation est d'autant plus nécessaire que certains stocks sont connectés (cf. synthèse scientifique). Les zones de gestion établies dans le cadre de l'APSOI sont importantes **pour atténuer d'éventuels impacts négatifs de la pêche aux abords de la ZEE de Crozet sur le stock de cette ZEE**. Le comité scientifique de l'APSOI a noté en mars 2022 l'existence d'une zone de pêche à la légine australe en dehors de la zone de gestion de Del Cano Rise mais dans une zone limitrophe. La réunion des parties de l'APSOI en juillet 2023 a adopté l'élargissement de la zone de Del Cano Rise mais pas l'établissement d'une nouvelle zone plus au nord-ouest comme recommandé par le comité scientifique (« South Indian Ridge » ; cf. rapport des pêches de 2022 ; rapport SC8 APSOI). L'établissement de cette zone de gestion devrait intervenir lors de la réunion annuelle de 2024.

Tableau 1: Définition et principal objectif des gestionnaires de la légine australe dans l'océan Indien sud.

	Définition	Objectif premier
Terres Australes et Antarctiques Françaises (TAAF)	Collectivité <i>sui generis</i> française créée par la loi du 6 août 1955	Sous l'autorité d'un préfet, cette administration assure des missions de souveraineté , de soutien à la recherche scientifique , de préservation de la biodiversité, et de logistique
Commission/Convention pour la conservation de la faune et la flore marines de l'Antarctique (CCAMLR)	Commission internationale formée de 27 Membres et de 10 autres pays qui ont adhéré à la Convention (depuis 1982)	D'après l'article 2 de cette Convention : « La présente Convention a pour objectif la conservation des ressources marines vivantes de l'Antarctique. Aux fins de la Convention, le terme "conservation" comprend la notion d'utilisation rationnelle.»
Accord des Pêches du Sud de l'Océan Indien (APSOI)	Organisation régionale de gestion des pêches dont l'accord est entré en vigueur en 2012, et qui est formée de 10 parties contractantes	D'après l'article 2 de cet accord, ce-dernier a pour objectif « d'assurer la conservation à long terme et l'utilisation durable des ressources halieutiques dans la Zone par la coopération entre les Parties contractantes et de promouvoir le développement durable des pêches dans la Zone, en tenant compte des besoins des États en développement riverains de la Zone qui sont Parties contractantes au présent Accord, en particulier les moins avancés d'entre eux et les petits États insulaires en développement ».

Influences entre les institutions à partir des textes réglementaires et historique des relations



Influences entre les institutions à partir de la connectivité physique entre les stocks gérés

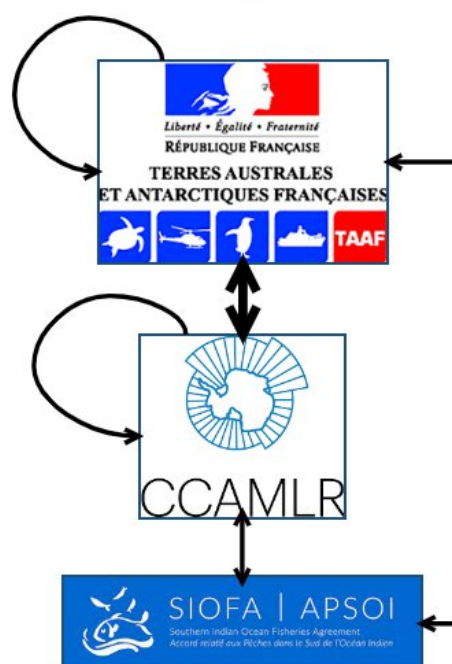


Figure 3: Schéma de principe illustrant les deux types de connectivité entre les gestionnaires: celle déterminée dans les textes réglementaires et de part leur évolution historique (à gauche) et celle du fait de la connectivité physique entre les stocks gérés (à droite). A noter que les flèches courbées sur un même gestionnaire

représentent la connectivité entre des stocks géographiquement distincts mais gérés par ce même gestionnaire. L'épaisseur des flèches représente l'intensité de la connectivité.

II - Objectifs de gestion

Que ce soit au sein de la CCAMLR, des TAAF ou de l'APSOI, les objectifs de gestion visent à assurer la durabilité de la ressource pour son exploitation. Assurer la durabilité de la ressource signifie permettre un renouvellement continué du stock, permettant sa stabilité dans le temps.

En ce sens, l'objectif de gestion vise à conserver une biomasse reproductrice de légine australe suffisante pour permettre un recrutement stable. **L'objectif de la CCAMLR est de conserver 50% de la biomasse reproductrice (par rapport à son niveau avant exploitation) à l'échelle de 35 ans.** A cela s'ajoute une cible pour éviter un déclin trop important de la biomasse. Les deux objectifs sont formulés sous forme probabiliste pour limiter les risques de ne pas les atteindre du fait de la variabilité introduite dans l'estimation du recrutement :

- Pas plus de 50% de probabilité d'atteindre une biomasse reproductrice inférieure à 50% de la biomasse reproductrice pré-exploitation.
- Pas plus de 10% de probabilité d'obtenir une biomasse reproductrice inférieure à 20% de la biomasse reproductrice pré-exploitation.

Les TAAF, par principe de **précaution**, ont fixé la cible à 60% de la biomasse reproductrice pré-exploitation (référence aussi notée « Bo ») au lieu de 50%. Ce principe de précaution est appliqué du fait d'incertitudes sur le modèle quant aux taux de déprédation élevés et du risque élevé de pêche INN ou extérieure aux ZEE pouvant impacter les stocks. Cet objectif ainsi que celui, comme pour la CCAMLR, de limiter la probabilité d'être inférieur à 20% de biomasse reproductrice, opérationnalisent l'objectif de gestion plus général : « **Conserver une biomasse reproductrice de légine australe à l'échelle de 35 ans suffisamment forte, pour préserver un capital reproducteur de l'espèce** face à tout type d'impact négatif sur la ressource (forte déprédation, pression de pêche illicite, non déclarée et non réglementée (INN), etc.) » mais contribuent également à l'objectif socio-économique : « Apporter de la **stabilité et de la visibilité** pour les acteurs économiques, en leur assurant une **pérennité** et en prenant en compte les lourds investissements requis dans la pêcherie » (plan de gestion de la légine australe des TAAF, 2019-2025).

Cet objectif est plus précautionneux que les objectifs adoptés pour d'autres gestions de la légine australe ou même dans le cadre des organisations régionales de gestion des pêches en général. Dans le cas des îles Falklands (Royaume-Uni) et des îles Prince Edward (Afrique du Sud), les objectifs sont fixés respectivement entre 40 et 45% et à 40% de la biomasse pré-exploitation (Brandao et Butterworth, 2017 ; Skeljo et al., 2022). Dans le cas de la gestion de la légine australe au Chili, l'objectif a été fixé à 50% de la biomasse associée à un rendement maximum durable (« Bmsy ») mais le stock est considéré comme épuisé (biomasse reproductrice estimée à 19% de Bo en 2018¹). Dans le cadre des organisations régionales de gestion des pêches, les points de référence cibles (« target reference point ») s'appuient le plus souvent sur le concept de rendement maximum durable ou RMD (« maximum sustainable yield » ou « MSY »), c'est-à-dire le niveau de prélèvement maximum de la ressource sans déplétion de long terme. Les objectifs de gestion peuvent alors cibler la biomasse associée à ce RMD (« Bmsy ») ou la mortalité due à la pêche qui permet de maintenir la biomasse au niveau de la

¹ Subsecretaria de Pesca y Acuicultura 2018. Acta del Comité de manejo de bacalao. Sesión n°06 – 2018, 12 y 13 de Septiembre de 2018.

« Bmsy » (« Fmsy »). Des travaux ont montré que la « Bmsy » correspond à environ 1/4 de la biomasse pré-exploitation et suivre la « Fmsy » conduirait à doubler le taux de mortalité actuelle due à la pêche (SC-CCAMLR-38/15).

Cependant, l'origine de cette valeur seuil de 50% de la biomasse pré-exploitation ne se fonde pas sur une compréhension fine de la dynamique de population de la légine australe. C'est une **valeur théorique**, qui, étant donné la gestion mondiale des pêches, semble précautionneuse, afin d'assurer un renouvellement du stock (Kock et al., 2000). Cet objectif inédit présente comme avantage d'être **robuste face à des changements de structure de la population** (changements dans la distribution des tailles ; SC-CAMLR-38/15) **mais il n'est pas adapté en cas de changement de productivité du stock**. Si la biomasse reproductrice d'équilibre réelle du stock diminue mais la biomasse reproductrice de référence est inchangée, alors l'objectif de gestion reste théoriquement atteint mais le TAC estimé n'est plus adapté et il y a un risque de surestimation de la productivité du stock (voir synthèse sur le changement climatique).

La gestion par l'APSOI s'est mise en place plus récemment, en 2019. Un objectif important sous-tendant la gestion de la légine australe dans cette instance est d'assurer une collaboration et complémentarité avec les mesures mises en place par la CCAMLR et de veiller à ce que la mortalité par la pêche dans les zones de Williams Ridge et Del Cano Rise « n'entraîne pas un dépassement des niveaux de capture biologiquement durables, compte tenu des liens entre les populations » (CMM 2021/15). Contrairement aux TAAF et à la CCAMLR qui ont des points de référence cibles fondés sur la biomasse, l'objectif de gestion actuel de l'APSOI mentionne des objectifs fondés sur la mortalité mais sans objectif opérationnel clairement identifié. Le quota de 55 tonnes à Del Cano Rise avait été adopté en 2019 sur la base des captures moyennes dans la région entre 2003 et 2015. Depuis, de récentes études suggèrent que cette valeur est plus élevée que le taux de capture historique moyen (SERAWG-02-11, 2020). Lors de la 10ème réunion des parties de l'APSOI en juillet 2023, **les parties ont approuvé l'organisation d'un atelier intersession conjoint gestionnaires-scientifiques pour définir les objectifs de gestion**. Le rapport de la 8ème réunion du comité scientifique recommande une approche similaire à celle de la CCAMLR dans un effort d'harmonisation des pratiques.

A retenir :

- L'objectif de gestion est l'indicateur principal justifiant de la durabilité du stock pêché.
- La gestion de la légine à la CCAMLR et aux TAAF s'appuie sur un objectif de gestion **précautionneux** par rapport aux pratiques usuelles de gestion des pêches.
- **Le choix de la référence (biomasse reproductrice pré-exploitation ou à l'état d'équilibre du stock) influence l'estimation du total admissible de capture**, et est donc un choix important pour assurer la durabilité du stock.

III – Mesures en place et gestion des risques

1. Mesures de gestion en place

La gestion de la pêche inclut une gestion de l'effort de la pêche et de son impact sur les écosystèmes. En ce sens, différents types de mesure de gestion ont été développés.

- Mise en place d'un total admissible de capture, ensuite réparti entre les différents pêcheurs (système de quotas).
- Mesures de régulations de l'espace, du temps et des techniques de pêche :
 - a. Pour assurer une gestion durable du stock ;
 - b. Pour limiter les impacts sur l'écosystème.

Les TAAF, la CCAMLR et l'APSOI visent à développer une **approche « écosystémique »**². Celle-ci s'opérationnalise par la minimisation des impacts de la pêche sur l'écosystème, notamment en évitant les prises accessoires d'espèces non ciblées (ex. fermeture de la pêche entre fin janvier et mi-mars pour diminuer le risque de mortalité aviaire).

Le détail des mesures de gestion et de conservation entre les différentes institutions est résumé dans l'annexe 1. On observe des différences dans la gestion entre les institutions mais parfois aussi au sein d'une même institution entre deux zones :

- Sur les techniques de pêche autorisées : la zone 58.5.2 (avec la ZEE de l'île de Heard) est la seule zone de la CCAMLR autorisant la pêche au chalut (Mesure de conservation 41-08, 2021) ; l'APSOI n'interdit pas explicitement des techniques de pêche autres que la palangre.
- **Les mesures de gestion des impacts de la pêche sur les écosystèmes sont beaucoup plus développées dans les réglementations des TAAF et de la CCAMLR que dans celle de l'APSOI** (cf. Annexe 1). La réglementation de l'APSOI prend en compte les risques de déprédation mais ne limite pas les potentielles captures accessoires de certains poissons (dont les raies) ou de certains oiseaux marins alors que c'est le cas pour les zones limitrophes de Crozet et de Heard, ce qui pourrait alors limiter l'efficacité des mesures mises en place dans ces zones.
- Au sein de l'APSOI, les mesures de gestion sont beaucoup plus contraignantes sur Williams' Ridge par rapport à Del Cano malgré un TAC plus élevé à Williams' Ridge. La gestion à Williams' Ridge est spatialisée avec des contraintes sur le nombre de navire, le nombre de lignes et des obligations de notification d'entrée et de sortie par point de grille de gestion.

On note dans le cadre de la CCAMLR, l'existence de pêcheries dites « **exploratoires** » (ex. zone 58.4.3a). Ce cadre particulier s'applique pour des pêcheries à des fins scientifiques, à l'exclusion de la pêche commerciale, et qui sont alors soumises à des règles spécifiques, principalement pour éviter une trop forte concentration de l'effort de pêche. Une pêcherie demeure exploratoire jusqu'à l'acquisition de données suffisantes pour i) estimer le rendement potentiel de la pêcherie, ii) mesurer l'impact potentiel de la pêcherie sur l'écosystème, et iii) « permettre au Comité scientifique de formuler et de fournir des avis à la Commission sur les niveaux de capture et d'effort de pêche souhaitables ainsi que sur les engins de pêche » (mesure de conservation 21-02).

2. Gestion des risques

Dans le cadre des TAAF, le plan de gestion prévoit que le TAC peut être revu à la baisse avant la fin des 3 ans « en cas **d'évènements majeurs** impactant les populations de légine ou les écosystèmes marins (reprise de la pêche INN, augmentation exponentielle de la déprédation,

² « Le principal but de l'approche écosystémique des pêches est de **prévoir**, de mettre en place et de gérer la pêche d'une manière qui réponde **aux besoins et désirs multiples des sociétés** sans mettre en péril les possibilités pour les **générations futures** de **profiter** de tout l'éventail des biens et services fournis par le milieu marin. » (Mise en pratique de l'approche écosystémique des pêches, FAO, 2006)

impacts conséquents sur les écosystèmes marins, etc.) ou en **fonction de l'évolution des connaissances** ». Le plan de gestion laisse la possibilité pour d'autres mesures d'être mises en place en complément : « Ces mesures ne sont pas exhaustives ; **elles peuvent être complétées par toute autre mesure spécifique permettant de réduire les impacts identifiés sur les populations de légine ou les écosystèmes marins** ». Un acte administratif du préfet peut aussi restreindre l'activité de pêche « dans l'espace et dans le temps ».

Une telle mesure est en cohérence avec l'application du principe de précaution. En effet, l'article 6 (application de l'approche de précaution) paragraphe 7 de l'Accord des Nations Unies sur les stocks de poissons chevauchants (UNFSA) indique : « *Si un **phénomène naturel a des effets néfastes notables sur l'état de stocks de poissons chevauchants ou de stocks de poissons grands migrants, les États adoptent d'urgence des mesures de conservation et de gestion pour que l'activité de pêche n'aggrave pas ces effets néfastes. Ils adoptent également d'urgence de telles mesures lorsque l'activité de pêche menace sérieusement la durabilité de ces stocks. Les mesures d'urgence sont de caractère temporaire et sont fondées sur les données scientifiques les plus fiables dont ces États disposent.*** ». On peut toutefois noter la distinction entre « événements majeurs » (plan de gestion des TAAF), qui suggère l'occurrence de processus ponctuels, et la mention de « phénomène naturel [ayant] des effets néfastes » (UNFSA) qui pourrait davantage recouvrir la réalité du changement climatique.

Dans le cadre de la CCAMLR ou de l'APSOI, **une telle flexibilité réglementaire n'est pas explicitement incluse dans les textes de gestion**. Dans le cadre de la CCAMLR **les TAC peuvent être adaptés chaque année** notamment puisque le groupe de travail sur l'évaluation des stocks halieutiques (WG-FSA), en charge entre autres de l'évaluation de l'état des stocks de la zone de la Convention, se réunit annuellement. Dans le cas de l'APSOI, le niveau de pêche est examiné chaque année uniquement à Williams' Ridge. Il est d'ailleurs indiqué dans les mesures de gestion de la légine à Williams' Ridge que cette mesure de conservation sera revue annuellement jusqu'à ce qu'une approche collaborative entre l'APSOI et la CCAMLR soit établie (CMM 2021/15). Toutefois, on peut noter la recommandation au paragraphe 51 du rapport du groupe de travail de la réunion des parties et du comité scientifique sur une pré-évaluation des stratégies d'exploitation dans l'APSOI (mars 2023) qui **introduit le besoin de considérer des règles d'arrêt de l'exploitation** (« dropout or breakout rules ») dans certains cas, notamment en cas de variabilité de la productivité du stock, de variabilité du changement climatique ou d'observations inhabituelles, qui rendraient les règles d'exploitation inadaptées ou inutiles. Cette recommandation a également été reprise par le comité scientifique, indiquant que les objectifs de gestion et la mise en œuvre de stratégies d'exploitation devraient aussi inclure des réponses à des « **circonstances exceptionnelles** » (paragraphe 189 rapport SC8).

La gestion du risque et des incertitudes est aussi incluse dans le **principe de précaution** présent dans l'ensemble des textes réglementaires et par l'objectif limite de 20% de la biomasse reproductrice. La revue de performance de l'APSOI (juillet 2023) note que l'approche de précaution n'est actuellement pas bien appliquée, notamment du fait de l'absence d'évaluation du stock de légine, avec à ce jour un taux de capture sans justification scientifique, et de l'absence de recommandation clairement opérationnelle de la part du comité scientifique qui conduit le plus souvent à l'inaction de la réunion des parties. Toutefois, les parties de l'APSOI ont approuvé lors de leur 10ème réunion en juillet 2023 des points de référence provisoires pour la gestion de légine similaires à ceux de la CCAMLR et ont montré leur volonté d'élaborer des stratégies de gestion adaptées.

3. Prise en compte du changement climatique

La CCAMLR reconnaît par les résolutions 30/XXVIII et 36/41 que le changement climatique peut induire des effets négatifs sur les écosystèmes marins de sa zone d'application, insistant sur l'**urgence d'agir**, notamment pour éviter des changements irréversibles. A travers ces résolutions, elle rappelle des grands principes de l'article II de la CCAMLR dont la « prévention de la diminution de la taille de toute population exploitée en-deçà du niveau **nécessaire au maintien de la stabilité du recrutement** », le « maintien des rapports écologiques entre les populations exploitées, dépendantes ou voisines des ressources marines vivantes de l'Antarctique » ou encore la « prévention des changements ou réduction maximale des risques de changement dans l'écosystème marin qui ne seraient potentiellement **réversibles en deux ou trois décennies**, compte tenu des **effets des changements environnementaux**, afin de permettre la conservation durable des ressources marines vivantes de l'Antarctique ». En effet, ces principes pourraient être remis en cause par le changement climatique et la CCAMLR « conseille vivement » de considérer les impacts du changement climatique pour **guider la gestion** et garantir que les mesures de conservation adoptées puissent demeurer efficaces dans le futur. Différentes initiatives scientifiques vont dans ce sens telles que le programme scientifique Integrating Climate and Ecosystem Dynamics ou le programme Southern Ocean Sentinel. Des sujets prioritaires de recherche ont également été identifiés lors du comité scientifique de la CCAMLR en 2022, notamment :

Dans le programme des travaux d'intersession du groupe de travail sur les statistiques, les évaluations et la modélisation (WG-SAM) :

- « Évaluation des règles de décision de la CCAMLR et autres règles potentielles de contrôle de l'exploitation pour les pêcheries évaluées »
- « Des stratégies de gestion des poissons résistantes au changement climatique » (pas de tâche attribuée)

Dans le programme des travaux d'intersession du groupe de travail sur le suivi et la gestion des écosystèmes (WG-EMM) :

- « Évaluation des stratégies de gestion des espèces visées (seconde évaluation de performance, recommandation 8) » : « Des stratégies de gestion des poissons résistantes au changement climatique » (urgence dite « faible »).
- « Suivi des effets du changement climatique, y compris de l'acidification, et adaptation » : « Développer des méthodes de détection des changements dans les écosystèmes, compte tenu de la variabilité et de l'incertitude (seconde évaluation de performance, recommandation 6) » (urgence dite « moyenne »).

En outre, les rapports des pêches incluent à présent une déclaration « Climate Change and environmental variability ». A ce jour, ces paragraphes présentent les mêmes informations pour les différents stocks, à savoir un résumé des potentiels impacts du changement climatique sur les pêches de l'océan austral d'après la FAO³ et en 2021 une déclaration générale « *There is no*

3

- « The Antarctic region is characterized by complex interaction of natural climate variability and anthropogenic climate change that produce high levels of variability in both physical and biological systems, including impacts on key fishery taxa such as Antarctic krill.
- The impact of anthropogenic climate change in the short-term could be expected to be related to changes in sea ice and physical access to fishing grounds, whereas longer-term implications are likely to include changes

formal evaluation of the impacts of climate change and environmental variability available for this particular fishery.» et en 2022 un rappel des actions menées par la CCAMLR sur la thématique du changement climatique. Certains groupes de travail prennent déjà en considération le changement climatique dans leurs travaux, comme rappelé dans le rapport du comité scientifique en 2022. En particulier, le comité scientifique a déjà indiqué que des changements des paramètres du modèle et des hypothèses sur la productivité pourraient être une manière utile de mettre en lumière les problématiques liées au changement climatique dans les avis de gestion pour les stocks de la CCAMLR (paragraphe 3.51 du rapport SC-CAMLR-XXXVII et le paragraphe 9.4 du rapport SC-CAMLR-38). En 2022, le comité scientifique « souligne la nécessité de tenir compte des impacts du changement climatique lors de l'évaluation des stratégies de gestion et **estime que les règles de décision de la CCAMLR pourraient être amenées à être révisées à la lumière du changement climatique** » (SC-CAMLR-41).

Un groupe de travail organisé dans le cadre de la CCAMLR sur le changement climatique, qui aura lieu du 4 au 8 septembre 2023, a pour objectif d'identifier les principaux effets du changement climatique sur les ressources marines, d'identifier les priorités scientifiques mais aussi de gestion avec **une visée d'opérationnalisation**.

Les textes réglementaires des TAAF et de l'APSOI ne font pas de mention explicite aux enjeux du changement climatique. Toutefois, la pêche à la légine australe aux TAAF s'effectue au sein de la Réserve Naturelle Nationale (RNN) dont un des objectifs opérationnels est par exemple « Identifier **les sources de pressions** sur les écosystèmes marins afin de mettre en place des mesures de gestion adaptées » (Fiche Action FS 14). De telles sources de pression peuvent inclure les effets du changement climatique, et les efforts de la RNN en ce sens pourraient être bénéfiques également à la résilience du stock de légine australe.

in ecosystem productivity affecting target stocks.

- There are no resident human populations or fishery-dependent livelihoods in the Commission for the Conservation of Antarctic Marine Living Resources (CCAMLR) Area, therefore climate change will have limited direct implications for regional food security. However, as an “under-exploited” fishery, there is potential for krill to play a role in global food security in the longer term.
- The institutional and management approach taken by CCAMLR, including the ecosystem-based approach, the establishment of large marine protected areas, and scientific monitoring programmes, provides measures of resilience to climate change. »

A retenir :

- La réglementation des TAAF évoque la possibilité d'évènements majeurs nécessitant une intervention d'urgence avec la possibilité de restreindre l'activité de pêche. Néanmoins, le changement climatique n'est à ce jour pas introduit comme une menace sur le long terme et **les projections sur lesquelles reposent la justification de la durabilité du stock exploité ne prennent pas en compte ce risque.**
- Ni des interventions d'urgence ni le changement climatique ne sont explicitement pris en considération dans le cadre de l'APSOI actuellement mais une recommandation allant dans ce sens a été formulée lors du groupe de travail sur la pré-évaluation des stratégies d'exploitation en mars 2023.
- **La CCAMLR reconnaît, dans le cadre de résolutions et à travers ses groupes de travail, l'importance de l'enjeu du changement climatique en insistant sur l'urgence d'agir mais n'a pas encore opérationnalisé cette prise de conscience.** L'organisation de groupes de travail et le soutien à des programmes scientifiques sur le sujet permettent d'amorcer la réflexion. Ces initiatives ne sont pas spécifiques au secteur de la pêche et contribuent **plus largement à une réflexion pour assurer l'efficacité de la conservation.**

Références

APSOI. CMM 2021/151 Conservation and Management Measure for the Management of Demersal Stocks in the Agreement Area (Management of Demersal Stocks).

APSOI/SIOFA. (22 – 31 mars 2023). Report of the Eighth Meeting of the Scientific Committee of the Southern Indian Ocean Fisheries Agreement (SIOFA) Spanish Institute of Oceanography, Santa Cruz de Tenerife, Spain / Hybrid Format.

APSOI/SIOFA (2023). 1st Performance Review Report by SIOFA Performance Review Panel. Présenté à la 10ème réunion des parties (MOP10).

APSOI/SIOFA (17-18 mars 2023). Report of the Joint Meeting of Parties and Scientific Committee Workshop on Harvest Strategy Pre-assessment of the Southern Indian Ocean Fisheries Agreement (SIOFA) Spanish Institute of Oceanography, Santa Cruz de Tenerife, Spain / Hybrid Format.

Brandão, A., and Butterworth, D.S. (2017). Assessment of the toothfish (*Dissostichus eleginoides*) resource in the Prince Edward Islands vicinity to include data from 1997 to 2016. DAFF Branch Fisheries document: FISHERIES/2017/SEP/SWG-DEM/27.

CCAMLR. Texte de la Convention sur la conservation de la faune et la flore marines de l'Antarctique et Déclaration du président de la conférence sur la conservation de la faune et la flore marines de l'Antarctique.

CCAMLR. Liste officielle des mesures de conservation en vigueur 2022/23 (adoptée par la Commission lors de la quarante-et-unième réunion, du 24 octobre au 4 novembre 2022)

Duhamel, G, Lord, C., and Pruvost, P. (2006). The Patagonian toothfish (*Dissostichus eleginoides*) fishery in the Kerguelen Islands (Indian Ocean sector of the Southern Ocean). CCAMLR science journal of the Scientific Committee and the Commission for the Conservation of Antarctic Marine Living Resources. 13. 1-25.

Kock, K.-H. (2000). Understanding CCAMLR approach to management.

Péron, C., Chazeau, C., Faure, J., Gasco, N., Martin, A., Massiot-Granier, F., Pruvost, P., Rajaonalison, F., and Selles, J. (2022). Rapport « Données statistiques de pêche des navires français et étrangers dans les zones économiques exclusives des îles Kerguelen, Crozet et Saint-Paul/Amsterdam et les eaux internationales CCAMLR et APSOI. Convention Ministère de l'Agriculture et de la Souveraineté Alimentaire (Direction générale des affaires maritimes, de la pêche et de l'aquaculture, DGAMPA) et Muséum National d'Histoire Naturelle.

SC-CAMLR-XXXVII (2018). Rapport de la trente-septième réunion du comité scientifique.

SC-CAMLR-38 (2019). Rapport de la trente-huitième réunion du comité scientifique.

SC-CAMLR-38/15 (2019). The CCAMLR Decision Rule, strengths and weaknesses. Délégation du Royaume-Uni.

SC-CAMLR-41 (2022). Rapport de la quarante-et-unième réunion du comité scientifique.

SERAWG-02-11 (2020). Preliminary analysis of the Patagonian toothfish fishing data of the Del Cano Rise SIOFA. 5 th Meeting of the Southern Indian Ocean Fisheries Agreement (SIOFA) Scientific Committee. Délégation de l'Union Européenne.

Skeljo F, Lee B and Winter A. (2022). 2021 Stock assessment report for Patagonian toothfish (*Dissostichus eleginoides*). Fisheries Report SA-2021-TOO. Fisheries Department, Directorate of Natural Resources, Falkland Islands Government, Stanley, Falkland Islands. 44 p.

Terres Australes et Antarctiques Françaises. Arrêté n°2019-59 du 2 juillet 2019 portant approbation du plan de gestion 2019-2025 de la pêcherie de la légine australe *Dissostichus eleginoides* dans les zones économiques exclusives des îles Kerguelen et de l'archipel Crozet.

Terres Australes et Antarctiques Françaises. Arrêté n°2022-128 du 16 septembre 2022 prescrivant les règles encadrant l'exercice de la pêche à la légine australe (*Dissostichus eleginoides*), dans les zones économiques exclusives de Crozet et de Kerguelen.

Terres Australes et Antarctiques Françaises. Arrêté n°2022-58 du 4 juillet 2022 portant fixation des totaux admissibles de capture de légine australe (*Dissostichus eleginoides*) dans les zones économiques exclusives des îles Kerguelen et de l'archipel Crozet pour les campagnes 2022-2023 à 2024-2025.

UNFSA (1995). Accord aux fins de l'application des dispositions de la Convention des Nations-Unies sur le droit de la mer du 10 décembre 1982 relatives à la conservation et à la gestion des stocks de poissons dont les déplacements d'effectuent tant à l'intérieur qu'au-delà des zones économiques exclusives (stocks chevauchants) et des stocks de poissons grands migrants.

ANNEXE 1. Tableau comparatif des mesures de gestion entre les TAAF, l'APSOI et la CCAMLR

	Zone 48.3	Zone 48.4 (toute espèce de légine)	Zone 58.4.3a	Zone 58.5.1 (Kerguelen)	Zone 58.5.2 (Heard)	Zone 58.6 (Crozet)
Mesure de conservation associée	41-02 (2019-2021) CADUQUE EN 2021	41-03, 2022	41-06, 2022	GESTION DES TAAF	41-08, 2021 (application aussi 2022/2023)	GESTION DES TAAF
Type de pêche	Établie	Établie	Exploratoire	Établie	Établie	Établie
Technique(s) de pêche autorisée(s)	Palangre et casiers	Uniquement palangre	Uniquement palangre Pêche dirigée interdite	Uniquement palangre et casier (casier sous demande d'autorisation et avec trappe biodégradable)	Chalut, casiers ou palangre	Idem zone 58.5.1
Limite de capture	Sous-zone A : 0 tonnes Sous-zone B : 698 tonnes Sous-zone C : 1629 tonnes	23 tonnes pour 2022 et 2023	0 tonnes	5200 tonnes pour 2021/2022	3010 tonnes pour 2021/2022	800 tonnes pour 2021/2022
Saison	Palangre : 16 avril au 14 septembre Casier : 1er décembre au 30 novembre	1er décembre au 30 novembre	1er décembre au 30 novembre	Fermeture fin janvier et mi-mars pour diminuer le risque de mortalité aviaire	Palangre : 1er mai au 14 septembre et 2 périodes d'extension : 1er au 30 avril et 15 septembre au 30 novembre	Idem zone 58.5.1
Mesures supplémentaires de gestion	Seulement une portion de cette zone autorisée à la pêche (3 sous-zones de gestion)	/	22-06 : règles sur les pêches de fond ¹ 22-07 : règles en cas de découverte d'EMV ¹ 22-08 : interdiction	Interdiction de pêche dans les zones de protection renforcée de Kerguelen Zone tampon de 1.5 milles marin où toute action de pêche est interdite	/	Interdiction de pêche dans les zones de protection renforcée de Crozet et dans certaines zones précises à proximité de Crozet

¹ « La présente mesure de conservation est applicable aux secteurs situés dans la zone de la Convention au sud de 60°S et au reste de la zone de la Convention, à l'exception des sous zones et divisions dans lesquelles une pêcherie établie était en place en 2006/07 avec une limite de capture supérieure à zéro. »

			<p>de pêche dans eaux inférieures à 550 m pour les pêcheries exploratoires</p> <p>41-01 : Mesures générales applicables aux pêcheries exploratoires de <i>Dissostichus</i> spp. (notamment « La pêche doit avoir lieu dans un intervalle géographique et bathymétrique aussi étendu que possible en vue de fournir les informations qui permettront de déterminer le potentiel de la pêcherie et d'éviter une trop forte concentration des captures et de l'effort de pêche »)</p>	<p>Pêche interdite à une profondeur inférieure à 500 m</p> <p>Chaque secteur statistique de pêche ne peut être exploité que par un seul navire de pêche autorisé à la fois ; un navire ne peut exploiter que deux secteurs simultanément (sauf dérogation)</p> <p>Un nombre maximum de sept palangriers en pêche simultanée (Arrêté n°2016-60)</p> <p>Mesure de déplacement en cas de fort taux de capture de légine australe de petite taille</p> <p>Potentielles zones d'exclusion dans le cas du franchissement d'un seuil de détection d'EMV (Écosystèmes Marins Vulnérables ; définition dans les mesures de conservation CCAMLR et transposé 2014 par les TAAF)</p>		<p>Pêche interdite à une profondeur inférieure à 500 m</p> <p>Chaque secteur statistique de pêche peut être exploité par deux navires au maximum simultanément, sans limite de durée d'exploitation</p> <p>Un nombre maximum de sept palangriers en pêche simultanée (Arrêté n°2016-60)</p> <p>Mesure de déplacement en cas de fort taux de capture de légine australe de petite taille</p> <p>Potentielles zones d'exclusion dans le cas du franchissement d'un seuil de détection d'EMV (Écosystèmes Marins Vulnérables ; définition dans les mesures de conservation CCAMLR et transposé 2014 par les TAAF)</p>
Capture accessoire Et atténuation des impacts	Relâcher les captures accessoires de crabes vivants	Limites/quotas sur les captures accessoires de certains poissons	33-03 : Limitation des captures accessoires dans les pêcheries	Système d'effarouchement des oiseaux Déclaration si interactions/captures	33-02 (quotas sur les captures accessoires) 25-03 (oiseaux et	Idem zone 58.5.1

sur les écosystèmes	Limites/quotas sur les captures accessoires de certains poissons (dont raies) Règle de déplacement 25-02 : Réduction de la mortalité accidentelle des oiseaux de mer au cours de la pêche à la palangre Limite sur la capture oiseau de mer (sinon palangre uniquement de nuit) Palangre uniquement la nuit	Règle du déplacement 25-02 : Réduction de la mortalité accidentelle des oiseaux de mer au cours de la pêche à la palangre Limite sur la capture oiseau de mer (sinon palangre uniquement de nuit)	25-02 : Réduction de la mortalité accidentelle des oiseaux de mer au cours de la pêche à la palangre Limite sur la capture oiseau de mer (sinon palangre uniquement de nuit)	accessoires mammifères marines ou oiseaux Procédure en cas de capture de raies Déclaration si découverte EMV Mesure de déplacement en cas de capture trop importante de raie Interdiction de pêche en présence d'orques, mesure d'éloignement ; secteur d'interaction et les 8 adjacents sont gelés pendant 10 jours avec des règles s'appliquant dans un rayon de 30 milles marins autour du point d'interaction. Transit direct entre Crozet et Kerguelen interdit	mammifères marines) ; 25-02 Limite sur la capture oiseau de mer (sinon palangre uniquement de nuit), sauf si pendant période d'extension, alors doit arrêter	
Observateurs	Au moins 1 observateur scientifique	Au moins 1 observateur scientifique	Au moins 1 observateur scientifique	Chaque navire a à son bord un contrôleur des pêches (cf. Code rural) ; 2 contrôleurs si le navire pêche à la palangre et au casier	Au moins 1 observateur scientifique Et 2 observateurs sur la période 1er au 30 avril	Idem zone 58.5.1
Données : capture et effort de pêche	23-01 : Système de déclaration de capture et d'effort de pêche par période de cinq jour 23-05 : Système de déclaration mensuelle des données	23-01 : Système de déclaration de capture et d'effort de pêche par période de cinq jour 23-04 : Système de déclaration mensuelle des données de	23-07 : Système de déclaration journalière de capture et d'effort de pêche pour les pêcheries exploratoires 23-04 : Système de	Conformément aux mesures de conservation de la CCAMLR et aux prescriptions techniques en vigueur, encadrant la pêche à la légine dans les eaux des TAAF, toutes les captures ciblées et accessoires sont comptabilisées par le	41-08/A (déclaration sous 10 jours et mensuelle) Nombre et poids total des rejets de légine australe à déclarer	Idem zone 58.5.1

	<p>biologiques à échelle précise applicable aux pêcheries au chalut, à la palangre et au casier</p> <p>Nombre et poids total des rejets de légine australe à déclarer</p> <p>Inclusion des captures pour la recherche dans la limite quotas 24-01</p>	<p>capture et d'effort de pêche à échelle précise applicable aux pêcheries au chalut, à la palangre et au casier</p>	<p>déclaration mensuelle des données de capture et d'effort de pêche à échelle précise applicable aux pêcheries au chalut, à la palangre et au casier</p>	<p>capitaine et figurent sur le carnet de pêche.</p>		
Données biologiques	<p>23-05 : Système de déclaration mensuelle des données biologiques à échelle précise applicable aux pêcheries au chalut, à la palangre et au casier</p>	<p>23-05 : Système de déclaration mensuelle des données biologiques à échelle précise applicable aux pêcheries au chalut, à la palangre et au casier</p> <p>Aussi programme de marquage</p>	<p>23-05 : Système de déclaration mensuelle des données biologiques à échelle précise applicable aux pêcheries au chalut, à la palangre et au casier</p> <p>Règles sur la recherche programme marquage...)</p>	<p>Collecte de données en cohérence avec le plan d'action de la Réserve Naturelle Nationale : (cf. actions FS 28, FS 29 et FS 30 du plan de gestion de la RNN)</p> <p><i>La France communique annuellement les données disponibles relatives à sa pêcherie de légine australe au comité scientifique de la CCAMLR afin qu'il puisse rendre un avis sur les prises (taille, captures accessoires et accidentelles, déprédation...) et sur le modèle de définition des TAC dans les ZEE australes françaises.</i></p>	<p>41-08/A (déclaration sous 10 jours et mensuelle)</p>	<p>Idem zone 58.5.1</p>

Protection environnementale (ex. Pollution)	26-01 : Protection générale de l'environnement par les navires de pêche	26-01 : Protection générale de l'environnement par les navires de pêche	26-01 : Protection générale de l'environnement par les navires de pêche	Contrôle et règle sur les rejets et gestion des déchets, biosécurité	26-01 : Protection générale de l'environnement par les navires de pêche	Idem zone 58.5.1
--	---	---	---	--	---	------------------

	Del Cano Rise	William's Ridge
Mesure de conservation associée	GESTION PAR L'APSOI CMM 2021/151	GESTION PAR L'APSOI CMM 2021/151
Type de pêche	Établie	Établie
Technique(s) de pêche autorisée(s)	Pas d'interdiction explicite mais semble principalement considérer la pêche à la palangre dans la gestion Les palangres ne doivent pas dépasser 3000 hameçons par ligne et doivent être fixées à au moins 3 milles marins les uns des autres.	Pas d'interdiction explicite mais semble principalement considérer la pêche à la palangre dans la gestion Les palangres ne doivent pas dépasser 6250 hameçons par ligne et ne doivent pas être placées sur plusieurs points de grille.
Limite de capture	55 tonnes (fermeture de la pêcherie quand 90% du quota est atteint) Pour les navires ne ciblant pas la légine australe, limite de 0.5 tonnes	140 tonnes (si limite dépassée, impact le TAC de l'année suivante) (fermeture de la pêcherie quand 90% du quota est atteint) Pour les navires ne ciblant pas la légine australe, limite de 0.5 tonnes Revue annuelle du niveau de TAC
Saison	1er décembre au 30 novembre	1er décembre au 30 novembre
Mesures supplémentaires de gestion	/	Zone de gestion découpée en une grille de 15'x15' pour une gestion spatialisée Un seul navire de pêche à la fois peut pêcher par point de grille Les CCPs doivent s'assurer qu'il n'y pas eu plus de deux lignes au total par point de grille sur la durée de la saison de pêche (ensuite point de grille fermé à la pêche). Les CCPs doivent s'assurer que leurs navires pêchant la légine à Williams Ridge applique une pause d'au moins 30 jours entre les voyages de pêche consécutifs à Williams Ridge

Capture accessoire Et atténuation des impacts sur les écosystèmes	<p>Mesures d'atténuation de la déprédation :</p> <ul style="list-style-type: none"> - « les navires sont encouragés à ne pas hisser de palangres en présence d'orques et sont découragés de hisser des palangres en présence d'odontocètes à dents. » - « Si des orques arrivent pendant les opérations de halage, les navires sont encouragés à cesser de remorquer, à attacher l'élingue à l'aide d'une bouée et à passer à autre chose. Le navire ne peut récupérer l'amarrage qu'une fois que les orques ne sont plus près de la ligne. » - « Les navires sont encouragés à établir des lignes à des profondeurs supérieures à 1 000 m. » <p>Depuis la 10ème réunion des parties (juillet 2023) : mesures pour une gestion durable de l'aiguillat commun (<i>Portuguese dogfish</i>) Travail en cours pour l'élaboration d'un programme de marquage des raies capturées vivantes</p>	<p>Mesures d'atténuation de la déprédation :</p> <ul style="list-style-type: none"> - « les navires sont encouragés à ne pas hisser de palangres en présence d'orques et sont découragés de hisser des palangres en présence d'odontocètes à dents. » - « Si des cachalots arrivent pendant les opérations de transport, les navires sont encouragés à cesser de remorquer, attacher l'élingue avec une bouée, et avancer. Le navire ne peut récupérer le navire attaché hors ligne que lorsque les cachalots ne sont plus près de la ligne. » <p>Depuis la 10ème réunion des parties (juillet 2023) : mesures pour une gestion durable de l'aiguillat commun (<i>Portuguese dogfish</i>) Travail en cours pour l'élaboration d'un programme de marquage des raies capturées vivantes.</p>
Observateurs	<p>Communiquer les données VMS toutes les heures quand navire dans la zone de Del Cano</p> <p>Au moins 1 observateur scientifique</p>	<p>Au moins 1 observateur scientifique</p>
Données : capture et effort de pêche	<p>Rapports mensuels des CCPs au secrétariat</p>	<p>Rapports journaliers des CCPs au secrétariat Système de notification au secrétariat quand un navire entre puis sort dans un point de la grille définie pour pêcher</p>
Données biologiques	<p>Programme de marquage</p>	<p>Programme de marquage Collecte de données représentatives (et échantillons) concernant les tailles, poids, sexes, stades de maturité, poids des gonades et les otolithes (notamment pour estimer les risques de déplétion).</p>
Protection environnementale (ex. Pollution)	<p>/</p>	

Synthèse relative aux implications du changement climatique pour la gestion de la légine australe

Par Clara Azarian, juillet 2023

Résumé

Le changement climatique peut impacter les stocks de poissons à travers différents processus ayant deux principaux impacts pour un stock donné : **la migration du stock et la diminution de sa biomasse**. Dans le cas de la légine australe, il semble peu probable qu'une migration des stocks ait lieu, cependant **on observe déjà une diminution de la biomasse reproductrice dans l'ensemble des stocks de légine australe gérés**. Cette diminution de biomasse a été associée à l'effet d'années de faible recrutement et a conduit l'Australie à adopter une approche précautionneuse de réduction des totaux admissibles de capture (TAC). Cependant, **les causes de ce déclin n'ont pas été clairement identifiées** (variabilité naturelle, changement de régime, événement extrême, tendance de fond, surpêche ?). Que le déclin actuel soit une conséquence de modifications environnementales ou non, le changement climatique peut entraîner de tels impacts et remettre en cause de nombreuses hypothèses sur lesquelles les scientifiques s'appuient pour évaluer l'état des stocks et estimer les TAC. La gestion actuelle de la légine repose sur une vision statique du stock et n'est pas adaptée à un stock aux propriétés changeantes dans le temps. Bien que des outils existent déjà pour permettre une gestion adaptée au changement climatique (le principe de précaution, la gestion fondée sur les écosystèmes), **la gestion actuelle pourrait ne plus être durable dans le futur**. Trois axes de travail sont ici identifiés : 1) un **axe méthodologique** à la fois pour les scientifiques (amélioration du modèle d'estimation des stocks) et pour les gestionnaires (réflexion sur le choix de l'objectif de gestion et des points de référence) ; 2) un **axe de gestion des risques** (approche par scénarios, vigilance et flexibilité dans la réglementation permettant de réagir à des événements extrêmes); 3) un **axe de résilience** (maximiser le potentiel de renouvellement du stock en adaptant la stratégie d'exploitation).

Les objectifs de cette synthèse :

- Identifier les principales hypothèses d'impact du changement climatique sur la légine australe.
- Analyser la pertinence de la réglementation actuelle et ses limites dans le contexte du changement climatique en vue de l'exploitation durable de la légine australe.
- Proposer des pistes d'amélioration de cette réglementation pour permettre une gestion durable du stock de légine australe.

I – Principales hypothèses d'impact du changement climatique sur la légine australe

De nombreuses études scientifiques alertent sur les potentiels impacts en cours et à venir du changement climatique sur les stocks de pêche (Pörtner et al., 2014 ; Cheung et al., 2022). Les deux impacts principaux sont : **une migration des stocks et une diminution de leur biomasse**. On observe notamment une **baisse du recrutement pour de nombreux stocks** : on estime que la capacité de recrutement moyenne des stocks dans le monde a décliné d'environ 3% du maximum historique par décennie (Britten et al., 2016). Néanmoins, on observe une grande hétérogénéité des impacts à l'échelle régionale et selon les espèces de poisson, ce qui nécessite une plus grande compréhension des mécanismes régionaux, en lien avec la gestion mise en place. De nombreux facteurs peuvent mener à ces impacts : allant d'une contrainte physiologique forte (ex. les nouvelles conditions de température et/ou d'oxygène altèrent l'efficacité du métabolisme d'un individu et/ou son comportement par exemple migratoire), à un impact physique sur une étape du cycle de vie (ex. les œufs sont transportés par les courants vers d'autres zones de nurseries ou dans des zones peu propices à leur développement) ou à un impact indirect à travers des effets sur la chaîne alimentaire ou la présence de prédateurs (Figure 1). Ces effets s'ajoutent alors aux pressions exercées par les activités anthropiques.

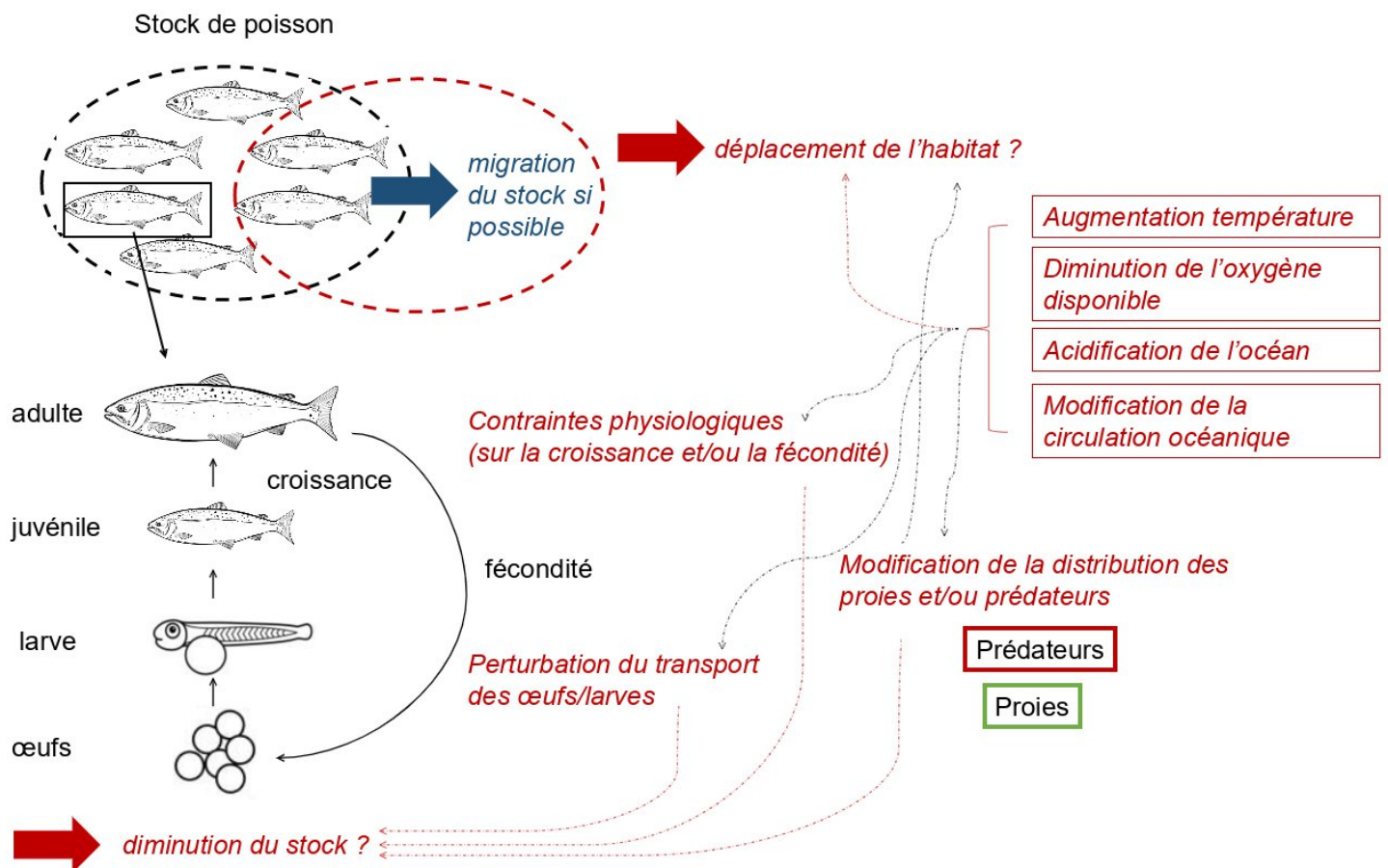


Figure 1: Schéma illustrant les différentes hypothèses d'impact du changement climatique sur les stocks de poissons.

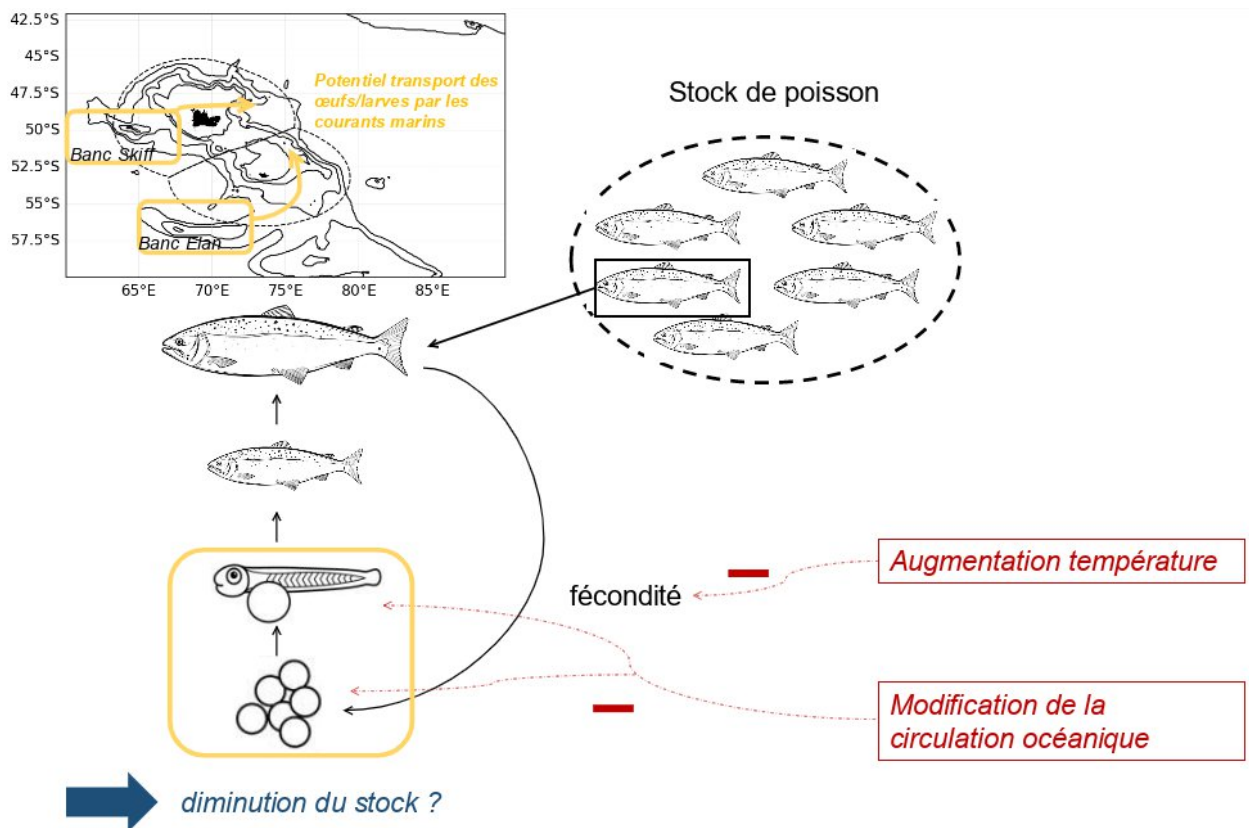


Figure 2: Schéma illustrant dans le cas de la légine australe les principales hypothèses d'impact du changement climatique sur les stocks de légine australe au niveau du Plateau de Kerguelen.

L'océan austral est un océan riche en oxygène, ainsi, bien que des variations en quantité d'oxygène puissent exercer une contrainte physiologique sur les individus, on ne considère pas que la désoxygénation soit la menace principale sur les stocks de légine dans la région. De même, bien que face à des conditions changeantes les individus adultes aient la capacité de migrer, **il est peu probable que l'on observe une migration du stock** car les premières phases du cycle de vie de la légine sont très fortement associées à la présence d'eaux peu profondes et donc ici à la présence du Plateau de Kerguelen.

Cependant, la région de l'océan Indien sud connaît déjà un réchauffement important qui devrait s'intensifier avec le changement climatique, entraînant également des événements de vagues de chaleur marines plus fréquents et plus intenses, en particulier au niveau des îles subantarctiques (Llovel et al., 2016 ; Azarian et al., 2023). D'autres modifications sont observées comme l'intensification du courant circumpolaire antarctique, circulant d'ouest en est (Fox-Kemper et al., 2021; Shi et al., 2021).

Les premières phases du cycle de vie de la légine sont sensibles aux changements des conditions environnementales que ce soit pour leur **développement** ou leur **transport** (voir synthèse scientifique). Une modification de la circulation océanique locale par exemple du fait de l'intensification du courant antarctique circumpolaire pourrait transporter les œufs et les larves de légine vers des zones peu propices à leur développement (ex. désynchronisation avec le bloom de phytoplancton source de nourriture, prédation plus élevée etc.) entraînant alors une **baisse de la productivité du stock**. A noter que de telles modifications hydrodynamiques peuvent être hétérogènes spatialement (ex. affectant une zone de ponte plutôt qu'une autre), il est donc important d'avoir une compréhension spatialisée des futurs changements.

En outre, **l'augmentation des températures pourrait entraîner une diminution de la taille et de la fécondité des individus matures** (Yates et al., 2019, Soeffker et al., 2022, voir la synthèse scientifique). Une telle baisse de maturité n'a pas été observée à ce jour mais a fait l'objet de débats, indépendamment de la question du changement climatique, ces dernières années au sein du groupe de travail sur l'évaluation des stocks de la CCAMLR (WG-FSA) pour la zone 48.3. En effet, depuis 2018, la délégation russe pointe une baisse de la biomasse des individus femelles et mâles matures impactant alors la capacité reproductrice du stock dans la zone 48.3 du fait des pratiques de pêche. La délégation russe recommande depuis plusieurs années la fermeture de cette pêcherie (WG-FSA-2021/41) et bloque l'adoption des limites de captures afférentes, malgré le fait que les résultats scientifiques de cette étude soient contestés par l'ensemble des autres membres de la CCAMLR. On note donc que certains arguments d'impacts sur le stock pourraient être récupérés par certains acteurs dans l'objectif de fermer certaines pêcheries pour de véritables raisons encore peu claires.

Bien qu'il n'y ait pas à ce jour de prévisions exactes sur les impacts du changement climatique sur la légine australe, les connaissances actuelles sur cette espèce et la comparaison avec d'autres stocks suggèrent que **le stock de légine australe pourrait voir sa dynamique changer, voire sa productivité baisser sous l'effet du changement climatique.**

II – Des limites de l'objectif de gestion opérationnel actuel ciblant la biomasse reproductrice

Les objectifs de gestion des TAAF et de la CCAMLR (et bientôt de l'APSOI ?) sont précautionneux en comparaison avec les pratiques usuelles de gestion des pêches dans d'autres régions (cf. synthèse réglementaire). Toutefois, nous observons deux limites à cet objectif dans un contexte de changement climatique :

- Cet objectif suppose une relation stable dans le temps entre biomasse reproductrice et recrutement ce qui n'est plus nécessairement valide ;
- L'assurance de l'atteinte de cet objectif repose sur des projections du modèle ne prenant pas en compte l'influence des facteurs environnementaux et leur dynamique.

A. Limite 1 : la relation entre biomasse reproductrice et recrutement n'est pas nécessairement stable dans le temps

Dans un contexte de changement climatique, certaines hypothèses associées à cet objectif peuvent être remises en question notamment la relation entre biomasse reproductrice et recrutement.

L'objectif opérationnel de gestion actuel, que ce soit pour les TAAF, la CCAMLR ou l'APSOI, consiste à assurer un niveau de biomasse reproductrice suffisant pour permettre une stabilité du recrutement et donc du stock. Ce niveau de biomasse reproductrice suffisant est estimé à 50% de la biomasse reproductrice pré-exploitation voire 60% dans le cas des TAAF par précaution. Cet objectif repose donc sur l'hypothèse que le lien entre biomasse reproductrice et recrutement est relativement stable. **Or les premiers stades du cycle de vie de la légine sont aussi les plus vulnérables aux conditions environnementales** (Dahlberg, 1979 ; Szuwalski et al., 2015a; Szuwalski et al., 2015b) **indépendamment du niveau de biomasse reproductrice.** Ce

découplage entre les deux indicateurs (recrutement et biomasse reproductrice) a déjà été observé dans diverses études (Myers, 2001) et certains cas suggèrent que le niveau de recrutement peut parfois davantage moduler le niveau de la biomasse reproductrice que l'inverse (Szuwalski et al., 2019).

Afin de permettre l'atteinte de l'objectif global du plan de gestion des TAAF¹, il semble que l'objectif opérationnel: « Conserver une biomasse reproductrice de légine australe à l'échelle de 35 ans suffisamment forte, pour préserver un capital reproducteur de l'espèce face à tout type d'impact négatif sur la ressource (forte déprédation, pression de pêche illicite, non déclarée et non réglementée (INN), etc.) » puisse ne plus être suffisant. En effet, il serait plus juste de viser **à assurer un recrutement suffisant**, ce dernier contribuant ensuite au capital reproducteur de l'espèce (l'inverse n'étant plus nécessairement vrai dans un contexte de changement climatique).

A ce jour, il semble difficile de développer un objectif de gestion fondé sur le recrutement étant donné le niveau d'incertitude associé à son estimation pour les stocks de légine australe. Néanmoins, il paraît crucial de pouvoir suivre l'évolution de cet indicateur afin d'avoir une meilleure visibilité sur l'état du stock, **en mettant par exemple un seuil critique de recrutement** permettant de déclencher un ensemble de mesures précautionneuses permettant d'adapter l'effort de pêche sur un stock fragilisé pour en faciliter la reconstitution. Estimer le niveau de recrutement dans un stock **nécessite alors des campagnes spécifiques régulières sur le terrain ciblant les jeunes individus**, à l'instar du programme scientifique annuel développé par l'Australie.

B. Limite 2 : les projections du modèle ne prennent pas en compte l'influence des facteurs environnementaux et leur dynamique

Si l'objectif de gestion demeure ciblé sur la biomasse reproductrice, compte tenu de l'usage et des données disponibles, il est important que la variabilité du recrutement puisse bien être prise en compte dans le modèle d'évaluation du stock. Dans le modèle actuellement utilisé (CASAL), l'étape du recrutement intègre implicitement de nombreux processus encore peu connus (ponte, développement larvaire etc.) qui peuvent être impactés différemment par les conditions environnementales. De nombreuses hypothèses sur lesquelles s'appuie le modèle actuel peuvent être remises en cause dans un contexte de changement climatique (Figure 3), notamment l'hypothèse de **stationnarité** qui suppose que l'ensemble des paramètres biologiques et leurs relations sont stables dans le temps. Cette hypothèse peut ne plus être valide dans le contexte du changement climatique, comme illustré précédemment pour les relations entre biomasse reproductrice et recrutement mais aussi pour d'autres paramètres clés comme la croissance, la mortalité naturelle et la reproduction (Szuwalski et al., 2016).

Pour d'autres stocks, des relations statistiques entre des paramètres d'abondance ou de recrutement et des paramètres environnementaux ont été établies et incluses dans les modèles d'évaluation des stocks. Néanmoins, cette méthode a des limites et nécessite des mises à jour régulières avec de nouvelles données. Par exemple, dans le cas de la sardine du Pacifique dans le courant de Californie, un lien statistique a été trouvé entre la relation stock-recrutement et la température de surface de la mer et utilisé pour conseiller la gestion (Jacobson et al., 1995). En revanche, cette relation a aussi été mise en défaut par de nouvelles données collectées

¹ « L'objectif global du plan de gestion est de garantir les conditions d'une exploitation durable et optimale de la légine australe, tant sur le plan environnemental que socioéconomique, dans un souci accru de visibilité et de transparence » (Plan de gestion 2019-2025).

(McClatchie et al., 2010 ; Lindegren et al., 2013) montrant alors la limite de n'utiliser qu'une variable comme proxy des conditions environnementales et la nécessité de réviser régulièrement ce type de relation statistique. La difficulté est que les relations statistiques ne permettent pas de comprendre par quel(s) mécanisme(s) le recrutement est impacté.

Le problème principal associé à l'absence d'inclusion des facteurs environnementaux dans le modèle est le moindre réalisme et donc la moindre fiabilité des projections qui doivent garantir que le total admissible de capture estimé est durable. En effet, les projections utilisent aléatoirement les niveaux de recrutement historiques et un niveau de total admissible de capture pour observer si après 35 ans la biomasse reproductrice reste au-dessus de l'objectif de 50% ou 60% de la biomasse reproductrice pré-exploitation. **Les projections sont donc fondées sur l'hypothèse que le passé se reproduira dans le futur, ce qui est remis en cause par le changement climatique.**

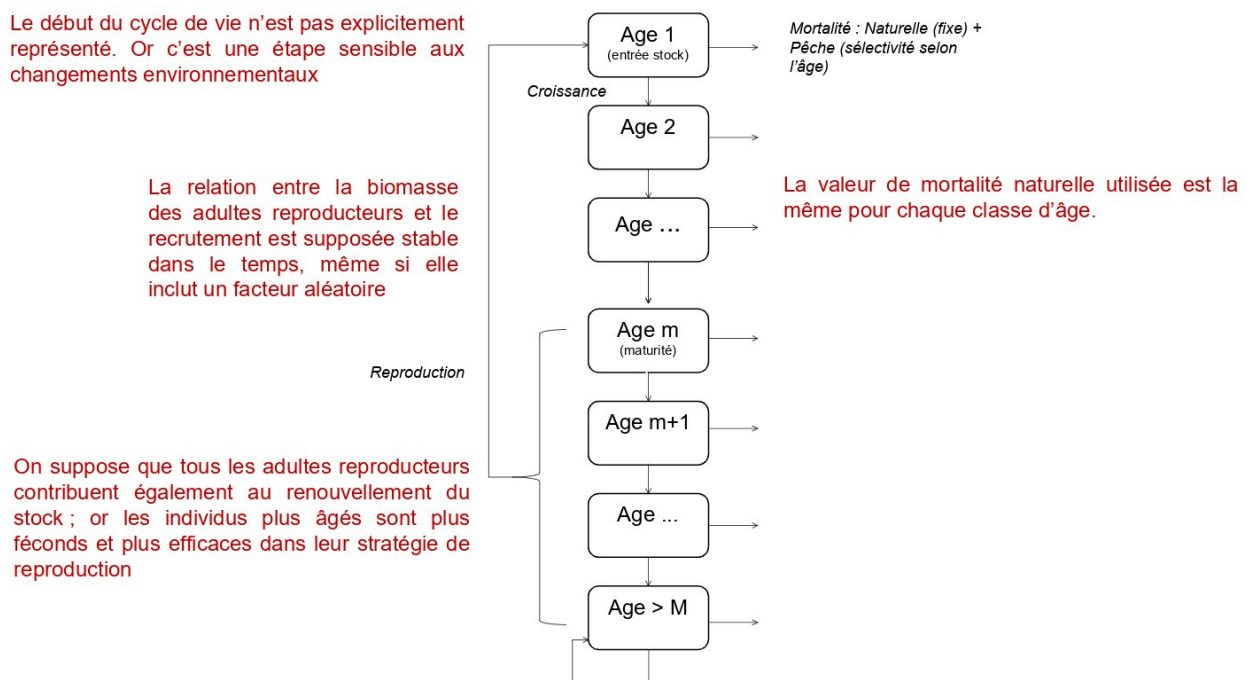


Figure 3: Schéma simplifié illustrant le principe du modèle structuré par âge permettant l'évaluation du stock et l'estimation du TAC permettant d'atteindre l'objectif de gestion et certaines hypothèses qui pourraient être des limites du modèle dans un contexte de changement climatique (en rouge).

A retenir :

- **L'objectif de gestion actuel**, bien que précautionneux par rapport aux objectifs adoptés dans d'autres organisations, **ne permet pas nécessairement d'assurer la durabilité du stock dans un contexte de changement climatique**, du fait de potentiels impacts sur le recrutement indépendamment du niveau de biomasse reproductrice.
- Le recrutement est une phase cruciale pour l'état du stock. Il est donc nécessaire d'améliorer nos connaissances sur cette étape encore mal représentée dans les modèles d'évaluation des stocks. Le **développement de programmes annuels de suivi du recrutement** pourrait alors permettre :
 - Une meilleure compréhension des facteurs impactant le recrutement (permettant ensuite une amélioration de la représentation du recrutement dans les modèles)
 - Une meilleure compréhension de l'état du stock et des tendances, permettant une **alerte plus précoce** lors de baisses importantes du recrutement, comme recommandé lors de l'examen indépendant de l'évaluation des stocks de la CCAMLR (SC-CAMLR-XXXVII/02 Rev. 1, 2018).

III – Déclin actuel de la biomasse reproductrice et implications pour les futurs totaux admissibles de capture

A. *Des tendances de déclin des biomasses reproductrices dans l'ensemble des stocks gérés de légine australe*

Actuellement la biomasse reproductrice de tous les stocks de légine australe est en déclin. On observe une diminution d'environ 31% de la biomasse reproductrice à Crozet et 54% à Heard et McDonald. Ces diminutions de la biomasse reproductrice sont associées à des baisses de recrutement, mais observées avec un délai d'environ 10 ans par exemple à Kerguelen (l'âge d'entrée d'un poisson dans le stock étant autour de 6-7 ans).

L'observation de ces tendances permet de soulever les points suivants :

- La tendance s'observe dans des stocks éloignés géographiquement et suivis indépendamment ce qui suggère un signal robuste qui n'est pas associé à des variabilités environnementales locales.
- Les stocks français de Kerguelen et de Crozet ont les objectifs de gestion les plus précautionneux et la baisse la plus tardive de biomasse reproductrice. Cela suggère que **les tendances observées pourraient être les conséquences des stratégies de gestion et d'exploitation.**
- **Suivre l'état du recrutement chaque année permettrait d'anticiper avec 10 ans d'avance** d'éventuelles fluctuations de la biomasse reproductrice.

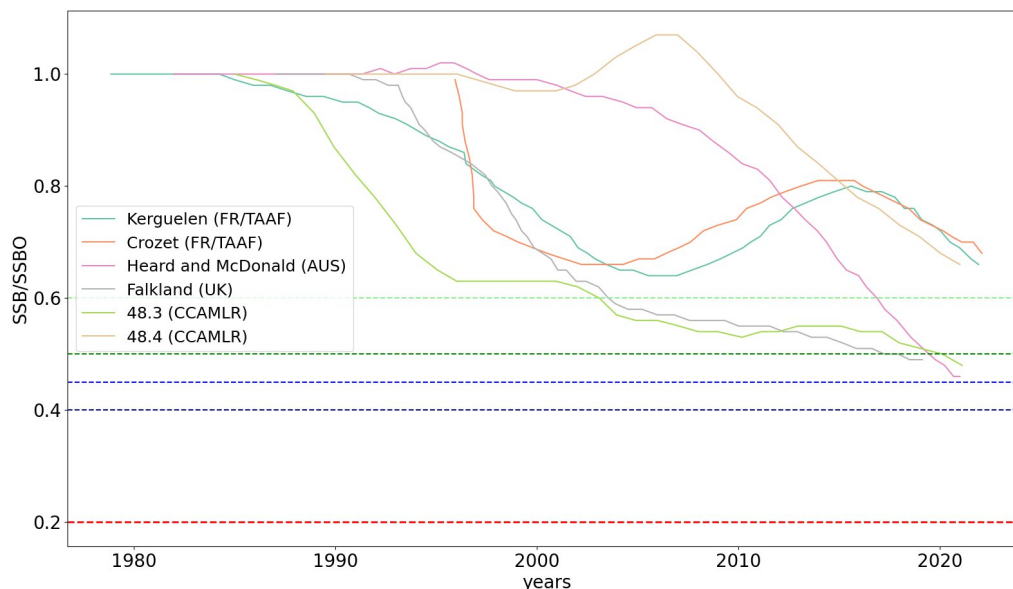


Figure 4: Évolution historique du ratio entre la biomasse reproductrice pour chaque année et la biomasse de référence (pré-exploitation). Données extraites des rapports d'évaluation des stocks 2022 pour les différents stocks. Les lignes horizontales marquent les objectifs de gestion (60% pour les TAAF, 50% pour la CCAMLR et entre 40 et 45% pour les îles Falklands ; 20% limite à ne pas dépasser).

Bien que le stock de la ZEE des îles Heard et McDonald ne soit pas considéré comme surexploité ou sujet à surexploitation (re-certifiée durable en 2017), un déclin dans la biomasse reproductrice est observé ces dernières années et les projections indiquent que l'objectif de gestion pourrait n'être atteint qu'à la fin des 35 ans de projection. Associé à ce déclin de la biomasse reproductrice, **une baisse dans l'intensité de recrutement a été observée** mais des incertitudes importantes demeurent autour de l'estimation des taux de recrutement **ce qui a conduit les autorités australiennes à prévoir une diminution des quotas de pêche** dans la zone pour les années à venir (de 3030 tonnes pour 2020/21 à 2510 tonnes pour 2022/23², Patterson et Tuynman, 2022).

Des tests préliminaires conduits par le Muséum National d'Histoire Naturelle sur le modèle CASAL avec des projections fondées sur les niveaux de recrutement des dernières années à Kerguelen (2013-2017) montrent qu'avec le niveau actuel de totaux admissibles de capture à Kerguelen, la biomasse reproductrice pourrait passer en-dessous de l'objectif de gestion, atteignant environ 30% de la biomasse pré-exploitation, tandis qu'en baissant le total admissible de capture à 2500 tonnes en 2030, ce déclin serait stabilisé à environ 40% de la biomasse pré-exploitation. Ces résultats préliminaires suggèrent donc qu'**une baisse du total admissible de capture pourrait permettre de compenser la diminution de biomasse due aux faibles niveaux de recrutement**.

B. Les causes de ce déclin demeurent incertaines mais la durabilité de la gestion actuelle pourrait être remise en cause dans un contexte de changement climatique

² <https://www.afma.gov.au/fisheries-management/management-tools/quota-and-total-allowable-catch>

Actuellement ces déclin de biomasse reproductrice sont principalement attribués à des baisses de recrutement. Ces baisses de recrutement peuvent refléter des réalités différentes :

- Une conséquence de l'effort de pêche (stratégie de gestion et/ou pêche INN)
- De la variabilité naturelle avec le passage d'un état d'équilibre à un autre
- Un événement extrême : baisse temporaire du recrutement
- Une tendance de fond : le recrutement va continuer à baisser

Il est complexe d'attribuer la baisse de recrutement à l'un de ces processus étant donné les données limitées à disposition. Toutefois, il est important de considérer que ces différents scénarios sont possibles et de s'interroger sur leurs implications pour la gestion de la légine australe. En particulier se posent les questions suivantes :

- Selon ces différents scénarios, l'objectif de gestion est-il toujours pertinent ?
 - La cible de l'objectif est-elle adaptée ? Représente-t-elle bien l'état du stock pour en garantir la durabilité ?
 - Le point de référence inclus dans l'objectif est-il adapté ? Quelles sont les implications de changer ou de garder la référence selon les scénarios ?

L'objectif de gestion de la pêcherie de légine australe repose sur l'estimation d'une biomasse reproductrice pré-exploitation, qui correspondrait à l'état d'équilibre du stock sans pêche. Dans le cas d'une baisse de productivité conduisant à un nouvel état d'équilibre, l'objectif de gestion actuel, si la biomasse de référence est inchangée, **reste précautionneux (SC-CAMLR-38/15) mais s'accompagne d'une baisse des totaux admissibles de captures plus importante**. Cela est possible dans la mesure où la nouvelle biomasse d'équilibre est supérieure à 50% de l'ancienne biomasse d'équilibre. Cependant, ajuster la biomasse de référence et donc l'objectif de gestion en cas de changement de régime peut aussi entraîner un taux d'exploitation de la ressource plus élevée sur une population déjà sous pression³ pouvant alors entraîner à son tour une baisse de la biomasse. **Il y a donc un danger d'accompagner le déclin d'un stock en adaptant régulièrement l'objectif** (Annexe 1).

C. Vers une prise en compte des incertitudes et une gestion des risques

Étant donné les données limitées à disposition et les incertitudes liées au changement climatique, il est essentiel de renforcer le cadre de gestion des risques de la pêcherie de légine australe. Nous suggérons ici deux axes de travail : i) un axe de long terme consistant à développer une approche par scénarios pour évaluer la robustesse des stratégies d'exploitation et ii) un axe de réponse à court terme permettant une plus grande réactivité aux événements extrêmes.

1] Développer une approche par scénario dans le choix de la stratégie d'exploitation.

L'**évaluation des stratégies de gestion** (ou « management strategy evaluation », MSE) permet la comparaison de différentes méthodes d'analyse et/ou règle de gestion afin de déterminer la stratégie la plus efficace pour atteindre un objectif de gestion donné. Cette procédure permet de prendre en compte les incertitudes et est considérée actuellement comme la piste la plus pertinente pour inclure les changements de régime dans la gestion des pêches (King et al., 2015),

³ ex. <https://meetings.npfmc.org/CommentReview/DownloadFile?p=3b7af7a3-419a-4284-983a-6a7e4a8a2d43.pdf&fileName=PPT%20Case%20Study%201%20Szuwalski.pdf>

notamment en posant la question des impacts de la prise en compte ou non des variables environnementales pour l'efficacité de la gestion.

A l'instar des méthodologies en science du climat pour gérer les incertitudes, il pourrait être pertinent de développer des scénarios de recrutement et d'évaluer les stratégies d'exploitation à l'aune de ces différents scénarios. Différentes approches peuvent être conduites pour développer les différents scénarios de recrutement. L'approche idéale serait de comprendre quels sont les mécanismes ou le mécanisme principal de la variabilité du recrutement et de faire le lien avec les projections des modèles de climat couplé utilisés pour l'exercice du GIEC, en utilisant différents scénarios d'émissions de CO₂. Une autre approche, plus faisable actuellement, serait de développer des scénarios à partir des données historiques, en particulier si un changement de régime a été observé, avec par exemple un scénario se fondant sur l'ensemble de la série temporelle (comme effectué actuellement), un autre seulement sur les dernières années de recrutement, etc. Les scientifiques pourraient présenter les différents TAC adaptés pour chaque scénario et la robustesse de ces TAC selon les autres scénarios (ex. Figure 5). Un niveau de risque acceptable serait alors à déterminer.

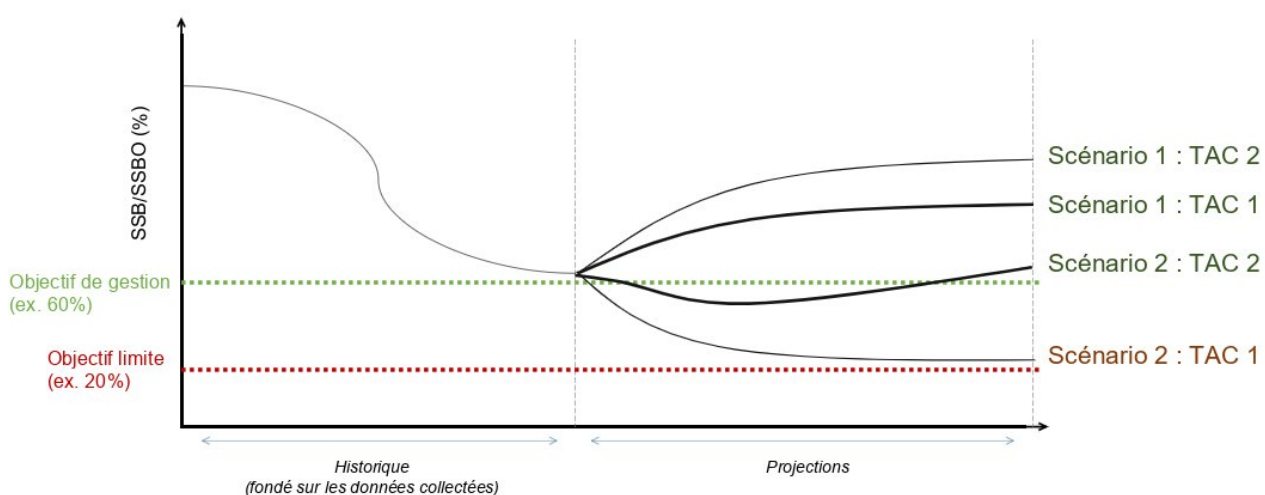


Figure 5: Exemple fictif d'une approche par scénario pour déterminer le TAC. On suppose que la baisse de la biomasse reproductrice (SSB) est associée à une baisse du recrutement. Pour les projections on envisage deux scénarios. Scénario 1: la baisse de recrutement est temporaire, la biomasse reproductrice va alors réaugmenter. Le TAC pertinent pour respecter l'objectif de gestion dans ce scénario est TAC 1. Scénario 2 : la baisse de recrutement se poursuit, la biomasse reproductrice va continuer à diminuer. Le TAC pertinent pour respecter l'objectif de gestion dans ce scénario est TAC 2 (a priori ce TAC sera plus faible que TAC 1). On évalue ensuite les conséquences des choix de gestion en fonction du scénario effectivement réalisé. Dans le cas où le scénario 1 se réalise mais le TAC 2 a été adopté, l'objectif de gestion reste atteint. Dans le cas où le scénario 2 se réalise mais le TAC 1 a été adopté, il y a un risque que l'objectif de gestion ne soit plus atteint.

2] Développer des mesures d'adaptation du TAC en cas d'évènement majeur de baisse du recrutement.

Le changement climatique peut induire une variabilité accrue dans les processus physiques et biologiques, ce qui peut nécessiter davantage de flexibilité réglementaire dans la gestion des stocks de pêche pour en assurer la durabilité.

En reprenant les arguments développés dans les sections II.A et III.A, il semble qu'une piste majeure est de préparer des réponses de la gestion en cas de baisse importante du recrutement.

Ces réponses peuvent être une **baisse de x% du TAC en cas de détection d'une baisse en-deçà d'un certain seuil de recrutement à déterminer**. L'objectif de cette baisse du TAC est de permettre une reconstitution du stock, permettant ensuite éventuellement de revenir à des niveaux de TAC plus élevés. Une analyse coûts-bénéfices pourrait être menée pour évaluer l'efficacité d'une telle action comparée à l'inaction.

IV – Assurer au maximum la résilience du stock

De par les diverses incertitudes, que ce soit sur la trajectoire d'émission qui va être suivie ou sur les mécanismes d'impact du changement climatique sur le stock de légine, il reste aujourd'hui difficile de prédire le futur du stock de légine australe dans la région et d'estimer quantitativement la valeur optimale de prélèvement assurant la pérennité du stock dans ce contexte changeant. Il est alors important de **maximiser la résilience du stock face à diverses perturbations**.

1] Continuer le développement d'une approche écosystémique de la pêche. Le développement d'approches écosystémiques intégrées que ce soit à travers des mesures de gestion ponctuelles, l'établissement d'aires marines protégées (par exemple en haute mer dans le cadre de la CCAMLR et de BBNJ) et les programmes de suivis scientifiques peuvent contribuer à la résilience du stock face au changement climatique. La gestion de la pêche fondée sur les écosystèmes peut permettre de diminuer le risque de déclin des stocks mais les avantages à long terme de cette approche sont limités par l'ampleur des changements climatiques projetés (Holsman et al., 2020).

2] La préservation de zones clés pour le renouvellement du stock de légine peut permettre d'augmenter la résilience du stock face à un environnement changeant. Les zones clés pour le renouvellement du stock de légine sont **les zones de pontes et les zones de nurseries** où les juvéniles se développent. Les zones de nurseries sont déjà protégées à travers les réglementations sur la profondeur de pêche autorisée (ex. pas de pêche à des profondeurs inférieures à 550m par exemple pour les TAAF) et par certaines limites de réserve naturelle (ex. protection stricte autour de l'île de Kerguelen). Des incertitudes demeurent sur l'ensemble des zones de pontes et leurs contributions aux différents stocks mais des campagnes ont pu identifier certaines zones comme étant particulièrement abondantes en individus matures notamment le banc Skiff et le banc Elan.

Le Banc Elan est une zone abritant une population de légines matures, ce qui suggère la présence d'une zone de pontes, et se situe entre les zones 58.5.2 et 58.4.3a de la CCAMLR. De par la circulation océanique sur le Plateau de Kerguelen, ce banc pourrait contribuer à la productivité des stocks de légine des ZEE de Heard et McDonald et de Kerguelen. Le rapport de l'arrêté de la pêche dans cette zone pourrait avoir un effet bénéfique sur le stock du Plateau de Kerguelen. La pêche de légine australe dans la zone 58.4.3a, en-dehors des juridictions nationales, est considérée comme exploratoire. La limite de capture était fixée à 24 tonnes pour la saison 2019/2020, à 19 tonnes pour 2020/2021 et 2021/2022 **puis réduite à 0 tonnes pour 2022/2023 par précaution** (mesure de conservation 41-06). **Il serait pertinent de conserver cette limitation du fait de l'importance potentielle de cette zone pour le renouvellement du stock de légine australe.**

3] Adapter le diagramme d'exploitation de la pêche pour maximiser la capacité de reproduction du stock.

Les adultes reproducteurs n'ont pas tous la même fécondité, celle-ci croissant avec la taille et l'âge des individus. Or les pêcheurs ne pêchent pas les mêmes quantités de poissons pour chaque classe d'âge. Il peut être intéressant de déterminer quel schéma de sélectivité de la pêche par classe d'âge permettrait d'optimiser la capacité reproductrice du stock. Les gestionnaires pourraient alors se saisir d'une telle information pour adapter la gestion par exemple à travers des limitations spatiales ou en profondeur.

V. Conclusion et généralisation

Les principes clés identifiés par le 5ème rapport du GIEC pour que les pêcheries puissent faire face au changement climatique sont : **la coopération, le principe de précaution et la gestion fondée sur les écosystèmes**. Ces principes sont présents dans les cadres réglementaires de la CCAMLR, des TAAF et de l'APSOI, la CCAMLR étant d'ailleurs considérée comme plutôt exemplaire dans l'intégration de ces principes (Wendebourg, 2020). Cependant, le changement climatique peut invalider de nombreuses hypothèses sur lesquelles est fondée la gestion actuelle, **remettant alors en question la durabilité de la gestion actuelle dans des scénarios de changement climatique futurs**. Adapter la gestion au changement climatique nécessite un changement de paradigme de la part des scientifiques et des gestionnaires. De potentielles mesures de gestion pour faire face aux changements climatiques sont ici résumées dans le Tableau 1 et trois axes de travail ont été identifiés :

- **Un axe méthodologique** (long terme) : une remise en question des hypothèses et des méthodes traditionnelles de gestion pour passer d'une vision statique ou à l'équilibre du stock à une vision dynamique ;
- **Un axe de gestion des risques** (moyen terme) : par le développement tant par les scientifiques que par les gestionnaires d'une approche par scénario et à travers l'élaboration de mesures d'urgence en cas d'évènement extrêmes de baisse du recrutement ;
- **Un axe de résilience** (court terme) : par un ensemble de mesures (parfois à travers des outils déjà existants) permettant de maximiser la capacité de reproduction du stock.

Les trois axes et les potentielles mesures de gestion présentés ici peuvent être généralisés à d'autres stocks pour faire face au risque d'une baisse de biomasse. Bien que le cas de la légine australe soit particulier, certains enjeux du changement climatique identifiés existent également pour d'autres pêcheries. En particulier, l'importance de la phase de recrutement concerne une grande partie des stocks pêchés. Or, une **baisse du recrutement a été observée pour de nombreux stocks** : on estime que la capacité de recrutement moyenne des stocks dans le monde a décliné d'environ 3% du maximum historique par décennie (Britten et al., 2016). L'enjeu de représentativité dans les modèles et de suivi de l'état du stock à travers l'objectif de gestion n'est donc pas spécifique à la légine et doit poser des questions pour tous les stocks réglementés/pêchés. De même, **des facteurs écosystémiques ou environnementaux ne sont inclus dans la gestion que d'environ 2% des stocks de pêche dans le monde** (Chavez-Molina et al., 2023).

Une étude de 2021 indique que si un grand nombre d'organisations régionales de gestion des pêches (ORGP) sont conscientes que le changement climatique va exercer une pression supplémentaire sur les stocks, **il manque encore une prise en compte opérationnelle de ces**

enjeux (Sumbly et al., 2021). Dans les ORGPs les plus avancées sur le sujet, les efforts sont principalement d'ordre procédural pour maintenir la prise de conscience et ce sujet à l'agenda et/ou pour appeler à prendre en compte le changement climatique dans la gestion. Des efforts pour davantage d'opérationnalisation de cette prise de conscience sont observés notamment avec la tenue les 11 et 12 juillet 2023 d'une réunion des experts de l'ICCAT sur le changement climatique lors de laquelle de nombreuses pistes de travail ont été discutées.

Parmi les principaux obstacles à l'opérationnalisation de la prise en compte du changement climatique dans la gestion des pêcheries on note les incertitudes associées aux impacts du changement climatique à l'échelle des unités de gestion (Sumbly et al., 2021) et la difficulté à définir des ruptures dans les dynamiques des stocks (Wendebourg et al., 2020). Le renforcement des outils existants à court terme pour augmenter la résilience du stock (axe 3) associé au développement à moyen terme d'approches par scénarios pour davantage intégrer les incertitudes à la prise de décision (axe 2) peuvent contribuer à pallier cette difficulté. Les autres principaux obstacles identifiés dans la littérature scientifique sont le manque de volonté politique pour prendre en compte des actions qui risquent de diminuer l'extraction de ressource à court terme (Sumbly et al., 2021) et le contraste entre la rapidité des changements environnementaux et la lenteur des procédures pour modifier les cadres réglementaires (Wendebourg et al., 2020). Une approche par scénario permettrait d'évaluer les coûts/bénéfices des différentes stratégies de gestion pouvant mettre en avant le coût économique de l'inaction ; et le développement de mesures de vigilance et de gestion des crises (Tableau 1) permettrait d'introduire de la flexibilité réglementaire permettant une plus grande réactivité en cas d'évènements extrêmes.

A noter que d'autres options d'adaptation au changement climatique n'ont pas été explorées dans cette synthèse, notamment en ce qui concerne les acteurs socio-économiques (ex. systèmes d'assurance, vers une diversification des pêcheries ou accompagnement vers leur fermeture etc.). Enfin, l'ampleur des efforts d'adaptation requis sont conditionnés à la trajectoire d'émissions de CO2 qui sera suivie : **les efforts d'atténuation dans le secteur de la pêche sont donc aussi essentiels pour permettre sur le long terme une adaptation possible.**

Tableau 1: Mesures de gestion potentielles pour adapter la gestion des pêches à la légine australe au changement climatique

Objectifs	Exemples de mesures de gestion
<i>Maximisation de la résilience du stock</i>	<ul style="list-style-type: none"> • Protection de zones clés pour maximiser le renouvellement du stock ; • Adapter le diagramme d'exploitation pour maximiser la reproduction (prenant en compte que les individus plus âgés sont plus féconds).
<i>Adaptation du modèle d'évaluation du stock</i>	Pistes d'amélioration de la structure du modèle : <ul style="list-style-type: none"> – Prise en compte de facteurs environnementaux sur le recrutement ; – Inclure les différents niveaux de fécondité selon les classes d'âge ; – Modèle spatialisé sur le Plateau de Kerguelen Pistes d'amélioration des projections : <ul style="list-style-type: none"> – Développer des scénarios de recrutement en lien avec la variabilité des conditions environnementales et selon différents scénarios de changement climatique.

<p><i>Vigilance et anticipation des impacts</i></p>	<ul style="list-style-type: none"> • Programme annuel de suivi du recrutement (avec seuil de recrutement à définir pour déclencher des mesures de gestion) ; • Développer des indicateurs environnementaux (ou biologiques) pour anticiper les événements extrêmes (aussi appelés « early warning signals » ; peut nécessiter un effort scientifique important).
<p><i>Gestion du risque et des incertitudes</i></p>	<ul style="list-style-type: none"> • Approche par scénarios avec les différentes parties prenantes et réflexion commune sur le niveau de préparation de la gestion et les potentielles solutions • Processus d'évaluation des stratégies de gestion (ou MSE) selon différents scénarios de changement climatique (et de ses impacts sur le recrutement) ; • Utilisation d'ensemble de modèles et/ou scénarios pour l'estimation du total admissible de capture ; • Développer des objectifs intermédiaires pour déclencher des mesures plus contraignantes (par exemple un seuil entre l'objectif de gestion et l'objectif limite de 20%) ;
<p><i>Réponse aux chocs et changements de régimes</i></p>	<ul style="list-style-type: none"> • Réduction du TAC ou fermeture de la pêche en cas d'évènement extrême (pour permettre la reconstitution plus rapide du stock) ; • Système d'assurance pour les pêcheurs en cas d'évènements extrêmes ; • Développement de nouvelles filières de valorisation et/ou diversification de la pêche.

Références

- Azarian, C., Bopp, L., Pietri, A., Sallée, J.B. and d'Ovidio, F., (2023). Current and projected patterns of warming and marine heatwaves in the Southern Indian Ocean. *Progress in Oceanography*, p.103036. doi.10.1016/j.pocean.2023.103036
- Bentley, J.W., Lundy, M.G., Howell, D., Beggs, S.E., Bundy, A., de Castro, F., Fox, C.J., Heymans, J.J., Lynam, C.P., Pedreschi, D., Schuchert, P., Serpetti, N., Woodlock, J. and Reid, D.G. (2021). Refining Fisheries Advice With Stock-Specific Ecosystem Information. *Front. Mar. Sci.* 8:602072. doi: 10.3389/fmars.2021.602072
- Britten, G.L., Dowd, M. et Worm, B. (2016). Changing recruitment capacity in global fish stocks. *Proceedings of the National Academy of Sciences*, 113 (1). <https://doi.org/10.1073/pnas.1504709112>.
- CCAMLR Secretariat (2023). Stock Assessment Report 2022: *Dissostichus eleginoides* at Heard Island (Division 58.5.2).
- CCAMLR Secretariat (2023). Stock Assessment Report 2022: *Dissostichus eleginoides* in Subarea 48.3.
- CCAMLR Secretariat (2023). Stock Assessment Report 2022: *Dissostichus eleginoides* and *Dissostichus mawsoni* in Subarea 48.4.
- Cheung, W. W. L., Palacios-Abrantes, J., Frölicher, T. L., Palomares, M. L., Clarke, T., Lam, V. W. Y., Oyinlola, M. A., Pauly, D., Reygondeau, G., Sumaila, U. R., Teh, L. C. L., and Wabnitz, C. C. C. (2022). Rebuilding fish biomass for the world's marine ecoregions under climate change. *Global Change Biology*, 28, 6254– 6267. <https://doi.org/10.1111/gcb.16368>
- Dahlberg, D. (1979). A review of survival rates of fish eggs and larvae in relation to impact assessments. *Mar. Fish. Rev.* 41, 1–12.
- Fox-Kemper, B., Hewitt, H.T., Xiao, C. , Aðalgeirsdóttir, G., Drijfhout, S.S., Edwards, T.L., Golledge, N.R., Hemer, M., Kopp, R.E., Krinner, G., Mix, A., Notz, D., Nowicki, S., Nurhati, I.S., Ruiz, L., Sallée, J.-B., Slangen, A.B.A., and Yu, Y. (2021). Ocean, Cryosphere and Sea Level Change. In *Climate Change, 2021. The Physical Science Basis. Contribution of Working Group I to the Sixth Assessment Report of the Intergovernmental Panel on Climate Change* [Masson-Delmotte, V., P. Zhai, A. Pirani, S.L. Connors, C. Péan, S. Berger, N. Caud, Y. Chen, L. Goldfarb, M.I. Gomis, M. Huang, K. Leitzell, E. Lonnoy, J.B.R. Matthews, T.K. Maycock, T. Waterfield, O. Yelekçi, R. Yu, and B. Zhou (eds.)]. Cambridge University Press, Cambridge, United Kingdom and New York, NY, USA, pp. 1211–1362, doi:10.1017/9781009157896.011
- Jacobson, L.D, and MacCall, A.D. (2011). Stock-recruitment models for Pacific sardine (*Sardinops sagax*). *Canadian Journal of Fisheries and Aquatic Sciences*. 52(3): 566-577. <https://doi.org/10.1139/f95-057>
- King, J.R., McFarlane, G.A., and Punt, A.E. (2015). Shifts in fisheries management: adapting to regime shifts. *Phil. Trans. R. Soc. B* 370: 20130277. <http://dx.doi.org/10.1098/rstb.2013.0277>
- Holsman, K.K et al (2019). Towards climate resiliency in fisheries management, *ICES Journal of Marine Science*, Volume 76, Issue 5, 09-10 , pp.1368–1378, <https://doi.org/10.1093/icesjms/fsz031>

- Lindegren, M., and Checkley, D.M.Jr. (2012). Temperature dependence of Pacific sardine (*Sardinops sagax*) recruitment in the California Current Ecosystem revisited and revised. *Canadian Journal of Fisheries and Aquatic Sciences*. **70**(2): 245-252. <https://doi.org/10.1139/cjfas-2012-0211>
- Llovel, W., and Terray, L. (2016). Observed southern upper-ocean warming over 2005–2014 and 1294 associated mechanisms. *Environmental Research Letters*, **11**(12), 124023. 1295 <https://doi.org/10.1088/1748-9326/11/12/124023>
- McClatchie, S., Goericke, R., Auad, G., and Hill, K. (2010). Re-assessment of the stock–recruit and temperature–recruit relationships for Pacific sardine (*Sardinops sagax*). *Canadian Journal of Fisheries and Aquatic Sciences*. **67**(11): 1782-1790. <https://doi.org/10.1139/F10-101>
- Myers, R. A. (2001). Stock and recruitment: generalizations about maximum reproductive rate, density dependence and variability using meta-analytic approaches. *ICES Journal of Marine Science* **58**, 937– 951.
- Holsman, K.K., Haynie, A.C., Hollowed, A.B. et al. (2020). Ecosystem-based fisheries management forestalls climate-driven collapse. *Nat Commun* **11**, 4579 . <https://doi.org/10.1038/s41467-020-18300-3>
- Patterson, H. and Tuynman, H. (2022). Chapter 24 Heard Island and MCDonal Islands Fishery, from Fishery status reports 2022, 2, Australian Bureau of Agricultural and Resource Economics and Sciences, Canberra. CC BY 4.0. <https://doi.org/10.25814/gx9r-3n90>.
- Pörtner, H.-O., Karl, D.M., Boyd, P.W., Cheung, W.W.L., Lluich-Cota, S.E., Nojiri, Y., Schmidt, D.N., and Zavialov, P.O. (2014). Ocean systems. In: *Climate Change 2014: Impacts, Adaptation, and Vulnerability. Part A: Global and Sectoral Aspects. Contribution of Working Group II to the Fifth Assessment Report of the Intergovernmental Panel on Climate Change* [Field, C.B., V.R. Barros, D.J. Dokken, K.J. Mach, M.D. Mastrandrea, T.E. Bilir, M. Chatterjee, K.L. Ebi, Y.O. Estrada, R.C. Genova, B. Girma, E.S. Kissel, A.N. Levy, S. MacCracken, P.R. Mastrandrea, and L.L.White (eds.)]. Cambridge University Press, Cambridge, United Kingdom and New York, NY, USA, pp. 411-484.
- SC-CAMLR-XXXVII/02 Rev. 1 (2018). Summary Report of the CCAMLR Independent Stock Assessment Review for Toothfish (Norwich, United Kingdom, 18 to 22 June 2018).
- SC-CAMLR-38/15 (2019). The CCAMLR Decision Rule, strengths and weaknesses. Délégation du Royaume-Uni.
- Shi, J.-R., Talley, L. D., Xie, S.-P., Peng, Q., and Liu, W. (2021). Ocean warming and accelerating Southern Ocean zonal flow. *Nature Climate Change*, **11**(12), 12. <https://doi.org/10.1038/s41558-021-92401212-5>
- Soeffker, M., Hollyman, P.R., Collins, M.A., Hogg, O.T., Riley, A., Laptikhovsky, V., Earl, T., Roberts, J., MacLeod, J.E., Belchier, M., and Darby, C. (2022). Contrasting life-history traits of two toothfish (*Dissostichus* spp.) species at their range edge around the South Sandwich Islands, *Deep Sea Res. Part II*, **201**,105098.
- Sumby, J., Haward, M., Fulton, E. A., and Pecl, G. T. (2021). Hot fish: The response to climate change by regional fisheries bodies. *Marine Policy*, **123**, 104284. <https://doi.org/10.1016/j.marpol.2020.104284>

Szuwalski, C.S., Vert-Pre, K.A., Punt, A.E., Branch, T.A. and Hilborn, R. (2015a), Examining common assumptions about recruitment: a meta-analysis of recruitment dynamics for worldwide marine fisheries. *Fish Fish*, 16: 633-648. <https://doi.org/10.1111/faf.12083>

Szuwalski, C.S., and Hiborn, R. (2015b). Environment drives forage fish productivity. *Proc. Natl. Acad. Sci. U.S.A.* 112, E3314-E3315.

Szuwalski, C.S. and Hollowed, A.B. (2016). Climate change and non-stationary population processes in fisheries management, *ICES Journal of Marine Science*, Volume 73, Issue 5, Pages 1297–1305, <https://doi.org/10.1093/icesjms/fsv229>

Szuwalski, C. S., Britten, G. L., Licandeo, R., Amoroso, R. O., Hilborn, R., and Walters, C. (2019). Global forage fish recruitment dynamics: A comparison of methods, time-variation, and reverse causality. *Fisheries Research*, 214, 56– 64. <https://doi.org/10.1111/faf.12083>.

Wendebourg, M. (2020). Southern Ocean fishery management: Is CCAMLR addressing the challenges posed by a changing climate? *Marine Policy*, 118, 103847. <https://doi.org/10.1016/j.marpol.2020.103847>

WG-FSA-2021/41 (2021). On the revision of the precautionary approach to ensure the rational use of the living resource (*Dissostichus eleginoides*) in Subarea 48.3. Delegation of the Russian Federation.

Yates, P., Ziegler, P., Welsford, D., Wotherspoon, S., Burch, P., and Maschette, D. (2019). Distribution of Antarctic toothfish *Dissostichus mawsoni* along East Antarctica: environmental drivers and management implications. *Fish. Res.* 219:105338. doi: 10.1016/j.fishres.2019.105338

Annexe 1 : Enjeu de modifier la valeur de biomasse reproductrice de référence B_0

L'objectif de cette annexe est d'illustrer les conséquences contradictoires que peut avoir un éventuel changement de la biomasse de référence utilisée pour l'objectif de gestion.

Cas 1 : la biomasse de référence est 200 000 tonnes. L'objectif de gestion est donc de maintenir une biomasse reproductrice supérieure à 100 000 tonnes avec donc une productivité qui peut atteindre autour de 10 000 tonnes. Le TAC calculé prend en compte cette productivité élevée du stock. Si en réalité un changement de régime a eu lieu qui correspond à une biomasse de référence plus faible mais que cela n'a pas été détecté par le modèle, on surestime donc la capacité réelle du stock à se renouveler et on risque de surexploiter le stock.

Cas 2 : la biomasse de référence passe de 200 000 tonnes à 100 000 tonnes et le changement de référence est effectué : on a alors une baisse de la biomasse reproductrice cible et une baisse du TAC associé. Un des risques est alors d'accompagner la baisse de biomasse reproductrice en adaptant fréquemment la valeur de la référence B_0 .

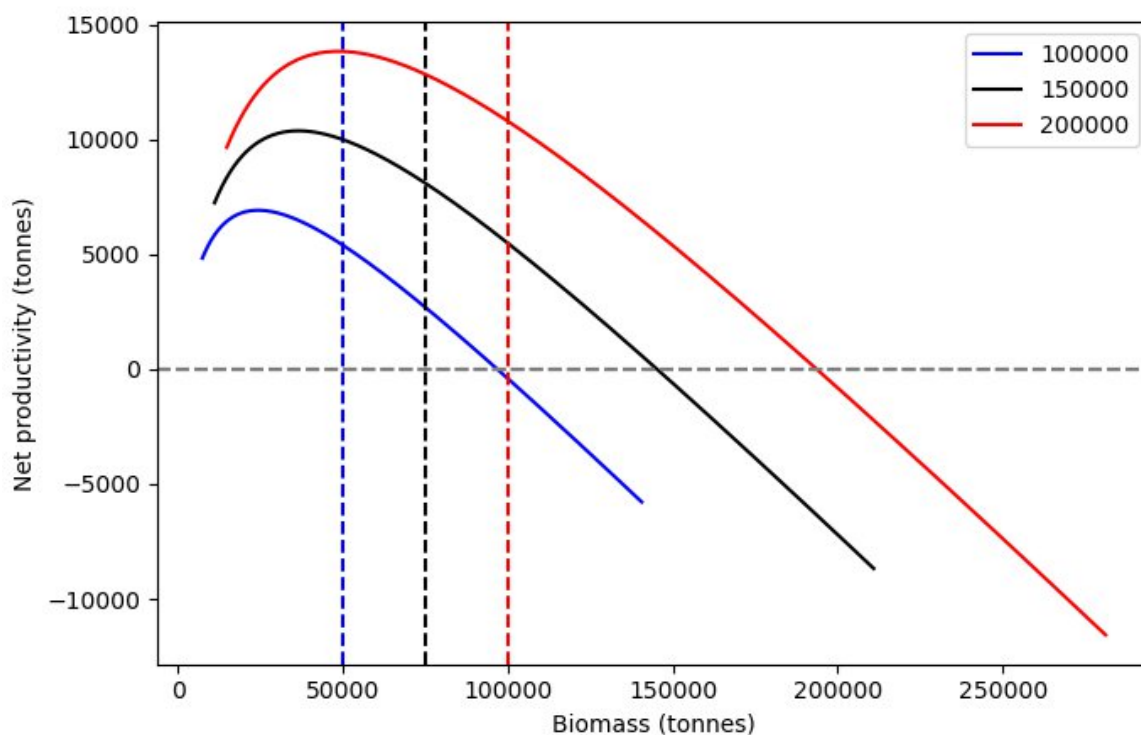


Figure 6: Productivité nette (biomasse moyenne sur toute les classes d'âge générée par le recrutement moins mortalité naturelle) en fonction de la biomasse reproductrice en tonnes selon différentes valeur de biomasse de référence (ou biomasse d'équilibre B_0) en utilisant les équations théoriques d'un modèle de population structuré par classe d'âge et sans prendre en compte la mortalité par la pêche. Les pointillés indiquent pour chaque cas de biomasse de référence, la biomasse cible pour la gestion (selon l'objectif de gestion de conserver 50% de B_0).

Annexe 2 : Figures de la littérature scientifique étudiant les effets du changement climatique sur les stocks de pêche à l'échelle globale.

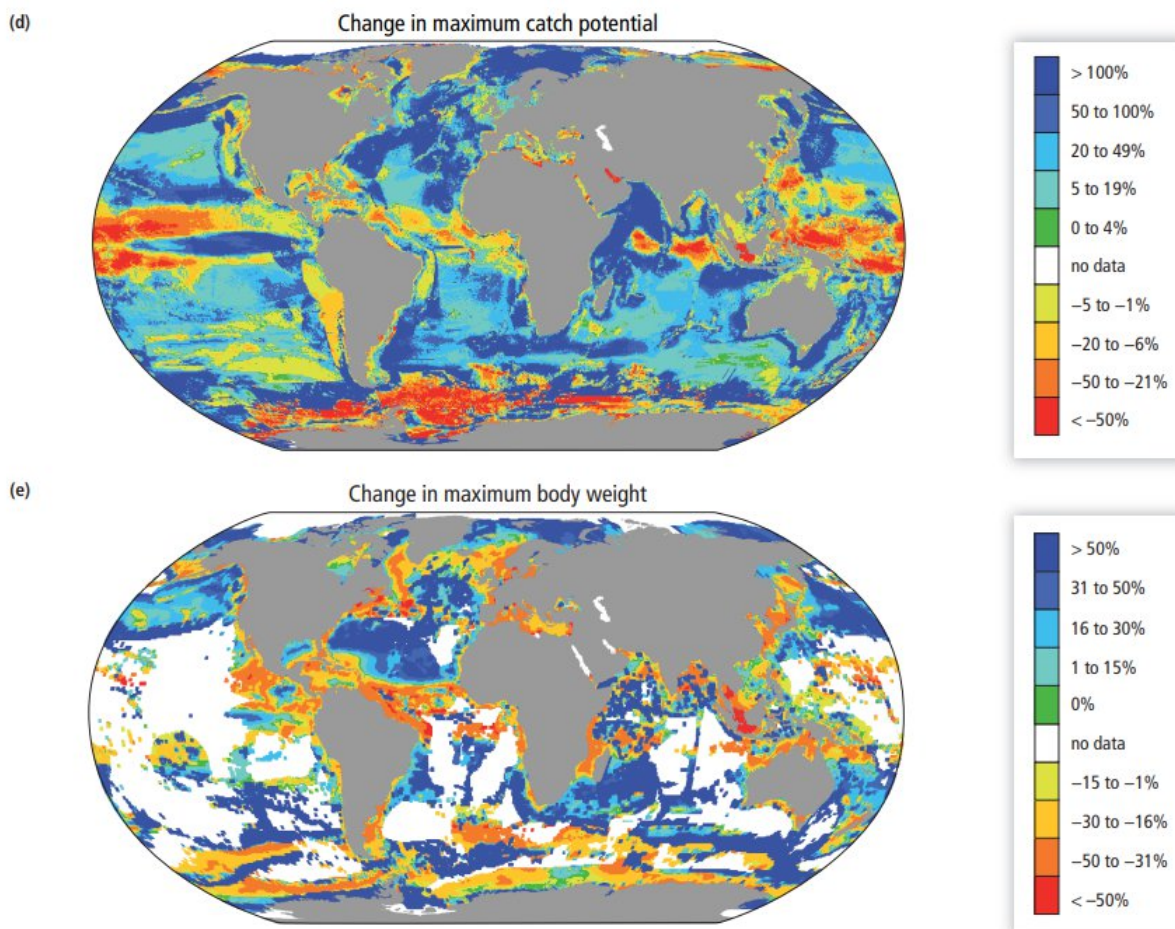


Figure 7: (d) Redistribution globale du potentiel de capture maximal en combinant les changements d'aire de répartition des espèces et les changements projetés de production primaire (analyse incluant environ 1000 espèces de poissons pêchés et d'invertébrés sous un scénario de réchauffement à 2°C, voir Cheung et al., 2010.) (e) Changement de la taille maximum de communautés de poissons issus des changements de distribution des espèces et des taux de croissance (analyse incluant environ 610 espèces de poissons, voir Cheung et al., 2013). Source : Pörtner et al., 2014 (AR5 WGII Chapitre 6).

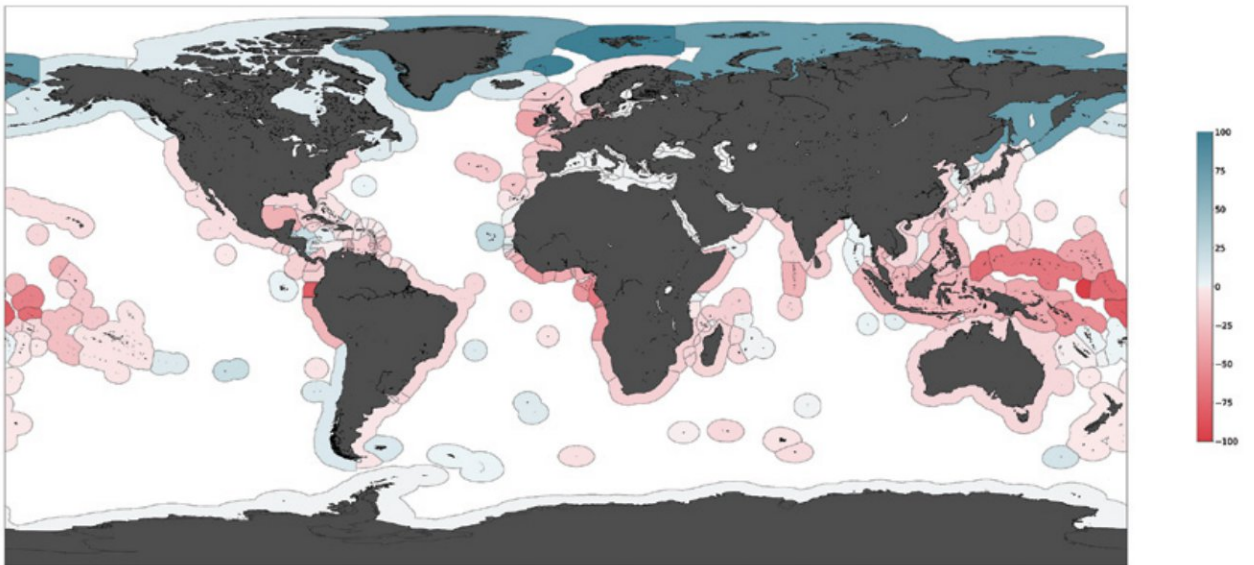


Figure 8: Variations prévues du potentiel de capture maximal (%) dans le cadre du scénario d'émission de CO2 le plus élevé (RCP8,5) d'ici 2050 (2046 à 2055) pour les projections du Modèle de bioclimat dynamique (DBEM). Source : Cheung et al., 2018.

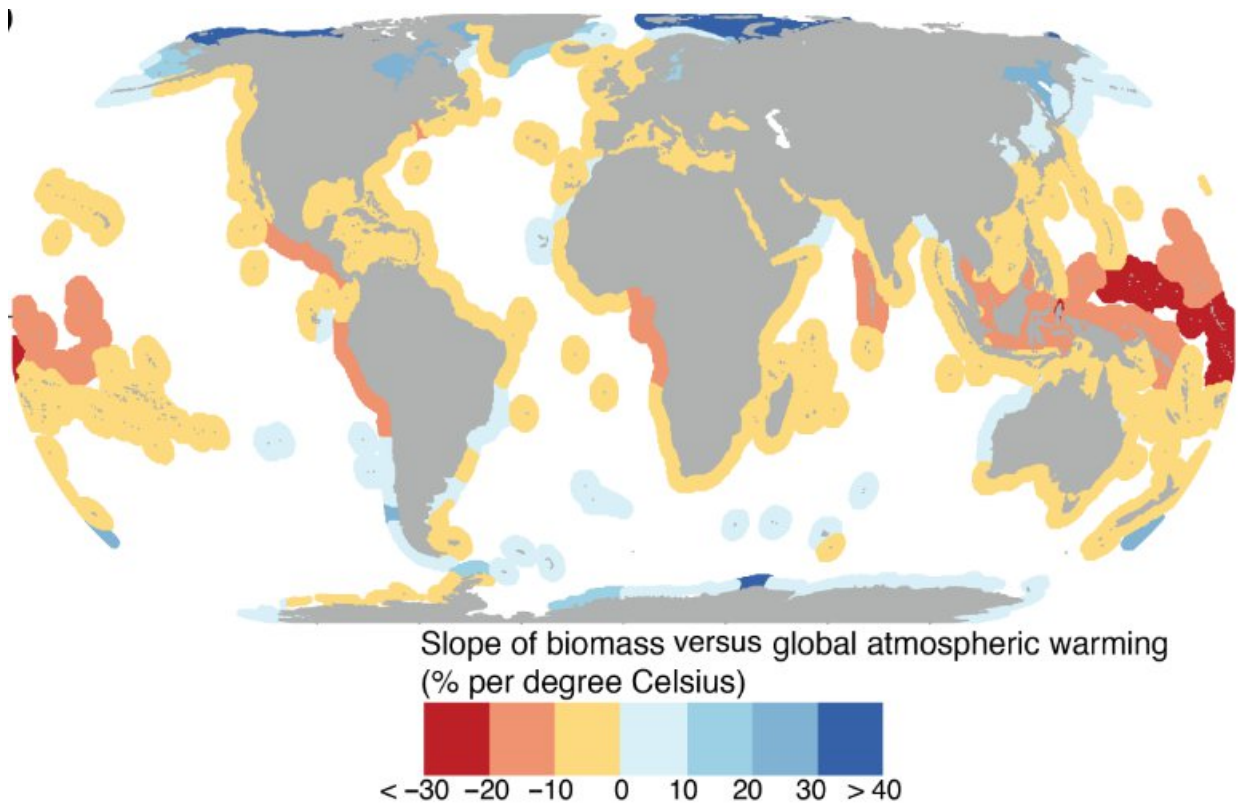


Figure 9: Carte des écorégions marines avec les pentes estimées entre la biomasse non exploitée projetée par rapport aux niveaux pré-industriels et les niveaux de réchauffement globaux (Source : Cheung et al., 2022).

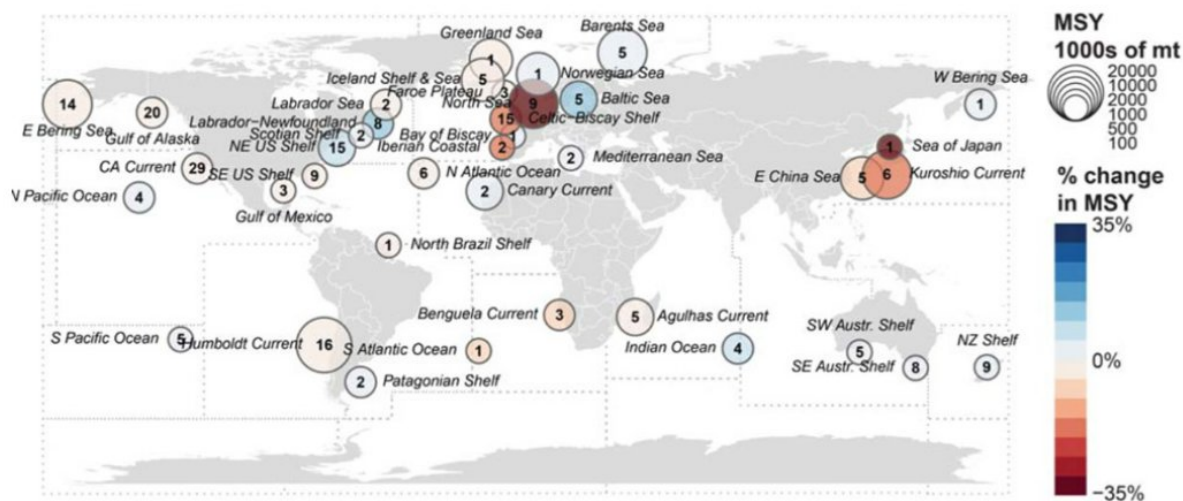


Figure 10: Impact du réchauffement de l'océan sur les stocks globaux de poissons. Les valeurs bleues indiquent une augmentation du rendement maximum durable entre les périodes 1930-39 et 2001-10 tandis que les valeurs rouges indiquent une diminution. La taille des cercles représente la taille des stocks de poissons (en millions de tonnes) et le nombre à l'intérieur du cercle montre le nombre de populations dans la région (Source : Free et al., 2019).

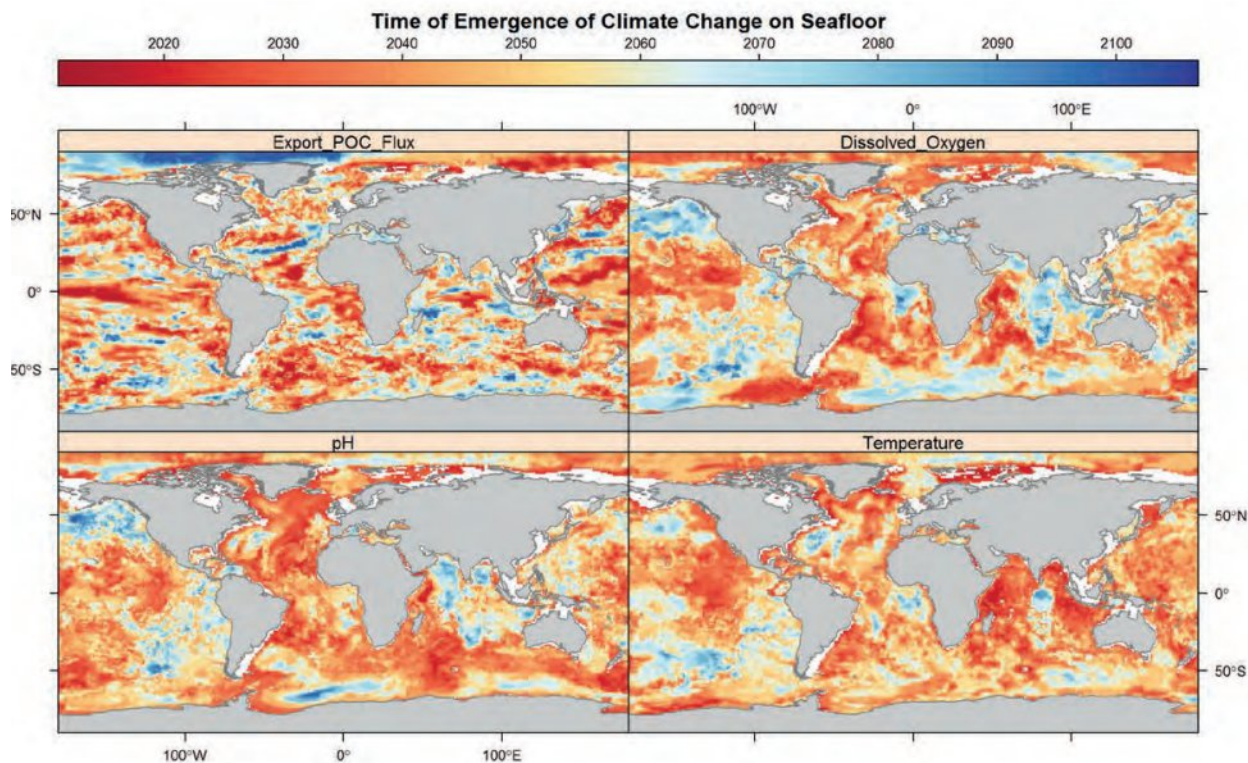


Figure 11: Temps d'émergence de signaux du changement climatique (flux d'export de carbone, oxygène dissous, pH et température) au niveau des fonds marins (Source : FAO, 2018).

Références pour les annexes

Cheung, W.W.L., V.W.Y. Lam, J.L. Sarmiento, K. Kearney, R. Watson, D. Zeller, and D. Pauly, (2010). Large-scale redistribution of maximum fisheries catch in the global ocean under climate change. *Global Change Biology*, 16(1), 24-35.

Cheung, W.W.L., J.L. Sarmiento, J. Dunne, T.L. Frölicher, V.W.Y. Lam, M.L.D. Palomares, R. Watson, and D. Pauly, 2013: Shrinking of fishes exacerbates impacts of global ocean changes on marine ecosystems. *Nature Climate Change*, 3(3), 254-258

Cheung, W.W.L, Burggeman, J., et Butenschön, M. (2018). Chapter 4 : Projected changes in global and national potential marine fisheries catch under climate change scenarios in the twenty-first century. In : *Impacts of climate change on fisheries and aquaculture : Synthesis of current knowledge, adaptation and mitigation options* [Barange, M., Bahri, T., Beveridge, M.C.M., Cochrane, K.L., Funge-Smith, S. and Poulain, F.]. FAO, Rome, Italy.

Cheung, W. W. L., Palacios-Abrantes, J., Frölicher, T. L., Palomares, M. L., Clarke, T., Lam, V. W. Y., Oyinlola, M. A., Pauly, D., Reygondeau, G., Sumaila, U. R., Teh, L. C. L., and Wabnitz, C. C. C. (2022). Rebuilding fish biomass for the world's marine ecoregions under climate change. *Global Change Biology*, 28, 6254–6267. <https://doi.org/10.1111/gcb.16368>

FAO. (2018). Deep-ocean climate change impacts on habitat, fish and fisheries, by Lisa Levin, Maria Baker, and Anthony Thompson (eds). FAO Fisheries and Aquaculture Technical Paper No. 638. Rome, FAO. 186 pp. Licence: CC BY-NC-SA 3.0 IGO.

Free, C.M., Thorson, J.T., Pinsky, M.L., Oken, K.L., Wiedenmann, J., and Jensen, O. (2019). Impacts of historical warming on marine fisheries production. *Science* 363:979-983

Pörtner, H.-O., Karl, D.M., Boyd, P.W., Cheung, W.W.L., Lluich-Cota, S.E., Nojiri, Y., Schmidt, D.N., and Zavialov, P.O. (2014). Ocean systems. In: *Climate Change 2014: Impacts, Adaptation, and Vulnerability. Part A: Global and Sectoral Aspects. Contribution of Working Group II to the Fifth Assessment Report of the Intergovernmental Panel on Climate Change* [Field, C.B., V.R. Barros, D.J. Dokken, K.J. Mach, M.D. Mastrandrea, T.E. Bilir, M. Chatterjee, K.L. Ebi, Y.O. Estrada, R.C. Genova, B. Girma, E.S. Kissel, A.N. Levy, S. MacCracken, P.R. Mastrandrea, and L.L. White (eds.)]. Cambridge University Press, Cambridge, United Kingdom and New York, NY, USA, pp. 411-484.

Bibliography

- Abernathy, R., Cerovecki, I., Holland, P., Newsom, E., Mazloff, M., and Talley, L. D., Water-mass transformation by sea ice in the upper branch of the Southern Ocean overturning. *Nature Geosci*, **9**, (2016), p. 596–601, doi:10.1038/ngeo2749.
- Alexander, M. A., Deser, C., and Timlin, M. S., The Reemergence of SST Anomalies in the North Pacific Ocean. *Journal of Climate*, **12**(8), (1999), pp. 2419 – 2433, doi: 10.1175/1520-0442(1999)012<2419:TROSAI>2.0.CO;2.
- Amaya, D., Jacox, M., Alexander, M., Scott, J. D., Deser, C., Capotondi, A., and Phillips, A. S., Bottom marine heatwaves along the continental shelves of North America. *Nat Commun*, **14**(1038), (2023a), pp. 1–15, doi:10.1038/s41467-023-36567-0.
- Amaya, D. J., Alexander, M. A., Capotondi, A., Deser, C., Karnauskas, K. B., Miller, A. J., and Mantua, N. J., Are Long-Term Changes in Mixed Layer Depth Influencing North Pacific Marine Heatwaves? *Bulletin of the American Meteorological Society*, **102**(1), (2021), pp. pp. S59–S66, ISSN 00030007, 15200477.
URL: <https://www.jstor.org/stable/27207255>
- Amaya, D. J., Jacox, M. G., Fewings, M. R., Saba, V. S., Stuecker, M. F., Rykaczewski, R. R., Ross, A. C., Stock, C. A., Capotondi, A., Petrik, C. M., Bograd, S. J., Alexander, M. A., Cheng, W., Hermann, A. J., Kearney, K. A., and Powell, B. S., Marine heatwaves need clear definitions so coastal communities can adapt. *Nature*, **616**, (2023b), pp. 29–32, doi:10.1038/d41586-023-00924-2.
- Andrews, O. D., Bindoff, N. L., Halloran, P. R., Ilyina, T., and Le Quéré, C., Detecting an external influence on recent changes in oceanic oxygen using an optimal fingerprinting method. *Biogeosciences*, **10**(3), (2013), pp. 1799–1813, doi: 10.5194/bg-10-1799-2013.
URL: <https://bg.copernicus.org/articles/10/1799/2013/>

Ardyna, M., Claustre, H., Sallée, J.-B., D'Ovidio, F., Gentili, B., van Dijken, G., D'Ortenzio, F., and Arrigo, K. R., Delineating environmental control of phytoplankton biomass and phenology in the Southern Ocean. *Geophysical Research Letters*, **44**(10), (2017), pp. 5016–5024, doi:10.1002/2016GL072428.

URL: <https://agupubs.onlinelibrary.wiley.com/doi/abs/10.1002/2016GL072428>

Ardyna, M., Lacour, L., Sergi, S., d'Ovidio, F., Sallée, J.-B., Rembauville, M., Blain, S., Tagliabue, A., Schlitzer, R., Jeandel, C., Arrigo, K. R., and Claustre, H., Hydrothermal vents trigger massive phytoplankton blooms in the Southern Ocean. *Nature Communications*, **10**(2451), (2019), pp. 1–8, doi:10.1038/s41467-019-09973-6.

Argo, Argo Float Data and Metadata from Global Data Assembly Centre (Argo GDAC)., (2000), doi:10.17882/42182.

Armour, K. C., Marshall, J., Scott, J. R., Donohoe, A., and Newsom, E. R., Southern Ocean warming delayed by circumpolar upwelling and equatorward transport. *Nature Geoscience*, **9**, (2016), p. 549–554, doi:10.1038/ngeo2731.

Artana, C., Ferrari, R., Bricaud, C., Lellouche, J.-M., Garric, G., Sennéchaël, N., Lee, J.-H., Park, Y.-H., and Provost, C., Twenty-five years of Mercator ocean reanalysis GLORYS12 at Drake Passage: Velocity assessment and total volume transport. *Advances in Space Research*, **68**(2), (2021), pp. 447–466, ISSN 0273-1177, doi: 10.1016/j.asr.2019.11.033, 25 Years of Progress in Radar Altimetry.

Arvon, H., La Philosophie du travail, PUF, (1961).

Atkinson, A., Hill, S., Pakhomov, E., Siegel, V., Reiss, C. S., Loeb, V. J., Steinberg, D. K., Schmidt, K., Tarling, G. A., Gerrish, L., and Sailley, S. F., Krill (*Euphausia superba*) distribution contracts southward during rapid regional warming. *Nature Climate Change*, **9**, (2019), pp. 142–147, doi:10.1038/s41558-018-0370-z.

Atkinson, A., Siegel, V., Pakhomov, E., and Rothery, P., Long-term decline in krill stock and increase in salps within the Southern Ocean. *Nature*, **432**, (2004), pp. 100–103, doi:10.1038/nature02996.

Aubert De La Rue, E., La pêche aux Iles Saint-Paul et Amsterdam. *Revue des Travaux de l'Institut des Pêches Maritimes*, **5**, (1932), pp. 53–109.

- Auger, M., Morrow, R., Kestenare, E., Sallée, J. B., and Cowley, R., Southern Ocean in-situ temperature trends over 25 years emerge from interannual variability. *Nature Communications*, **12**(1), (2021), p. 514, doi:10.1111/gcb.12943.
- Azam, C.-S., Thellier, T., Verdier, A.-G., and Marteau, C., The French Southern Lands marine protected area: genesis of one the largest marine protected areas in the world. In *The Kerguelen Plateau: Marine Ecosystem and Fisheries*, in *Proceedings of the Second Symposium* (Edited by Welsford, D., Dell, J., and Duhamel, G.), The Department of the Environment and Energy, Australian Antarctic Division, Kingston, (2019).
- Azarian, C., Bopp, L., Pietri, A., Sallee, J., and d'Ovidio, F., Current and projected patterns of warming and marine heatwaves in the Southern Indian Ocean. *Progress in Oceanography*, (103036), (2023), pp. 1–19, doi:10.1016/j.pocean.2023.103036.
- Azarian, C., Bopp, L., Sallee, J., Swart, S., Guinet, C., and d'Ovidio, F., Marine heatwaves and global warming impacts on winter waters in the southern indian ocean. *Journal of Marine Systems*, **243**, (2024), pp. 1–14, doi:10.1016/j.jmarsys.2023.103962.
- Bailleul, F., Cotté, C., and Guinet, C., Mesoscale eddies as foraging area of a deep-diving predator, the southern elephant seal. *Mar Ecol Prog Ser*, **408**, (2010), pp. 251–264, doi:10.3354/meps08560.
- Bakun, A., *Patterns in the Ocean: Ocean Processes and Marine Population Dynamics*, in *California Sea Grant. Cooperation with Centro de Investigaciones Biológicas del Noroeste: La Paz, Mexico.*, (1996).
- Banzon, V., Smith, T. M., Chin, T. M., Liu, C., and Hankins, W., A long-term record of blended satellite and in situ sea-surface temperature for climate monitoring, modeling and environmental studies. *Earth System Science Data*, **8**(1), (2016), pp. 165–176, doi:10.5194/essd-8-165-2016.
URL: <https://essd.copernicus.org/articles/8/165/2016/>
- Barange, M., Bahri, T., Beveridge, M. C., Cochrane, K., Funge-Smith, S., and Poulain, F., *Impacts of Climate Change on Fisheries and Aquaculture: Synthesis of Current Knowledge, Adaptation and Mitigation Options*, (2018), doi:10.1038/nclimate1301.
URL: <http://www.fao.org/3/i9705en/i9705en.pdf>

- Barbraud, C., Delord, K., Bost, C. A., Chaigne, A., Marteau, C., and Weimerskirch, H., Population trends of penguins in the French Southern Territories. *Polar Biology*, **43**(7), (2020), p. 835–850, doi:10.1007/s00300-020-02691-6.
URL: <https://doi.org/10.1007/s00300-020-02691-6>
- Bashevkin, S. M., Dibble, C. D., Dunn, R. P., Hollarsmith, J. A., Ng, G., Satterthwaite, E. V., and Morgan, S. G., Larval dispersal in a changing ocean with an emphasis on upwelling regions. *Ecosphere*, **11**(1), (2020), p. e03015, doi:10.1002/ecs2.3015.
- Baudena, A., Ser-Giacomi, E., D’Onofrio, D., Capet, X., Cotté, C., Cherel, Y., and D’Ovidio, F., Fine-scale structures as spots of increased fish concentration in the open ocean. *Scientific Reports*, **11**(15805), (2021), pp. 1–13, doi:10.1038/s41598-021-94368-1.
- Baudena, A., Ser-Giacomi, E., López, C., Hernández-García, E., and d’Ovidio, F., Cross-roads of the mesoscale circulation. *Journal of Marine Systems*, **192**, (2019), pp. 1–14, ISSN 0924-7963, doi:10.1016/j.jmarsys.2018.12.005.
URL: <https://www.sciencedirect.com/science/article/pii/S092479631830040X>
- Baudouin, V., From sustainability to sobriety., in *Sustainability research in the upper Rhine region – Concepts and case studies* (Edited by Hamman, P. and Vuilleumier, S.), pp. 27–37, Presses universitaires de Strasbourg, (2019).
- Beadling, R. L., Russell, J. L., Stouffer, R. J., Mazloff, M., Talley, L. D., Goodman, P. J., Sallée, J. B., Hewitt, H. T., Hyder, P., and Pandde, A., Representation of Southern Ocean Properties across Coupled Model Intercomparison Project Generations: CMIP3 to CMIP6. *Journal of Climate*, **33**(15), (2020), pp. 6555 – 6581, doi: 10.1175/JCLI-D-19-0970.1.
- Beaumont, L. J., Hughes, L., and Poulsen, M., Predicting species distributions: use of climatic parameters in BIOCLIM and its impact on predictions of species’ current and future distributions. *Ecological Modelling*, **186**(2), (2005), pp. 251–270, ISSN 0304-3800, doi:10.1016/j.ecolmodel.2005.01.030.
URL: <https://www.sciencedirect.com/science/article/pii/S0304380005000530>
- Beets, J. and Manuel, M., Temporal and seasonal closures used in fisheries management: A review with application to Hawaii, pp. 1–13, Department of Marine Science University of Hawaii-Hilo, (2007).

Belchier, M. and Collins, M. A., Recruitment and body size in relation to temperature in juvenile Patagonian toothfish (*Dissostichus eleginoides*) at South Georgia. *Marine Biology*, **155**, (2008), pp. 493–503, doi:10.1007/s00227-008-1047-3.

Belkin, I., Front, in *Interdisciplinary Encyclopedia of Marine Sciences* (Edited by Nybakken, J. W., Broenkow, W. W., , and Vallier, T. L.), pp. 433–436, Grolier Academic Reference, Danbury, Connecticut, (2003).

Bestley, S., Ropert-Coudert, Y., Bengtson, N. S., Brooks, C., Cotté, C., Dewar, M., Friedlaender, A., Jackson, J., Labrousse, S., Lowther, A., McMahon, C., Phillips, R., Pistorius, P., Puskic, P., Reis, A., Reisinger, R., Santos, M., Tarszisz, E., Tixier, P., Trathan, P., M, W., and Wienecke, B., Marine Ecosystem Assessment for the Southern Ocean: Birds and Marine Mammals in a Changing Climate. *Front. Ecol. Evol.*, **8**(566936), (2020), pp. 1–39, doi:10.3389/fevo.2020.566936.

URL: <https://doi.org/10.3389/fevo.2020.566936>

BirdLife International, World Database of Key Biodiversity Areas, (2022), developed by the KBA Partnership: BirdLife International, International Union for the Conservation of Nature, American Bird Conservancy, Amphibian Survival Alliance, Conservation International, Critical Ecosystem Partnership Fund, Global Environment Facility, Re:Wild (formerly Global Wildlife Conservation), NatureServe, Rainforest Trust, Royal Society for the Protection of Birds, Wildlife Conservation Society and World Wildlife Fund. March 2022 version.

URL: <http://keybiodiversityareas.org/kba-data/request>

Biuw, M., Boehme, L., Guinet, C., Hindell, M., Costa, D., Charrassin, J.-B., Roquet, F., Bailleul, F., Meredith, M., Thorpe, S., Tremblay, Y., McDonald, B., Park, Y.-H., Rintoul, S. R., Bindoff, N., Goebel, M., Crocker, D., Lovell, P., Nicholson, J., Monks, F., and Fedak, M. A., Variations in behavior and condition of a Southern Ocean top predator in relation to in situ oceanographic conditions. *Proceedings of the National Academy of Sciences*, **104**(34), (2007), pp. 13705–13710, doi:10.1073/pnas.0701121104.

URL: <https://www.pnas.org/doi/abs/10.1073/pnas.0701121104>

Blain, S., Quéguiner, B., Armand, L., Belviso, S., Bombled, B., Bopp, L., Bowie, A., Brunet, C., Brussaard, C., Carlotti, F., Christaki, U., Corbière, A., Durand, I., Ebersbach, F., Fuda, J.-L., Garcia, N., Gerringa, L., Griffiths, B., Guigue, C., Guillerm, C.,

- Jacquet, S., Jeandel, C., Laan, P., Lefèvre, D., Lo Monaco, C., Malits, A., Mosseri, J., Obernosterer, I., Park, Y.-H., Picheral, M., Pondaven, P., Remenyi, T., Sandroni, V., Sarthou, G., Savoye, N., Scouarnec, L., Souhaut, M., Thuiller, D., Timmermans, K., Trull, T., Uitz, J., van Beek, P., Veldhuis, M., Vincent, D., Viollier, E., Vong, L., and Wagener, T., Effect of natural iron fertilization on carbon sequestration in the Southern Ocean. *Nature*, **446**, (2007), p. 1070–1074, doi:10.1038/nature05700.
- Blain, S., Tréguer, P., Belviso, S., Bucciarelli, E., Denis, M., Desabre, S., Fiala, M., Martin Jézéquel, V., Le Fèvre, J., Mayzaud, P., Marty, J.-C., and Razouls, S., A biogeochemical study of the island mass effect in the context of the iron hypothesis: Kerguelen Islands, Southern Ocean. *Deep Sea Research Part I: Oceanographic Research Papers*, **48**(1), (2001), pp. 163–187, ISSN 0967-0637, doi:10.1016/S0967-0637(00)00047-9.
URL: <https://www.sciencedirect.com/science/article/pii/S0967063700000479>
- Boscolo-Galazzo, F., Crichton, K., Barker, S., and Pearson, P., Temperature dependency of metabolic rates in the upper ocean: A positive feedback to global climate change? *Global and Planetary Change*, **170**, (2018), pp. 201–212, doi:10.1111/gcb.13104.
- Bost, C., Cotte, C., Terray, P., Barbraud, C., Bon, C., Delord, K., Gimenez, O., Handrich, Y., Naito, Y., Guinet, C., and Weimerskirch, H., Large-scale climatic anomalies affect marine predator foraging behaviour and demography. *Nature Communications*, **6**(8220), (2015), pp. 1–9, doi:10.1038/ncomms9220.
URL: <https://doi.org/10.1038/ncomms9220>
- Bracegirdle, T. J., Holmes, C. R., Hosking, J. S., Marshall, G. J., Osman, M., Patterson, M., and Rackow, T., Improvements in Circumpolar Southern Hemisphere Extratropical Atmospheric Circulation in CMIP6 Compared to CMIP5. *Earth and Space Science*, **7**(6), (2020), p. e2019EA001065, doi:10.1029/2019EA001065.
URL: <https://agupubs.onlinelibrary.wiley.com/doi/abs/10.1029/2019EA001065>
- Brander, K., Impacts of climate change on fisheries. *Journal of Marine Systems*, **79**(3), (2010), pp. 389–402, ISSN 0924-7963, doi:10.1016/j.jmarsys.2008.12.015.
URL: <https://www.sciencedirect.com/science/article/pii/S0924796309000931>
- Bris, A. L., Mills, K. E., Wahle, R. A., Chen, Y., Alexander, M. A., Allyn, A. J., Schuetz, J. G., Scott, J. D., and Pershing, A. J., Climate vulnerability and resilience

- in the most valuable North American fishery. *Proceedings of the National Academy of Sciences*, **115**(8), (2018), pp. 1831–1836, doi:10.1073/pnas.1711122115.
URL: <https://www.pnas.org/doi/abs/10.1073/pnas.1711122115>
- Brisson-Curadeau, E., Elliott, K., and Bost, C.-A., Contrasting bottom-up effects of warming ocean on two king penguin populations. *Global Change Biology*, **29**(4), (2023), pp. 998–1008, doi:10.1111/gcb.16519.
- Brito-Morales, I., García Molinos, J., Schoeman, D. S., Burrows, M. T., Poloczanska, E. S., Brown, C. J., Ferrier, S., Harwood, T. D., Klein, C. J., McDonald-Madden, E., Moore, P. J., Pandolfi, J. M., Watson, J. E., Wenger, A. S., and Richardson, A. J., Climate Velocity Can Inform Conservation in a Warming World. *Trends in Ecology Evolution*, **33**(6), (2018), pp. 441–457, ISSN 0169-5347, doi:10.1016/j.tree.2018.03.009.
URL: <https://www.sciencedirect.com/science/article/pii/S0169534718300636>
- Brito-Morales, I., Schoeman, D. S., Everett, J. D., Klein, C. J., Dunn, D. C., García Molinos, J., Burrows, M. T., Buenafe, K. C. V., Dominguez, R. M., Possingham, H. P., and Richardson, A. J., Towards climate-smart, three-dimensional protected areas for biodiversity conservation in the high seas. *Nature Climate Change*, **12**, (2022), p. 402–407, doi:10.1038/s41558-022-01323-7.
- Brito-Morales, I., Schoeman, D. S., Molinos, J. G., Burrows, M. T., Klein, C. J., Arafeh-Dalmau, N., Kaschner, K., Garilao, C., Kesner-Reyes, K., and Richardson, A. J., Climate velocity reveals increasing exposure of deep-ocean biodiversity to future warming. *Nature Climate Change*, **10**(6), (2020), pp. 576–581, ISSN 1758-6798, doi:10.1038/s41558-020-0773-5.
URL: <https://doi.org/10.1038/s41558-020-0773-5>
- Britten, G. L., Dowd, M., and Worm, B., Changing recruitment capacity in global fish stocks. *Proceedings of the National Academy of Sciences*, **113**(1), (2016), pp. 134–139, doi:10.1073/pnas.1504709112.
URL: <https://www.pnas.org/doi/abs/10.1073/pnas.1504709112>
- Brodie, S., Jacox, M., Bograd, S., Welch, H., Dewar, H., Scales, K., Maxwell, S., Briscoe, D., Edwards, C., Crowder, L., Lewison, R., and Hazen, E., Integrating Dynamic Subsurface Habitat Metrics Into Species Distribution Models. *Front. Mar. Sci.*, **5**(219), (2018), pp. 1–13, doi:10.3389/fmars.2018.00219.

- Brooks, C., Chown, S., Douglass, L., Raymond, B., Shaw, J., Sylvester, Z., and et al., Progress towards a representative network of Southern Ocean protected areas. *PLoS ONE*, **15**(4), (2020), p. e0231361, doi:10.1371/journal.pone.0231361.
URL: <https://doi.org/10.1371/journal.pone.0231361>
- Brooks, C., Epstein, G., and Ban, N., Managing Marine Protected Areas in Remote Areas: The Case of the Subantarctic Heard and McDonald Islands. *Front. Mar. Sci.*, **6**, (2019), p. 631, doi:10.3389/fmars.2019.00631.
URL: <https://doi.org/10.3389/fmars.2019.00631>
- Brooks, C. M., Ainley, D. G., Abrams, P. A., Dayton, P. K., Hofman, R. J., Jacquet, J., and Siniff, D. B., Antarctic fisheries: Factor climate change into their management. *Nature*, **558**(7709), (2001), p. 177–180.
- Bruno, J., Bates, C., A.E.and Cacciapaglia, Pike, E. P., Amstrup, S. C., van Hooedonk, R., Henson, S. A., and Aronson, R. B., Climate change threatens the world’s marine protected areas. *Nature Climate Change*, **8**, (2018), pp. 499–503, doi:10.1038/s41558-018-0149-2.
- Bryndum-Buchholz, A., Tittensor, D. P., Blanchard, J. L., Cheung, W. W. L., Coll, M., Galbraith, E. D., Jennings, S., Maury, O., and Lotze, H. K., Twenty-first-century climate change impacts on marine animal biomass and ecosystem structure across ocean basins. *Global Change Biology*, **25**(2), (2019), pp. 459–472, doi:10.1111/gcb.14512.
URL: <https://onlinelibrary.wiley.com/doi/abs/10.1111/gcb.14512>
- Bull, B., Casal (c++ algorithmic stock assessment laboratory) casal user manual v2.30-2012/03/2, p. 282, (2012).
- Byju, P., Dommenget, D., and Alexander, M. A., Widespread Reemergence of Sea Surface Temperature Anomalies in the Global Oceans, Including Tropical Regions Forced by Reemerging Winds. *Geophysical Research Letters*, **45**(15), (2018), pp. 7683–7691, doi:10.1029/2018GL079137.
- Béhagle, N., Cotté, C., Lebourges-Dhaussy, A., Roudaut, G., Duhamel, G., Brehmer, P., Josse, E., and Cherel, Y., Acoustic distribution of discriminated micronektonic organisms from a bi-frequency processing: The case study of eastern Kerguelen oceanic

waters. *Progress in Oceanography*, **156**, (2017), pp. 276–289, ISSN 0079-6611, doi:10.1016/j.pocean.2017.06.004.

URL: <https://www.sciencedirect.com/science/article/pii/S0079661115300239>

Caccavo, J., Christiansen, H., Constable, A., Ghigliotti, L., Trebilco, R., Brooks, C., Cotte, C., Desvignes, T., Dornan, T., Jones, C., Koubbi, P., Saunders, R., Strobel, A., Vacchi, M., van de Putte, A., Walters, A., Waluda, C., Woods, B., and Xavier, J., Productivity and Change in Fish and Squid in the Southern Ocean. *Front. Ecol. Evol.*, **9**(624918), (2021), pp. 1–25, doi:10.3389/fevo.2021.624918.

Cai, W., Cowan, T., Godfrey, S., and Wijels, S., Simulations of processes associated with the fast warming rate of the southern midlatitude ocean. *J. Climate*, **23**, (2010), p. 197–206.

Canadell, J., Monteiro, P., Costa, M., da Cunha, L. C., Cox, P., Eliseev, A., Henson, S., Ishii, M., Jaccard, S., Koven, C., Lohila, A., Patra, P., Piao, S., Rogelj, J., Syampungani, S., Zaehle, S., , and Zickfeld, K., Global Carbon and other Biogeochemical Cycles and Feedbacks, in *In Climate Change 2021: The Physical Science Basis. Contribution of Working Group I to the Sixth Assessment Report of the Intergovernmental Panel on Climate Change* (Edited by Masson-Delmotte, V., Zhai, P., Pirani, A., Connors, S., Pean, C., Berger, S., Caud, N., Chen, Y., Goldfarb, L., Gomis, M., Huang, M., Leitzell, K., Lonnoy, E., Matthews, J., Maycock, T., Waterfield, T., Yelekçi, O., Yu, R., and Zhou, B.), p. 673–816, Cambridge University Press, (2021), doi:10.1017/9781009157896.007.

Caputi, N., Kangas, M., Chandrapavan, A., Hart, A., Feng, M., Marin, M., and Lestang, S. d., Factors Affecting the Recovery of Invertebrate Stocks From the 2011 Western Australian Extreme Marine Heatwave. *Frontiers in Marine Science*, **6**, ISSN 2296-7745, doi:10.3389/fmars.2019.00484.

URL: <https://www.frontiersin.org/articles/10.3389/fmars.2019.00484>

Carpenter-Kling, T., Handley, J., Connan, M., Crawford, R., Makhado, A., Dyer, B., Froneman, W., Lamont, T., Wolfaardt, A., Landman, M., Sigqala, M., and Pistorius, P., Gentoo penguins as sentinels of climate change at the sub-Antarctic Prince Edward Archipelago, Southern Ocean. *Ecological Indicators*, **101**, (2019), pp. 163–172, ISSN 1470-160X, doi:10.1016/j.ecolind.2019.01.008.

URL: <https://www.sciencedirect.com/science/article/pii/S1470160X19300081>

Carr, M., Woodson, C., Cheriton, O., Malone, D., McManus, M., and Raimondi, P., Knowledge through partnerships: Integrating marine protected area monitoring and ocean observing systems. *Frontiers in Ecology and the Environment*, **9**, (2011), p. 342–350, doi:10.2307/23034443.

Carter, L., McCave, I., and Williams, M. J., Chapter 4 Circulation and Water Masses of the Southern Ocean: A Review, in *Antarctic Climate Evolution* (Edited by Florindo, F. and Siegert, M.), volume 8 of *Developments in Earth and Environmental Sciences*, pp. 85–114, Elsevier, (2008), doi:10.1016/S1571-9197(08)00004-9.

URL: <https://www.sciencedirect.com/science/article/pii/S1571919708000049>

Chapman, C. C., Lea, M.-A., Meyer, A., Sallée, J.-B., and Hindell, M., Defining Southern Ocean fronts and their influence on biological and physical processes in a changing climate. *Nature Climate Change*, **10**(3), (2020), pp. 209–219, ISSN 1758-6798, doi: 10.1038/s41558-020-0705-4.

URL: <https://doi.org/10.1038/s41558-020-0705-4>

Charrassin, J.-B. and Bost, C.-A., Utilisation of the oceanic habitat by king penguins over the annual cycle. *Marine Ecology Progress Series*, **221**, (2001), pp. 285–298, doi:10.3354/meps221285.

Charrassin, J.-B., Park, Y.-H., Le Maho, Y., and Bost, C.-A., Fine resolution 3D temperature fields off Kerguelen from instrumented penguins. *Deep Sea Research Part I: Oceanographic Research Papers*, **51**(12), (2004), pp. 2091–2103, ISSN 0967-0637, doi:10.1016/j.dsr.2004.07.019.

URL: <https://www.sciencedirect.com/science/article/pii/S0967063704001578>

Chavez-Molina, V., Nocito, E. S., Carr, E., Cavanagh, R. D., Sylvester, Z., Becker, S. L., Dorman, D. D., Wallace, B., White, C., and Brooks, C. M., Managing for climate resilient fisheries: Applications to the Southern Ocean. *Ocean and Coastal Management*, **239**, (2023), p. 106580, ISSN 0964-5691, doi:10.1016/j.ocecoaman.2023.106580.

URL: <https://www.sciencedirect.com/science/article/pii/S0964569123001059>

Chen, D., Rojas, M., Samset, B., Cobb, K., Niang, A. D., Edwards, P., Emori, S., Faria, S., Hawkins, E., Hope, P., Huybrechts, P., Meinshausen, M., Mustafa, S., Plattner, G.-K., and Tréguier, A.-M., Framing, Context, and Methods, in *Climate*

- Change 2021: The Physical Science Basis. Contribution of Working Group I to the Sixth Assessment Report of the Intergovernmental Panel on Climate Change* (Edited by Masson-Delmotte, V., Zhai, P., Pirani, A., Connors, S., Péan, C., Berger, S., Caud, N., Chen, Y., Goldfarb, L., Gomis, M., Huang, M., Leitzell, K., Lonnoy, E., Matthews, J., Maycock, T., Waterfield, T., Yelekçi, O., Yu, R., and Zhou, B.), p. 147–286, Cambridge University Press, (2021), doi:10.1017/9781009157896.003.
- Cheung, W. W., Lam, V. W., and Pauly, D., *Dynamic bioclimate envelope model to predict climate-induced changes in distribution of marine fishes and invertebrates*, volume 16, (2008).
- Cheung, W. W., Lam, V. W., Sarmiento, J. L., Kearney, K., Watson, R., and Pauly, D., Projecting global marine biodiversity impacts under climate change scenarios. *Fish and Fisheries*, **10**(3), (2009), pp. 235–251, ISSN 1467-2960, doi:10.1111/j.1467-2979.2008.00315.x, publisher: John Wiley Sons, Ltd.
URL: <https://doi.org/10.1111/j.1467-2979.2008.00315.x>
- Cheung, W. W. L., The future of fishes and fisheries in the changing oceans. *Journal of Fish Biology*, **92**(3), (2018), pp. 790–803, doi:10.1111/jfb.13558.
URL: <https://onlinelibrary.wiley.com/doi/abs/10.1111/jfb.13558>
- Choi, Y. and Nam, S., East–west contrasting changes in Southern Indian Ocean Antarctic Bottom Water salinity over three decades. *Sci Rep*, **12**(12175), (2022), pp. 1–10, doi:10.1038/s41598-022-16331-y.
- Cinner, J. E., McClanahan, T. R., Graham, N. A. J., Pratchett, M. S., Wilson, S. K., and Raina, J.-B., Gear-based fisheries management as a potential adaptive response to climate change and coral mortality. *Journal of Applied Ecology*, **46**(3), (2009), pp. 724–732, doi:10.1111/j.1365-2664.2009.01648.x.
- Cipollini, P., Vignudelli, S., and Benveniste, J., The Coastal Zone: A Mission Target for Satellite Altimeters. *Eos, Transactions American Geophysical Union*, **95**(8), (2014), pp. 72–72, doi:10.1002/2014EO080006.
URL: <https://agupubs.onlinelibrary.wiley.com/doi/abs/10.1002/2014EO080006>
- Civel-Mazens, M., Crosta, X., Cortese, G., Michel, E., Mazaud, A., Ther, O., Ikehara, M., and Itaki, T., Antarctic Polar Front migrations in the Kerguelen Plateau region, Southern Ocean, over the past 360 kyrs. *Global and Planetary Change*, **202**, (2021),

p. 103526, ISSN 0921-8181, doi:10.1016/j.gloplacha.2021.103526.

URL: <https://www.sciencedirect.com/science/article/pii/S0921818121001119>

Cochrane, K. L., Reconciling sustainability, economic efficiency and equity in marine fisheries: Has there been progress in the last 20 years? *Fish and Fisheries*, **22**(2), (2021), pp. 298–323, doi:10.1111/faf.12521.

Collins, M., Ross, K., Belchier, M., and Reid, K., Distribution and diet of juvenile Patagonian toothfish on the South Georgia and Shag Rocks shelves (Southern Ocean). *Marine Biology*, **152**, (2007), p. 135–147, doi:10.1007/s00227-007-0667-3.

Collins, M. A., Brickle, P., Brown, J., and Belchier, M., Chapter Four - The Patagonian Toothfish: Biology, Ecology and Fishery, volume 58 of *Advances in Marine Biology*, pp. 227–300, Academic Press, (2010), doi:10.1016/B978-0-12-381015-1.00004-6.

URL: <https://www.sciencedirect.com/science/article/pii/B9780123810151000046>

Comiso, J. C., McClain, C. R., Sullivan, C. W., Ryan, J. P., and Leonard, C. L., Coastal zone color scanner pigment concentrations in the Southern Ocean and relationships to geophysical surface features. *Journal of Geophysical Research: Oceans*, **98**(C2), (1993), pp. 2419–2451, doi:10.1029/92JC02505.

Constable, A., Melbourne-Thomas, J., Corney, S., Arrigo, K., Barbraud, C., Barnes, D., Bindoff, N., Boyd, P., Brandt, A., Costa, D., Davidson, A., Ducklow, H., Emmerson, L., Fukuchi, M., Gutt, J., Hindell, M., Hofmann, E., Hosie, G., Iida, T., Jacob, S., Johnston, N., Kawaguchi, S., Kokubun, N., Koubbi, P., Lea, M.-A., Makhado, A., Massom, R., Meiners, K., Meredith, M., Murphy, E., Nicol, S., Reid, K., Richerson, K., Riddle, M., Rintoul, S., Smith, J., W.O., Southwell, C., Stark, J., Sumner, M., Swadling, K., Takahashi, K., Trathan, P., Welsford, D., Weimerskirch, H., Westwood, K., Wienecke, B., Wolf-Gladrow, D., Wright, S., Xavier, J., and Ziegler, P., Climate change and Southern Ocean ecosystems I: how changes in physical habitats directly affect marine biota. *Glob Change Biol*, **20**, (2014), pp. 3004–3025, doi:10.1111/gcb.12623.

Constable, A., Melbourne-Thomas, J., Muelbert, M., McCormack, S., Brasier, M., Caccavo, J., Cavanagh, R., Grant, S., Griffiths, H., Gutt, J., Henley, S., Höfer, J., Hollowed, A., Johnston, N., Morley, S., Murphy, E., Pinkerton, M., Schloss, I., Swadling, K., and Van de Putte, A., Marine Ecosystem Assessment for the Southern

- Ocean: Summary for Policymakers. Integrated Climate and Ecosystem Dynamics in the Southern Ocean, Scientific Committee on Antarctic Research, Scientific Committee on Oceanic Research, (2023), doi:10.5281/zenodo.8359585.
- Constable, A. J. and Welsford, D. C., Developing a precautionary, ecosystem approach to managing fisheries and other marine activities at Heard Island and McDonald Islands in the Indian Sector of the Southern Ocean, pp. 233–255, (2011).
- Cotté, C., Ariza, A., Berne, A., Habasque, J., Lebourges-Dhaussy, A., Roudaut, G., Espinasse, B., Hunt, B., Pakhomov, E., Henschke, N., Péron, C., Conchon, A., Koedooder, C., Izard, L., and Cherel, Y., Macrozooplankton and micronekton diversity and associated carbon vertical patterns and fluxes under distinct productive conditions around the Kerguelen Islands. *Journal of Marine Systems*, **226**, (2022), p. 103650, ISSN 0924-7963, doi:10.1016/j.jmarsys.2021.103650.
URL: <https://www.sciencedirect.com/science/article/pii/S0924796321001457>
- Cotté, C., d'Ovidio, F., Dragon, A.-C., Guinet, C., and Lévy, M., Flexible preference of southern elephant seals for distinct mesoscale features within the Antarctic Circumpolar Current. *Progress in Oceanography*, **131**, (2015), pp. 46–58, ISSN 0079-6611, doi:10.1016/j.pocean.2014.11.011.
URL: <https://www.sciencedirect.com/science/article/pii/S0079661114002006>
- Cury, P. and Roy, C., Optimal Environmental Window and Pelagic Fish Recruitment Success in Upwelling Areas. *Canadian Journal of Fisheries and Aquatic Sciences*, **46**(4), (1989), pp. 670–680, doi:10.1139/f89-086.
- Darmaraki, S., Somot, S., Sevault, F., and Nabat, P., Past Variability of Mediterranean Sea Marine Heatwaves. *Geophysical Research Letters*, **46**(16), (2019), pp. 9813–9823, doi:10.1029/2019GL082933.
- de Beauvoir, S., Le deuxième sexe, Deuxième partie, Chapitre I , pp. 124–125, Édition du Club France Loisirs, La Bibliothèque du XXe siècle, (1949).
- de Boer, A. M., Hutchinson, D. K., Roquet, F., Sime, L. C., Burls, N. J., and Heuzé, C., The Impact of Southern Ocean Topographic Barriers on the Ocean Circulation and the Overlying Atmosphere. *Journal of Climate*, **35**(18), (2022), pp. 5805 – 5821, doi:10.1175/JCLI-D-21-0896.1.

de Boyer Montégut, C., Madec, G., Fischer, A. S., Lazar, A., and Iudicone, D., Mixed layer depth over the global ocean: An examination of profile data and a profile-based climatology. *Journal of Geophysical Research: Oceans*, **109**(C12), (2004), pp. 1–20, doi:10.1029/2004JC002378.

URL: <https://agupubs.onlinelibrary.wiley.com/doi/abs/10.1029/2004JC002378>

Del Castillo, C. E., Signorini, S. R., Karaköylü, E. M., and Rivero-Calle, S., Is the Southern Ocean Getting Greener? *Geophysical Research Letters*, **46**(11), (2019), pp. 6034–6040, doi:10.1029/2019GL083163.

URL: <https://agupubs.onlinelibrary.wiley.com/doi/abs/10.1029/2019GL083163>

Della Penna, A., De Monte, S., Kestenare, E., Guinet, C., and d'Ovidio, F., Quasi-planktonic behavior of foraging top marine predators. *Sci Rep*, **5**(18063), (2015), pp. 1–10, doi:10.1038/srep18063.

Della Penna, A. and Gaube, P., Mesoscale Eddies Structure Mesopelagic Communities. *Frontiers in Marine Science*, **7**(454), (2020), pp. 1–9, ISSN 2296-7745, doi:10.3389/fmars.2020.00454.

URL: <https://www.frontiersin.org/articles/10.3389/fmars.2020.00454>

Della Penna, A., Koubbi, P., Cotté, C., Bon, C., Bost, C.-A., and d'Ovidio, F., Lagrangian analysis of multi-satellite data in support of open ocean Marine Protected Area design. *Future of oceanic animals in a changing ocean*, **140**, (2017), pp. 212–221, ISSN 0967-0645, doi:10.1016/j.dsr2.2016.12.014.

URL: <https://www.sciencedirect.com/science/article/pii/S0967064516304222>

Della Penna, A., Llort, J., Moreau, S., Patel, R., Kloser, R., Gaube, P., Strutton, P., and Boyd, P. W., The Impact of a Southern Ocean Cyclonic Eddy on Mesopelagic Micronekton. *Journal of Geophysical Research: Oceans*, **127**(11), (2022), p. e2022JC018893, doi:10.1029/2022JC018893.

URL: <https://agupubs.onlinelibrary.wiley.com/doi/abs/10.1029/2022JC018893>

Della Penna, A., Trull, T. W., Wotherspoon, S., De Monte, S., Johnson, C. R., and d'Ovidio, F., Mesoscale Variability of Conditions Favoring an Iron-Induced Diatom Bloom Downstream of the Kerguelen Plateau. *Journal of Geophysical Research: Oceans*, **123**(5), (2018), pp. 3355–3367, doi:10.1029/2018JC013884.

- Delord, K., Barbraud, C., Bost, Y., C.A.and Cherel, Guinet, C., and Weimerskirch, H., Atlas of top predators from French Southern Territories in the Southern Indian Ocean, CNRS, (2014), doi:10.15474/AtlasTopPredatorsOLCEBC.CNRS-FrenchSouthernTerritorie.
- Deppeler, S. and Davidson, A., Southern Ocean Phytoplankton in a Changing Climate. *Front. Mar. Sci.*, **4**(40), (2017), pp. 1–28, doi:10.3389/fmars.2017.00040.
- Descartes, R., Discours de la méthode, p. sixième partie, (1637).
- Dong, S., Sprintall, J., Gille, S. T., and Talley, L., Southern Ocean mixed-layer depth from Argo float profiles. *Journal of Geophysical Research: Oceans*, **113**(C6), (2008), pp. 1–12, doi:10.1029/2006JC004051.
URL: <https://agupubs.onlinelibrary.wiley.com/doi/abs/10.1029/2006JC004051>
- Donohue, K. A., Tracey, K. L., Watts, D. R., Chidichimo, M. P., and Chereskin, T. K., Mean Antarctic Circumpolar Current transport measured in Drake Passage. *Geophysical Research Letters*, **43**(22), (2016), pp. 11,760–11,767, doi:10.1002/2016GL070319.
URL: <https://agupubs.onlinelibrary.wiley.com/doi/abs/10.1002/2016GL070319>
- d’Ovidio, F., Della Penna, A., Trull, T. W., Nencioli, F., Pujol, M.-I., Rio, M.-H., Park, Y.-H., Cotté, C., Zhou, M., and Blain, S., The biogeochemical structuring role of horizontal stirring: Lagrangian perspectives on iron delivery downstream of the Kerguelen Plateau. *Biogeosciences*, **12**(19), (2015), pp. 5567–5581, doi:10.5194/bg-12-5567-2015.
URL: <https://bg.copernicus.org/articles/12/5567/2015/>
- Doxa, A., Almpnidou, V., Katsanevakis, S., Queirós, A. M., Kaschner, K., Garilao, C., Kesner-Reyes, K., and Mazaris, A. D., 4D marine conservation networks: Combining 3D prioritization of present and future biodiversity with climatic refugia. *Global Change Biology*, **28**(15), (2022), pp. 4577–4588, doi:10.1111/gcb.16268.
URL: <https://onlinelibrary.wiley.com/doi/abs/10.1111/gcb.16268>
- Dragon, A.-C., Monestiez, P., Bar-Hen, A., and Guinet, C., Linking foraging behaviour to physical oceanographic structures: Southern elephant seals and mesoscale eddies east of Kerguelen Islands. *3rd GLOBEC OSM: From ecosystem function to ecosystem prediction*, **87**(1), (2010), pp. 61–71, ISSN 0079-6611, doi:10.1016/j.pocean.2010.09.

025.

URL: <https://www.sciencedirect.com/science/article/pii/S0079661110001370>

Duhamel, G., *The Pelagic Fish Community of the Polar Frontal Zone off the Kerguelen Islands*, pp. 63–74, Springer Milan, Milano, (1998), ISBN 978-88-470-2157-0, doi: 10.1007/978-88-470-2157-0_5.

Duhamel, G., Hulley, P.-A., Causse, R., Koubbi, P., Vacchi, M., Pruvost, P., Vignetta, S., Irisson, J.-O., Mormede, S., Belchier, M., Dettai, A., Detrich, H. W., Gutt, J., Jones, C. D., Kock, K.-H., Lopez Abellan, L. J., and Van de Putte, A., Biogeographic patterns of fish, in *Biogeographic Atlas of the Southern Ocean* (Edited by De Broyer, C., Koubbi, P., Griffiths, H., Raymond, B., d’Udekem d’Acoz, C., Van de Putte, A., Danis, B., David, B., Grant, S., Gutt, J., Held, C., Hosie, G., Huettmann, F., Post, A., and Ropert-Coudert, Y.), pp. 328–362, Cambridge, Scientific Committee on Antarctic Research, (2014).

Duhamel, G., Pruvost, P., Bertignac, M., Gasco, N., and Hauteceur, M., Major fishery events in Kerguelen Islands: *Notothenia rossi*, *Champscephalus gunnari*, *Dissostichus eleginoides*-Current distribution and status of stocks. **35**, (2011), pp. 275–286.

d’Ovidio, F., De Monte, S., Della Penna, A., Cotté, C., and Guinet, C., Ecological implications of eddy retention in the open ocean: a Lagrangian approach. *Journal of Physics A: Mathematical and Theoretical*, **46**(25), (2013), p. 254023.

Eayrs, C., Li, X., Raphael, M. N., and Holland, D. M., Rapid decline in Antarctic sea ice in recent years hints at future change. *Nature Geoscience*, **14**, (2021), pp. 460–464, doi:10.1038/s41561-021-00768-3.

Egerton, F. N., Changing Concepts of the Balance of Nature. *The Quarterly Review of Biology*, **48**(2), (1973), pp. 322–350, doi:10.1086/407594.

Elzahaby, Y. and Schaeffer, A., Observational Insight Into the Subsurface Anomalies of Marine Heatwaves. *Frontiers in Marine Science*, **6**, (2019), p. 745, ISSN 2296-7745, doi:10.3389/fmars.2019.00745.

URL: <https://www.frontiersin.org/article/10.3389/fmars.2019.00745>

Elzahaby, Y., Schaeffer, A., Roughan, M., and Delaux, S., Oceanic Circulation Drives the Deepest and Longest Marine Heatwaves in the East Australian Current System. *Geophysical Research Letters*, **48**(17), (2021), p. e2021GL094785, doi: 10.1029/2021GL094785.

URL: <https://agupubs.onlinelibrary.wiley.com/doi/abs/10.1029/2021GL094785>

Elzahaby, Y., Schaeffer, A., Roughan, M., and Delaux, S., Why the Mixed Layer Depth Matters When Diagnosing Marine Heatwave Drivers Using a Heat Budget Approach. *Frontiers in Climate*, **4**(838017), (2022), pp. 1–15, ISSN 2624-9553, doi:10.3389/fclim.2022.838017.

URL: <https://www.frontiersin.org/articles/10.3389/fclim.2022.838017>

Eyring, V., Bony, S., Meehl, G. A., Senior, C. A., Stevens, B., Stouffer, R. J., and Taylor, K. E., Overview of the Coupled Model Intercomparison Project Phase 6 (CMIP6) experimental design and organization. *Geoscientific Model Development*, **9**(5), (2016), pp. 1937–1958, ISSN 1991-959X, doi:10.5194/gmd-9-1937-2016, publisher: Copernicus GmbH.

URL: <https://gmd.copernicus.org/articles/9/1937/2016/gmd-9-1937-2016.html>

FAO, The State of World Fisheries and Aquaculture 2022: Towards Blue Transformation., FAO, Rome, (2022), doi:10.4060/cc0461en.

Faulkner, K. T., Clusella-Trullas, S., Peck, L. S., and Chown, S. L., Lack of coherence in the warming responses of marine crustaceans. *Functional Ecology*, **28**(4), (2014), pp. 895–903, doi:10.1111/1365-2435.12219.

URL: <https://besjournals.onlinelibrary.wiley.com/doi/abs/10.1111/1365-2435.12219>

Fernandes, J. A., Rutterford, L., Simpson, S. D., Butenschön, M., Frölicher, T. L., Yool, A., Cheung, W. W. L., and Grant, A., Can we project changes in fish abundance and distribution in response to climate? *Global Change Biology*, **26**(7), (2020), pp. 3891–3905, doi:10.1111/gcb.15081.

URL: <https://onlinelibrary.wiley.com/doi/abs/10.1111/gcb.15081>

Fjeld, K., Tiller, R., Grimaldo, E., Grimsmo, L., and Standal, I.-B., Mesopelagics—New gold rush or castle in the sky? *Marine Policy*, **147**, (2023), p. 105359, ISSN 0308-597X, doi:10.1016/j.marpol.2022.105359.

URL: <https://www.sciencedirect.com/science/article/pii/S0308597X22004067>

Flynn, E. E., Bjelde, B. E., Miller, N. A., and Todgham, A. E., Ocean acidification exerts negative effects during warming conditions in a developing Antarctic fish. *Conservation Physiology*, **3**(1), (2015), p. cov033, ISSN 2051-1434, doi: 10.1093/conphys/cov033.

URL: <https://doi.org/10.1093/conphys/cov033>

Forster, P., Storelvmo, T., Armour, K., Collins, W., Dufresne, J.-L., Frame, D., Lunt, D., Mauritsen, T., Palmer, M., Watanabe, M., Wild, M., and Zhan, H., The Earth's Energy Budget, Climate Feedbacks, and Climate Sensitivity., in *Climate Change, 2021. The Physical Science Basis. Contribution of Working Group I to the Sixth Assessment Report of the Intergovernmental Panel on Climate Change*. (Edited by Masson-Delmotte, V., Zhai, P., Pirani, A., Connors, S., Pean, C., Berger, S., Caud, N., Chen, Y., Goldfarb, L., Gomis, M., Huang, M., Leitzell, K., Lonnoy, E., Matthews, J., Maycock, T., Waterfield, T., Yelekçi, O., Yu, R., and Zhou, B.), pp. 923–1054, Cambridge University Press, (2021), doi:10.1017/9781009157896.009.

Fox-Kemper, B., Hewitt, H., Xiao, C., Adalgeirsdottir, G., Drijfhout, S., Edwards, T., Golledge, N., Hemer, M., Kopp, R., Krinner, G., Mix, A., Notz, D., Nowicki, S., Nurhati, I., Ruiz, L., Sallee, J.-B., Slangen, A., and Yu, Y., Ocean, cryosphere and sea level change, in *Climate Change, 2021. The Physical Science Basis. Contribution of Working Group I to the Sixth Assessment Report of the Intergovernmental Panel on Climate Change*. (Edited by Masson-Delmotte, V., Zhai, P., Pirani, A., Connors, S., Pean, C., Berger, S., Caud, N., Chen, Y., Goldfarb, L., Gomis, M., Huang, M., Leitzell, K., Lonnoy, E., Matthews, J., Maycock, T., Waterfield, T., Yelekçi, O., Yu, R., and Zhou, B.), p. 1211–1362, Cambridge University Press, (2021), doi:10.1017/9781009157896.011.

Fragkopoulou, E., Sen Gupta, A., Costello, M. J., Wernberg, T., Araújo, M. B., Serrão, E. A., De Clerck, O., and Assis, J., Marine biodiversity exposed to prolonged and intense subsurface heatwaves. *Nature Climate Change*, **13**, (2023), p. 1114–1121, doi: 10.1038/s41558-023-01790-6.

URL: <https://doi.org/10.1038/s41558-023-01790-6>

Freer, J. J., Tarling, G. A., Collins, M. A., Partridge, J. C., and Genner, M. J., Predicting future distributions of lanternfish, a significant ecological resource within the Southern Ocean. *Diversity and Distributions*, **25**(8), (2019), pp. 1259–1272, doi:10.1111/ddi.

12934.

URL: <https://onlinelibrary.wiley.com/doi/abs/10.1111/ddi.12934>

Frölicher, T., Sarmiento, J., Paynter, D., Dunne, J., Krasting, J., and Winton, M., Dominance of the southern ocean in anthropogenic carbon and heat uptake in CMIP5 models. *J. Clim.*, **28**(2), (2015), p. 862–886, doi:10.1175/JCLI-D-14-00117.1.

Gaines, S. D., White, C., Carr, M. H., and Palumbi, S. R., Designing marine reserve networks for both conservation and fisheries management. *Proceedings of the National Academy of Sciences*, **107**(43), (2010), pp. 18286–18293, doi:10.1073/pnas.0906473107.

URL: <https://www.pnas.org/doi/abs/10.1073/pnas.0906473107>

Game, E. T., Grantham, H. S., Hobday, A. J., Pressey, R. L., Lombard, A. T., Beckley, L. E., Gjerde, K., Bustamante, R., Possingham, H. P., and Richardson, A. J., Pelagic protected areas: the missing dimension in ocean conservation. *Trends in Ecology and Evolution*, **24**(7), (2009), pp. 360–369, doi:10.1016/j.tree.2009.01.011.

URL: <https://doi.org/10.1016/j.tree.2009.01.011>

Gao, L., Rintoul, S., and Yu, W., Recent wind-driven change in Subantarctic Mode Water and its impact on ocean heat storage. *Nature Clim Change*, **8**, (2018), p. 58–63, doi:10.1038/s41558-017-0022-8.

Garcia-Soto, C., Cheng, L., Caesar, L., Schmidtko, S., Jewett, E., Cheripka, A., Rigor, I., Caballero, A., Chiba, S., Báez, J., Zielinski, T., and Abraham, J., An Overview of Ocean Climate Change Indicators: Sea Surface Temperature, Ocean Heat Content, Ocean pH, Dissolved Oxygen Concentration, Arctic Sea Ice Extent, Thickness and Volume, Sea Level and Strength of the AMOC (Atlantic Meridional Overturning Circulation). *Front. Mar. Sci.*, **8**(642372), (2021), pp. 1–24, doi:0.3389/fmars.2021.642372.

URL: <https://doi.org/0.3389/fmars.2021.642372>

García Molinos, J., Burrows, M., and Poloczanska, E., Ocean currents modify the coupling between climate change and biogeographical shifts. *Sci Rep*, **7**(1332), (2017), pp. 1–9, doi:10.1038/s41598-017-01309-y.

García Molinos, J., Halpern, B. S., Schoeman, D. S., Brown, C. J., Kiessling, W., Moore, P. J., Pandolfi, J. M., Poloczanska, E. S., Richardson, A. J., and Burrows, M. T., Climate velocity and the future global redistribution of marine biodiversity. *Nature*

- Climate Change*, **6**(1), (2016), pp. 83–88, ISSN 1758-6798, doi:10.1038/nclimate2769.
URL: <https://doi.org/10.1038/nclimate2769>
- Garnesson, P., Mangin, A., Fanton d'Andon, O., Demaria, J., and Bretagnon, M., The CMEMS GlobColour chlorophyll-a product based on satellite observation: multi-sensor merging and flagging strategies. *Ocean Science*, **15**(3), (2019), pp. 819–830, doi:10.5194/os-15-819-2019.
URL: <https://os.copernicus.org/articles/15/819/2019/>
- Geary, W. L., Bode, M., Doherty, T. S., Fulton, E. A., Nimmo, D. G., Tulloch, A. I. T., Tulloch, V. J. D., and Ritchie, E. G., A guide to ecosystem models and their environmental applications. *Nat Ecol Evol*, **4**, (2020), pp. 1459–1471, doi:10.1038/s41559-020-01298-8.
- Giddy, I. S., Fer, I., Swart, S., and Nicholson, S.-A., Vertical Convergence of Turbulent and Double-Diffusive Heat Flux Drives Warming and Erosion of Antarctic Winter Water in Summer. *Journal of Physical Oceanography*, **53**(8), (2023), pp. 1941 – 1958, doi:10.1175/JPO-D-22-0259.1.
URL: <https://journals.ametsoc.org/view/journals/phoc/53/8/JPO-D-22-0259.1.xml>
- Gilbert, E. and Holmes, C., 2023's Antarctic sea ice extent is the lowest on record. *Weather*, **79**, (2024), pp. 46–51, doi:10.1002/wea.4518.
- Gille, S. T., Float Observations of the Southern Ocean. Part I: Estimating Mean Fields, Bottom Velocities, and Topographic Steering. *Journal of Physical Oceanography*, **33**(6), (2003), pp. 1167 – 1181, doi:10.1175/1520-0485(2003)033<1167:FOOTSO>2.0.CO;2.
- Goldsworthy, L. and Brennan, E., Climate change in the Southern Ocean: Is the Commission for the Convention for the Conservation of Antarctic Marine Living Resources doing enough? *Marine Policy*, **130**, (2021), p. 104549, ISSN 0308-597X, doi: 10.1016/j.marpol.2021.104549.
URL: <https://www.sciencedirect.com/science/article/pii/S0308597X21001603>
- Good, S., Fiedler, E., Mao, C., Martin, M., Maycock, A., Reid, R., Roberts-Jones, J., Searle, T., Waters, J., While, J., and Worsfold, M., The current configuration of the OSTIA system for operational production of foundation sea surface temperature

- and ice concentration analyses. *Remote Sens.*, **12**(4), (2020), p. 720, doi:10.3390/rs12040720.
- Gordon, A. L., An Antarctic oceanographic section along 1701E. *Deep Sea Res.*, **22**, (1975), p. 357–377.
- Grafton, R. Q., Adaptation to climate change in marine capture fisheries. *Marine Policy*, **34**(3), (2010), pp. 606–615, doi:10.1016/j.marpol.2009.11.011.
URL: <https://www.sciencedirect.com/science/article/pii/S0308597X09001845>
- Grilly, E., Reid, K., Lenel, S., and Jabour, J., The price of fish: A global trade analysis of Patagonian (*Dissostichus eleginoides*) and Antarctic toothfish (*Dissostichus mawsoni*). *Marine Policy*, **60**, (2015), pp. 186–196, ISSN 0308-597X, doi:10.1016/j.marpol.2015.06.006.
URL: <https://www.sciencedirect.com/science/article/pii/S0308597X15001657>
- Gruber, N., Boyd, P. W., Frölicher, T. L., and Vogt, M., Biogeochemical extremes and compound events in the ocean. *Nature*, **600**, (2021), pp. 395–407, doi:10.1038/s41586-021-03981-7.
- Guinet, C., Koudil, M., Bost, C., Durbec, J., Georges, J., Mouchot, M., and Jouventin, P., Foraging behaviour of satellite-tracked king penguins in relation to sea-surface temperatures obtained by satellite telemetry at Crozet Archipelago, a study during three austral summers. *Marine Ecology Progress Series*, **150**, (1997), pp. 11–20, doi:10.3354/meps150011.
- Guinet, C., Vacquié-Garcia, J., Baptiste, P., Bessigneul, G., Lebras, Y., Dragon, A., Viviant, M., Arnould, J., and Bailleul, F., Southern elephant seal foraging success in relation to temperature and light conditions: Insight into prey distribution. *Marine Ecology Progress Series*, **499**, (2014), pp. 285–301, doi:10.3354/meps10660.
- Gulev, S., Thorne, P., Ahn, J., Dentener, F., Domingues, C., Gerland, S., Gong, D., Kaufman, D., Nnamchi, H., Quaas, J., Rivera, J., Sathyendranath, S., Smith, S., Trewin, B., von Schuckmann, K., and Vose, R., *Changing State of the Climate System*, p. 287–422, Cambridge University Press, (2021), doi:10.1017/9781009157896.004.
- Hadot, P., *Le Voile d’Isis, Essai sur l’histoire de l’idée de Nature*, p. 143, Folio-Essais, (2004).

- Hallgren, A. and Hansson, A., Conflicting Narratives of Deep Sea Mining. *Sustainability*, **13**(9), (2021), p. 5261, doi:10.3390/su13095261.
- Harden-Jones, F., Fish migration, p. 325, Edward Arnold, London, (1968).
- Haumann, F., Gruber, N., Münnich, M., Frenger, I., and Kern, S., Sea-ice transport driving Southern Ocean salinity and its recent trends. *Nature*, **537**, (2016), p. 89–92, doi:10.1038/nature19101.
- Hausfather, Z. and Peters, G., Emissions – the ‘business as usual’ story is misleading. *Nature*, **577**(7792), (2020), p. 618–620, doi:10.1038/d41586-020-00177-3.
- Heikkinen, R. K., Luoto, M., Araújo, M. B., Virkkala, R., Thuiller, W., and Sykes, M. T., Methods and uncertainties in bioclimatic envelope modelling under climate change. *Progress in Physical Geography: Earth and Environment*, **30**(6), (2006), pp. 751–777, doi:10.1177/0309133306071957.
- Heinze, C., Blenckner, T., Martins, H., Rusiecka, D., Döscher, R., Gehlen, M., Gruber, N., Holland, E., Øystein Hov, Joos, F., Matthews, J. B. R., Rødven, R., and Wilson, S., The quiet crossing of ocean tipping points. *Proceedings of the National Academy of Sciences*, **118**(9), (2021), p. e2008478118, doi:10.1073/pnas.2008478118.
URL: <https://www.pnas.org/doi/abs/10.1073/pnas.2008478118>
- Heller, N. E. and Zavaleta, E. S., Biodiversity management in the face of climate change: A review of 22 years of recommendations. *Biological Conservation*, **142**(1), (2009), pp. 14–32, ISSN 0006-3207, doi:10.1016/j.biocon.2008.10.006.
URL: <https://www.sciencedirect.com/science/article/pii/S000632070800387X>
- Henschke, N., Blain, S., Cherel, Y., Cotte, C., Espinasse, B., Hunt, B. P., and Pakhomov, E. A., Population demographics and growth rate of *Salpa thompsoni* on the Kerguelen Plateau. *Journal of Marine Systems*, **214**, (2021), p. 103489, ISSN 0924-7963, doi: 10.1016/j.jmarsys.2020.103489.
URL: <https://www.sciencedirect.com/science/article/pii/S0924796320301846>
- Henson, S. A., Beaulieu, C., and Lampitt, R., Observing climate change trends in ocean biogeochemistry: when and where. *Global Change Biology*, **22**(4), (2016), pp. 1561–1571, doi:10.1111/gcb.13152.
URL: <https://onlinelibrary.wiley.com/doi/abs/10.1111/gcb.13152>

- Herger, N., Sanderson, B. M., and Knutti, R., Improved pattern scaling approaches for the use in climate impact studies. *Geophysical Research Letters*, **42**(9), (2015), pp. 3486–3494, doi:10.1002/2015GL063569.
- Herraiz-Borreguero, L. and Naveira Garabato, A., Poleward shift of Circumpolar Deep Water threatens the East Antarctic Ice Sheet. *Nature Climate Change*, **12**, (2022), pp. 728–734, doi:10.1038/s41558-022-01424-3.
- Hersbach, H., Bell, B., Berrisford, P., Biavati, G., Horányi, A., Muñoz Sabater, J., Nicolas, J., Peubey, C., Radu, R., Rozum, I., Schepers, D., Simmons, A., Soci, C., Dee, D., and Thépaut, J.-N., ERA5 hourly data on single levels from 1940 to present., (Accessed on 26-10-2023), (2023), doi:10.24381/cds.adbb2d47.
- Heupink, T. H., van den Hoff, J., and Lambert, D. M., King penguin population on Macquarie Island recovers ancient DNA diversity after heavy exploitation in historic times. *Biology Letters*, **8**(4), (2012), pp. 586–589, doi:10.1098/rsbl.2012.0053.
- Hewitt, H., Fox-Kemper, B., Pearson, B., Roberts, M., and Klocke, D., The small scales of the ocean may hold the key to surprises. *Nature Climate Change*, **12**, (2022), p. 496–499, doi:10.1038/s41558-022-01386-6.
- Hewitt, J. E. and Thrush, S. F., Monitoring for tipping points in the marine environment. *Journal of Environmental Management*, **234**, (2019), pp. 131–137, ISSN 0301-4797, doi:10.1016/j.jenvman.2018.12.092.
URL: <https://www.sciencedirect.com/science/article/pii/S0301479718315147>
- Hill, S. L., Atkinson, A., Pakhomov, E. A., and Siegel, V., Evidence for a decline in the population density of Antarctic krill *Euphausia superba* Dana, 1850 still stands. A comment on Cox et al. *Journal of Crustacean Biology*, **39**(3), (2019), pp. 316–322, ISSN 0278-0372, doi:10.1093/jcbiol/ruz004.
URL: <https://doi.org/10.1093/jcbiol/ruz004>
- Hill, S. L., Phillips, T., and Atkinson, A., Potential Climate Change Effects on the Habitat of Antarctic Krill in the Weddell Quadrant of the Southern Ocean. *PLOS ONE*, **8**(8), (2013), pp. 1–12, doi:10.1371/journal.pone.0072246.
URL: <https://doi.org/10.1371/journal.pone.0072246>
- Hindell, M. A., McMahon, C. R., Bester, M. N., Boehme, L., Costa, D., Fedak, M. A., Guinet, C., Herraiz-Borreguero, L., Harcourt, R. G., Huckstadt, L., Kovacs, K. M.,

Lydersen, C., McIntyre, T., Muelbert, M., Patterson, T., Roquet, F., Williams, G., and Charrassin, J.-B., Circumpolar habitat use in the southern elephant seal: implications for foraging success and population trajectories. *Ecosphere*, **7**(5), (2016), p. e01213, doi:10.1002/ecs2.1213.

URL: <https://esajournals.onlinelibrary.wiley.com/doi/abs/10.1002/ecs2.1213>

Hindell, M. A., McMahon, C. R., Jonsen, I., Harcourt, R., Arce, F., and Guinet, C., Inter- and intrasex habitat partitioning in the highly dimorphic southern elephant seal. *Ecology and Evolution*, **11**(4), (2021), pp. 1620–1633, doi:10.1002/ece3.7147.

URL: <https://onlinelibrary.wiley.com/doi/abs/10.1002/ece3.7147>

Hindell, M. A., Reisinger, R. R., Ropert-Coudert, Y., Hückstädt, L. A., Trathan, P. N., Bornemann, H., Charrassin, J.-B., Chown, S. L., Costa, D. P., Danis, B., Lea, M.-A., Thompson, D., Torres, L. G., Van de Putte, A. P., Alderman, R., Andrews-Goff, V., Arthur, B., Ballard, G., Bengtson, J., Bester, M. N., Blix, A. S., Boehme, L., Bost, C.-A., Boveng, P., Cleeland, J., Constantine, R., Corney, S., Crawford, R. J. M., Dalla Rosa, L., de Bruyn, P. J. N., Delord, K., Descamps, S., Double, M., Emmerson, L., Fedak, M., Friedlaender, A., Gales, N., Goebel, M. E., Goetz, K. T., Guinet, C., Goldsworthy, S. D., Harcourt, R., Hinke, J. T., Jerosch, K., Kato, A., Kerry, K. R., Kirkwood, R., Kooyman, G. L., Kovacs, K. M., Lawton, K., Lowther, A. D., Lydersen, C., Lyver, P. O., Makhado, A. B., Márquez, M. E. I., McDonald, B. I., McMahon, C. R., Muelbert, M., Nachtsheim, D., Nicholls, K. W., Nordøy, E. S., Olmastroni, S., Phillips, R. A., Pistorius, P., Plötz, J., Pütz, K., Ratcliffe, N., Ryan, P. G., Santos, M., Southwell, C., Staniland, I., Takahashi, A., Tarroux, A., Trivelpiece, W., Wakefield, E., Weimerskirch, H., Wienecke, B., Xavier, J. C., Wotherspoon, S., Jonsen, I. D., and Raymond, B., Tracking of marine predators to protect Southern Ocean ecosystems. *Nature*, **580**, (2020), pp. 87–92, doi:10.1038/s41586-020-2126-y.

Hobday, A. J., Alexander, L. V., Perkins, S. E., Smale, D. A., Straub, S. C., Oliver, E. C., Benthuisen, J. A., Burrows, M. T., Donat, M. G., Feng, M., Holbrook, N. J., Moore, P. J., Scannell, H. A., Sen Gupta, A., and Wernberg, T., A hierarchical approach to defining marine heatwaves. *Progress in Oceanography*, **141**, (2016), pp. 227–238, ISSN 0079-6611, doi:10.1016/j.pocean.2015.12.014.

URL: <https://www.sciencedirect.com/science/article/pii/S0079661116000057>

Holmes, C. R., Bracegirdle, T. J., and Holland, P. R., Antarctic Sea Ice Projections Constrained by Historical Ice Cover and Future Global Temperature Change. *Geophysical Research Letters*, **49**(10), (2022), p. e2021GL097413, doi:10.1029/2021GL097413, e2021GL097413 2021GL097413.

URL: <https://agupubs.onlinelibrary.wiley.com/doi/abs/10.1029/2021GL097413>

Houde, E., Emerging from Hjort's shadow. *Journal of Northwest Atlantic Fishery Science*, **41**, (2008), pp. 53,70.

Howell, D., Schueller, A., Bentley, J., Buchheister, A., Chagaris, D., Cieri, M., Drew, K., Lundy, M., Pedreschi, D., Reid, D., and Townsend, H., Combining Ecosystem and Single-Species Modeling to Provide Ecosystem-Based Fisheries Management Advice Within Current Management Systems. *Front. Mar. Sci.*, **7**(607831), (2021), pp. 1–10, doi:10.3389/fmars.2020.607831.

Hu, S., Li, S., Zhang, Y., Guan, C., Du, Y., Feng, M., Ando, K., Wang, F., Schiller, A., and Hu, D., Observed strong subsurface marine heatwaves in the tropical western Pacific Ocean. **16**(10), (2021), p. 104024, ISSN 1748-9326, doi:10.1088/1748-9326/ac26f2, publisher: IOP Publishing.

URL: <https://doi.org/10.1088/1748-9326/ac26f2>

Hunt, B. and Swadling, K., Macrozooplankton and micronekton community structure and diel vertical migration in the Heard Island Region, Central Kerguelen Plateau. *Journal of Marine Systems*, **221**, (2021), p. 103575, ISSN 0924-7963, doi:10.1016/j.jmarsys.2021.103575.

Inchausti, P., Guinet, C., Koudil, M., Durbec, J.-P., Barbraud, C., Weimerskirch, H., Cherel, Y., and Jouventin, P., Inter-annual variability in the breeding performance of seabirds in relation to oceanographic anomalies that affect the Crozet and the Kerguelen sectors of the Southern Ocean. *Journal of Avian Biology*, **34**(2), (2003), pp. 170–176, doi:10.1034/j.1600-048X.2003.03031.x.

URL: <https://onlinelibrary.wiley.com/doi/abs/10.1034/j.1600-048X.2003.03031.x>

IPBES, Summary for policymakers of the global assessment report on biodiversity and ecosystem services of the Intergovernmental Science-Policy Platform on Biodiversity and Ecosystem Services, IPBES secretariat, Bonn, Germany, (2019), doi:10.5281/zenodo.3553458.

IPCC, Annex I: Glossary, in *Climate Change 2023: Synthesis Report. Contribution of Working Groups I, II and III to the Sixth Assessment Report of the Intergovernmental Panel on Climate Change [Core Writing Team, H. Lee and J. Romero (eds.)]* (Edited by Reisinger, A., Cammarano, D., Fischlin, A., Fuglestedt, J., Hansen, G., Jung, Y., Ludden, C., Masson-Delmotte, V., Matthews, R., Mintenbeck, J., Orendain, D., Pirani, A., Poloczanska, E., and Romero, J.), pp. 119–130, IPCC, Geneva, Switzerland, (2023), doi:10.59327/IPCC/AR6-9789291691647.002.

IUCN, A Global Standard for the Identification of Key Biodiversity Areas, volume Version 1.0, (2016a), ISBN 978-2-8317-1835-4.

IUCN, Adapting to Climate Change: Guidance for protected area managers and planners., in *Best Practice Protected Area Guidelines Series* (Edited by Gross, J. E., Woodley, S., Welling, L. A., and Watson, J. E.), volume 24, pp. xviii + 129, IUCN, Gland, Switzerland, (2016b).

IUCN MMPATF, Global Dataset of Important Marine Mammal Areas (IUCN-IMMA), (2023), made available under agreement on terms of use by the IUCN Joint SSC/WCPA Marine Mammal Protected Areas Task Force. Accessed in December 2023. **URL:** www.marinemammalhabitat.org/imma-atlas

Ivanchenko, The structure and quantitative developments of phytoplankton in the waters of the Kerguelen islands, in *Les rapports des campagnes à la mer. Campagnes SKALP 1987 et 1988 aux îles Kerguelen à bord des navires "SKIF" et "KALPER"* (Edited by Duhamel, G.), volume 93-01, pp. 73–83, L'Institut Français pour la Recherche et la Technologie Polaires. Expéditions Paul-Emile Victor, (1993).

Izard, L., Fonville, N., Merland, C., Koubbi, P., Nerini, D., Habasque, J., Lebourges-Dhaussy, A., Monaco, C. L., Roudaut, G., d'Ovidio, F., Charrassin, J.-B., and Cotté, C., Decomposing acoustic signal reveals the pelagic response to a frontal system. *Journal of Marine Systems*, **243**, (2024), p. 103951, ISSN 0924-7963, doi:10.1016/j.jmarsys.2023.103951.

URL: <https://www.sciencedirect.com/science/article/pii/S0924796323000957>

- Jackson, L., Hughes, C. W., and Williams, R. G., Topographic Control of Basin and Channel Flows: The Role of Bottom Pressure Torques and Friction. *Journal of Physical Oceanography*, **36**(9), (2006), pp. 1786 – 1805, doi:10.1175/JPO2936.1.
URL: <https://journals.ametsoc.org/view/journals/phoc/36/9/jpo2936.1.xml>
- Johannessen, O., A review of oceanic fronts, in *Oceanic Acoustic Modelling* (Edited by Bachmann, W. and Williams, R.), p. 28–1 to 28–33, Rep. CP-17, pt. 5, SACLANT Undersea Research Centre, La Spezia, Italy, (1975).
- Johnson, J. E. and Welch, D. J., Marine Fisheries Management in a Changing Climate: A Review of Vulnerability and Future Options. *Reviews in Fisheries Science*, **18**(1), (2009), pp. 106–124, doi:10.1080/10641260903434557.
- Johnston, N., Murphy, E., Atkinson, A., Constable, A., Cotté, C., Cox, M., Daly, K., Driscoll, R., Flores, H., Halfter, S., Henschke, N., Hill, S., Höfer, J., Hunt, B., Kawaguchi, S., Lindsay, D., Liszka, C., Loeb, V., Manno, C., Meyer, B., Pakhomov, E., Pinkerton, M., Reiss, C., Richerson, K., Smith, W. J., Steinberg, D., Swadling, K., Tarling, G., Thorpe, S., Veytia, D., Ward, P., Weldrick, C., and Yang, G., Status, Change, and Futures of Zooplankton in the Southern Ocean. *Front. Ecol. Evol.*, **9**(624692), (2022), pp. 1–41, doi:10.3389/fevo.2021.624692.
- Jonas, H., *Le Principe Responsabilité. Une éthique pour la civilisation technologique*, (1979), ISBN 9782081307698.
- Jones, K. R., Watson, J. E., Possingham, H. P., and Klein, C. J., Incorporating climate change into spatial conservation prioritisation: A review. *Biological Conservation*, **194**, (2016), pp. 121–130, ISSN 0006-3207, doi:10.1016/j.biocon.2015.12.008.
URL: <https://www.sciencedirect.com/science/article/pii/S0006320715301877>
- Juza, M., Fernández-Mora, A., and Tintoré, J., Sub-Regional Marine Heat Waves in the Mediterranean Sea From Observations: Long-Term Surface Changes, Sub-Surface and Coastal Responses. *Front. Mar. Sci.*, **9**(785771), (2022), pp. 1–25, doi:10.3389/fmars.2022.785771.
- Keppel, G., Mokany, K., Wardell-Johnson, G. W., Phillips, B. L., Welbergen, J. A., and Reside, A. E., The capacity of refugia for conservation planning under climate

- change. *Frontiers in Ecology and the Environment*, **13**(2), (2015), pp. 106–112, doi:10.1890/140055.
URL: <https://esajournals.onlinelibrary.wiley.com/doi/abs/10.1890/140055>
- Klein, E. S., Hill, S. L., Hinke, J. T., Phillips, T., and Watters, G. M., Impacts of rising sea temperature on krill increase risks for predators in the Scotia Sea. *PLOS ONE*, **13**(1), (2018), pp. 1–21, doi:10.1371/journal.pone.0191011.
URL: <https://doi.org/10.1371/journal.pone.0191011>
- Koenigstein, S., Mark, F. C., Göbbling-Reisemann, S., Reuter, H., and Poertner, H.-O., Modelling climate change impacts on marine fish populations: process-based integration of ocean warming, acidification and other environmental drivers. *Fish and Fisheries*, **17**(4), (2016), pp. 972–1004, doi:10.1111/faf.12155.
- Kolodziejczyk, N., Llovel, W., and Portela, E., Interannual variability of upper ocean water masses as inferred from Argo Array. *Journal of Geophysical Research: Oceans*, **124**, (2019), p. 6067–6085, doi:10.1029/2018JC014866.
- Kooijman, S. A. L. M., Dynamic energy and mass budgets in biological systems, Cambridge university press., (2000).
- Kooyman, G. L., Cherel, Y., Maho, Y. L., Croxall, J. P., Thorson, P. H., Ridoux, V., and Kooyman, C. A., Diving Behavior and Energetics During Foraging Cycles in King Penguins. *Ecological Monographs*, **62**(1), (1992), pp. 143–163, doi:10.2307/2937173.
URL: <https://esajournals.onlinelibrary.wiley.com/doi/abs/10.2307/2937173>
- Kooyman, G. L., Davis, R. W., Croxall, J. P., and Costa, D. P., Diving Depths and Energy Requirements of King Penguins. *Science*, **217**(4561), (1982), pp. 726–727, doi:10.1126/science.7100916.
URL: <https://www.science.org/doi/abs/10.1126/science.7100916>
- Koubbi, P., Influence of the frontal zones on ichthyoplankton and mesopelagic fish assemblages in the Crozet Basin (Indian sector of the Southern Ocean). *Polar Biol*, **13**, (1993), pp. 557–564, doi:10.1007/BF00236398.
- Koubbi, P., Duhamel, G., Hecq, J.-H., Beans, C., Loots, C., Pruvost, P., Tavernier, E., Vacchi, M., and Vallet, C., Ichthyoplankton in the neritic and coastal zone of Antarctica and Subantarctic islands: A review. *Journal of Marine Systems*, **78**(4),

(2009), pp. 547–556, ISSN 0924-7963, doi:10.1016/j.jmarsys.2008.12.024, revisiting the Role of Zooplankton in Pelagic Ecosystems.

URL: <https://www.sciencedirect.com/science/article/pii/S0924796309001043>

Koubbi, P., Guinet, C., Alloncle, N., Améziane, N., Azam, C.-S., Baudena, A., Bost, C., Romain, C., Chazeau, C., Coste, G., Cotte, C., d'Ovidio, F., Karine, D., Duhamel, G., Forget, A., Gasco, N., Hauteceur, M., Lehodey, P., Lo Monaco, C., and Weimerskirch, H., Ecoregionalisation of the Kerguelen and Crozet islands oceanic zone. Part I: Introduction and Kerguelen oceanic zone, (2016), doi:10.13140/RG.2.2.17278.18246.

Koubbi, P., Hulley, P., B., R., Penot, F., Gasparini, S., Labat, J.-P., Pruvost, P., Mormède, S., Irisson, J., Duhamel, G., and Mayzaud, P., Estimating the biodiversity of the sub-Antarctic Indian part for ecoregionalisation: Part I. Pelagic realm of CCAMLR areas 58.5.1 and 58.6, pp. 1–39, (2011).

Koubbi, P., Ibanez, F., and Duhamel, G., Environmental influences on spatio-temporal oceanic distribution of ichthyoplankton around the Kerguelen Islands (Southern Ocean). *Marine Ecology Progress Series*, **72**(3), (1991), pp. 225–238, ISSN 01718630, 16161599.

Kricher, J. C., *The Balance of Nature: Ecology's Enduring Myth*, (2009), ISBN 9780691138985.

Kwiatkowski, L., Torres, O., Bopp, L., Aumont, O., Chamberlain, M., Christian, J. R., Dunne, J. P., Gehlen, M., Ilyina, T., John, J. G., Lenton, A., Li, H., Lovenduski, N. S., Orr, J. C., Palmieri, J., Santana-Falcón, Y., Schwinger, J., Séférian, R., Stock, C. A., Tagliabue, A., Takano, Y., Tjiputra, J., Toyama, K., Tsujino, H., Watanabe, M., Yamamoto, A., Yool, A., and Ziehn, T., Twenty-first century ocean warming, acidification, deoxygenation, and upper-ocean nutrient and primary production decline from CMIP6 model projections. *Biogeosciences*, **17**(13), (2020), pp. 3439–3470, doi:10.5194/bg-17-3439-2020.

URL: <https://bg.copernicus.org/articles/17/3439/2020/>

Labrousse, S., Vacquié-Garcia, J., Heerah, K., Guinet, C., Sallée, J.-B., Authier, M., Picard, B., Roquet, F., Bailleul, F., Hindell, M., and Charrassin, J.-B., Winter use of sea ice and ocean water mass habitat by southern elephant seals: The length and

- breadth of the mystery. *Progress in Oceanography*, **137**, (2015), pp. 52–68, ISSN 0079-6611, doi:10.1016/j.pocean.2015.05.023.
URL: <https://www.sciencedirect.com/science/article/pii/S0079661115001287>
- Laptikhovsky, V. and Brickle, P., The Patagonian toothfish fishery in Falkland Islands' waters. *Fisheries Research*, **74**(1), (2005), pp. 11–23, ISSN 0165-7836, doi:10.1016/j.fishres.2005.04.006.
URL: <https://www.sciencedirect.com/science/article/pii/S016578360500127X>
- Lasker, R., Field criteria for survival of anchovy larvae: the relation between inshore chlorophyll maximum layers and successful first feeding. *U.S. Fish. Bull.*, **73**, (1975), pp. 453–462.
- Lasker, R., The role of a stable ocean in larval fish survival and subsequent recruitment. *Marine fish larvae: morphology, ecology and relation to fisheries*, **1**, (1981), pp. 80–89.
- Laws, R., Seals and whales of the Southern Ocean. *Phil Trans R Soc Lond B*, **279**, (1977), pp. 81–96.
- Lawson, K. N., Lang, K. M., Rabaiotti, D., and Drew, J., Predicting climate change impacts on critical fisheries species in Fijian marine systems and its implications for protected area spatial planning. *Diversity and Distributions*, **29**(10), (2023), pp. 1226–1244.
- Lee, J.-Y., Marotzke, J., Bala, G., Cao, L., Corti, S., Dunne, J., Engelbrecht, F., Fischer, E., Fyfe, J., Jones, C., Maycock, A., Mutemi, J., Ndiaye, O., Panickal, S., and Zhou, T., Future Global Climate: Scenario-Based Projections and Near-Term Information, in *Climate Change 2021: The Physical Science Basis. Contribution of Working Group I to the Sixth Assessment Report of the Intergovernmental Panel on Climate Change*. (Edited by Masson-Delmotte, V., Zhai, P., Pirani, A., Connors, S., Péan, C., Berger, S., Caud, N., Chen, Y., Goldfarb, L., Gomis, M., Huang, M., Leitzell, K., Lonnoy, E., Matthews, J., Maycock, T., Waterfield, T., Yelekçi, O., Yu, R., and Zhou, B.), p. 553–672, Cambridge University Press, (2021), doi:10.1017/9781009157896.006.
- Lellouche, J., Le Galloudec, O., Greiner, E., Garric, G., Regnier, C., Drevillon, M., and Le Traon, P., The Copernicus Marine Environment Monitoring Service global ocean 1/12 physical reanalysis GLORYS12V1: description and quality assessment. *Egu general assembly conference abstracts*, **20**, (2018a), p. 19806.

- Lellouche, J.-M., Greiner, E., Le Galloudec, O., Garric, G., Regnier, C., Drevillon, M., Benkiran, M., Testut, C.-E., Bourdalle-Badie, R., Gasparin, F., Hernandez, O., Levier, B., Drillet, Y., Remy, E., and Le Traon, P.-Y., Recent updates to the copernicus marine service global ocean monitoring and forecasting real-time 1/12 high-resolution system. *Ocean Science*, **14**(5), (2018b), pp. 1093–1126, doi:10.5194/os-14-1093-2018.
URL: <https://os.copernicus.org/articles/14/1093/2018/>
- Lenton, T. M., Held, H., Kriegler, E., Hall, J. W., Lucht, W., Rahmstorf, S., and Schellnhuber, H. J., Tipping elements in the Earth's climate system. *Proceedings of the National Academy of Sciences*, **105**(6), (2008), pp. 1786–1793, doi:10.1073/pnas.0705414105.
- Leopold, A., *A Sand County Almanac: And Sketches Here and There*, (1949).
- Leseurre, C., Lo Monaco, C., Reverdin, G., Metzl, N., Fin, J., Mignon, C., and Benito, L., Summer trends and drivers of sea surface fCO₂ and pH changes observed in the southern Indian Ocean over the last two decades (1998–2019). *Biogeosciences*, **19**, (2022), p. 2599–2625, doi:10.5194/bg-19-2599-2022.
URL: <https://bg.copernicus.org/articles/19/2599/2022/>
- Leung, S., Cabré, A., and Marinov, I., A latitudinally banded phytoplankton response to 21st century climate change in the Southern Ocean across the CMIP5 model suite. *Biogeosciences*, **12**(19), (2015), pp. 5715–5734, doi:10.5194/bg-12-5715-2015.
URL: <https://bg.copernicus.org/articles/12/5715/2015/>
- Levin, L. A., Manifestation, Drivers, and Emergence of Open Ocean Deoxygenation. *Annual Review of Marine Science*, **10**, (2018), pp. 229–260, ISSN 1941-0611, doi:doi.org/10.1146/annurev-marine-121916-063359.
URL: <https://www.annualreviews.org/content/journals/10.1146/annurev-marine-121916-063359>
- Li, G., Cheng, L., Zhu, J., Trenberth, K. E., Mann, M. E., and Abraham, J. P., Increasing ocean stratification over the past half-century. *Nature Climate Change*, **10**, (2020), pp. 1116–1123, doi:10.1038/s41558-020-00918-2.
- Llovel, W. and Terray, L., Observed southern upper-ocean warming over 2005–2014 and associated mechanisms. *Environmental Research Letters*, **11**(12), (2016), p. 124023,

ISSN 1748-9326, doi:10.1088/1748-9326/11/12/124023, publisher: IOP Publishing.

URL: <http://dx.doi.org/10.1088/1748-9326/11/12/124023>

Loarie, S. R., Duffy, P. B., Hamilton, H., Asner, G. P., Field, C. B., and Ackerly, D. D., The velocity of climate change. *Nature*, **462**(7276), (2009), pp. 1052–1055, ISSN 1476-4687, doi:10.1038/nature08649.

URL: <https://doi.org/10.1038/nature08649>

Loeb, V., Siegel, V., Holm-Hansen, O., Hewitt, R., Fraser, W., Trivelpiece, W., and S., T., Effects of sea-ice extent and krill or salp dominance on the Antarctic food web. *Nature*, **387**, (1997), pp. 897–900, doi:10.1038/43174.

Long, M. C., Deutsch, C., and Ito, T., Finding forced trends in oceanic oxygen. *Global Biogeochemical Cycles*, **30**(2), (2016), pp. 381–397, doi:10.1002/2015GB005310.

URL: <https://agupubs.onlinelibrary.wiley.com/doi/abs/10.1002/2015GB005310>

Lotze, H. K., Tittensor, D. P., Bryndum-Buchholz, A., Eddy, T. D., Cheung, W. W. L., Galbraith, E. D., Barange, M., Barrier, N., Bianchi, D., Blanchard, J. L., Bopp, L., Büchner, M., Bulman, C., Carozza, D. A., Christensen, V., Coll, M., Dunne, J., Fulton, E. A., Jennings, S., Jones, M., Mackinson, S., Maury, O., Niiranen, S., OliverosRamos, R., Roy, T., Fernandes, J. A., Schewe, J., Shin, Y.-J., Silva, T. A. M., Steenbeek, J., Stock, C. A., Verley, P., Volkholz, J., and Walker, N. D., Ensemble projections of global ocean animal biomass with climate change, p. 467175, Cold Spring Harbor Laboratory, (2018), doi:10.1101/467175.

URL: <https://www.biorxiv.org/content/early/2018/11/09/467175>

Lévy, M., Franks, P., and Smith, K., The role of submesoscale currents in structuring marine ecosystems. *Nat Commun*, **9**(4758), (2018), pp. 1–16, doi:10.1038/s41467-018-07059-3.

López-Farrán, Z., Guillaumot, C., Vargas-Chacoff, L., Paschke, K., Dulière, V., Danis, B., Poulin, E., Saucède, T., Waters, J., and Gérard, K., Is the southern crab *Hali carcinus planatus* (Fabricius, 1775) the next invader of Antarctica? *Global Change Biology*, **27**(15), (2021), pp. 3487–3504, doi:10.1111/gcb.15674.

URL: <https://onlinelibrary.wiley.com/doi/abs/10.1111/gcb.15674>

- Maas, T., Pauwelussen, A., and Turnhout, E., Co-producing the science–policy interface: towards common but differentiated responsibilities. *Humanit Soc Sci Commun*, **9**(93), (2022), pp. 1–11, doi:10.1057/s41599-022-01108-5.
- Magris, R. A., Pressey, R. L., Weeks, R., and Ban, N. C., Integrating connectivity and climate change into marine conservation planning. *Biological Conservation*, **170**, (2014), pp. 207–221, ISSN 0006-3207, doi:10.1016/j.biocon.2013.12.032.
URL: <https://www.sciencedirect.com/science/article/pii/S0006320713004539>
- Makhado, A., Koubbi, P., Huggett, J., Cotte, C., Reisinger, R., Swadling, K., Azarian, C., Barnerias, C., d'Ovidio, F., Gauthier, L., Goberville, E., Leroy, B., Lombard, A., Muller, L., van de Putte, A., and workshop participants, Ecoregionalisation of the pelagic zone in the Subantarctic and Subtropical Indian Ocean, pp. 1–32, (2023).
- Makhado, A., Lowther, A., Koubbi, P., Anson, I., Brooks, C., Cotté, C., Crawford, R., Dzulisa, S., d'Ovidio, F., Fawcett, S., Freeman, D., Grant, S., Huggett, J., Hindell, M., Hulley, P., Kirkman, S., Lamont, T., Lombard, M., Masothla, M., Lea, M.-A., Oosthuizen, W., Orgeret, F., Reisinger, R., Samaai, T., Sergi, S., Swadling, K., Somhlaba, S., Van de Putte, A., Von de Meden, C., and Yemane, D., Expert Workshop on Pelagic Spatial Planning for the eastern subantarctic region (Domains 4, 5 and 6), (2019).
- Maraldi, C., Mongin, M., Coleman, R., and Testut, L., The influence of lateral mixing on a phytoplankton bloom: Distribution in the Kerguelen Plateau region. *Deep Sea Research Part I: Oceanographic Research Papers*, **56**(6), (2009), pp. 963–973, ISSN 0967-0637, doi:10.1016/j.dsr.2008.12.018.
URL: <https://www.sciencedirect.com/science/article/pii/S0967063709000053>
- Martinez-Moreno, J., Hogg, A. M., England, M. H., Constantinou, N. C., Kiss, A. E., and Morrison, A. K., Global changes in oceanic mesoscale currents over the satellite altimetry record. *Nature Climate Change*, **11**, (2021), pp. 397–403, doi:10.1038/s41558-021-01006-9.
- Martínez-Moreno, J., Hogg, A. M., Kiss, A. E., Constantinou, N. C., and Morrison, A. K., Kinetic Energy of Eddy-Like Features From Sea Surface Altimetry. *Journal of Advances in Modeling Earth Systems*, **11**(10), (2019), pp. 3090–3105, doi:10.1029/

2019MS001769.

URL: <https://agupubs.onlinelibrary.wiley.com/doi/abs/10.1029/2019MS001769>

McCartney, M. S., Subantarctic mode water, in *Voyage of Discovery: George Deacon 70th Anniversary Volume, Supplement to Deep-Sea Research*. (Edited by Angel, M.), p. 103–119, Pergamon Press, Oxford, (1977).

McCormack, S., Melbourne-Thomas, J., Trebilco, R., Griffith, G., Hill, S., Hoover, C., Johnston, N., Marina, T., Murphy, E., Pakhomov, E., Pinkerton, M., Plaganyi, E., Saravia, L., Subramaniam, R., Van de Putte, A., and AJ, C., Southern Ocean Food Web Modelling: Progress, Prognoses, and Future Priorities for Research and Policy Makers. *Front. Ecol. Evol.*, **9**(624763), (2021), pp. 1–21, doi:10.3389/fevo.2021.624763.

McDonald, A., Gold, M., and Ziegler, P., Summary Report from Australia's Heard Island and McDonald Islands Fishery Climate Adaptation Workshop, CCAMLR, (2023).

McKay, D. I. A., Staal, A., Abrams, J. F., Winkelmann, R., Sakschewski, B., Loriani, S., Fetzer, I., Cornell, S. E., Rockström, J., and Lenton, T. M., Exceeding 1.5°C global warming could trigger multiple climate tipping points. *Science*, **377**(6611), (2022), p. eabn7950, doi:10.1126/science.abn7950.

URL: <https://www.science.org/doi/abs/10.1126/science.abn7950>

McLeod, E., Anthony, K. R., Mumby, P. J., Maynard, J., Beeden, R., Graham, N. A., Heron, S. F., Hoegh-Guldberg, O., Jupiter, S., MacGowan, P., Mangubhai, S., Marshall, N., Marshall, P. A., McClanahan, T. R., Mcleod, K., Nyström, M., Obura, D., Parker, B., Possingham, H. P., Salm, R. V., and Tamelander, J., The future of resilience-based management in coral reef ecosystems. *Journal of Environmental Management*, **233**, (2019), pp. 291–301, ISSN 0301-4797, doi: 10.1016/j.jenvman.2018.11.034.

URL: <https://www.sciencedirect.com/science/article/pii/S0301479718312994>

McLeod, E., Green, A., Game, E., Anthony, K., Cinner, J., Heron, S. F., Kleypas, J., Lovelock, C. E., Pandolfi, J. M., Pressey, R. L., Salm, R., Schill, S., and Woodroffe, C., Integrating Climate and Ocean Change Vulnerability into Conservation Planning. *Coastal Management*, **40**(6), (2012), pp. 651–672, doi:10.1080/08920753.2012.728123.

McLeod, E., Salm, R., Green, A., and Almany, J., Designing marine protected area networks to address the impacts of climate change. *Frontiers in Ecology and the Environment*, **7**(7), (2009), pp. 362–370, doi:10.1890/070211.

URL: <https://esajournals.onlinelibrary.wiley.com/doi/abs/10.1890/070211>

McMahon, C. R., Bester, M. N., Burton, H. R., Hindell, M. A., and Bradshaw, C. J. A., Population status, trends and a re-examination of the hypotheses explaining the recent declines of the southern elephant seal *Mirounga leonina*. *Mammal Review*, **35**(1), (2005), pp. 82–100, doi:10.1111/j.1365-2907.2005.00055.x.

URL: <https://onlinelibrary.wiley.com/doi/abs/10.1111/j.1365-2907.2005.00055.x>

McMahon, C. R., Hindell, M. A., Charrassin, J.-B., Corney, S., Guinet, C., Harcourt, R., Jonsen, I., Trebilco, R., Williams, G., and Bestley, S., Finding mesopelagic prey in a changing Southern Ocean. *Scientific Reports*, **9**(19013), (2019), pp. 1–11, doi:10.1038/s41598-019-55152-4.

Meehl, G. A., Arblaster, J. M., Chung, C. T. Y., Holland, M. M., DuVivier, A., Thompson, L., Yang, D., and Bitz, C. M., Sustained ocean changes contributed to sudden Antarctic sea ice retreat in late 2016. *Nature Communications*, **10**(14), (2019), pp. 1–9, doi:10.1038/s41467-018-07865-9.

Meilland, J., Fabri-Ruiz, S., Koubbi, P., Monaco, C. L., Cotte, C., Hosie, G. W., Sanchez, S., and Howa, H., Planktonic foraminiferal biogeography in the Indian sector of the Southern Ocean: Contribution from CPR data. *Deep Sea Research Part I: Oceanographic Research Papers*, **110**, (2016), pp. 75–89, ISSN 0967-0637, doi:10.1016/j.dsr.2015.12.014.

Melbourne-Thomas, J., Corney, S. P., Trebilco, R., Meiners, K. M., Stevens, R. P., Kawaguchi, S., Sumner, M. D., and Constable, A. J., Under ice habitats for Antarctic krill larvae: Could less mean more under climate warming? *Geophysical Research Letters*, **43**(19), (2016), pp. 10,322–10,327, doi:10.1002/2016GL070846.

Melo-Merino, S. M., Reyes-Bonilla, H., and Lira-Noriega, A., Ecological niche models and species distribution models in marine environments: A literature review and spatial analysis of evidence. *Ecological Modelling*, **415**, (2020), p. 108837, ISSN 0304-3800, doi:10.1016/j.ecolmodel.2019.108837.

URL: <https://www.sciencedirect.com/science/article/pii/S030438001930345X>

- Meredith, M., Sommerkorn, M., Cassotta, S., Derksen, C., Ekaykin, A., Hollowed, A., Kofinas, G., Mackintosh, A., Melbourne-Thomas, J., Muelbert, M., Ottersen, G., Pritchard, H., and Schuur, E., Polar Regions, in *IPCC Special Report on the Ocean and Cryosphere in a Changing Climate* (Edited by Pörtner, H.-O., Roberts, D., Masson-Delmotte, V., Zhai, P., Tignor, M., Poloczanska, E., Mintenbeck, K., Alegría, A., Nicolai, M., Okem, A., Petzold, J., Rama, B., and Weyer, N.), p. 203–320, Cambridge University Press, (2019), doi:10.1017/9781009157964.005.
- Merland, C., Azarian, C., d’Ovidio, F., and Cotté, C., Physical and biogeochemical regionalisations and climate velocities in the epipelagic and mesopelagic Southern Indian Ocean, in *CCAMLR Science*, (under review).
- Mestre, J., Authier, M., Cherel, Y., Harcourt, R., McMahon, C. R., Hindell, M. A., Charrassin, J.-B., and Guinet, C., Decadal changes in blood $\delta^{13}\text{C}$ values, at-sea distribution, and weaning mass of southern elephant seals from Kerguelen Islands. *Proc. R. Soc. B.*, (28720201544), (2020), pp. 1–10, doi:10.1098/rspb.2020.1544.
- Mills, K. E., Pershing, A. J., Brown, C. J., Chen, Y., Chiang, F.-S., Holland, D. S., Lehuta, S., Nye, J. A., Sun, J. C., Thomas, A. C., and Wahle, R. A., Fisheries Management in a Changing Climate: Lessons from the 2012 Ocean Heat Wave in the Northwest Atlantic. *Oceanography*, **26**(2), (2013), pp. 191–195, ISSN 10428275, 2377617X.
URL: <http://www.jstor.org/stable/24862052>
- Miyama, T., Minobe, S., and Goto, H., Marine Heatwave of Sea Surface Temperature of the Oyashio Region in Summer in 2010–2016. *Frontiers in Marine Science*, **7**, (2021), p. 1150, ISSN 2296-7745, doi:10.3389/fmars.2020.576240.
URL: <https://www.frontiersin.org/article/10.3389/fmars.2020.576240>
- Mongin, M., Molina, E., and Trull, T. W., Seasonality and scale of the Kerguelen plateau phytoplankton bloom: A remote sensing and modeling analysis of the influence of natural iron fertilization in the Southern Ocean. *Deep Sea Research Part II: Topical Studies in Oceanography*, **55**(5), (2008), pp. 880–892, ISSN 0967-0645, doi:10.1016/j.dsr2.2007.12.039, kEOPS: Kerguelen Ocean and Plateau compared Study.
URL: <https://www.sciencedirect.com/science/article/pii/S0967064508000295>

- Moore, J. K. and Abbott, M. R., Phytoplankton chlorophyll distributions and primary production in the Southern Ocean. *Journal of Geophysical Research: Oceans*, **105**(C12), (2000), pp. 28709–28722, doi:10.1029/1999JC000043.
- Moore, J. K., Abbott, M. R., and Richman, J. G., Location and dynamics of the Antarctic Polar Front from satellite sea surface temperature data. *Journal of Geophysical Research: Oceans*, **104**(C2), (1999), pp. 3059–3073, doi:10.1029/1998JC900032
URL: <https://agupubs.onlinelibrary.wiley.com/doi/abs/10.1029/1998JC900032>
- Mori, M., Corney, S. P., Melbourne-Thomas, J., Welsford, D. C., Klocker, A., and Ziegler, P. E., Using satellite altimetry to inform hypotheses of transport of early life stage of Patagonian toothfish on the Kerguelen Plateau. *Ecological Modelling*, **340**, (2016), pp. 45–56, ISSN 0304-3800, doi:10.1016/j.ecolmodel.2016.08.013.
URL: <https://www.sciencedirect.com/science/article/pii/S0304380016303325>
- Mori, M., Mizobata, K., Ichii, T., Ziegler, P., and Okuda, T., Modeling the egg and larval transport pathways of the Antarctic toothfish (*Dissostichus mawsoni*) in the East Antarctic region: New insights into successful transport connections. *Fisheries Oceanography*, **31**(1), (2022), pp. 19–39, doi:10.1111/fog.12560.
URL: <https://onlinelibrary.wiley.com/doi/abs/10.1111/fog.12560>
- Morris, M., Stanton, B. R., and Neil, H. L., Subantarctic oceanography around New Zealand: Preliminary results from an ongoing survey. *N. Z. J. Mar. Freshwater Res.*, **35**, (2001), p. 499–519.
- Morrison, A. K., Griffies, S. M., Winton, M., Anderson, W. G., and Sarmiento, J. L., Mechanisms of Southern Ocean Heat Uptake and Transport in a Global Eddyng Climate Model. *J. Climate*, **29**, (2016), p. 2059–2075, doi:10.1175/JCLI-D-15-0579.1.
- Mujica, A., Peñailillo, D., Reyes, A., and Nava, M., Embryonic and larval development of *Dissostichus eleginoides* (Pisces: Nototheniidae). *Revista de biología marina y oceanografía*, **51**, (2016), pp. 675–680, doi:10.4067/S0718-19572016000300018.
- Nie, Y., Uotila, P., Cheng, B., Massonnet, F., Kimura, N., Cipollone, A., and Lv, X., Southern Ocean sea ice concentration budgets of five ocean-sea ice reanalyses. *Clim Dyn*, **59**, (2022), pp. 3265–3285, doi:10.1007/s00382-022-06260-x.

- Niu, Y., Cheng, X., Qin, J., Ou, N., Yang, C., and Huang, D., Mechanisms of Inter-annual Variability of Ocean Bottom Pressure in the Southern Indian Ocean. *Front. Mar. Sci.*, **9**(916592), (2022), pp. 1–11, doi:10.3389/fmars.2022.916592.
- Nocedal, J. and Wright, S., Numerical Optimization, Springer, (2006).
- N'Diaye, A., La nature est-elle au fondement de nos normes ? *Philosophie Magazine*, (147), (2021), p. 82.
- Ohayon, S., Granot, I., and Belmaker, A meta-analysis reveals edge effects within marine protected areas. *Nat Ecol Evol*, **5**, (2021), p. 1301–1308, doi:10.1038/s41559-021-01502-3.
- Oliver, E. C., Benthuisen, J. A., Darmaraki, S., Donat, M. G., Hobday, A. J., Holbrook, N. J., Schlegel, R. W., and Sen Gupta, A., Marine Heatwaves. *Annual Review of Marine Science*, **13**(1), (2021), pp. 313–342, ISSN 1941-1405, doi: 10.1146/annurev-marine-032720-095144, publisher: Annual Reviews.
URL: <https://doi.org/10.1146/annurev-marine-032720-095144>
- Oliver, E. C. J., Donat, M. G., Burrows, M. T., Moore, P. J., Smale, D. A., Alexander, L. V., Benthuisen, J. A., Feng, M., Sen Gupta, A., Hobday, A. J., Holbrook, N. J., Perkins-Kirkpatrick, S. E., Scannell, H. A., Straub, S. C., and Wernberg, T., Longer and more frequent marine heatwaves over the past century. *Nature Communications*, **9**(1), (2018), p. 1324, ISSN 2041-1723, doi:10.1038/s41467-018-03732-9.
URL: <https://doi.org/10.1038/s41467-018-03732-9>
- O'Neill, B. C., Tebaldi, C., van Vuuren, D. P., Eyring, V., Friedlingstein, P., Hurtt, G., Knutti, R., Kriegler, E., Lamarque, J.-F., Lowe, J., Meehl, G. A., Moss, R., Riahi, K., and Sanderson, B. M., The Scenario Model Intercomparison Project (ScenarioMIP) for CMIP6. *Geoscientific Model Development*, **9**(9), (2016), pp. 3461–3482, doi:10.5194/gmd-9-3461-2016.
URL: <https://gmd.copernicus.org/articles/9/3461/2016/>
- Orsi, A. H., Johnson, G. C., and Bullister, J. L., Circulation, mixing and production of Antarctic Bottom Water. *Prog. Oceanogr.*, **43**, (1999), p. 55–109.
- Orsi, A. H., Whitworth III, T., and Nowlin, W. D. J., On the meridional extent and fronts of the Antarctic Circumpolar Current. *Deep Sea Res.*, **42**, (1995), p. 641–673.

- Pakhomov, A., Perissinotto, R., and McQuaid, C. D., Comparative structure of the macrozooplankton/micronekton communities of the Subtropical and Antarctic Polar Fronts. *Marine Ecology Progress Series*, **111**, (1994), pp. 155–169.
- Pankhurst, N. W. and Munday, P. L., Effects of climate change on fish reproduction and early life history stages. *Marine and Freshwater Research*, **62**, (2011), pp. 1015–1026, doi:10.1071/MF10269.
- Park, Y., Charriaud, E., and Fieux, M., Thermohaline structure of the antarctic surface water/winter water in the Indian sector of the Southern Ocean. *Journal of Marine Systems*, **17**, (1998), pp. 5–23.
- Park, Y.-H. and Durand, I., Altimetry-Derived Antarctic Circumpolar Current Fronts., (2019), doi:10.17882/59800.
- Park, Y.-H., Durand, I., Kestenare, E., Rougier, G., Zhou, M., d'Ovidio, F., Cotté, C., and Lee, J.-H., Polar Front around the Kerguelen Islands: An up-to-date determination and associated circulation of surface/subsurface waters. *Journal of Geophysical Research: Oceans*, **119**(10), (2014), pp. 6575–6592, doi:10.1002/2014JC010061.
URL: <https://agupubs.onlinelibrary.wiley.com/doi/abs/10.1002/2014JC010061>
- Park, Y.-H., Fuda, J.-L., Durand, I., and Naveira Garabato, A. C., Internal tides and vertical mixing over the Kerguelen Plateau. *Deep Sea Research Part II: Topical Studies in Oceanography*, **55**(5), (2008a), pp. 582–593, ISSN 0967-0645, doi:10.1016/j.dsr2.2007.12.027, kEOPS: Kerguelen Ocean and Plateau compared Study.
URL: <https://www.sciencedirect.com/science/article/pii/S0967064508000118>
- Park, Y.-H., Roquet, F., Durand, I., and Fuda, J.-L., Large-scale circulation over and around the Northern Kerguelen Plateau. *Deep Sea Research Part II: Topical Studies in Oceanography*, **55**(5), (2008b), pp. 566–581, ISSN 0967-0645, doi:10.1016/j.dsr2.2007.12.030, kEOPS: Kerguelen Ocean and Plateau compared Study.
URL: <https://www.sciencedirect.com/science/article/pii/S0967064508000106>
- Park, Y.-H., Roquet, F., Durand, I., and Fuda, J.-L., Large-scale circulation over and around the Northern Kerguelen Plateau. *KEOPS: Kerguelen Ocean and Plateau compared Study*, **55**(5), (2008c), pp. 566–581, ISSN 0967-0645, doi:10.1016/j.dsr2.2007.12.030.
URL: <https://www.sciencedirect.com/science/article/pii/S0967064508000106>

- Pascual, A., Faugère, Y., Larnicol, G., and Le Traon, P.-Y., Improved description of the ocean mesoscale variability by combining four satellite altimeters. *Geophysical Research Letters*, **33**(2), (2006), p. L02611, doi:10.1029/2005GL024633.
- Patterson, H. and Tuynman, H., Chapter 24 : Heard Island and McDonald Islands Fishery, in *Fishery status reports 2022*, pp. 340–348, (2022).
- Pauthenet, E., Roquet, F., Madec, G., Guinet, C., Hindell, M., McMahon, C. R., Harcourt, R., and Nerini, D., Seasonal Meandering of the Polar Front Upstream of the Kerguelen Plateau. *Geophysical Research Letters*, **45**(18), (2018), pp. 9774–9781, doi: 10.1029/2018GL079614.
URL: <https://agupubs.onlinelibrary.wiley.com/doi/abs/10.1029/2018GL079614>
- Pauthenet, E., Roquet, F., Madec, G., and Nerini, D., A linear decomposition of the Southern Ocean thermohaline structure. *Journal of Physical Oceanography*, **47**(1), (2017), p. 29–47, doi:10.1175/JPO-D-16-0083.1.
- Pentz, B., Klenk, N., Ogle, S., and Fisher, J. A., Can regional fisheries management organizations (RFMOs) manage resources effectively during climate change? *Marine Policy*, **92**, (2018), pp. 13–20, ISSN 0308-597X, doi:10.1016/j.marpol.2018.01.011.
URL: <https://www.sciencedirect.com/science/article/pii/S0308597X17305560>
- Petitgas, P., Rijnsdorp, A. D., Dickey-Collas, M., Engelhard, G. H., Peck, M. A., Pinnegar, J. K., Drinkwater, K., Huret, M., and Nash, R. D. M., Impacts of climate change on the complex life cycles of fish. *Fisheries Oceanography*, **22**(2), (2013), pp. 121–139, doi:10.1111/fog.12010.
URL: <https://onlinelibrary.wiley.com/doi/abs/10.1111/fog.12010>
- Pinkerton, M. H., Boyd, P. W., Deppeler, S., Hayward, A., Höfer, J., and Moreau, S., Evidence for the Impact of Climate Change on Primary Producers in the Southern Ocean. *Frontiers in Ecology and Evolution*, **9**, (2021), p. 134, ISSN 2296-701X, doi: 10.3389/fevo.2021.592027.
URL: <https://www.frontiersin.org/article/10.3389/fevo.2021.592027>
- Pinkerton, M. H., Décima, M., Kitchener, J. A., Takahashi, K. T., Robinson, K. V., Stewart, R., and Hosie, G. W., Zooplankton in the Southern Ocean from the continuous plankton recorder: Distributions and long-term change. *Deep Sea Research*

- Part I: Oceanographic Research Papers*, **162**, (2020), p. 103303, ISSN 0967-0637, doi: 10.1016/j.dsr.2020.103303.
URL: <https://www.sciencedirect.com/science/article/pii/S0967063720300911>
- Pinones, A. and Fedorov, A. V., Projected changes of Antarctic krill habitat by the end of the 21st century. *Geophysical Research Letters*, **43**(16), (2016), pp. 8580–8589, doi:10.1002/2016GL069656.
URL: <https://agupubs.onlinelibrary.wiley.com/doi/abs/10.1002/2016GL069656>
- Pinsky, M., Worm, B., Fogarty, M., Sarmiento, J., and Levin, S., Marine taxa track local climate velocities. *Science*, **341**, (2013), pp. 1239–42.
- Pinsky, M. L. and Mantua, N. J., Emerging Adaptation Approaches for Climate-Ready Fisheries Management. *Oceanography*, **27**(4), (2014), pp. 146–159.
- Pistevos, J., Nagelkerken, I., Rossi, T., and Connell, S. D., Ocean acidification alters temperature and salinity preferences in larval fish. *Oecologia*, **183**, (2017), p. 545–553, doi:10.1007/s00442-016-3778-z.
- Plecha, S. M. and Soares, P. M. M., Global marine heatwave events using the new CMIP6 multi-model ensemble: from shortcomings in present climate to future projections. *Environmental Research Letters*, **15**(12), (2020), p. 124058, doi:10.1088/1748-9326/abc847.
- Portela, E., Kolodziejczyk, N., Maes, C., and Thierry, V., Interior Water-Mass Variability in the Southern Hemisphere Oceans during the Last Decade. *J. Phys. Oceanogr.*, **50**, (2020), p. 361–381, doi:10.1175/JPO-D-19-0128.1.
- Press, W. H. and Teukolsky, S. A., Adaptive Step-size Runge-Kutta Integration. *Computer in Physics*, **6**(2), (1992), pp. 188–191, ISSN 0894-1866, doi:10.1063/1.4823060.
- Purich, A. and Doddridge, E., Record low Antarctic sea ice coverage indicates a new sea ice state. *Communications Earth and Environment*, **4**(1), (2023), p. 314.
- Purich, A. and England, M. H., Historical and Future Projected Warming of Antarctic Shelf Bottom Water in CMIP6 Models. *Geophysical Research Letters*, **48**(10), (2021), p. e2021GL092752, doi:10.1029/2021GL092752.
- Péron, C., Chazeau, C., Faure, J., Gasco, N., Martin, A., Massiot-Granier, F., Pruvost, P., Rajaonalison, F., and Selles, J., Données statistiques de pêche des navires français

- et étrangers dans les zones économiques exclusives des îles Kerguelen, Crozet et Saint-Paul/Amsterdam et les eaux internationales CCAMLR et APSOI., in *Rapport 2022*, (2022).
- Péron, C., Welsford, D. C., Ziegler, P., Lamb, T. D., Gasco, N., Chazeau, C., Sinègre, R., and Duhamel, G., Modelling spatial distribution of Patagonian toothfish through life-stages and sex and its implications for the fishery on the Kerguelen Plateau. *Progress in Oceanography*, **141**, (2016), pp. 81–95, ISSN 0079-6611, doi:10.1016/j.pocean.2015.12.003.
URL: <https://www.sciencedirect.com/science/article/pii/S007966111530015X>
- Qu, T., Gao, S., and Fine, R. A., Variability of the Sub-Antarctic Mode Water subduction rate during the Argo period. *Geophysical Research Letters*, **47**(13), (2020), p. e2020GL088248, doi:10.1029/2020GL088248.
- Quetin, L. B. and Ross, R. M., Episodic recruitment in Antarctic krill *Euphausia superba* in the Palmer LTER study region. *Marine Ecology Progress Series*, **259**, (2003), pp. 185–200.
- Raphael, M. and Handcock, M., A new record minimum for Antarctic sea ice. *Nat Rev Earth Environ*, **3**(4), (2022), pp. 215–216.
- Rayfuse, R., Climate Change and Antarctic Fisheries: Ecosystem Management in CCAMLR. *Ecology Law Quarterly*, **45**(1), (2018), p. 53–82.
URL: <https://www.jstor.org/stable/26568787>
- Rayner, N. A., Parker, D. E., Horton, E. B., Folland, C. K., Alexander, L. V., Rowell, D. P., Kent, E. C., and Kaplan, A., Global analyses of sea surface temperature, sea ice, and night marine air temperature since the late nineteenth century. *Journal of Geophysical Research: Atmospheres*, **108**(D14), (2003), p. 4407, doi: 10.1029/2002JD002670.
- Reisinger, R. R., Brooks, C. M., Raymond, B., Freer, J. J., Cotté, C., Xavier, J. C., Trathan, P. N., Bornemann, H., Charrassin, J.-B., Costa, D. P., Danis, B., Hückstädt, L., Jonsen, I. D., Lea, M.-A., Torres, L., Van de Putte, A., Wotherspoon, S., Friedlaender, A. S., Ropert-Coudert, Y., and Hindell, M., Predator-derived bioregions

- in the Southern Ocean: Characteristics, drivers and representation in marine protected areas. *Biological Conservation*, **272**, (2022), p. 109630, ISSN 0006-3207, doi: 10.1016/j.biocon.2022.109630.
- URL:** <https://www.sciencedirect.com/science/article/pii/S0006320722001835>
- Reisinger, R. R., Raymond, B., Hindell, M. A., Bester, M. N., Crawford, R. J. M., Davies, D., de Bruyn, P. J. N., Dilley, B. J., Kirkman, S. P., Makhado, A. B., Ryan, P. G., Schoombie, S., Stevens, K., Sumner, M. D., Tosh, C. A., Wege, M., Whitehead, T. O., Wotherspoon, S., and Pistorius, P. A., Habitat modelling of tracking data from multiple marine predators identifies important areas in the Southern Indian Ocean. *Divers Distrib.*, **24**, (2018), p. 535–550, doi:10.1111/ddi.12702.
- Reynolds, R. W., Rayner, N. A., Smith, T. M., Stokes, D. C., and Wang, W., An Improved In Situ and Satellite SST Analysis for Climate. *Journal of Climate*, **15**(13), (2002), pp. 1609 – 1625, doi:10.1175/1520-0442(2002)015(1609:AIISAS)2.0.CO;2.
- Reynolds, R. W., Smith, T. M., Liu, C., Chelton, D. B., Casey, K. S., and Schlax, M. G., Daily High-Resolution-Blended Analyses for Sea Surface Temperature. *Journal of Climate*, **20**(22), (2007), pp. 5473 – 5496, doi:10.1175/2007JCLI1824.1.
- Rilov, G., Mazaris, A. D., Stelzenmüller, V., Helmuth, B., Wahl, M., Guy-Haim, T., Mieszkowska, N., Ledoux, J.-B., and Katsanevakis, S., Adaptive marine conservation planning in the face of climate change: What can we learn from physiological, ecological and genetic studies? *Global Ecology and Conservation*, **17**, (2019), p. e00566, ISSN 2351-9894, doi:10.1016/j.gecco.2019.e00566.
- URL:** <https://www.sciencedirect.com/science/article/pii/S2351989418301720>
- Rintoul, S. R., The global influence of localized dynamics in the Southern Ocean. *Nature*, **558**, (2018), pp. 209–218, doi:10.1038/s41586-018-0182-3.
- Rintoul, S. R., Hughes, C. W., and Olbers, D., The Antarctic Circumpolar Current system., in *Ocean Circulation and Climate: Observing and Modelling the Global Ocean*. (Edited by G. Siedler, J., Church, J., and Gould, J.), p. 271–302, Academic Press, London, (2001).
- Rintoul, S. R. and Naveira Garabato, A., Chapter 18 - Dynamics of the Southern Ocean Circulation. *International Geophysics*, **103**, (2013), pp. 471–492, doi: 10.1016/B978-0-12-391851-2.00018-0.

Roach, L. A., Dörr, J., Holmes, C. R., Massonnet, F., Blockley, E. W., Notz, D., Rackow, T., Raphael, M. N., O'Farrell, S. P., Bailey, D. A., and Bitz, C. M., Antarctic Sea Ice Area in CMIP6. *Geophysical Research Letters*, **47**(9), (2020), p. e2019GL086729, doi:10.1029/2019GL086729, e2019GL086729 10.1029/2019GL086729.

URL: <https://agupubs.onlinelibrary.wiley.com/doi/abs/10.1029/2019GL086729>

Roemmich, D., Church, J., Gilson, J., Monselesan, D., Sutton, P., and Wijffels, S., Unabated planetary warming and its ocean structure since 2006. *Nature Clim Change*, **5**, (2015), pp. 240–245, doi:10.1038/nclimate2513.

Rogers, A., Frinault, B., Barnes, D., Bindoff, N., Downie, R., Ducklow, H., Friedlaender, A., Hart, T., Hill, S., Hofmann, E., Linse, K., McMahon, C., Murphy, E., Pakhomov, E., Reygondeau, G., Staniland, I., Wolf-Gladrow, D., and Wright, R., Antarctic Futures: An Assessment of Climate-Driven Changes in Ecosystem Structure, Function, and Service Provisioning in the Southern Ocean. *Annual Review of Marine Science*, **12**, (2020), pp. 87–120, ISSN 1941-0611, doi:doi.org/10.1146/annurev-marine-010419-011028.

URL: <https://www.annualreviews.org/content/journals/10.1146/annurev-marine-010419-011028>

Rombough, P. J., The effects of temperature on embryonic and larval development. **61**, (1997), pp. 177–224.

Roquet, F., Williams, G., Hindell, M. A., Harcourt, R., McMahon, C., Guinet, C., Charrassin, J.-B., Reverdin, G., Boehme, L., Lovell, P., and Fedak, M., A Southern Indian Ocean database of hydrographic profiles obtained with instrumented elephant seals. *Scientific Data*, **1**(1), (2014), p. 140028, ISSN 2052-4463, doi:10.1038/sdata.2014.28.

URL: <https://doi.org/10.1038/sdata.2014.28>

Rosso, I., Hogg, A. M., Strutton, P. G., Kiss, A. E., Matear, R., Klocker, A., and van Sebille, E., Vertical transport in the ocean due to sub-mesoscale structures: Impacts in the Kerguelen region. *Ocean Modelling*, **80**, (2014), pp. 10–23, ISSN 1463-5003, doi:10.1016/j.ocemod.2014.05.001.

URL: <https://www.sciencedirect.com/science/article/pii/S146350031400064X>

- Rousselet, L., d'Ovidio, F., Izard, L., Della Penna, A., Petrenko, A., Barrillon, S., Nencioli, F., and A., D., A Software Package for an Adaptive Satellite-based Sampling for Oceanographic cruises (SPASSOv2.0): tracking fine scale features for physical and biogeochemical studies. (in preparation).
- Ruby, P. and Ahilan, B., An overview of climate change impact in fisheries and aquaculture. *Climate Change*, **4**(13), (2018), pp. 87–94.
- Ryan-Keogh, T. J., Thomalla, S. J., Monteiro, P. M. S., and Tagliabue, A., Multidecadal trend of increasing iron stress in Southern Ocean phytoplankton. *Science*, **379**(6634), (2023), pp. 834–840, doi:10.1126/science.abl5237.
URL: <https://www.science.org/doi/abs/10.1126/science.abl5237>
- Sabu, P., Libera, S. A., Chacko, R., Anilkumar, N., Subeesh, M., and Thomas, A. P., Winter water variability in the Indian Ocean sector of Southern Ocean during austral summer. *Understanding the link between atmospheric, physical and biogeochemical processes in the Indian sector of the Southern Ocean*, **178**, (2020), p. 104852, ISSN 0967-0645, doi:10.1016/j.dsr2.2020.104852.
URL: <https://www.sciencedirect.com/science/article/pii/S0967064519301560>
- Sala, E., Mayorga, J., Bradley, D., Cabral, R. B., Atwood, T. B., Auber, A., Cheung, W., Costello, C., Ferretti, F., Friedlander, A. M., Gaines, S. D., Garilao, C., Goodell, W., Halpern, B. S., Hinson, A., Kaschner, K., Kesner-Reyes, K., Leprieur, F., McGowan, J., Morgan, L. E., Mouillot, D., Palacios-Abrantes, J., Possingham, H. P., Rechberger, K. D., Worm, B., and Lubchenco, J., Protecting the global ocean for biodiversity, food and climate. *Nature*, **592**, (2021), p. 397–402, doi:10.1038/s41586-021-03371-z.
- Sallée, J.-B., Southern Ocean Warming. *Oceanography*, **31**(2), (2018), pp. 52–62, ISSN 10428275, 2377617X, publisher: Oceanography Society.
URL: <https://www.jstor.org/stable/26542651>
- Sallée, J.-B., Pellichero, V., Akhoudas, C., Pauthenet, E., Vignes, L., Schmidtko, S., Garabato, A. N., Sutherland, P., and Kuusela, M., Summertime increases in upper-ocean stratification and mixed-layer depth. *Nature*, **591**(4), (2021), pp. 592–598, doi: 10.1038/s41586-021-03303-x.
URL: <https://doi.org/10.1038/s41586-021-03303-x>

- Scannell, H. A., Johnson, G. C., Thompson, L., Lyman, J. M., and Riser, S. C., Sub-surface Evolution and Persistence of Marine Heatwaves in the Northeast Pacific. *Geophysical Research Letters*, **47**(23), (2020), p. e2020GL090548, ISSN 0094-8276, doi:10.1029/2020GL090548, place: Washington Publisher: Amer Geophysical Union WOS:000598677000038.
- Scannell, H. A., Pershing, A. J., Alexander, M. A., Thomas, A. C., and Mills, K. E., Frequency of marine heatwaves in the North Atlantic and North Pacific since 1950. *Geophysical Research Letters*, **43**(5), (2016), pp. 2069–2076, ISSN 0094-8276, doi: 10.1002/2015GL067308, publisher: John Wiley Sons, Ltd.
URL: <https://doi.org/10.1002/2015GL067308>
- Schaeffer, A. and Roughan, M., Subsurface intensification of marine heatwaves off southeastern Australia: The role of stratification and local winds. *Geophysical Research Letters*, **44**(10), (2017), pp. 5025–5033, ISSN 0094-8276, doi:10.1002/2017GL073714, publisher: John Wiley Sons, Ltd.
URL: <https://doi.org/10.1002/2017GL073714>
- Scheffer, A., Bost, C., and Trathan, P., Frontal zones, temperature gradient and depth characterize the foraging habitat of king penguins at South Georgia. *Marine Ecology Progress Series*, **465**, (2012), pp. 281–297, doi:10.3354/meps09884.
- Scheffer, A., Trathan, P. N., Edmonston, J. G., and Bost, C.-A., Combined influence of meso-scale circulation and bathymetry on the foraging behaviour of a diving predator, the king penguin (*Aptenodytes patagonicus*). *Progress in Oceanography*, **141**, (2016), pp. 1–16, ISSN 0079-6611, doi:10.1016/j.pocean.2015.10.005.
URL: <https://www.sciencedirect.com/science/article/pii/S0079661115002141>
- Schmidtko, S., Heywood, K. J., Thompson, A. F., and Aoki, S., Multidecadal warming of Antarctic waters. *Science*, **346**(6214), (2014), p. 1227–1231.
- Schmidtko, S., Stramma, L., and Visbeck, M., Decline in global oceanic oxygen content during the past five decades. *Nature*, **542**, (2017), pp. 335–339, doi:10.1038/nature21399.
- Sergi, S., Baudena, A., Cotté, C., Ardyna, M., Blain, S., and d’Ovidio, F., Interaction of the Antarctic Circumpolar Current With Seamounts Fuels Moderate Blooms but Vast Foraging Grounds for Multiple Marine Predators. *Frontiers in Marine Science*,

- 7, (2020), p. 416, ISSN 2296-7745, doi:10.3389/fmars.2020.00416.
URL: <https://www.frontiersin.org/articles/10.3389/fmars.2020.00416>
- Serres, M., *Le Contrat naturel*, Flammarion, (2020).
- Shi, J.-R., Talley, L. D., Xie, S.-P., Peng, Q., and Liu, W., Ocean warming and accelerating Southern Ocean zonal flow. *Nature Climate Change*, **11**, (2021), pp. 1090–1097, doi:10.1038/s41558-021-01212-5.
- Shu, Q., Wang, Q., Song, Z., Qiao, F., Zhao, J., Chu, M., and Li, X., Assessment of Sea Ice Extent in CMIP6 With Comparison to Observations and CMIP5. *Geophysical Research Letters*, **47**(9), (2020), p. e2020GL087965, doi:10.1029/2020GL087965, e2020GL087965 2020GL087965.
URL: <https://agupubs.onlinelibrary.wiley.com/doi/abs/10.1029/2020GL087965>
- Siegert, M., Bentley, M., Atkinson, A., Bracegirdle, T., Convey, P., Davies, B., Downie, R., Hogg, A., Holmes, C., Hughes, K., Meredith, M., Ross, N., Rumble, J., and Wilkinson, J., Antarctic extreme events. *Front. Environ. Sci.*, **11**, (2023), p. 1229283, doi:10.3389/fenvs.2023.1229283.
- Sillero, N., Arenas-Castro, S., Enriquez-Urzelai, U., Vale, C. G., Sousa-Guedes, D., Martínez-Freiría, F., Real, R., and Barbosa, A., Want to model a species niche? A step-by-step guideline on correlative ecological niche modelling. *Ecological Modelling*, **456**, (2021), p. 109671, ISSN 0304-3800, doi:10.1016/j.ecolmodel.2021.109671.
URL: <https://www.sciencedirect.com/science/article/pii/S0304380021002301>
- Silvy, Y., Guilyardi, E., Sallee, J.-B., and Durack, P., Human-induced changes to the global ocean water masses and their time of emergence. *Nature Climate Change*, **20**, (2020), p. 1030–1036, doi:10.1038/s41558-020-0878-x.
- Skern-Mauritzen, M., Ottersen, G., Handegard, N. O., Huse, G., Dingsør, G. E., Stenseth, N. C., and Kjesbu, O. S., Ecosystem processes are rarely included in tactical fisheries management. *Fish and Fisheries*, **17**(1), (2016), pp. 165–175, doi: 10.1111/faf.12111.
URL: <https://onlinelibrary.wiley.com/doi/abs/10.1111/faf.12111>

Smale, D., Wernberg, T., and Vanderklift, M., Regional-scale variability in the response of benthic macroinvertebrate assemblages to a marine heatwave. *Marine Ecology Progress Series*, **568**, (2017), pp. 17–30.

URL: <https://www.int-res.com/abstracts/meps/v568/p17-30/>

Smale, D. A., Wernberg, T., Oliver, E. C. J., Thomsen, M., Harvey, B. P., Straub, S. C., Burrows, M. T., Alexander, L. V., Benthuisen, J. A., Donat, M. G., Feng, M., Hobday, A. J., Holbrook, N. J., Perkins-Kirkpatrick, S. E., Scannell, H. A., Sen Gupta, A., Payne, B. L., and Moore, P. J., Marine heatwaves threaten global biodiversity and the provision of ecosystem services. *Nature Climate Change*, **9**(4), (2019), pp. 306–312, ISSN 1758-6798, doi:10.1038/s41558-019-0412-1.

URL: <https://doi.org/10.1038/s41558-019-0412-1>

Smith, K. E., Burrows, M. T., Hobday, A. J., Gupta, A. S., Moore, P. J., Thomsen, M., Wernberg, T., and Smale, D. A., Socioeconomic impacts of marine heatwaves: Global issues and opportunities. *Science*, **374**(6566), (2021), p. eabj3593, doi:10.1126/science.abj3593.

URL: <https://www.science.org/doi/abs/10.1126/science.abj3593>

Smith, K. E., Burrows, M. T., Hobday, A. J., King, N. G., Moore, P. J., Sen Gupta, A., Thomsen, M. S., Wernberg, T., and Smale, D. A., Biological Impacts of Marine Heatwaves. *Annual Review of Marine Science*, **15**(Volume 15, 2023), (2023), pp. 119–145, ISSN 1941-0611, doi:doi.org/10.1146/annurev-marine-032122-121437.

URL: <https://www.annualreviews.org/content/journals/10.1146/annurev-marine-032122-121437>

Sokolov, S. and Rintoul, S. R., Structure of Southern Ocean fronts at 140°E. *Journal of Marine Systems*, **37**(1), (2002), pp. 151–184, ISSN 0924-7963, doi:10.1016/S0924-7963(02)00200-2, physics and Biology of Ocean Fronts.

URL: <https://www.sciencedirect.com/science/article/pii/S0924796302002002>

Solodoch, A., Stewart, A. L., Hogg, A. M., Morrison, A. K., Kiss, A. E., Thompson, A. F., Purkey, S. G., and Cimoli, L., How Does Antarctic Bottom Water Cross the Southern Ocean? *Geophysical Research Letters*, **49**(7), (2022), p. e2021GL097211, doi:10.1029/2021GL097211, e2021GL097211 2021GL097211.

URL: <https://agupubs.onlinelibrary.wiley.com/doi/abs/10.1029/2021GL097211>

- Southwell, C., Emmerson, L., McKinlay, J., Newbery, K., Takahashi, A., Kato, A., Barbraud, C., DeLord, K., and Weimerskirch, H., Spatially Extensive Standardized Surveys Reveal Widespread, Multi-Decadal Increase in East Antarctic Adélie Penguin Populations. *PLOS ONE*, **10**, (2015), pp. 1–18, doi:10.1371/journal.pone.0139877.
URL: <https://doi.org/10.1371/journal.pone.0139877>
- Stewart, R. I., Dossena, M., Bohan, D. A., Jeppesen, E., Kordas, R. L., Ledger, M. E., Meerhoff, M., Moss, B., Mulder, C., Shurin, J. B., Suttle, B., Thompson, R., Trimmer, M., and Woodward, G., Chapter Two - Mesocosm Experiments as a Tool for Ecological Climate-Change Research, in *Global Change in Multispecies Systems: Part 3* (Edited by Woodward, G. and O’Gorman, E. J.), volume 48 of *Advances in Ecological Research*, pp. 71–181, Academic Press, (2013), doi:10.1016/B978-0-12-417199-2.00002-1.
URL: <https://www.sciencedirect.com/science/article/pii/B9780124171992000021>
- Stock, C. A., Cheung, W. W., Sarmiento, J. L., and Sunderland, E. M., Chapter 2 - Changing ocean systems: A short synthesis, in *Predicting Future Oceans* (Edited by Cisneros-Montemayor, A. M., Cheung, W. W., and Ota, Y.), pp. 19–34, Elsevier, (2019), ISBN 978-0-12-817945-1, doi:10.1016/B978-0-12-817945-1.00002-2.
URL: <https://www.sciencedirect.com/science/article/pii/B9780128179451000022>
- Su, Z., Pilo, G. S., Corney, S., Holbrook, N. J., Mori, M., and Ziegler, P., Characterizing Marine Heatwaves in the Kerguelen Plateau Region. *Frontiers in Marine Science*, **7**, (2021), p. 1119, ISSN 2296-7745, doi:10.3389/fmars.2020.531297.
URL: <https://www.frontiersin.org/article/10.3389/fmars.2020.531297>
- Subramaniam, R. C., Melbourne-Thomas, J., Corney, S. P., Alexander, K., Péron, C., Ziegler, P., and Swadling, K. M., Time-Dynamic Food Web Modeling to Explore Environmental Drivers of Ecosystem Change on the Kerguelen Plateau. *Frontiers in Marine Science*, **7**, (2020), p. 641, ISSN 2296-7745, doi:10.3389/fmars.2020.00641.
URL: <https://www.frontiersin.org/article/10.3389/fmars.2020.00641>
- Sulman, M. H., Huntley, H. S., Lipphardt, B., and Kirwan, A., Leaving flatland: Diagnostics for Lagrangian coherent structures in three-dimensional flows. *Physica D: Nonlinear Phenomena*, **258**, (2013), pp. 77–92, ISSN 0167-2789, doi:10.1016/j.physd.2013.05.005.
URL: <https://www.sciencedirect.com/science/article/pii/S0167278913001450>

- Sumaila, U. R., Cheung, W. W. L., Lam, V. W. Y., Pauly, D., and Herrick, S., Climate change impacts on the biophysics and economics of world fisheries. *Nature Climate Change*, **15**(12), (2011), pp. 1758–6798, doi:10.1038/nclimate1301.
- Sumbly, J., Haward, M., Fulton, E. A., and Pecl, G. T., Hot fish: The response to climate change by regional fisheries bodies. *Marine Policy*, **123**, (2021), p. 104284, ISSN 0308-597X, doi:10.1016/j.marpol.2020.104284.
URL: <https://www.sciencedirect.com/science/article/pii/S0308597X20309301>
- Sun, D., Li, F., Jing, Z., Hu, S., and Zhang, B., Frequent marine heatwaves hidden below the surface of the global ocean. *Nat. Geosci*, **16**, (2023), pp. 1099–1104, doi: 10.1038/s41561-023-01325-w.
- Sunday, J., Pecl, G., Frusher, S., Hobday, A., Hill, N., Holbrook, N., Edgar, G., Stuart-Smith, R., Barrett, N., Wernberg, T., Watson, R., Smale, D., Fulton, E., Slawinski, D., Feng, M., Radford, B., Thompson, P., and Bates, A., Species traits and climate velocity explain geographic range shifts in an ocean-warming hotspot. *Ecol Lett*, **18**, (2015), pp. 944–953, doi:10.1111/ele.12474.
- Swart, N. C. and Fyfe, J. C., Observed and simulated changes in the Southern Hemisphere surface westerly wind-stress. *Geophys. Res. Lett.*, **39**(16), (2012), p. L16711, doi:10.1029/2012GL052810.
- Talley, L. D., *The Southern Ocean*, chapter 13, pp. 437–471, Academic Press, (2011).
- Thiers, L., Delord, K., Bost, C.-A., Guinet, C., and Weimerskirch, H., Important marine sectors for the top predator community around Kerguelen Archipelago. *Polar Biol*, **40**, (2017), p. 365–378, doi:10.1007/s00300-016-1964-4.
- Thomas, J. L., Waugh, D. W., and Gnanadesikan, A., Southern Hemisphere extratropical circulation: Recent trends and natural variability. *Geophys. Res. Lett.*, **42**, (2015), p. 5508–5515, doi:10.1002/2015GL064521.
- Tittensor, D. P., Beger, M., Boerder, K., Boyce, D. G., Cavanagh, R. D., Cosandey-Godin, A., Crespo, G. O., Dunn, D. C., Ghiffary, W., Grant, S. M., Hannah, L., Halpin, P. N., Harfoot, M., Heaslip, S. G., Jeffery, N. W., Kingston, N., Lotze, H. K., McGowan, J., McLeod, E., McOwen, C. J., O’Leary, B. C., Schiller, L., Stanley, R. R. E., Westhead, M., Wilson, K. L., and Worm, B., Integrating climate adaptation

and biodiversity conservation in the global ocean. *Science Advances*, **5**(11), (2019), p. eaay9969, doi:10.1126/sciadv.aay9969.

URL: <https://www.science.org/doi/abs/10.1126/sciadv.aay9969>

Tittensor, D. P., Eddy, T. D., Lotze, H. K., Galbraith, E. D., Cheung, W., Barange, M., Blanchard, J. L., Bopp, L., Bryndum-Buchholz, A., Büchner, M., Bulman, C., Carozza, D. A., Christensen, V., Coll, M., Dunne, J. P., Fernandes, J. A., Fulton, E. A., Hobday, A. J., Huber, V., Jennings, S., Jones, M., Lehodey, P., Link, J. S., Mackinson, S., Maury, O., Niiranen, S., Oliveros-Ramos, R., Roy, T., Schewe, J., Shin, Y.-J., Silva, T., Stock, C. A., Steenbeek, J., Underwood, P. J., Volkholz, J., Watson, J. R., and Walker, N. D., A protocol for the intercomparison of marine fishery and ecosystem models: Fish-mip v1.0. *Geoscientific Model Development*, **11**(4), (2018), pp. 1421–1442, doi:10.5194/gmd-11-1421-2018.

URL: <https://gmd.copernicus.org/articles/11/1421/2018/>

Toggweiler, J., Shifting Westerlies. *Science*, **323**(5920), (2009), pp. 1434–1435, doi:10.1126/science.1169823.

Toole, J. M., Sea ice, winter convection, and the temperature minimum layer in the Southern Ocean. *Journal of Geophysical Research: Oceans*, **86**(C9), (1981), pp. 8037–8047, doi:10.1029/JC086iC09p08037.

URL: <https://agupubs.onlinelibrary.wiley.com/doi/abs/10.1029/JC086iC09p08037>

Traon, P. Y. L., Nadal, F., and Ducet, N., An Improved Mapping Method of Multisatellite Altimeter Data. *Journal of Atmospheric and Oceanic Technology*, **15**(2), (1998), pp. 522 – 534, doi:10.1175/1520-0426(1998)015<0522:AIMMOM>2.0.CO;2.

Treasure, A. M., Roquet, F., Ansorge, I. J., Bester, M. N., Bornemann, L. B. H., Charrassin, J.-B., Chevallier, D., Costa, D. P., Fedak, M. A., Guinet, C., Hammill, M. O., Harcourt, R. G., Hindell, M. A., Kovacs, K. M., Lea, M.-A., Lovell, P., Lowther, A. D., Lydersen, C., McIntyre, T., McMahon, C. R., Muelbert, M. M., Nicholls, K., Picard, B., Reverdin, G., Trites, A. W., Williams, G. D., and de Bruyn, P. N., Marine Mammals Exploring the Oceans Pole to Pole: A Review of the MEOP Consortium. *Oceanography*, **30**(2), (2017), pp. 132–138, doi:10.5670/oceanog.2017.234.

Turner, J., Holmes, C., Caton Harrison, T., Phillips, T., Jena, B., Reeves-Francois, T., Fogt, R., Thomas, E. R., and Bajish, C. C., Record Low Antarctic Sea Ice Cover

in February 2022. *Geophysical Research Letters*, **49**(12), (2022), p. e2022GL098904, doi:10.1029/2022GL098904, e2022GL098904 2022GL098904.

URL: <https://agupubs.onlinelibrary.wiley.com/doi/abs/10.1029/2022GL098904>

Uggla, Y., What is this thing called 'natural'? The nature-culture divide in climate change and biodiversity policy. *Journal of Political Ecology*, **17**(1), (2010), pp. 79–91, doi:10.2458/v17i1.21701.

UNEP-WCMC and IUCN, Protected Planet: The World Database on Protected Areas (WDPA) and World Database on Other Effective Area-based Conservation Measures (WD-OECM), Cambridge, UK: UNEP-WCMC and IUCN, (2023).

URL: www.protectedplanet.net

van Beek, P., Bourquin, M., Reyss, J.-L., Souhaut, M., Charette, M., and Jeandel, C., Radium isotopes to investigate the water mass pathways on the Kerguelen Plateau (Southern Ocean). *Deep Sea Research Part II: Topical Studies in Oceanography*, **55**(5), (2008), pp. 622–637, ISSN 0967-0645, doi:10.1016/j.dsr2.2007.12.025, kEOPS: Kerguelen Ocean and Plateau compared Study.

URL: <https://www.sciencedirect.com/science/article/pii/S0967064508000155>

van Wijk, E. M., Rintoul, S. R., Ronai, B. M., and Williams, G. D., Regional circulation around Heard and McDonald Islands and through the Fawn Trough, central Kerguelen Plateau. *Deep Sea Research Part I: Oceanographic Research Papers*, **57**(5), (2010), pp. 653–669, ISSN 0967-0637, doi:10.1016/j.dsr.2010.03.001.

URL: <https://www.sciencedirect.com/science/article/pii/S0967063710000439>

Venegas-Li, R., Levin, N., Possingham, H., and Kark, S., 3D spatial conservation prioritisation: Accounting for depth in marine environments. *Methods in Ecology and Evolution*, **9**(3), (2018), pp. 773–784, doi:10.1111/2041-210X.12896.

Waldman, R. and Giordani, H., Ocean Barotropic Vorticity Balances: Theory and Application to Numerical Models. *Journal of Advances in Modeling Earth Systems*, **15**(4), (2023), p. e2022MS003276, doi:10.1029/2022MS003276, e2022MS003276 2022MS003276.

URL: <https://agupubs.onlinelibrary.wiley.com/doi/abs/10.1029/2022MS003276>

- Wang, R., Nan, F., Yu, F., and Wang, B., Subantarctic mode water variations in the three Southern Hemisphere ocean basins during 2004–2019. *Journal of Geophysical Research: Oceans*, **127**(7), (2022), p. e2021JC017906, doi:10.1029/2021JC017906.
- Weimerskirch, H., Le Bouard, F., Ryan, P. G., and Bost, C., Massive decline of the world's largest king penguin colony at Ile aux Cochons, Crozet. *Antarctic Science*, **30**(4), (2018), p. 236–242, doi:10.1017/S0954102018000226.
- Weller, R. A. and Plueddemann, A. J., Observations of the vertical structure of the oceanic boundary layer. *Journal of Geophysical Research: Oceans*, **101**(C4), (1996), pp. 8789–8806, doi:10.1029/96JC00206.
- Welsford, D. C., Constable, A. J., and Nowara, G. B., The Heard Island and McDonald Islands marine reserve and conservation zone: a model for Southern Ocean marine reserves, pp. 297–304, (2011).
- Wendebourg, M. R., Southern Ocean fishery management - Is CCAMLR addressing the challenges posed by a changing climate? *Marine Policy*, **118**, (2020), p. 103847, ISSN 0308-597X, doi:10.1016/j.marpol.2020.103847.
URL: <https://www.sciencedirect.com/science/article/pii/S0308597X18308121>
- Williamson, P. and Guinder, V. A., Chapter 5 - Effect of climate change on marine ecosystems, in *The Impacts of Climate Change* (Edited by Letcher, T. M.), pp. 115–176, Elsevier, (2021), ISBN 978-0-12-822373-4, doi:10.1016/B978-0-12-822373-4.00024-0.
URL: <https://www.sciencedirect.com/science/article/pii/B9780128223734000240>
- Wilson, K. L., Tittensor, D. P., Worm, B., and Lotze, H. K., Incorporating climate change adaptation into marine protected area planning. *Global Change Biology*, **26**(6), (2020), pp. 3251–3267, doi:10.1111/gcb.15094.
URL: <https://onlinelibrary.wiley.com/doi/abs/10.1111/gcb.15094>
- WMO, State of the Global Climate 2023, World Meteorological Organization, (2024), ISBN 978-92-63-11347-4.
URL: <https://library.wmo.int/records/item/68835-state-of-the-global-climate-2023>
- Wolfe, C. L., Cessi, P., McClean, J. L., and Maltrud, M. E., Vertical heat transport in eddy ocean models. *Geophys. Res. Lett.*, **35**(23), (2008), p. L23605, doi:10.1029/2008GL036138.

- Xu, L., Ding, Y., and Xie, S.-P., Buoyancy and wind driven changes in Subantarctic Mode Water during 2004–2019. *Geophysical Research Letters*, **48**(8), (2021), p. e2021GL092511, doi:10.1029/2021GL092511.
- Xu, X., Chassignet, E. P., Firing, Y. L., and Donohue, K., Antarctic Circumpolar Current Transport Through Drake Passage: What Can We Learn From Comparing High-Resolution Model Results to Observations? *Journal of Geophysical Research: Oceans*, **125**(7), (2020), p. e2020JC016365, doi:10.1029/2020JC016365.
- Xu, Y. and Fu, L.-L., The Effects of Altimeter Instrument Noise on the Estimation of the Wavenumber Spectrum of Sea Surface Height. *Journal of Physical Oceanography*, **42**(12), (2012), pp. 2229 – 2233, doi:10.1175/JPO-D-12-0106.1.
- Yang, C., Leonelli, F. E., Marullo, S., Artale, V., Beggs, H., Nardelli, B. B., Chin, T. M., Toma, V. D., Good, S., Huang, B., Merchant, C. J., Sakurai, T., Santoleri, R., Vazquez-Cuervo, J., Zhang, H.-M., and Pisano, A., Sea Surface Temperature Intercomparison in the Framework of the Copernicus Climate Change Service (C3S). *Journal of Climate*, **34**(13), (2021), pp. 5257 – 5283, doi:10.1175/JCLI-D-20-0793.1.
- Yates, P., Ziegler, P., Welsford, D., McIvor, J., Farmer, B., and Woodcock, E., Spatio-temporal dynamics in maturation and spawning of Patagonian toothfish *Dissostichus eleginoides* on the sub-Antarctic Kerguelen Plateau. *Journal of Fish Biology*, **92**(1), (2018), pp. 34–54, doi:10.1111/jfb.13479.
URL: <https://onlinelibrary.wiley.com/doi/abs/10.1111/jfb.13479>
- Young, E. F., Tysklind, N., Meredith, M. P., de Bruyn, M., Belchier, M., Murphy, E. J., and Carvalho, G. R., Stepping stones to isolation: Impacts of a changing climate on the connectivity of fragmented fish populations. *Evolutionary Applications*, **11**(6), (2018), pp. 978–994, doi:10.1111/eva.12613.
URL: <https://onlinelibrary.wiley.com/doi/abs/10.1111/eva.12613>
- Zhang, L., Delworth, T. L., Yang, X., Zeng, F., Lu, F., Morioka, Y., and Bushuk, M., The relative role of the subsurface Southern Ocean in driving negative Antarctic Sea ice extent anomalies in 2016–2021. *Weather*, **3**(1), (2022), p. 302, doi:10.1038/s43247-022-00624-1.
- Zhang, Y., Du, Y., Feng, M., and Hobday, A. J., Vertical structures of marine heatwaves. *Nature Communications*, **14**(1), (2023), p. 6483, doi:10.1038/s41467-023-42219-0.

- Ziegler, P. and Welsford, D., The Patagonian toothfish (*Dissostichus eleginoides*) fishery at Heard Island and McDonald Islands (HIMI) – population structure and history of the fishery stock assessment, in *The Kerguelen Plateau: Marine Ecosystem and Fisheries* (Edited by Duhamel, G. and Welsford, D.), Kingston, TAS: Société française d'ichtyologie, (2019).
- Zscheischler, J., Westra, S., van den Hurk, B. J. J. M., Seneviratne, S. I., Ward, P. J., Pitman, A., AghaKouchak, A., Bresch, D. N., Leonard, M., Wahl, T., and Zhang, X., Future climate risk from compound events. *Nature Climate Change*, **8**, (2018), pp. 469–477, doi:10.1038/s41558-018-0156-3.